

Universidade de Lisboa

Faculdade de Farmácia

Departamento de Química Farmacêutica e Terapêutica



**New synthetic methodologies for the transformation of
biomass derived intermediates to valuable molecules**

Jaime Alfredo da Silva Coelho

Doutoramento em Farmácia

Especialidade em Química Farmacêutica e Terapêutica

2014

Universidade de Lisboa

Faculdade de Farmácia

Departamento de Química Farmacêutica e Terapêutica



**New synthetic methodologies for the transformation of
biomass derived intermediates to valuable molecules**

Jaime Alfredo da Silva Coelho

Tese orientada pelo Prof.^o Doutor Carlos A. M. Afonso e
Doutor Alexandre F. Trindade, especialmente elaborada para a
obtenção do grau de doutor no ramo de Farmácia,
especialidade de Química Farmacêutica e Terapêutica

Abstract

The efficient use of biomass has recently attracted considerable attention as a potential alternative to limited fossil resources. 5-Hydroxymethylfurfural (HMF), which can be obtained from carbohydrates, has been identified as a promising bio-platform molecule for the synthesis of building block chemicals, pharmaceutical active compounds and biofuel products. To overcome the lack of efficient methods for HMF isolation, a process that uses wet tetraethylammonium bromide (TEAB) as solvent was developed, allowing the quantitative isolation of HMF in high purity, and reaction medium reutilization by crystallization. Based on that, two new efficient and reusable methodologies for the efficient synthesis and isolation of HMF were developed: the direct dehydration of fructose into HMF using Amberlyst® 15 and the more challenging integrated chemo-enzymatic synthesis from D-glucose that combines sweetzyme®-promoted D-glucose–D-fructose isomerization and HNO₃-catalyzed fructose dehydration into HMF. Furthermore, the impact of HMF and derivatives in human skin fibroblast cells was studied, where, in opposite to other derivatives, HMF was found as non-cytotoxic (94% cell viability).

In order to develop novel and competitive synthetic methodologies for HMF valorization, and according to precedent literature regarding transformation of furans into cyclopent-2-enones, the reactivity of 5-substituted furfurals with amines and Lewis acid catalysis was extensively investigated. Remarkably, two novel transformations were found and further studied: a unique and selective ϵ -functionalization of 5-substituted furfurals *via* trienamine intermediates and the synthesis of triarylmethanes bearing secondary anilines by Friedel-Crafts reaction of (hetero)aryl aldehydes and the corresponding secondary anilines. Both methodologies resulted in the synthesis of new furan-containing scaffolds that showed important antiproliferative activity against cancer cell lines. Furthermore, it was demonstrated that extreme high pressure (9 kbar) has a significant effect on the rate of the catalytic Friedel-Crafts alkylation studied.

Finally, the results towards the total synthesis of the natural products Modiolin and Fusanolide A using functionalized and stereodefined diene carboxylates through the thermal 4 π -electrocyclic ring-opening of cyclobutene precursors are shown. Two main strategies were proposed for the synthesis of the key 1,4-*cis*-substituted cyclobutene: one by direct alkylation of halocyclobutenes and the other by kinetic protonation of the easily synthesized *trans*-cyclobutene isomer. Unfortunately, no competitive methodology was discovered.

Keywords: 5-hydroxymethylfurfural (HMF), trienamines, bisvinylogous Mannich addition, high-pressure, triarylmethanes, total synthesis.

Resumo

A utilização eficiente de biomassa tem-se evidenciado cada vez mais como uma potencial alternativa às fontes fósseis vulgarmente usadas. O 5-Hidroximetilfurfural (HMF), que pode ser obtido a partir de carboidratos, tem-se mostrado como uma molécula promissora para a bio-refinaria na síntese de compostos químicos, compostos farmacologicamente activos e biocombustíveis. Foi desenvolvido um processo que utiliza brometo de tetraetilamonio (TEAB) como solvente, possibilitando o isolamento quantitativo do HMF com um grau de pureza elevado através da imediata cristalização do meio reaccional. Assim sendo, foram desenvolvidas duas metodologias eficientes e reutilizáveis para a síntese e isolamento do HMF: a desidratação directa da D-fructose em HMF utilizando Amberlyst® 15 e um processo químico-enzimático integrado para a preparação do HMF a partir da D-glucose que combina a isomerização D-glucose–D-fructose promovida pela sweetzyme® e a desidratação da fructose a HMF catalisada por HNO₃. Foi também estudado o impacto do HMF e vários derivados em células fibroblásticas de pele humana, revelando, ao contrário de outros derivados, a não citotoxicidade do HMF (94% de viabilidade celular).

Com o intuito de desenvolver novas metodologias sintéticas competitivas para a valorização do HMF, e de acordo com a literatura referente à transformação de furanos em ciclopent-2-enonas, foi extensivamente investigada a reactividade de derivados do HMF na presença de aminas e ácidos de Lewis. Contrariamente ao esperado, o estudo da reactividade do HMF demonstrou que ocorreram duas novas transformações: a funcionalização selectiva na posição ϵ de furfuraldeídos substituídos na posição 5, através de trienaminas como intermediários; ou a alquilação de Friedel-Crafts entre aldeídos aromáticos e anilinas secundárias resultando na síntese eficiente de triarilmetanos. Ambas as metodologias resultaram na síntese de novos compostos contendo o grupo furano com actividade antiproliferativa relevante contra linhas celulares cancerígenas. Foi também demonstrado que a alta pressão (9 kbar) tem um elevado impacto no aumento da velocidade da reacção de Friedel-Crafts estudada.

Finalmente, são apresentados os resultados relativos à tentativa de síntese total dos produtos naturais Modiolin e Fusanolide A partindo de carboxilatos dienoicos funcionalizados. Foram propostas duas estratégias para a síntese do *cis*-ciclobuteno chave: uma por alquilação directa de halociclobutenos e a outra por protonação cinética do isómero *trans*. Infelizmente, não foi descoberta nenhuma metodologia competitiva.

Palavras-chave: 5-hidroximetilfurfural (HMF), trienaminas, adição de Mannich bisvinílica, alta-pressão, triarilmetanos, síntese total.

Acknowledgements

Gostaria de agradecer ao Prof. Carlos A. M. Afonso, meu orientador, por todas as discussões, incentivos e entusiasmo que cedo fizeram despertar o meu gosto por Química Orgânica. Agradeço também a enorme disponibilidade demonstrada em todas as fases que levaram à concretização deste trabalho e contribuíram para a minha formação científica.

Ao Dr. Alexandre F. Trindade, meu co-orientador, agradeço toda a orientação, dedicação e competência, fundamentais para a realização desta tese de Doutoramento.

Ao Prof. Nuno Maulide gostaria de agradecer a oportunidade de poder trabalhar no seu laboratório (no *Max-Planck-Institut für Kohlenforschung*), e por todas as discussões motivadoras. To Dr. Caroline Souris I would like to thank for all the guidance at Maulide laboratory.

Ao Prof. Luís F. Veiros quero agradecer toda a disponibilidade e discussões sobre DFT. À Dr^a. Vânia André e Prof. M. Teresa Duarte quero agradecer a colaboração e análise de Raios-X.

To my friend and colleague Svilen Simeonov I would like to thank for all the great collaborations, for all the fruitful discussions and for all the nice moments inside and outside the workplace. À Dr^a. Raquel Frade quero agradecer pela realização de todos os estudos de actividade biológica descritos nesta tese, assim como todas as explicações relacionadas com os ensaios e a enorme disponibilidade. À Ana Reis, André Riscado, Jorge Silva e Rafael Gomes gostaria de agradecer por todo o trabalho realizado e interesse demonstrado.

Ao meu amigo e colega, Dr. Carlos Monteiro, agradeço toda a ajuda dentro e fora do laboratório e sobretudo o seu apoio. À minha amiga e colega de laboratório e de corridas, Dr. Filipa Siopa, agradeço pela disponibilidade e boa disposição.

Aos meus colegas de laboratório Dr^a. Andreia Rosatella, Dr^a. Catarina Rodrigues, Dr. Nuno Candeias, M.S. Fábio Santos, Dr. João Rosa, Dr. Luís Frija, Dr. Luís Gomes, M.S. Pedro Cal, M.S. Roberta Paterna, agradeço pelas discussões, ensinamentos e bons momentos passados durante todo o meu percurso pelo laboratório do Prof. Carlos Afonso.

To Maulide group colleagues, and all the great people that I met at *Max-Planck-Institut* I thank for all the fruitful discussions and great moments.

Quero também agradecer o apoio financeiro da Fundação para a Ciência e Tecnologia (SFRH/BD/73971/2010), da Fundação Calouste Gulbenkian (Prémio de Estimulo à Investigação 2012) e Acções Integradas Luso-Alemãs 2011 (Proj. 268) pelo apoio financeiro. Quero também agradecer à rede Nacional de NMR (REDE/1518/REM/2005) por disponibilizar o acesso ao equipamento de MS e NMR.

Por último, mas não menos importante, gostaria de agradecer a todos os meus amigos e familiares por todo o apoio.

Abbreviations

Ac	Acetyl
app	Apparent
AZT	Azidothymidine
BIAB	[bis(acetoxy)iodo]benzene
BINAP	2,2'-Bis(diphenylphosphino)-1,1'-binaphthyl
BINOL	1,1'-Bi(2-naphthol)
Bn	Benzyl
Boc	<i>tert</i> -Butyloxycarbonyl
BOX	2,2'-Isopropylidenebis[(4 <i>S</i>)-4- <i>tert</i> -butyl-2-oxazoline]
brsm	Based on recovered starting material
bs	Broad singlet
Bt	1 <i>H</i> -Benzotriazole
Bz	Benzoyl
CAFAM	5-Carboxylic-2-furoylamino-methane
CAFG	5-Carboxylic-2-furoyl-glycine
COD	1,5-Cyclooctadiene
CPME	Cyclopentyl methyl ether
CSA	10-Camphorsulfonic acid
Cy	Cyclohexyl
d	duplet
DCC	<i>N,N'</i> -Dicyclohexylcarbodiimide
DCE	1,2-Dichloroethane
DCM	Dichloromethane
DDQ	2,3-Dichloro-5,6-dicyano-1,4-benzoquinone
DFT	Density functional theory
DIBAL-H	Diisobutylaluminium hydride
DMA	Dimethylacetamide
DMAP	4-Dimethylaminopyridine
DME	1,2-Dimethoxyethane
DMF	<i>N,N</i> -dimethylformamide
DMP	Dimethoxypropane
DMPES	Dimethylphenethylsilane
DMSO	Dimethyl sulfoxide
dpppe	1,5-bis(diphenylphosphino)pentane
DU145	Human prostate cancer cell lines
EDG	Electron donating group
ee	Enantiomeric excess
ES	Ethyl 2-hydroxybenzoate
ESI	Electrospray ionization
EtOAc	Ethyl acetate
EWG	Electron withdrawing group
FDA	U. S. Food and drug administration
FDCA	2,5-Furan dicarboxylic acid
GC	Gas chromatography
GFI	D-Glucose/D-fructose isomerization
hex	<i>n</i> -Hexane
HIV	Human immunodeficiency virus
HMF	5-Hydroxymethylfurfural
HMFA	5-Hydroxymethyl-2-furoic acid
HMFG	5-Hydroxymethyl-2-furoyl glycine
HMPA	Hexamethylphosphoramide
HOMO	Higher occupied molecular orbital

HPLC	High-performance liquid chromatography
Hz	Hexanoyl
IC ₅₀	Half maximal inhibitory concentration
ILs	Ionic liquids
<i>J</i>	Nuclear magnetic resonance coupling constant
KIE	Kinetic isotope effect
LA	Lewis acid
LNCaP	Epithelial cell line derived from a human prostate carcinoma
LUMO	Lower unoccupied molecular orbital
m	multiplet
m. p.	melting point
mCPBA	<i>meta</i> -Chloroperoxybenzoic acid
Mim	<i>N</i> -methylimidazole
min	minutes
MS	Mass spectra
MTBE	Methyl <i>tert</i> -butyl ether
MW	Microwave irradiation
NBS	<i>N</i> -bromosuccinimide
NMR	Nuclear magnetic resonance
OTf	Trifluoromethanesulfonate
PCM	Polarizable continuum model
pent	<i>n</i> -pentane
PG	Protective group
Ph	Phenyl
PMA	Phosphomolibdic acid.
PPA	Polyphosphoric acid
ppm	parts per million
PTC	Phase transfer catalyst
PTSA	<i>p</i> -Toluenesulfonic acid
<i>p</i> -TSO	<i>p</i> -Tolyl sulfoxide
PyBOX	2,6-Bis[(4 <i>R</i>)-4-phenyl-2-oxazoliny] pyridine
q	quartet
RB	Rose Bengal
R _f	Retention factor
R _t	Retention time
RT	Room temperature
s	singlet
SIBX	Stabilized 2-iodoxybenzoic acid
SIMes	1,3-bis(2,4,6-trimethylphenyl)imidazol-2-ylidene
SIPr	1,3-bis-(2,6-diisopropylphenyl)imidazol-2-ylidene
SMF	5-[(Sulfooxy)-methyl]furfural
t	triplet
TBAF	Tetra- <i>n</i> -butylammonium fluoride
TBDMS	<i>tert</i> -Butyldimethylsilane
TBDPS	<i>tert</i> -Butyldiphenylsilane
^t Bu	<i>tert</i> -Butyl
TEA	Triethylamine
TEAB	Tetraethylammonium bromide
TEAC	Tetraethylammonium chloride
Tf	Trifluoromethylsulfonyl
TFA	Trifluoroacetic acid
THF	Tetrahydrofuran
THS	Trihexylsilane
TIPS	Triisopropylsilane
TLC	Thin-layer chromatography

TMS	Tetramethylsilane
TPAB	Tetrapropylammonium bromide
TPAC	Tetrapropylammonium chloride
TRAM	Triarylmethane
TRIP	(<i>R</i>)-3,3'-Bis(2,4,6-triisopropylphenyl)-1,1'-binaphthyl-2,2'-diyl
Ts	<i>para</i> -Toluenesulfonyl
UV	Ultra-violet
VAPOL	(<i>R</i>)-2,2'-Diphenyl-3,3'-biphenanthryl-4,4'-diyl phosphate
XPhos	2-Dicyclohexylphosphino-2',4',6'-triisopropylbiphenyl

Table of Contents

I.	Introduction	1
I.1.	Nucleosides	3
I.2.	Functionalized cyclopent-2-enones	6
I.2.1.	Conversion of furans into cyclopent-2-enones	7
I.2.2.	Conversion of furfuryl alcohol motives into cyclopent-2-enones.....	8
I.2.3.	Conversion of furfuraldehyde motives into cyclopent-2-enones	21
I.3.	5-Hydroxymethylfurfural (HMF)	26
I.4.	Objectives.....	27
II.	Synthesis, isolation and cytotoxicity of 5-Hydroxymethylfurfural and derivatives	31
II.1.	Introduction.....	33
II.1.1.	Preparation of 5-Hydroxymethylfurfural (HMF).....	33
II.1.2.	Enzymatic isomerization of D-glucose to D-fructose	34
II.1.3.	Mechanism	35
II.1.4.	Cytotoxicity	35
II.2.	Results	37
II.2.1.	Production and isolation of HMF from carbohydrates.....	37
II.2.2.	Integrated chemo-enzymatic production of HMF from glucose	41
II.2.3.	Guidelines for human exposure of furfural-related compounds.....	50
II.3.	Conclusions and Perspectives	53
II.4.	Experimental	56
II.4.1.	General Remarks.....	56
II.4.2.	Experimental procedures of Section II.2.1	57
II.4.3.	Experimental procedures of Section II.2.2.....	63
II.4.4.	Preparation of furanic compounds for cytotoxicity studies.....	65
III.	New synthetic methodologies for 5-Hydroxymethylfurfural (HMF) valorization	71
III.1.	Introduction.....	73
III.1.1.	Preliminary Results.....	73
III.1.2.	Extreme high pressure induced reactions	76
III.2.	ϵ -Functionalization of 5-substituted Furfurals <i>via</i> Trienamines Intermediates.....	80
III.2.1.	Introduction	80
III.2.2.	Results and Discussion	85
III.2.3.	Conclusions	105

III.3. Synthesis and Biological Activity of New Triarylmethanes	106
III.3.1. Introduction	106
III.3.2. Results and Discussion	115
III.3.3. Conclusions	130
III.4. Experimental	131
III.4.1. General Methods	131
III.4.2. Experimental part for Section III.1.1	134
III.4.3. Experimental part for Section III.2	134
III.4.4. Experimental part for Section III.3	145
IV. Towards total synthesis of Modiolin, Fusanolide A and FR256523	155
IV.1. Towards total synthesis of Modiolin and Fusanolide A	157
IV.1.1. Introduction	157
IV.1.2. Results	160
IV.2. Towards total synthesis of FR256523.....	171
IV.3. Conclusions and Perspectives.....	175
IV.4. Experimental	177
IV.4.1. General Remarks	177
IV.4.2. Towards total synthesis of Modiolin and Fusanolide A	177
IV.4.3. Towards total synthesis of FR256523.....	189
V. Conclusions	193
VI. References.....	197
Supporting information	278

Chapter 1

Introduction

This chapter aims to present the background and the initial objectives of the current thesis. After a brief introduction on carbocyclic nucleosides as target molecules, the state of the art on cyclopent-2-enones synthesis from furan-containing molecules will be comprehensively described followed by a description of 5-hydroxymethylfurfural (HMF) as starting material.

I. Introduction	1
I.1. Nucleosides.....	3
I.2. Functionalized cyclopent-2-enones.....	6
I.2.1. Conversion of furans into cyclopent-2-enones	7
I.2.2. Conversion of furfuryl alcohol motives into cyclopent-2-enones	8
I.2.3. Conversion of furfuraldehyde motives into cyclopent-2-enones.....	21
I.3. 5-Hydroxymethylfurfural (HMF)	26
I.4. Objectives	27

I.1. Nucleosides

Nucleosides have been used for a long time as building units for antisense oligonucleotides preparation and widely studied as potential antitumor, anti-inflammatory and antiviral agents. Since human immunodeficiency virus (HIV) was discovered, extensive fundamental research work has been carried out to identify compounds with antiviral activity against this virus.¹ In fact, nucleosides such as AZT (**1**) (**Figure I.1**), that exhibited significant antiviral activity were approved by the FDA for the treatment of HIV infection as reverse transcriptase inhibitors.

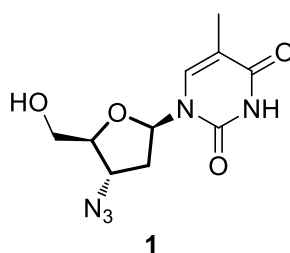


Figure I.1. Structure of azidothymidine (AZT).

The clinical application of these nucleosides is limited not only due to elevated toxicity and side effects but also because virus can acquire resistance.¹ For these reasons, the demand for more stable and less toxic anti-HIV agents which are not crossresistant with existing drugs has increased.

Carbocyclic nucleosides, where the furanose oxygen atom of the normal nucleosides is replaced by a methylene group, changing the furanose ring into cyclopentane, have received extraordinary attention over the last two decades. For example, the natural occurring carbocyclic nucleosides aristeromycin (**2**) and neplanocin A (**3**) (**Figure I.2**) have been isolated from *Streptomyces citricolor* and *Actinoplanacea ampullariella*, respectively, possessing both pronounced activity. Furthermore, it was found that synthetic carbocyclic nucleosides [e.g., carbovir (**4**) and abacavir (**5**), **Figure I.2**] also exhibited good activity against HIV. This replacement results in greater metabolic stability toward the phosphorylase enzymes which cleave glycosidic linkages of normal nucleosides. Furthermore, they have comparatively higher lipophilicity which is potentially beneficial for increasing oral efficiency and cell wall penetration.¹

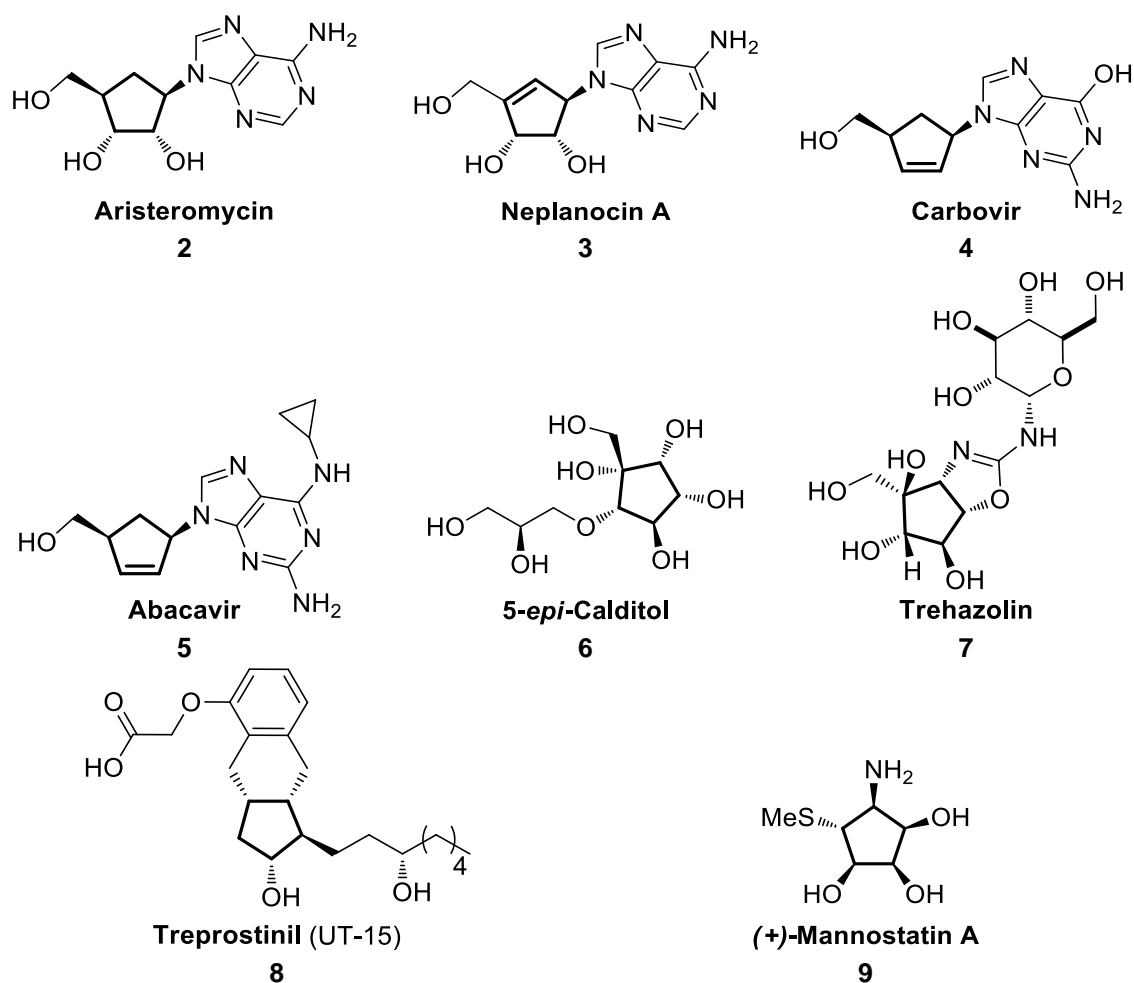
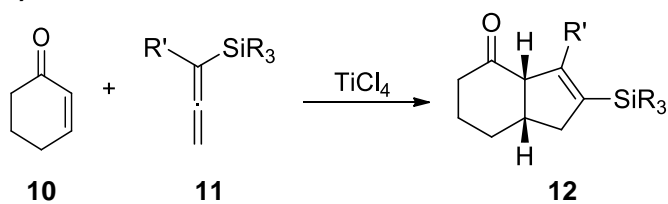
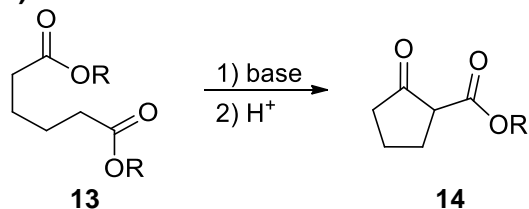
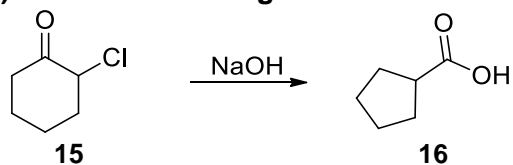
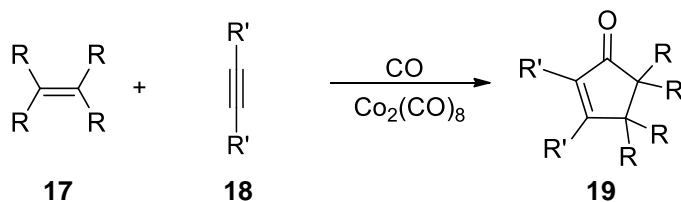
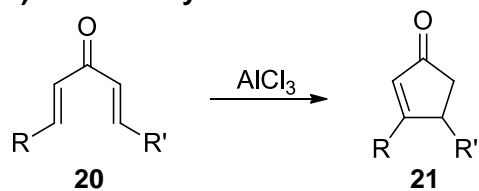
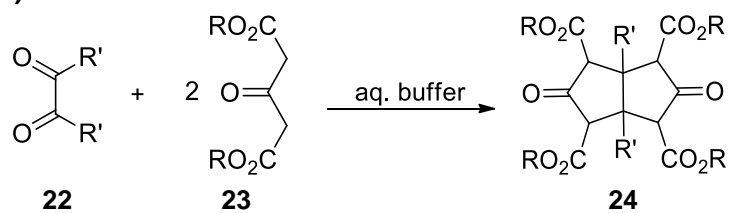


Figure I.2. Examples of carbocyclic nucleosides.

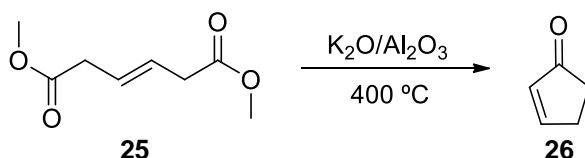
Two key points can be highlighted for the preparation of carbocyclic nucleosides: the synthesis of the required carbocyclic sugar moiety bearing the suitable functional groups and the construction or introduction of the base moiety. The first point corresponds to the main synthetic organic work done in this area, while the second one can be easily achieved through convergent approaches with high regio- and stereoselectivity.²

Five-membered carbocycles structures can be generally achieved from six main type of reactions: Danheiser annulation, Dieckmann condensation, Favorskii rearrangement, Nazarov cyclization, Pauson-Khand reaction and Weiss-Cook reaction (**Scheme I.1**).³⁻⁴ It is noteworthy mentioning that functionalized cyclopent-2-enones (e.g., **19** and **21**) are interesting derivatives for the synthesis of carbocyclic nucleosides.

a) Danheiser annulation**b) Dieckmann condensation****c) Favorskii rearrangement****d) Pauson–Khand reaction****e) Nazarov Cyclization****f) Weiss–Cook reaction****Scheme I.1.** Synthesis of five-membered carbocycles motives.

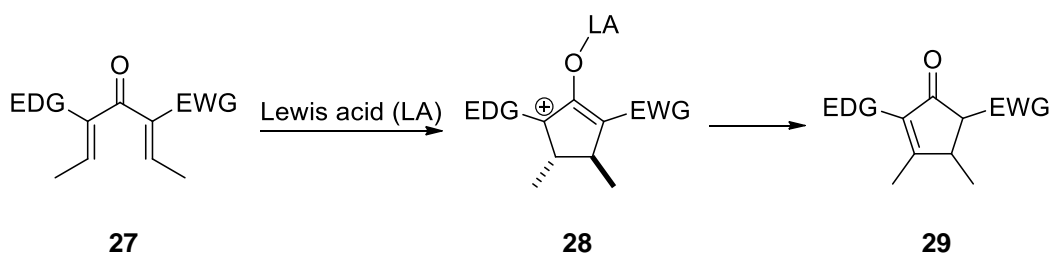
I.2. Functionalized cyclopent-2-enones

Industrially, simple cyclopent-2-enones are commonly obtained by Claisen condensation of hexenedioic acids or their corresponding diesters as shown in **Scheme I.2**. Generally, alkyl, alkenyl or aryl substituents can be used in a temperature range of 150 to 450 °C.⁵ Moreover functionalized cyclopent-2-enones can be typically obtained by Nazarov cyclization or by Pauson-Khand reaction (**Scheme I.1**).



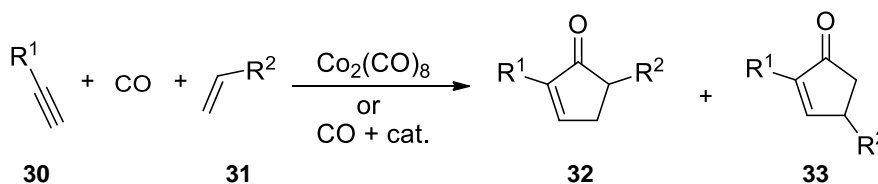
Scheme I.2. Cyclization of dimethyl hex-3-ene-1,6-dioate (**25**) into cyclopent-2-enone (**26**).

Nazarov cyclization is a Lewis acid-catalyzed 4π conrotatory electrocyclic reaction that allows the synthesis of cyclopent-2-enones **29** from divinyl ketones **27** (**Scheme I.3**). According to the mechanism the diastereoselectivity involving the new formed σ bond is lost after proton elimination.^{4,6}



Scheme I.3. Nazarov cyclization.

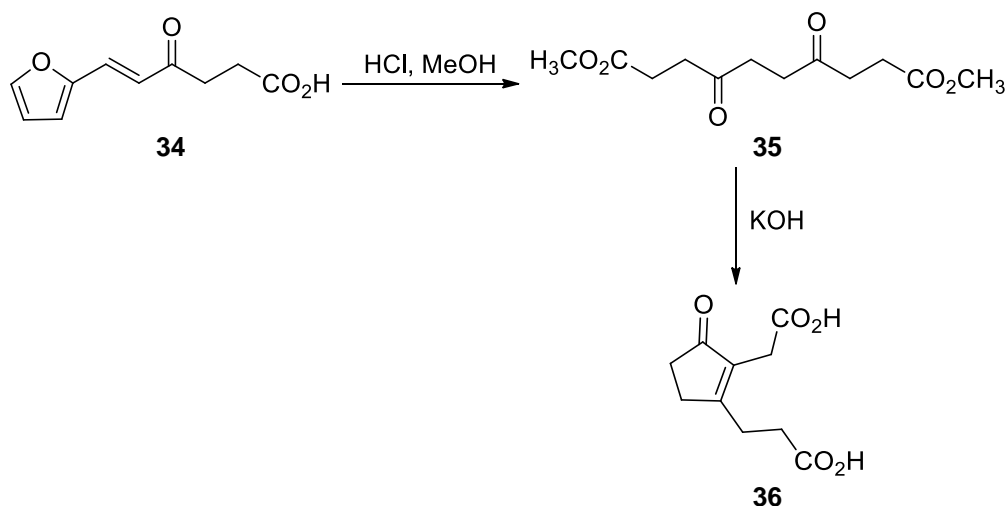
Pauson-Khand reaction is a $[2+2+1]$ cycloaddition between an alkyne, an alkene and carbon monoxide. In this case, the stereochemistry of the complexation of the alkene at cobalt is guided by steric repulsions between the R^1 and R^2 groups favoring the formation of only 2 isomers as represented in **Scheme I.4**.^{4,7}



Scheme I.4. Pauson-Khand reaction.

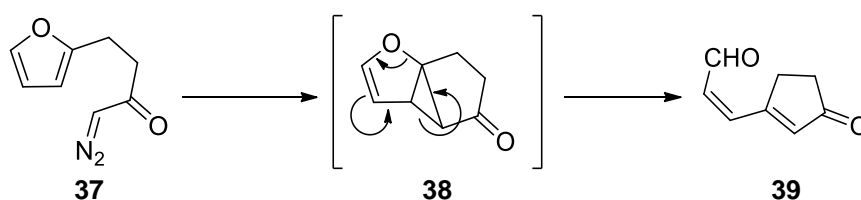
I.2.1. Conversion of furans into cyclopent-2-enones

Conversion of furan-containing scaffolds into cyclopent-2-enones can be achieved *via* a variety of different reactions. Alkylfurans can generate cyclopent-2-enones through 1,4-dicarbonyl compounds and *via* oxidation reactions. Furylidene ketones **34** can undergo acidic ring-opening followed by cyclization into the corresponding cyclopent-2-enones **36** as shown in **Scheme I.5**.⁸



Scheme I.5. Acidic ring opening conversion of 2-furylidenelevulinic acid (**34**) into the symmetrical dimethyl 4,7-dioxodecandioate (**35**) followed by cyclization under basic conditions.⁹

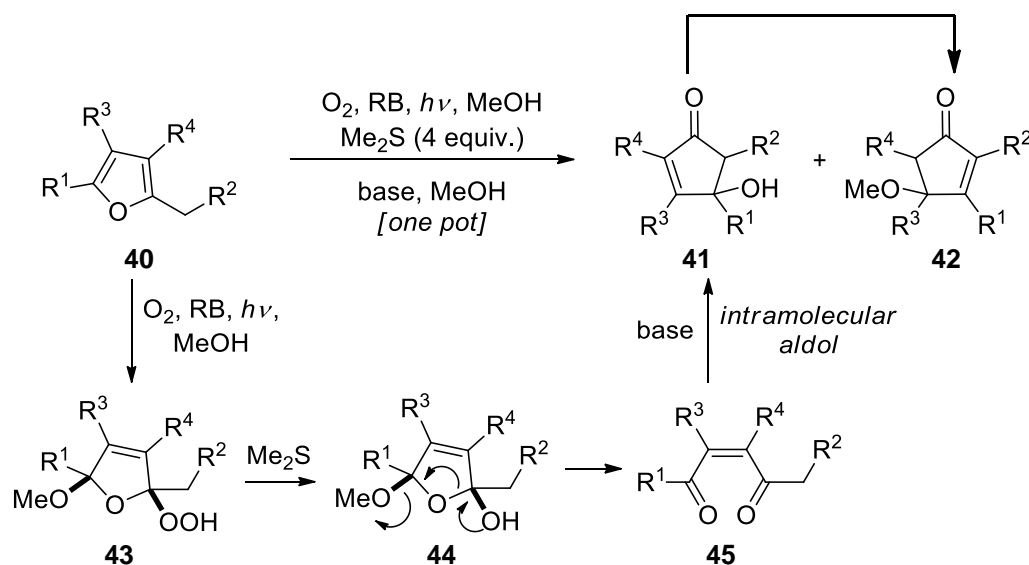
Furthermore, few examples showed that cyclopent-2-enones **39** can be obtained *via* carbene cyclopropanation in the furan ring proceeded by ring opening rearrangements as depicted in **Scheme I.6**.⁸



Scheme I.6. Bicyclo **38** formed by cyclopropanation undergoes electrocyclic ring opening to generate the cyclopent-2-enone **39**.¹⁰

Very recently, Vassilikogiannakis *et al.* developed an efficient one-pot transformation of readily accessible furans **40** into 4-hydroxycyclopent-2-enones **41** and **42** in H₂O, using singlet oxygen as oxidant as depicted in **Scheme I.7**.¹¹ The direct oxidation of the furan nucleus mediated by agents such as mCPBA, NBS, Br₂ and H₂O₂ are already widely

described in literature,¹² however the novelty of this approach is related to the one-pot protocol for the synthesis of cyclopent-2-enones.



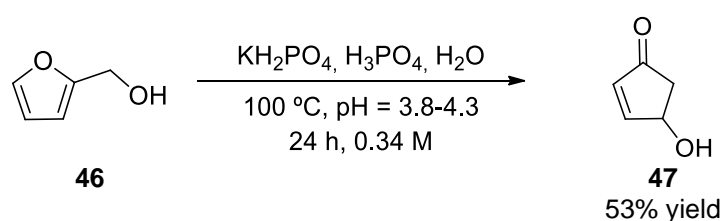
Scheme I.7. One-pot transformation of simple furans **40** into 4-hydroxycyclopent-2-enones **41** and **42**. RB = Rose bengal.

Furylcarbinols, furfuraldehydes or stenhouse salts are also susceptible of conversion to the corresponding cyclopent-2-enones. In the following pages a comprehensive review on conversion of these motives into cyclopent-2-enones will be described.

I.2.2. Conversion of furfuryl alcohol motives into cyclopent-2-enones

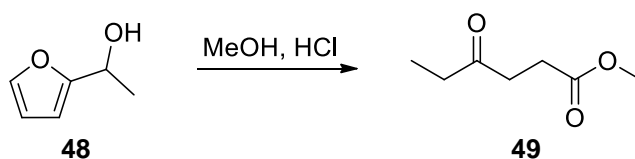
The seminal work reported by Nanni *et al.* in 1982 describes the rearrangement of furfuryl alcohol (**46**) into (\pm)-4-hydroxycyclopent-2-enone (**47**).¹³⁻¹⁴ Today, this transformation is a well-established synthetic method, whose usefulness was demonstrated in several total synthesis.¹⁵⁻²⁴ Sodium or potassium dihydrogenphosphate and phosphoric acid in water or 1,4-dioxane in a pH range of 4 to 5 for around 40 hours at 99 °C are generally the optimal conditions to perform the transformation. The reported yield range is from 30 to 53%, which reflects the low efficiency of the transformation. Consequently, some recent reaction conditions optimization studies were reported by several authors.^{23,25} For example, during the synthesis of carbocyclic nucleoside MDL 201449A in 1998, Webster *et al.* used the optimized reaction conditions described in **Scheme I.8** to perform the rearrangement.²³ The authors reported that furfuryl alcohol (**46**) concentration is important for the reaction yield, in which higher concentration (2.55 M) led to lower yields (17%). In other example, Ulbrich *et al.* studied in 2010 the rearrangement assisted by both microwave and microreactor, reporting a very impressive good yield of 87% in subcritical water and in absence of any catalyst.²⁵

The synthesis of enantiomerically pure cyclopent-2-enone **47** is very important for further preparation of nucleosides and prostaglandins, hence several methods for its enantioselective preparation were reported in literature including desymmetrizations, classical and kinetic resolutions and D-tartaric acid derivatives synthesis. Furthermore, a short review on the specific cyclopent-2-enone **47** was published in 2010 by Roche and Aitken.²⁶ Despite the moderate enantioselectivity, the most interesting process in a scale-up point of view is the enzymatic kinetic resolution of the racemic cyclopent-2-enone **47** using Lipozyme IM as described by Ghorpade and co-workers. In this process the enzymatic kinetic resolution studies of (±)-**47** were taken up in organic solvents by transesterification with vinyl acetate followed by alcoholysis.²⁷



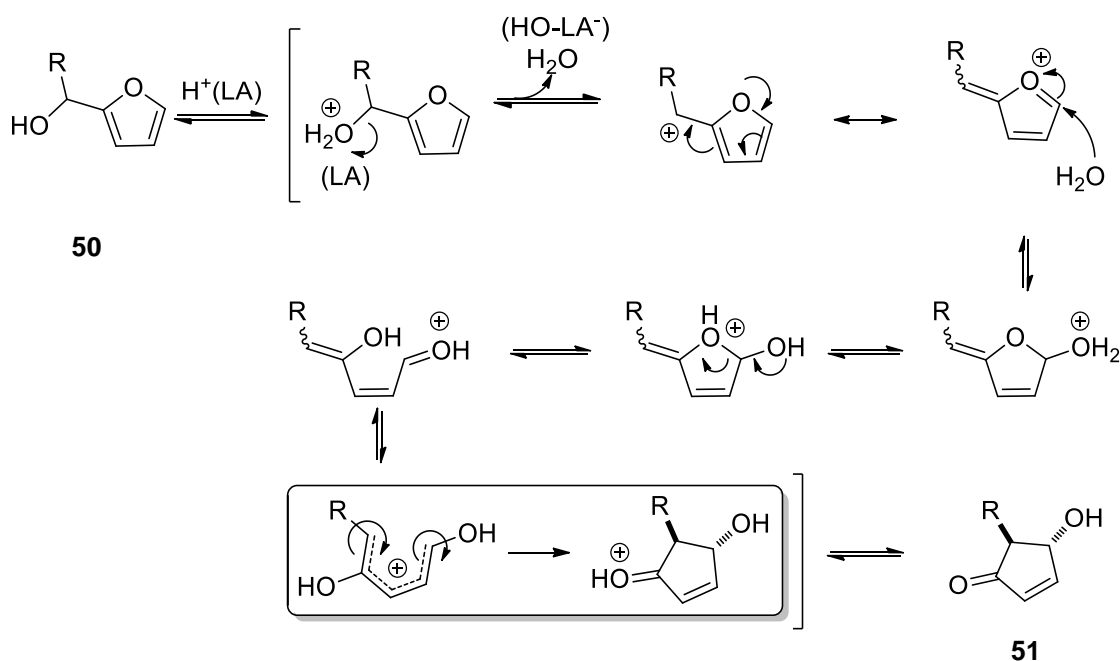
Scheme I.8. Furfuryl alcohol (**46**) rearrangement into (±)-4-hydroxycyclopent-2-enone (**47**).

Secondary furfuryl alcohol derivatives **50** (2-furylcarbinols) are also susceptible of conversion into the respective cyclopent-2-enones **51** under appropriate controlled conditions such as the solvent, temperature and catalyst. Aqueous media containing buffers and strong acid catalysts (e.g., formic, polyphosphoric or *p*-toluenesulfonic acids) are commonly used in a temperature around $100\text{ }^\circ\text{C}$. In many others procedures, a co-solvent such as acetone²⁸⁻²⁹, dioxane, or dimethoxyethane is also used.^{8,30} The pH plays a very important role in this transformation due to the formation of several byproducts under strong acid conditions³¹⁻³². Another issue that influences the yield is the reaction concentration, where in general a solvent/substrate ratio of 30:1 seems to be the best.³⁰ Furthermore, it is noteworthy that 2-furylcarbinols can also undergo Marckwald-type reactions under specific acidic conditions to give levulinic acid derivatives **49** (**Scheme I.9**).³³



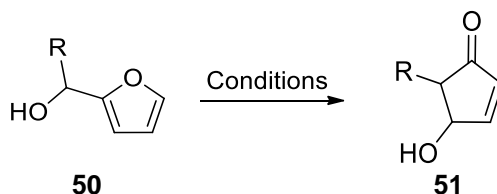
Scheme I.9. Marckwald-type reaction of 1-(furan-2-yl)ethanol (**48**) to yield methyl 4-oxohexanoate (**49**).

Today the rearrangement of 2-furylcarbinols **50** into cyclopent-2-enones **51** is known as Piancatelli reaction because it dates back to the seminal reports of the Italian chemist Giovanni Piancatelli, who first described this reaction in 1976.²⁸ The same group continued to systematically investigate the rearrangement resulting in several reports.⁸ The overall mechanism of this transformation is believed to proceed through a cascade sequence that terminates with a 4π electrocyclic ring closure of a pentadienyl cation, analogous to the Nazarov cyclization. In **Scheme I.10** is represented the mechanism proposed by Faza *et al.* established by computational studies.³⁴



Scheme I.10. Proposed mechanism of the Piancatelli reaction.³⁴ LA = Lewis acid

Several 2-furylcarbinols derivatives **50** can be converted into the corresponding cyclopent-2-enones **51**, as shown in a variety of different reports (**Table I.1**). Starting materials having an aromatic substituent as R are particularly reactive.^{8,35} For some cases, milder conditions such as zinc(II) chloride can also be applied. However, when the side chain is an alkyl or cycloalkyl group the starting materials are less prone to rearrange. 2-Furylcarbinols bearing a steroid nucleus has unusual stability in a mildly acidic medium, being necessary treatment with concentrated sulfuric acid as catalyst.³⁶

Table I.1. Overview of reported conversion of 2-furylcarbinols **50** into corresponding cyclopent-2-enones **51**.

Entry	R	Conditions	Yield (%)
1 ²⁸	phenyl	HCOOH, H ₂ O/acetone (2:1), 50 °C, 24 h	65
2 ³⁷⁻³⁹	phenyl	ZnCl ₂ , DME/H ₂ O, 60 °C, 96 h	28
3 ²⁵	phenyl	H ₂ O, 200 °C, 300 W, 15 bar, 2 min	96
4 ²⁸	methyl	PTSA, H ₂ O/acetone (2:1), 50 °C, 24 h	30
5 ^{28,31}	<i>n</i> -hexyl	PPA, H ₂ O/acetone (2:1), 50 °C, 24 h	70
6 ⁴⁰	<i>n</i> -heptyl	PPA, H ₂ O/acetone, 65 °C, 48 h	50
7 ²⁵	<i>n</i> -ethyl	H ₂ O, 200 °C, 300 W, 15 bar, 15 min	54
8 ²⁵	<i>n</i> -pentyl	H ₂ O, 200 °C, 300 W, 15 bar, 15 min	65
9 ²⁵	<i>n</i> -dodecyl	H ₂ O, 200 °C, 300 W, 15 bar, 30 min	NR
10 ²⁹	cyclohexyl	PPA, H ₂ O/acetone, 55 °C, 48 h	85
11 ⁴¹	(CH ₂) ₆ CO ₂ (<i>t</i> -C ₄ H ₉)	PPA, H ₂ O/acetone, 50 °C, 24 h	51
12 ⁴²	CH ₂ CH ₂ Ph	H ₂ SO ₄ , DME/H ₂ O, 80 °C, 3 h	72
13 ^{38,43}	3,4,5-(OCH ₃) ₃ -C ₆ H ₂	ZnCl ₂ , dioxane/H ₂ O, reflux, 24 h	85
14 ²⁵	CH ₂ CH=CHCH ₃	H ₂ O, 200 °C, 300 W, 15 bar, 5 min	73
15 ³⁶	steroid	H ₂ SO ₄ , H ₂ O/acetone, 50 °C, 30 h	90

NR – No reaction, PPA - Polyphosphoric Acid, DME - 1,2-Dimethoxyethane, MW - Microwave irradiation. PTSA - *p*-toluenesulfonic acid

Although less explored, C-5 substituted 2-furylcarbinols derivatives are also susceptible to conversion into cyclopent-2-enones (**Table I.2**). The presence of electron-withdrawing nitro group at C-5 of the furan ring stabilizes the starting material avoiding the rearrangement even under harsh conditions.⁸ Furthermore, an electron-donor methoxy group favors the formation of 4-ylidenebutenolides **53** (**Scheme I.11** and **Table I.2**, entry 10).⁴⁴ The same result is obtained using chloro as substituent (**Table I.2**, entry 11).⁴⁵

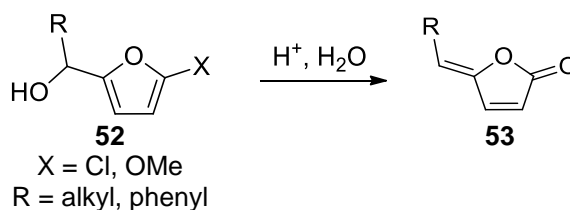
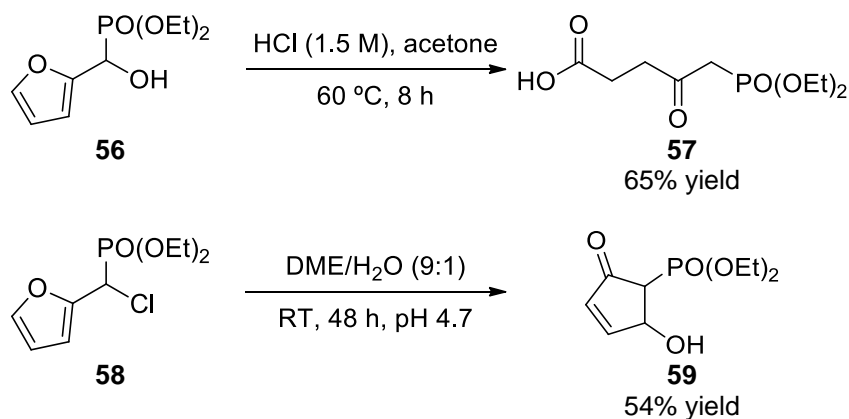
**Scheme I.11.** Formation of 4-ylidenebutenolides products **53** from C-5 substituted 2-furylcarbinols **52**.

Table I.2. Conversion of C-5 substituted 2-furylcarbinols derivatives **54** into corresponding cyclopent-2-enones **55**.

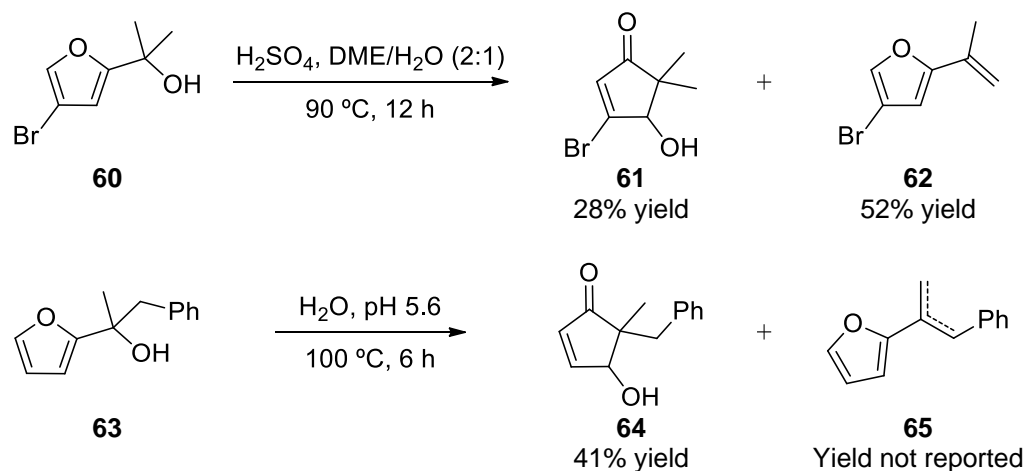
Entry	R ¹	R ²	Conditions	Yield (%)
1 ^{28,31}	CH ₃	allyl	ZnCl ₂ , H ₂ O/acetone, 55 °C, 96 h	35
2 ³⁰	CH ₃	allyl	H ₂ O, pH 5-5.5, 100 °C, 12 h	85
3 ²⁹	CH ₃	propargyl	PPA, H ₂ O/acetone, 55 °C, 96 h	46
4 ³⁰	CH ₃	propargyl	H ₂ O, pH 4.5-5.0, 100 °C, 13 h	74
5 ³⁰	CH ₃	<i>n</i> -butyl	H ₂ O, pH 5-5.5, 100 °C, 30 h	70
6 ²⁸	CH ₃	thiophene-2-yl	ZnCl ₂ , H ₂ O/acetone, 4 h	85
7 ³⁰	CH ₃	<i>p</i> -chlorobenzyl	H ₂ O, pH 4.0-5.7, 100 °C, 30 h	88
8 ²⁸	CH ₃	cyclohexyl	ZnCl ₂ , H ₂ O/acetone, 60 °C, 72 h	16
9 ⁴⁶	NO ₂	<i>n</i> -pentyl	H ⁺ , H ₂ O/acetone, 60 °C	NR
10 ⁴⁴	OCH ₃	<i>n</i> -octyl	H ⁺ , H ₂ O	^a
11 ⁴⁵	Cl	phenyl	H ⁺ , H ₂ O	^a

PPA - Polyphosphoric Acid, ^a4-ylidenebutenolide product (see Scheme I.11). NR - No reaction

Interestingly, a different reactivity for 2-furylcarbinols bearing a phosphonate group in the side chain is observed, giving normally the levulinic acid derivative through Marckwald-type reaction (**Scheme I.12**, top).⁴⁷ However, replacement of the hydroxyl group in the side chain with a more efficient leaving group such as chloride greatly enhances the furan reactivity through cyclopent-2-enone formation (**Scheme I.12**, bottom). For this cases, due to hydrogen chloride liberating an appropriate buffer solution has to be used to prevent a fall in pH.⁴⁸

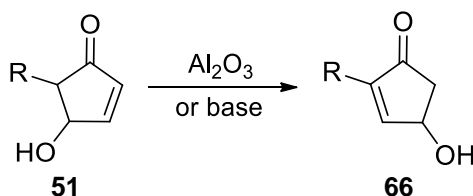
**Scheme I.12.** Reactivity of 2-furylcarbinols bearing phosphonate groups in the side chain.⁴⁷⁻⁴⁸

Tertiary 2-furylcarbinols can also undergo rearrangement into cyclopent-2-enones, however dehydration of starting tertiary alcohol into alkenes is the major reaction (**Scheme I.13**).⁸



Scheme I.13. Reactivity of tertiary 2-furylcarbinols.⁸

Another interesting feature of this rearrangement is the fact that 5-substituted 4-hydroxycyclopent-2-enones **51** can undergo further rearrangement into the thermodynamically more stable 2-substituted 4-hydroxycyclopent-2-enones **66** (**Scheme I.14**). Alumina or basic conditions are the common methods used to perform the isomerization.⁸



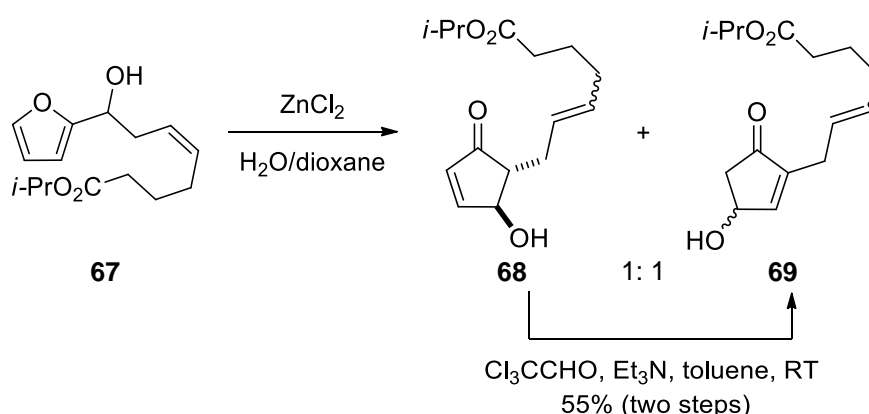
Scheme I.14. Isomerization of 5-substituted 4-hydroxycyclopent-2-enones **51** into 2-substituted 4-hydroxycyclopent-2-enones **66**.

In some cases, MgCl_2 or ZnCl_2 at high temperatures can also be used to obtain directly the 2-substituted 4-hydroxycyclopent-2-enone **56** (**Table I.3**).

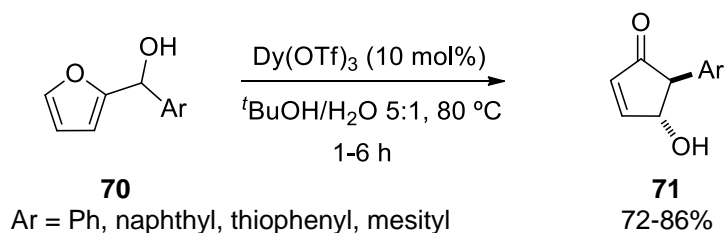
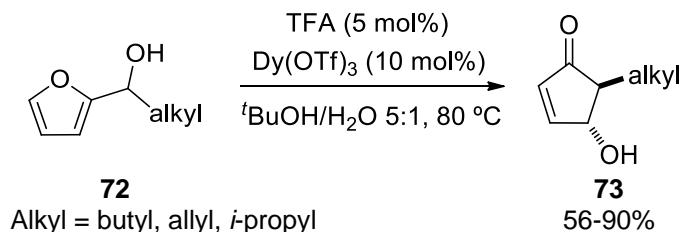
Table I.3. Selected examples of direct conversion and isomerization of 2-furylcarbinols **50** into corresponding cyclopent-2-enones **66**.

Entry	R	Conditions	Yield (%)
1 ⁴⁹	allyl	H ₂ O, MgCl ₂ , 180 °C, pH 6.0, 3.5 h	84
2 ⁵⁰	CH ₂ CH ₂ CHCFCO ₂ C ₂ H ₅	ZnCl ₂ , H ₂ O, dioxane, 180 °C, 32 h	27

Some of the current drawbacks of the Piancatelli rearrangement are the use of stoichiometric quantities of Brønsted or Lewis acid, the moderate isolated yields and the formation of polymeric byproducts that are difficult to remove, especially when performing gram scale reactions.¹⁵ Moreover, the rearrangement often results in an inseparable mixture of the 4-hydroxycyclopent-2-enone isomers.⁵¹⁻⁵² For example, rearrangement of 2-furylcarbinol **67** in the presence of ZnCl₂ gives a 1:1 mixture of **68** and **69**, that can be further isomerized to a single isomer **69** by exposure to basic conditions (**Scheme I.15**).⁵²

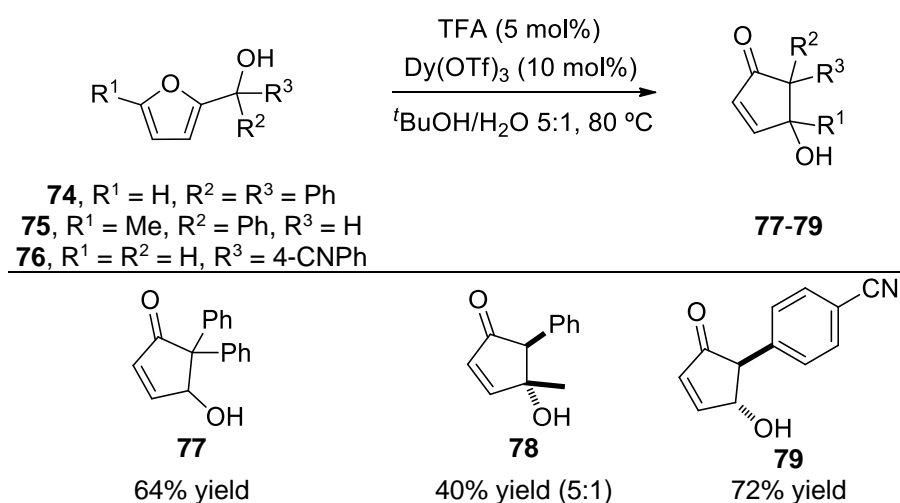
**Scheme I.15.** Piancatelli rearrangement of 2-carbinol **67**.⁵²

Very recently (2014), Alaniz *et al.* addressed these problems by using catalytic dysprosium(III) trifluoromethanesulfonate in the Piancatelli rearrangement of both aryl and alkyl substituted furylcarbinols to *trans*-4-hydroxycyclopent-2-enones.⁵³ The authors reported good yield when simple aryl carbinols are used (**Scheme I.16a**). For alkyl carbinols, combination of Dy(OTf)₃ and trifluoroacetic acid (TFA) catalysis was necessary to achieve good yields (**Scheme I.16b**).

a) Rearrangement of aryl carbinols **70**b) Rearrangement of alkyl carbinols **72**

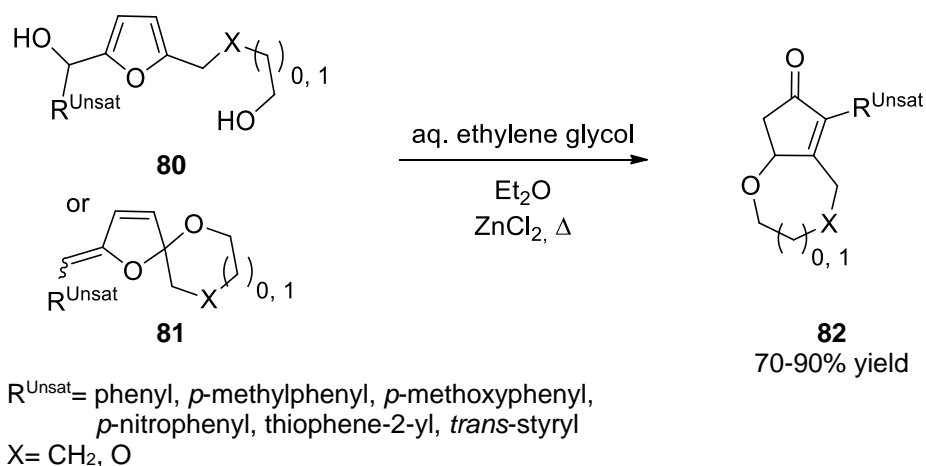
Scheme I.16. Dual Dy(OTf)_3 and TFA catalyzed Piancatelli rearrangement of aryl and alkyl carbinols **70** and **72**.⁵³

Moreover, the authors reported that this dual catalysis was beneficial for the more challenging substrates **c** (**Scheme I.17**).



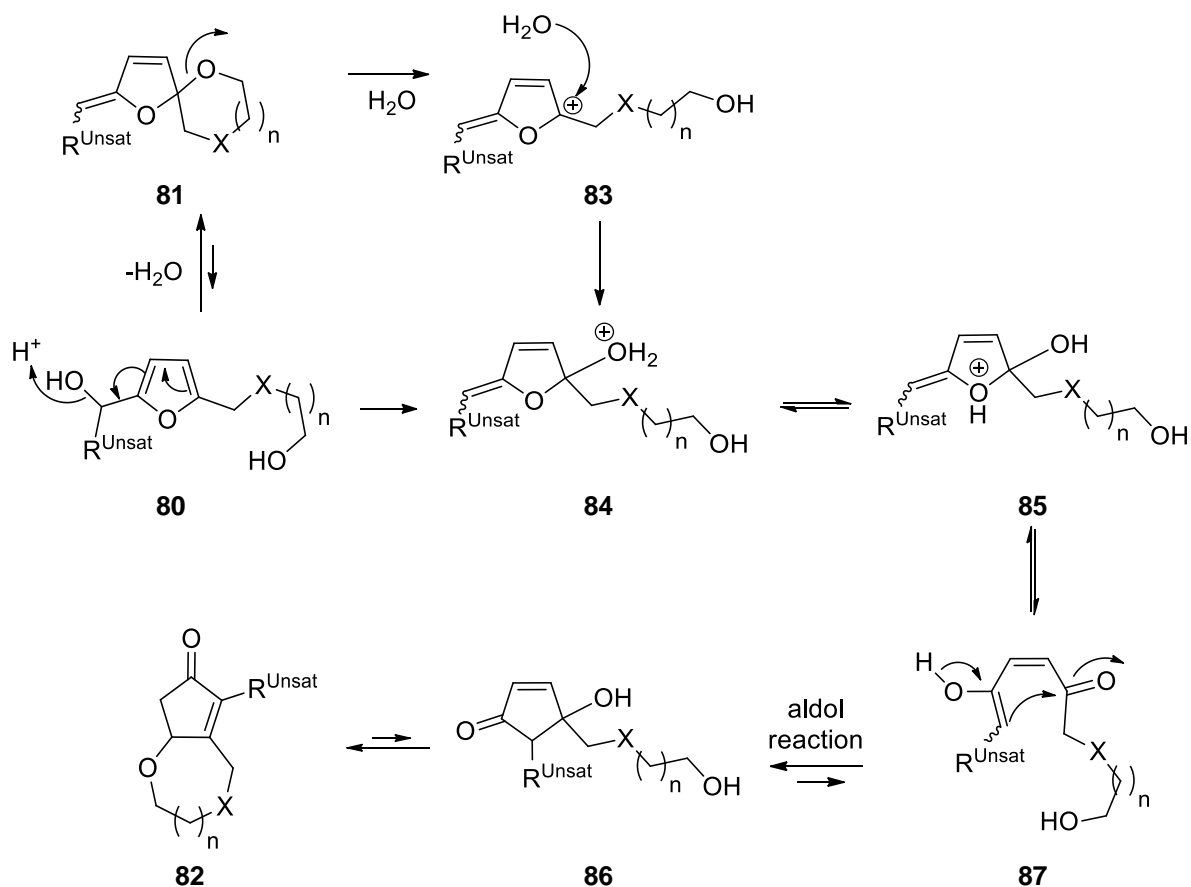
Scheme I.17. Dual Dy(OTf)_3 and TFA catalyzed Piancatelli rearrangement of carbinols **74-76**.⁵³

In 2009, Lai *et al.* reported a novel conversion of 2-furylcarbinols **80**, bearing a hydroxyl in the side chain at the 5-position of the furan ring, into corresponding oxabicyclic cyclopent-2-enones **82** in good to excellent yields (**Scheme I.18**).⁵⁴ Dehydration-spiroacetalized product **81** of starting furandiols **80** was observed as reaction intermediate. Using these intermediates as starting materials similar reaction yields were observed under the same reaction conditions.



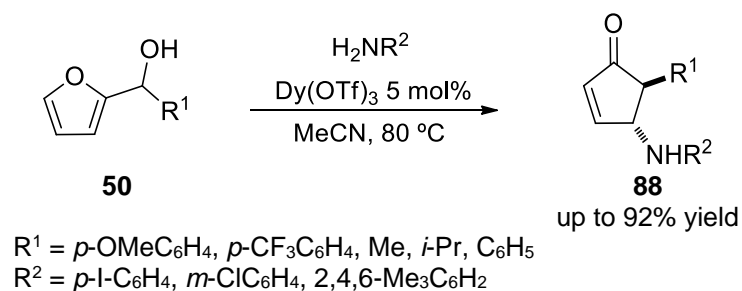
Scheme I.18. Conversions of furandiols **80** and spiroacetal enol ethers **81** into cyclopent-2-enones **82**.

After mechanistic investigation, and supported by the observation that water could catalyzed the reaction of the spiroacetal enols **80**, an intramolecular aldol condensation reaction was proposed (**Scheme I.19**) instead of the reported 4 π -electron electrocycloization mechanism of 2-furylcarbinols rearrangement.



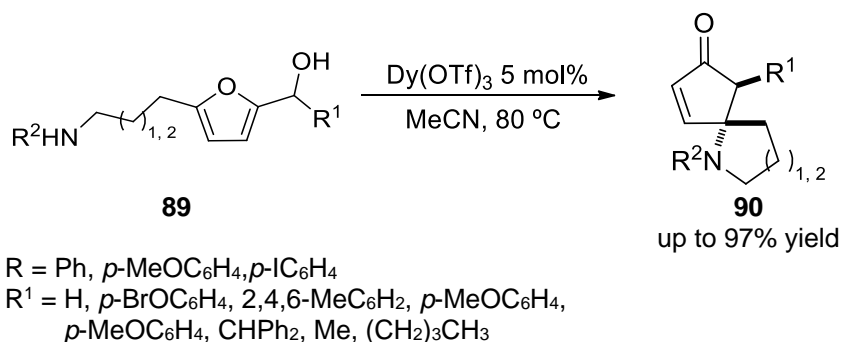
Scheme I.19. Proposed mechanism for conversion of furandiols **80** and spiroacetal enol ethers **81** into cyclopent-2-enones **82**.⁵⁴

In 2010, Alaniz *et al.* reported the efficient aza-Piancatelli rearrangement as a mild catalytic single-step procedure for the synthesis of *trans*-substituted 4-amino-5-alkylcyclopent-2-enones **88** (**Scheme I.20**).⁵⁵ Remarkably, the typical product isomerization does not occur in aza-Piancatelli rearrangement presumably because of the mild nature of the Dy(OTf)₃ catalyst.



Scheme I.20. Scope of the aza-Piancatelli rearrangement.

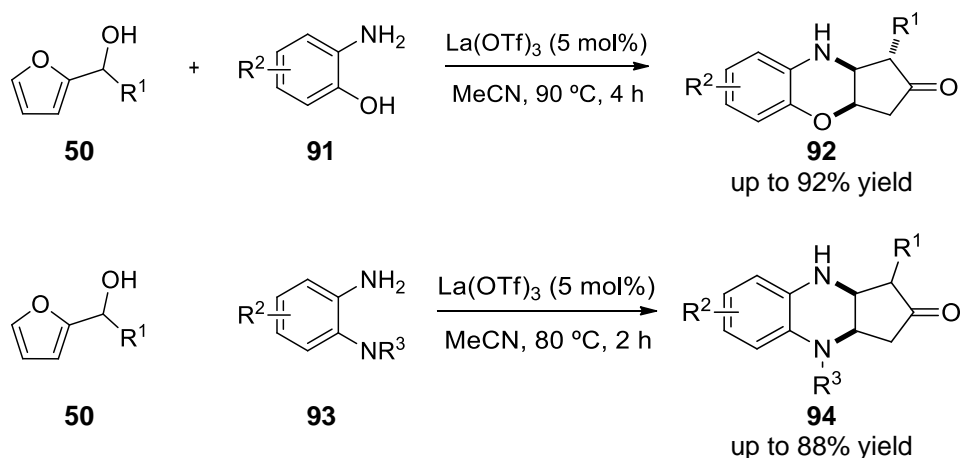
Later in 2011, the same group reported the intramolecular aza-Piancatelli rearrangement.⁵⁶ The intramolecular version constructs a fully substituted carbon center bearing a nitrogen atom and a spirocyclic ring system in a single step as depicted in **Scheme I.21**. For the mechanistic point of view the authors suggested a 4 π -electrocyclization because the azaspirocycles **90** formed were obtained as the *trans* diastereoisomer.



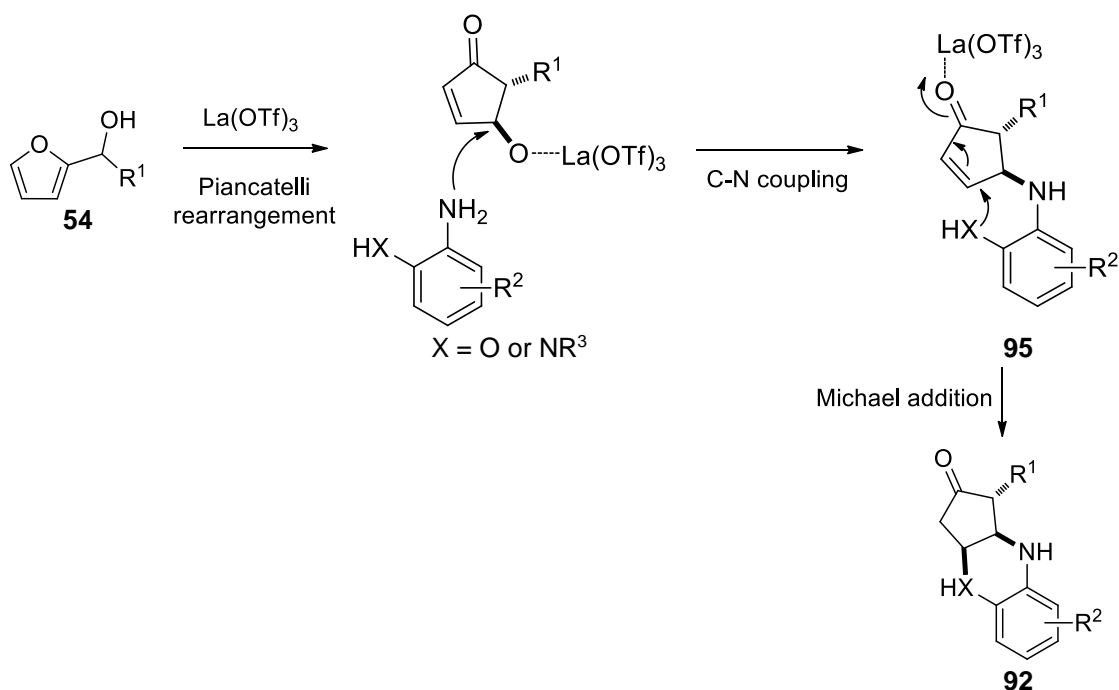
Scheme I.21. Scope of the intramolecular aza-Piancatelli rearrangement of **89**.

Wang *et al.* reported a domino synthesis of benzo-1,4-heterocycle compounds **92** via a Piancatelli/C-N coupling/Michael addition process promoted by La(OTf)₃ (**Scheme I.22**).⁵⁷ Noteworthy is the fact that the C-N coupling resemble the work reported by Alaniz and co-workers.⁵⁵⁻⁵⁶ When *o*-aminophenol derivatives **91** were used, 1,4-benzoxazine **92** were obtained as single diastereoisomers whereas when using derivatives **93** gives the corresponding products **94** as a mixture of diastereoisomers, and the diastereoisomeric

composition changed over time. It was suggested that this may be due to the steric effect of the R^3 groups.⁵⁷



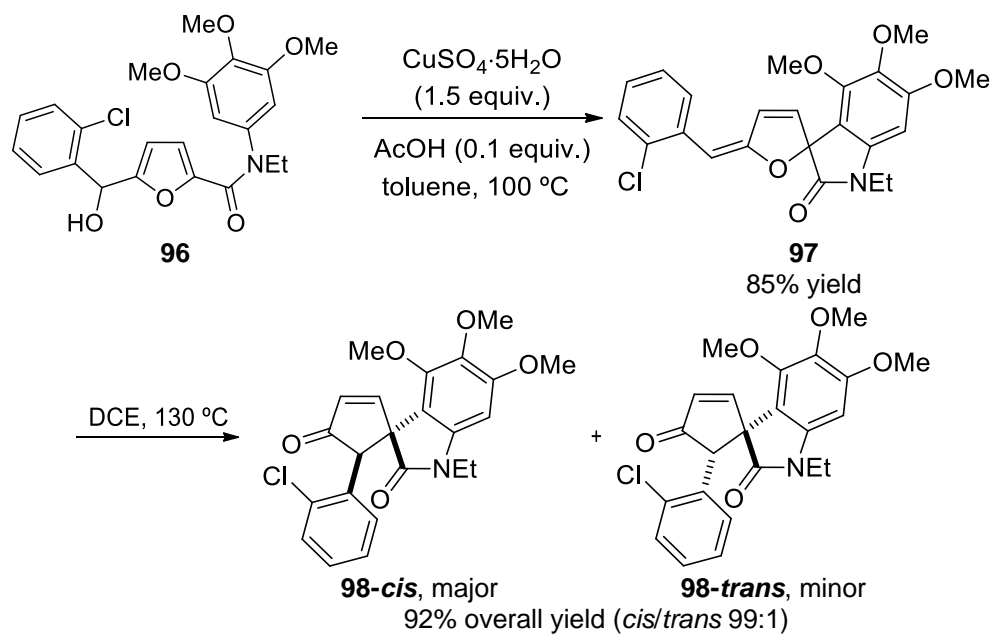
Scheme I.22. La(OTf)_3 -promoted domino Piancatelli/C–N coupling/Michael addition process.⁵⁷



Scheme I.23. Proposed mechanism for the domino Piancatelli/C–N coupling/Michael addition reaction.⁵⁷

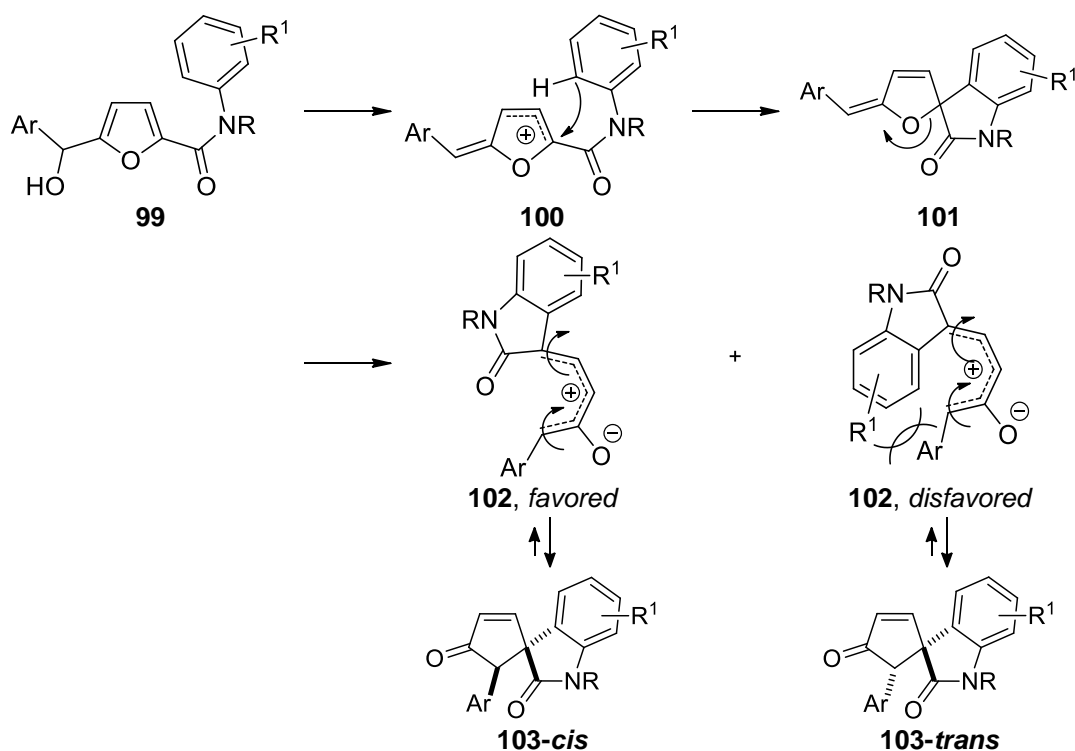
Very recently, Yin *et al.* reported the rearrangement of 2-furylcarbinols **96** into spiroentenoneoxindoles **98** through a stepwise C-Piancatelli rearrangement.⁵⁸ The first step of the methodology is a tandem dearomatization of furan ring and intramolecular Friedel-Crafts reaction of 5-substituted 2-aryl carbinols promoted by CuSO_4 to give spirofurooxindoles **97**,⁵⁹ followed by a thermal conrotatory electrocyclozation of the 4π -electron system to yield the final spiroentenoneoxindoles **98** as two diastereoisomers.⁶⁰

An extensive study on substrate scope was performed and the best result is depicted in **Scheme I.24**. Tertiary 2-carbinols derivatives were also studied but failed to yield the desired product in the second step of the procedure. Remarkably, some of the spirooxindole products showed promising cytotoxic activities against the DU145 and LNCaP tumor cell lines.



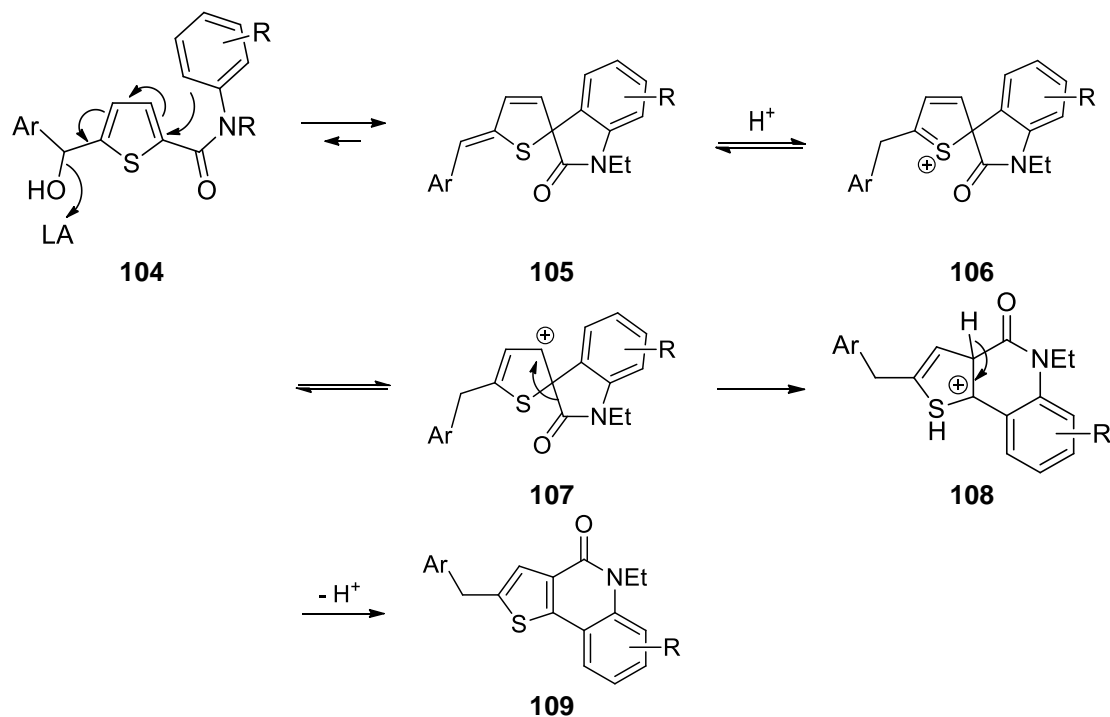
Scheme I.24. Stepwise C-Piancatelli rearrangement.⁵⁸

The rearrangement of spirofurooxindoles **102** into spiroentenoneoxindoles **103** provides additional evidence for the thermal conrotatory electrocyclization of the 4π -electron mechanism as shown in **Scheme I.25**. In addition, DFT studies using Gaussian 09/B3LYP/6-31+G* showed a difference in the cyclization energy barrier of 8 kcal/mol favoring the formation of the *cis* isomer.⁵⁸



Scheme I.25. Proposed mechanism for the rearrangement of spirofurooxindoles **99** into spiroindenoneoxindoles **103**.⁵⁸

Interestingly, spirothienooxindoles derivatives **105**⁶¹ do not presented the same reactivity, giving thieno[2,3-*c*]quinolin-4-ones **109** *via* the proposed mechanism depicted in **Scheme I.26**.⁵⁸



Scheme I.26. Proposed mechanism for the formation of thieno[2,3-*c*]quinolin-4-ones **109**.⁵⁸

I.2.3. Conversion of furfuraldehyde motives into cyclopent-2-enones

Cyclopent-2-enones can be obtained by reaction of 2-furaldehyde (**99**) with two moles of anilines (**Table I.4**).⁶²⁻⁶⁴ Nevertheless, Stenhouse salts **110** (**Figure I.3**), that were reported in 1850,⁶⁵ can also be obtained from the reaction of 2-furaldehyde with primary aromatic amines in the presence of hydrochloric acid.⁶⁵⁻⁶⁶ Furthermore, basic subsequent treatments of this salt give the respective cyclopent-2-enone. Remarkably, treatment of Stenhouse salts with other amines, malonate anion or sodium bicarbonate methanolic solution promotes the nucleophilic displacement of the anilino group to give the 4-nucleophile substituted 5-amino cyclopent-2-enones.⁶⁷⁻⁶⁹

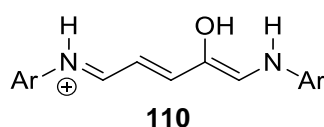
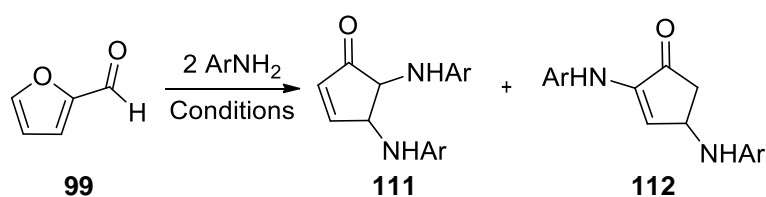


Figure I.3. General structure of Stenhouse salts.

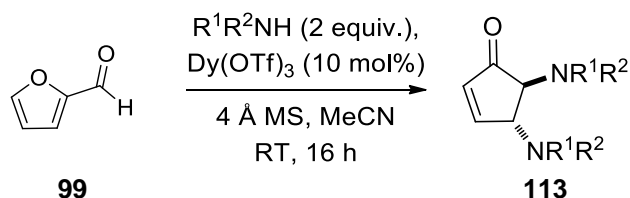
Although in different reaction conditions, the reaction of 2-furaldehyde (**99**) with two equivalents of aniline gives cyclopent-2-enone **112** as product, whereas in reaction with *p*-nitroaniline only 4,5-di(*p*-nitroanilino)cyclopent-2-enone **111** is formed.⁶² This difference was attributed to the basicity of the amine. In this way, *m*-nitroaniline is a borderline case where both isomers were isolable.⁶² Furthermore, heating of 4,5-products **111** in presence of the respective amines result in conversion into the more stable 2,4-products **112**.⁶² In addition, it was observed that bulky or very electron deficient aromatic groups such as 2,4-dinitroaniline, 3,5-dinitroaniline or 2,4,6-tribromoaniline inhibit the cyclopent-2-enones formation.⁶⁷ Recently, Qiang-Li *et al.* performed this reaction to prepare a diaminocyclopent-2-enone that was used as a highly selective and sensitive turn-on catalytic chemodosimeter for Cu(II) in aqueous solution (**Table I.4**, entry 7).⁷⁰

Table I.4. Reaction of 2-furaldehyde (**99**) with anilines.

Entry	Ar	Conditions	111 Yield (%)	112 Yield (%)
1 ⁶²⁻⁶⁴	C ₆ H ₅	Et ₂ O	ND	50
2 ⁷¹	C ₆ H ₅	Sodium sulfate, 0.5 h, RT	10.3	ND
3 ⁶²	<i>p</i> -NO ₂ -C ₆ H ₄	Reflux, 4 h	75	ND
5 ⁶²	<i>p</i> -Cl, <i>m</i> -NO ₂ -C ₆ H ₃	Et ₂ O, RT	ND	50
6 ⁶⁷	<i>N</i> -methylaniline	100 °C, 5 h	60	ND
7 ⁷⁰	<i>m</i> -COOH-C ₆ H ₄	EtOH	85	ND

ND = Not determined.

In 2007 the pioneering report of Li and Batey describes the diastereoselective formation of *trans*-4,5-diaminocyclopent-2-enone derivatives **113** by Lewis acid catalyzed reaction of 2-furaldehyde (**99**) and secondary amines in good to excellent yields (**Table I.5**).⁷²

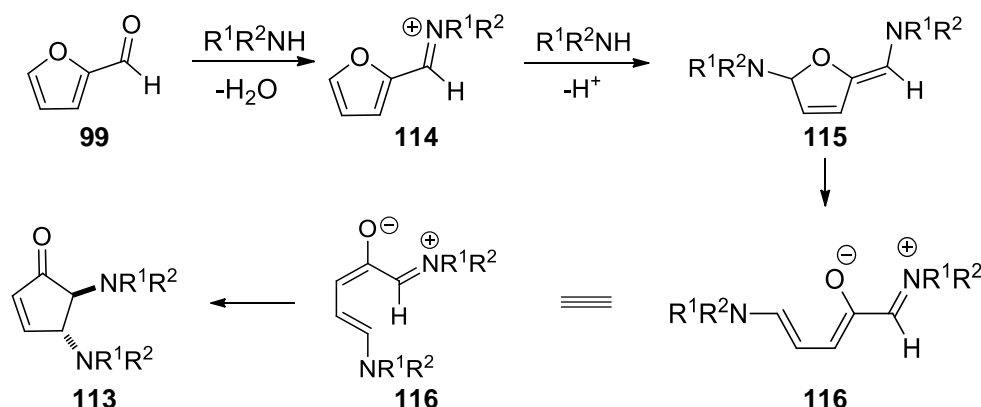
Table I.5. Dysprosium triflate catalyzed reaction of 2-furaldehyde (**99**) with secondary amines.⁷²

Entry	Amine	Yield (%)
1	morpholine	quantitative
2	diallylamine	82
3	dibenzylamine	98
4	bis(4-methoxybenzyl)amine	quantitative
5	1,2,3,4-tetrahydroisoquinoline	92
6	<i>N</i> -methylaniline	78
7	1,2,3,4-tetrahydroquinoline	81
8	indoline	99
9	benzylamine	NR
10	aniline	17

NR = No reaction.

According to previous experimental observations and supported by computational studies the authors proposed a domino condensation/ring-opening/electrocyclization

process (**Scheme I.27**). An initial condensation of 2-furaldehyde (**99**) and one molecule of dialkylamine take place to form the iminium ion intermediate **114**. A second condensation of dialkylamine in the 5-position of furan ring promotes the furan opening to yield the deprotonated Stenhouse salt **116**. As previously demonstrated, isolated Stenhouse salts can undergo cyclization to form cyclopent-2-enones. Therefore, the authors proposed a conrotatory 4π electrocyclic reaction to yield the final *trans* 4,5-diaminocyclopent-2-enone derivatives **113** as a single diastereoisomer.⁷²

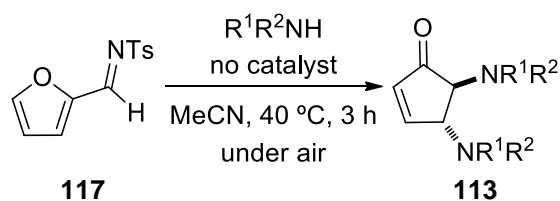


Scheme I.27. Proposed mechanism for the formation of 4,5-diaminocyclopent-2-enones **113**.⁷²

More recently, Ramesh *et al.* reported that acidic ionic liquid 1-methylimidazolium tetrafluoroborate ($[\text{HMim}]^+[\text{BF}_4]^-$) can be successfully employed as a reusable catalyst for the same reaction in the absence of solvent. Remarkably, same or better yields were obtained in very fast reactions (up to 5 min). According to the authors, the significant enhancement in the reaction rate resulted from the inherent Brønsted acidity and high polarity of ionic liquid.⁷³

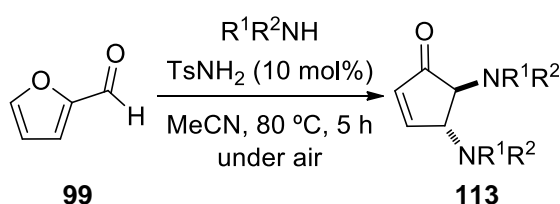
Later, Sindona *et al.* reported the use of Erbium(III) chloride hexahydrate in ethyl lactate as environmentally sustainable alternative system for the synthesis of the *N,N*-substituted 4,5-diaminocyclopent-2-enones **113**. Remarkably, comparable yields to those reported by Batey *et al.* were obtained under these conditions in a short reaction time (20 to 30 min).⁷⁴

In other study, Wang *et al.* reported a new protocol for the preparation of 4,5-diaminocyclopent-2-enones *via* the reaction of *N*-sulfonylimine **117** with secondary amines, with *p*-toluenesulfonamide acting as a leaving group, affording the products in moderate yields (**Scheme I.28**).⁷⁵



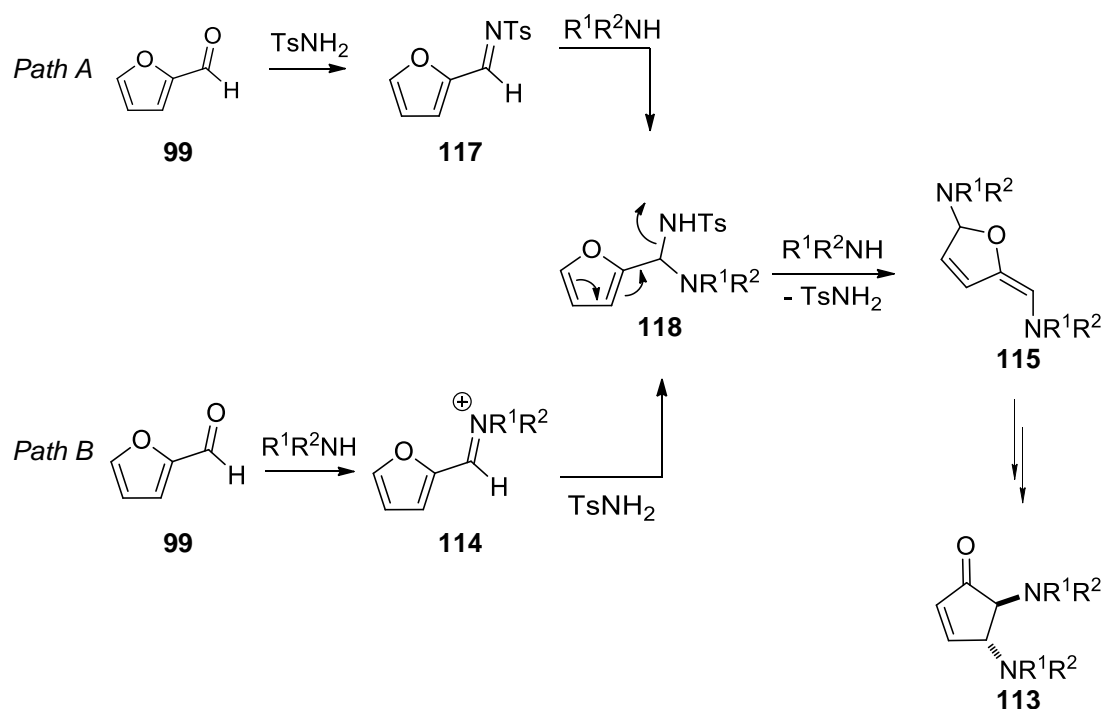
Scheme I.28. Reaction of *N*-(furan-2-ylmethylene)-4-methylbenzenesulfonamide (**117**) with secondary amines.

In addition, *p*-toluenesulfonamide worked well as a catalyst for the reaction of 2-furaldehyde (**99**) and secondary amines to afford the corresponding products **113** in higher yields (**Scheme I.29**).⁷⁵



Scheme I.29. *p*-Toluenesulfonamide-catalyzed synthesis of 4,5-diaminocyclopent-2-enones **113**.

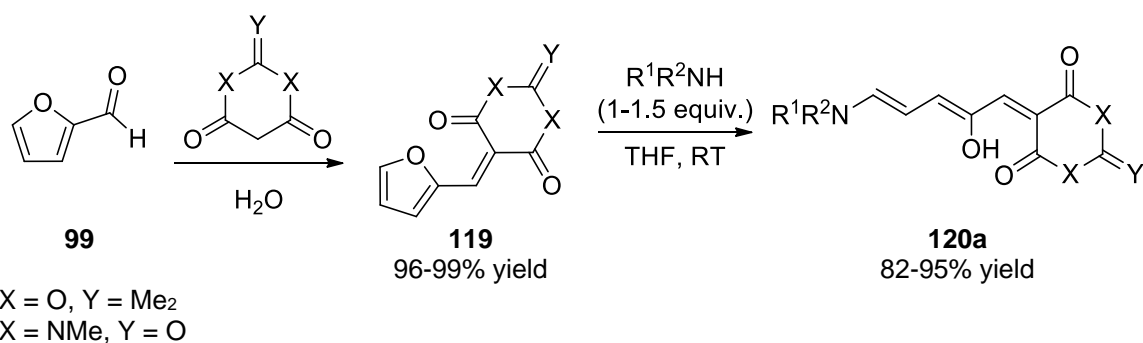
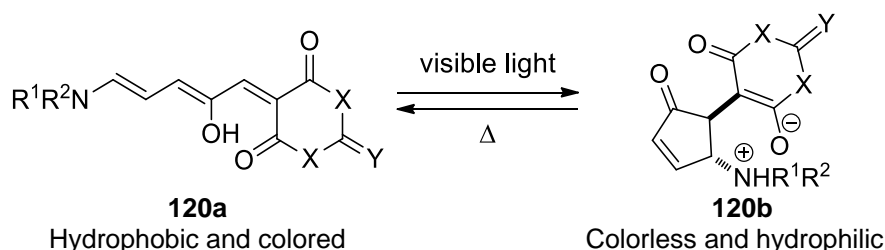
Mechanistic studies were performed to understand the role of *p*-toluenesulfonamide. Two paths were proposed for a possible mechanism (**Scheme I.30**). The authors proposed that 2-furaldehyde (**99**) is first converted into imine **117** (*Path A*) and iminium-ion **114** (*Path B*), which could be detected by LC-MS analysis (**Scheme I.30**). Then, amine and *p*-toluenesulfonamide attacked **117** and **114**, respectively to form intermediate **118** that despite being too reactive to be isolated, was detected by LC-MS. In addition, it was observed that potassium carbonate inhibits the reaction, suggesting that *p*-toluenesulfonamide also work as a mild acid.



Scheme I.30. Proposed mechanism for the *p*-toluenesulfonamide catalyzed synthesis of 4,5-diaminocyclopent-2-enones **113**.

Very recently, Alaniz *et al.* published a very remarkable work on the creation of a new class of organic photochromic molecules based on the rearrangement of Stenhouse salts into cyclopent-2-enones.⁷⁶ For that, furfural (**99**) was activated either with Meldrum's or with 1,3-dimethyl barbituric acids to form derivatives **119**. Treatment of these activated furans with secondary aliphatic, cyclic, or functional amine derivatives, such as diethylamine, diallylamine, and tetrahydroisoquinoline provided photoswitches with the general structure **120** (**Scheme I.31**). These derivatives offer an unprecedented combination of physical properties including tunable photoswitching using visible light, excellent fatigue resistance, and large polarity changes. Moreover, these derivatives can be routinely accessed at the multigram scale in excellent yields over the two-step procedure (**Scheme I.31**).⁷⁶

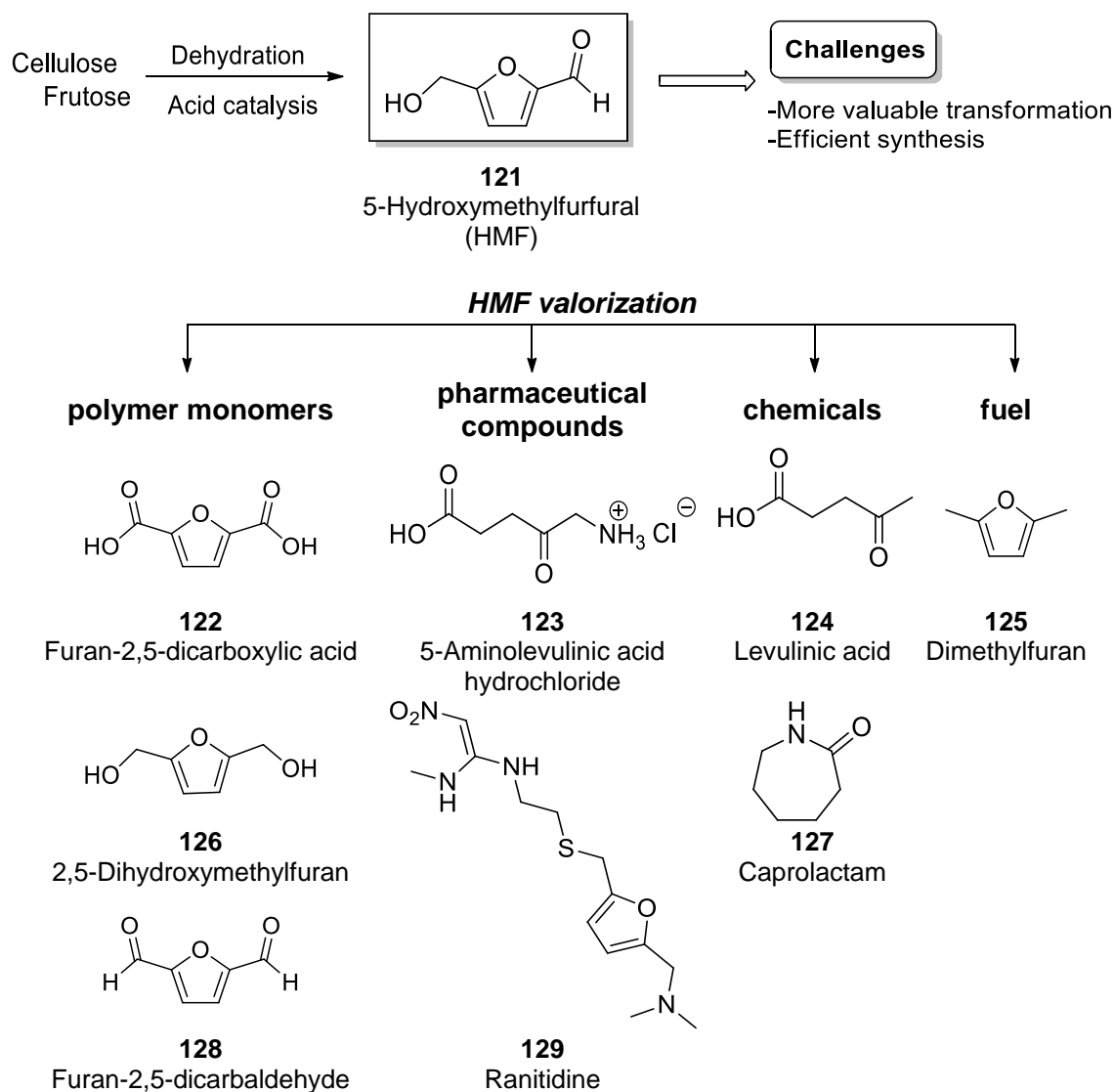
a) Synthesis of new photochromic molecules

b) Photoswitching and thermal reversion of triene **120a** to cyclopent-2-enone **120b**

Scheme I.31. Synthesis of new photochromic molecules **120** and respective mode of action.⁷⁶

I.3. 5-Hydroxymethylfurfural (HMF)

The increasing price of fossil fuels, the limited availability of these non-renewable carbon resources and the environmental impact have motivated the use of renewable and abundant biomass as the source for sustainable production of fuels and chemicals. As a result, today we are looking to a gradual replacement of petrochemical refineries by long term more economic biorefineries.⁷⁷⁻⁷⁹ Among several building blocks derived from renewable resources such as furfural (**99**),^{77,80-82} 5-hydroxymethylfurfural (HMF, **121**) has been identified as a very versatile starting building block for different applications such as biofuel, polymer monomers, active pharmaceutical compounds,⁸³⁻⁸⁴ and many other valuable molecules (**Scheme I.32**)⁸⁵⁻⁸⁸.



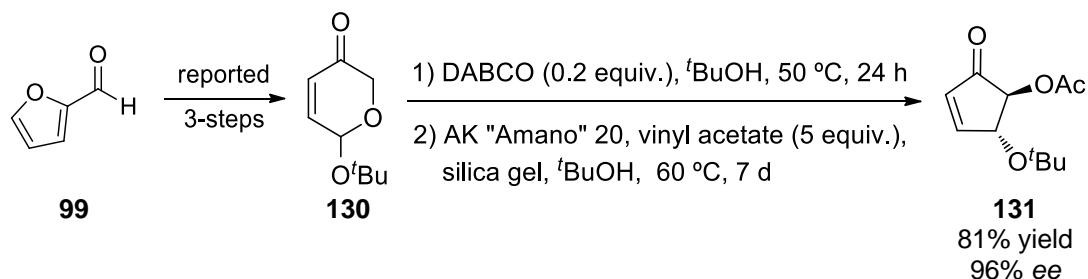
Scheme I.32. 5-Hydroxymethylfurfural as a bio-platform.

Further overview on synthetic methods for the preparation of HMF is described in **Chapter II**.

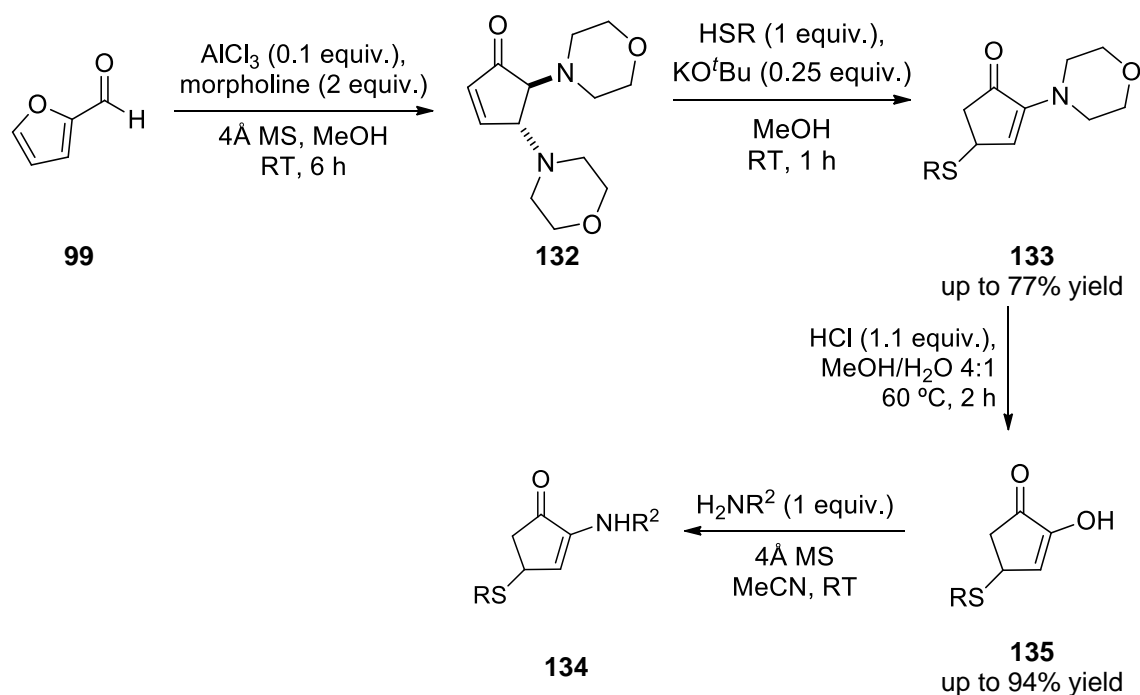
I.4. Objectives

Recently, this team have been interested in the development of synthetic routes that allows the formation of functionalized cyclopent-2-enones. In one approach was reported a methodology for the generation of enantiomerically pure *trans*-4,5-dioxygenated-cyclopent-2-enones **131** by organocatalyzed rearrangement of pyranones (derived from furfuryl alcohol) and enzymatic dynamic kinetic resolution (**Scheme I.33**).⁸⁹ In another and more recent approach was reported the formation of 2-amino-4-thio-cyclopent-2-enones **134** through condensation of 2-furaldehyde (**99**) and morpholine followed by 1,4-addition

of nucleophiles (**Scheme I.34**).⁹⁰ Both synthetic methodologies were achieved by a strategy based on comprehensive catalyst screening experiments. Moreover, a cheaper protocol for the condensation of 2-furaldehyde (**99**) and morpholine comparing to Batey's protocol was found (**Scheme I.34**).

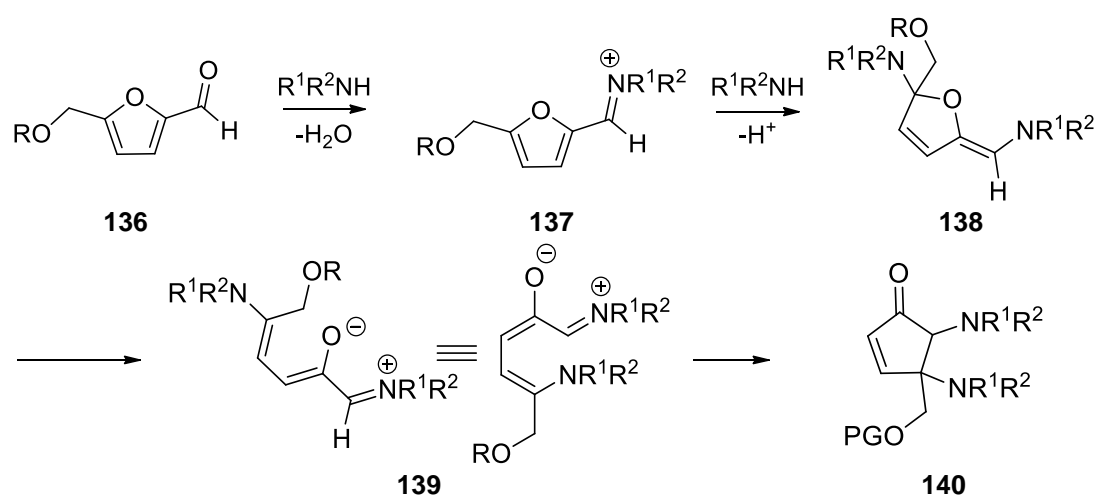


Scheme I.33. New methodologies for the synthesis of *trans*-4,5-dioxygenated-cyclopent-2-enones.



Scheme I.34. New methodologies for the synthesis of 2-amino-4-thio-cyclopent-2-enones.

The main goal of this thesis is the valorization of HMF molecule. When this project was initiated, it was sought to take advantage of precedent information regarding conversion of furans into cyclopent-2-enones and the experience of this team in cyclopent-2-enones synthesis, so it was believed that it would be possible to successfully transform HMF into highly functionalized cyclopent-2-enones bearing a quaternary center (**Scheme I.35**), and, to further manipulate the product into carbocycles using reported methodologies.



Scheme I.35. Proposed strategy for the conversion of HMF into cyclopent-2-enones.

Chapter 2

Synthesis, isolation and cytotoxicity of 5-Hydroxymethylfurfural and derivatives

The several contributions of our group for the synthesis and isolation of HMF from carbohydrates will be presented in this chapter. In addition, the cytotoxicity of HMF and other bioplateform derivatives will be described.

The work reported herein was described in the following 3 publications:

1) “An Integrated Approach for the Production and Isolation of 5-Hydroxymethylfurfural from Carbohydrates”, Svilen P. Simeonov, Jaime A. S. Coelho and Carlos A. M. Afonso, *ChemSusChem*, **2012**, 5, 1388;

2) “Integrated Chemo-Enzymatic Production of 5-Hydroxymethylfurfural from Glucose”, Svilen P. Simeonov, Jaime A. S. Coelho and Carlos A. M. Afonso, *ChemSusChem*, **2013**, 6, 997;

3) “An emerging platform from renewable resources: selection guidelines for human exposure of furfural-related compounds”, Raquel F. M. Frade, Jaime A. S. Coelho, Svilen P. Simeonov and Carlos A. M. Afonso, *Toxicol. Res.*, **2014**, 3, 311.

II. Synthesis, isolation and cytotoxicity of 5-Hydroxymethylfurfural and derivatives.....	31
II.1. Introduction	33
II.1.1. Preparation of 5-Hydroxymethylfurfural (HMF).....	33
II.1.2. Enzymatic isomerization of D-glucose to D-fructose	34
II.1.3. Mechanism	35
II.1.4. Cytotoxicity	35
II.2. Results	37
II.2.1. Production and isolation of HMF from carbohydrates	37
II.2.2. Integrated chemo-enzymatic production of HMF from glucose	41
II.2.3. Guidelines for human exposure of furfural-related compounds.....	50
II.3. Conclusions and Perspectives	53
II.4. Experimental	56
II.4.1. General Remarks	56
II.4.2. Experimental procedures of Section II.2.1.....	57
II.4.3. Experimental procedures of Section II.2.2.....	63
II.4.4. Preparation of furanic compounds for cytotoxicity studies	65

II.1. Introduction

II.1.1. Preparation of 5-Hydroxymethylfurfural (HMF)

Increasing interest in 5-hydroxymethylfurfural (HMF, see **Section I.3**) led to notable progress in the HMF synthesis from carbohydrates and multiple conditions are now known.^{87,91} Ideally, more abundant bio-renewable resources like cellulose and inulin could be used as starting materials for HMF production.⁷⁹ However, the efficient direct transformation of cellulose to HMF appears less feasible mainly due to 1) the occurrence of side reactions (e.g., formation of humins); 2) different involved reactivity pathways that require complementary catalysts (e.g., acid and bases); and 3) experimental conditions that are non-compatible with the HMF stability.⁸⁷ The most explored synthetic route for HMF formation is based on multistep approach consisted of cellulose hydrolysis to D-glucose, D-glucose isomerization to D-fructose and D-fructose dehydration to HMF. Since the D-fructose dehydration to HMF is less demanding, the one-pot transformation of D-glucose to HMF has also been intensively explored, in which chromium dichloride or trichloride appears to be the best catalysts to date, requiring temperatures above 100 °C.^{87,92} Currently, the most efficient reported methods allow the formation of HMF in a range from 45 to 90% yield (**Table II.1**).

Table II.1. Selected examples for the preparation of HMF from D-Glucose.

Entry	Catalyst	Reaction medium	T (°C)	Yield (%)
1 ⁹²	CrCl ₂	Ionic liquid	100	68
2 ⁹³	CrCl ₃	Ionic liquid	100 ^a	90
3 ⁹⁴	CrCl ₂	DMA-LiCl-ionic liquid	100	62
4 ⁹⁵	SnCl ₄	Ionic liquid	100	60
5 ⁹⁶	Al(OTf) ₃	DMSO	140	60
6 ⁹⁷	AlCl ₃	HCl/biphasic: water and 2-sec-butylphenol	170	62
7 ⁹⁸	MgCl ₂ (2 equiv.) and 2-carboxyphenylboronic acid (1 equiv.)	DMA	120	54
8 ⁹⁹	Sn-β and Amberlyst® 70	THF/methyltetrahydrofuran	130	63
9 ¹⁰⁰	Zeolite (100 mg/mL)	Ionic liquid	110	45

^aUnder MW irradiation.

In the case of D-fructose dehydration to HMF a broader range of efficient catalysts has been reported, where in general homogeneous and heterogeneous mineral and organic acids, at temperatures from room temperature to above 100 °C are used.⁸⁷ In addition, this transformation is also feasible in absence of catalysts, promoted by specific solvents such as DMSO and ionic liquids, although requiring higher temperatures (up to 120 °C).⁸⁷

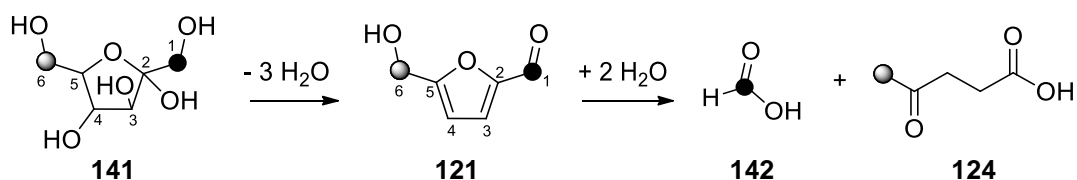
The HMF isolation from the reaction mixture is a very important issue due to the specific properties of HMF such as 1) high solubility in aqueous media and polar solvents; 2) low vapour pressure (114-116 °C/1 mbar)¹⁰¹; 3) low melting point (30-34 °C)¹⁰¹; 4) thermal and chemical instability that complicates its high scale isolation namely by solvent extraction, distillation or crystallization. In fact, the main reported literature provides the HMF conversion and/or yields based on HPLC analysis and in less extend by GC analysis of the reaction mixture instead of isolated yields.⁸⁷ In the case of the best traditional organic solvent, DMSO, the isolation method requires partial distillation of HMF under vacuum followed by column chromatography.^{13,87,102} For ionic liquids based on imidazolium, choline cations and betaine hydrochloride-based media, has been reported the extraction with diethyl ether, methyl isobutyl ketone or 2-sec-butylphenol⁹⁷ in which continuous or repeated extractions are required.^{87,103} More recently, the use of entrainer-intensified vacuum reactive distillation has been demonstrated by using IrCl₃ and CrCl₃ in ionic liquid.¹⁰⁴ At the initial stage of the work reported in this thesis there was still not reported in the literature a combined methodology for the production and isolation of HMF that could be applicable for a big scale production. In this context, one of the goals of this work was the development of an integrated methodology for the preparation and isolation of HMF, as well to be available for further catalysis screenings. Thus, in **Section II.2.1** is described the approach from D-fructose and in **Section II.2.2** the chemo-enzymatic approach from D-glucose.

II.1.2. Enzymatic isomerization of D-glucose to D-fructose

The enzymatic isomerization of D-glucose to D-fructose in water by using glucose isomerase, namely sweetzyme[®], is a well-established industrial process for the production of high D-fructose syrup, which provides a 1:1 equilibrium mixture of D-glucose/D-fructose by using a temperature of approximately 60 °C and a pH range of 6.5-8.2.¹⁰⁵⁻¹⁰⁶ The isomerization is also possible in the presence of an ionic liquid, for example *N,N*-dimethylisopropanolammonium propionate (80% w/w)¹⁰⁷ or ethanol (85% w/w).¹⁰⁸ The transformation of D-glucose to HMF has already been successfully demonstrated by using sweetzyme[®]-promoted D-glucose–D-fructose isomerization (GFI), followed by chemical dehydration. Huang *et al.* reported improved GFI in the presence of sodium tetraborate at 70 °C, followed by simultaneous D-fructose dehydration-extraction with 1-butanol at 190 °C to give HMF in 63% yield.¹⁰⁹ Grande *et al.* reported GFI in seawater that contained phosphate buffer, followed by D-fructose dehydration–extraction in the presence of oxalic acid, which provided HMF in a 40% overall yield. Remarkable, this method also allowed the reuse of the enzyme.¹¹⁰

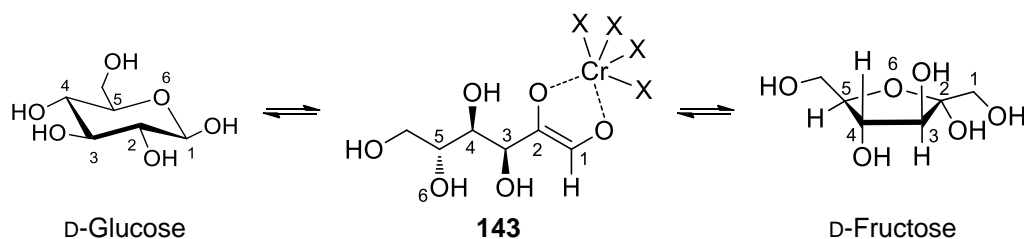
II.1.3. Mechanism

The mechanism for the conversion of D-fructose into HMF consists of three acid catalyzed dehydrations and a keto-enol tautomerism. Very recently, Zhang and Weitz reported an *in situ* NMR study of the mechanism for the catalytic conversion of D-fructose (**141**) to 5-hydroxymethylfurfural (**121**) and then to levulinic acid (**124**) using ^{13}C labeled D-fructose. The data obtained in different solvents and with different catalysts are consistent with the proposed mechanisms for the formation of HMF, levulinic and formic acids.¹¹¹⁻¹¹⁶ The corresponding ^{13}C -labeled results shown that the carbon C-1 in D-fructose maps onto the aldehyde carbon in HMF. For the rehydration of HMF, the results show that C-1 and C-6 carbon of HMF are transformed to the carbon of formic acid and methyl carbon of levulinic acid, respectively (**Scheme II.1**).¹¹⁷



Scheme II.1. ^{13}C -labeled mechanism study for the conversion of D-fructose to HMF and then to levulinic acid.

Regarding the conversion of D-glucose into HMF is believed that chromium plays a critical role in the isomerization of glucose to D-fructose by effecting a formal hydride transfer plausible *via* formation of the chromium enolate **143** as the key intermediate as depicted in **Scheme II.2**.^{92,94}



Scheme II.2. Proposed role of chromium species in the isomerization of glucopyranose to fructofuranose.

II.1.4. Cytotoxicity

5-Hydroxymethylfurfural (HMF) is produced during thermal treatment of carbohydrates-containing foods such as plum juice beverage (707.7 mg/kg), plum butter/jam (410.9 mg/kg), chocolates/praline (273.8 mg/kg), almonds, roasted and coated (155.5 mg/kg), rye-wheat bread (44.5 mg/kg) and cereal bar (43.2 mg/kg).¹¹⁸ The estimated intake range per person is 4-30 mg/day.¹¹⁸ HMF is formed during reaction of hexoses with amino acids

or proteins (Maillard reaction) and it is not detectable in fresh food, being therefore used as an indicator of food quality. For example, a maximum limit of 40 mg/Kg has been fixed in honey by the Codex Alimentarius standard sets.¹¹⁹

Studies in rats demonstrated that HMF can be a potent carcinogen, but in contrast, it was considered a weak carcinogen in mice.¹²⁰⁻¹²³ To determine the toxicological impact of HMF in humans, several experimental studies have been developed. HMF metabolites have been detected and quantified in the urine, but they are different depending on the *in vivo* subjects. In rats urine, 5-hydroxymethyl-2-furoic acid (HMFA), 2,5-furan dicarboxylic acid (**122**, FDCA) and 5-hydroxymethyl-2-furoyl glycine (HMFG) have been found, whereas in human urine, new other metabolites such as 5-carboxylic-2-furoyl-glycine (CAFG) and 5-carboxylic-2-furoylamino-methane (CAFAM) have been detected in addition to HMFA, FDCA and HMFG.¹²⁴⁻¹²⁷ The current data for human HMF exposure has not revealed any significant carcinogenic or genotoxic potential effects and a maximum HMF dose of 80-100 mg/kg per day was observed not to cause adverse effects regarding acute and subacute toxicity in animal experiments.^{118,123}

HMF can be metabolized into 5-sulfoxymethylfurfural (SMF) by sulfotransferases, which in some studies was seen as potential genotoxic and mutagenic.¹²⁸⁻¹³⁰ Different sulfotransferase activity within the used experimental models was suggested as a possible explanation for the discrepant conclusions within the several reported studies.^{118,122-123}

In addition to the intense ongoing research that already allowed the identification of potential building blocks and synthetic routes, it is extremely important the anticipation of their toxic impact in environment¹³¹⁻¹³² and humans (see **Table II.2** for reported toxicity data of selected compounds). In this context, the toxicology of HMF, SMF and a range of HMF derivatives in immortalized human skin fibroblast cells (CRL-1502) was studied with the aim to provide key guidelines about the most human-friendly building blocks.

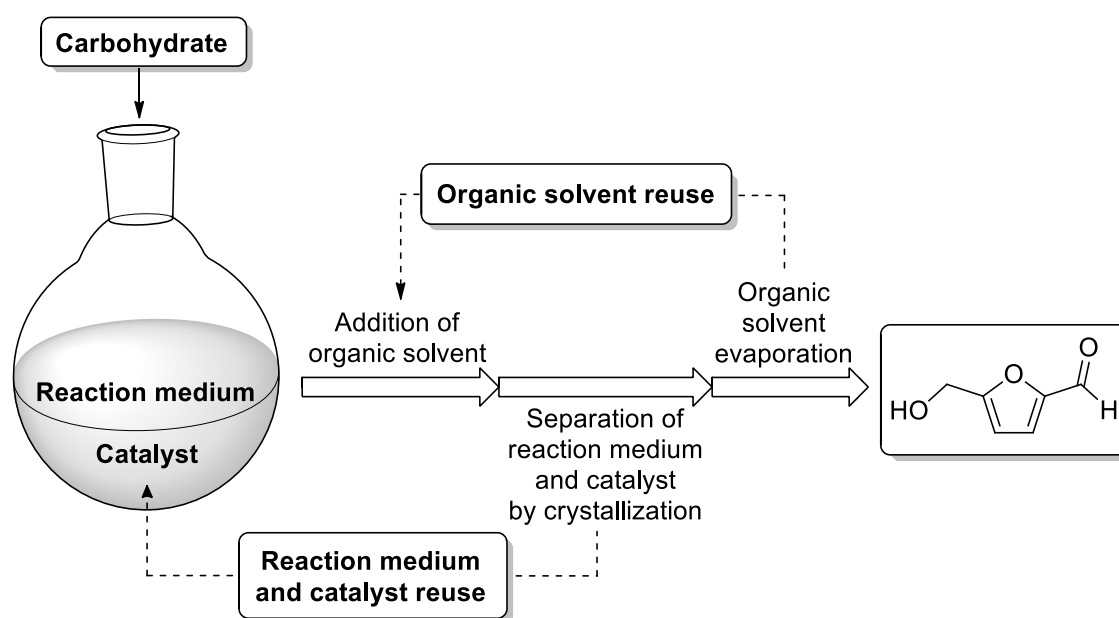
Table II.2. Selected reported toxicity data (LD₅₀) for furfural, furfuryl alcohol and levulinic acid.¹³³

Compound	LD ₅₀ (mg.kg ⁻¹)
Furfural (99)	65 (rat, oral)
	102 (mouse, intraperitoneal)
	0.3 (human, inhalation)
	950 (dog, oral)
Furfuryl alcohol (46)	177 (rat, oral)
	160 (mouse, oral)
	360 (mammal, oral)
Levulinic acid (124)	1850 (rat, oral)
	450 (mouse, intraperitoneal)
	>5000 (rabbit, skin)

II.2. Results

II.2.1. Production and isolation of HMF from carbohydrates

Among the separation processes, crystallization methods are one of the best to use in industry. Based on that, we explored the possibility of using readily available, easily crystallized, and low-volatility solids as efficient reaction media in an integrated process as described in **Scheme II.3**. For that, the selected solid must promote the production of HMF under homogeneous conditions by melting of the reaction media and solubilization of carbohydrates at the temperature required for the reaction, and, after cooling, must precipitate using the appropriate organic solvent, allowing isolation of the HMF in the mother liquor just by evaporation of the organic solvent, which can then be reused.



Scheme II.3. Proposed integrated approach for the production and isolation of HMF from carbohydrates.

Considering that DMSO was shown to be one of the best solvents for HMF dehydration into D-fructose,^{87,102,134-135} the use of solid sulfoxides such as *p*-tolyl sulfoxide (m.p. 94-96 °C)¹⁰¹ in the presence of Amberlyst® 15 as catalyst was initially explored according to the proposed integrated process. Under these conditions, 90% of the *p*-tolyl sulfoxide could be recovered by crystallization. Unfortunately, the isolated yield of HMF was very low (28%) compared to DMSO (70%; **Table II.3**, entries 1 and 2). Furthermore, purification by chromatography was still required to afford HMF in high purity (94%).

Based on literature precedents describing the efficient use of imidazolium-based cations (bearing in mind some concerns about instability) and choline-based eutectic

mixtures,¹⁰³ this team then explored ammonium salts as potential reaction media as summarized in **Table II.3**.^{13,15} Pleasantly, tetrapropylammonium bromide (TPAB) and tetraethylammonium bromide (TEAB) provided outstanding results (up to 91% isolated yield) in reactions catalyzed by Amberlyst® 15 (10% w/w) at 100 °C (**Table II.3**, entries 6 and 7). The TEAB salt was selected for further studies because it is more appropriate for the integrated process since the crystallization is easier and also because it is commercial available at a moderate price (15 €/kg)¹³⁶. It is noteworthy to mention that a report on the use of tetraethylammonium chloride (TEAC) as efficient promoter and/or reaction medium for the conversion of D-fructose and D-glucose to HMF also appeared in the literature in the course of this study.¹³⁷⁻¹³⁹

The D-fructose dehydration also occurred in the absence of catalyst, although more slowly and at a higher temperature (110 °C; **Table II.3**, entries 3-5). Further optimization showed that the use of 10-15% (w/w) Amberlyst® 15 and the presence of small amounts of water (10-15%, w/w) were important to achieve a very selective transformation (**Table II.3**, entries 6-8). In addition, an initial preheating (10 min, from 80 to 100 °C) proved to be important to achieve higher yields of HMF (91% and quantitative) and outstanding purity (97 and 99%), using TEAB containing 10% (w/w) water in 1:5 and 1:10 D-fructose/TEAB (w/w), respectively.

This transformation has already been reproduced more than 50 times by different researchers of our lab using the optimized conditions in 1:5 D-fructose/TEAB (w/w) media and in a scale up to 20 g of D-fructose (100 g of TEAB), providing an average HMF yield of 93% and outstanding purity (98%, **Table II.3**, entry 10).

As proposed, HMF was isolated by crystallization of the reaction medium, first dissolving the reaction mixture in the minimum amount of hot ethanol followed by the addition of ethyl acetate, filtration, and evaporation of the ethanol-ethyl acetate solvent system (**Table II.3**, entries 7 and 11).

Table II.3. Selection of the reaction media (**RM**) for the synthesis of HMF from D-fructose (**F**).

Entry	F (g)	RM ^a	Water (%w/w)	F:RM (w/w)	Cat. (%w/w)	T (°C)	t (min)	Yield (%) ^b	Purity (%) ^c
1	6	DMSO	dry	1:37	6.7	120	150	70	98
2	1	<i>p</i> -TSO	dry	1:3	10	120	120	28	94
3 [†]	1	TPAB	^d	1:5		110 ⁱ	60 90	37 71	99 99
4 [†]	1	TEAB	14 ^e	1:5		110 ⁱ	30	79	^f
5 [†]	1	TPAB	3 ^g	1:5		100	30	77	98
6 [†]	2	TPAB	^d	1:5	10	100 ^j	15	91	70
					5			71	96
7	2	TEAB	10 ^h	1:5	10	100 ^j	15	91	97
					15			90	95
8	2	TEAB	5 ^h 15 ^h	1:5	15	100 ^j	15	80 71	77 98
9	5	TEAB	10 ^h	1:20	10 20	100 ^j	15	29 57	99 99
10 [†]	20	TEAB	10 ^h	1:5	15	100 ^j	15	93	98
11	10 2	TEAB	10 ^h	1:10	10	100 ^j	15	97 100	99 99

^aReaction media: DMSO = dimethyl sulfoxide, *p*-TSO = *p*-tolyl sulfoxide, TEAB = tetraethylammonium bromide, TPAB = tetrapropylammonium bromide.

^bIsolated yield. ^cPurity of HMF determined by HPLC. ^dUsed commercial sample of ammonium salt. ^eOld (>15 years) and wet (average water content of 14% w/w) sample. ^fIsolated HMF pure by TLC. ^gUsed commercial sample of ammonium salt followed by addition of water. ^hDetermined by Karl Fisher on the commercial sample followed by addition of water. ⁱPreheating from 80 °C to 110 °C for 12min. ^jPreheating from 80 °C to 100 °C for 10min. [†]Experiments performed by Svilen P. Simeonov.

Next the possibility to reuse the reaction medium and the catalyst was investigated. In an experiment using 20 g of D-fructose and 100 g of TEAB, the reaction medium and the catalyst were efficiently reused for three cycles (**Table II.4**). Furthermore, excellent recycling results were obtained when using a 1:10, instead of 1:5, D-fructose/TEAB ratio (w/w, 2 g scale), providing high isolated yields (94% overall yield) and purity (>96%) over six cycles (**Table II.4**). During the 7th cycle an erosion on the reaction performance was observed (63% yield); however, after reloading of the catalyst an isolated yield of 123% was obtained. This corresponds to an overall yield of 93% for the combined 7th and 8th cycles, due to transformation of the D-fructose accumulated in the previous cycle.

Table II.4. Catalyst and reaction medium reuse for the preparation of HMF from D-fructose (F)^a

Cycle	F/TEAB (1:5), catalyst (15% w/w)		F/TEAB (1:10), catalyst (10% w/w)	
	Yield (%) ^b	Purity (%) ^c	Yield (%) ^b	Purity (%) ^c
1	92	98	98	99
2	86	97	95	99
3	93	93	94	99
4	64	91	91	99
5			89	99
6			97	96
7			63	95
8 ^d			123	94

^aAll experiments were performed by adding D-fructose (commercial grade from supermarket) and Amberlyst® 15 to TEAB containing 10% (w/w) of water and heated for 10 min from 80 °C to 100 °C, followed by more 15 min at 100 °C. ^bIsolated yield. ^cPurity of HMF determined by HPLC. ^dThe recovered TEAB was purified and added fresh Amberlyst® 15 (10% w/w).

The continuous transformation of D-fructose to HMF was also explored by this team by passing D-fructose dissolved in TEAB containing 25% (w/w) of water through Amberlyst® 15 (3.5 g) supported in a housemade glass tube reactor at 100 °C, giving yields in the range of 81-90% and purities of 91-97% as summarized in **Table II.5**.

Table II.5. Continuous preparation of HMF from D-fructose.^a (Experiments performed by Svilen P. Simeonov.)

Entry	D-Fructose/TEAB ratio (w/w)	Flow (mL/min)	Yield (%) ^b	Purity (%) ^c
1	1:20	0.3	90	91
2	1:20	0.9	90	97
3	1:15	0.9	91	93
4	1:10	0.9	85	92

^aAll experiments were performed by passing continuously 1 g of D-fructose, TEAB containing 25% (w/w) of water, through a glass reactor containing Amberlyst® 15 (3.5 g) at 100 °C in a commercial domestic oven. ^bIsolated yield. ^cPurity of the isolated product determined by HPLC analysis.

This integrated process was also explored for the direct transformation of D-glucose, inulin, and sucrose to HMF, using some catalysts already reported for this transformation. The developed process showed to be compatible with all the catalysts tested because HMF was easily isolated from the reaction mixtures in good purity. Unfortunately, all the catalysts tested so far under non-optimized conditions showed that the transformation occurred in low to moderate isolated yields (**Table II.6**).

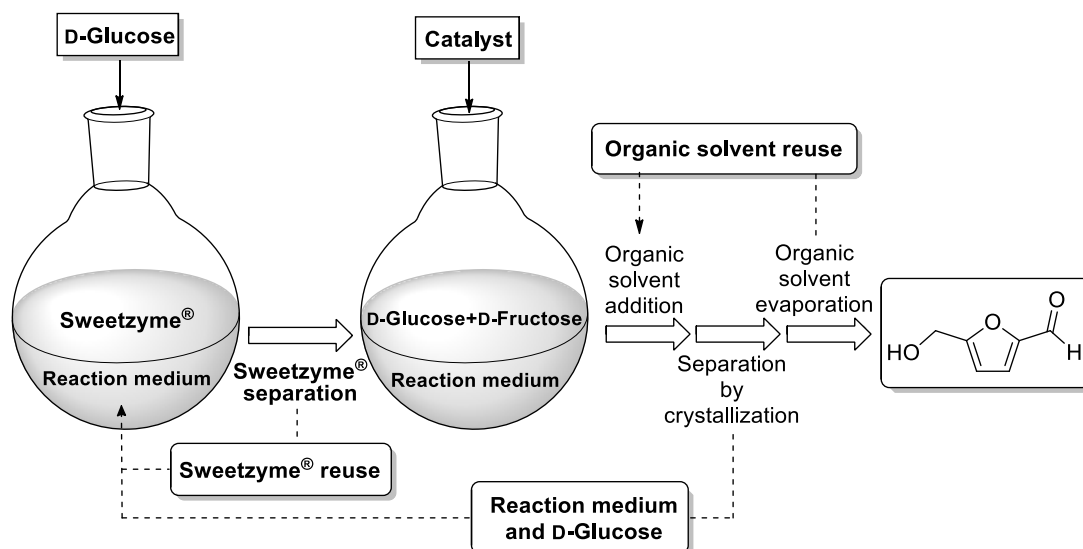
Table II.6. Preparation of HMF from other carbohydrates in TEAB.^a

Entry	Carbohydrate	Catalyst	Catalyst amount (%w/w)	Yield (%) ^b	Purity (%) ^c
1 [†]	Sucrose	Amberlyst® 15	10	32	90
2 [†]	Inulin	Amberlyst® 15	10	55	98
3 [†]	D-Glucose	PMA	10	15	87
4 [†]	D-Glucose	Boric acid	34	26	85
5	D-Glucose	CrCl ₃ ·6H ₂ O	3	35	82

^aAll experiments were performed in a 2.0 g scale of carbohydrate and TEAB containing 10% (w/w) of water and carbohydrate/TEAB ratio (w/w) of 1:5 and catalyst. For PMA and Boric acid reactions, 100 °C for 90 min were applied instead of 15 min reaction. ^bIsolated yield. ^cPurity of HMF determined by HPLC. PMA=Phosphomolibdic acid. [†]Experiments performed by Svilen P. Simeonov.

II.2.2. Integrated chemo-enzymatic production of HMF from glucose

The method previously developed is very efficient for the conversion of D-fructose into HMF, however, lower yields (up to 35%) were obtained for D-glucose by using the best reported catalysts (*i.e.*, boric acid, CrCl₃, and phosphomolibdic acid).¹⁴⁰ As mentioned above, the transformation of glucose to HMF is more demanding and so the goal herein was the development of an integrated process for the transformation of glucose into HMF. Thus, by taking advantage of the reported sweetzyme® performance and our previously described approach, this team explored an integrated process derived from glucose as depicted in **Scheme II.4**. This approach is based on the following key features: a) the enzymatic isomerization of D-glucose to D-fructose in the reaction medium later required for D-fructose dehydration to HMF and HMF isolation, b) the stability of the remaining D-glucose that was derived from the equilibrated D-glucose-D-fructose mixture during the selective catalyzed transformation of D-fructose to HMF, and c) the recovery of the remaining glucose and reaction medium for the next enzymatic isomerization.



Scheme II.4. Integrated approach for the production and isolation of HMF from D-glucose.

From the previously studies, wet TEAB (10% w/w) was identified as an efficient promoter for the dehydration of D-fructose to HMF, which can be improved in the presence of the Amberlyst® 15 acid catalyst. To achieve the integrated D-glucose-D-fructose-HMF transformation and HMF isolation, D-glucose-D-fructose isomerization (GFI) was explored by using sweetzyme® (3% w/w) at 70 °C for 14 h in TEAB/water. The initial reaction conditions were chosen according to the reported GFI reactions in the presence of ethanol, *N,N*-dibutylethanolammonium octanoate ionic liquid¹⁰⁷ and seawater.¹¹⁰ Since the D-fructose dehydration step takes place in relative low amounts of water (**Section II.2.1**) the impact of the water content in the GFI was initially studied. According to the results depicted in **Figure II.1**, the enzyme did not lose activity until the amount of water was lower than 50% (w/w), at which 47% conversion to D-fructose was achieved. Thus, a 1:1 (w/w) ratio of TEAB/water was selected for the further studies.

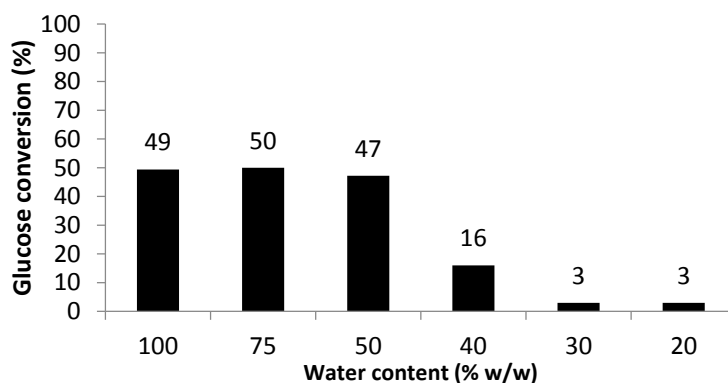


Figure II.1. The effect of water content on D-glucose-D-fructose isomerization by using sweetzyme® in TEAB at 70 °C for 14 h. (Experiments performed by Svilen P. Simeonov).

To achieve a higher GFI rate the experimental conditions (e.g., enzyme concentration and temperature) were further optimized. To compare the data, the rate constants k_1 and k_2 of the single step formation of D-fructose into glucose were determined and summarized in **Table II.7** and **Figure II.2**. The GFI was only slightly slower in 1:1 TEAB/water than in pure water (**Table II.7**, entries 1 and 3 and **Figure II.2a**). The known promoter in water, MgSO_4 , was almost inactive in 1:1 TEAB/water (**Table II.7**, entries 2 and 4 and **Figure II.2b**). As expected, higher enzyme loading and temperature (70 °C vs. 60 °C) resulted in improved performance (**Table II.7**, entries 3 and 5-7 and **Figure II.2c** and **Figure II.2d**). For further studies, 6% w/w of the enzyme was chosen.

Table II.7. Observed GFI by using sweetzyme® in wet TEAB.^{a, †}

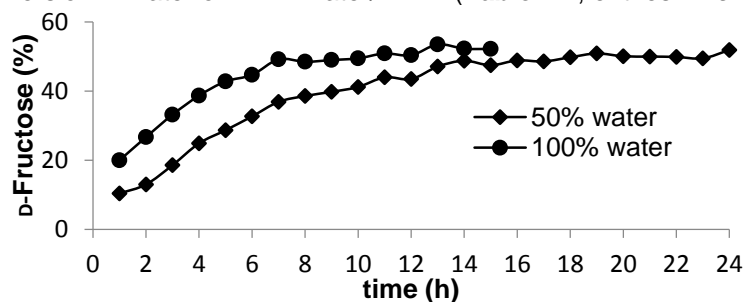
Entry	Enzyme conc. (% w/w)	H ₂ O:TEAB w/w	T (°C)	$k_1 (\times 10^{-3} \text{ h}^{-1})^b$	$k_2 (\times 10^{-3} \text{ h}^{-1})^b$	t_{25} (h) ^c	t_{42} (h) ^c
1	3	10:0	70	112	105	2.8	6.9
2 ^d	3	10:0	70	162	150	1.8	4.8
3	3	5:5	70	75	69	4.4	9.8
4 ^d	3	5:5	70	80	73	4.0	10.3
5	6	5:5	70	203	172	1.2	3.5
6	6	5:5	60	90	85	3.2	8.2
7	10	5:5	70	297	254	1.1	1.9

^aGlucose: 1.2 g in 10 mL of water (entries 1 and 2) or 10 g of 1:1 TEAB/water w/w (entries 3-7).

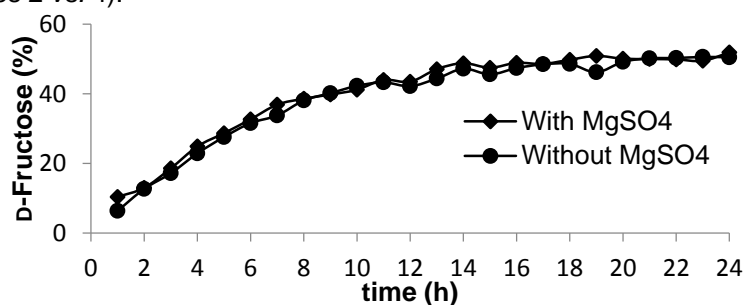
^b k_1 and k_2 are the determined rate constants ($-\text{d}[G]/\text{d}t = k_1[G] - k_2[F]$), in which $[G]$ and $[F]$ are D-glucose and D-fructose concentrations, respectively). ^c t_{25} = time required to achieve 25% of D-fructose, and t_{42} = time required to achieve 42% of D-fructose, as determined by using HPLC.

^dWith 20 mg MgSO_4 . [†]Apart from data processing, the experiments were performed by Svilen P. Simeonov.

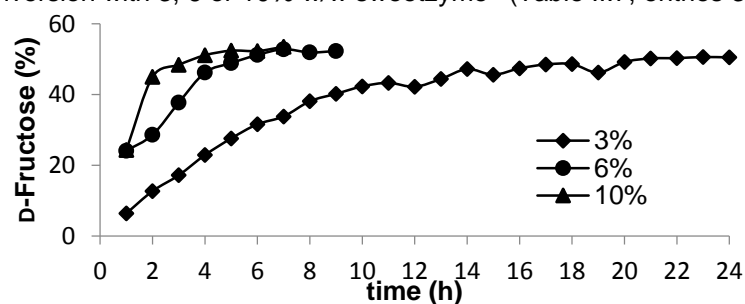
a) D-Glucose conversion in water or in 1:1 water/TEAB (Table II.7, entries 1 vs. 3).



b) D-Glucose conversion in the presence or absence of 20 mg of MgSO_4 in TEAB:water 1:1 w/w (Table II.7, entries 2 vs. 4).



c) D-Glucose conversion with 3, 6 or 10% w/w sweetzyme® (Table II.7, entries 3 vs. 5 vs. 7).



d) D-Glucose conversion at 60 and 70 °C (Table II.7, entries 3 vs. 6).

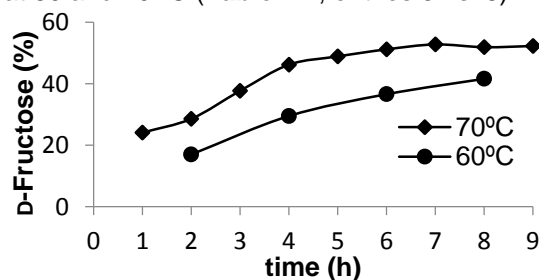


Figure II.2. Study of D-Glucose conversion into D-fructose. (Experiments performed by Svilen P. Simeonov)

Next, the efficient D-fructose dehydration to HMF and HMF isolation without degradation of the remaining D-glucose was explored by studying a range of readily available acid catalysts (e.g., H_2SO_4 , HCl , H_3PO_4 , HNO_3 , and Amberlyst® 15) under conditions that could be integrated with the previous GFI step through prior enzyme filtration and partial water evaporation (Figure II.3). By using a 1:1 mixture of D-glucose/D-

fructose it was possible to determine the conditions for each catalyst (catalyst loading, temperature, and time) that resulted in the conversion of D-fructose above 85%.

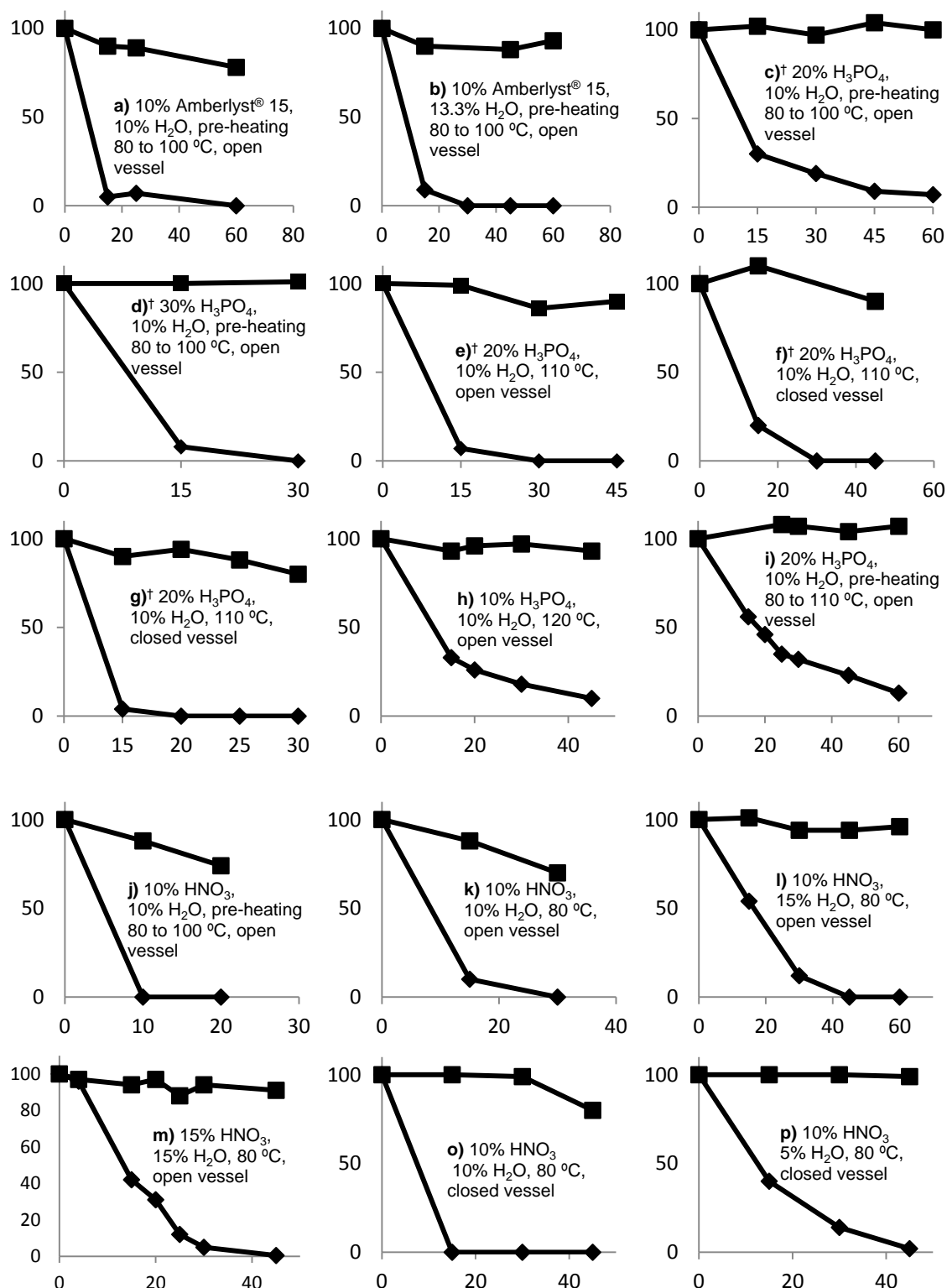


Figure II.3. Data plots of the reaction optimization of the selective transformation of D-fructose to HMF in the presence of D-glucose. X-axis is the time (min) and Y-axis is the remaining sugar (D-Glucose-square, D-Fructose-rhombus) Conditions: The acid was added at RT (a-f and j-p) or at 110 °C (g), 120 °C (h) or 80 °C (i). The reaction was performed in an open vessel (a-e and j-l) or closed vessel (f-i and n-p). The reaction scale was 2 g sugar/15 g rm (a-b and e-p) or 3 g sugar/15 g rm (c-d). †Experiments performed by Svilen P. Simeonov.

In addition, for the HNO_3 and H_3PO_4 catalysts, outstanding stability of D-glucose was observed. Improved results were obtained by performing the reaction in a closed vessel, which avoided the evaporation of water during the reaction. For the HNO_3 (10% w/w, 80 °C, 15 min) and H_3PO_4 (30% w/w, 100 °C, 30 min) catalysts, complete conversion of D-fructose was observed almost without any conversion of D-glucose (**Figure II.4**).

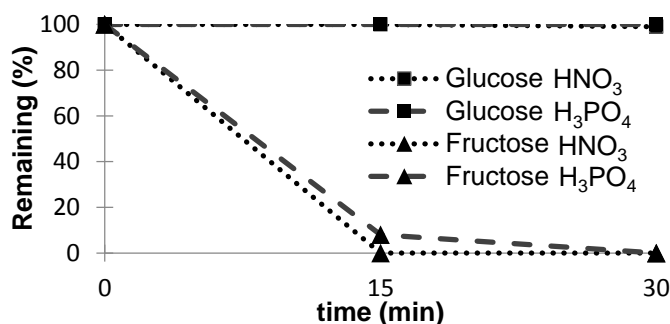


Figure II.4. Selective transformation of D-fructose to HMF in the presence of D-glucose: 1:1 mixture of D-glucose/D-fructose (2.0 g scale) in TEAB/water 10% (w/w), at 80 °C with 10% (w/w) HNO_3 [**Figure II.3**, entry o)] and at 100 °C with 30% (w/w) H_3PO_4 [**Figure II.3**, entry d)]; the yields were determined by using HPLC.

The experimental conditions were further explored by studying the isolation of HMF through the neutralization of the reaction medium and subsequent precipitation of the TEAB/D-glucose/neutralized catalyst mixture by using the sequential addition of ethanol and ethyl acetate (**Table II.8**). The transformation was feasible in high yields and purities for a range of readily available protic acids. The best isolated yields of 89% and 91% and purities of 99% and 90% were observed for H_3PO_4 and HNO_3 , respectively (**Table II.8**, entries 1 and 2). In addition, the continuous dehydration was possible for the two H_2SO_4 and HNO_3 catalysts (**Table II.8**, entries 4 and 5), which provided HMF in 80% and 87% yields and purities of 97% and 99%, respectively.

Table II.8. Production and isolation of HMF from D-fructose in the presence of D-glucose.^a

Entry	Catalyst, conc. (% w/w)	T (°C)	t (min)	Isolated HMF yield (%) ^b	HMF Purity (%) ^c	Remaining D-glucose (%) ^c
1 [†]	H_3PO_4 , 30	100	30	89	99	94
2	HNO_3 , 10	80	15	91	90	99
3 [†]	HCl, 10	90	15	85	87	73
4 [†]	H_2SO_4 , 25	95	0.5 ^d	80	97	89
5 [†]	HNO_3 , 15	95	0.5 ^d	87 ^c	99	-

^a1:1 mixture of D-glucose and D-fructose (entries 1 and 2 = 2 g, entry 3 = 3 g, and entries 4 and 5 = 4 g) in TEAB/water (entry 1 = 10 g with 10% w/w water, entry 2 = 15 g with 10% w/w water, entry 3 = 15 g with 15% w/w water, and entries 4 and 5 = 35 g with 28% w/w water) with catalyst in a closed vessel (entries 1 and 2), an open vessel (entry 3), or under flow conditions (entries 4 and 5: homemade glass reactor with 5 mm internal diameter, and 12 mL internal volume).

^bIsolated yield based on D-fructose. ^cDetermined by using HPLC. ^dReaction flow in mL.min⁻¹.

[†]Experiments performed by Svilen P. Simeonov.

Finally, the integrated process for the big scale production and isolation of HMF from D-glucose (10 g of D-glucose for each cycle), that is, GFI, exclusive D-fructose dehydration to HMF, isolation of HMF and reuse of the unreacted D-glucose, was performed by using sweetzyme[®], reaction medium and HNO₃. Initially, the GFI was performed at 70 °C, which led to a loss of the enzymatic activity after 4 cycles (**Table II.9** and **Figure II.5**). This loss of activity is not related with the reaction medium because by just adding freshly enzyme was enough to achieve 1.0 ratio after 6 hours enzymatic reaction. It is noteworthy the fact that using more than 10% (w/w) of water in the reaction medium led to a low yield in the dehydration reaction (and so less D-glucose was added to perform the next cycle, **Table II.9**, cycle 2).

Table II.9. Reutilization experiments by performing GFI at 70 °C.

Cycle	Reaction	F loading (g)	G loading (g)	Isolated HMF (g)	HMF purity (%)	G Conv. (%)	F Conv. (%)	F/G ratio after enzymatic reaction
1	Dehyd. ^a	5	5	2.7 (77% yield)	98	0	94	
	GFI ^b		5					1.0
2 ^a	Dehyd. ^a			1.8	100	0	55	
	GFI ^b		2.5					1.1
3	Dehyd. ^a			2.8	99	3	95	
	GFI ^b		5					0.9
4	Dehyd. ^a			2.5	100	0	94	
	GFI ^b		5					0.6
5	Dehyd. ^a			2.1	98	3	98	
	GFI ^b		5					0.3 (1.0) ^c
Total		5	27.5	11.9				

^aD-Glucose-D-fructose isomerization (GFI) performed at 70 °C in 1:1 w/w water/TEAB with 6% w/w of sweetzyme[®]. ^bDehydration reaction (Dehyd.) performed using 10% w/w HNO₃ (added at 80 °C) in TEAB with 10% w/w H₂O, at 80 °C, in a closed vessel, scale 10 g sugar/75 g RM. For entry 2 more than 10% w/w H₂O was used. ^cDue to low D-glucose conversion, freshly enzyme was replaced and 1.0 ratio was obtained after 6 hours of enzymatic reaction. F = D-Fructose. G = D-Glucose

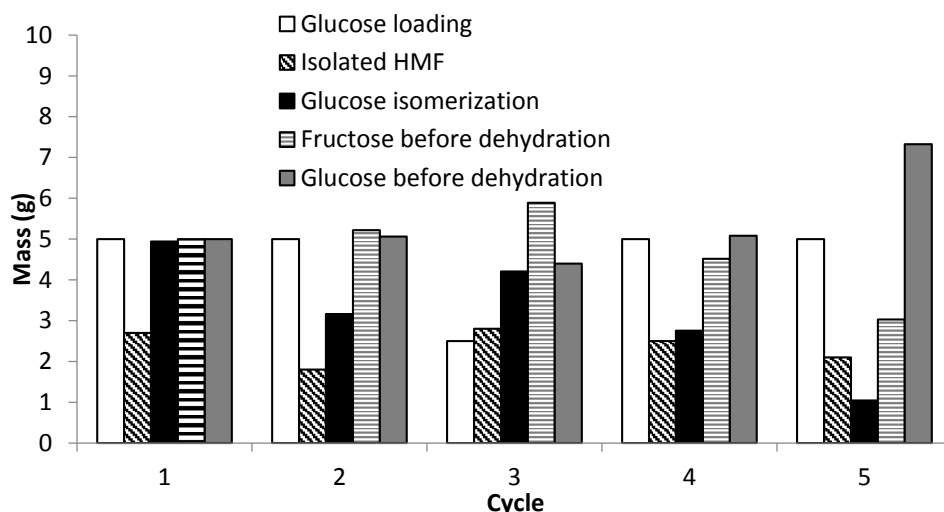


Figure II.5. Reutilization experiments by performing GFI at 70 °C.

Very gratifyingly, performing the GFI at 60 °C instead of 70 °C led to a later decrease of the enzymatic activity (**Table II.10** and **Figure II.6**). For each cycle, approximately half of the D-glucose was isomerized to D-fructose and further transformed to HMF; therefore, considering the overall process, the remaining D-glucose was isolated as 21.1 g of pure HMF, which corresponded to an overall yield of 87% over eight cycles. Per cycle, the average total-mass and D-glucose-loss was 1.1 % and 1.6 %, respectively. As the number of cycles increased, a loss of the enzymatic activity was observed, which could be attributed to the presence of high concentration of NaNO_3 derived from HNO_3 neutralization. Notably, with the exception of the HNO_3 catalyst, all components were reused in the overall process. In addition, the use of the H_3PO_4 catalyst could provide a more efficient integrated process because it formed the neutralized phosphoric acid salt, which is also commercially valuable. In fact, after the addition of ethanol, which caused precipitation, the salt was isolated in a 95% yield.

Table II.10. Reutilization experiments by performing GFI at 60 °C.

Cycle	Reaction	G loading (g)	Isolated HMF (g)	HMF purity (%)	G conv. (%)	F Conv. (%)	F/G ratio after enzymatic reaction
1	GFI ^a	10					1.0
	Dehyd. ^b		2.8	100	7	84	
2	GFI ^a	5					0.9
	Dehyd. ^b		3.0	100	1	94	
3	GFI ^a	5					0.8
	Dehyd. ^b		2.6	100	7	83	
4	GFI ^a	5					0.9
	Dehyd. ^b		2.6	100	1	83	
5	GFI ^a	5					1.0
	Dehyd. ^b		2.5	100	1	74	
6	GFI ^a	5					0.8
	Dehyd. ^b		2.1	100	5	64	
7	GFI ^a	5					0.7
	Dehyd. ^b		2.6	100	2	72	
8	GFI ^a	5					0.6
	Dehyd. ^b		2.9	100	6	96	
Total		45	21.1				

^aDehydration reaction (Dehyd.) performed using 10% w/w HNO₃ (added at 80 °C) in TEAB with 10% w/w H₂O, at 80 °C, in a closed vessel, scale 10 g sugar/75 g RM. ^bD-Glucose-D-fructose isomerization (GFI) performed at 60 °C in 1:1 w/w water/TEAB with 6% w/w of sweetzyme®. F = D-Fructose. G = D-Glucose

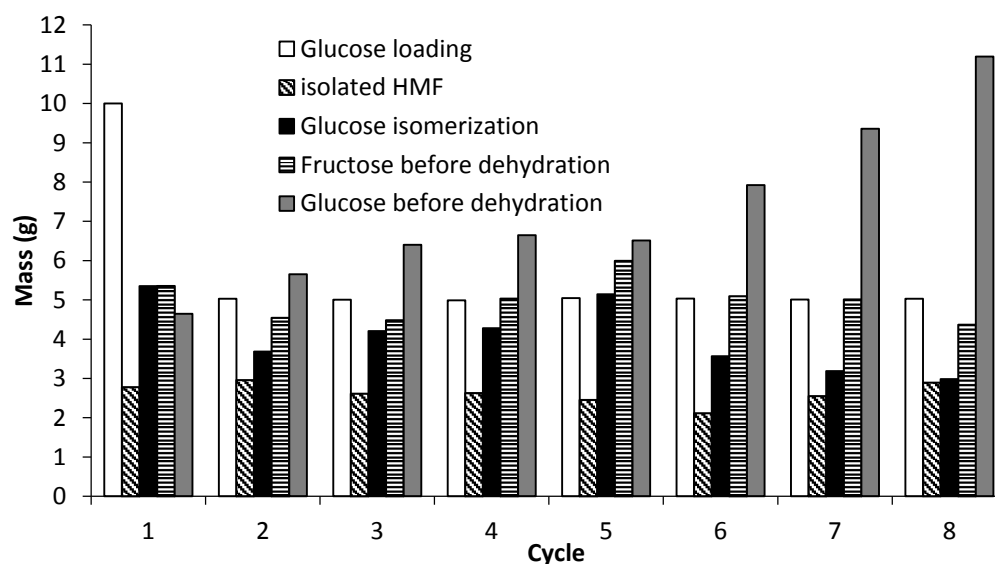


Figure II.6. Integrated chemo-enzymatic production and isolation of HMF from D-glucose by using HNO₃ catalyst. For each cycle: isomerization step with D-glucose (10 g, for cycles 2-8 5 g of D-glucose was added), TEAB/water (1:1 w/w, 135 g), sweetzyme® (0.6 g, 6% w/w, 60 °C, overnight); and the dehydration step with HNO₃ (10% w/w), TEAB/water (9:1 w/w), 80 °C, 25 min.

II.2.3. Guidelines for human exposure of furfural-related compounds

To provide key guidelines about the most human-friendly building blocks the toxic impact of HMF, SMF and a range of HMF derivatives (in a total of 22 compounds) in immortalized human skin fibroblast cells (CRL-1502) were studied. CRL-1502 is a non-tumor cell line which was chosen to resemble human healthy tissue, allowing the prediction of the impact of such compounds in humans. The viability and the ability of the compounds to generate oxidative stress in treated cells were assessed. Furthermore, the studied was also extended to the already in use and established bioplatfrom furan-based molecules such as furfural (**99**) and furfuryl alcohol (**46**) and levulinic acid (**124**) to allow the comparison with the new potentially emerging molecules.

For the viability studies, the CRL-1502 cells were incubated with 100–500 μ M of the tested compounds for 72 hours and the corresponding toxicity curves analyzed (**Table II.11**). Treatment with SMF (**144**) induced a decline in viability of about 30%, whereas HMF (**121**) was not seen to lead to detectable variations. A one-way ANOVA analysis demonstrated that these differences are statistically significant ($p < 0.05$) and we may assume that SMF (**144**) constitutes a compound with a slightly higher probability to generate cytotoxicity (**Table II.11**, entry 2 vs. 1).

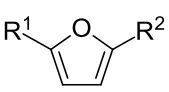
The promising candidates for polymer production **122** and **126** and the potential biofuel replacement **125** were also included in this study (**Table II.11**, entries 12, 17 and 18). The first two did not affect significantly cell viability whereas compound **125** induced a viability decrease to 65%, a similar extent as SMF; and results were statistically significant ($p < 0.05$) when compared to the control molecule HMF.

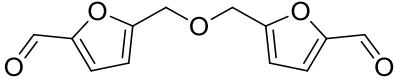
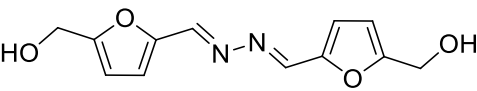
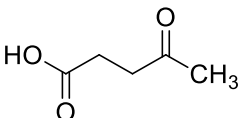
For compounds **145**, **147**, **148**, **149** and **151**, CRL-1502 cells experienced a weak decrease in viability at the maximum tested dose, which did not go below 60% (**Table II.11**, entries 3, 5-7 and 9). However, in the presence of the more lipophilic compound **150**, the induced cytotoxicity was undoubtedly enhanced, producing 80% viability decline at a 500 μ M dose (**Table II.11**, entry 8). Compound **128** and **156** were the second and third most toxic compounds producing 70% and 50% viability decline, respectively (**Table II.11**, entry 10 and 20).

Finally, compounds **46**, **99**, **124**, **146**, **152**, **153**, **154**, **155** and **157** did not decreased the viability of this model up to 500 μ M.

For the assessment of reactive oxygen species (ROS), CRL-1502 cells were incubated with 250 μ M of the compounds for a period of 90 min. This concentration was chosen because at 500 μ M the high cytotoxicity of some of the compounds could not allow ROS determination.

Table II.11. Percentage of viability and ROS determined for treated CRL-1502 cells. Viability was assayed after 72 hours incubation and presented values correspond to a 500 μ M concentration. For the determination of ROS, cells were incubated with 250 μ M of compound for 90 min.[†]



Entry	R ¹	R ²	Compound	Viability \pm SD (%)	ROS \pm SD (%)
1	CHO	CH ₂ OH	121	94 \pm 3	106 \pm 7
2	CHO	CH ₂ OSO ₃ Na	144	68 \pm 5 ^a	120 \pm 11
3	CHO	CH ₂ Cl	145	70 \pm 10 ^a	379 \pm 60 ^a
4 [‡]	CHO	CH ₂ OEt	146	90 \pm 15	107 \pm 22
5	CHO	CH ₂ OBn	147	72 \pm 13 ^a	177 \pm 14 ^a
6	CHO	CH ₂ OTBDMS	148	75 \pm 24 ^a	158 \pm 36 ^a
7	CHO	CH ₂ OAc	149	86 \pm 11	108 \pm 34
8	CHO	CH ₂ OH _z	150	22 \pm 3 ^a	370 \pm 44 ^a
9	CHO	CH ₂ OBz	151	62 \pm 7 ^a	153 \pm 17 ^a
10 [‡]	CHO	CHO	128	32 \pm 2 ^a	113 \pm 12
11	CHO	H	99	95 \pm 8	101 \pm 30
12	CH ₂ OH	CH ₂ OH	126	96 \pm 10	254 \pm 32 ^a
13 [‡]	CH ₂ OH	CH ₂ OEt	152	95 \pm 10	116 \pm 7
14 [‡]	CH ₂ OH	COONa	153	95 \pm 17	89 \pm 13
15	CH ₂ OH	H	46	99 \pm 6	101 \pm 28
16 [‡]	CH ₂ OEt	CH ₂ OEt	154	114 \pm 15	97 \pm 21
17	COOH	COOH	122	93 \pm 11	86 \pm 7
18	CH ₃	CH ₃	125	65 \pm 8 ^a	172 \pm 20 ^a
19	CH ₃	H	155	93 \pm 6	84 \pm 20
20 [‡]			156	51 \pm 6 ^a	134 \pm 19
21 [‡]			157	109 \pm 5 ^a	109 \pm 19
22	Levulinic acid		124	98 \pm 5	122 \pm 52

[†]Viability assays and ROS determination experiments were performed by the team member Dr. Raquel Frade. [‡]Prepared by Svilen P. Simeonov. ^ap<0.05. Bz = Benzoyl; Bn = Benzyl; Hz = Hexanoyl; Ac = Acetyl.

With the exception of compounds **144**, **128** and **156**, data showed that compounds that affect viability lead to considerable ROS generation. Within such compounds, the decreasing trend of oxidant potential is: compounds **145** \approx **150** \gg **147** \approx **125** $>$ **148** \approx **151**,

where the most toxic is the halogenated compound **145** (**Table II.11**). This effect was not detected in cells exposed to HMF.

The increment of ROS does not seem to represent the key player for the detected cytotoxicity because: 1) the highly and moderately toxic compounds **128** and **156**, respectively, did not increment ROS that much; 2) weakly toxic compounds such as **145**, **147** and **125** enhanced significantly ROS levels; and 3) compound **126** which did not lead to detectable changes in viability was an important ROS generator.

Interestingly, comparing the results obtained for compounds **126**, **153** and **46**, it is clear that the functionalization of the furan ring with methylhydroxyl groups increases the potentiality of the compound to cause harmful effects on a long term basis due to the formation of oxidative stress. If we compare the results for compounds **125** and **155**, the same observations is also valid for the dimethylated compound.

This information could not be concluded from the viability assay discussed previously, which demonstrates the importance of this assessment. Compounds **46**, **121**, **122**, **146**, **149**, **99**, **152**, **153**, **154**, **155**, **157** and **124** were not seen to affect the oxidative status in addition to their lack of cytotoxicity in the neutral red assay, meaning that these are very likely the safest studied compounds (**Table II.11**).

II.3. Conclusions and Perspectives

To overcome the lack of reported integrated methodologies for the synthesis and isolation of HMF this team contributed to this field resulting in the development of two novel methodologies.

In the first one is reported an integrated, simple, efficient, reusable and scalable method for the transformation of carbohydrates (mainly D-fructose) into HMF that overcome the major problem in big scale HMF production that is the isolation and purification. In conclusion, simple crystallization (precipitation) of the reaction medium (TEAB) using renewable solvents ethanol and ethyl acetate followed by solvent evaporation provides HMF in excellent yields and purity without any further purification (**Figure II.7**). In addition, this method opens the opportunity to discover more efficient catalytic system that may allow the direct conversion of D-glucose, or ultimately cellulose to HMF under conditions that can more easily transferred to large scale production.

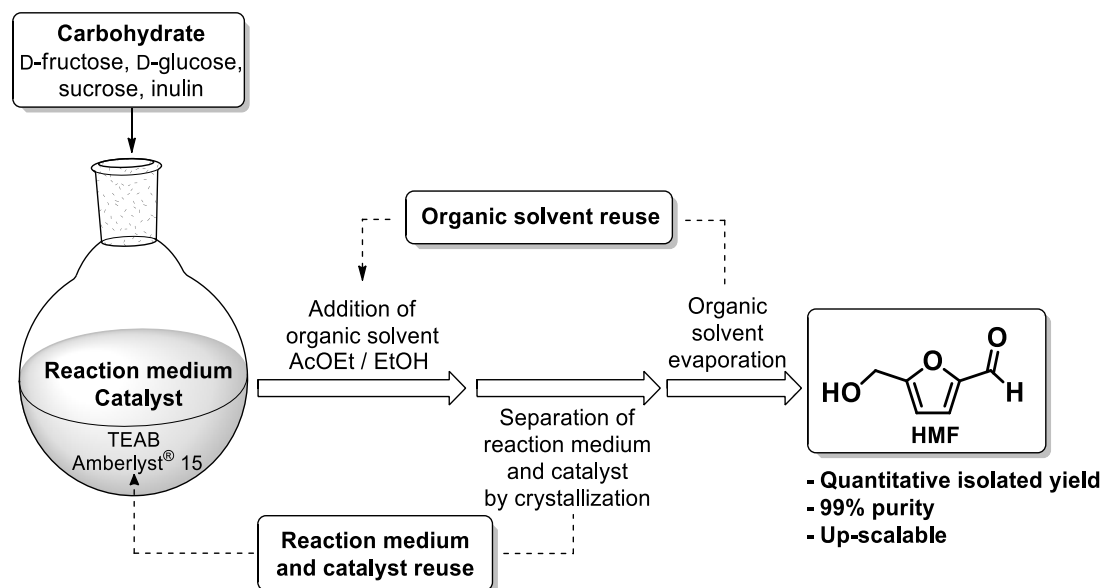


Figure II.7. Integrated production and isolation of HMF from carbohydrates.

In the second methodology we reported the first integrated process for the production and isolation of HMF from D-glucose, which achieves yields up to 87% and extremely high purity (>99 %). In conclusion, the overall process is a combination of enzymatic GFI, selective D-fructose dehydration to HMF, and HMF isolation (**Figure II.8**). The isolation of HMF through the precipitation of the reaction medium allows the reuse of the enzyme and the reaction medium, TEAB, which also acts as a dehydration promoter. This process took advantage of the sweetzyme® that is already used in the large industrial-scale production of D-glucose-D-fructose syrup in water. The combination of this well established technology with robust D-fructose dehydration and HMF isolation processes, which are based on

reaction medium precipitation and solvent evaporation, demonstrates the required overall features for future industrial applications in the production of highly pure HMF.

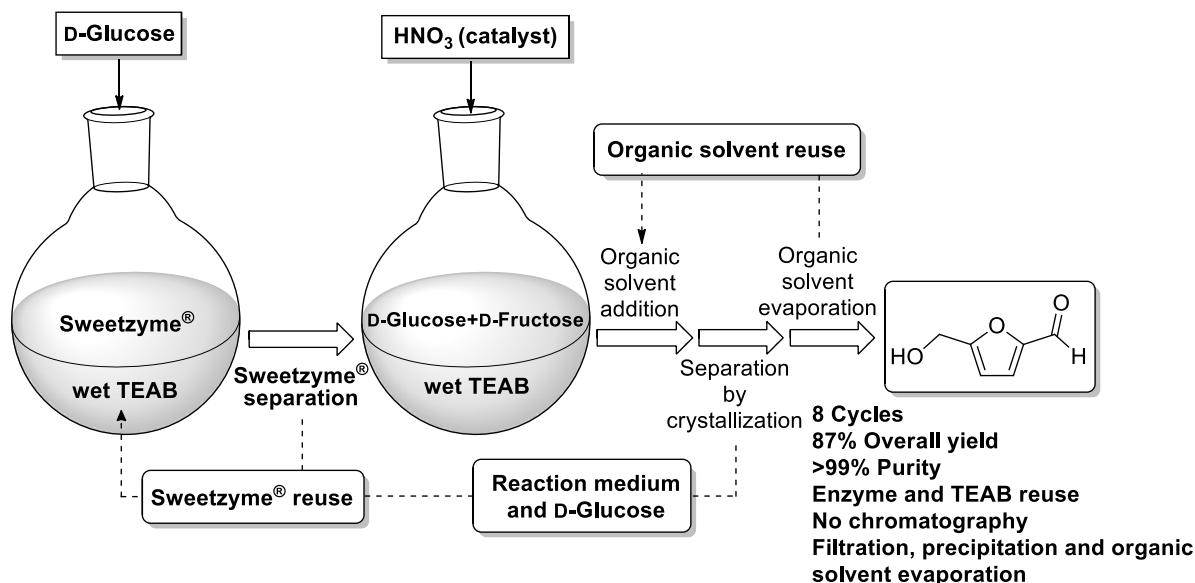
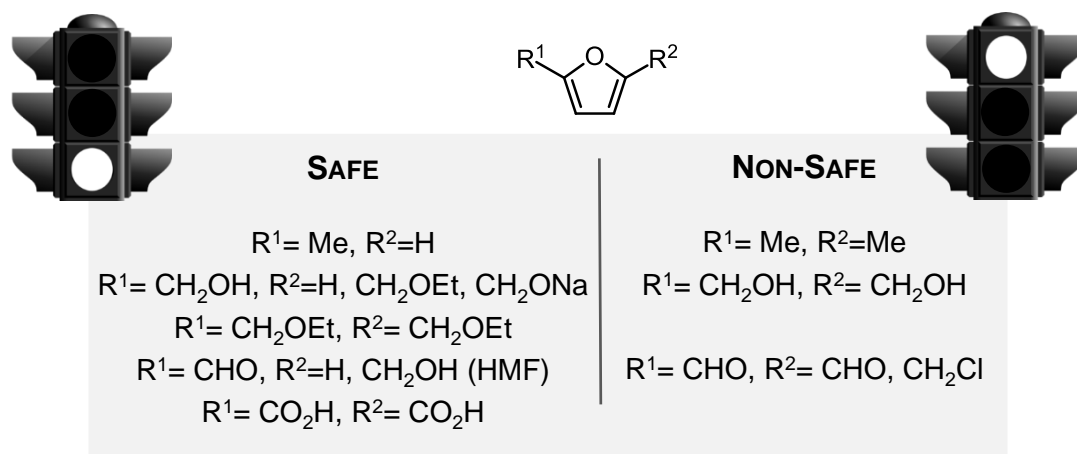


Figure II.8. Integrated chemo-enzymatic production of HMF from D-glucose.

Regarding the results of the cytotoxicity studies of HMF and derivatives, it was possible to organize them in two different groups (**Figure II.9**): one group constituted by compounds that did not decrease viability and did not enhance ROS levels (compounds **46, 99, 121, 122, 124, 146, 149, 152, 153, 154, 155, 157**); and a second group formed by the remaining compounds. In this last group, three different types of compounds can be distinguished: i) compounds not involved in ROS generation but weakly cytotoxic (compound **144**) or extremely cytotoxic (compound **128**); ii) others that induced both ROS and viability decrease (compounds **125, 145, 147, 148, 150, 151** and **156**; and iii) compound **126** that was not seen to decrease viability but it was seen to form ROS in a significant way. This suggests other major players being responsible for the induced cytotoxicity rather than oxidative stress.

Regarding the controversial data in the literature for HMF toxicological impact, it was not seen any significant cellular impact in this work. In addition, SMF was shown to be just a moderated cytotoxic compound in the tested model.



SAFE	NON-SAFE
$R^1 = \text{Me}, R^2 = \text{H}$	$R^1 = \text{Me}, R^2 = \text{Me}$
$R^1 = \text{CH}_2\text{OH}, R^2 = \text{H}, \text{CH}_2\text{OEt}, \text{CH}_2\text{ONa}$	$R^1 = \text{CH}_2\text{OH}, R^2 = \text{CH}_2\text{OH}$
$R^1 = \text{CH}_2\text{OEt}, R^2 = \text{CH}_2\text{OEt}$	
$R^1 = \text{CHO}, R^2 = \text{H}, \text{CH}_2\text{OH}$ (HMF)	$R^1 = \text{CHO}, R^2 = \text{CHO}, \text{CH}_2\text{Cl}$
$R^1 = \text{CO}_2\text{H}, R^2 = \text{CO}_2\text{H}$	

Figure II.9. Guidelines for selected furan-containing biomass derivatives.

At the moment this team are working on a new novel methodology for the one step protocol of HMF production from D-glucose using CrCl_3 supported in ion exchange resins in the same reaction medium described before. Additionally, the preliminary cytotoxicity results opens the opportunity to perform more studies regarding to the involved mode of action.

II.4. Experimental

II.4.1. General Remarks

All solvents were freshly distilled from commercial grade sources. Commercially available reagents were used as received without further purification otherwise notice. TEAB: Sigma Ref. N° 14023-1kg (water content 1% w/w) or old source from Laboratórios Azevedos Sociedade (>15 years, average water content of 14 % w/w), TEAB: Industrial Farmacêutica Lisboa, TPAB: Alfa Aesar Ref. N° A11522, Amberlyst® 15 (wet): Ref. N° 216399-500G, D-Fructose: Merck extra pure or commercial grade from supermarket. HNO₃ 65% solution: Merck, H₃PO₄ 85% solution: Merck pro analysis, HCl 36% solution: Scharlau, D(+)-Glucose anhydrous: Merck Ref. N° 8337.

Preparative thin-layer chromatography plate was prepared with silica gel 60 GF₂₅₄ Merck (Ref 1.07730.1000), whereas flash chromatography was carried out on silica gel 60M purchased from MN (Ref. 815381). Reaction mixtures were analyzed by TLC using ALUGRAM SIL G/UV254 from MN (Ref. 818133, silica gel 60), and visualization by UV and phosphomolybdic acid stain.

The HMF purity was determined using HPLC analysis on Dionex P680 pump, Dionex UVD 340S diode array detector, detection at 275 and 225 nm, manual injector with 20 µL loop, column HICHROM C18, 250×4.6mm, R_t (HMF) = 9.5 min or Kromasil 100, C18, 250 × 4.6mm, R_t (HMF) = 11.4 min. Mobile phase gradient from 1:99 to 50:50 for 40 min acetonitrile:water, and then 50:50 for the time indicated in the chromatogram, flow 1 mL/min, The HPLC purity was determined by comparing the integration area of the main signal with other observed minor peaks and are represented in the chromatograms by relative area.

The D-glucose and D-fructose HPLC analysis was performed on Shimadzu LC-20AT pump, Merck Differential Refractometer RI-71, Manual injector with 20µL loop. The analysis has been performed using Phenomenex Luna-NH₂ 250 × 4.6mm 5 µm column, flow 2 mL/min and mobile phase acetonitrile and water 87:13. R_t (D-Fructose) = 5.4 min and R_t (D-Glucose) = 7.2 min.

The determination of water content in the ammonium salt was performed on Metrohm Karl Fisher coulometer (831KF coulometer Metrohm, 768KF oven Metrohm, 703TI stand Metrohm) equipped with oven: temperature for the analysis was 220 °C.

NMR spectra were recorded at room temperature in a Bruker AMX 300 or Bruker AMX 400 using CDCl₃, D₂O or DMSO-d₆ as solvents and (CH₃)₄Si(¹H) as internal standard.

All the biological studies were performed by Dr. Raquel F. M. Frade.

II.4.2. Experimental procedures of Section II.2.1

General procedure for the transformation of D-fructose to HMF using dimethyl sulfoxide (DMSO) based on reported procedure.¹⁰² To an round bottom flask equipped with an distillation apparatus (N₂ or evacuation can be also used to take out the produced water) was added 200 mL of DMSO, 6.0 g of D-fructose and 0.4 g of Amberlyst® 15 powders. The mixture was stirred at 120 °C for 2.5 hours. After reaction, the catalyst was filter out and 190 mL of dimethyl sulfoxide was distilled at 31 °C/ 0.6 mbar (oil bath temperature: 60 °C, complete distillation led to HMF degradation) to obtain a dark orange oil which was finally purified by column chromatography to give light yellow liquid (that crystalizes in freezer) of HMF (2.94 g, 70%) with 98% purity by HPLC. Spectral data (¹H NMR, ¹³C NMR) identical to those reported.

General procedure for the transformation of D-fructose to HMF and isolation using *p*-tolyl sulfoxide. To 3.0 g of melted *p*-tolyl sulfoxide at 120 °C was added 1.0 g of D-fructose and 100 mg of Amberlyst® 15 powders. The mixture was stirred for 2 hours. After reaction, EtOAc was added, filtered through a pad of silica gel and the solvent evaporated to give a yellow solid. This solid was then recrystallized of diethyl ether/hexanes to give 2.7 g (90%) of *p*-tolyl sulfoxide as a brown solid. Finally the HMF present in solution was purified by column chromatography to give brown liquid (197 mg, 28%) with 94% purity determined by HPLC analysis.

General procedure for the synthesis of HMF under batch conditions. D-Fructose (commercial grade, purchased locally) and catalyst (Amberlyst® 15, unless stated otherwise) were added to the reaction medium (TEAB, unless stated otherwise) and heating in an open flask for 10 min, from 80 °C to 100 °C, followed by an additional 15 min at 100 °C. Isolation of HMF was performed by dissolution of the reaction mixture in ethanol followed by precipitation with EtOAc, filtration, and removal of ammonium salt traces by filtration with silica. HMF purity was determined by HPLC.

Procedures for the recycling experiments for the transformation of D-fructose (20 g scale) to HMF (Table II.4, left):

1st Cycle. To 91 g of TEAB (1% w/w water content) was added 9.0 mL of water. The resulting mixture (100 g, 10% w/w water content) was mixed with 20.0 g of D-fructose and 2 g of smashed Amberlyst® 15 (10% w/w). The mixture was placed at 80 °C and heat up to 100 °C for 10 min. Then was stirred at 100 °C for 15 min. The mixture was cooled down to RT and the resulting solid was washed with EtOAc (200 mL). The solvent was decanted

and the solid was dissolved in hot EtOH (10 mL) then under vigorous stirring was added EtOAc (1 L). The resulting precipitated was filtered out and the combined solutions were filtered through a pad of silica gel (20 g) and evaporated to give brown liquid of crude HMF (12.9 g, 92%) with 99% purity by HPLC analysis.

2nd Cycle. The recovered TEAB was recrystallized additionally from EtOH and EtOAc and dried for 5 h under vacuum (rotatory pump, <1 mmHg) resulting in 86 g. The amount of water was determined by Karl Fisher – 2%, then 7.6 mL of water was added to achieve 10% w/w water amount and 20.0 g of D-fructose was added. The mixture was placed at 80 °C and heat up to 100 °C for 10 min. Then was stirred at 100 °C for 15 min. The mixture was cooled down to RT and the resulting solid was washed with EtOAc (200 mL). The solvent was decanted and the solid was dissolved in hot EtOH (10 mL) then under vigorous stirring was added EtOAc (1 L). The resulting precipitated was filtered out and the combined solutions were filtered through a pad of silica gel (20 g) and evaporated to give brown liquid of crude HMF (12.0 g, 86%) with 97% purity by HPLC and ¹H NMR analysis.

3rd Cycle. The recovered TEAB was recrystallized additionally from EtOH and EtOAc and dried for 5 h under vacuum (rotatory pump, <1 mmHg) resulting in 68 g. The amount of water was determined by Karl Fisher – 3%. 5.3 mL of water was added to achieve 10% w/w water amount and 14.0 g of D-fructose was added. The mixture was placed at 80 °C and heat up to 100 °C for 10 min. Then was stirred at 100 °C for 15 min. The mixture was cooled down to RT and the resulting solid was washed with EtOAc (200 mL). The solvent was decanted and the solid was dissolved in hot EtOH (10 mL) then under vigorous stirring was added EtOAc (1 L). The resulting precipitated was filtered out and the combined solutions were filtered through a pad of silica gel (20 g) and evaporated to give brown liquid of crude HMF (9.1 g, 93%) with 93% purity by HPLC analysis.

4th Cycle. The recovered TEAB was recrystallized additionally from EtOH and EtOAc and dried for 5 h under vacuum (rotatory pump, <1 mmHg) resulting in 60 g. The amount of water was determined by Karl Fisher – 2%, then 31 g of new TEAB was added together with 8.4 mL of water to achieve 10% w/w water amount then 20 g of D-fructose was added. The mixture was placed at 80 °C and heat up to 100 °C for 10 min. Then was stirred at 100 °C for 15 min. The mixture was cooled down to RT and the resulting solid was washed with EtOAc (200 mL). The solvent was decanted and the solid was dissolved in hot EtOH (10 mL) then under vigorous stirring was added EtOAc (1 L). The precipitation was not good forming gum type brown solid. It was filtered out and the combined solutions was filtered through a pad of silica gel (20 g) and evaporated to give brown liquid of crude HMF (9.0 g, 64%) with 91% purity by HPLC analysis.

Procedures for the recycling experiments for the transformation of D-fructose (2 g scale) to HMF in 1:10 D-fructose/TEAB ratio (w/w) (Table II.4, right):

1st to 7th Cycles. To 18.2 g of TEAB (1% w/w water content) was added 1.8 mL of water. The resulting mixture (10 g, 10% w/w water content) was mixed with 2.0 g of D-fructose and 0.2 g of smashed Amberlyst® 15. The mixture was placed at 80 °C and heat up to 100 °C for 10 min and then stirred at 100 °C for 15 min. The reaction was cooled down to RT and the water from the resulting solid mixture was evaporated. Then it was dissolved in hot EtOH (10 mL) and under vigorous stirring was added EtOAc (500 mL). The resulting precipitated was filtered out and the solution was filtered through a pad of silica gel (10 g) and evaporated to give HMF as orange oil (1.37 g, 98%) with 99% purity by HPLC analysis.

The collected TEAB mixed with Amberlyst® 15 was dried under vacuum (4-5 h, rotator pump, <1 mmHg) and recycled using the same conditions for seven times.

8th Cycle. The recovered TEAB and Amberlyst® 15 from the seventh cycle was dissolved in 300 mL MeOH, and 4 g of charcoal was added. The mixture was heated with stirring until it started to boil and was immediately filtered through celite. The solvent was evaporated to give 14 g of purified TEAB. To the purified TEAB (14 g), water (1.6 mL) was added. The resulting mixture (15.6 g, 10% w/w water content) was mixed with 1.6 g of D-fructose and 160 mg of smashed Amberlyst® 15. The mixture was placed at 80 °C and heat up to 100 °C for 10 min and then stirred at 100 °C for 15 min. The reaction was cooled down to RT and the water from the resulting solid mixture was evaporated. Then it was dissolved in hot EtOH (10 mL) and under vigorous stirring EtOAc (500 mL) was added. The resulting precipitated was filtered out and the solution was filtered through a pad of silica gel (10 g) and evaporated to give HMF as orange oil (1.38 g, 123%) with 94% purity by HPLC. The observed 123% yield is due to the transformation of accumulated non-reacted D-fructose from the previous cycle which corresponds to a combined yields of 7th and 8th cycles of 93%.

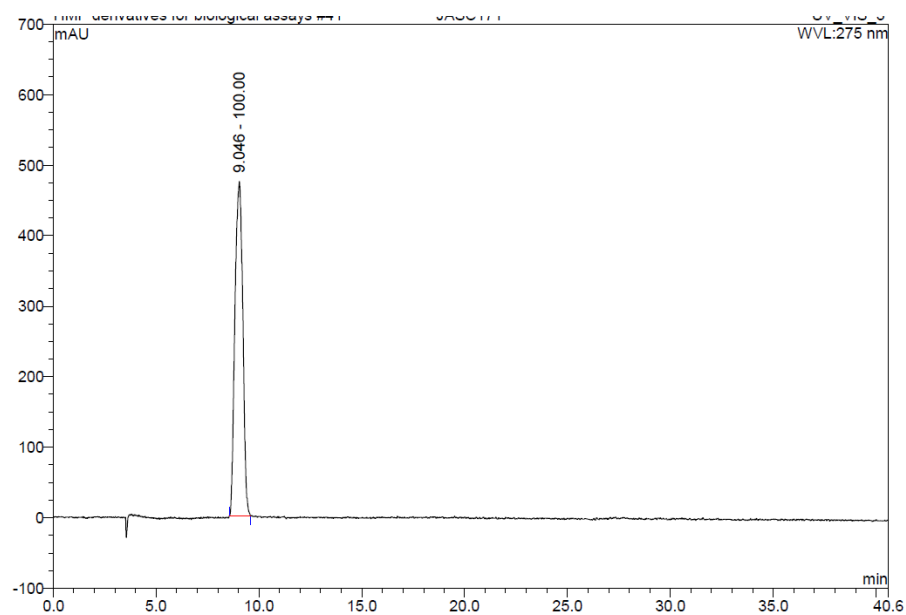


Figure II.10. HPLC chromatogram of HMF (100% purity by HPLC analysis) obtained from recycling experiment (1st cycle, D-fructose/TEAB ratio 1:10 w/w).

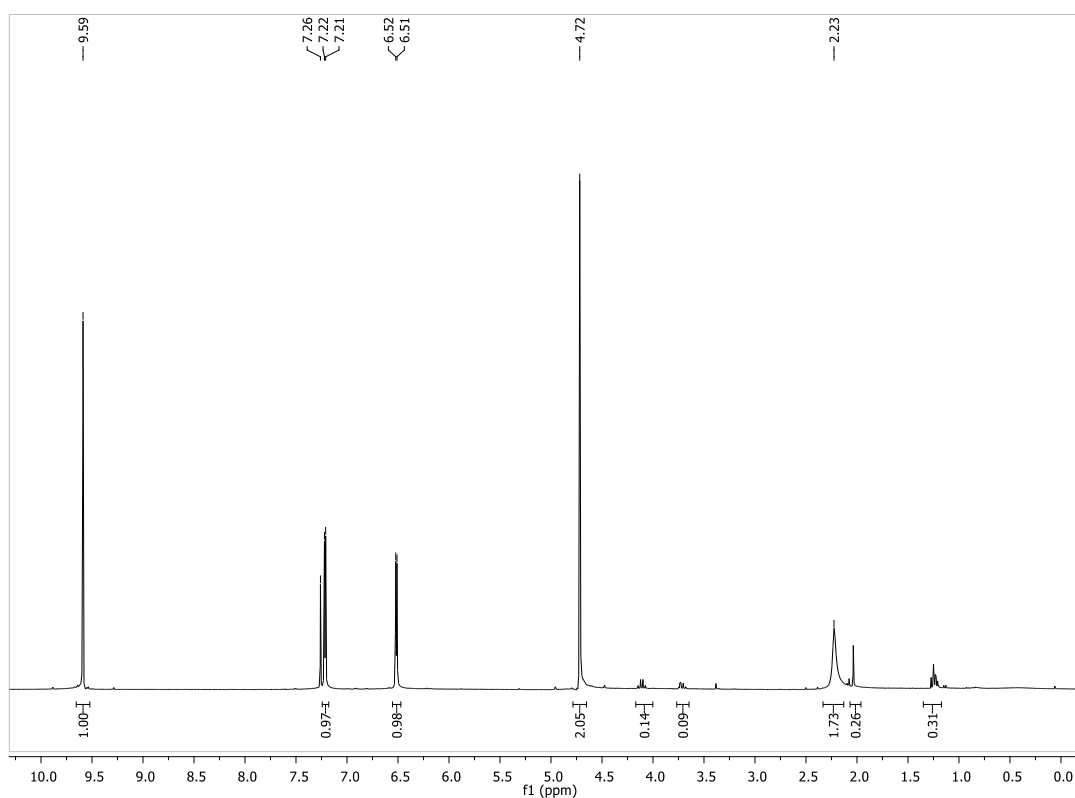


Figure II.11. ¹H NMR spectrum of HMF (100% purity by HPLC analysis) obtained from recycling experiment (1st cycle, D-fructose/TEAB ratio 1:10 w/w).

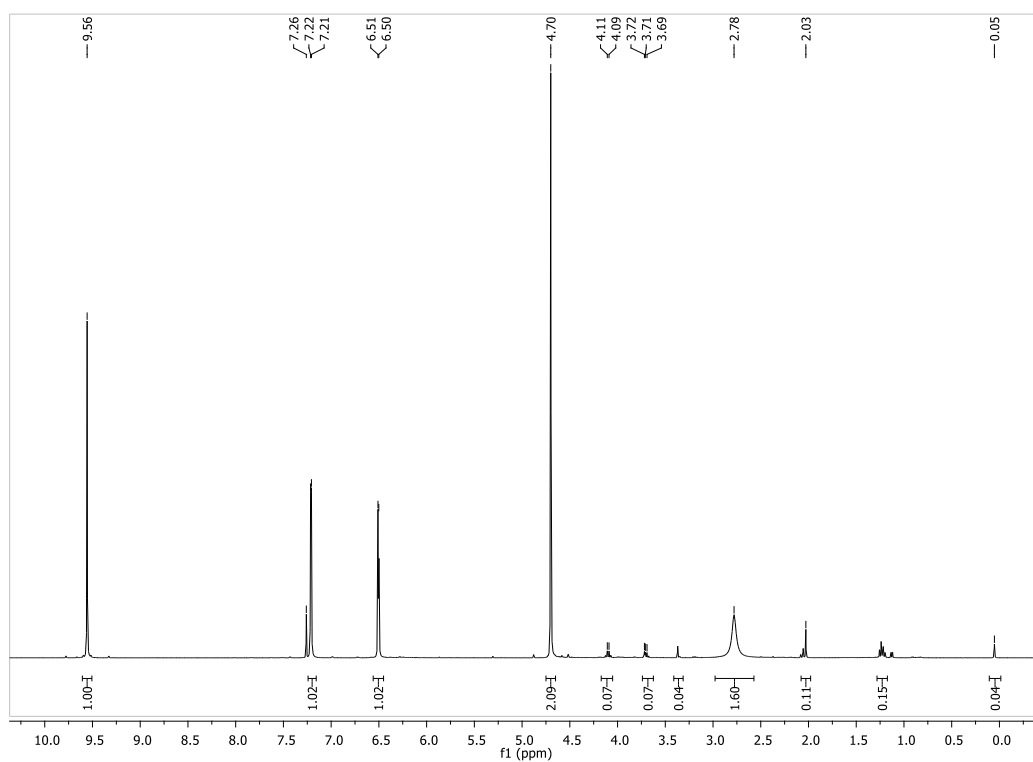


Figure II.12. ¹H NMR spectrum of HMF (98.7% purity by HPLC analysis) obtained from recycling experiment (2nd cycle, D-fructose/TEAB ratio 1:10 w/w).

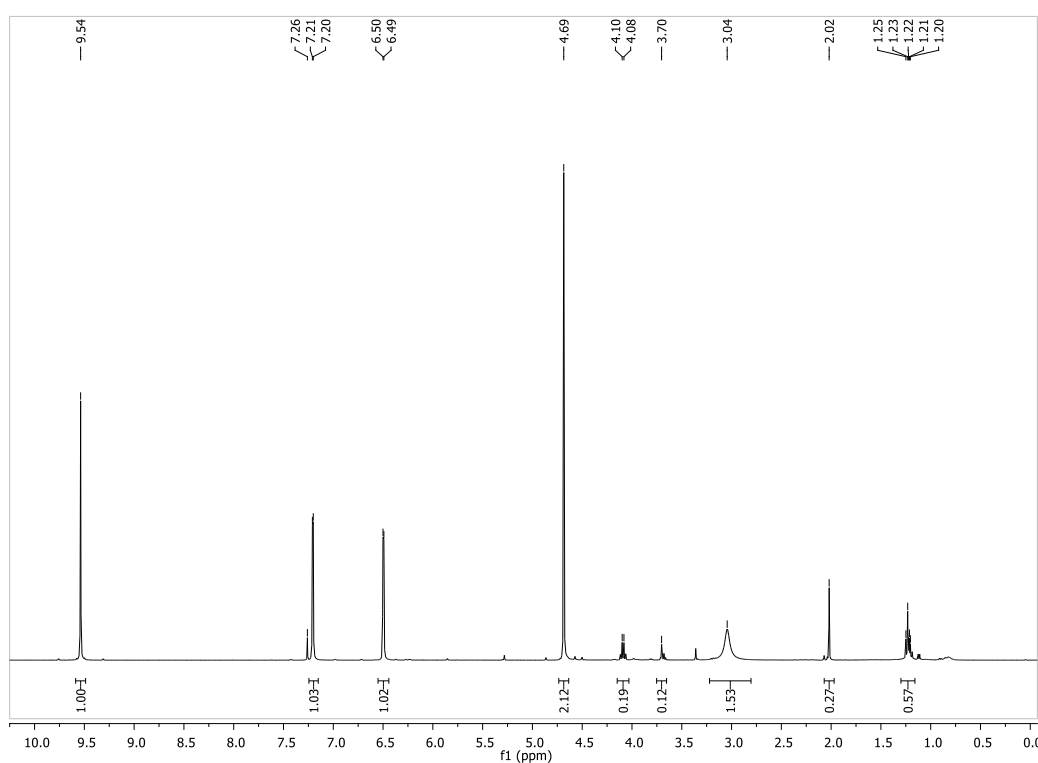


Figure II.13. ¹H NMR spectrum of HMF (99.5% purity by HPLC analysis) obtained from recycling experiment (3rd cycle, D-fructose/TEAB ratio 1:10 w/w).

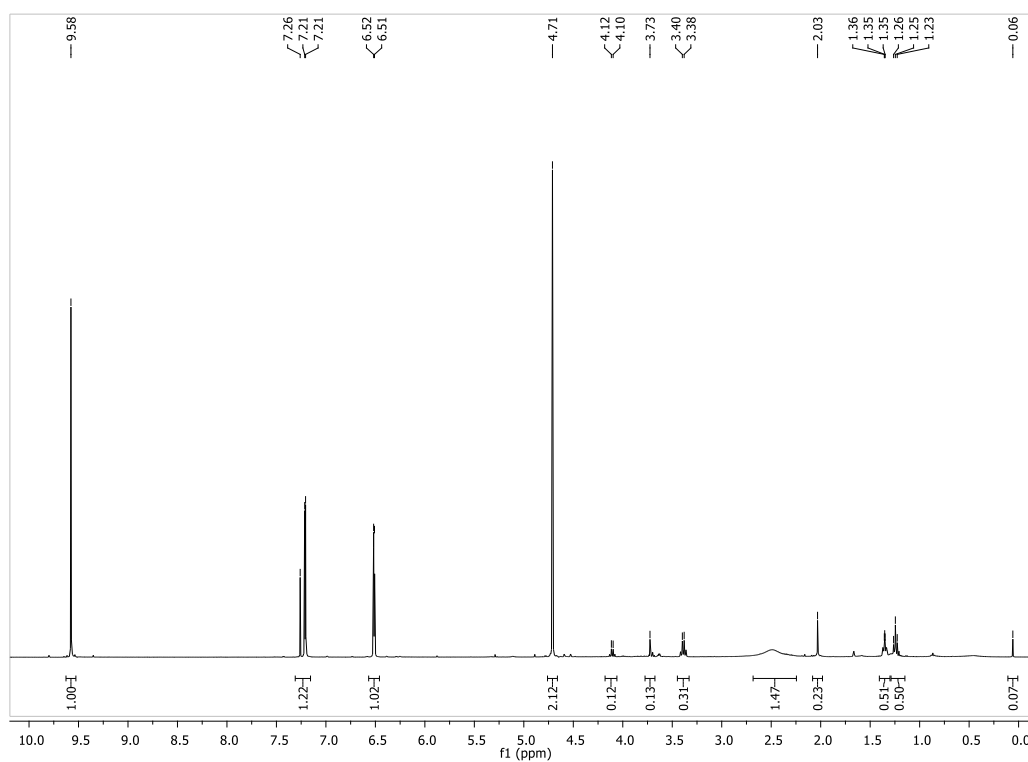


Figure II.14. ^1H NMR spectrum of crude HMF before filtration through a pad of silica gel obtained from recycling experiment (6th cycle, D-fructose/TEAB ratio 1:10 w/w).

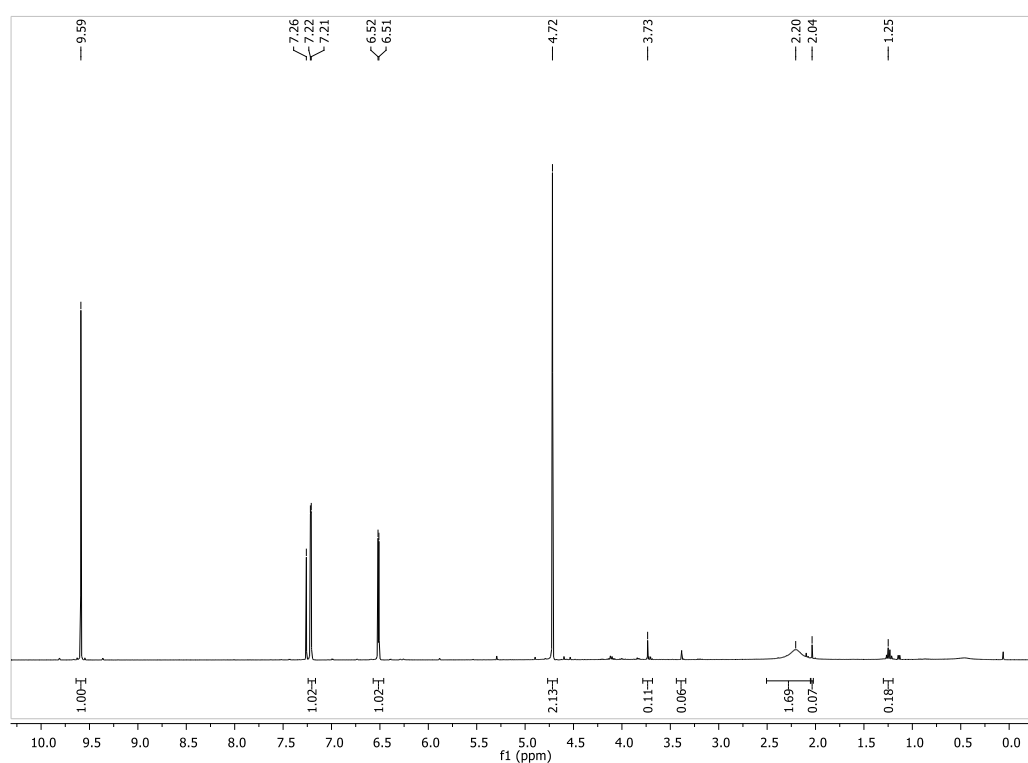


Figure II.15. ^1H NMR spectrum of HMF (96.3% purity by HPLC analysis) obtained from recycling experiment (6th cycle, D-fructose/TEAB ratio 1:10 w/w).

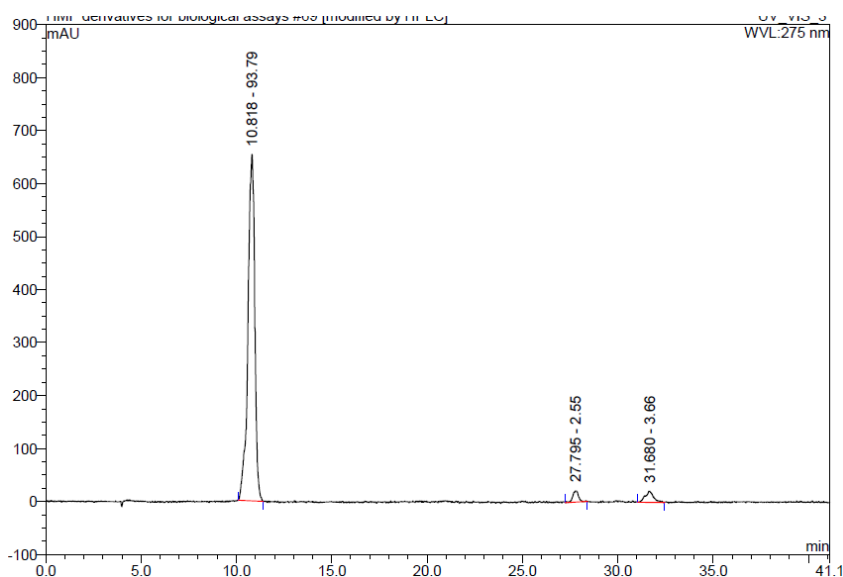


Figure II.16. HPLC chromatogram of HMF (93.8% purity by HPLC analysis) obtained from recycling experiment (8st cycle, D-fructose/TEAB ratio 1:10 w/w).

II.4.3. Experimental procedures of Section II.2.2

General procedure for the kinetic studies of GFI (Table II.7, entry 3). TEAB (5 g) was dissolved in water (5 mL) then 1.2 g of D-glucose and 36 mg of enzyme have been added and the mixture was placed in Kugelrohr at 70 °C and 50 rpm. Samples on every 1 hour have been analyzed by HPLC to generate the graphical data. A single step formation of D-fructose into D-glucose was used as model and the two associated rate constants k_1 and k_2 were evaluated using Excel software and Runge-Kutta fourth order algorithm and the least square method for minimization of errors.

General procedure for the dehydration reactions screening [Figure II.3, entry o]. TEAB (13.5 g) was mixed with D-Fructose (1.0 g) and D-Glucose (1.0 g) then H₂O (1.5 mL) and HNO₃ 65% aq. sol. (0.11 mL, 10% w/w) were added. The mixture was placed to stir at 80 °C in a closed vessel reactor and samples have been taken on every 15 min to be analysed in HPLC.

General procedures for the preparation of HMF from D-glucose and recycling experiments (GFI at 70 °C, Table II.9)

D-Fructose dehydration step. To a closed vessel reactor, reaction mixture containing TEAB in water (10% w/w), D-fructose and D-glucose were added. The mixture was stirred at 80 °C until a homogeneous solutions was obtained. Then 0.55 mL of 65% HNO₃ (10% w/w) was added and the mixture was stirred at 80 °C for 25 min. 100 mg of the reaction

mixture was collected at 0 and 25 min for HPLC analysis. The reaction mixture was then dissolved in absolute EtOH and transferred to a round bottom flask. The acid was neutralized with equimolar amount of NaHCO₃ (667.5 mg) and the solvent evaporated. The obtained solid mixture was extracted with EtOAc and then dissolved in hot absolute EtOH and the TEAB, NaNO₃ and D-glucose were crystalized with the addition of EtOAc. The precipitate was filtered and all the collected organic phases were passed through a pad of silica gel. The solvent was evaporated to give HMF as orange oil.

D-Glucose to D-fructose step. The reaction medium was dissolved in 50% w/w of H₂O and passed through a pad of activated carbon and celite. To the mixture, D-Glucose (5.0 g) and sweetzyme® (600 mg used for the 1st cycle, which was reuse in the next cycles) were added and the mixture was placed in rotavap at 70 °C and 50 rpm overnight. The D-glucose/D-fructose ratio was determined by HPLC analysis. Sweetzyme® was decanted and stored in the fridge for the next cycle. Water was evaporated and the obtained solid was used for the D-fructose dehydration reaction.

General procedures for the preparation of HMF from D-glucose and recycling experiments (GFI at 60 °C, Table II.10):

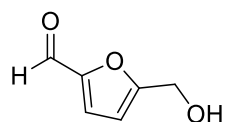
D-Glucose to D-fructose step. A mixture of D-glucose (10 g), TEAB (67.5 g), H₂O (67.5 mL), and sweetzyme® (600 mg) was placed in a flask on a rotary evaporator at 60 °C and 50 rpm for overnight reaction. The D-glucose/D-fructose ratio was determined by using HPLC analysis. The sweetzyme® was decanted and stored in the fridge for the next cycle and the water was evaporated to obtain the solid, which was used for the D-fructose dehydration reaction.

D-Fructose dehydration step. The reaction mixture from the GFI step was placed in a closed vessel reactor and water (7.5 mL) was added. The mixture was stirred at 80 °C until a homogeneous solution was obtained. Then, 65% HNO₃ (0.55 mL, 10% w/w) was added and the mixture was stirred at 80 °C for 25 min. A portion of the reaction mixture (100 mg) was collected at 0 and 25 min for HPLC analysis. The reaction mixture was then dissolved in absolute ethanol (50 mL) and transferred to a round bottom flask. The acid was neutralized with an equimolar amount of NaHCO₃ (667.5 mg) and the solvent was evaporated under reduced pressure. The obtained solid mixture was extracted with EtOAc (2 × 100 mL) and then dissolved in hot absolute ethanol (25 mL). TEAB, NaNO₃, and D-glucose were crystalized with the addition of EtOAc (800 mL). The precipitate was filtered

and all of the collected organic phases were passed through pad of silica gel (10 g). The solvent was evaporated to yield HMF as orange oil.

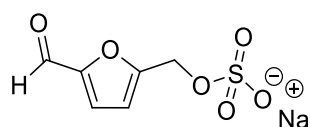
II.4.4. Preparation of furanic compounds for cytotoxicity studies

5-(Hydroxymethyl)furfural, HMF (121)



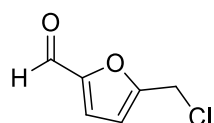
Prepared according to the literature.¹⁰² To a round-bottom flask D-fructose (6 g, 33.3 mmol) and DMSO (200 mL) were added followed by the addition of Amberlyst® 15 powder (0.4 g, 15% w/w). The reaction was allowed to stir for 120 min at 120 °C under inert atmosphere. After reaction the DMSO was removed by distillation and the crude reaction mixture was purified by column chromatography (hex/EtOAc 1:1) to yield the product (2.9 g, 70% yield) as a pale yellow oil that crystallizes in the freezer (0 °C). Spectral data are in accordance with those reported in the literature.¹⁰² ¹H NMR (300 MHz, CDCl₃) δ 2.59 (s, 1H), 4.71 (s, 2H), 6.51 (d, *J* = 3.5 Hz, 1H), 7.21 (d, *J* = 3.5 Hz, 1H), 9.58 (s, 1H); ¹³C NMR (100 MHz, CDCl₃) δ 57.7, 110.1, 123.1, 152.4, 160.8, 177.9.

Sodium (5-formylfuran-2-yl)methyl sulfate, SMF (144)



Prepared according to the literature.¹⁴¹ To a solution of *N,N'*-dicyclohexylcarbodiimide (1.0 g, 5 mmol) in DMF (3 mL) at 0 °C, HMF (128 mg, 1 mmol) dissolved in DMF (0.5 mL) was added with vigorous stirring. A cold solution of sulfuric acid (2 mmol) in DMF (1 mL) was added. The mixture was allowed to stir at 0 °C for 1 h. The mixture was then centrifuged and the solution neutralized with methanolic NaOH 1 M. The resulting solution was once again centrifuged. The precipitate was washed with DMF and centrifuged. The collected organic phases were concentrated under vacuum and the crude dissolved in ethanol and centrifuged. To the solution 10 volumes of Et₂O was slowly added and the precipitate centrifuged. The precipitate was then washed with Et₂O to give the product as a pale orange solid (55 mg, 24% yield); **m.p.** = 128 °C (lit. = 128 °C)¹⁴¹.

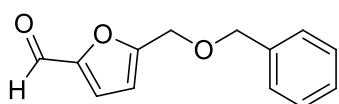
5-(Chloromethyl)furan-2-carbaldehyde (145)



Prepared according to the literature.¹⁴² To a flame dried round bottom flask, HMF (1 g, 7.9 mmol) and anhydrous CHCl₃ were added. Trimethylsilyl chloride (6 mL, 47.3 mmol, 6 equiv.) was added dropwise at 45 °C and the resulting mixture stirred for 24 h at 45 °C under inert atmosphere. The mixture was then quenched with saturated aqueous solution of NaHCO₃ and extracted with DCM. The collected organic layers were dried over Na₂SO₄ and the solvent removed.

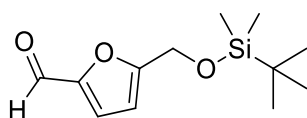
The crude product was purified by dissolution in hot hexane and filtration through a pad of celite and activated carbon. The solvent was removed under vacuum to give the desired product (0.7 g, 61% yield). Spectral data are in accordance with those reported in the literature.¹⁴² **¹H NMR (300 MHz, CDCl₃)** δ 4.59 (s, 2H), 6.57 (d, J = 3.57 Hz, 1H), 7.19 (d, J = 3.57 Hz, 1H), 9.60 (s, 1H).

5-((Benzyloxy)methyl)furan-2-carbaldehyde (147)



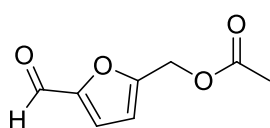
Prepared according to the literature.¹⁴³ Benzyl bromide (3.8 g, 22.2 mmol) and silver oxide (2.6 g, 11.1 mmol) were successively added to a stirred solution of HMF (1.4 g, 11.1 mmol) dissolved in anhydrous DMF (15 mL). The mixture was stirred for 50 h at RT. The solution was evaporated under reduced pressure and the residue was purified by column chromatography (hex/EtOAc 1:1) to give the desired product (1.2 g, 50 % yield). Spectral data are in accordance with those reported in the literature.¹⁴³ **¹H NMR (300 MHz, CDCl₃)** δ 0.87 (t, J = 6.9 Hz, 3H), 1.27-1.31 (m, 4H), 1.63 (quint, J = 7.4 Hz, 2H), 2.35 (t, J = 7.6, 2H), 5.12 (s, 2H), 6.58 (d, J = 3.55 Hz, 1H), 7.21 (d, J = 3.55 Hz, 1H), 9.63 (s, 1H); **¹³C NMR (100 MHz, CDCl₃)** δ 64.2, 73.0, 111.4, 122.0, 128.0, 128.1, 128.6, 137.3, 152.7, 158.5, 177.8.

5-(((tert-Butyldimethylsilyl)oxy)methyl)furan-2-carbaldehyde (148)



Prepared according to the literature.¹⁴⁴ To a solution of HMF (1.6 g, 12.7 mmol) in anhydrous DMF (3.2 mL), imidazole (2.2 g, 31.7 mmol, 2.5 equiv.) and *tert*-butyldimethylsilyl chloride (2.3 g, 15.2 mmol, 1.2 equiv.) were added. The solution was stirred for 22 h. The silylated compound was extracted with hexane (5 x 20 mL). The collected organic layers were washed with brine, dried over Na₂SO₄, and the solvent removed to give the crude product that was distilled (100 °C/0.8 mbar) giving the product (1.9 g, 63% yield) as a light yellow liquid that solidifies in the freezer (0 °C). Spectral data are in accordance with those reported in the literature.¹⁴⁴ **¹H NMR (300 MHz, CDCl₃)** δ 0.08 (s, 6H), 0.89 (s, 9H), 4.71 (s, 2H), 6.45 (d, J = 3.53 Hz, 1H), 7.19 (d, J = 3.53 Hz, 1H), 9.56 (s, 1H); **¹³C NMR (100 MHz, CDCl₃)** δ - 5.3, 18.4, 25.8, 58.7, 109.5, 122.6, 152.3, 161.5, 175.6.

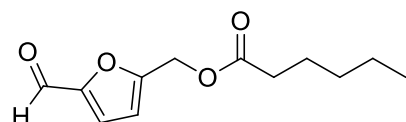
(5-Formylfuran-2-yl)methyl acetate (149)



Prepared according to the literature.¹⁴³ To a flame dried round-bottom flask, HMF (3.5 g, 27.8 mmol), anhydrous MeCN (50 mL) and acetic anhydride (4.3 mL, 45.6 mmol) were added followed by catalytic amount of anhydrous pyridine (0.5 mL, 6.2 mmol). The reaction mixture was

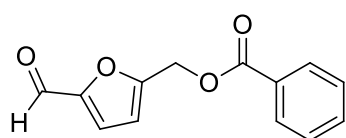
allowed to stir at room temperature for 22 h under argon atmosphere. The solvent was removed and the product purified by column chromatography (hex/EtOAc 8:2) to give the product (4.3 g, 93% yield) as a pale yellow oil that crystallized in the freezer (0 °C). Spectral data are in accordance with those reported in the literature.¹⁴³ **¹H NMR (300 MHz, CDCl₃)** δ 2.11 (s, 3H), 5.12 (s, 2H), 6.58 (d, *J* = 3.55 Hz, 1H), 7.21 (d, *J* = 3.55 Hz, 1H), 9.64 (s, 1H); **¹³C NMR (100 MHz, CDCl₃)** δ 20.8, 57.9, 112.7, 121.8, 153.0, 155.6, 170.5, 178.0.

(5-Formylfuran-2-yl)methyl hexanoate (150)

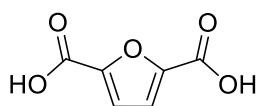


Prepared by a procedure similar to that in the literature.¹⁴⁵ To a flame dried round-bottom flask, HMF (250 mg, 1.98 mmol), anhydrous MeCN (10 mL) and hexanoic anhydride (0.51 mL, 2.2 mmol, 1.1 equiv.) were added, followed by a catalytic amount of pyridine (32 µL, 0.4 mmol, 0.2 equiv.). The reaction mixture was allowed to stir at room temperature for 66 h under argon atmosphere. The mixture was quenched with cold water, acidified with HCl 1 M and extracted with Et₂O. The combined organic layers were dried over MgSO₄, filtered and the solvent removed to give the crude product that was purified by column chromatography (hex/EtOAc 8:2) to give the product (315 mg, 71% yield) as a pale yellow oil. **¹H NMR (300 MHz, CDCl₃)** δ 0.87 (t, *J* = 6.9 Hz, 3H), 1.27-1.31 (m, 4H), 1.63 (quint, *J* = 7.4 Hz, 2H), 2.35 (t, *J* = 7.6, 2H), 5.12 (s, 2H), 6.58 (d, *J* = 3.55 Hz, 1H), 7.21 (d, *J* = 3.55 Hz, 1H), 9.63 (s, 1H); **¹³C NMR (100 MHz, CDCl₃)** δ 14.0, 22.4, 24.6, 31.3, 34.06, 57.8, 112.6, 121.9, 152.9, 155.8, 173.3, 178.0.

(5-Formylfuran-2-yl)methyl benzoate (151)



Prepared according to the literature.¹⁴⁶ To a flame dried round-bottom flask, HMF (1.0 g, 7.9 mmol) and pyridine (4 mL) were added followed by benzoyl chloride (1 mL, 8.7 mmol, 1.1 equiv.). The reaction mixture was allowed to stir at reflux for 1.5 h under argon atmosphere. The mixture was quenched with cold water (50 mL), acidified with HCl 1 M and extracted with Et₂O. The combined organic layers were dried over MgSO₄, filtered and the solvent removed to give the crude product that was recrystallized from Et₂O/hexane as a pale orange solid (0.86 g, 47% yield). Spectral data are in accordance with those reported in the literature.¹⁴⁶ **¹H NMR (300 MHz, CDCl₃)** δ 5.38 (s, 2H), 6.68 (d, *J* = 3.55 Hz, 1H), 7.24 (d, *J* = 3.55 Hz, 1H), 7.46 (t, *J* = 7.7 Hz, 2H), 7.58 (tt, *J* = 7.45, 1.30 Hz, 1H), 8.06 (m, 2H), 9.65 (s, 1H).

Furan-2,5-dicarboxylic acid, FDCA (122)

Prepared according to the literature.¹⁴⁷ To a solution of sodium hydroxide (958 mg, 23 mmol) in water (10 mL), HMF (126 mg, 1 mmol) was added at 20 °C, followed by the addition of potassium permanganate (363 mg, 2.3 mmol). After 10 min stirring at 20 °C the precipitate was filtered off and a concentrated HCl solution was added to the filtrate until pH 1. The resulted precipitate was separated by filtration, washed with water and dried under vacuum to give FDCA (106 mg, 68% yield) as a white powder. ¹H NMR (300 MHz, D₂O) δ 7.25 (s).

Furan-2,5-dicarbaldehyde (128), Furan-2,5-diyl dimethanol (126), (5-(Ethoxymethyl)furan-2-yl)methanol (152), Sodium 5-(hydroxymethyl)furan-2-carboxylate (153), 2,5-Bis(ethoxymethyl)furan (154), (5,5'-(Oxybis(methylene))bis(furan-5,2-diyl))dimethanol (156), (5,5'-((1E,1'E)-hydrazine-1,2-diylidenebis(methanylylidene))bis(furan-5,2-diyl))dimethanol (157), 5-(Ethoxymethyl)furan-2-carbaldehyde (146) were synthesized by Svilen P. Simeonov.

Commercial available furan-2-carbaldehyde (99) and furan-2-ylmethanol (46) were purified by distillation under vacuum to give a colorless oil.

The commercial available 2,5-dimethylfuran (125), 2-methylfuran (155) and levulinic acid (124) were used as received.

Cell culture. (Experiments performed by Dr. Raquel F. M. Frade). Human skin fibroblasts (CRL-1502) were purchased from ATCC and cultivated in RPMI-1640 medium with L-glutamine and supplemented with 10% fetal bovine serum (FBS), antibiotic and antimycotic solutions and kept under a humidified atmosphere with 5% CO₂ and at 37 °C.

Toxicity assays. (Experiments performed by Dr. Raquel F. M. Frade). Cells were plated in 96-well plates and grown until confluence to form a monolayer. Cells were incubated with the tested compounds pre-dissolved in ethanol or dimethyl sulfoxide (percentage of organic solvent in contact with the cells ≤1%). Compounds were diluted in the same cell culture medium with only 0.5% FBS and added to the cells that were kept for 72 h in the incubator. Tested concentrations were 100, 200, 250 and 500 μM. Afterwards the medium was removed, cells were washed with phosphate buffer saline (PBS) and incubated with fresh medium containing 50 μg mL⁻¹ neutral red. Three hours later, cell monolayers were washed with PBS and the amount of neutral red retained by the cells was extracted and dissolved with an organic solution (19.96 mL distilled water, 20 mL ethanol and 400 μL

glacial acetic acid). Absorbance of the wells was measured at 540 nm in a plate reader. Viability was determined by the ratio of absorbance of treated cells and control cells. The presented results are the average \pm standard deviation (SD). Analysis of variance was performed in GraphPad Prism 5 and with one-way ANOVA and using the Dunnett's multiple comparison test with 95% confidence intervals, and data was compared with the HMF as the control compound.

Determination of reactive oxygen species. (Experiments performed by Dr. Raquel F. M. Frade). Cells were plated in 96-well plates and grown until reaching approximately confluence. They were washed with Hank's balanced salt solution (HBSS) supplemented with CaCl_2 (0.14 g L^{-1}) and MgSO_4 (0.20 g L^{-1}) and incubated for 15 min with $8 \text{ }\mu\text{M}$ of the probe 2',7'-dichlorofluorescein diacetate (DCF-DA) in supplemented HBSS. Cells were washed again with supplemented HBSS and incubated for 90 min with $250 \text{ }\mu\text{M}$ of the compounds diluted in the same buffer. Afterwards, compounds were removed, and cells were washed and trypsinized ($30 \text{ }\mu\text{L}$ of trypsin/EDTA per well). To neutralize trypsin, $100 \text{ }\mu\text{L}$ of buffer was added to each well. The plate was read for fluorescence in a Guava easyCyte high throughput flow cytometer (Millipore). Percentage of ROS was determined using the ratio of two fluorescence means (treated cells/control cells) $\times 100$. Data were analyzed in GraphPad Prism 5. The presented results are the average \pm standard deviation (SD). Analysis of variance was performed in GraphPad Prism 5 and with one-way ANOVA and using the Dunnett's multiple comparison test with 95% confidence intervals, and data was compared with HMF as the control compound.

Chapter 3

New synthetic methodologies for 5-Hydroxymethylfurfural (HMF) valorization

In the current chapter is described the new methodologies discovered for the HMF valorization. The chapter is divided in three topics: i) Preliminary screening studies of HMF reactivity; ii) Bisvinillogous Mannich reaction of HMF derivatives via trienamine catalysis; iii) High-pressure accelerated Friedel-Crafts Alkylation of secondary anilines with furfurals: synthesis and biological activity of new triarylmethanes.

The work reported herein are described in 3 publications:

- 1) "NHC catalysed direct addition of HMF to diazo compounds: synthesis of acyl hydrazones with antitumor activity", João P. M. António, Raquel F. M. Frade, Fábio M. F. Santos, Jaime A. S. Coelho, Carlos A. M. Afonso, Pedro M. P. Gois and Alexandre F. Trindade, *RSC Adv.*, **2014**, 4, 29352.
- 2) "Trienamines derived from 5-substituted furfurals: remote ε -functionalization of 2,4-dienals", Jaime A. S. Coelho, Alexandre F. Trindade, Vânia André, M. Teresa Duarte, Luís F. Veiros and Carlos A. M. Afonso, *Org. Biom. Chem.*, **2014**, 12, 9324.
- 3) "High-pressure accelerated Friedel-Crafts Alkylation of secondary anilines with furfurals: synthesis and biological activity of new triarylmethanes", Rafael F. A. Gomes, Jaime A. S. Coelho, Carlos A. M. Afonso, *manuscript in preparation*.

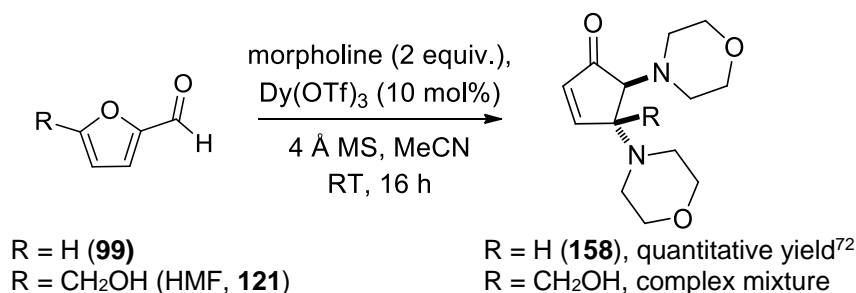
III. New synthetic methodologies for 5-Hydroxymethylfurfural (HMF) valorization.....	71
III.1. Introduction.....	73
III.1.1. Preliminary Results.....	73
III.1.2. Extreme high pressure induced reactions	76
III.2. ϵ -Functionalization of 5-substituted Furfurals <i>via</i> Trienamines Intermediates.....	80
III.2.1. Introduction.....	80
III.2.2. Results and Discussion	85
III.2.3. Conclusions	105
III.3. Synthesis and Biological Activity of New Triarylmethanes	106
III.3.1. Introduction.....	106
III.3.2. Results and Discussion	115
III.3.3. Conclusions	130
III.4. Experimental	131
III.4.1. General Methods	131
III.4.2. Experimental part for Section III.1.1	134
III.4.3. Experimental part for Section III.2	134
III.4.4. Experimental part for Section III.3	145

III.1. Introduction

The main goal of the current work was the creation of a novel and competitive synthetic methodology for the valorization of the biomass intermediate 5-hydroxymethylfurfural (HMF, **121**). To achieve this goal the transformation of HMF derivatives into functionalized cyclopent-2-enones and further manipulation into target carbocycles was initially proposed. The feasibility of this transformation was based on precedent literature of furfural and furfuryl alcohol derivatives chemistry and on the accumulated experience of this laboratory in this area (see **Chapter 1** for details).

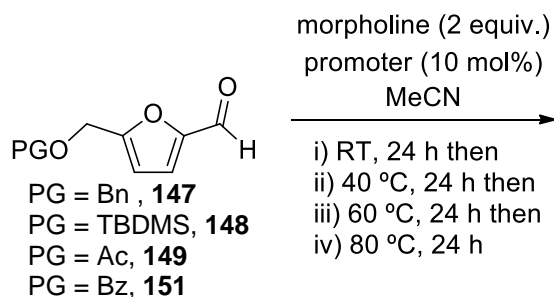
III.1.1. Preliminary Results

To discover the appropriate combination of substrate structure of HMF derivative, catalyst nature and experimental conditions for the desirable rearrangement of HMF this work started by employing the reactions conditions reported by Batey *et al.*⁷² to HMF (**121**). Unfortunately, reaction of HMF (**121**) with 2 equivalents of morpholine, 10 mol% of Dy(OTf)₃ as catalyst, 4 Å molecular sieves in acetonitrile at room temperature for 16 h resulted in a complex reaction mixture (**Scheme III.1**).



Scheme III.1. Reactivity of furfural (**99**) and HMF (**121**) in the presence of secondary amines.

Next, the reactivity of several HMF derivatives with secondary amines under Lewis acid catalysis was studied (**Scheme III.2**). HMF (**121**) and four O-protected HMF derivatives: **147** (PG = Bn), **148** (PG = TBDMS), **149** (PG = Ac), **151** (PG = Bz) were tested, along with a series of transition metal salts and complexes [e.g., Pd(II), Cu(II), Au(I), Ag(I), Ru(III), Co(II), Zn(II), Gd(III), Cu(I), Ni(II), Zr(II), Dy(III) and La(III)], at different temperatures and up to 4 days reaction time (in general, the screening was performed at RT for 24 h, followed by 24 h at 40 °C, then 24 h at 60 °C and finally 24 h at 80 °C). From this extensive screening two promising results were selected and further studied in detail as described in this Chapter.



Scheme III.2. Screening experiments for the HMF derivatives valorization.

From the screening study using HMF (**121**) as substrate (**Figure III.1**), several products that resulted mainly from oxidation reactions were found, and $\text{FeCl}_3 \cdot 6\text{H}_2\text{O}$ was identified as the most promising promoter.

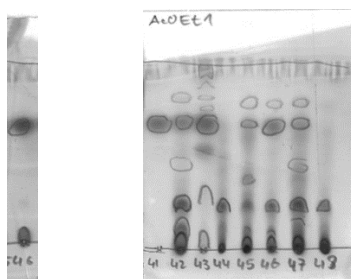
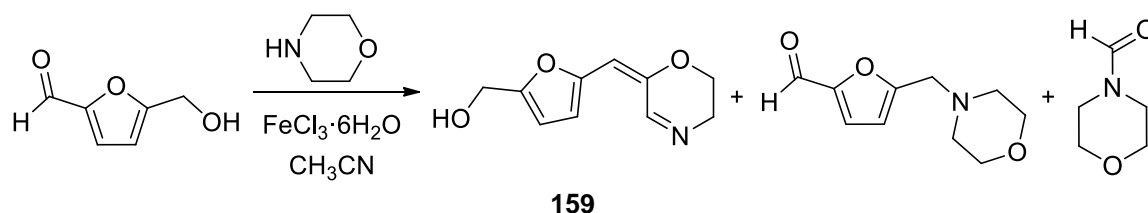


Figure III.1. Representative TLC of HMF screening after 3 days reaction time (24 h at RT then 24 h at 40 °C and finally 24 h at 60 °C). In the left is the initial reaction mixture with HMF ($R_F=0.7$) and morpholine ($R_F=0.1$). In the right is an example of obtained TLC for 7 different Lewis acids. #44 corresponds to $\text{FeCl}_3 \cdot 6\text{H}_2\text{O}$ and #48 to $\text{BF}_3 \cdot \text{Et}_2\text{O}$. #41 is the control reaction only with HMF.

From all the products already identified from this reaction (**Scheme III.3**), compound **159** is the most interesting one because is believed to be formed through oxidation of the morpholine to the cyclic enamine followed by addition to HMF and finally aldol condensation. Unfortunately, this product seems to be very unstable in silica hindering its purification and quantification. After a very long time consuming study on this reaction, we believe that Pd/C-catalyzed hydrogenation can give a more stable derivative that could be used for further reaction study. To the date, 5 equivalents of morpholine and atmospheric air were found to be benefic for the reaction, providing **159** in low isolated yield (8%). It is also believed that furan-2,5-diylidimethanol can accelerate the reaction probably due to the formation of an more active iron catalyst. The complete study of the reaction is still undergoing and will be reported in due time.



Scheme III.3. Reaction of HMF with morpholine catalyzed by iron(III) chloride.

Unlike HMF (**121**), derivative **148** was found as a very stable compound, and no conversion of the starting material was observed in the blank reaction without catalyst. From this screening, an unprecedented reactivity of this formal 2,4-dienal was disclosed when catalysts such as Dy(OTf)₃, GdCl₃ and ZrCl₄ were used (**Figure III.2**). These results are discussed in detail in **Section III.2**.

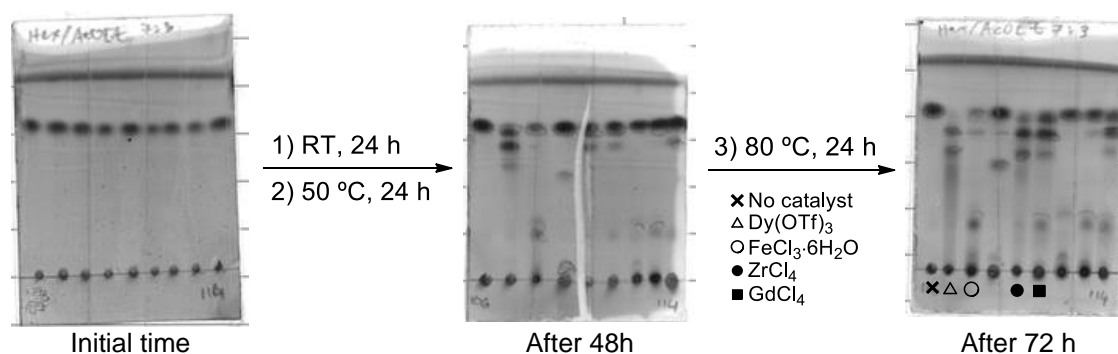
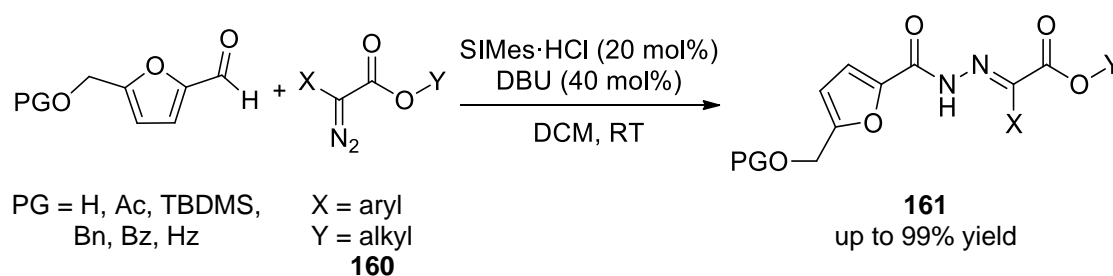


Figure III.2. Representative TLC of Lewis acid screening using **148** as substrate.

During the substrate scope study of the reaction of **148** with amines, a novel reactivity was observed when anilines were employed as amines. These results are discussed in detail in **Section III.3**.

In a different approach, desired *N*-acylhydrazones bearing furan derivatives were synthesized through NHC-catalyzed direct addition of HMF and derivatives to diazo compounds (**Scheme III.4**).¹⁴⁸ This strategy showed to be an interesting alternative to the usual multistep synthesis of acylhydrazones and enabled the direct access to an unexplored family of HMF-based acylhydrazones.



Scheme III.4. NHC-catalyzed formation of *N*-acylhydrazones **161** from HMF derivatives.

Gratifyingly, the new acylhydrazones displayed promising anti-tumor activity. The preliminary screening of *O*-protecting groups allowed the identification of the TBDMS group as being essential for the desired biological activity, where compound **162** was found to be very active against MCF-7 breast cell line ($IC_{50} = 3.60 \mu M$) together with a much lower toxicity in differentiated CaCo-2 monolayer (**Figure III.3**).

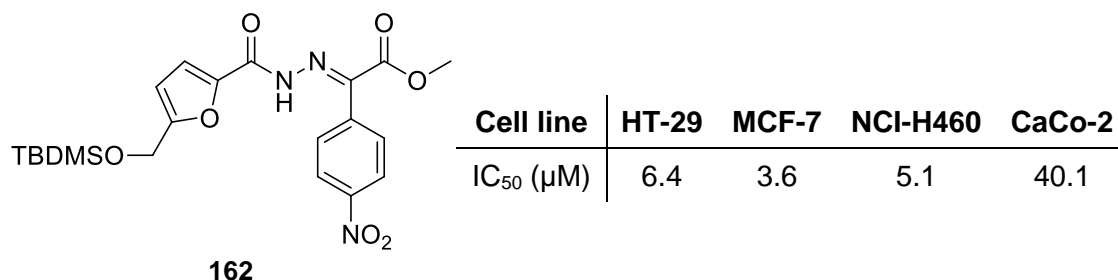


Figure III.3. Biological activity of *N*-acylhydrazones **162** in different cell lines.

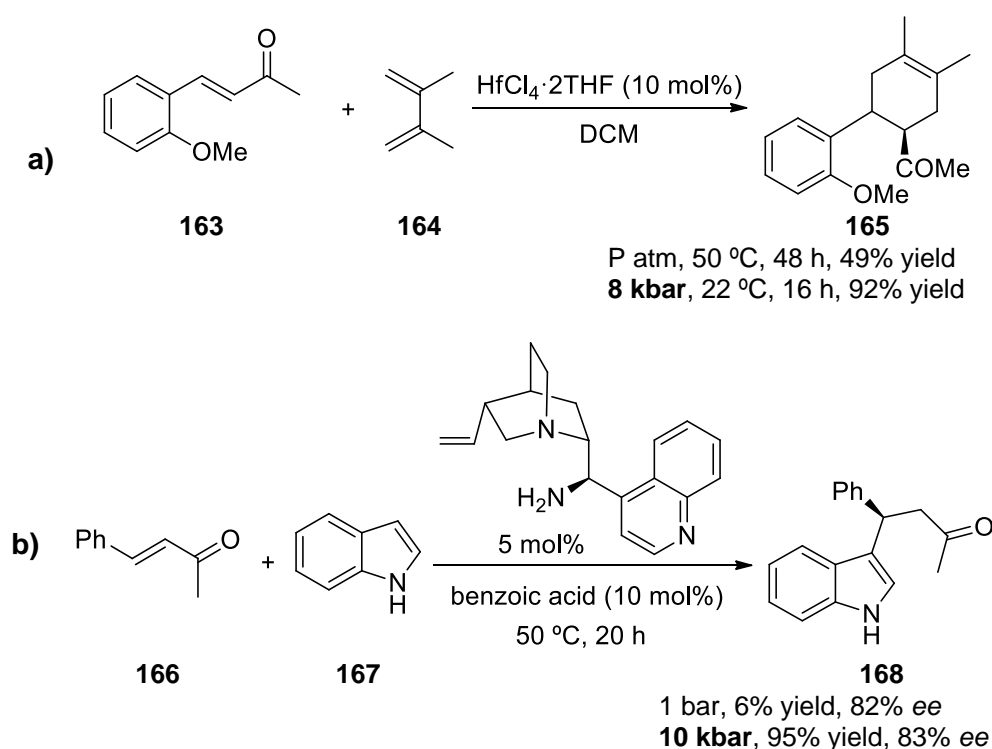
III.1.2. Extreme high pressure induced reactions

Extreme high pressure is applied today in several areas of science such as food chemistry (as a non-thermal sterilization process), polymerization chemistry, enzymatic reactions and organic reactions. Pressure in the range of 1-20 kbar (1 kbar = 1013.25 atm) can strongly influences the rate and the chemical equilibrium of chemical reactions. Every reaction is characterized by a volume of activation (ΔV^\ddagger) defined as the difference between the partial molar volume occupied by the transition state and that occupied by the reactants ($\Delta V^\ddagger = V_{TS} - V_R$). Thus, processes accompanied by a decrease in volume are accelerated by pressure and the equilibria are shifted toward the products, while those accompanied by an increase of volume are retarded and the equilibria are shifted toward reactants. Moreover pressure can also influence the reaction free energy and the regio- and stereoselectivity of organic reactions due to the different partial molar volumes of the products. Cycloadditions, condensations and domino reactions are typical examples of pressure-accelerated/induced reactions due to their negative activation volumes (**Table III.1**).

Table III.1. Typical values for the volumes of activation (left)¹⁴⁹ and contributions to account for activation volumes of various elementary processes (right)¹⁵⁰.

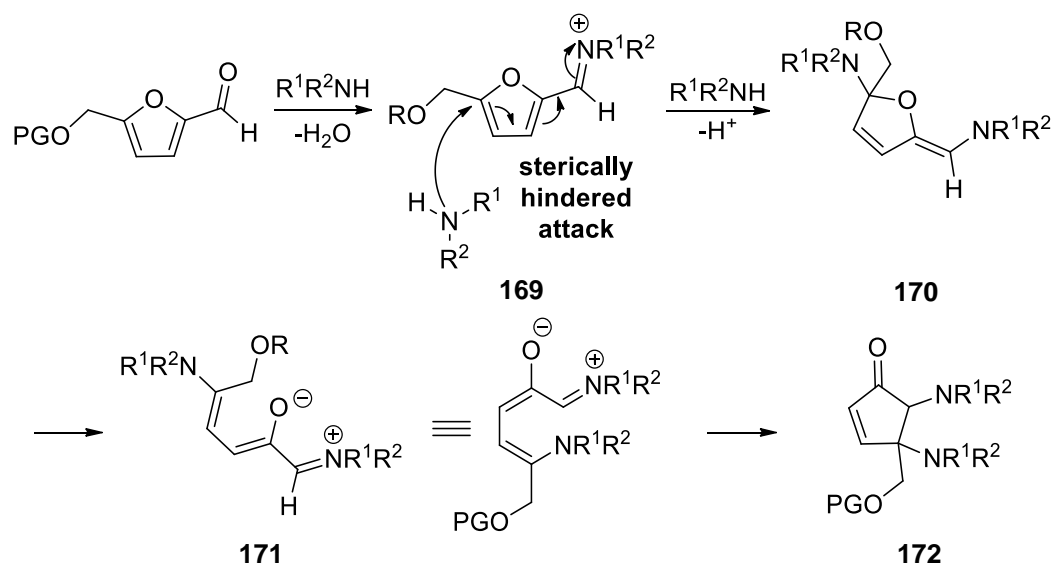
Reaction	$\Delta V^\ddagger(\text{cm}^3\text{mol}^{-1})$	Mechanistic feature	Contribution in $\text{cm}^3\text{mol}^{-1}$
Homolysis	+5 to +20	Homolytic bond cleavage	+10
Radical polymerization	ca. -20	Homolytic association	-10
Cycloadditions	-25 to -55	Bond deformation	0
Ester hydrolysis	-10 to -15	Ionization	-20
Epoxide-ring opening	-15 to -20	Neutralization	+20
H ₂ transfer	-25	Charge dispersal	+5
Aldol reaction	-10 to -30	Displacement	-5
Baylis-Hillman reactions	< -50	Steric hindrance	(-)
Wittig reactions	-20 to -30	Diffusion control	+20

In the recent examples is highlighted the high-pressure (8-11 kbar) activation of the regioselective Diels-Alder cycloadditions between benzylideneacetones and 1,3-butadienes reported by Piermatti *et al.* (**Scheme III.5a**)¹⁵¹ and the high-pressure acceleration of organocatalytic Friedel-Crafts alkylation of indoles with unsaturated ketones, with enantioselectivity up to 90%, reported by Kwiatkowski and co-workers (**Scheme III.5b**).¹⁵²

**Scheme III.5.** Selected examples of recently reported high-pressure induced reactions.

Since the initial mechanistic pathway proposed for the HMF transformation into cyclopent-2-enones has two steps (condensation of amine and iminium ion and

electrocyclization, **Scheme III.6**) that is thought to have negative activation volumes, it was suggested to further investigate the HMF reactivity under extreme high-pressure.



Scheme III.6. Proposed mechanism for the transformation of HMF derivatives into cyclopent-2-enones.

There are two general approaches to generate and apply high pressure for use in a chemical reaction: dynamic and static. The dynamic methods are based on a shock wave compression generated by gas guns, pulsed lasers, high pulsed electrical currents. The accessible pressure range of these methods are extremely high, however, there are always produced together with very high temperatures and during very short time, which limit their applicability. On the other hand, static pressures are produced through the application of a mechanical force perpendicularly to the surface of the sample. Two main devices can be selected: Piston-cylinder and diamond anvil cell (DAC). For very small samples volume ($<1 \text{ mm}^3$) DAC is the most reliable tool to study the matter under pressure because, among other advantages, optical techniques can be used to monitor the changes in the sample. High pressure organic reactions on a preparative scale are mostly carried on in a piston-cylinder type apparatus. This apparatus comprises external rings surrounding an internal steel conical vessel containing flexible Teflon ampoules used as liquid media reaction containers. The cylindrical high pressure space is closed from below with a steel stopper and from above by a mobile piston moved by an independent hydraulic force. The piston and the stopper are sealed with resin O-rings and brass rings that should be changed from time to time do to wear. Higher temperatures reaction can be performed using an external heating jacket.^{149-150,153}

High pressure reaction carried out in solution can be limited by solvent-related properties. This is due to the effect of pressure on the behavior of organic liquids. The property most affected is the freezing pressure (p_f). To prevent the drawback involved in solvent freezing under high pressure, temperature elevation is mostly used. For the same purpose, reactions may be carried out in solvent mixtures, which usually exhibit a substantial increase in solidification pressure, as compared to pure components. This laboratory is equipped with a *Unipress (Warsaw, Poland)* equipment (**Figure III.4**) that allow the execution of 4 simultaneous reactions inside a Teflon ampoules (2.5 mL) to up 9 kbar.

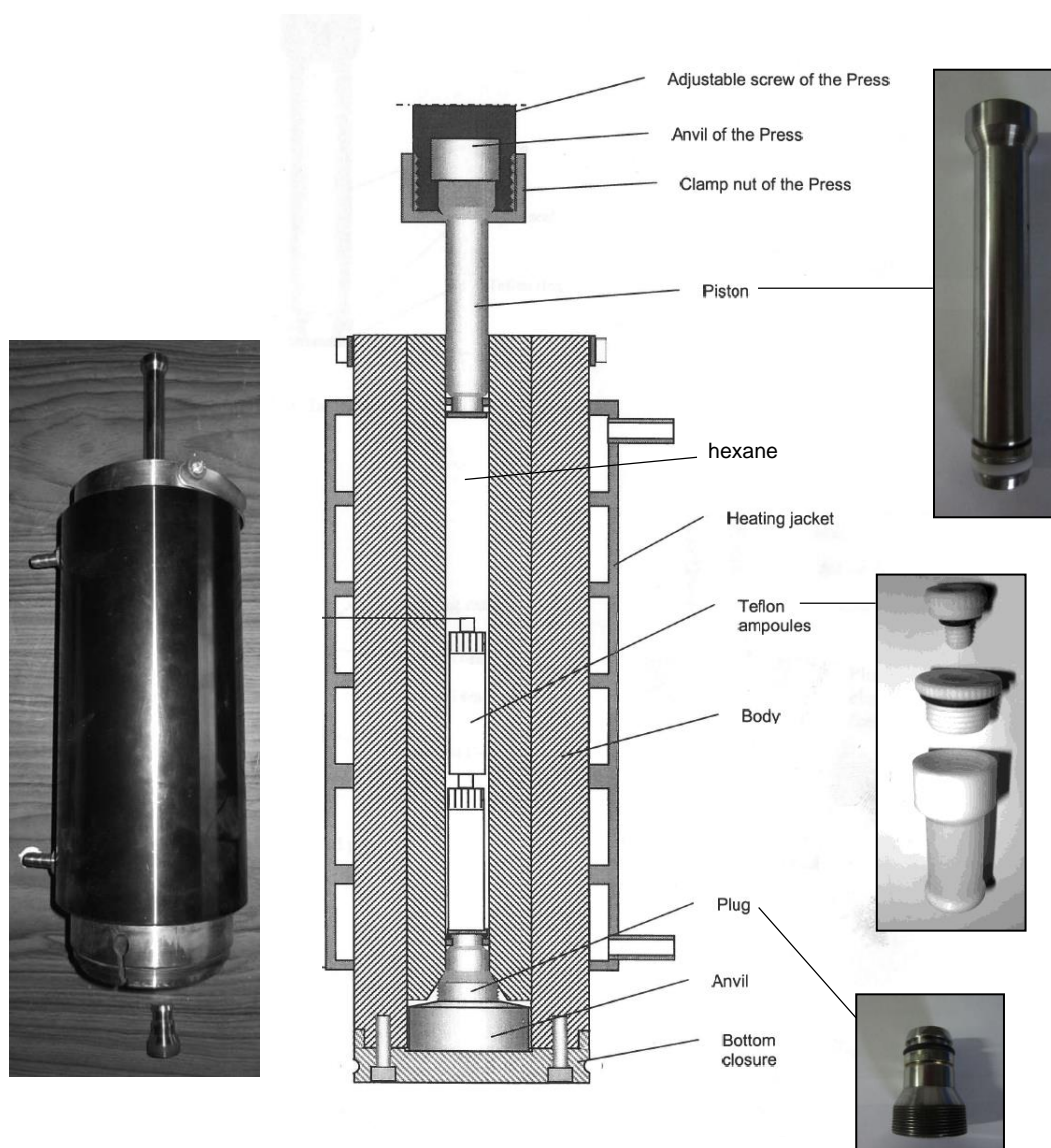
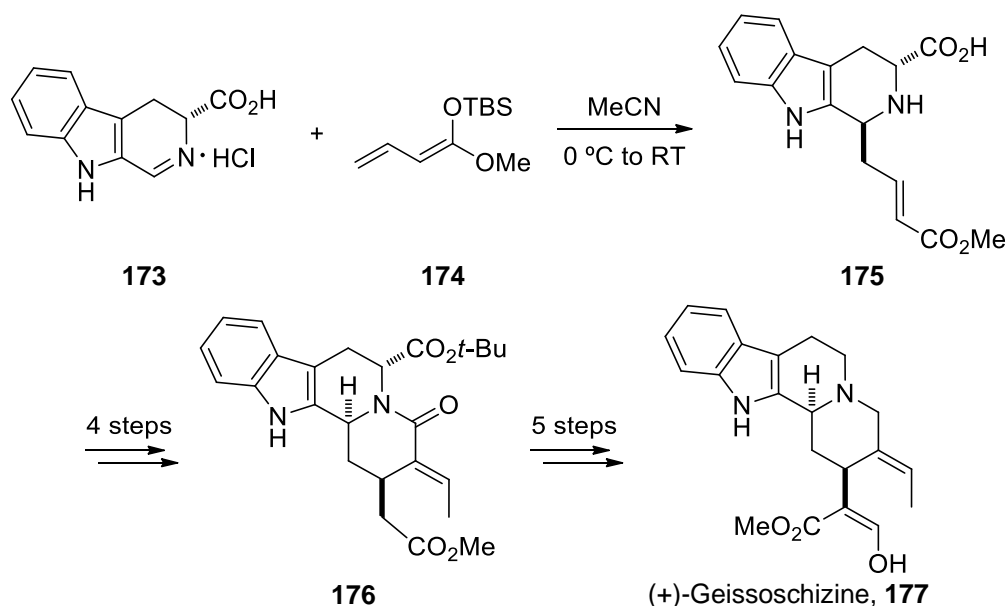


Figure III.4. Liquid piston vessel LV30/16.

III.2. ϵ -Functionalization of 5-substituted Furfurals via Trienamines Intermediates

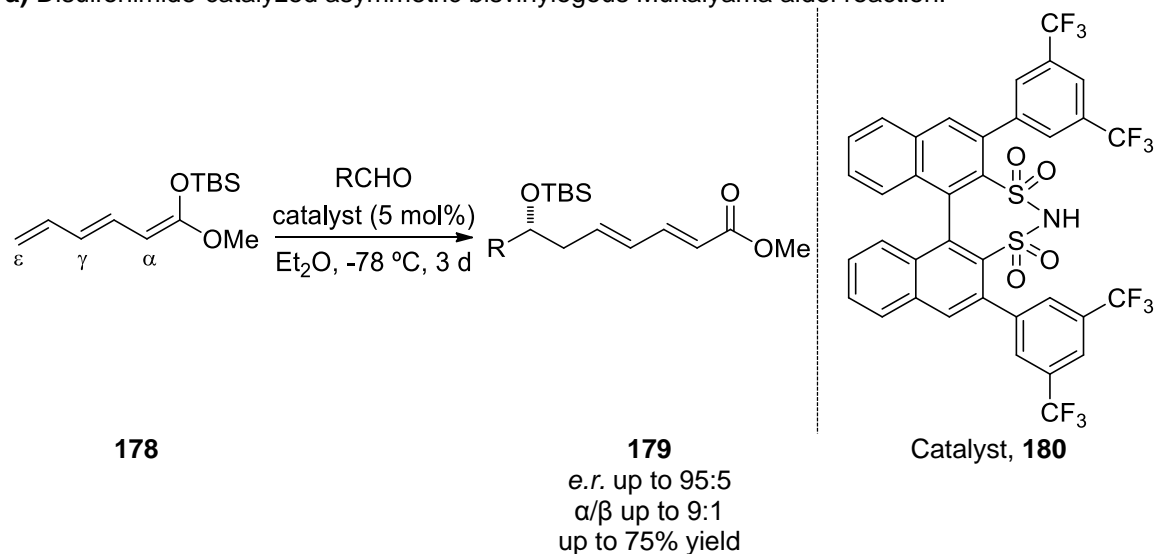
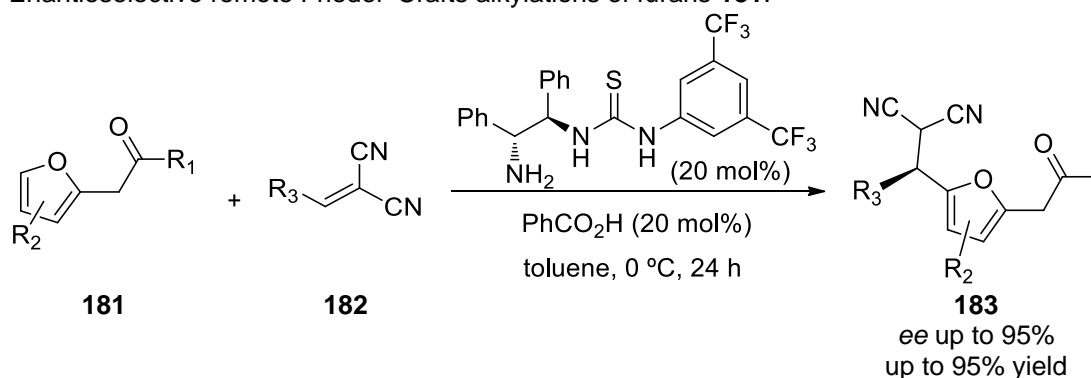
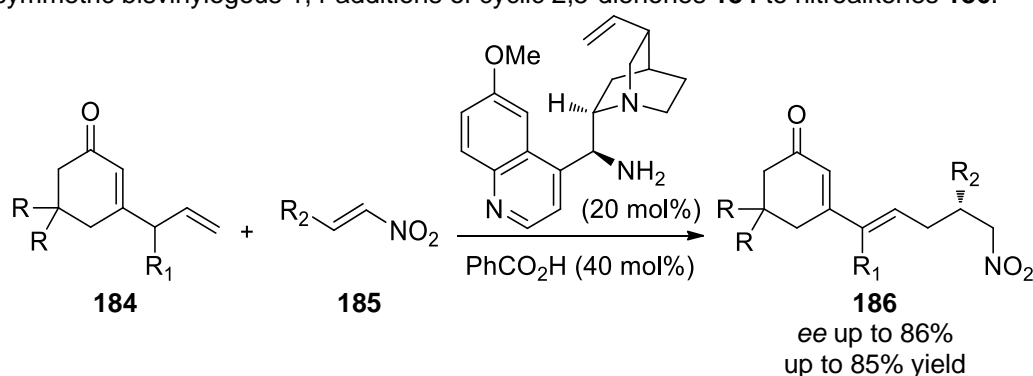
III.2.1. Introduction

Vinylogous Mannich addition reaction is a powerful synthetic methodology for carbon-carbon bond formation that produces useful synthons for the synthesis of a variety of molecules from simple pyrrolidine and piperidine heterocycles to complex naturally occurring alkaloidal compounds (e.g., Geissoschizine, **Scheme III.7**).¹⁵⁴⁻¹⁵⁵



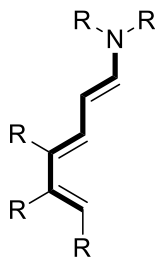
Scheme III.7. Total synthesis of (+)-Geissoschizine **177**.¹⁵⁶

Extension to the bisvinylogous version seems to be much more challenging, and to the best of our knowledge has not been described to date. Nevertheless, very limited attempts in bisvinylogous additions were reported in Mukaiyama aldol reaction (**Scheme III.8a**), Friedel-Crafts alkylation (**Scheme III.8b**) and Michael addition (**Scheme III.8c**).¹⁵⁷⁻¹⁵⁹

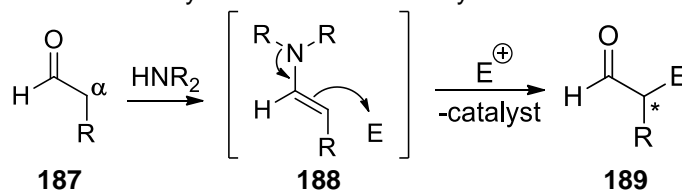
a) Disulfonimide-catalyzed asymmetric bisvinylogous Mukaiyama aldol reaction.¹⁵⁷b) Enantioselective remote Friedel–Crafts alkylations of furans **181**.¹⁵⁹c) Asymmetric bisvinylogous 1,4-additions of cyclic 2,5-dienones **184** to nitroalkenes **186**.¹⁵⁸

Scheme III.8. Selected examples of bisvinylogous reactions.

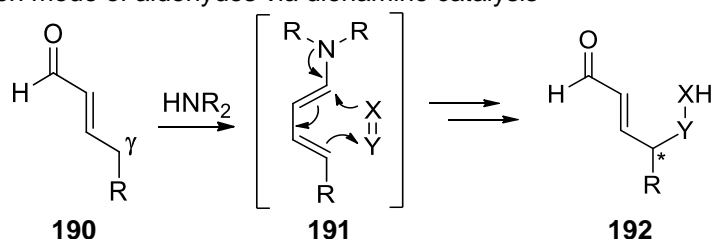
Firstly reported in 2011 by Jørgensen *et al.*,¹⁶⁰ trienamine (**Figure III.5**) catalysis has emerged as a new activation mode as an extension of the well-known amine catalysis, namely enamine (**Scheme III.9a**), dienamine (**Scheme III.9b**) and iminium-ion catalysis (**Scheme III.9c**).^{52,161-169}

**Figure III.5.** General structure of trienamines.

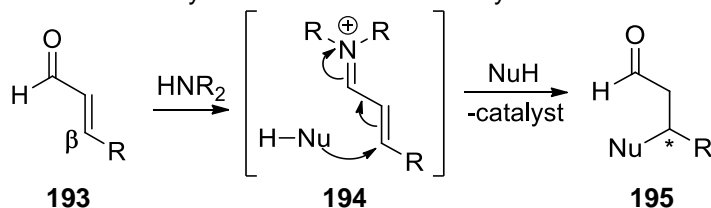
a) HOMO-activation mode of aldehydes *via* enamine catalysis



b) HOMO-activation mode of aldehydes *via* dienamine catalysis

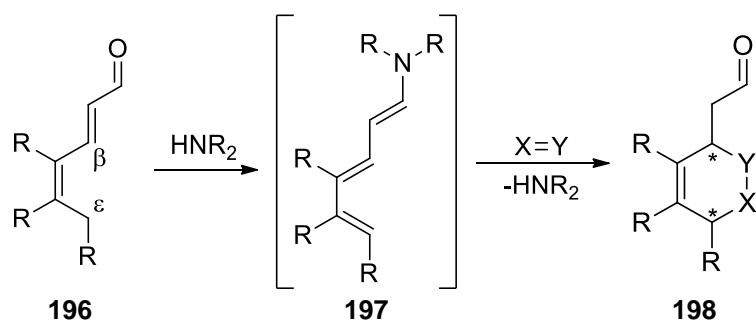


c) LUMO-activation mode of aldehydes *via* iminium-ion catalysis

**Scheme III.9.** General amine catalysis.

Both vinylogous iminium-ion activation by LUMO-lowering and trienamine activation by HOMO-raising have been demonstrated as powerful strategies for modifications of 2,4-dienals.^{160,167-173}

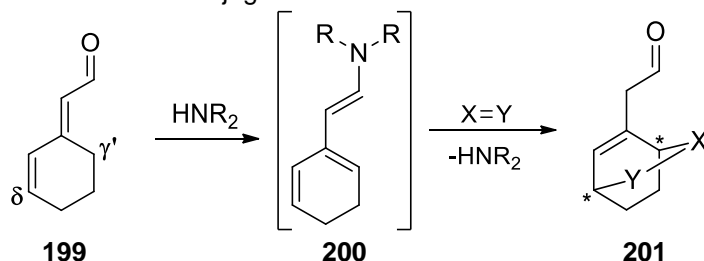
Linear trienamine intermediates effectively react with dienophiles yielding formal cycloadducts products having up to four contiguous stereocenters through direct β,ϵ -functionalization of 2,4-dienals (**Scheme III.10**).¹⁶⁰



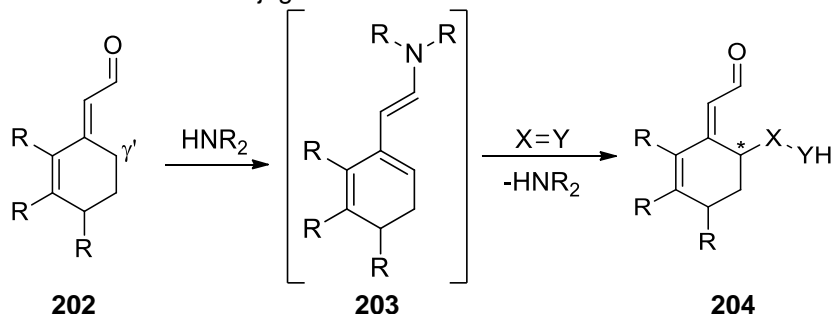
Scheme III.10. β,ϵ -functionalization *via* linear trienamine.

Furthermore, cross-trienamines intermediates can undergo γ',δ -functionalization by reaction with dienophiles (**Scheme III.11a**) or γ' -functionalization by selective additions to polarized olefins (**Scheme III.11b**).¹⁷⁰

a) γ',δ -Functionalization *via* cross-conjugated trienamine

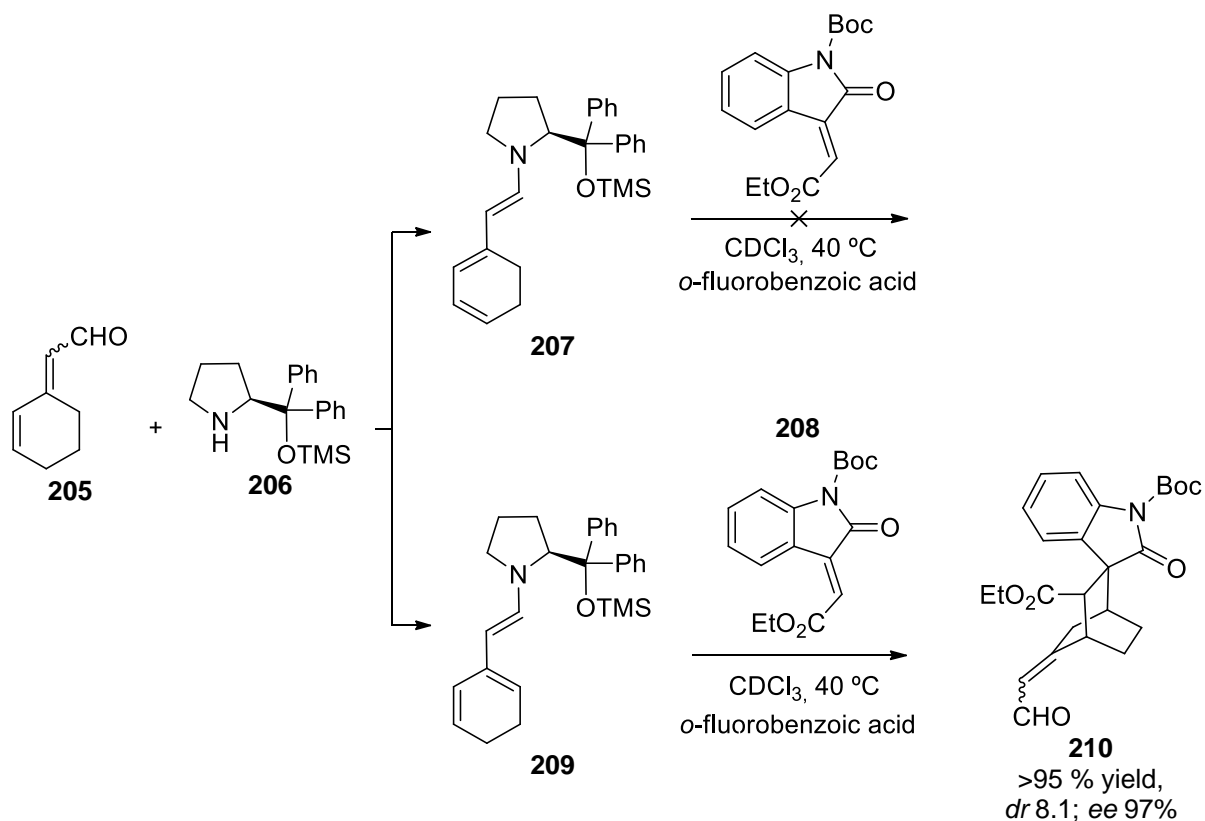


b) γ' -functionalization *via* cross-conjugated trienamine



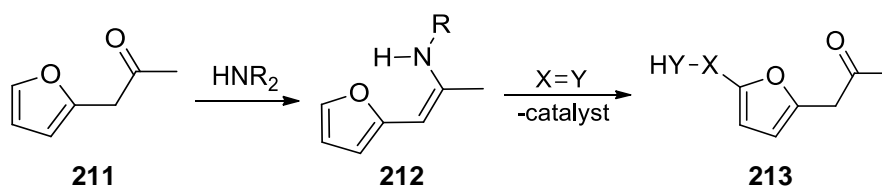
Scheme III.11. Cross-conjugated trienamine functionalizations.

It is noteworthy to highlight that specific substitution patterns of the starting carbonyl compounds are usually required to achieve high regioselectivity in these transformations.¹⁶⁹ Furthermore, high stereoselectivity can be achieved either by steric effects or hydrogen bonding on the chiral amine catalyst in this type of remote activation. Despite the fact that functionalization of the γ' -position of 2,4-dienals have been achieved by reaction with highly reactive Michael acceptors, ϵ -functionalization was not observed (**Scheme III.12**).¹⁷⁴ This is believed to be a result of kinetic control, in which the cross-conjugated trienamine **209** is preferred compared to the thermodynamically linear-trienamine **207** as proposed independently by the groups of Jørgensen and Houk.^{170,175}



Scheme III.12. Experimentally observed regioselectivities in Diels-Alder-reactions of trienamines **207** and **209** and oxindole **208**.¹⁵⁷

Very recently (2014), Chen *et al.* reported the remote Friedel–Crafts alkylation of furans through a formal-trienamine catalysis using simple bifunctional primary amine-thiourea derived from chiral 1,2-diphenylethanediamine (**Scheme III.13**).¹⁵⁹ Exclusive regioselective alkylation at the 5-position occurred with alkylidenemalononitriles, and high reactivity and excellent enantioselectivity (up to 95% ee) was obtained by this remote activation.

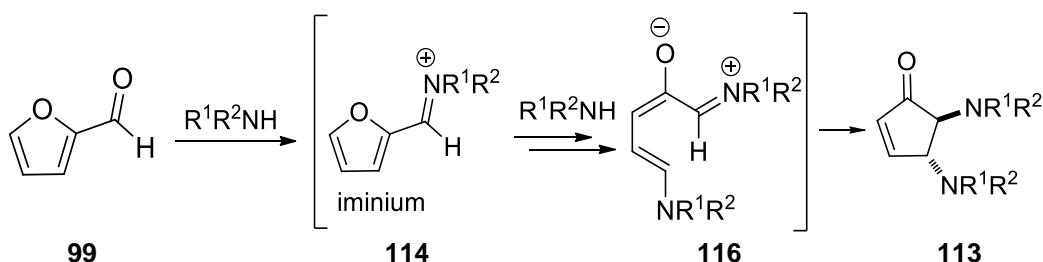


Scheme III.13. ϵ -Selective Friedel–Crafts alkylation of furans *via* formal-trienamine.

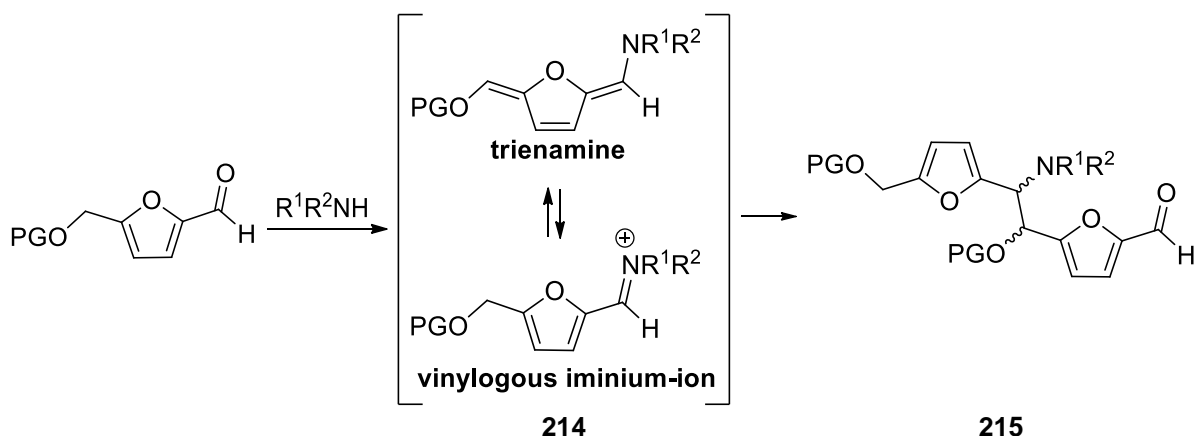
To the best of our knowledge, linear-trienamine catalysis has been limited to Diels-Alder reactions, and ϵ -functionalization of 2,4-dienals *via* trienamine catalysis is not reported.

III.2.2. Results and Discussion

From the extensive screening studies described above in **Section III.1.1**, an unprecedented reactivity of O-protected 5-hydroxymethyl furfurals was discovered. Unsuccessful attempts to use this type of compounds as starting material for the synthesis of cyclopent-2-enones *via* Nazarov type reaction (**Scheme III.14**)^{72,90} led to the isolation of an unexpected product, as depicted in **Scheme III.15**.



Scheme III.14. Furfural reactivity: formation of cyclopent-2-enones from furfural by conrotatory 4 π -electrocyclization.

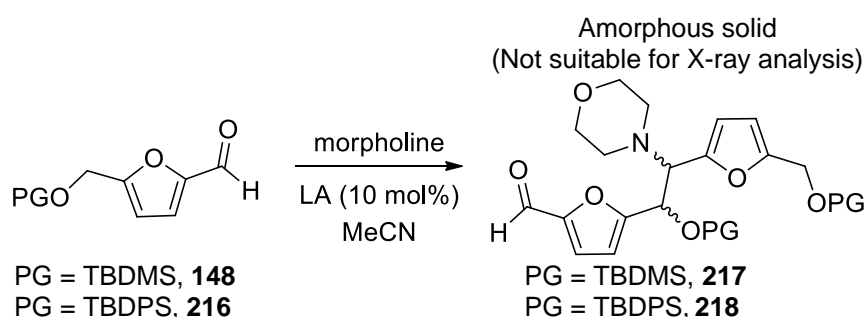


Scheme III.15. 5-Substituted furfural reactivity: new furanic scaffolds by homo Mannich reaction of trienamine/iminium-ion pair.

Remarkably, the new scaffold contains two furan units linked by a new formed C-C bond and a C-N bond bearing the secondary amine. This different reactivity is believed to be a result of increased steric effects at the 5-position of the furan moiety. As will be discussed later, it is proposed that a reaction between the linear-trienamine intermediate and its corresponding iminium-ion pair is taking place (homo-Mannich type reaction) to afford the product bearing two stereocenters. Thus, this is the first example of a bisvinyllogous Mannich reaction.

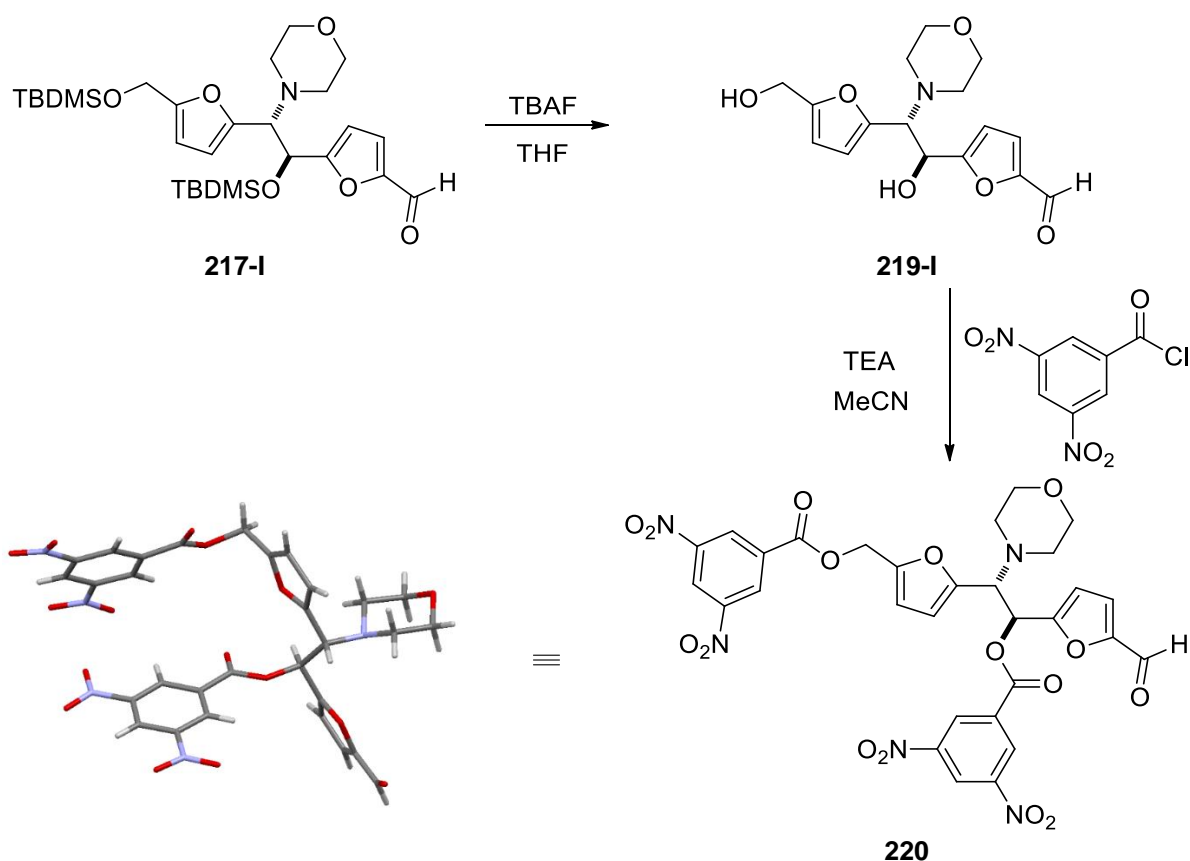
Structural Elucidation

From the initial screening of Lewis acids as catalyst for the reaction of **148** with morpholine, two products were observed by TLC analysis. Since the reactivity of O-protected 5-hydroxymethyl furfurals was not known, structural elucidation of the products was only possible with the help of X-ray analysis, performed by Dr. Vânia André from Instituto Superior Técnico. Since the products did not give suitable crystals for X-ray analysis, we first changed the protecting group of the starting aldehyde from TBDMS to TBDPS. Despite the reaction gave the same products patterns, once again no suitable crystals for X-ray analysis were achieved (**Scheme III.16**).



Scheme III.16. Bisvinylogous homo-Michael addition. LA = Lewis acid

Gratefully, further modification of one of the diastereoisomers (**217-I**), by reaction of the free alcohols with dinitrobenzoyl chloride, allowed the confirmation of the structure by X-ray analysis (**Scheme III.17**).



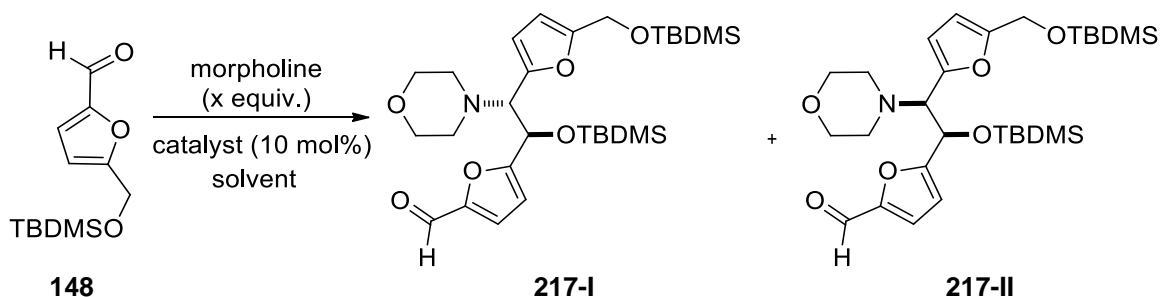
Scheme III.17. Synthesis of compound **220** and corresponding X-ray structure.

Reaction Optimization

The study was continued by screening different acid catalysts for the homo-bisvinyllogous Mannich reaction between **148** and morpholine (**Table III.2**). Despite the fact that Brønsted acids are known catalysts for amine catalysis, no reaction was observed when TFA or PTSA were used at 50 °C (**Table III.2**, entry 1). However, increasing the temperature to 80 °C afforded complex mixtures with a moderate yields of **217** (**Table III.2**, entries 2-5). Using the most promising Lewis acids catalysts found in the initial screening, moderate to very good conversions were obtained together with low to moderate yields of **217** at 80 °C (**Table III.2**, entries 6-12). Dysprosium and Scandium triflates were identified as the most reactive catalysts, leading to full conversion of aldehyde **148** at 80 °C (**Table III.2**, entries 8 and 12). Since these results were accompanied by low yields of **217**, we hypothesize that the product may not be stable under the reaction conditions. Gratifyingly, decreasing the temperature to 40 °C improved the yields, being dysprosium triflate slight better catalyst (**Table III.2**, entries 19 and 20). Unfortunately, the reaction was very slow at 30 °C (**Table III.2**, entry 21). Increasing the reaction time at 40 °C improved the yield to 73% (**Table III.2**, entry 22). Optimization of the catalyst loading led to improved yield of 85% using 20 mol% of catalyst but due to the high

price of dysprosium triflate, these conditions were abandoned (**Table III.2**, entries 23 and 24). Optimization of the amine stoichiometry allowed to decrease its quantity from 2 to 1 equivalent without changing both conversion and yield (**Table III.2**, entries 25 and 26).

Table III.2. Optimization of the reaction conditions.^a



Entry	Catalyst	x	t (h)	T (°C)	Conv. (%) ^b	Yield (%) ^b	d.r. ^b
1	Brønsted acids ^c	2	16	50	-	NR	-
2	H ₂ SO ₄	2	16	80	46	23	1:0.9
3	TFA	2	16	80	97	20	1:2.3
4	PTSA	2	16	80	82	59	1:1.4
5	HCOOH	2	16	80	38	8	1:0.8
6	ZrCl ₄	2	16	80	70	48	1:1.4
7	GdCl ₃	2	16	80	68	64	1:1.3
8	Dy(OTf) ₃	2	16	80	96	6	1:0.6
9	FeCl ₃	2	16	80	76	13	1:0.1
10	CeCl ₃	2	16	80	67	42	1:1.3
11	AlCl ₃	2	16	80	96	35	1:2.6
12	Sc(OTf) ₃	2	16	80	100	6	1:5.5
13	ZrCl ₄	2	16	50	47	23	1:0.8
14	GdCl ₃	2	16	50	51	18	1:0.8
15	DyOTf ₃	2	16	50	93	42	1:1.5
16	FeCl ₃	2	16	50	67	25	1:0.9
17	CeCl ₃	2	16	50	31	11	1:0.8
18	AlCl ₃	2	16	50	32	17	1:0.8
19	Dy(OTf) ₃	2	16	40	47	47	1:0.9
20	Sc(OTf) ₃	2	16	40	44	44	1:0.9
21	Dy(OTf) ₃	2	16	30	21	11	1:0.8
22	Dy(OTf) ₃	2	48	40	73	73	1:1.0
23	Dy(OTf) ₃ ^d	2	48	40	57	57	1:0.9
24	Dy(OTf) ₃ ^e	2	48	40	85	85	1:1.1
25	Dy(OTf)₃	1	48	40	74	74	1:1.0
26	Dy(OTf) ₃	0.55	48	40	51	38	1:1.1
27	GdCl ₃	2	6	80	63	34	1:1.0
28	GdCl ₃	2	48	80	95	33	1:2.6

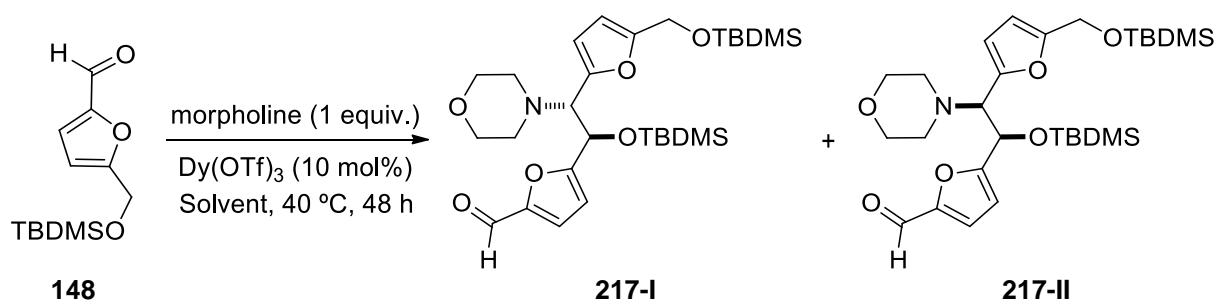
^aReaction conditions: 10 mol% of catalyst, 0.125 mmol of **148**, 1.5 mL of acetonitrile.

^bDetermined by HPLC of the crude reaction mixture, ratio **217-II:217-I**. ^cSulfuric acid, trifluoroacetic acid, *p*-toluenesulfonic acid (PTSA), formic acid were tested. ^d5 mol% of catalyst.

^e20 mol% of catalyst. NR = No reaction was observed by TLC.

No improvement in the yield was observed when other solvents were screened (**Table III.3**, entries 1-8). Increasing the reaction concentration further increased the combined overall yield to 88% for the two diastereoisomers (**Table III.3**, entries 9 and 10). Finally, the use of molecular sieves or the use of commercial grade acetonitrile (not dried) did not improve the yields (**Table III.3**, entries 11 and 12).

Table III.3. Solvent and concentration optimization.^a



Entry	Solvent	Conc. (M)	Conv. (%) ^b	Yield (%) ^b	d.r. ^b
1	Hexane	0.08	25	traces	-
2	MeOH	0.08	62	3	1:0.3
3	DCE	0.08	91	33	1:1.8
4	THF	0.08	60	22	1:0.9
5	DCM	0.08	77	59	1:1.3
6	DMSO	0.08	16	traces	-
7	DMF	0.08	24	traces	-
8	H ₂ O	0.08	71	traces	-
9	MeCN	0.04	68	68	1:1.3
10	MeCN	0.17	88	88	1:1.1
11	MeCN	0.08 ^c	77	55	1:1.1
12	MeCN	0.08 ^d	62	62	1:1.3

^aReaction conditions: 10 mol% of Dy(OTf)₃, 0.125 mmol of **148** and 0.125 mmol of morpholine, in the mentioned solvent at mentioned concentration.

^bDetermined by HPLC of the crude reaction mixture, ratio **217-II:217-I**.

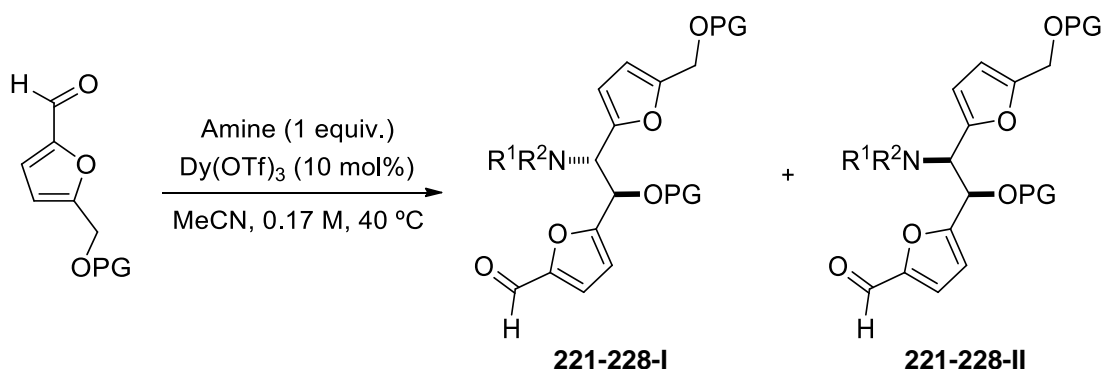
^c10% w/w molecular sieves was used as additive. ^dUsed commercial HPLC grade MeCN, not dried.

In conclusion, optimization of the reaction conditions, namely catalyst, catalyst loading, amine stoichiometry, solvent, temperature, time and additives, led to a high overall yield of 88% for the two products **217-I** and **217-II** (**Table III.3**, entry 10).

Reaction Scope

With the optimized conditions in hands, the substrate scope was explored (**Table III.4**). Several secondary amines were used under the optimized reaction conditions (until full conversion of **148**) using **148** as formal 2,4-dienal. It was observed that the reaction outcome depends strongly on the nucleophilicity of the nitrogen atom. Several amines were successfully applied in this transformation in moderate to good yields (**Table III.4**, entries 1-5). Steric hindered amines such as bis(1-phenylethyl)amine, 2,2,6,6-tetramethylpiperidine and *N*-benzyl-2-methylpropan-2-amine did not react even in refluxing acetonitrile. Furthermore imidazole, pyrrole, diethanolamine and diphenylamine also did not react. Very interestingly, the formation of other type of products were observed when secondary anilines were used as amines (see **Section III.3** for the complete study of these reactions). Highly reactive amines such as pyrrolidine or piperidine, which led to full conversion of **148**, furnished only traces or moderate yields of the corresponding products, respectively. These results can be explained by the stability of the product under the reaction conditions. In fact, for extended reaction times the yield of the product bearing a piperidine (**225**) decreases (**Table III.4**, entry 5, 24 h, 48 % vs. 48 h 38 %). Furthermore it was observed that product **217** is not stable in the presence of pyrrolidine (leading to a complex mixture), but is stable in the presence of morpholine. *N*-methylbutan-1-amine, diallylamine, piperazine and proline were also used as amines but very complex mixtures were obtained.

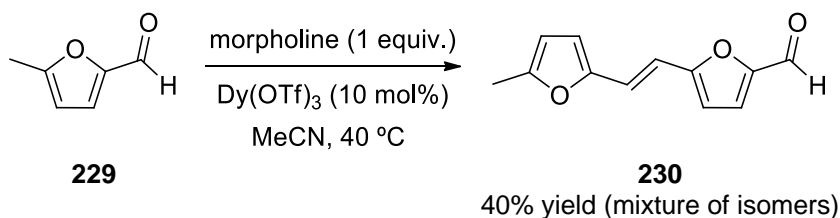
The effect of the alcohol protecting group was also investigated (**Table III.4**, entries 6-9). When the protection group (PG) is benzoyl (Bz) or benzyl (Bn) moderate yields were obtained (full conversion was not achieved using non-optimized conditions). When acetate (Ac) was employed as PG the observed yield drops to 29%, while HMF gave 44% yield of the corresponding product. These results highlights the importance of the protection group in the reaction efficiency, most probably by offering additional steric stabilization to the trienamine. Remarkably when 5-(chloromethyl)furfural was used instead of **148**, no reaction took place under the optimized reaction conditions.

Table III.4. Amine and O-protecting group scope^a

Entry	Amine	PG	t (h)	Yield (%) ^b	Product	d.r. ^c
1	dibenzylamine	TBDMS (148)	41	86	221	ND
2	diethylamine	TBDMS (148)	24	78	222	ND
3	<i>N</i> -methylpiperazine	TBDMS (148)	24	37	223	1:1.0
4	<i>N</i> -ethylbutylamine	TBDMS (148)	20	60	224	1:0.25
5	piperidine	TBDMS (148)	24 48	48 38	225	ND
6	morpholine	Bz (151)	54	58 (99)	226	1:1.0
7	morpholine	Bn (147)	54	58 (69)	227	1:0.8
8	morpholine	H (121)	54	44 (78)	219	1:1.1
9	morpholine	Ac (149)	54	29 (80)	228	1:1.0

^aReaction conditions: 10 mol % of catalyst, 0.125 mmol of aldehyde, 0.125 mmol of amine, 1.5 mL of acetonitrile. ^bIsolated yield after column chromatography. Conversions are present in parentheses. ^cDetermined by ¹H NMR. ND – not determined.

Very interestingly, employing 5-methylfurfuraldehyde (**229**) under the optimized conditions, bisvinylogous aldol condensation reaction took place as depicted in **Scheme III.18**, producing a mixture of isomers **230** in 40% yield. This result was not further studied because there is a precedent in literature using potassium hydroxide in water to give 8% of **230-trans** and 60% of recovered starting material **229**.¹⁷⁶

**Scheme III.18.** Bisvinylogous aldol condensation reaction.

During reaction conditions optimization, it was observed that high-pressure (ca. 9 kbar) is not benefic for the bisvinylogous Mannich reaction. Despite the higher conversion of the

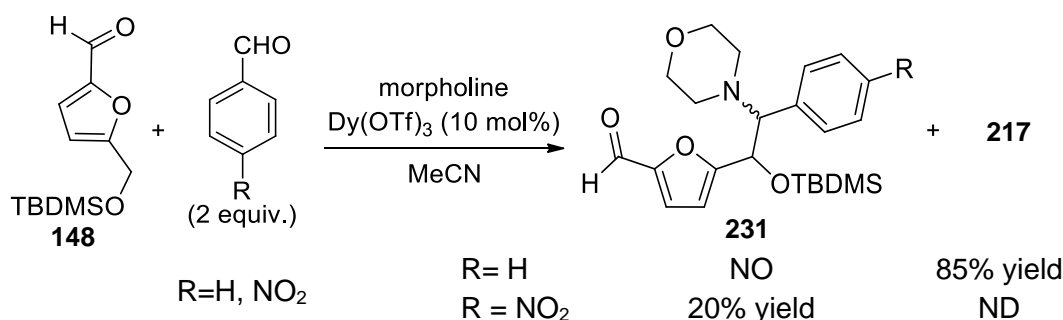
starting aldehydes, there was no increase in the yield, probably due to the formation of side-products as very complex reaction mixtures were obtained (**Figure III.4**).

Table III.5. Bisvinylous Mannich reaction under high-pressure conditions.^a

Entry	PG	Atm. Pressure		9800 atm	
		Conv. (%) ^b	Yield (%) ^b	Conv. (%) ^b	Yield (%) ^b
1	Bz	48	37	63	13
2	Bn	40	17	74	11
3	Ac	40	33	77	14

^aReaction conditions: 10 mol% of Dy(OTf)₃, 0.375 mmol of aldehyde, 0.375 mmol morpholine, in 2.4 mL of MeCN. ^bIsolated yield.

Next we aimed to achieve a cross reaction by intersecting the trienamine intermediate with other electrophiles (**Scheme III.19**). Several electrophiles such as substituted benzaldehydes, chalcone, *N*-protected isatine and acrylonitrile were tested using different ratios of **148**/substrate/amine. 4-Nitro benzaldehyde was found to react with this intermediate to give the cross-product **231** (**Scheme III.19**). It is noteworthy the great selectivity relatively to the homo-reaction as **217** was isolated as the major product using other electrophiles (for the reaction in presence of benzaldehyde, **217** was isolated in 85% yield).



Scheme III.19. Cross-reaction experiments. NO = Not observed by TLC analysis and preparative chromatography. ND = Not determined.

Asymmetric version

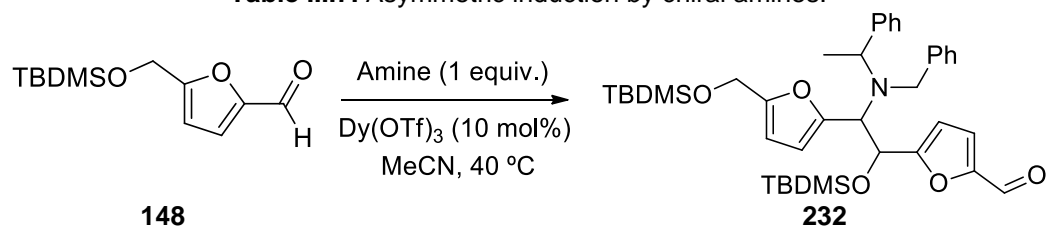
The possibility to perform the asymmetric reaction was also examined. Both Brønsted (eg., chiral phosphoric acids) and Lewis [eg., Sc(OTf)₃/chiral bis(oxazoline) ligands system] acid catalysts were explored (**Table III.6**). In all the cases the reaction did not display significant diastereo- or enantio- selectivities (**Table III.6**).

Table III.6. Reaction of **148** with morpholine using asymmetric-induced conditions.

Entry	Catalyst	Ligand	Conditions	Yield ^a	ee ^b
1	Dy(OTf) ₃	(S)-BINOL	MeCN, 40 °C, 2 days	Good	racemic
2	Dy(OTf) ₃	BOX	MeCN, 40 °C, 2 days	Good	racemic
3	Dy(OTf) ₃		MeCN, 40 °C, 2 days	Good	racemic
4 ^c	Sc(OTf) ₃	PyBOX	MeCN, 40 °C, 2 days	Good	racemic
5 ^c	Sc(OTf) ₃		DCM, 40 °C, 2 days	Good	racemic
6	(R)-BINOL Hydrogenphosphate	-	DCE, 80 °C, 3 days	Low	racemic
7 ^d	(R)-VAPOL Hydrogenphosphate	-	DCE, 80 °C, 5 days	Low	racemic
8	(R)-TRIP	-	DCE, 70 °C, 5 days	Moderate	racemic
9 ^d	(S)-CSA	-	MeCN, 80 °C, 2 days	Moderate	racemic

^aQualitative yield obtained by TLC analysis of crude reaction mixture; ^bDetermined by HPLC of crude reaction mixture; ^cThe catalyst and the ligand were pre-mixed before for 2 h at RT; ^dNo reaction observed at 40 °C for 2 d. (S)-BINOL = (S)-(-)-1,1'-Bi(2-naphthol); BOX = 2,2'-Isopropylidenebis[(4S)-4-*tert*-butyl-2-oxazoline]; PyBOX = 2,6-Bis[(4R)-4-phenyl-2-oxazoliny] pyridine; (R)-BINOL hydrogenphosphate = (R)-(-)-1,1'-Binaphthyl-2,2'-diyl hydrogenphosphate; (R)-VAPOL hydrogenphosphate = (R)-2,2'-Diphenyl-3,3'-biphenanthryl-4,4'-diyl phosphate; (R)-TRIP = (R)-3,3'-Bis(2,4,6-triisopropylphenyl)-1,1'-binaphthyl-2,2'-diyl hydrogenphosphate; (S)-CSA = (1S)-(+)-10-Camphorsulfonic acid.

Encouraged by the reported asymmetric trienamine reaction using chiral amines,¹⁶⁰ it was observed a great selectivity of 1:1:0:0 when a chiral amine is employing vs. 1:1:0.4:0.3 for the reaction with racemic amine (**Table III.7** and **Figure III.6**). These results suggest the existence of an interaction between the amine moieties from the iminium-ion and the trienamine, resulting in a chiral induction from a very remote position.

Table III.7. Asymmetric induction by chiral amines.^a

Entry	Amine	<i>d.r.</i> ^b
1		NR
2		1:1:0.4:0.3 ^c
3		1:1:0:0 ^d
4		1:1:0:0 ^e

^aReaction conditions: 10 mol% of catalyst, 0.125 mmol of aldehyde, 0.125 mmol of amine, 1.5 mL of solvent. ^bDetermined by ¹H NMR. ^c15% isolated yield after column chromatography. ^dYield not determined. ^e13% isolated yield after column chromatography. NR = No reaction was observed by ¹H NMR.

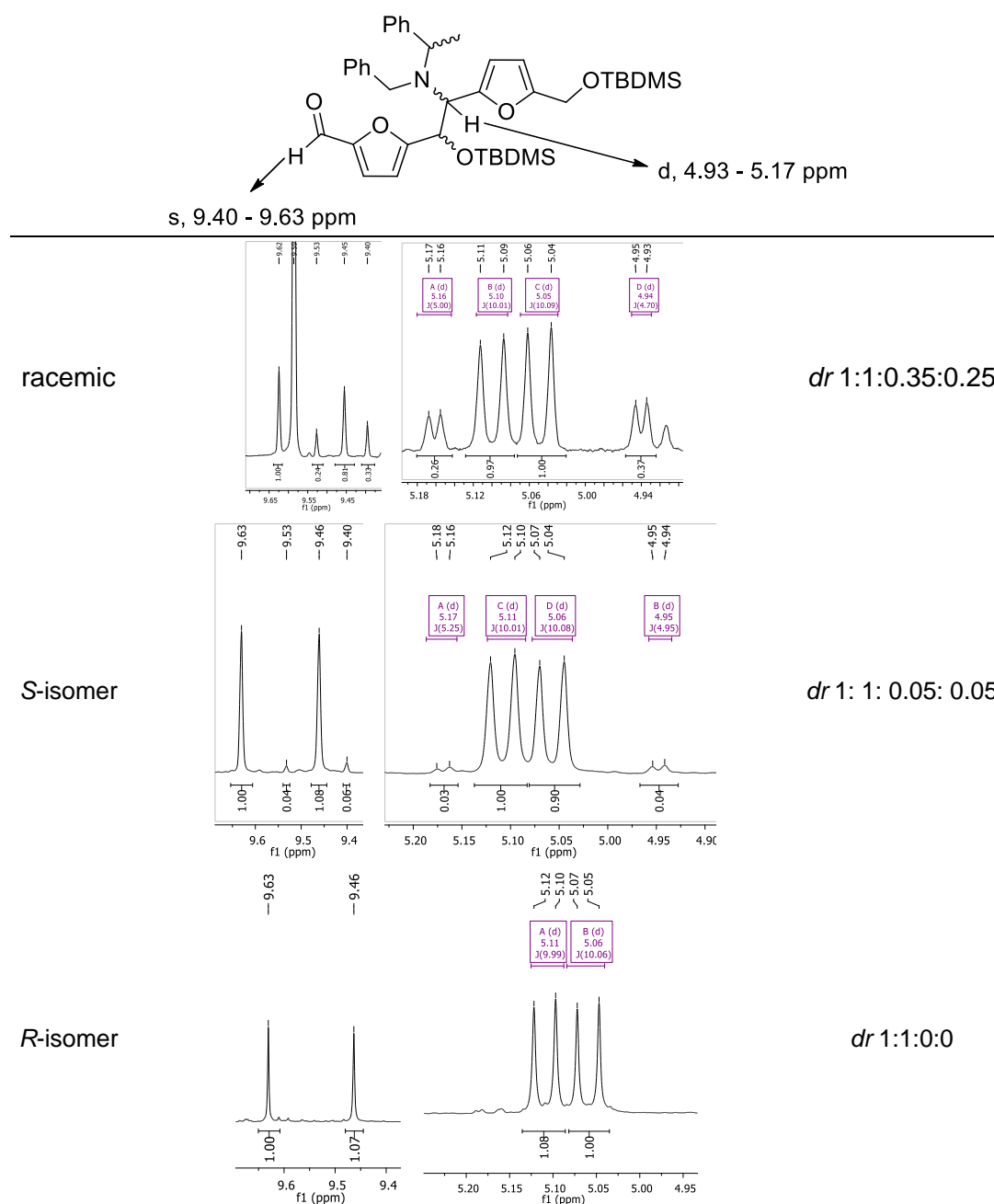


Figure III.6. ^1H NMR analysis of the asymmetric reactions using racemic and enantiopure amines.

Mechanism

To gain insights into the mechanism of the transformation, the reaction of **148** with secondary amines was followed by ^1H NMR. Surprisingly, formation of the corresponding aminal was observed as the only intermediate of the reaction. In **Figure III.7** is shown the proton NMR spectra for the initial time and after 16 h.

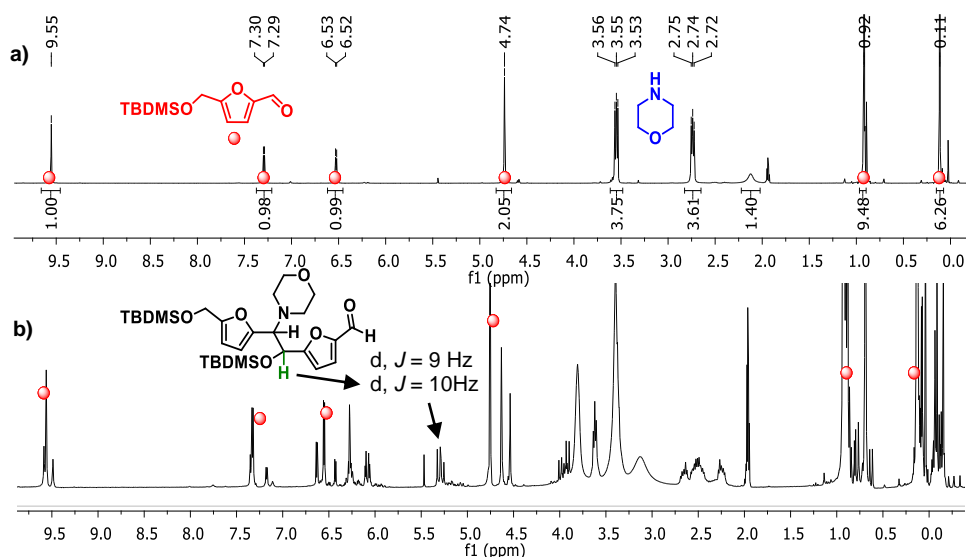


Figure III.7. ^1H NMR spectra of the reaction of **148** with morpholine and 10 mol% of $\text{Sc}(\text{OTf})_3$ in CD_3CN at 40°C for **a)** $t = 0$ (before the addition of catalyst) and **b)** $t = 16$ h (after the addition of catalyst).

The formation of the aminal immediately occurs when the aldehyde is added to the amine, even at room temperature and in absence of the catalyst (an equimolar amount of **148** and the aminal is reached after 4 h when morpholine is used as amine, **Figure III.8**).

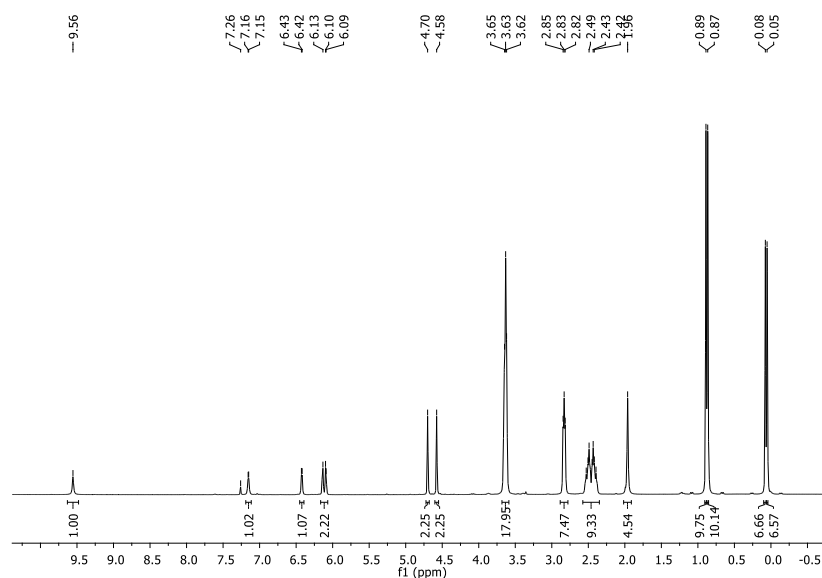


Figure III.8. ^1H NMR spectrum of the reaction mixture of **148** with morpholine in CDCl_3 after 4 h at RT.

For the unreactive amines, such as bis(1-phenylethyl)amine, no aminal was observed, explaining why no reaction took place (**Figure III.9**).

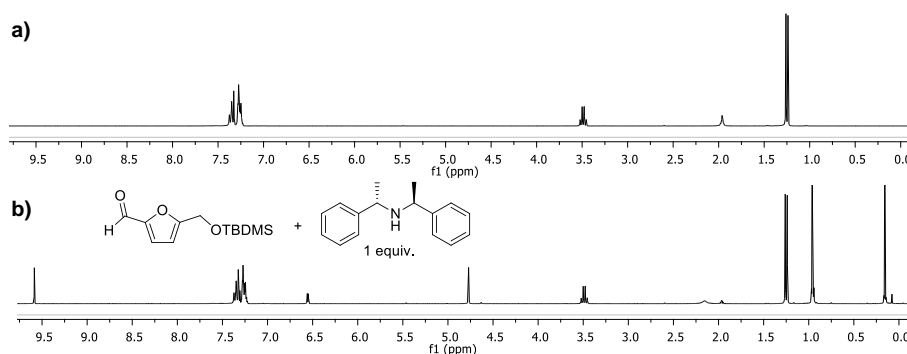


Figure III.9. ^1H NMR spectra in CD_3CN of **a)** bis(1-phenylethyl)amine and **b)** reaction mixture of bis(1-phenylethyl)amine and **148** after 16 h at RT.

The uncatalyzed reaction of **148** and pyrrolidine was also followed by ^1H NMR. By comparing the two reactions, it is clear that pyrrolidine is giving a complex mixture whereas morpholine is giving a clean NMR even after 2 days (**Figure III.10** vs. **Figure III.11**).

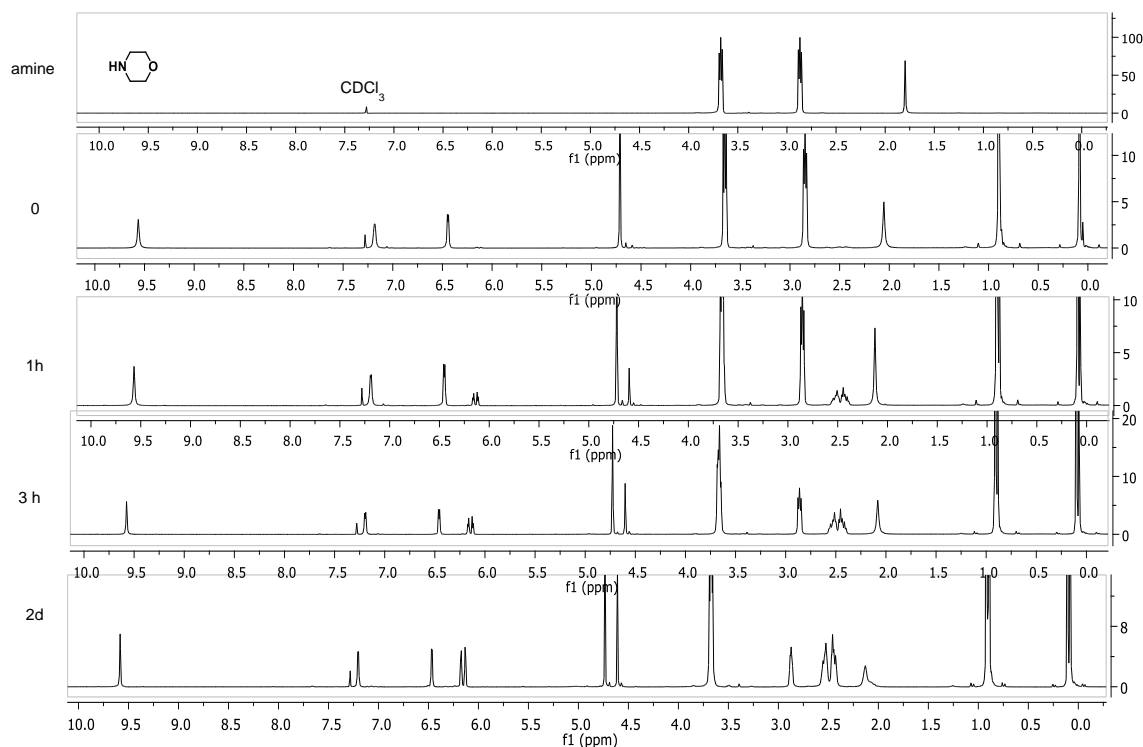


Figure III.10. ^1H NMR spectra of the reaction of **148** and morpholine in CDCl_3 after 1 h, 3 h and 2 days.

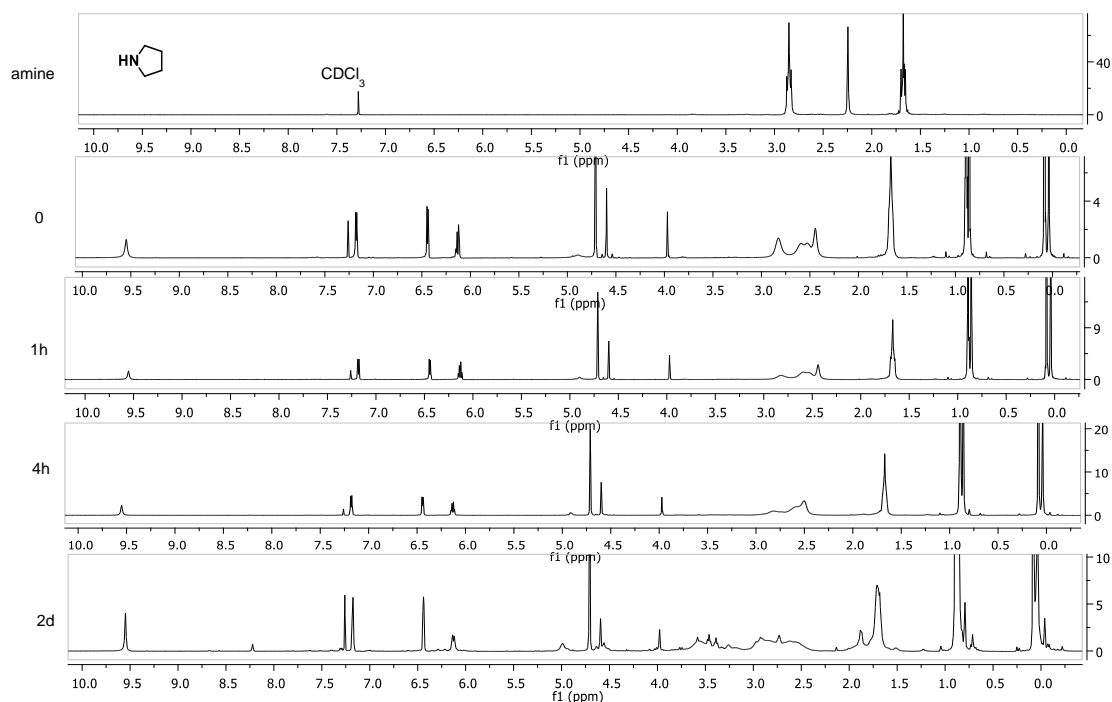


Figure III.11. ^1H NMR spectra of the reaction of **148** and pyrrolidine in CDCl_3 after 1 h, 4 h and 2 days.

Noteworthy is the fact that no further reaction takes place if catalyst is not added, even at 80 °C. Following the reaction catalyzed by $\text{Sc}(\text{OTf})_3$ in acetonitrile- d_3 at 40 °C, did not led to the identification of other intermediates, apart from the amination and products (diastereoisomers I and II, **Figure III.7**). In particular, there was the interest to identify the proposed trienamine intermediate. With this goal in mind, the optimized reaction was performed in the presence of D_2O or using *N*-deuterated morpholine, however no incorporation of deuterium into the final product was found.

These observations led us to hypothesize that the formation of the trienamine is the rate-limiting step (RLS). In fact, by preparing the bisdeuterated derivative **148-d₂** and submitting a 1:1 mixture of **148** and **148-d₂** to optimized conditions (**Figure III.12**), primary hydrogen kinetic isotope effect was observed ($\text{KIE} = 4.0$, **Figure III.12**). The existence of this substantial isotope effect is a strong evidence that the carbon-hydrogen/deuterium bond is being broken in the RLS. The determination of the kinetic isotope effect is based on the data summarized in the same figure.

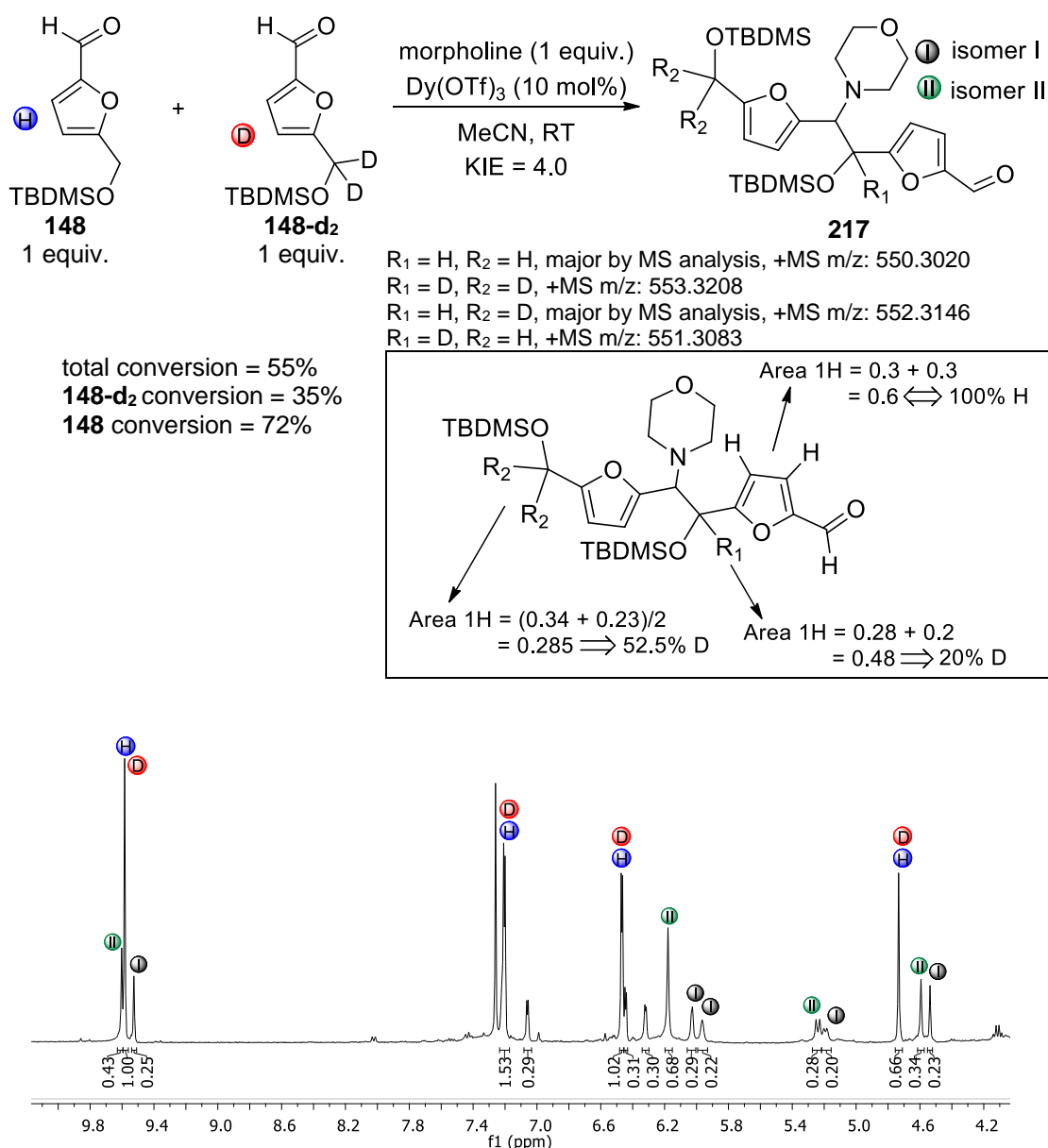
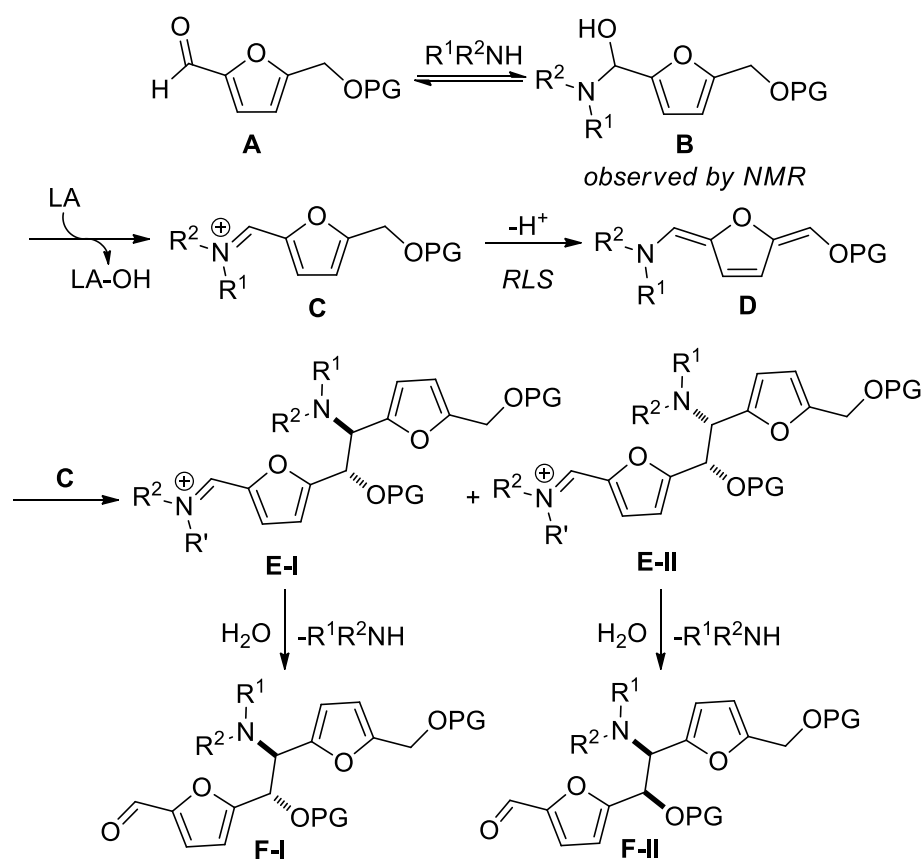


Figure III.12. Kinetic isotope effect experiment.

Based on the total starting material conversion, $\text{KIE} = \frac{33.1}{13.9} = 2.4$. However, since two molecules of the starting material are involved in the reaction in a different way, there are different KIE that can be determined. In fact, the enrichment of the isotope is different for R₁ (trienamine) and for R₂ (iminium) as shown by the different deuterium enrichment for R₁ and R₂. To calculate the desired KIE, the deuterium enrichment in the products was taking in consideration. Thus, $\text{KIE for R}_1 = \frac{0.48}{0.6 - 0.48} = 4.0$ and $\text{KIE for R}_2 = \frac{0.57}{0.6 \times 2 - 0.57} = 0.9$.

Taking in consideration these observations it is proposed the mechanism depicted in **Scheme III.20**. The great ϵ -selectivity of this transformation (vs. other possible additions) is believed to be due to the rearomatization of the furan ring of **D**.



Scheme III.20. Proposed mechanism for the bisvinylogous homo-Mannich reaction.

DFT Studies

Density Functional Theory (DFT)¹⁷⁷ studies were performed, under the guidance of Prof. Luis Veiros from Instituto Superior Técnico, to evaluate the proposed mechanism. Three steps were considered independently: i) the formation of iminium-ion **C** by dehydration of aminal **B**, ii) conversion of iminium-ion **C** into trienamine **D** and finally iii) the reaction of trienamine **D** with iminium-ion **C**. After geometries optimization for all the species using B3LYP functional and a standard 6-31G(d,p) basis set, the solvent effect (acetonitrile) was taken in consideration by single point energy calculations using the polarizable continuum model, with radii and non-electrostatic terms of the SMD solvation model. For these single point energy calculations three different functionals were screened (B3LYP, PBE1PBE and M06-2X) together with the 6-311++G(d,p) basis set. A full description of the computational details and the respective references is presented in the Experimental **Section III.4**. From this extensive study, M06-2X/6-311++G(d,p)//B3LYP/6-31G(d,p) was selected as the level that best corroborates with the experimental data and thus best describe the reaction. Although all the functionals suggest a similar energetic path, calculations with B3LYP and PBE1PBE resulted in very high global

energies that are not in agreement with a reaction that takes place at 40 °C. In addition, for PBE1PBE functional, the trienamine formation was not identified as the RLS.

The conversion of iminium-ion **C** into trienamine **D** exhibited the highest energy barrier (23 kcal.mol⁻¹, **Figure III.14**), which is in agreement with this being the RLS. On the other hand, conversion of aminal **B** into iminium-ion **C** displayed the lowest energy barrier (9 kcal.mol⁻¹, **Figure III.13**). Finally, reaction of **D** with **C** to give the two iminium-ions products **E-I** and **E-II** exhibited energy barriers of 19 and 15 kcal.mol⁻¹, respectively (**Figure III.15**).

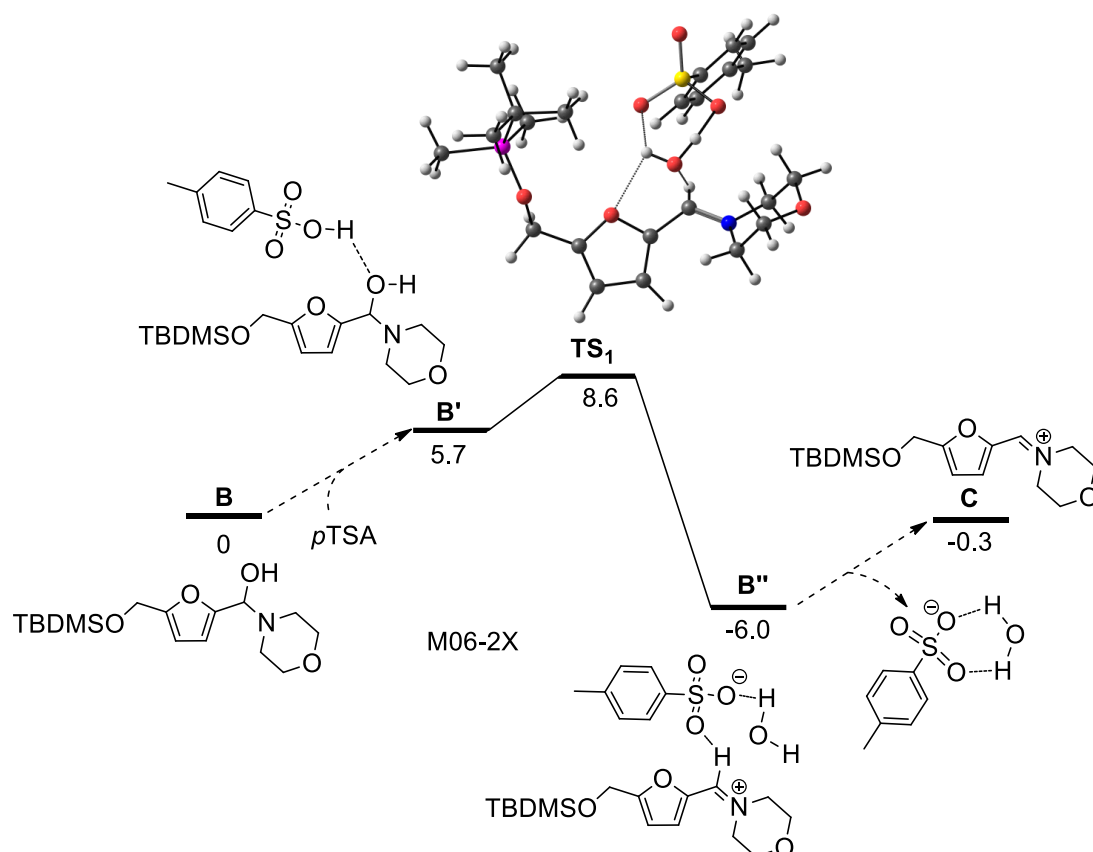


Figure III.13. Free energy profile (kcal.mol⁻¹) calculated for the formation of iminium-ion **C** by dehydration of aminal **B** catalyzed by *para*-toluenesulfonic acid (PTSA). The minima and the transition state were optimized and the energy values are referred to **B** after thermal correction to Gibbs Free Energy in acetonitrile using M06-2X functional. PTSA was used as the acid due to computational convenience.

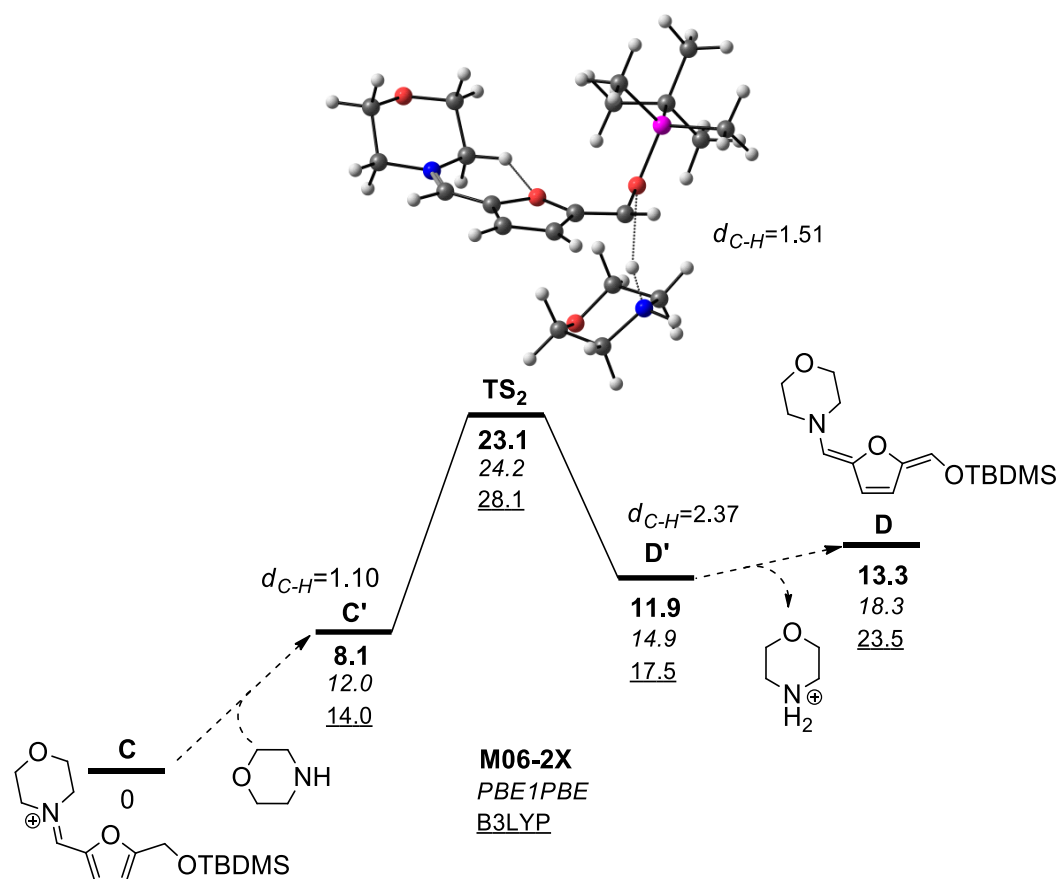


Figure III.14. Free energy profile (kcal.mol⁻¹) calculated for the conversion of iminium-ion **C** into trienamine **D** using morpholine as a base. The minima and the transition state were optimized and the energy values are referred to **C** after thermal correction to Gibbs Free Energy in acetonitrile using M06-2X, PBE1PBE or B3LYP functionals. The lengths (Å) of the C-H that is being broken are indicated for the relevant structures.

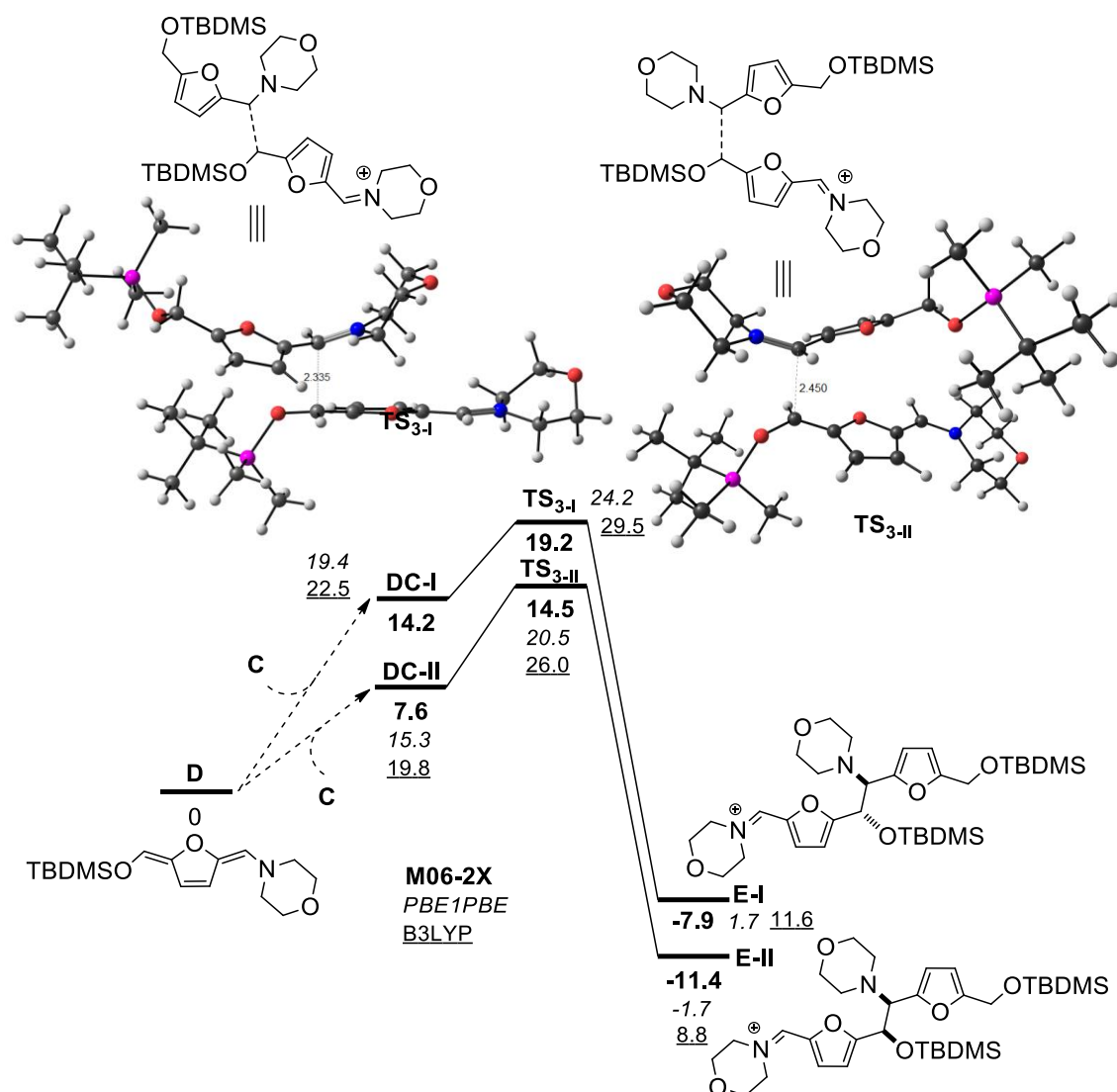


Figure III.15. Free energy profile (kcal.mol⁻¹) calculated for the reaction of trienamine **D** with iminium-ion **C** to yield the two diastereoisomers **E-I** and **E-II**. The minima and the transition state were optimized and the energy values are referred to **D** after thermal correction to Gibbs Free Energy in acetonitrile using M06-2X, PBE1PBE or B3LYP functionals. The lengths (Å) of the C-C that is being formed are indicated for the transition state structures.

Biological Activity

This unprecedented family of furanic scaffolds were evaluated, by the team member Dr. Raquel F. M. Frade, for their antiproliferative activity towards human cancer cell lines from colon (HT-29), lung (NCI-H460) and breast (MCF-7) origin (**Table III.8**). Compounds **217** and **223** induced an important cancer cell growth inhibition in contrast to compounds **221**, **222** and **224**, which suggests that a cyclic amine is important for the observed biological activity. Determined concentration of **217** to reduce 50% of NCI-H460 cell viability was 13.2 μM (IC₅₀) whereas for HT-29 and MCF-7, IC₅₀ was below 10 μM. Promising IC₅₀ were also determined for **223** (<10 μM) in all cell models (**Table III.8**). Human colon adenocarcinoma cells (CACO-2), able to mimetic human intestinal

epithelium, and human normal skin fibroblasts cells (CRL-1502) were also used to test toxicity of compounds **217** and **223** and data demonstrates that larger doses of these compounds are required to attain the IC_{50} in these models. Therefore, the compounds bearing a cyclic secondary amine present interesting biological activity which motivates the exploitation of this new scaffold. Further investigation on the biological activity showed that compounds with an alcohol protective group different from TBDMS (e.g., Bz, Bn, TIPS, THS, DMPES) did not show relevant biological activity for concentrations lower than 10 μ M. Finally, changes in the *N*-substituent of piperazine led to the conclusion that the introduction of a carboxyl group (e.g., Ac, Boc) did not provide better activity. On the other hand the *N*-methyl and *N*-butylpiperazine provided promising activity against MCF-7 and NCI-H460 cell lines.

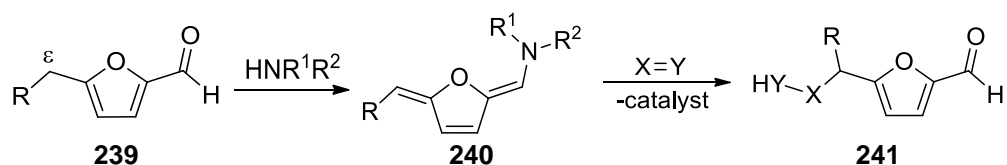
Table III.8. Biological activity of the synthesized compounds.

Amine	R		IC ₅₀ (μM) ± SD					
			CACO-2	CRL-1502	HT-29	MCF-7	NCI-H460	
Morpholine	TBDMS	217	>15	10<IC ₅₀ <20	5.3±2.9	8.6±2.0	13.2±2.0	
Dibenzylamine	TBDMS	221	-	-	>50	>50	>50	
Diethylamine	TBDMS	222	-	-	>50	>50	>50	
<i>N</i> -methylpiperazine	TBDMS	223	>15	10<IC ₅₀ <20	4.7±1.2	5.8±1.3	4.9±1.1	
<i>N</i> -ethylbutylamine	TBDMS	224	-	-	>50	>50	>50	
Morpholine	Bz	226	-	-	>10	>10	>10	
Morpholine	Bn	227	-	-	>10	>10	>10	
Morpholine	Ac	228	-	-	>10	>10	>10	
Morpholine	H	219	-	-	>10	>10	>10	
Morpholine	TIPS	233 [†]	-	-	-	-	>10	
Morpholine	THS	234 [†]	-	-	-	-	≥10	
Morpholine	DMPES	235 [†]	-	-	>10	>10	>10	
<i>N</i> -Butylpiperazine	TBDMS	236 [†]	-	-	>10	6.0±3.1	10.5±1.1	
<i>N</i> -Acylpiperazine	TBDMS	237 [†]	-	-	>10	>10	>10	
<i>N</i> -Bocpiperazine	TBDMS	238 [†]	-	-	>10	>10	>10	
<div style="text-align: center;"> </div>			231	-	-	>8	6<IC ₅₀ <8	>8

SD = standard deviation; HT-29 = human colorectal adenocarcinoma cell line; NCI-H460 = human non-small cell lung cancer cells; MCF-7 = breast cancer cell line; CACO-2 = continuous cell of heterogeneous human epithelial colorectal adenocarcinoma cells; CRL-1502 = human normal skin fibroblasts cells. [†]Prepared by Master students under my supervision.

III.2.3. Conclusions

The selective ε -functionalization of 2,4-dienals *via* trienamine intermediates was reported (**Scheme III.21**), that to the best of our knowledge, is the first example in the literature since linear-trienamine catalysis has been limited to Diels-Alder reactions. Several amines were successfully applied producing a new highly functionalized skeleton. Asymmetric version using chiral amines revealed the existence of an interaction between the amine moieties from the iminium-ion and the trienamine resulting in a relevant stereoselectivity. Specific patterns in 5-substituted furfural showed to be important to achieve good yields. Mechanistic studies suggested that formation of vinylogous iminium-ion is the rate limiting step, which is different from the known amine catalysis. DFT studies also corroborate the proposed mechanism. Preliminary biological assays results indicate that these new compounds exhibited promising antitumor activities when a cyclic secondary amine is present resulting. Furthermore, for piperazines, *N*-alkyl substituents offer better results than carboxyl group. Hence, derivatives bearing different *N*-alkyl substituents are going to be prepared and evaluated against the mentioned cell lines.



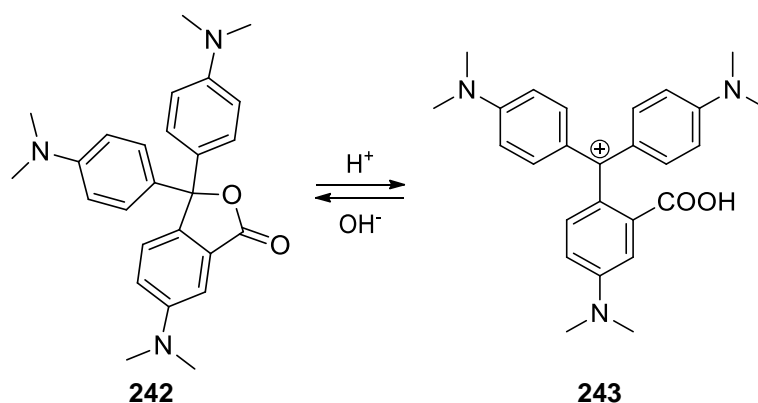
Scheme III.21. Selective ε -functionalization of 5-substituted furfurals *via* trienamine intermediate.

III.3. Synthesis and Biological Activity of New Triarylmethanes

III.3.1. Introduction

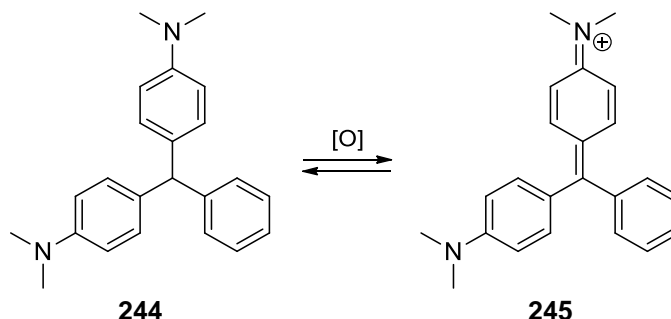
Triarylmethanes (TRAM) and related structures has attracted much attention in the area of medicinal chemistry and materials science.¹⁷⁸⁻¹⁸⁰ Indeed, the triarylmethane motif is ubiquitous in dyes,¹⁸⁰⁻¹⁸⁴ fluorescent probes,¹⁸⁵⁻¹⁸⁹ natural products,¹⁹⁰⁻¹⁹² and biologically active compounds.¹⁹³⁻¹⁹⁵

As dyes, this class of compounds are known as leuco dyes because they can have two structural forms, usually one colorless and other extremely colored. For example, crystal violet lactone can undergo reactions in response to acid and base to give a colored cation, and thus serve as pH indicator (**Scheme III.22**).¹⁹⁶



Scheme III.22. Transformation between leuco and colored form of crystal violet lactone.

In other example, they can undergo on hydride abstraction by oxidizing agents such as the example of malachite green (**Scheme III.23**). Malachite green is traditionally used as dye, however is also used medicinally in dilute solution as a local antiseptic as it is effective against fungi and gram-positive bacteria.



Scheme III.23. Leuco malachite green (LMG) and malachite green (MG) structures.

Other common examples of triarylmethane dyes are methyl violet and phenol red (**Figure III.16**). For the case of methyl violet, the color of the dye can be changed

depending on the amount of methyl groups attached to the nitrogen (R_1 and R_2 in **Figure III.16**). This compound is mainly used as a purple dye for textiles and to give deep violet colors in paint and ink. Phenol red is a pH indicator that is frequently used in cell biology laboratories and in home swimming pool test kits.

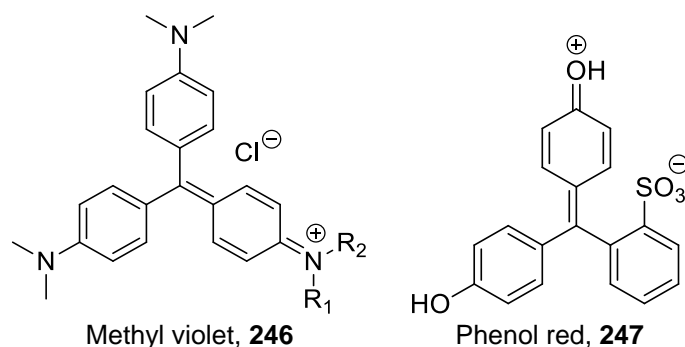


Figure III.16. Examples of synthetic organic triarylmethane dyes.

Triarylmethanes are also known for having various medicinal properties. Among others they are reported to have anti-breast cancer, antitubercular, antiimplantation, and antiproliferative activities (**Figure III.17**).¹⁹⁷⁻²⁰³

Notably, the antifungal agent clotrimazole **248** inhibits the growth of cancer cells in culture, and has shown efficacy in various mouse models of cancer. Further studies indicate that this compound arrests cells in the G1-phase of the cell cycle. The anticancer properties of clotrimazole have been linked to its ability to affect intracellular Ca^{2+} levels thereby inhibiting translation, in addition to inhibition of glycolysis by inducing the detachment of mitochondrial-bound hexokinase.¹⁹⁷ However, inhibition of cytochrome P450 enzymes by clotrimazole limits its therapeutic value.¹⁹⁸ More recently, Chandy *et al.* reported a rational design strategy that resulted in the development of the clotrimazole analog **249**, a potential immunosuppressant that selectively inhibits *IKCa1* without blocking cytochrome P450 enzymes.¹⁹⁸ In other study, Young *et al.* studied the antiproliferative activity of clotrimazole derivatives **250** without the imidazole moiety, which is responsible for the hepatotoxicity. The majority of the analogues demonstrate *in vitro* antiproliferative activity ranging from submicromolar to micromolar concentrations.¹⁹⁹

Bisacodyl **251**, a pyridine-containing TRAM, is a stimulant laxative drug, typically prescribed for relief of constipation and for the management of neurogenic bowel dysfunction.

A method of treating a disorder associated with KSP kinesin activity using a series of simple triphenylmethanes **252** have been protected with a patent.²⁰⁰

Hergenrother *et al.* identified several triphenylmethanides **253** as quite potent inducers of apoptotic death in melanoma cell lines ($IC_{50} \sim 0.5 \mu M$), and importantly, are comparatively nontoxic to normal cells isolated from the bone marrow of healthy donors.²⁰¹

Bis-(indolyl)arylmethanes **254**, a particular class of TRAMS, are found in bioactive metabolites of terrestrial and marine origin and present antimicrobial activity.²⁰²

The triarylmethane **255**, containing a phenanthrene and a basic amino side chain, was reported in 2006 as a new anticancer agent, showing good antiproliferative activity against MCF-7 cell line with IC_{50} in the range of $3.5\text{--}22.3 \mu M$.²⁰³

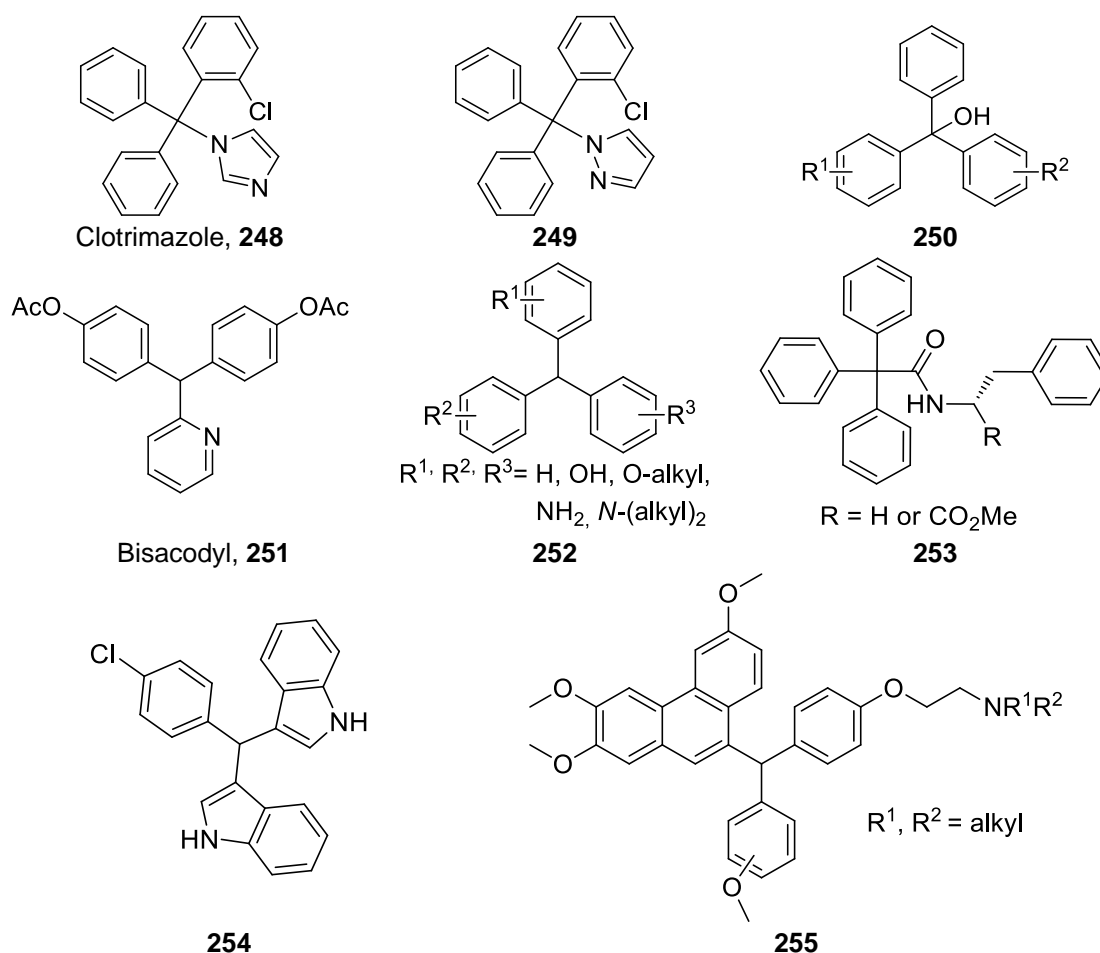
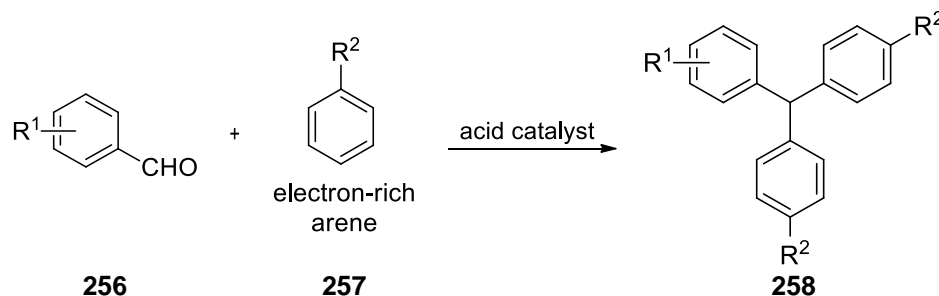


Figure III.17. Structure of bioactive TRAM.

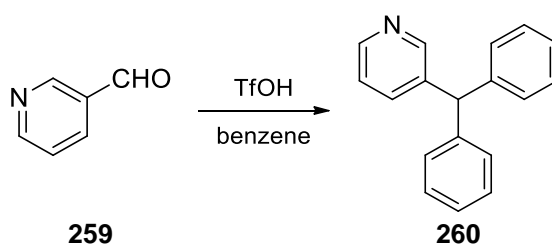
Due to their important physical, chemical and biological properties, a variety of methods are known for the synthesis of triarylmethane motifs. Friedel-Crafts alkylation and Grignard reaction are typically employed. Since they are text book reaction, a brief overview of the transformations is going to be showed. Next, some specific examples of other transformations for TRAM synthesis are going to be presented.

Possibly, the most widely used synthetic method for the preparation of TRAMs is the reaction of aromatic aldehydes with electron-rich arenes (such as phenols and anilines) in the presence of acid catalysts (**Scheme III.24**).¹⁷⁸⁻¹⁷⁹



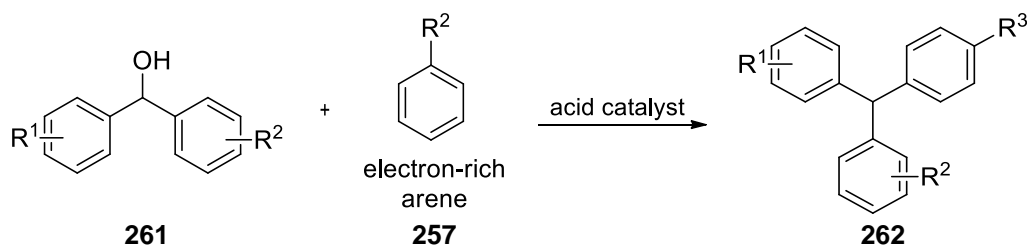
Scheme III.24. Two-fold Friedel-Craft alkylation of aromatic aldehydes.

There are however some examples where unactivated arenes are employed as nucleophile. For that cases was shown that the use of strong acids and heteroaromatic aldehydes facilitates the transformation (**Scheme III.25**).²⁰⁴⁻²⁰⁶



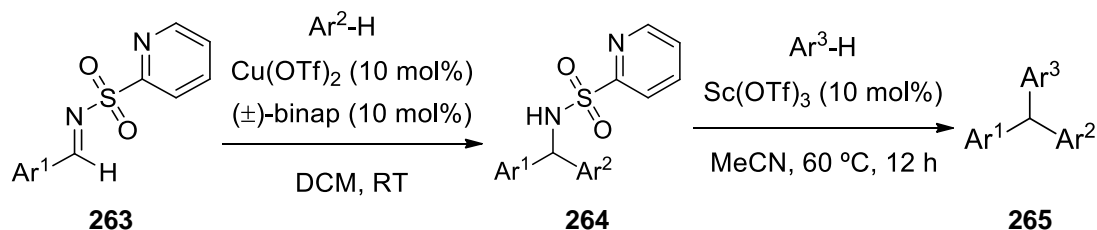
Scheme III.25. Friedel-Crafts alkylation using unactivated arenes.

Other substrates that can yield TRAM by Friedel-Crafts alkylation are diarylmethanols, by condensation with electron-rich arenes or heteroarenes. An important feature of this synthetic method is that both symmetric and unsymmetrical TRAM can be obtained (**Scheme III.26**).¹⁸⁴



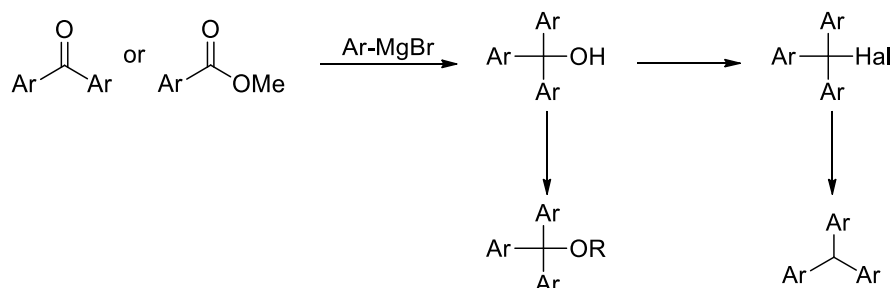
Scheme III.26. Condensation of diarylmethanols with arenes under Friedel-Crafts conditions.

Recently, Carretero *et al.* reported the synthesis of unsymmetrical triarylmethanes by two-steps protocol involving first a Cu(II)-catalyzed aza-Friedel-Crafts reaction of *N*-(2-pyridyl)sulfonyl aldimines with electron-rich arenes followed by a second electrophilic aromatic substitution in the presence of Sc(OTf)₃ (**Scheme III.27**).²⁰⁷



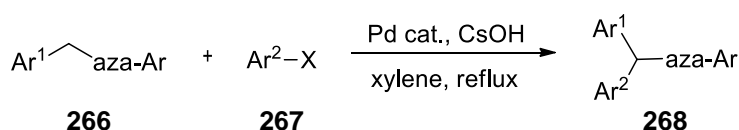
Scheme III.27. Synthesis of triarylmethanes by copper(II)-catalyzed aza-Friedel-Crafts reaction of *N*-(2-pyridyl)sulfonyl aldimines.

Addition of aryl Grignard reagents to carbonyls (such as diarylketones or aryl ester) yields triarylmethanols. This can be halogenated by refluxing in AcCl/toluene or converted into alkyl ether by reaction with alcohol in glacial acetic acid. Triarylmethyl halogenides can be reduced to the desired triarylmethanes by dialkylamides. Oxidation of triarylmethanes into triarylmethanols can take place under oxidizing conditions such as $\text{PbO}_2/\text{CH}_3\text{CO}_2\text{H}/\text{DDQ}$.¹⁷⁸



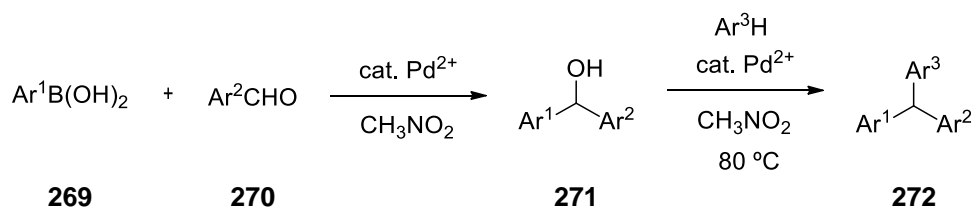
Scheme III.28. Synthesis of TRAM from triarylmethanols.

Various others procedures have been reported in the literature for the preparation of triarylmethane compounds. Oshima and co-workers reported a new method to synthesize TRAM having at least one azaaryl group through the palladium-catalyzed direct benzylic arylation of aryl(azaaryl)methanes (**Scheme III.29**).²⁰⁸



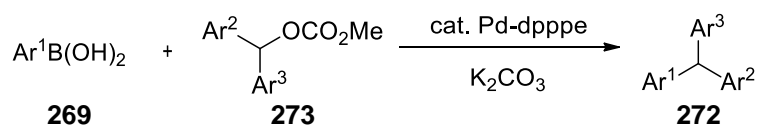
Scheme III.29. Palladium-catalyzed direct arylation of aryl(azaaryl)methanes **266** with aryl halides providing triarylmethanes **268**.

Lu and Co-workers reported the synthesis of unsymmetrical TRAM *via* cationic Pd(II)/bipyridine-catalyzed addition of arylboronic acids to arylaldehydes (**Scheme III.30**).²⁰⁹



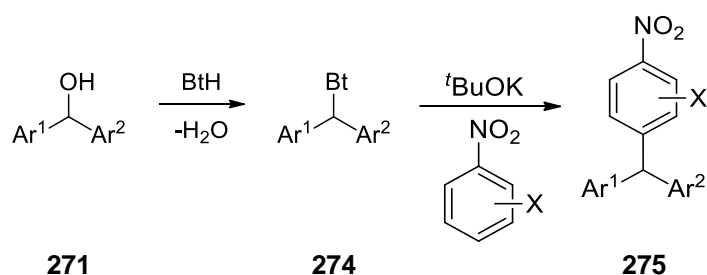
Scheme III.30. Cationic Pd(II)/bipyridine-catalyzed addition of arylboronic acids to arylaldehydes.

Kuwano *et al.* reported a novel synthesis of unsymmetrical TRAM *via* Suzuki-Miyaura coupling of diarylmethyl carbonates with arylboronic acids in the presence of [Pd(η^3 -C₃H₅)Cl]₂-dpppe catalyst (**Scheme III.31**).²¹⁰



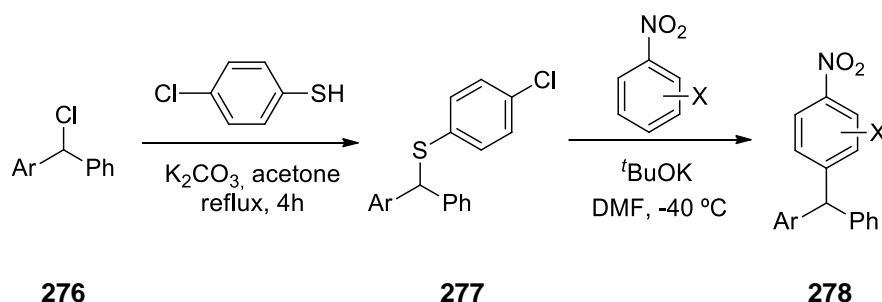
Scheme III.31. Suzuki-Miyaura coupling of diarylmethyl carbonates with arylboronic acids.²¹⁰

Toader *et al.* reported a general regiospecific method for the synthesis of (*p*-Nitroaryl)diarylmethanes from diarylmethanols and substituted nitrobenzenes *via* vicarious nucleophilic substitution of hydrogen. The method makes use of the quantitative reaction between benzotriazole and diarylmethanols under acidic catalysis. In the presence of Brønsted or Lewis acids, diarylmethanols are highly electrophilic, reacting with electron-rich arenes in Friedel-Crafts fashion. In contrast, (diarylmethyl)benzotriazoles **274** in the presence of strong bases become highly nucleophilic, allowing reactions with electron poor arenes. Hence, this substitution procedure complements Friedel-Crafts approaches to similar compounds.²¹¹



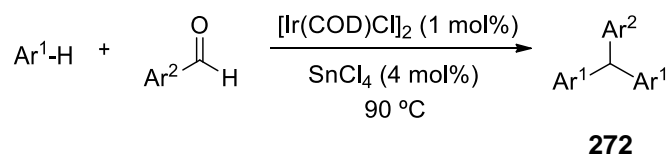
Scheme III.32. Synthesis of (*p*-nitroaryl)diarylmethanes **275** *via* vicarious nucleophilic substitution of hydrogen.²¹¹

Later, Voskresensky *et al.* reported the use of diarylmethyl *p*-chlorophenyl sulfide instead of the intermediate containing Bt as depicted in **Scheme III.33**.²¹²



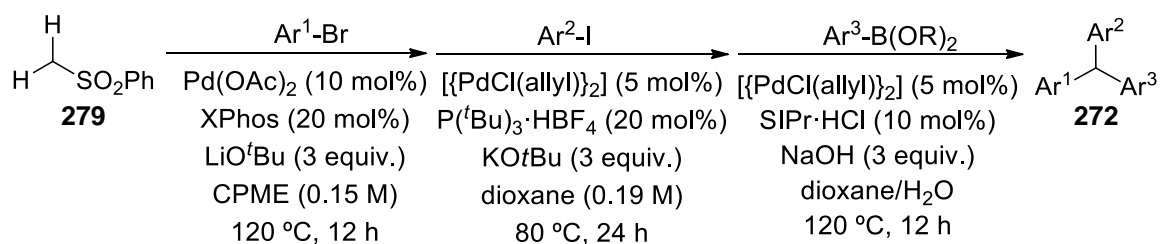
Scheme III.33. Synthesis of (*p*-nitroaryl)diarylmethanes via vicarious nucleophilic substitution of hydrogen using *p*-chlorophenyl sulfide.²¹²

Roy *et al.* reported the synthesis of TRAM by reaction of arenes and heteroarenes with aromatic aldehydes in the presence of a catalytic combination of $[\text{Ir}(\text{COD})\text{Cl}]_2$ and SnCl_4 .²¹³



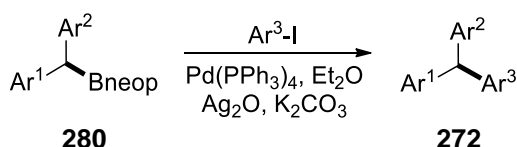
Scheme III.34. Dual-reagent catalysis: highly selective alkylation of arenes and heteroarenes with aromatic aldehydes.²¹³

Very recently, Crudden *et al.* reported the synthesis of triarylmethanes through Palladium-catalyzed sequential arylation of methyl phenyl sulfone **279**. The three aryl groups are installed through two sequential palladium-catalyzed C-H arylation reactions, followed by an arylation and desulfonation as depicted in **Scheme III.35**.²¹⁴



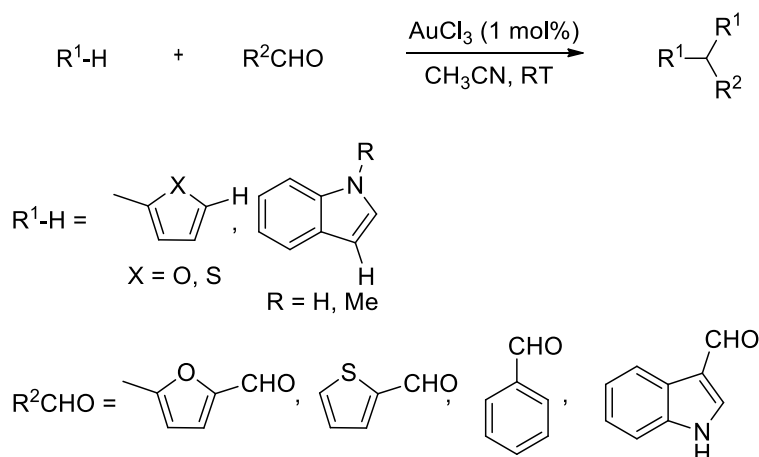
Scheme III.35. Modular synthesis of triarylmethanes through palladium-catalyzed sequential arylation of methyl phenyl sulfone **279**.²¹⁴

Very recently Crudden *et al.* published the synthesis of enantiomerically enriched triarylmethanes by enantiospecific Suzuki-Miyaura cross-coupling reactions.²¹⁵



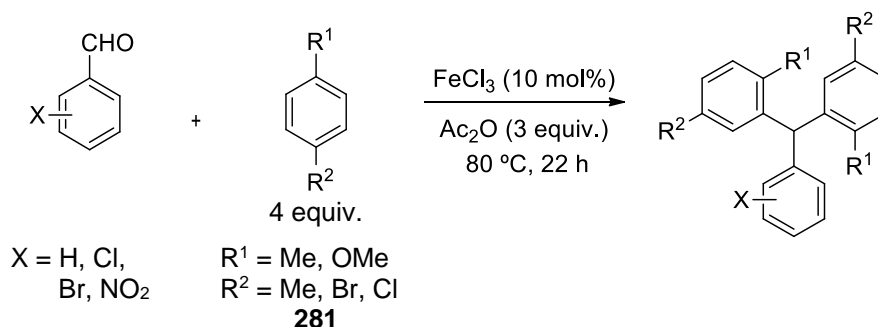
Scheme III.36. Synthesis of enantiomerically enriched triarylmethanes **272** by enantiospecific Suzuki-Miyaura cross-coupling reactions.²¹⁵

Vidya *et al.* reported a practical synthesis of triheteroarylmethanes by reaction of aldehydes and activated arenes promoted by gold(III) chloride (**Scheme III.37**).²¹⁶

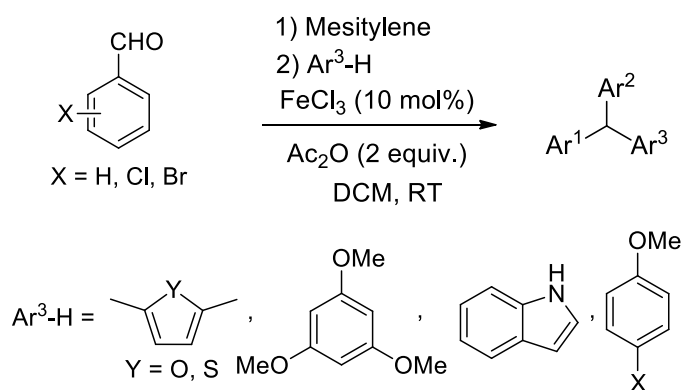


Scheme III.37. Practical synthesis of triheteroarylmethanes by reaction of aldehydes and activated arenes promoted by gold(III) chloride.²¹⁶

Wu *et al.* reported the synthesis of triarylmethane derivatives of aromatic aldehydes and electron-rich arenes catalyzed by FeCl_3 . This method provides a facile and direct access to symmetrical (**Scheme III.38**) and unsymmetrical (**Scheme III.39**) triarylmethane and diarylmethane derivatives. The presence of acetic anhydride is crucial to this FeCl_3 catalyzed TRAM formation. From a mechanistic point of view, the authors proposed that aldehydes react with acetic anhydride to form the more reactive geminal diacetates that undergo arylation to provide TRAM or diarylmethane derivatives.²¹⁷

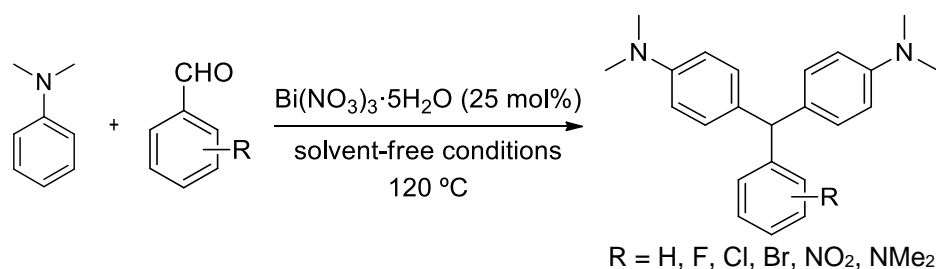


Scheme III.38. A simple access to triarylmethane derivatives from aromatic aldehydes and electron-rich arenes catalyzed by FeCl_3 .²¹⁷



Scheme III.39. One-pot FeCl_3 -catalyzed unsymmetrical triarylmethanes formation.²¹⁷

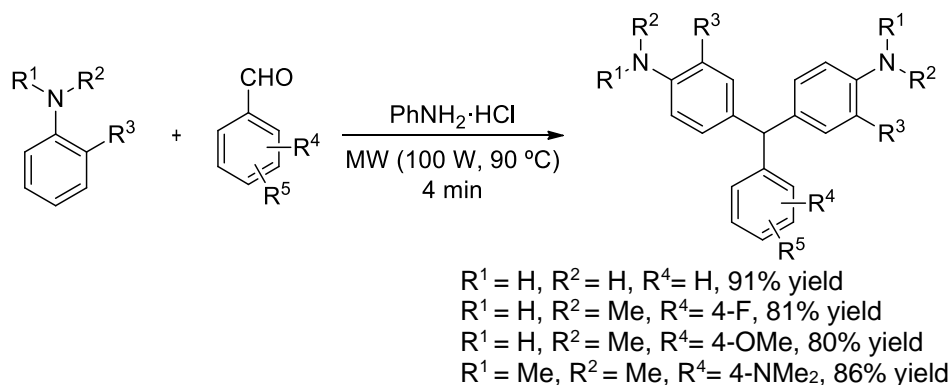
Jafarpour and Bardajee reported the synthesis of diaminotriarylmethane derivatives with dimethylamino functional groups. These compounds were synthesized by the tandem regio-selective electrophilic aromatic substitution reaction of *N,N*-dimethylaniline with aryl aldehydes to form the corresponding diaminotriarylmethane compounds, using $\text{Bi}(\text{NO}_3)_3$ as a catalyst under solvent free conditions to afford the desired products in good to excellent yields (**Scheme III.40**).²¹⁸



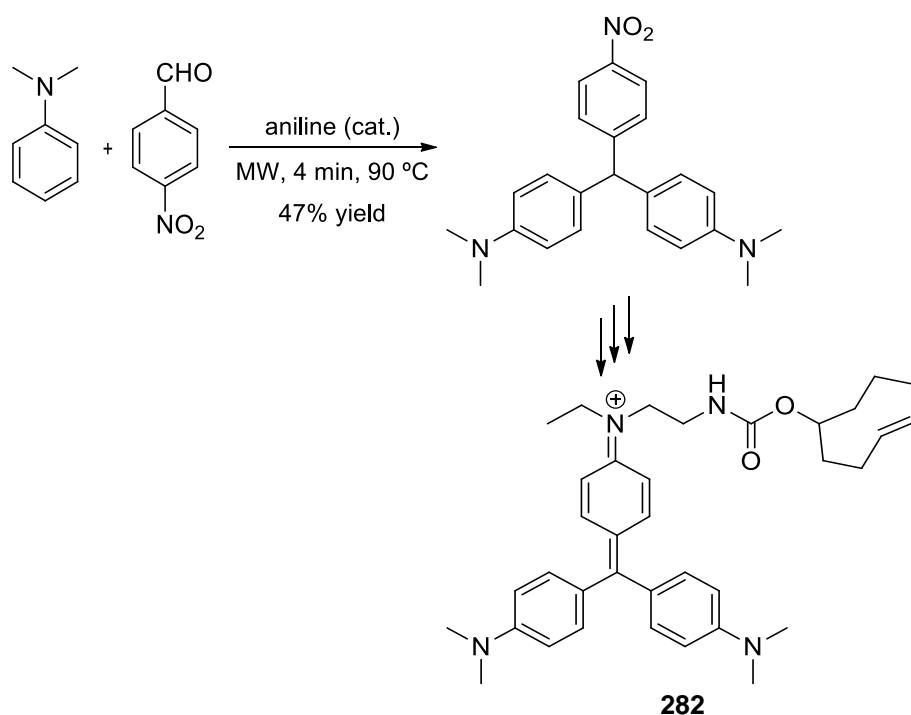
Scheme III.40. $\text{Bi}(\text{NO}_3)_3 \cdot 5\text{H}_2\text{O}$ -mediated synthesis of 4,4'-diaminotriarylmethane leuco malachite compounds under solvent-free conditions.²¹⁸

Several other research groups described the synthesis of triarylmethanes in solvent-free conditions. Rahmdel *et al.* in 2009 reported the versatile and solvent-free synthesis of diaminotriarylmethanes by treating *N,N*-dimethylaniline with some arylaldehydes over 30 mol% of zirconium(IV) oxide chloride ($\text{ZrOCl}_2 \cdot 8\text{H}_2\text{O}$).²¹⁹ Bardajee in 2011 reported the simple, efficient, and mild procedure for a solvent-free one-step synthesis of various diaminotriarylmethane derivatives in the presence of antimony trichloride as catalyst.²²⁰

In a different approach, Martínez-Palou *et al.* reported a fast, efficient and versatile route for the synthesis of diaminotriphenylmethanes under microwave irradiation and aniline hydrochloride as catalyst (**Scheme III.41**).²²¹ In this reported is described one of the very few examples of the use of secondary anilines, giving an 81% yield.²²¹ Later, a variation of this method with aniline as catalyst was used by Weissleder *et al.* in the synthesis of crystal violet-*trans*-cyclooctene (**Scheme III.42**).²²²



Scheme III.41. Microwave-assisted synthesis of diaminotriphenylmethanes.²²¹



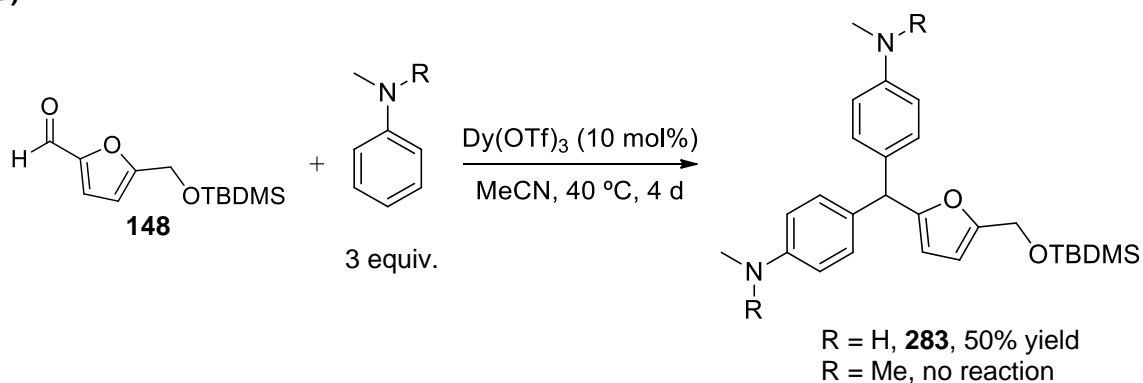
Scheme III.42. Synthesis of crystal violet *trans*-cyclooctene (**282**).²²²

III.3.2. Results and Discussion

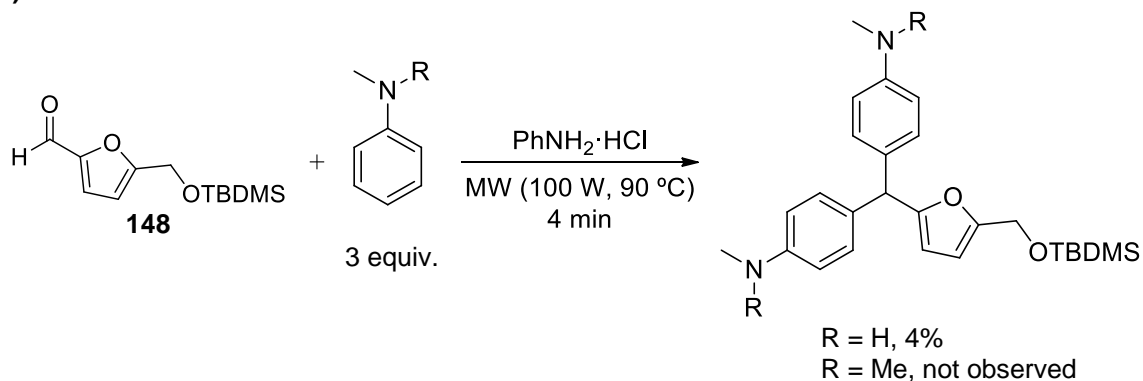
As mentioned in **Section III.2**, when secondary anilines were used as amines under the optimized bisvinylogous Mannich reaction conditions, the unexpected formation of triarylmethanes derivatives were observed. For *N*-methylaniline, the corresponding triarylmethane **283** was obtained in a moderate yield (50%), whereas employing the more C-nucleophilic *N,N*-dimethylaniline under the same reaction conditions, no reaction took place (**Scheme III.43a**). This observation was very intriguing due to the lack of literature examples regarding triarylmethanes bearing secondary anilines, leading us to believe that the current methods for TRAM formation are mainly limited to tertiary anilines. In fact, following the reported conditions for the microwave-assisted synthesis of triarylmethanes

catalyzed by $\text{PhNH}_2\cdot\text{HCl}$, led to a very low yield (4%) for the reaction of **148** and *N*-methylaniline (**Scheme III.43b**).²²¹ Furthermore, no reaction was observed using *N,N*-dimethylaniline (**Scheme III.43b**). Because is described good results for substituted benzaldehyde derivatives (**Scheme III.41**), is believed that 5- substituted furfurals are less reactive through TRAM formation. Intriguingly, reaction with benzaldehyde gave again no product with *N,N*-dimethylaniline and 50% yield for the reaction with *N*-methylaniline, concluding that the microwave-assisted reaction conditions are quite specific for activated aldehydes (**Scheme III.43c**). Motivated by these interesting results and taking into account the potential biological activity of triarylmethanes we became interested in studying this reaction in more detail.

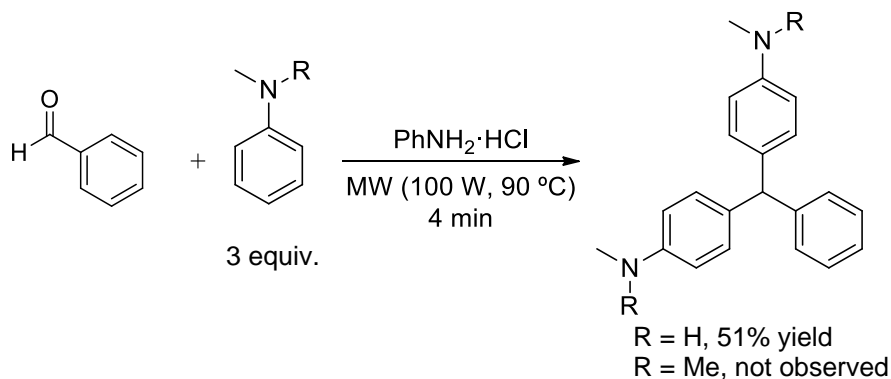
a)



b)



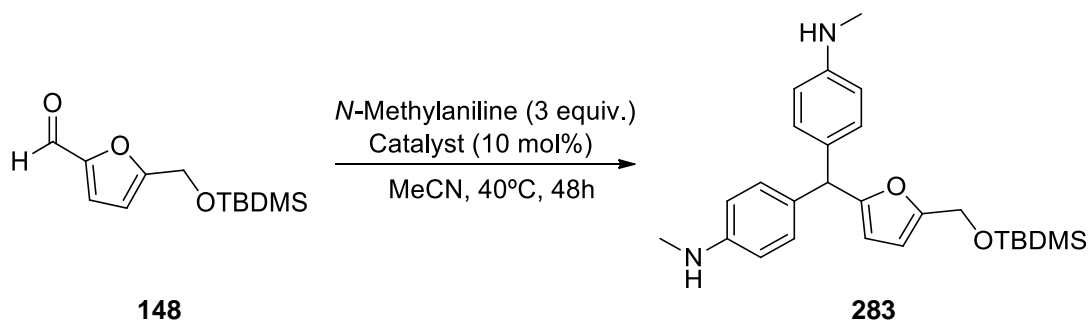
c)



Scheme III.43. Preliminary results on triarylmethanes formation.

The initial screening with aldehyde **148**, *N*-methylaniline and diverse Lewis acids (**Table III.9**) revealed that Yb(OTf)₃, LaCl₃·7H₂O and AlCl₃ are the most suitable catalysts for this transformation, giving up to 82% yield of **283** and full conversion of **148** (**Table III.9**, entries 17-19). Under the same reaction conditions the protic acid *p*TSOH only provided 33% yield (**Table III.9**, entry 13). After extensive reaction conditions optimization studies, LaCl₃·7H₂O and AlCl₃ were not further studied because unreproducible results were obtained probably due to the heterogeneity or uncontrolled degree of moisture. In fact, the formation of by-product **284** resulting from the deprotection of the silyl ether was taking place explaining the discrepancy between the conversion and the yield. In addition, it is noteworthy the fact that the reaction in the absence of any catalyst gave 50% of conversion of **148** together with no yield of the desired product, which suggest the existence of an intermediate (**Table III.9**, entry 1).

Table III.9. Catalyst screening for the reaction of **148** with *N*-Methylaniline.

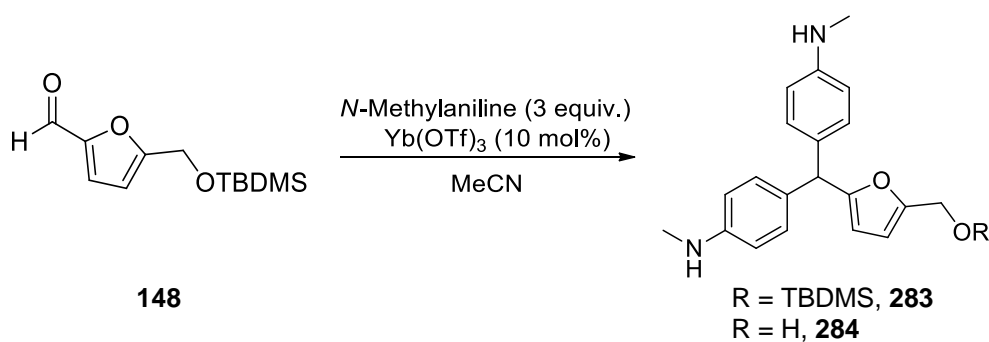


Entry	Catalyst	Conversion (%) ^a	Yield (%) ^a
1	-	50	NO
2	BaCl ₂	52	NO
3	Ti(O ⁱ Pr) ₄	50	NO
4	FeCl ₃ ·6H ₂ O	93	Traces
5	RuCl ₃ ·xH ₂ O	94	6
6	NiCl ₂	60	12
7	Dy(OTf) ₃	91	15
8	ZnI ₂	55	17
9	AgOTf	61	19
10	CeCl ₃	63	24
11	ZrCl ₄	76	26
12	CoCl ₂ ·6H ₂ O	58	29
13	<i>p</i> TSOH	67	33
14	Cu(OTf) ₂	67	41
15	GdCl ₃ ·6H ₂ O	88	50
16	ZrCl ₄	82	52
17	Yb(OTf) ₃	100	61
18	LaCl ₃ ·7H ₂ O	100	72
19	AlCl ₃	94	82

^aDetermined by HPLC analysis of crude reaction mixture.
NO = Not observed by HPLC analysis.

After extensive reaction conditions optimization, namely temperature, time and concentration, we were very pleased to find that carrying the reaction for 34 h at 40 °C in 0.1 M acetonitrile offered the product in a quantitative yield (**Table III.10**, entry 6). Formation of by-product **284** was observed under harsher conditions, resulting in a lower yield of **283** (**Table III.10**, entries 3 and 4). This deprotection is believed to occur once the triarylmethane **283** is formed because no HMF was observed in the reaction medium. In fact, by subjecting triarylmethane **283** to the optimized reaction conditions led to the formation of the deprotected product **284** (**Scheme III.44**), showing the importance of the reaction time control.

Table III.10. Reaction conditions optimization using Yb(OTf)₃ as catalyst.



Entry	Conc. (M)	time (h)	T (°C)	Yield (%) ^a
1	0.1	48	40	61 (60 ^b)
2	0.1	24	40	53
3	0.1	24	50	45 ^c
4	0.1	24	60	25 ^c
5	0.1	32	40	81
6	0.1	34	40	100 (98 ^b)
7	0.05	27	40	57
8	0.2	30	40	62

^aDetermined by HPLC analysis of crude reaction mixture. ^bIsolated yield after purification by column chromatography. ^cDeprotected product **284** detected by TLC analysis of crude reaction mixture.



Scheme III.44. Triarylmethane **283** stability experiment under the reaction conditions.

Reaction of HMF with *N*-methylaniline catalyzed by Yb(OTf)₃ also smoothly produced the corresponding triarylmethane **284** (Table III.11, entry 1). Gratifyingly, decreasing the reaction time to 28 h further increased the yield to 91% (Table III.11, entry 2). Subsequently, a number of aryl aldehydes were used in the reaction with *N*-methylaniline catalyzed by Yb(OTf)₃ under the same reaction conditions. As summarized in Table III.11, 5-substituted furfurals bearing hydroxyl protecting groups are well tolerated, and the corresponding triarylmethanes were generally obtained in good yields (Table III.11, entries 3-5). In addition, *p*-substituted benzaldehydes also produced the triarylmethanes derivatives, however longer times were needed to achieve higher conversions of the starting aldehyde (Table III.11, entries 6-9). Salicylaldehyde showed lower reactivity under the same reaction conditions giving the corresponding triarylmethane in 30% yield (Table III.11, entry 10). Unfortunately, more sluggish reaction was observed for 5-methylfurfuraldehyde (Table III.11, entry 11).

Table III.11. Scope of the aldehydes.

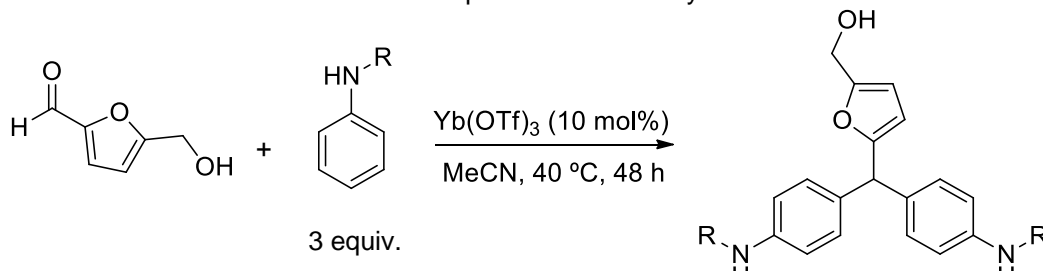
284-293

Entry	ArCHO	t (h)	Product	Yield (%) ^a
1	R = H	48	284	60
2	R = H	28	284	91
3	R = Ac	28	285	91
4	R = Bz	28	286	80
5	R = Bn	28	287	56
6	R = H	48h	288	68
7	R = 4-Me	48h	289	65
8	R = 4-OMe	48h	290	50
9	R = 4-NO ₂	48h	291	97
10	R = 2-OH	48h	292	30
11		48	293	6

^aIsolated yield after purification by column chromatography.

Next, the substrates scope of anilines in the reaction with HMF catalyzed by $\text{Yb}(\text{OTf})_3$ was studied (**Table III.12**). Secondary anilines bearing benzyl or alkyl substituents reacted to give the corresponding triarylmethanes in low yields (**Table III.12**, entries 2-4). Diphenylamine did not react with HMF even at reflux acetonitrile.

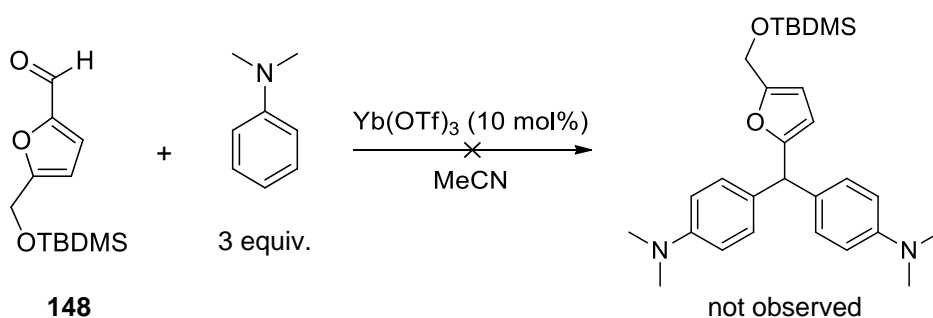
Table III.12. Scope of the secondary anilines



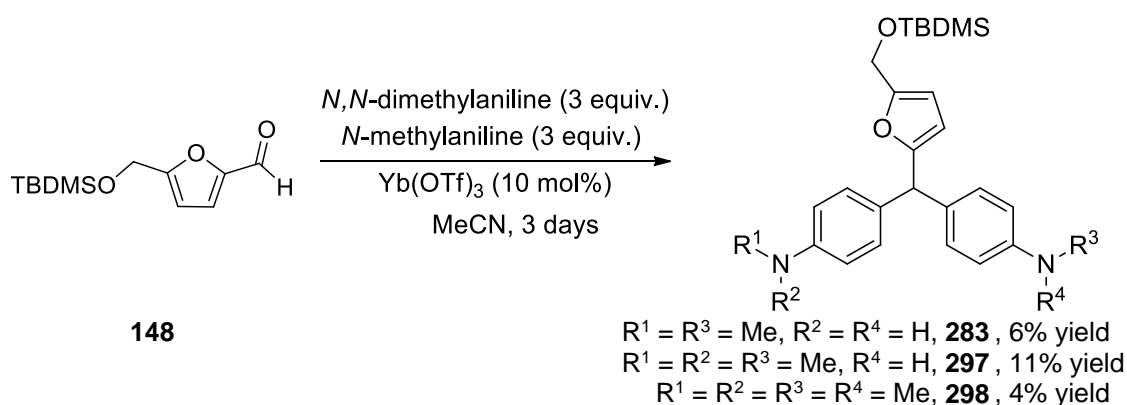
121		294-296	
Entry	R	Product	Yield (%) ^a
1	Ph		NR
2	CH_2Ph	294	20
3	CH_2Cy	295	14
4	Cy	296	NR

^aIsolated yield after purification by column chromatography. NR – No reaction. Cy = cyclohexyl.

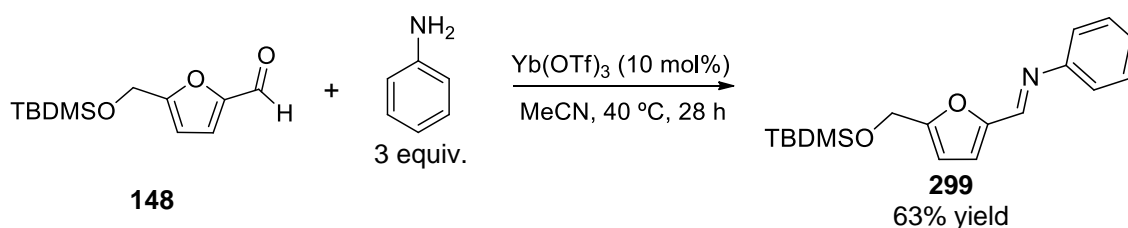
In addition, as mentioned above, tertiary aniline *N,N*-dimethylaniline did not react in our reaction conditions (**Scheme III.45**). It was hypothesized that an iminium ion could be an intermediate of the reaction, thus a catalytic amount of *N*-methylaniline in the reaction of **148** and *N,N*-dimethylaniline could lead to the desired product, however once again no reaction took place. Nevertheless, a competitive reaction between *N*-methylaniline and *N,N*-dimethylaniline (3.5:3 equivalents) led to the isolation of the three possible products as despite in **Scheme III.46**. Furthermore, simple aniline did not give the desired product, yielding imine **299** in 63% yield after 28 h (**Scheme III.47**).



Scheme III.45. Reaction of *N,N*-dimethyl aniline with **148** catalyzed by $\text{Yb}(\text{OTf})_3$.

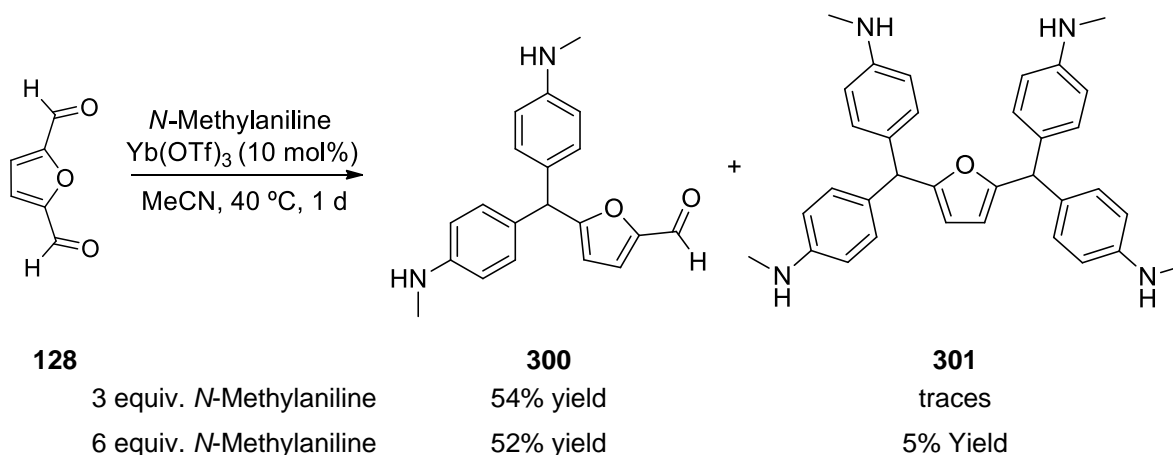


Scheme III.46. Reaction of N,N -dimethyl aniline and N -methylaniline with **148** catalyzed by $\text{Yb}(\text{OTf})_3$.



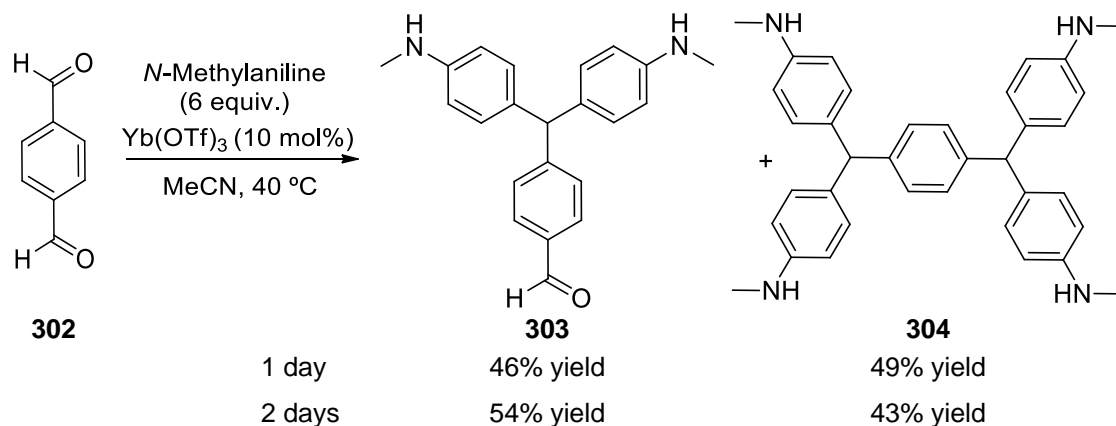
Scheme III.47. Reaction of aniline with **148** catalyzed by $\text{Yb}(\text{OTf})_3$.

The more challenging substrates terephthalaldehyde (**302**) and 2,5-diformylfuran (**128**) were also study as arylaldehydes for triarylmethane formation. Reaction of 2,5-diformylfuran (**128**) reacted smoothly to selectively produce the mono-triarylmethane **301** even when 6 equivalents of N -methylaniline was used (**Scheme III.48**). Furthermore, increasing the reaction time to 2 days led to a very complex mixture with only traces of the product suggesting decomposition.



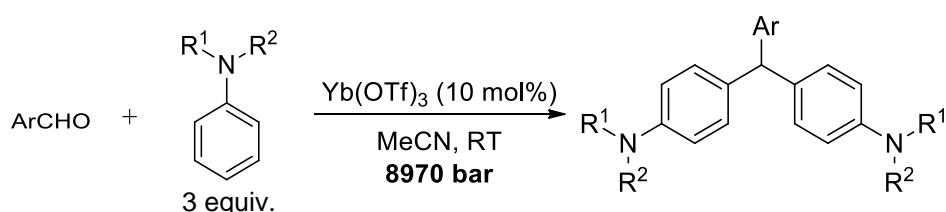
Scheme III.48. Reaction of 2,5-diformylfuran (**128**) with N -methylaniline catalyzed by $\text{Yb}(\text{OTf})_3$.

Interestingly, when terephthalaldehyde was subjected to the same reaction conditions using 6 equivalents of *N*-methylaniline, an unselective reaction occurred to yield the corresponding mono- (**303**) and bis-triarylmethane (**304**) as depicted in **Scheme III.49**.



Scheme III.49. Reaction of terephthalaldehyde (**302**) with *N*-methylaniline catalyzed by Yb(OTf)₃.

We envisioned that formation of triarylmethanes, being a condensation reaction, could occur by a decrease in the activation volume and consequently be accelerated by extreme high-pressure (see Section III.1.2). Remarkably, the reaction of HMF (**121**) with *N*-methylaniline catalyzed by Yb(OTf)₃ was extremely accelerated at 8970 bar, yielding the corresponding product in 86% after only 30 min reaction at RT (**Table III.13**, entry 4). Moreover, performing the same reaction at normal pressure resulted in only traces of the product. Unfortunately, for the reaction with **148**, formation of the TBDMS deprotected product **284** was again observed, being minimized for 1 h reaction time, which gave 60% yield of the desired product **283** together with 20% of **284** (**Table III.13**, entries 5-7). It is believed that the formation of this deprotected product can be suppress by reaction time optimization. Gratifyingly, the reaction with other arylaldehydes was also accelerated in this conditions as summarized in **Table III.13**. Several alcohol protecting groups of HMF were well tolerated offering the corresponding triarylmethane in 79 to 90% yield (**Table III.13**, entries 8-11). Substituted benzaldehydes also smoothly reacted to yield the corresponding products in up to 94% yield (**Table III.13**, entries 15-19). Finally, secondary anilines *N*-benzylaniline and *N*-cyclohexylmethylaniline offered 84% and 31% yield of the corresponding triarylmethanes, respectively. As observed for the reaction at normal pressure, *N*-cyclohexylaniline and diphenylamine did not react under this conditions (**Table III.13**, entries 20-23).

Table III.13. Extreme high pressure induced reaction

Entry	ArCHO	R ¹	R ²	t (h)	Product	Yield (%) ^a
1	121	H	CH ₃	8	284	92 [40]
2	121	H	CH ₃	4	284	90
3	121	H	CH ₃	1	284	90
4	121	H	CH ₃	0.5	284	86 [traces]
5	148	H	CH ₃	4	283	53 ^b
6	148	H	CH ₃	1	283	60 + 20 ^c
7	148	H	CH ₃	0.5	283	30 ^d
8	149	H	CH ₃	1	290	82
9	151	H	CH ₃	1	291	90
10	147	H	CH ₃	1	292	86
11	146	H	CH ₃	1	305	79
12	128	H	CH ₃	4	300	NO
13	128	H	CH ₃	1	300	NO
14	128	H	CH ₃	0.5	300	41
15	PhCHO	H	CH ₃	1	288	50
16	4-Me-PhCHO	H	CH ₃	1	289	88
17	4-OMe-PhCHO	H	CH ₃	1	290	80
18	4-NO₂-PhCHO	H	CH ₃	1	291	94
19	2-OH-PhCHO	H	CH ₃	1	292	78
20	121	H	CH ₂ Ph	8	294	84
21	121	H	CH ₂ Cy	8	295	31
22	121	H	Cy	8	-	NO
23	121	H	Ph	4	-	NO
24	121	CH ₃	CH ₃	8	306	42

^aIsolated yield after purification by column chromatography. In brackets is showed the yield obtained by performing the reaction at atmospheric pressure for the same time. ^bThe TBDMS deprotected product **284** observed by TLC analysis but not quantified. ^cIsolated yield of TBDMS deprotected product **284**. ^dTBDMS deprotected product **284** was not detected. NO = Not observed by preparative chromatography. Cy = cyclohexyl.

To gain insights into the mechanism of the transformation, the reaction of **148** with *N*-methylaniline in acetonitrile-*d*₃ catalyzed by Yb(OTf)₃ was followed by ¹H NMR (**Figure III.18**). Although the reaction was very slow and no full conversion was observed after 4 days, possible intermediates were observed as depicted in **Figure III.18** (the chemical

shifts are in agreement with similar structures from iminium-ions²²³ and tertiary anilines²²⁴). Unfortunately the full characterization of the intermediates was not possible since there are no stable in silica and were not detected in GC-MS analysis.

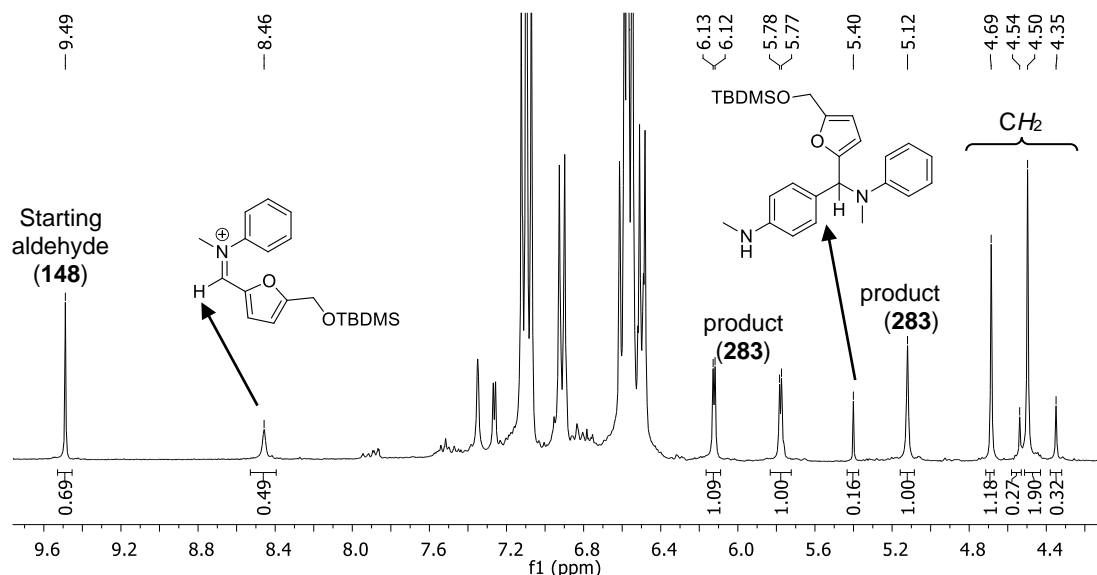
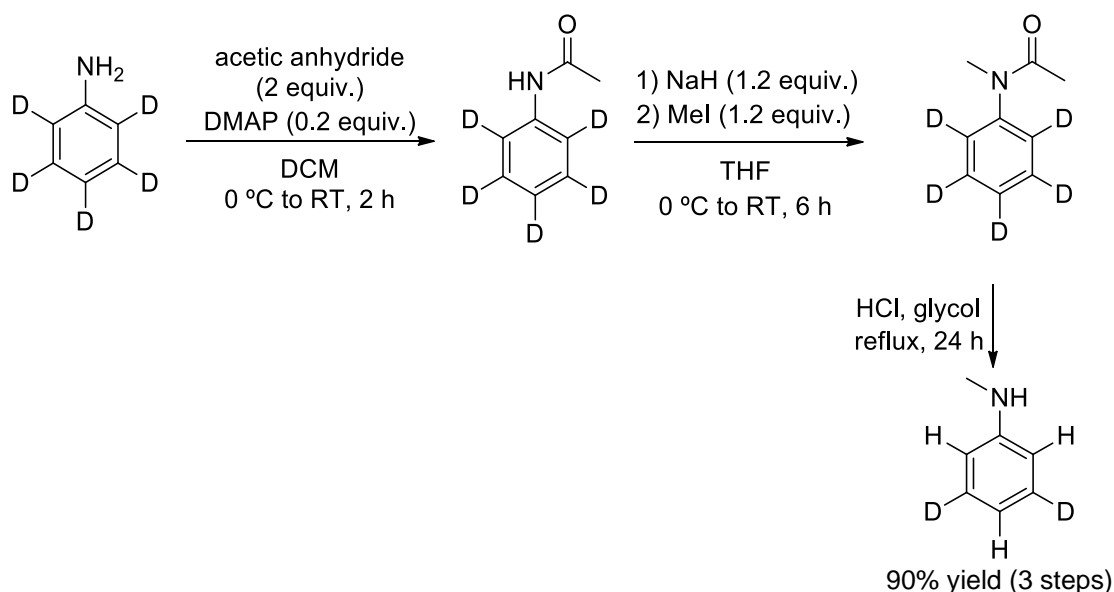


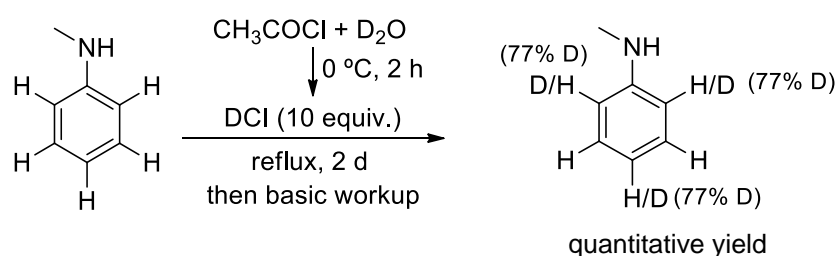
Figure III.18. ¹H NMR spectrum of the crude reaction mixture of **148** with *N*-methylaniline in acetonitrile-*d*₃ (Complete data is in experimental part).

Considering this Yb(III)-catalyzed transformation includes C-H break steps, it was proposed to study the kinetic isotope effect (KIE) to probe the mechanism, therefore, deuterated aniline derivative was required. Because aniline-*d*₆ is commercial available, it was planned to prepare *N*-methylaniline-2,3,4,5,6-*d*₅ by mono methylation methods. Unfortunately, following reported one-step procedures for the selective mono-*N*-alkylation of anilines, such as MeI/ILs²²⁵ and Ph₃P/DDQ,²²⁶ offered a mixture of mono- and di-alkylation products. Next, a three step reported protocol, comprising acetylation, alkylation and acetyl removal,²²⁷ was performed. Although the selective mono-*N*-alkylation was achieved in quantitative yield, complete D/H exchange of the *ortho* and *para* positions was observed for the final product (**Scheme III.50**).



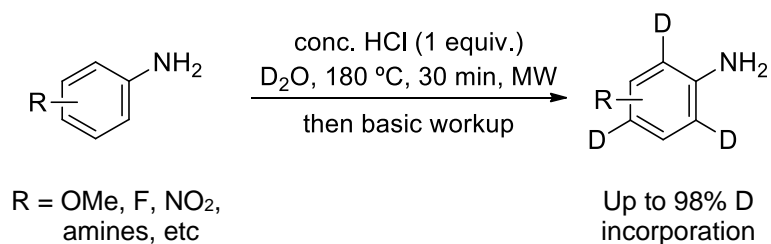
Scheme III.50. Alkylation of aniline-2,3,4,5,6-d₅ following reported 3-steps protocol.²²⁷

Based on this result, *N*-methylaniline-2,4,6-d₃ was prepared by H/D exchange using DCl prepared *in situ* by reaction of acetyl chloride and D₂O. The desired product was obtained with a 77% D incorporation after 2 days (**Scheme III.51**).



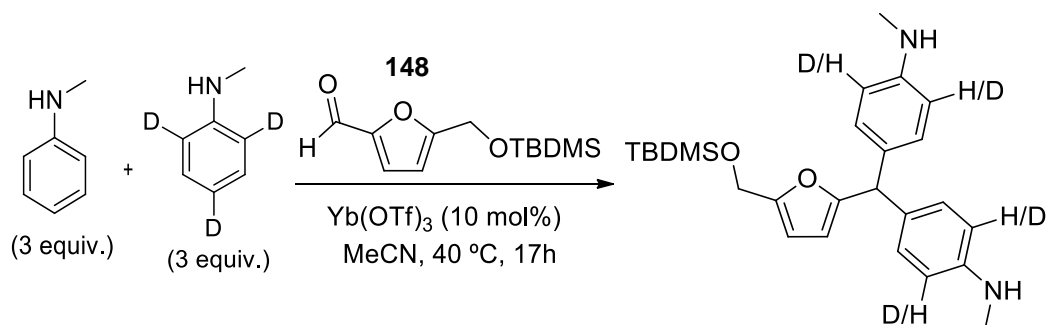
Scheme III.51. Preparation of *N*-methylaniline-d₃.

In fact, further literature study revealed that anilines can undergo H/D exchange in acidic conditions.²²⁸ In particular, Lautens *et al.* reported in 2008 a highly effective regioselective deuteration of anilines at the *ortho* and *para* positions with respect to the nitrogen in the presence of 1 equiv. of HCl (0.2 M) in D₂O (**Scheme III.52**).²²⁹ Interestingly, the authors emphasize the need of microwave irradiation, as conventional heating did not afford comparable degrees of deuteration.

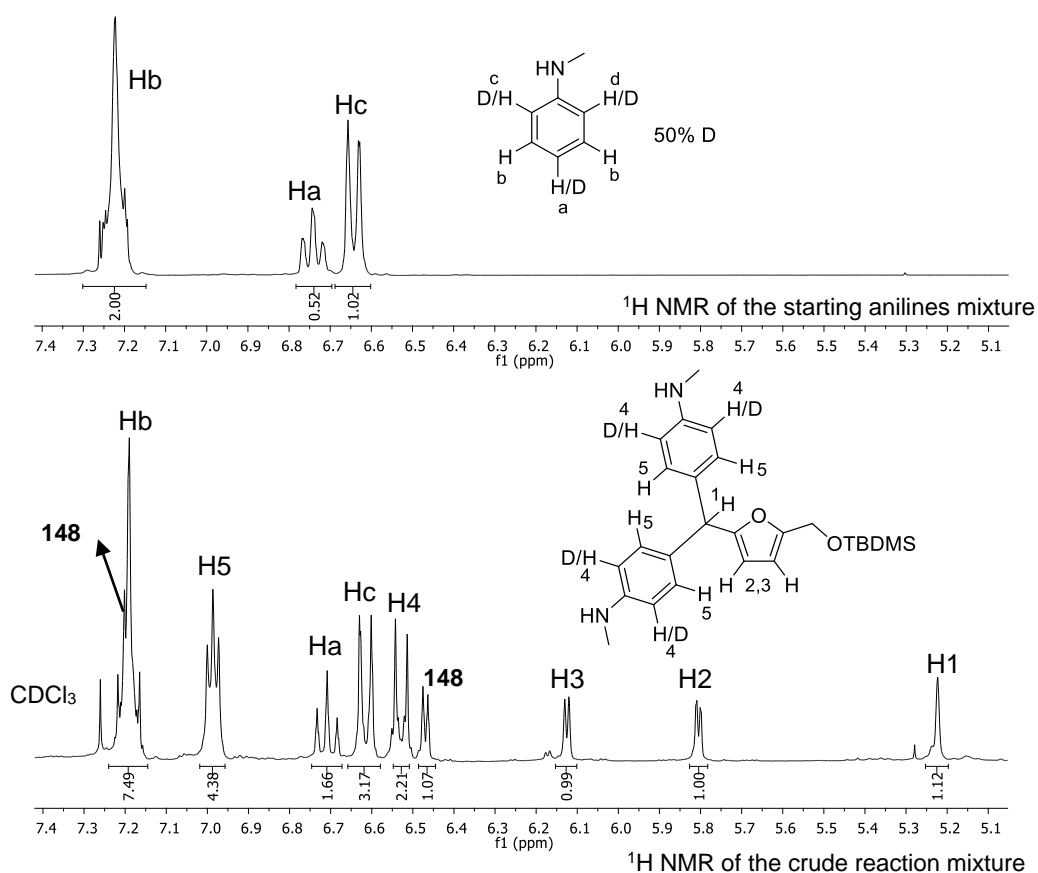


Scheme III.52. Regioselective deuteration of anilines in the presence of 1 equiv. of conc HCl in D₂O.²²⁹

With the desired deuterated aniline in hands, KIE study was conducted by submitting a 1:1 mixture of *N*-methylaniline and *N*-methylaniline-2,4,6-d₃ to intermolecular competition experiment (**Scheme III.53**).²³⁰ The observed absence of an isotope effect (KIE = 1.02) shows that C-H bond cleavage does not occur during the rate-determining step (RLS).²³⁰ In fact, it is known from the text books that the attack of the aryl moiety is the RLS in the Friedel-Crafts reactions.

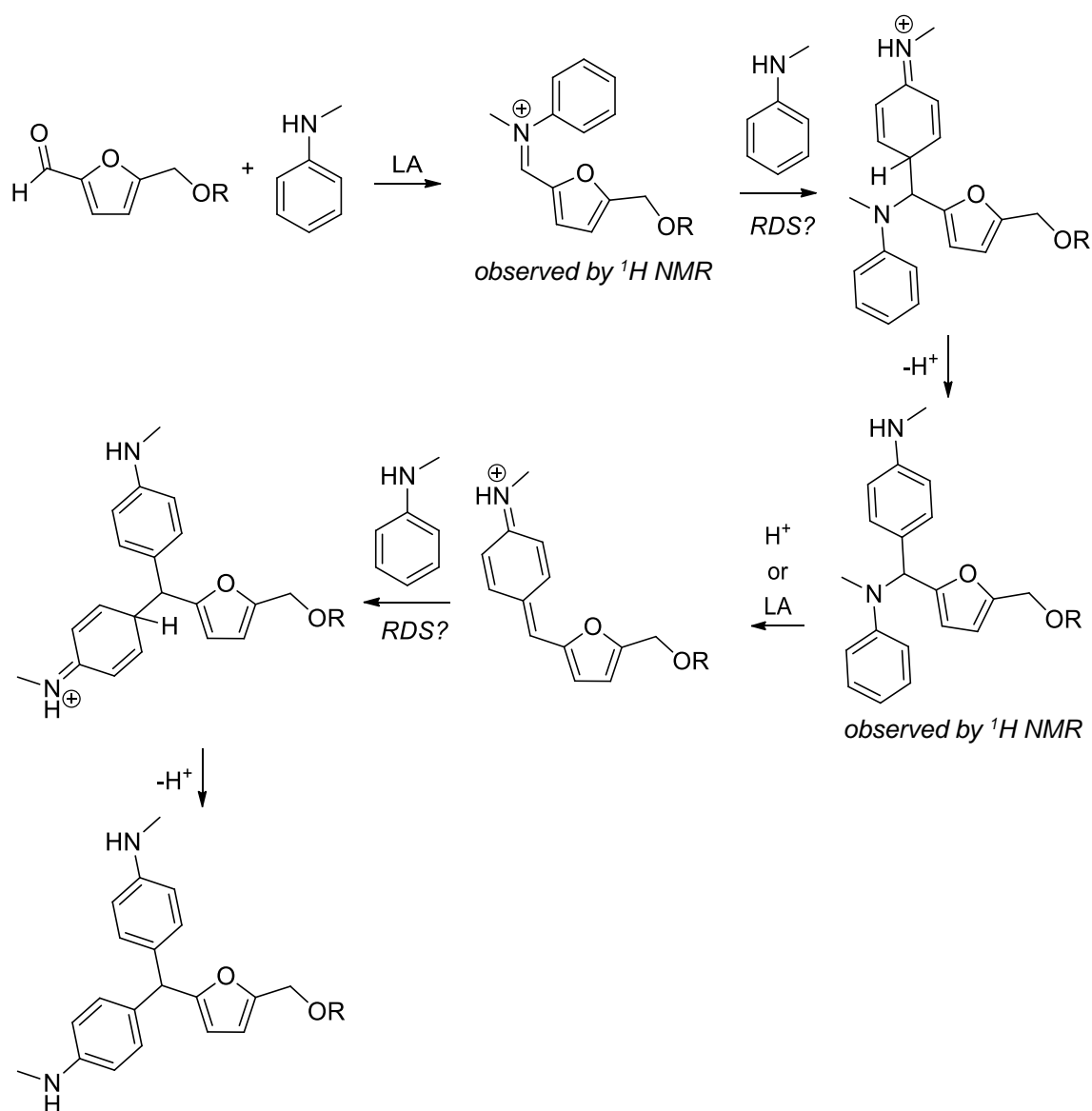


$$\text{KIE} = \frac{P_H}{P_D} = \frac{A(\text{H4})}{A(\text{H5}) - A(\text{H4})} = \frac{2.21}{(4.38 - 2.21)} = 1.02$$



Scheme III.53. Intermolecular competition reaction of *N*-methylaniline and *N*-methylaniline-2,4,6- d_3 for kinetic isotope effect study.

On the basis of these experimental results, a plausible mechanism for the reaction of 5-substituted furfurals with secondary anilines is proposed in **Scheme III.54**. DFT calculations are now under investigation and will be reported in due time.

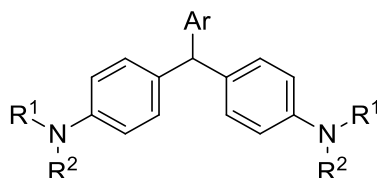


Scheme III.54. Proposed mechanism for triarylmethanes formation.

This unprecedented family of triarylmethanes was evaluated, by the team member Dr. Raquel F. M. Frade, for their antiproliferative activity towards human cancer cell lines from colon (HT-29), lung (NCI-H460) and breast (MCF-7) origin (**Table III.14**). Triarylmethanes bearing HMF derivatives did not show relevant activity when the aldehyde, the free alcohol, or acyl and benzyl O-protecting groups were present (**Table III.14**, entries 1-4). On the other hand, remarkable activity against all the three cell lines tested was observed for ether protective groups, in particular, for silyl ether protective groups (**Table III.14**, entries 5-7). Introduction of a bulky group in the secondary aniline instead of a methyl group, resulted in an important activity enhancing for HMF-containing triarylmethanes (**Table III.14**, entries 8-9). Furthermore, triarylmethane bearing HMF and *N,N*-dimethylaniline did not show activity against the tested cell lines. Interesting, great selectivity towards HT-29 cell line was observed for the triarylmethane bearing a phenyl

group and two *N*-methylanilines (**Table III.14**, entry 11). From the others triarylmethanes synthesized from substituted benzaldehydes, an outstanding activity was observed when 4-methylbenzaldehyde was used, with an IC₅₀ of 1.74 µM against HT-29 (**Table III.14**, entry 13).

Table III.14. Biological activity of the new synthesized triarylmethanes.



Entry	Ar	R ¹	R ²	Compound	IC ₅₀ (µM) ± SD		
					NCI-H460	MCF-7	HT-29
1	HOCH ₂ Furyl	H	CH ₃	284	> 20	> 20	> 20
2	AcOCH ₂ Furyl	H	CH ₃	285	> 20	> 20	> 20
3	BzOCH ₂ Furyl	H	CH ₃	286	> 20	ND	> 20
4	CHO ₂ Furyl	H	CH ₃	300	> 20	> 20	> 20
5	BnOCH ₂ Furyl	H	CH ₃	287	8.2±1.6	10.3±1.1	4.76±2.96
6	TBDMSOCH ₂ Furyl	H	CH ₃	283	5.0±1.1	7.69±1.31	5.8±1.2
7	TIPSOCH ₂ Furyl	H	CH ₃	307	5.28±2.70	7.58±1.24	4.38±1.09
8	HOCH ₂ Furyl	H	CyCH ₂	295	4.84±1.23	5.94±1.02	5.37±1.16
9	HOCH ₂ Furyl	H	Bn	294	4.29±1.35	4.84±1.23	3.58±1.23
10	HOCH ₂ Furyl	CH ₃	CH ₃	306	> 15	> 15	> 15
11	Ph	H	CH ₃	288	> 20	> 20	5.1 ±3.3
12	CHOPh	H	CH ₃	303	> 20	> 20	> 20
13	4-Me-Ph	H	CH₃	289	> 20	7.81±1.02	1.74±2.32
14	4-MeO-Ph	H	CH ₃	290	> 15	12.44±1.11	12.80±1.12
15	4-NO ₂ -Ph	H	CH ₃	291	> 20	12.08±1.04	7.97±3.13
16	2-OH-Ph	H	CH ₃	292	> 15	> 15	> 15
17	4-((4-NHMe-Ph) ₂)-Ph	H	CH ₃	304	> 20	> 20	> 20

SD = standard deviation; HT-29 = human colorectal adenocarcinoma cell line; NCI-H460 = human non-small cell lung cancer cells; MCF-7 = breast cancer cell line; Bn = benzyl; Bz = benzoyl; Cy = Cyclohexyl.

Compounds **283**, **286**, **287** and **288** were also tested for their *in vitro* antibacterial activity, but no promising results were obtained. This study was carried out using Gram-positive bacteria (S.a. - *Staphylococcus aureus* ATCC 25923, MRSA (Methicillin-resistant *Staphylococcus aureus*, B.s.- *Bacillus subtilis* ATCC 6633, E.f. - *Enterococcus faecalis* ATCC 29212 and vancomycin-resistant enterococci (VRE)- isolated strain), Gram-negative bacteria (E.c. - *Escherichia coli* ATCC 25922, P.a. - *Pseudomonas aeruginosa* ATCC 27853 and K.p. - *K. pneumonia* ATCC 9997).

III.3.3. Conclusions

In conclusion is described a mild and efficient synthesis of triarylmethanes bearing secondary anilines by Friedel-Crafts reaction of (hetero)aryl aldehydes and the corresponding secondary anilines catalyzed by ytterbium(III) triflate. In addition we have demonstrated that extreme high pressure (8970 bar) has a significant effect on the rate of the catalytic Friedel-Crafts alkylation. Several triarylmethanes were synthesized in 50-94% yield in 1 hour at RT and 8970 bar. Remarkably, some of the triarylmethanes presented important antiproliferative activity against cancer cell lines, especially from colon origin (HT-29).

III.4. Experimental

III.4.1. General Methods

All solvents were freshly dried and distilled before use. All reactions were performed in flame dried glassware under argon atmosphere otherwise notice. Commercially available reagents were used as received without further purification otherwise notice. 3,3'-bis(2,4,6-triisopropylphenyl)-2,2'-binaphtholate ((*R*)-TRIP) was kindly provided by Prof. Dr. Benjamin List.

Flash column chromatography was carried out on silica gel 60M purchased from MN (Ref. 815381). Reaction mixtures were analyzed by TLC using ALUGRAM SIL G/UV254 from MN (Ref. 818133, silica gel 60), and visualization by UV and phosphomolybdic acid stain. NMR spectra were recorded at room temperature in a Bruker AMX 300 or Bruker AMX 400 using CDCl₃, D₂O or DMSO-d₆ as solvents and (CH₃)₄Si(¹H) as internal standard. All coupling constants are expressed in Hz. Electrospray ionization (ESI) mass spectra were recorded in a mass spectrometer (Micromass Quattro Micro API, Waters, Ireland) with a Triple Quadrupole (TQ) and with an electrospray ion source operating in positive mode. Elemental analysis was performed in a Flash 2000 CHNS-O analyzer (ThermoScientific, UK).

HPLC analysis was performed on a VWR Hitachi apparatus with a diode array detector L-2455 coupled to a pump L-2130 and using a KROMASIL 100 SIL 5.0 column, manual injector with 20 µL loop. Mobile phase gradient from 100:0 to 98:2 in 30 min hex/2-propanol, flow 1 mL/min.

GC-MS analyses were performed on Gas Chromatograph Mass Spectrometer-QP2010S, Shimadzu by using the column TRB-5MS-Teknokroma (30 m × 0.25 mm × 0.25 µm). GC program: column oven $T_{\text{initial}} = 50.0\text{ }^{\circ}\text{C}$, $T_{\text{final}} = 250.0\text{ }^{\circ}\text{C}$, slope = 5 °C/min; injection temperature: 250 °C; pressure: 77.9 kPa, total flow: 17.7 mL/min; column flow: 1.34 mL/min; linear velocity: 42.0 cm/sec; purge flow: 3.0 mL/min split ratio: 10.0, high press. inj. pressure: 100.0 kPa, high press. inj. time: 1.00 min. MS program: start time: 3.00 min; end time: 50.00 min; event time: 0.50 s; scan speed: 666; start: $m/z = 40.00$; end: $m/z = 350.00$.

The preparation of HMF derivatives are described in **Section II.4**.

Antibacterial studies was performed by Dr. Patrícia Rijo from Universidade Lusófona.

High pressure reactions were performed in a 4 mL Teflon ampoules in a Liquid pressure vessel LV 30/16 coupled to a laboratory hydraulic press U101 from High pressure center, Polish Academy of Sciences. The pressure inside the vessel (P_v) is related to the pressure from the press according to the following expression: $P_v [\text{MPa}] = 3.9 \times P_p [\text{bar}]$.

Computational Details

All calculations were performed using the Gaussian 09 software package.²³¹ The optimized geometries were obtained using B3LYP²³² functional and a standard 6-31G(d,p) basis set,²³³⁻²³⁷ without symmetry constraints. B3LYP functional includes the Becke three parameter hybrid functional devised by Becke in 1993²³² and the correlation functional LYP of Lee, Yang, and Parr, which includes both local and non-local terms²³⁸⁻²³⁹. Transition state optimizations were performed with the Synchronous Transit-Guided Quasi-Newton Method (STQN) developed by Schlegel *et al.*,²⁴⁰⁻²⁴¹ following extensive searches of the potential energy surface. Frequency calculations were performed to confirm the nature of the stationary points, yielding one imaginary frequency for the transition states and none for the minima. Each transition state was further confirmed by following its vibrational mode downhill on both sides and obtaining the minima presented on the energy profile. Single point energy (E2) calculations were performed using M06-2X functional and the 6-311++G(d,p)²⁴²⁻²⁵⁰ basis set, with solvent effects (acetonitrile) calculated by means of the Polarizable Continuum Model (PCM) initially devised by Tomasi and coworkers,²⁵¹⁻²⁵⁴ with radii and non-electrostatic terms of the SMD solvation model, developed by Truhler *et al.*²⁵⁵ M06-2X is a hybrid meta-GGA functional developed by Truhlar and Zhao,²⁵⁶ and it was shown to perform very well for main-group kinetics, providing a good description of long range effects such as van der Waals interactions or π – π stacking.²⁵⁷⁻²⁵⁸ The electronic energies (E_1) obtained at the B3LYP/6-31G(d,p) level of theory were converted to free energy at 298.15 K and 1 atm (G_1) by using zero point energy and thermal energy corrections based on structural and vibration frequency data calculated at the same level. The free energy values presented along the text (G_2^{soln}) were derived from the electronic energy values obtained at the M06-2X/6-311++G(d,p)//B3LYP/6-31G(d,p) level, including solvent effects (E_2^{soln}), according to the following expression: $G_2^{\text{soln}} = E_2^{\text{soln}} + G_1 - E_1$.

Biological assays

All the assays were performed by Dr. Raquel F. M. Frade.

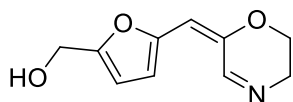
Cell Culture. Human colon adenocarcinoma (CaCo-2 and HT-29), lung cancer (NCI-H460) and breast cancer (MCF-7) cell lines from ATCC were cultivated in RPMI-1640 media supplemented with L- glutamine, 10% fetal bovine serum (FBS) and antibiotic antimycotic solution (A5955, Sigma) and were grown in an incubator with a 5% CO₂ humidified atmosphere and at 37 °C.

Anti-proliferative assay. Each cell line was plated in 96-well plates with a density of approximately 5x10⁴ (NCI-H460), 1x10⁵ (HT-29) and 1,5x10⁵ (MCF-7) cells/mL. Plates were incubated overnight and treated the next day with the samples to be tested. Compounds were pre-dissolved in ethanol and then diluted with the cell culture media with only 0.5% FBS (percentage of organic solvent is <1% (v/v)). Cells were incubated for 48 (or 72) hours with the compounds, media was then removed and cells washed with phosphate buffer saline (PBS). 0.5% FBS fresh cell culture media containing 50 µg/ml neutral red was added to the plate and left for 3 hours. Cells were then washed with PBS and the amount of neutral red retained by the cells extracted and dissolved with an organic solution (19.96 ml distilled water, 20 ml ethanol and 400 µl glacial acetic acid). Plate was gently shake and read at 540 nm in a plate reader. Viability was determined by the ratio of absorbance of treated cells and non-treated cells (control). For each experimental condition, 4 replicates were done. IC₅₀ were determined using GraphPad Prism software.

Toxicity assays. Caco-2 cells were plated in 96-well plates and cultured more 3-days after reaching total confluency whereas CRL-1502 cells were left in the incubator until reaching confluency. Monolayers were incubated with the tested compounds pre-dissolved in ethanol and diluted in the cell culture media with only 0.5% FBS (percentage of organic solvent is 1% (v/v)). Media was removed and cells were washed with phosphate buffer saline (PBS) after 24 hours incubation. Viability was determined likewise described previously. For each experimental condition, 4 replicates were done.

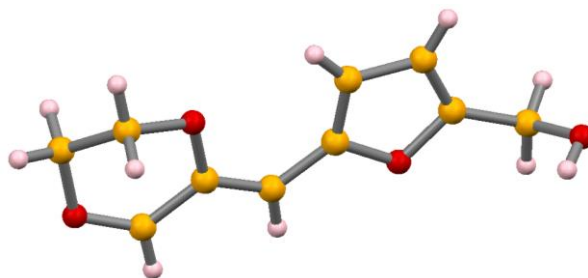
III.4.2. Experimental part for Section III.1.1

Compound 159 (Scheme III.3)



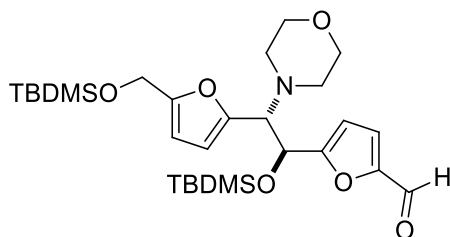
To a solution of HMF **121** (630 mg, 5 mmol) in anhydrous acetonitrile (60 mL), morpholine (4 equiv., 20 mmol) was added followed by the addition of $\text{FeCl}_3 \cdot 6\text{H}_2\text{O}$ (140 mg, 10 mol%) in one portion. The reaction mixture was allowed to stir at 60 °C for 2 days. To the final reaction mixture was added water (100 mL) and extracted with DCM. The combined organic layers were dried over K_2CO_3 , filtered and the solvent removed to give the crude product that was purified by column chromatography (hex/EtOAc from 1:1 to 0:1) to give the impure product (200 mg) that was recrystallized from hex/EtOAc to yield the pure product as a orange solid (66 mg, 8% yield). **^1H NMR (300 MHz, CDCl_3)** δ 2.37 (bs, 1H), 3.81 (m, 2H), 4.14 (t, $J = 4.89$ Hz, 2H), 4.62 (s, 2H), 5.80 (s, 1H), 6.40 (d, $J = 3.25$ Hz, 1H), 6.76 (d, $J = 3.24$ Hz, 1H), 7.78 (s, 1H). **^{13}C NMR (100 MHz, CDCl_3)** δ 47.9, 57.5, 63.2, 104.5, 110.5, 113.3, 142.4, 150.0, 154.2, 156.6. **Melting point:** 116-117 °C.

Preliminary X-ray structure:



III.4.3. Experimental part for Section III.2

Synthesis and characterization of 217

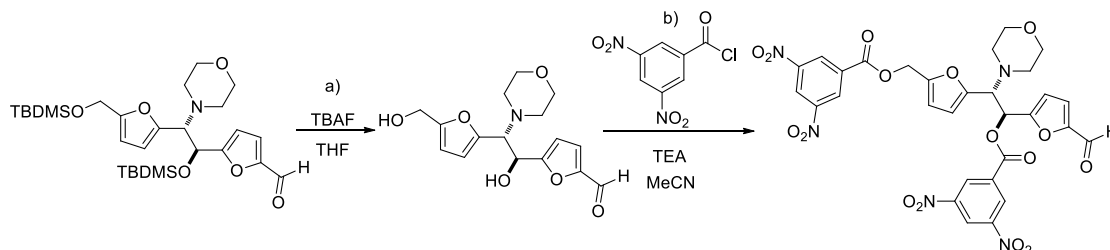


Diastereoisomer 217-I. To a solution of **148** (90 mg, 0.375 mmol) in anhydrous acetonitrile, morpholine (1 equiv., 0.375 mmol) was added *via* gas-tight syringe followed by the addition of $\text{Dy}(\text{OTf})_3$ (10 mol%) in one portion. The reaction mixture was allowed to stir at

40 °C for 2 d. The solvent was then evaporated and the two diastereoisomers **217-I** ($R_f=0.55$, 8:2 Hex/EtOAc) and **217-II** ($R_f=0.65$, 8:2 Hex/EtOAc) were purified by flash chromatography (hex/EtOAc). **^1H NMR (400 MHz, CDCl_3)** δ -0.17 (s, 3H), -0.13 (s, 3H), 0.09 (s, 3H), 0.10 (s, 3H), 0.69 (s, 9H) 0.91 (s, 9H), 2.29 (m, 2H), 2.59 (m, 2H), 3.46 (m, 4H), 3.82 (d, $J = 9.04$ Hz, 1H), 4.60 (s, 2H), 5.24 (d, $J = 9.07$ Hz, 1H), 6.18 (s, 2H), 6.44 (d, $J = 3.53$ Hz, 1H), 7.22 (d, $J = 3.47$ Hz, 1H), 9.61 (s, 1H). **217-I and 217-II ^{13}C NMR (100 MHz, CDCl_3)** δ 177.7, 177.6, 163.8, 162.3, 153.9, 153.8, 151.8, 151.8, 150.2, 150.1,

122.8, 122.0, 110.9, 110.1, 110.1, 109.5, 107.8, 107.6, 68.7, 68.3, 68.2, 67.5, 67.4, 58.3, 58.2, 50.9, 50.8, 26.0, 25.9, 25.8, 25.5, 18.5, 18.5, 18.3, 18.0, -4.8, -4.9, -5.0, -5.0, -5.4, -18.7. **HRMS** Calculated for $C_{28}H_{47}NO_6Si_2Na$: 572.283414 m/z, found: 572.283506 m/z. **ESI⁺** Calculated for $[C_{28}H_{47}NO_6Si_2]^+$: 550.3020 m/z, found: 550.3015 m/z.

Synthesis of compound **220** - crystals suitable for X-Ray analysis:



a) To a solution of **217-I** (100 mg, 0.18 mmol) in anhydrous THF (1 mL), TBAF·3H₂O (4 equiv., 215 mg) was added at 0 °C and the mixture was allowed to stir for 15 min. The product was purified by column chromatography to yield the product as a pale yellow oil (58 mg, 99% yield). **¹H NMR (400 MHz, CDCl₃)** δ 2.54 (m, 4H), 3.66 (m, 4H), 3.87 (d, *J* = 6.11 Hz, 1H), 4.54 (d, *J* = 5.87 Hz, 2H), 5.33 (d, *J* = 6.08 Hz, 1H), 6.14 (dd, *J* = 9.96, 2.85 Hz, 2H), 6.39 (d, *J* = 3.48 Hz, 1H), 7.13 (d, *J* = 3.50 Hz, 1H), 9.51 (s, 1H).

b) To a mixture of compound **219-I** (58 mg, 0.18 mmol) in MeCN (1 mL) 3,5-dinitrobenzoyl chloride (2.2 equiv.) was added and the reaction mixture was allowed to stir at RT. After 1 h, triethylamine (2.2 equiv.) was added slowly and the reaction mixture was allowed to stir for 1 h. The product was then purified by column chromatography to yield a yellow solid (83.6 mg, 65% yield) that was recrystallized from hex/EtOAc.

X-ray Crystallographic Analysis:

Crystals of **220** suitable for X-ray diffraction studies were mounted on a loop with protective oil. X-ray data were collected at 150K on a Bruker AXS-KAPPA APEX II diffractometer using graphite monochromated Mo-K α radiation (λ =0.71069 Å) and operating at 50kV and 30 mA. Cell parameters were retrieved using Bruker SMART software and refined using Bruker SAINT²⁵⁹ on all observed reflections. Absorption corrections were applied using SADABS²⁶⁰. Structure solution and refinement were performed using direct methods with program SIR97²⁶¹ and SHELXL97²⁶², both included in the package of programs WINGX-Version 1.80.05²⁶³. A full-matrix least-squares refinement was used for the non-hydrogen atoms with anisotropic thermal parameters. All hydrogen atoms connected to carbons were inserted in idealized positions and allowed to refine riding in the parent carbon atom.

Crystallographic data for **220** (CCDC 1011693, **Figure III.19**): C₃₀H₂₃N₅O₁₆, fw=709.53, monoclinic, space group *P*2₁, *a*=6.462(3) Å, *b*=21.405(2) Å, *c*=11.722(4) Å, β = 105.001(1)

$^{\circ}$, $V = 1566.1(9) \text{ \AA}^3$, $Z=2$, $T=150\text{K}$, $d_{\text{calc}}=1.505 \text{ mg.m}^{-3}$, $\mu = 0.125 \text{ mm}^{-1}$, $F(000)=732$. Of 22063 reflections collected, 6354 were independent ($R_{\text{int}} = 0.0725$); 461 variables refined with 6354 reflections to final R indices $R_1(I > 2\sigma(I))=0.0544$, $wR_2(I > 2\sigma(I))=0.1136$, $R_1(\text{all data})=0.0988$, $wR_2(\text{all data})=0.1284$, $\text{GOF} = 0.967$.

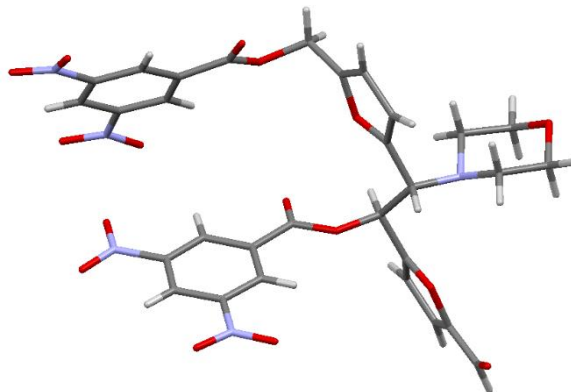
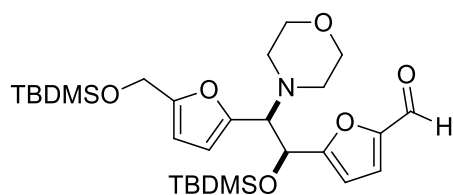


Figure III.19. X-ray structure of **220**.

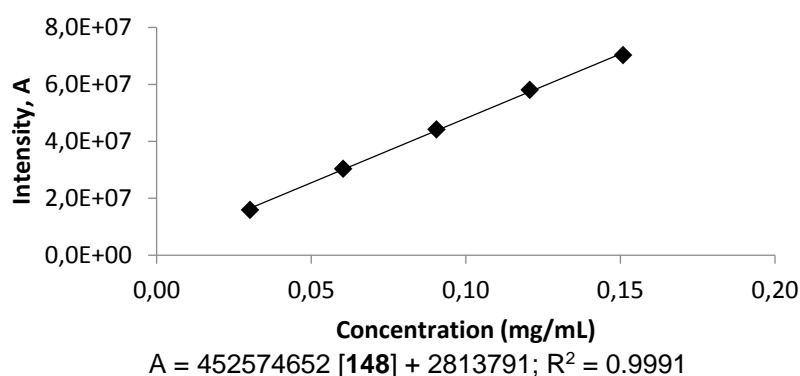
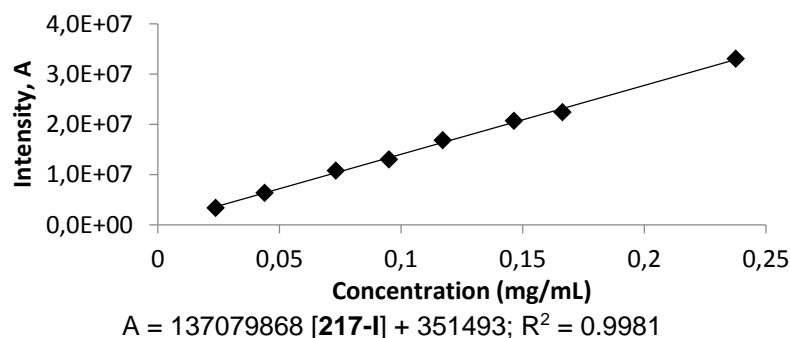
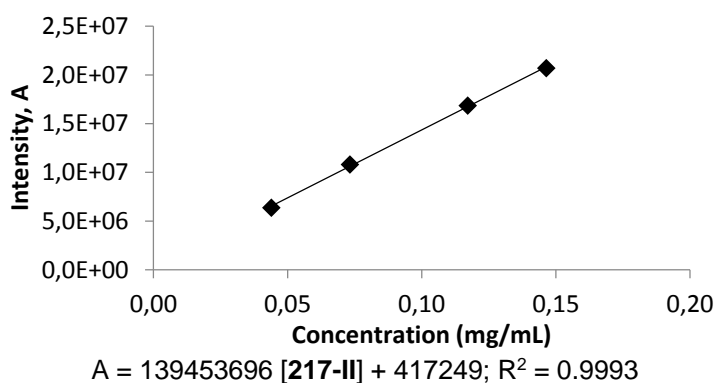
Diastereoisomer 217-II



^1H NMR (400 MHz, CDCl_3) δ -0.13 (s, 3H), 0.07 (s, 9H), 0.86 (s, 9H), 0.89 (s, 9H), 2.50 (m, 2H), 2.70 (m, 2H), 3.66 (m, 4H), 3.96 (d, $J = 8.20 \text{ Hz}$, 1H), 4.54 (s, 2H), 5.19 (d, $J = 8.21 \text{ Hz}$, 1H), 5.96 (d, $J = 2.98 \text{ Hz}$, 1H), 6.03 (d, $J = 2.92 \text{ Hz}$, 1H), 6.32 (d, $J = 3.49 \text{ Hz}$, 1H), 7.06 (d, $J = 3.55 \text{ Hz}$, 1H), 9.53 (s, 1H). **HRMS** Calculated for $\text{C}_{28}\text{H}_{47}\text{NO}_6\text{Si}_2\text{Na}$: 572.283414 m/z , found: 572.283506 m/z .

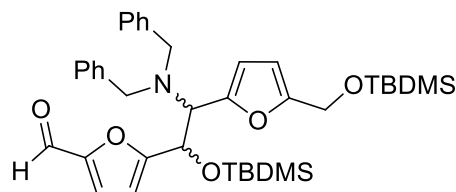
General protocol for reaction conditions optimization (Table III.2, Table III.3)

To a solution of **148** (30 mg, 0.125 mmol) in the desired anhydrous solvent, morpholine was added *via* gas-tight syringe. The catalyst was added in one portion and the mixture was allowed to stir at the mentioned temperature and time. The solvent was then evaporated and the crude reaction mixture was filtered through a small pad of silica gel using 10 mL hex/EtOAc 7:3. The solvent was evaporated and hexane was used to dilute the mixture to the appropriate concentration for HPLC analysis. R_t (**148**) = 4.78 min, λ_{\max} =275 nm; R_t (**217-II**) = 5.21 min, 282 nm; R_t (**217-I**) = 7.05 min, λ_{\max} =282 nm.

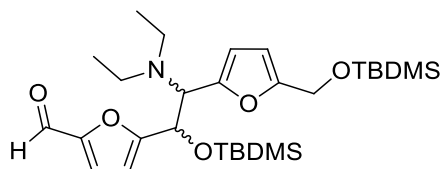
Calibration curves for quantitative HPLC analysis**Calibration curve for 148****Calibration curve for 217-I****Calibration curve for 217-II**

General protocol for amine scope (Table III.4).

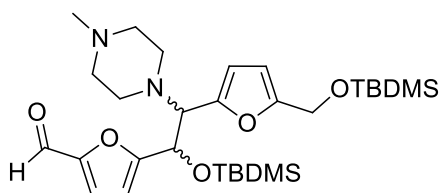
To a solution of **148** (90 mg, 0.375 mmol) in anhydrous acetonitrile (2.25 mL), amine (1 equiv., 0.375 mmol) was added followed by the addition of Dy(OTf)₃ (10 mol%) in one portion. The reaction mixture was allowed to stir at 40 °C until full consumption of **148** (followed by TLC). The solvent was then evaporated and the product was purified by column chromatography (hex/EtOAc).

Compound 221

Isolation of the different diastereoisomers, **221-I** and **221-II** (not stable), ratio not determined. **221-I** - ¹H NMR (400 MHz, CDCl₃) δ -0.24 (s, 3H), -0.19 (s, 3H), 0.16 (s, 3H), 0.16 (s, 3H), 0.60 (s, 9H) 0.96 (s, 9H), 3.13 (d, *J* = 13.78 Hz, 2H), 3.88 (d, *J* = 13.69 Hz, 2H), 4.06 (d, *J* = 10.09 Hz, 1H), 4.68 (s, 2H), 5.33 (d, *J* = 10.12 Hz, 1H), 6.20 (d, *J* = 2.47 Hz, 1H), 6.27 (d, *J* = 2.50 Hz, 1H), 6.30 (d, *J* = 3.47 Hz, 1H), 7.06 (m, 4H), 7.22 (m, 6 H), 7.29 (d, *J* = 3.36 Hz, 1H), 9.59 (s, 1H). ¹³C NMR (100 MHz, CDCl₃) δ -5.5, -5.2, -4.9, 18.0, 18.6, 25.4, 26.1, 29.9, 50.0, 55.4, 58.4, 61.7, 67.8, 107.9, 110.4, 111.8, 127.1, 128.3, 128.9, 139.3, 150.4, 152.0, 153.9, 163.2, 178.4. HRMS Calculated for C₃₈H₅₃NO₅Si₂Na: 682.335451 m/z, found: 682.335489 m/z.

Compound 222

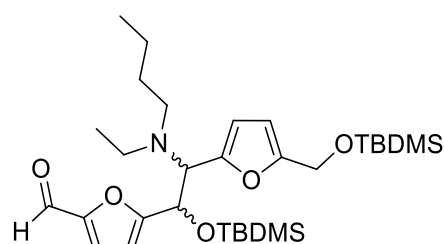
Isolated as a mixture of diastereoisomers **222-I** and **222-II**, ratio not determined. **222-I** and **222-II** - ¹H NMR (400 MHz, CDCl₃) δ -0.20 – -0.15 (6H), 0.00 – 0.12 (6H), 0.75 – 1.00 (18H), 0.5 – 0.7 (6H), 2.00 – 3.00 (4H), 4.03 – 4.13 (1H), 4.59-4.74 (s, 2H), 5.00 – 5.18 (1H), 6.08 - 6.14 (2H), 6.38 - 6.40 (1H), 7.09 - 7.23 (1H), 9.54 - 9.59 (1H). ¹³C NMR (100 MHz, CDCl₃) δ -5.4, -5.2, -4.1, -5.0, 13.9, 18.0, 18.6, 25.6, 25.8, 25.9, 26.0, 44.9, 58.4, 60.6, 63.3, 69.0, 107.7, 107.8, 109.5, 109.6, 109.9, 110.2, 122.2, 151.7, 153.4, 164.3, 177.7. HRMS Calculated for C₂₈H₄₉NO₅Si₂Na: 558.304147 m/z, found: 558.304643 m/z.

Compound 223

Isolated as a mixture of diastereoisomers, **223-I** and **223-II**, ratio 1:1.0. **223-I** - ¹H NMR (400 MHz, CDCl₃) δ -0.18 (s, 3H), -0.15 (s, 3H), 0.07 (s, 3H), 0.08 (s, 3H), 0.68 (s, 9H) 0.90 (s, 9H), 2.14 (s, 3H), 2.30-2.72 (m, 8H), 3.84 (d, *J* = 9.1 Hz, 1H), 4.56 (s, 2H), 5.22 (d, *J* = 9.09 Hz, 1H), 6.14 (m, 2H), 6.44

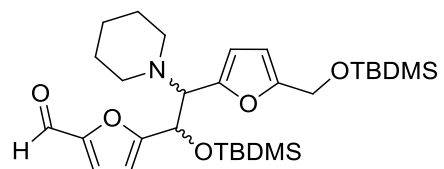
(d, $J = 3.46$ Hz, 1H), 7.21 (d, $J = 3.39$ Hz, 1H), 9.60 (s, 1H). **223-II** – ^1H NMR (400 MHz, CDCl_3) δ -0.10 (s, 3H), 0.05 (s, 9H), 0.84 (s, 9H) 0.88 (s, 9H), 1.25-1.55 (m, 6H), 2.24 (s, 3H), 2.30-2.72 (m, 8H), 3.98 (d, $J = 8.12$ Hz, 1H), 4.51 (s, 2H), 5.18 (d, $J = 8.12$ Hz, 1H), 5.94 (d, $J = 2.4$ Hz, 1H), 5.98 (d, $J = 2.75$ Hz, 1H), 6.30 (d, $J = 3.43$ Hz, 1H), 7.05 (d, $J = 3.46$ Hz, 1H), 9.51 (s, 1H). **223-I + 223-II** – ^{13}C NMR (100 MHz, CDCl_3) δ 177.69, 177.67, 164.1, 162.4, 153.8, 153.7, 151.8, 150.1, 149.9, 122.5, 121.0, 110.8, 110.1, 109.4, 107.8, 107.6, 68.5, 67.9, 67.0, 66.6, 58.2, 58.1, 55.4, 55.3, 45.7, 26.1, 26.0, 25.8, 25.6, 18.6, 18.5, 18.3, 18.0, -4.8, -4.9, -5.0, -5.4. **HRMS** Calculated for $\text{C}_{29}\text{H}_{50}\text{N}_2\text{O}_5\text{Si}_2\text{Na}$: 585.315053 m/z, found: 585.315022 m/z.

Compound 224



Isolated as a mixture of diastereoisomers, **224-I** and **224-II**, ratio 1:0.25. **224-I** – ^1H NMR (400 MHz, CDCl_3) δ -0.20 (s, 3H), -0.17 (s, 3H), 0.09 (s, 3H), 0.10 (s, 3H), 0.66 (s, 9H), 0.74-0.81 (m, 6H), 0.91 (s, 9H), 1.04-1.31 (m, 4H), 2.11 (m, 2H), 2.37 (m, 1H), 2.64 (m, 1H), 4.03 (d, $J = 9.78$ Hz, 1H), 4.59 (s, 2H), 5.18 (d, $J = 9.79$ Hz, 1H), 6.12 (d, $J = 2.7$ Hz, 1H), 6.16 (d, $J = 2.7$ Hz, 1H), 6.44 (d, $J = 3.52$ Hz, 1H), 7.21 (d, $J = 3.51$ Hz, 1H), 9.61 (s, 1H). ^{13}C NMR (100 MHz, CDCl_3) δ 177.7, 164.2, 153.3, 151.7, 151.6, 122.2, 110.4, 109.7, 107.8, 68.7, 63.5, 58.4, 50.7, 45.1, 30.5, 26.0, 25.8, 25.5, 20.4, 20.3, 18.6, 18.1, 18.0, 14.2, 13.9, -5.0, -5.1, -5.5. Calculated for $\text{C}_{30}\text{H}_{53}\text{NO}_5\text{Si}_2\text{Na}$: 586.335452 m/z, found: 586.335467 m/z. **224-II** – Calculated for $\text{C}_{30}\text{H}_{53}\text{NO}_5\text{Si}_2\text{Na}$: 586.335452 m/z, found: 586.335797 m/z.

Compound 225



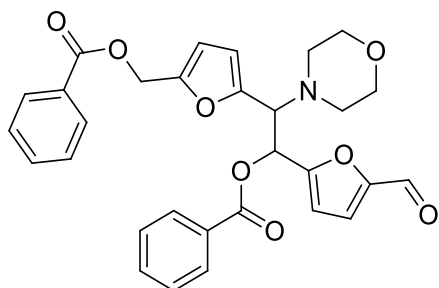
Isolation of the different diastereoisomers, **225-I** and **225-II**. **225-I** – ^1H NMR (400 MHz, CDCl_3) δ -0.17 (s, 3H), -0.15 (s, 3H), 0.09 (s, 3H), 0.10 (s, 3H), 0.68 (s, 9H) 0.91 (s, 9H), 1.20-1.31 (m, 6H), 2.17 (m, 2H), 2.53 (m, 2H), 3.81 (d, $J = 9.24$ Hz, 1H), 4.60 (s, 2H), 5.24 (d, $J = 9.24$ Hz, 1H), 6.13 (d, $J = 2.93$ Hz, 1H), 6.17 (d, $J = 2.95$ Hz, 1H), 6.45 (d, $J = 3.56$ Hz, 1H), 7.21 (d, $J = 3.55$ Hz, 1H), 9.61 (s, 1H). ^{13}C NMR (100 MHz, CDCl_3) δ 177.77, 151.76, 109.49, 107.84, 68.54, 58.33, 51.70, 26.00, 25.57, 18.54, 18.02, -5.00, -5.04, -5.36. Calculated for $\text{C}_{29}\text{H}_{49}\text{NO}_5\text{Si}_2\text{Na}$: 570.304151 m/z, found: 570.303693 m/z. **225-II** – ^1H NMR (400 MHz, CDCl_3) δ -0.07 (s, 3H), 0.06 (s, 6H), 0.09 (s, 3H), 0.85 (s, 9H) 0.89 (s, 9H), 1.25-1.55 (m, 6H), 2.38 (m, 2H), 2.63 (m, 2H), 3.95 (d, $J = 8.73$ Hz, 1H), 4.53 (s, 2H), 5.18 (d, $J = 8.69$ Hz, 1H), 5.90 (d, J

= 2.94 Hz, 1H), 6.00 (d, J = 2.96 Hz, 1H), 6.30 (d, J = 3.51 Hz, 1H), 7.05 (d, J = 3.56 Hz, 1H), 9.51 (s, 1H). ^{13}C NMR (100 MHz, CDCl_3) δ 178.1, 151.7, 110.0, 107.8, 68.4, 58.2, 51.7, 29.9, 25.8, 18.5, 18.33, -4.73, -5.0, -5.4.

General protocol for aldehyde scope (Table III.4)

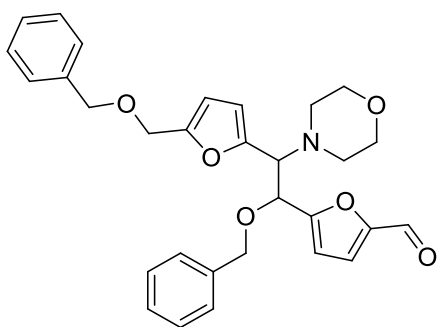
To a solution of aldehyde (0.375 mmol) in anhydrous acetonitrile (2.25 mL), morpholine (1 equiv., 0.375 mmol) was added *via* gas-tight syringe followed by the addition of $\text{Dy}(\text{OTf})_3$ (10 mol%) in one portion. The reaction mixture was allowed to stir at 40 °C for 54h. The solvent was then evaporated and the product (mixture of diastereoisomers) was purified by column chromatography (hex/EtOAc).

Compound 226



Isolated as a mixture of diastereoisomers, **226-I** and **226-II**, ratio 1:1.0. **226-I** and **226-II** – ^1H NMR (400 MHz, CDCl_3) δ 2.32-2.40 (m, 4H), 2.67 (m, 2H), 3.78 (m, 2H), 3.50 (m, 8H), 4.35 (d, J = 10.42 Hz, 1H), 4.47 (d, J = 9.97 Hz, 1H), 5.20 (s, 2H), 5.22 (s, 2H), 6.12 (d, J = 3.10 Hz, 1H), 6.31 (d, J = 2.76 Hz, 2H), 6.40 (d, J = 3.11 Hz, 1H), 6.43 (d, J = 3.53 Hz, 1H), 6.60 (d, J = 9.97 Hz, 1H), 6.63 (d, J = 3.53 Hz, 1H), 6.73 (d, J = 10.40 Hz, 1H), 6.91 (d, J = 3.54 Hz, 1H), 7.18 (d, J = 3.53 Hz, 1H), 7.26-7.57 (m, 12H), 7.80 (d, J = 7.44 Hz, 2H), 7.90 (d, J = 7.41 Hz, 2H), 8.01 (d, J = 7.39 Hz, 2H), 8.06 (d, J = 7.36 Hz, 2H), 9.49 (s, 1H), 9.61 (s, 1H). ^{13}C NMR (75 MHz, CDCl_3) δ 177.8, 177.8, 166.2, 166.1, 165.6, 165.3, 157.7, 156.4, 152.7, 152.5, 150.7, 149.8, 149.7, 149.7, 133.4, 133.4, 133.1, 130.0, 129.9, 129.9, 129.8, 129.8, 129.3, 128.7, 128.6, 128.6, 128.5, 128.5, 128.4, 127.2, 122.1, 122.1, 121.6, 121.5, 112.3, 112.3, 111.4, 111.3, 111.0, 111.0, 67.3, 67.3, 67.0, 66.1, 64.8, 64.2, 58.6, 58.5, 50.5, 50.3. **CHN** Calculated for $(\text{C}_{30}\text{H}_{27}\text{NO}_8)_4\text{H}_2\text{O}$: C: 67.47; H: 5.19; N: 2.62, found: C: 67.45; H: 5.29; N: 2.42.

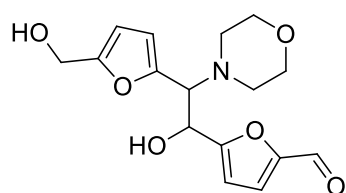
Compound 227



Isolated as a mixture of diastereoisomers, **227-I** and **227-II**, ratio 1:0.8. **227-I** – ^1H NMR (400 MHz, CDCl_3) δ 2.28 (m, 2H), 2.58 (m, 2H), 3.68 (m, 4H), 4.19 (d, J = 9.12 Hz, 1H), 4.36 (d, J = 12.21 Hz, 1H), 4.39 (d, J = 12.14 Hz, 1H), 4.38 (s, 2H), 4.46 (d, J = 2.88 Hz, 2H), 4.98 (d, J = 9.11 Hz, 2H), 6.02 (d, J = 2.99 Hz, 1H), 6.13 (d, J = 2.95 Hz, 1H), 6.39 (d, J = 3.51 Hz, 1H), 7.03 (d, J = 3.51 Hz, 1H), 7.23-7.36 (m, 10H), 9.63 (s, 1H). **227-II** – ^1H NMR (400

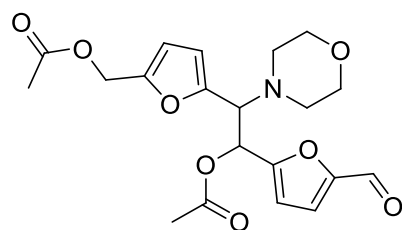
MHz, CDCl₃) δ 2.28 (m, 2H), 2.58 (m, 2H), 3.68 (m, 4H), 4.01 (d, J = 9.12 Hz, 1H), 4.42 (s, 2H), 4.50 (s, 2H), 4.53 (d, J = 11.81 Hz, 1H), 4.67 (d, J = 12.07 Hz, 1H), 5.04 (d, J = 9.16 Hz, 2H), 6.22 (d, J = 2.96 Hz, 1H), 6.33 (d, J = 2.95 Hz, 1H), 6.50 (d, J = 3.49 Hz, 1H), 7.09 (d, J = 3 Hz, 1H), 7.23-7.36 (m, 10H), 9.52 (s, 1H). **227-I and 227-II – ¹³C NMR (100 MHz, CDCl₃)** δ 177.8, 177.7, 161.0, 159.5, 152.5, 152.4, 151.4, 151.3, 150.8, 150.8, 150.5, 150.3, 138.0, 137.9, 137.3, 137.2, 128.6, 128.5, 128.4, 128.3, 128.2, 127.9, 127.8, 127.8, 122.2, 121.5, 111.7, 110.8, 110.6, 110.4, 110.3, 110.1, 74.0, 72.9, 72.1, 71.6, 71.5, 67.3, 66.2, 65.5, 64.0, 63.8, 50.6, 50.3. **CHN** Calculated for (C₃₀H₃₁NO₆)₂(H₂O): C: 70.57; H: 6.32; N: 2.74, found: C: 70.37; H: 6.12; N: 2.84.

Compound 219

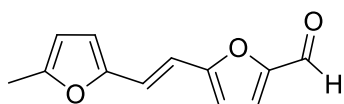


Isolated as a mixture of diastereoisomers, **219-I** and **219-II**, ratio 1:1.1. **219-I – ¹H NMR (400 MHz, CDCl₃)** δ 2.50 (m, 4H), 3.6 – 3.7 (m, 4H), 3.50-3.86 (d, 1H), 4.53 (d, J = 4.97 Hz, 2H), 5.28 (d, J = 6.40 Hz, 1H), 6.14 (dd, J = 9.96, 2.85, 2H), 6.39 (d, J = 3.48 Hz, 1H), 7.13 (d, J = 3.50 Hz, 1H), 9.51 (s, 1H). **219-II – ¹H NMR (400 MHz, CDCl₃)** δ 2.75 (m, 4H), 3.6 – 3.7 (m, 4H), 3.82 (d, J = 9.69 Hz, 1H), 4.54 (s, 2H), 5.12 (d, J = 10.51 Hz, 1H), 6.08 (s, 1H), 6.10 (s, 1H), 6.45 (d, J = 3.48 Hz, 1H), 7.10 (d, J = 3.50 Hz, 1H), 9.45 (s, 1H). **219-I and 219-II – ¹³C NMR (100 MHz, CDCl₃)** δ 177.6, 177.5, 161.1, 160.5, 155.0, 154.4, 152.3, 152.0, 149.9, 148.4, 122.6, 119.6, 111.5, 111.4, 110.7, 109.8, 109.1, 108.3, 67.3, 67.2, 67.1, 67.0, 66.8, 66.5, 66.2, 64.1, 57.5, 57.3.

Compound 228



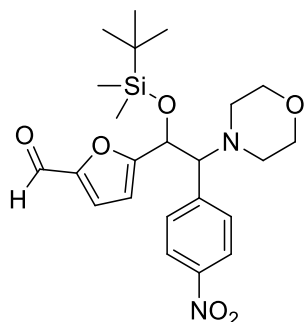
Isolated as a mixture of diastereoisomers, **228-I** and **228-II**, ratio 1:1.05. **228-I – ¹H NMR (400 MHz, CDCl₃)** δ 1.90-2.15 (2 x s, 2 x 3H), 3.25-3.80 (m, 4H or 2 x 2H), 3.4-3.7 (m, 4H), 4.16 (d, J = 10.56 Hz, 1H), 5.00 (d, J = 9.57 Hz, 2H), 6.21 (m, t_{ap} , J = 3.0 Hz, 2H), 6.47 (d, J = 10.56 Hz, 1H), 6.56 (d, J = 3.49 Hz, 1H), 7.20 (d, J = 3.52 Hz, 1H), 9.62 (s, 1H). **228-II – ¹H NMR (400 MHz, CDCl₃)** δ 1.90-2.15 (2 x s, 2 x 3H), 3.25-3.80 (m, 4H or 2 x 2H), 3.4-3.7 (m, 4H), 4.27 (d, J = 10.34 Hz, 1H), 4.93 (s, 2H), 6.04 (d, J = 3.08 Hz, 1H), 6.34 (d, J = 3.40 Hz, 1H), 6.37 (d, J = 11.02 Hz, 1H), 6.39 (d, J = 3.70 Hz, 1H), 7.04 (d, J = 3.54 Hz, 1H), 9.53 (s, 1H). **228-I and 228-II – ¹³C NMR (100 MHz, CDCl₃)** δ 177.8, 177.8, 170.7, 170.6, 169.8, 169.5, 157.7, 156.4, 152.6, 152.4, 150.6, 150.5, 149.7, 149.6, 122.0, 121.4, 112.1, 112.0, 111.1, 111.1, 110.9, 110.6, 67.5, 67.2, 66.1, 65.1, 64.6, 63.9, 58.2, 58.0, 50.3, 50.3, 21.1, 21.1, 21.0, 20.7. **CHN** Calculated for C₂₀H₂₃NO₈: C: 59.25; H: 5.72; N: 3.46, found: C: 59.4; H: 5.78; N: 3.18.

Compound 230

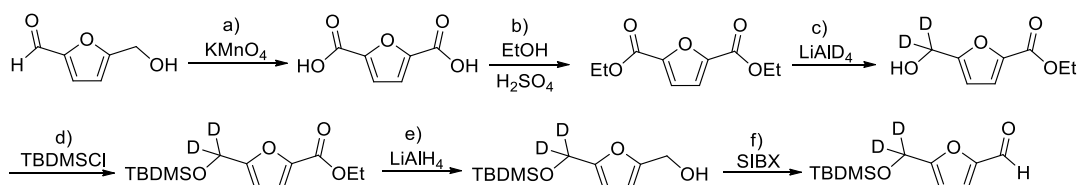
To a solution of 5-methylfurfural (41.5 mg, 0.375 mmol) in acetonitrile (2.25 mL), morpholine (1 equiv., 0.375 mmol) was added *via* gas-tight syringe followed by the addition of Dy(OTf)₃ (10 mol%) in one portion. The reaction mixture was allowed to stir at 40 °C for 17 h. The solvent was then evaporated and column chromatography (hex/EtOAc 7:3) offered two products in a 40% overall yield. Spectral data are in accordance with those reported in the literature.¹⁷⁶ **230-*trans*** ¹H NMR (400 MHz, CDCl₃) δ 2.35 (s, 3 H), 6.05 (dd, *J* = 0.98, 3.23 Hz, 1H), 6.37 (d, *J* = 3.21 Hz, 1H), 6.44 (d, *J* = 3.71 Hz, 1 H), 6.74 (d, *J* = 15.95 Hz, 1 H), 7.09 (d, *J* = 15.87 Hz, 1 H), 7.23 (d, *J* = 3.70 Hz, 1 H), 9.55 (s, 1 H).

General procedure for cross-reaction experiments:

To a solution of **148** (90 mg, 0.375 mmol) and the desired aldehyde (2 equiv., 0.75 mmol) in anhydrous acetonitrile (3 mL), morpholine (2 equiv., 0.75 mmol) was added *via* gas-tight syringe followed by the addition of Dy(OTf)₃ (10 mol%) in one portion. The reaction mixture was allowed to stir at 40 °C for 3 d. The solvent was then evaporated and the product was purified by column chromatography (hex/EtOAc). Compound **231** was isolated in 20% yield when 4-nitrobenzaldehyde was used as aldehyde.

Compound 231

231-I – ¹H NMR (400 MHz, CDCl₃) δ -0.18 (s, 3H), 0.00 (s, 3H), 0.77 (s, 9H), 2.44 (m, 4H), 3.58 (m, 4H), 3.76 (d, *J* = 5.58 Hz, 1H), 5.35 (d, *J* = 5.58 Hz, 1H), 6.10 (d, *J* = 3.42 Hz, 1H), 7.10 (d, *J* = 3.44 Hz, 1H), 7.34 (d, *J* = 8.43 Hz, 1H), 8.12 (d, *J* = 8.42 Hz, 1H), 9.57 (s, 1H). ¹³C NMR (400 MHz, CDCl₃) δ -5.1, -4.5, 18.1, 25.6, 51.5, 67.1, 68.3, 74.4, 110.5, 122.8, 130.56, 130.60, 144.0, 147.5, 151.8, 162.3, 177.4. CHN Calculated for (C₂₃H₃₂N₂O₆Si)₅ (CHCl₃)₃: C: 53.26; H: 6.17; N: 5.26, found: C: 53.53; H: 6.14; N: 5.19. **231-II** – ¹H NMR (400 MHz, CDCl₃) δ -0.12 (s, 3H), 0.05 (s, 3H), 0.86 (s, 9H), 2.45 (m, 2H), 2.66 (m, 2H), 3.58 (m, 4H), 3.69 (d, *J* = 5.5 Hz, 1H), 5.33 (d, *J* = 5.52 Hz, 1H), 6.00 (d, *J* = 3.4 Hz, 1H), 7.07 (d, *J* = 3.4 Hz, 1H), 7.34 (d, *J* = 8.4 Hz, 1H), 8.05 (d, *J* = 8.4 Hz, 1H), 9.55 (s, 1H).

Synthesis of 148-d₂

a) **Furan-2,5-dicarboxylic acid, FDCA.** To a solution of sodium hydroxide (30 g) in water (300 mL), HMF (4.1 g, 32.5 mmol) was added at 20 °C, followed by the addition of potassium permanganate (11 g, 70 mmol). After 10 min stirring at 20 °C the precipitate was filtered off and a concentrated HCl solution was added to the filtrate until pH 1. The resulted precipitate was separated by filtration, washed with water and dried under vacuum to give FDCA (4.26 g, 84% yield) as a white powder. ¹H NMR (300 MHz, D₂O) δ 7.25 (s).

b) **Diethyl furan-2,5-dicarboxylate.** To a round bottom flask equipped with a Dean-Stark a solution of FDCA (2.53 g, 16.2 mmol) in ethanol (70 mL) was charged, followed by the addition of a catalytic amount of sulfuric acid (3 drops). The mixture was allowed to stir at reflux for 16h. The mixture was neutralized with a saturated aqueous solution of NaHCO₃, extracted with EtOAc, dried over MgSO₄, filtered and evaporated to give the crude product as a yellow solid. The product was purified by column chromatography to give the product as a white solid (1.36 g, 40% yield). ¹H NMR (400 MHz, CDCl₃) δ 1.39 (t, *J* = 7.12 Hz, 6H), 4.40 (t, *J* = 7.13 Hz, 2H), 7.20 (s_{app}, 2H). ¹³C NMR (100 MHz, CDCl₃) δ 14.4, 61.8, 118.4, 147.1, 158.2.

c) **Ethyl 5-(hydroxymethyl)furan-2-carboxylate-d₂.** To a suspension of LiAlD₄ (19 mg, 2 equiv.) in THF (1 mL), a solution of diethyl furan-2,5-dicarboxylate (47.8 mg, 0.225 mmol) in anhydrous THF (1 mL) was added slowly at 0 °C. The mixture was allowed to stir for 22h at RT. Water was added and the product extracted with EtOAc (3 x 10 mL). The product was then purified by column chromatography to yield the product as a yellow oil (9 mg, 23% yield). *Notes:* Scale up of the reaction was not reproducible, so small scale reactions were performed to synthesize the compound. The full reduction (incorporation of four D atoms) occurred as side reaction to give the diol as a minor product. The low overall yield of the reaction was due to low conversion of the starting material. ¹H NMR (400 MHz, CDCl₃) δ 1.36 (t, *J* = 7.13 Hz, 3H), 2.34 (bs, 1H) 4.35 (t, *J* = 7.13 Hz, 2H), 6.40 (d, *J* = 3.40 Hz, 1H), 7.12 (d, *J* = 3.39 Hz, 1H).

d) **Ethyl 5-(((tert-butyldimethylsilyl)oxy)methyl)furan-2-carboxylate-d₂.** To a solution of ethyl 5-(hydroxymethyl)furan-2-carboxylate-d₂ (43.9 mg, 0.255 mmol) in anhydrous DCM (0.4 mL) were added imidazole (35 mg, 0.5 mmol, 2 equiv.) and *tert*-butyldimethylsilyl chloride (58 mg, 0.382 mmol, 1.5 equiv.) at 0 °C. The solution was stirred for 15 min at RT. The reaction was quenched with water and the silylated compound was extracted with DCM (5 x 20 mL). The collected organic layers were dried over MgSO₄, and

the solvent removed to give the crude product as a pale yellow oil that was used without further purification in the next step.

e) **5-(((tert-butyldimethylsilyl)oxy)methyl)furan-2-yl)methanol-d₂**. To a suspension of LiAlH₄ (20 mg, 2 equiv.) in anhydrous THF (1.5 mL), a solution of ethyl 5-(((tert-butyldimethylsilyl)oxy)methyl)furan-2-carboxylate-d₂ (0.255 mmol) in THF (1 mL) was added slowly at 0 °C. The mixture was allowed to stir for 15 min at RT and then the reaction was quenched with water. The product was extracted with EtOAc (3 x 10 mL), dried over Mg₂SO₄ and filtered to give the crude product (51.4 mg) that was used in the next step without further purification.

f) **5-(((tert-butyldimethylsilyl)oxy)methyl)furan-2-carbaldehyde-d₂**. To a solution of crude 5-(((tert-butyldimethylsilyl)oxy)methyl)furan-2-yl)methanol-d₂ (51.4 mg) in anhydrous THF (1.5 mL), stabilized 2-iodoxybenzoic acid (SIBX, 1.6 equiv.) was added and the mixture was allowed to stir for 8h at 60 °C. The crude product was purified by column chromatography to yield the desired product (22.7 mg, 37% yield - 3 steps). **¹H NMR (400 MHz, CDCl₃)** δ 0.11 (s, 6H), 0.92 (s, 9H), 6.47 (d, *J* = 3.53 Hz, 1H), 7.20 (d, *J* = 3.52 Hz, 1H), 9.59 (s, 1H). **¹³C NMR (100 MHz, CDCl₃)** δ -5.2, 18.5, 25.9, 109.6, 122.7, 152.3, 161.5, 177.7. **HRMS** Calculated for [C₁₂H₁₉D₂O₃Si]⁺: 243.1380 m/z, found: 243.1380 m/z.

Procedure for determination of kinetic isotope effect:

To a mixture of **148** (11 mg, 45.76 μmol) and **148-d₂** (9.6 mg, 39.61 μmol), anhydrous acetonitrile (0.5 mL), morpholine (7.3 μL, 2 equiv.) and DyOTf₃ (5 mg, 10 mol%) were added. The mixture was allowed to stir for 59 h at 40 °C. The mixture was filtered through a pad of silica gel and the crude reaction mixture was analyzed by ¹H NMR.

General protocol for unsuccessful asymmetric version using chiral catalysts (Table III.6). To a solution of **148** (15 mg, 0.06 mmol) in the desired anhydrous solvent (0.4 mL), morpholine (1 equiv., 0.06 mmol), catalyst (10 mol%) and the ligand (for the Lewis acid examples, 10 mol%) were added. The reaction mixture was allowed to stir for the time and Temperature described. The solvent was then evaporated and the catalyst was filtrated through a pad of silica gel using hex/EtOAc and the crude mixture analyzed by HPLC. **HPLC analysis** was performed on a Shimadzu apparatus with a diode array detector SPD-M20A coupled to a pump LC-20AT and using a CHIRALCEL OD column, manual injector with 20 μL loop. Mobile phase gradient from 99:1 hex/2-propanol, flow 1 mL/min.

General protocol using chiral amines:

To a solution of **148** (90 mg, 0.375 mmol) in anhydrous acetonitrile (2.25 mL), *N*-benzyl-1-phenylethanamine (1 equiv., racemic, (*R*)- or (*S*)-isomers) was added followed by the addition of Dy(OTf)₃ (10 mol%) in one portion. The reaction mixture was allowed to stir at 40 °C for 4 days. The solvent was then evaporated and the catalyst was filtrated through a pad of silica gel using hexane/ethyl acetate and the starting material/products were analyzed by ¹H NMR. HRMS for the product **232** using racemic amine: Calculated for C₃₉H₅₆NO₅Si₂: 674.3692 m/z, found: 674.3690 m/z.

III.4.4. Experimental part for Section III.3

The experimental procedures reported herein were performed mainly by Rafael Gomes under my supervision as part of his 7th semester plan project.

General protocol for reaction conditions optimization (Table III.9)

To a solution of **148** (30 mg, 0.125 mmol) anhydrous acetonitrile (1.3 mL, 0.1 M), *N*-methylaniline (40 µL, 3 equiv.) was added *via* gas-tight syringe. The catalyst was added in one portion and the mixture was allowed to stir at the mentioned temperature and time under argon atmosphere. The solvent was then evaporated and the crude reaction mixture was filtered through a small pad of silica gel. The solvent was evaporated and hex/*i*-propanol was used to dilute the mixture to the appropriate concentration for HPLC analysis. R_t (**148**) = 6.2 min, λ_{max}=275 nm; R_t (**283**) = 16.2 min, λ_{max}=252 nm. HPLC conditions: column - KROMASIL 100 SIL 5.0 column and Mobile phase gradient from 99:1 to 98:2 in 10 min hex/2-propanol, flow 0.7 to 1 mL/min in 10 min.

General procedure for the synthesis of triarylmethanes at atmospheric pressure. To a solution of aldehyde in anhydrous acetonitrile (0.1 M), desired aniline (3 equiv.) was added followed by the addition of Yb(OTf)₃ (10 mol%) in one portion. The reaction mixture was allowed to stir at the desired temperature and time described in **Table III.11** and **Table III.12** under argon atmosphere. The solvent was then evaporated and the product purified by column chromatography using hex/EtOAc.

Protocol for stability of 283 experiment (Scheme III.44). To a solution of **283** (54.5 mg, 0.125 mmol) in anhydrous acetonitrile (0.1 M), *N*-methylaniline (40 µL, 3 equiv.) was added followed by the addition of Yb(OTf)₃ (10 mol%) in one portion. The reaction mixture was allowed to stir at 40 °C for 48 h under argon atmosphere. The solvent was then evaporated and the crude reaction mixture was filtered through a small pad of silica gel. The solvent

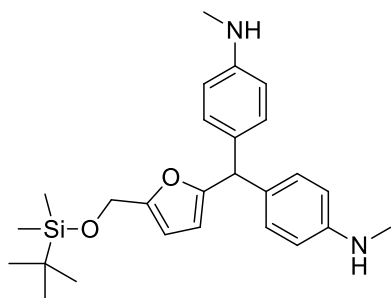
was evaporated and hex/*i*-propanol was used to dilute the mixture to the appropriate concentration for HPLC analysis.

General procedure for the synthesis of triarylmethanes under high pressure. To a proper teflon vessel, the corresponding aldehyde (0.26 mmol, 1 equiv.), aniline (3 equiv.), anhydrous acetonitrile (1 mL) and Yb(OTf)₃ (10 mol%) were added (without argon atmosphere). Next the reactor was filled to the top with acetonitrile until the total volume of 2.4 mL. The reactor was introduced in the high pressure apparatus and kept for the time described in **Table III.13**. The solvent was then evaporated and the product purified by column chromatography using hex/EtOAc.

General procedure for amine competition experiment (Scheme III.46). *N,N*-Dimethylaniline (50 μ L, 0.39 mmol, 3 equiv.), *N*-methylaniline (42 μ L, 0.39 mmol, 3 equiv.) and Yb(OTf)₃ (8 mg, 0.013 mmol, 10 mol%) were added to a solution of **148** (30 mg, 0.13 mmol, 1 equiv.) in anhydrous acetonitrile (1.3 mL, 0.1 M). The reaction mixture was allowed to stir for 89 h at 40 °C under argon atmosphere. The solvent was evaporated and the crude mixture was purified by column chromatography to yield the products **283**, **297**, **298**.

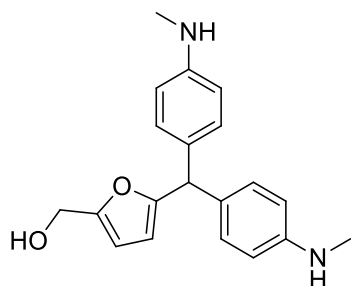
Triarylmethanes characterization

Compound 283

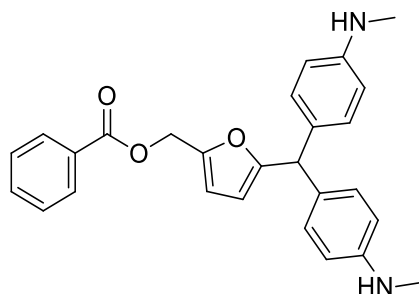


Isolated as a brown viscous liquid. **¹H NMR (300 MHz, CDCl₃)** δ 0.03 (s, 6H), 0.87 (s, 9H), 2.81 (s, 6H), 4.57 (s, 2H), 5.22 (s, 1H), 5.79 (d, *J* = 2.76 Hz, 1H), 6.12 (d, *J* = 2.68 Hz, 1H), 6.55 (d, *J* = 8.1 Hz, 4H), 6.98 (d, *J* = 8.3 Hz, 4H). **¹³C NMR (100 MHz, CDCl₃)** δ 5.1, 18.5, 26.0, 31.2, 49.4, 58.5, 107.8, 108.4, 112.7, 129.6, 131.9, 147.7,

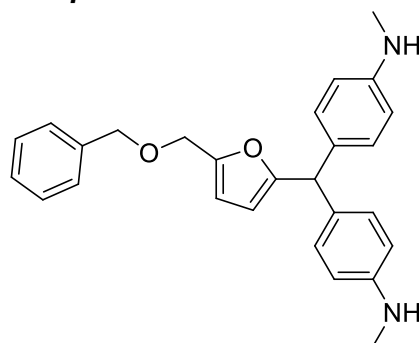
153.5, 157.8. **CHN** Calculated for (C₂₆H₃₆N₂O₂Si): C: 71.51; H: 8.31; N: 6.42, found: C: 71.12; H: 8.44; N: 6.69.

Compound 284

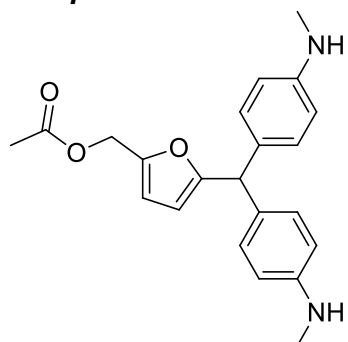
Isolated as a dark green viscous oil. **¹H NMR (300 MHz, CDCl₃)** δ 2.81 (s, 6H), 4.53 (s, 2H), 5.23 (s, 1H), 5.80 (d, *J* = 3.1 Hz, 1H), 6.18 (d, *J* = 2.9 Hz, 1H), 6.54 (d, *J* = 8.6 Hz, 4H), 6.98 (d, *J* = 8.29 Hz, 4H). **¹³C NMR (100 MHz, CDCl₃)** δ 30.9, 49.4, 57.6, 108.3, 108.6, 112.5, 129.5, 131.3, 148.0, 153.2, 158.5.

Compound 286

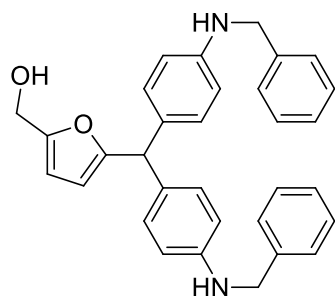
Isolated as a green viscous oil. **¹H NMR (300 MHz, CDCl₃)** δ 2.81 (s, 6H), 5.24 (s, 1H), 5.25 (s, 1H), 5.85 (s, 1H), 6.38 (s, 1H), 6.56 (d, *J* = 7.80 Hz, 4H), 6.99 (d, *J* = 7.70, 4H), 7.42 (t, *J* = 7.23 Hz, 2H), 7.55 (t, *J* = 6.60 Hz, 1H), 8.03 (d, *J* = 6.85 Hz, 2H). **¹³C NMR (100 MHz, CDCl₃)** δ 30.4, 49.4, 59.0, 108.9, 111.5, 112.4, 128.4, 129.5, 129.8, 130.1, 131.1, 133.0, 148.0, 148.4, 159.4, 166.3.

Compound 287

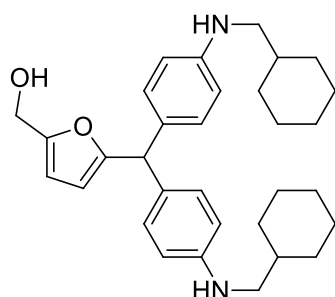
Isolated as a green viscous oil. **¹H NMR (300 MHz, CDCl₃)** δ 2.82 (s, 6H), 4.43 (s, 2H), 4.50 (s, 2H), 5.26 (s, 1H), 5.83 (d, *J* = 3.1 Hz, 1H), 6.24 (d, *J* = 3.1 Hz, 1H), 6.54 (d, *J* = 8.6 Hz, 4H), 6.99 (d, *J* = 8.3 Hz, 4H), 7.31 (m, 5H). **¹³C NMR (100 MHz, CDCl₃)** δ 31.0, 49.4, 64.2, 71.7, 108.6, 110.2, 112.5, 127.7, 128.1, 128.5, 129.6, 131.4, 138.2, 148.0, 150.9, 158.9.

Compound 285

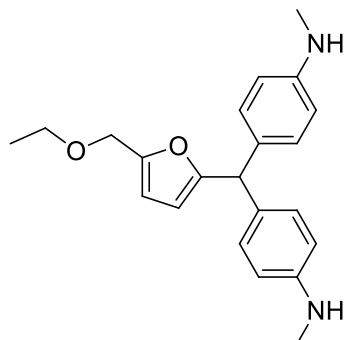
Isolated as a light green viscous oil. **¹H NMR (300 MHz, CDCl₃)** δ 2.06 (s, 3H), 2.82 (s, 6H), 4.99 (s, 2H), 5.25 (s, 1H), 5.84 (d, *J* = 3.1 Hz, 1H), 6.30 (d, *J* = 3.1 Hz, 1H), 6.56 (d, *J* = 8.5 Hz, 4H), 6.98 (d, *J* = 8.4 Hz, 4H). **¹³C NMR (100 MHz, CDCl₃)** δ 21.1, 31.0, 64.2, 49.4, 58.6, 108.9, 111.4, 112.0, 129.5, 131.2, 148.0, 148.4, 159.5, 170.8.

Compound 294

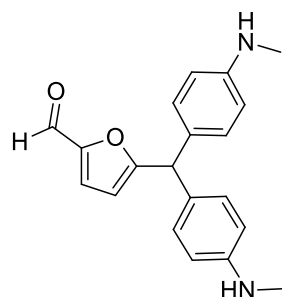
Isolated as a green oil. $^1\text{H NMR}$ (300 MHz, CDCl_3) δ 4.29 (s, 4H), 4.53 (s, 2H), 5.30 (s, 1H), 5.80 (d, $J = 3.1$ Hz, 1H), 6.17 (d, $J = 3.1$ Hz, 1H), 6.56 (d, $J = 8.6$ Hz, 4H), 6.95 (d, $J = 8.4$ Hz, 4H), 7.22 - 7.41 (m, 10H). $^{13}\text{C NMR}$ (100 MHz, CDCl_3) δ 48.5, 49.3, 57.7, 108.3, 108.6, 112.8, 127.2, 127.6, 128.6, 129.5, 131.4, 139.5, 146.8, 153.0, 158.4.

Compound 295

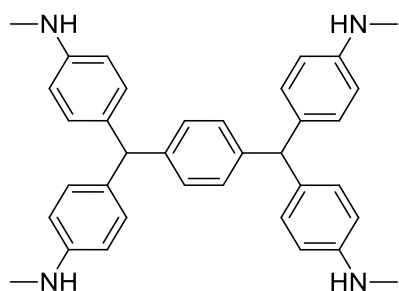
Isolated as a green oil. $^1\text{H NMR}$ (300 MHz, CDCl_3) δ 0.87 - 1.82 (m, 22H), 2.85 (d, $J = 6.6$ Hz, 4H), 4.46 (s, 2H), 5.13 (s, 1H), 5.73 (d, $J = 3.2$ Hz, 1H), 6.11 (d, $J = 3.1$ Hz, 1H), 6.44 (d, $J = 8.6$ Hz, 4H), 6.87 (d, $J = 8.4$ Hz, 4H). $^{13}\text{C NMR}$ (100 MHz, CDCl_3) δ 26.1, 26.7, 31.4, 37.7, 49.4, 50.9, 57.8, 108.4, 108.6, 112.6, 129.5, 130.9, 147.3, 153.1, 158.8.

Compound 305

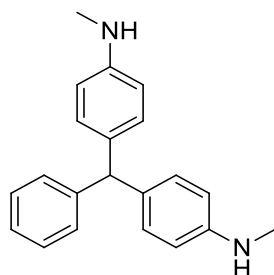
Isolated as a green oil. $^1\text{H NMR}$ (300 MHz, CDCl_3) δ 1.23 (t, $J = 7.0$ Hz, 3H), 2.81 (s, 6H), 3.54 (d, $J = 7.0$ Hz, 2H), 4.41 (s, 2H), 5.28 (s, 1H), 5.84 (d, $J = 3.0$ Hz, 1H), 6.24 (d, $J = 3.0$ Hz, 1H), 6.56 (d, $J = 8.6$ Hz, 4H), 7.01 (d, $J = 8.4$ Hz, 4H). $^{13}\text{C NMR}$ (100 MHz, CDCl_3) δ 15.3, 31.0, 49.4, 64.8, 65.5, 108.6, 109.7, 112.4, 129.6, 131.4, 148.0, 151.1, 158.8.

Compound 300

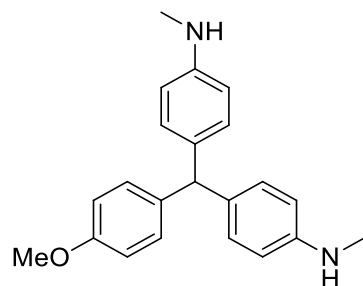
Isolated as a dark viscous oil. $^1\text{H NMR}$ (300 MHz, CDCl_3) δ 2.81 (s, 6H), 5.33 (s, 1H), 6.14 (d, $J = 3.55$ Hz, 1H), 6.55 (m, 4H), 6.97 (m, 4H), 7.16 (d, $J = 3.54$ Hz, 1H), 9.55 (s, 1H). $^{13}\text{C NMR}$ (100 MHz, CDCl_3) δ 31.3, 50.1, 111.6, 113.0, 124.9, 130.1, 133.2, 148.7, 152.8, 166.3, 178.3.

Compound 304

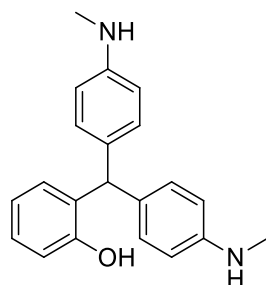
Isolated as a blue crystals. $^1\text{H NMR}$ (300 MHz, CDCl_3) δ 2.80 (s, 12H), 5.29 (s, 2H), 6.53 (d, $J = 8.6$, 8H), 6.93 (d, $J = 8.3$ Hz, 8H), 7.0 (s, 4H). $^{13}\text{C NMR}$ (100 MHz, CDCl_3) δ 31.0, 55.0, 112.4, 129.1, 130.2, 134.0, 142.8, 147.6. **CHN** Calculated for ($\text{C}_{36}\text{H}_{38}\text{N}_4$): C: 82.09; H: 7.27; N: 10.64, found: C: 82.38; H: 7.30; N: 10.43.

Compound 288

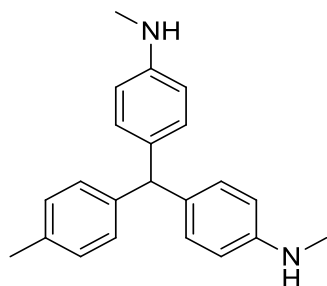
Isolated as a blue viscous oil. $^1\text{H NMR}$ (300 MHz, CDCl_3) δ 2.84 (s, 6H), 5.39 (s, 1H), 6.60 (d, $J = 7.8$ Hz, 4H), 6.97 (d, $J = 7.8$ Hz, 4H), 7.15 - 7.29 (m, 5H). $^{13}\text{C NMR}$ (100 MHz, CDCl_3) δ 31.0, 55.3, 112.4, 125.9, 128.2, 129.5, 130.2, 133.6, 145.6, 147.6.

Compound 290

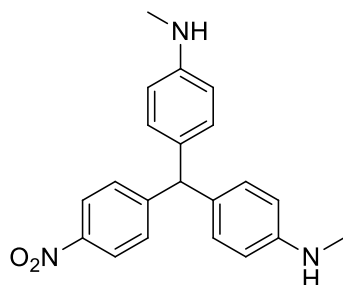
Isolated as a green oil. $^1\text{H NMR}$ (300 MHz, CDCl_3) δ 2.82 (s, 6H), 3.78 (s, 3H), 5.31 (s, 1H), 6.54 (d, $J = 8.6$ Hz, 4H), 6.81 (d, $J = 8.7$ Hz, 2H), 6.94 (d, $J = 8.5$ Hz, 4H), 7.05 (d, $J = 8.6$ Hz, 2H). $^{13}\text{C NMR}$ (100 MHz, CDCl_3) δ 30.9, 54.4, 55.2, 112.3, 113.5, 130.0, 130.2, 132.9, 137.7, 147.5, 157.7. **CHN** Calculated for ($\text{C}_{22}\text{H}_{24}\text{N}_2\text{O}$): C: 79.48; H: 7.28; N: 8.43, found: C: 79.40; H: 7.55; N: 8.67.

Compound 292

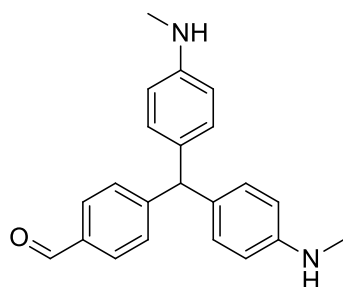
Isolated as a green crystals. $^1\text{H NMR}$ (300 MHz, CDCl_3) δ 2.82 (s, 6H), 5.42 (s, 1H), 6.57 (d, $J = 8.6$ Hz, 4H), 6.82 (m, 3H), 6.97 (d, $J = 8.4$ Hz, 4H), 7.13 (m, 1H). $^{13}\text{C NMR}$ (100 MHz, CDCl_3) δ 30.9, 49.8, 112.7, 116.3, 120.5, 127.7, 130.1, 130.4, 131.5, 148.0, 153.9.

Compound 289

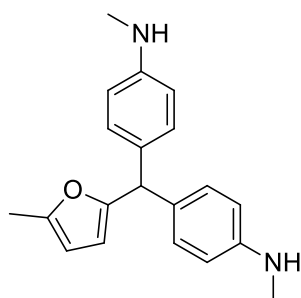
Isolated as a green oil. $^1\text{H NMR}$ (300 MHz, CDCl_3) δ 2.32 (s, 3H), 2.83 (s, 6H), 5.29 (s, 1H), 6.57 (d, $J = 8.6$ Hz, 4H), 6.94 (d, $J = 8.2$ Hz, 4H), 7.01 (d, $J = 8.1$ Hz, 2H), 7.07 (d, $J = 8.1$ Hz, 2H). $^{13}\text{C NMR}$ (100 MHz, CDCl_3) δ 21.1, 31.3, 55.0, 112.8, 128.9, 129.3, 130.2, 134.3, 135.4, 142.5, 147.2.

Compound 291

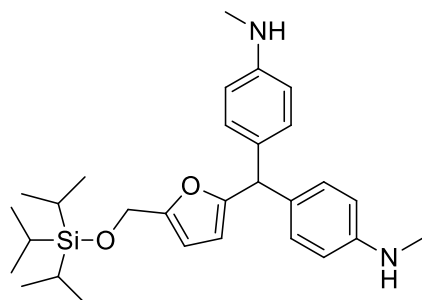
Isolated as a yellow oil. $^1\text{H NMR}$ (300 MHz, CDCl_3) δ 2.82 (s, 6H, s), 5.43 (s, 1H), 6.55 (d, $J = 8.6$ Hz, 4H), 6.90 (d, $J = 8.5$, 4H), 7.29 (d, $J = 8.6$ Hz, 2H), 8.11 (d, $J = 8.8$ Hz, 2H). $^{13}\text{C NMR}$ (100 MHz, CDCl_3) δ 30.9, 55.2, 112.5, 123.5, 130.1, 130.2, 131.8, 146.3, 148.1, 153.6.

Compound 303

Isolated as a green oil. $^1\text{H NMR}$ (300 MHz, CDCl_3) δ 2.82 (s, 6H), 5.40 (s, 1H), 6.59 (d, $J = 8.6$ Hz, 4H), 6.91 (d, $J = 8.3$ Hz, 4H), 7.30 (d, $J = 8.3$ Hz, 2H), 7.71 (d, $J = 8.3$ Hz, 2H), 9.97 (s, 1H). $^{13}\text{C NMR}$ (100 MHz, CDCl_3) δ 30.9, 55.6, 112.5, 129.8, 130.1, 130.2, 132.4, 134.6, 148.0, 153.1, 192.2.

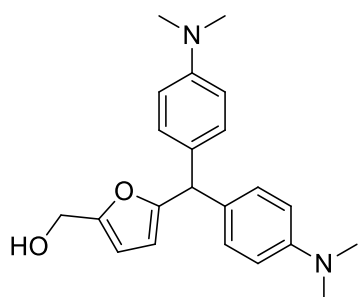
Compound 293

Isolated as a brown oil. $^1\text{H NMR}$ (300 MHz, CDCl_3) δ 2.23 (s, 3H, s), 2.81 (s, 6H), 5.19 (s, 1H), 5.71 (app s, 1H), 5.85 (app s, 1H), 6.54 (d, $J = 8.6$ Hz, 4H), 6.98 (d, $J = 8.2$ Hz, 4H).

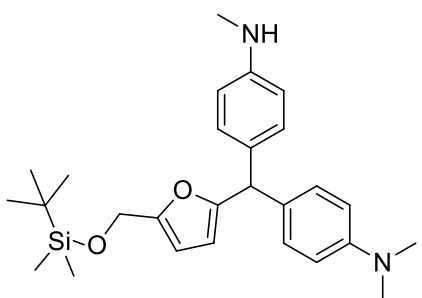
Compound 307

To a solution of **284** (50 mg, 0.16 mmol, 1 equiv.) in anhydrous DCM (1.6 mL, 0.1 M) at 0 °C, imidazole (21 mg, 0.32 mmol, 2 equiv.) and TIPSCl (0.07 mL, 0.32 mmol, 2 equiv.) were added. The reaction mixture was allowed to stir for 12 h at RT under argon atmosphere. The solvent was evaporated and the product was

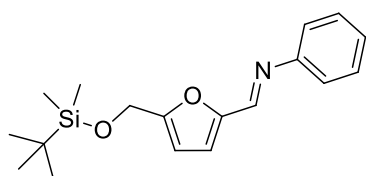
purified by column chromatography using hex/EtOAc to give the pure product (83% yield) as a yellow oil. **¹H NMR (300 MHz, CDCl₃)** δ 1.11 (m, 21H), 2.82 (s, 6H), 4.69 (s, 2H), 5.24 (s, 1H), 5.84 (d, *J* = 3.1 Hz, 1H), 6.17 (d, *J* = 3.1 Hz, 1H), 6.55 (d, *J* = 8.6 Hz, 4H), 7.02 (d, *J* = 8.3 Hz, 4H). **¹³C NMR (100 MHz, CDCl₃)** δ 12.2, 18.1, 31.0, 49.4, 58.8, 107.3, 108.2, 112.4, 129.6, 131.6, 147.9, 153.7, 157.7.

Compound 306

Isolated as a brown oil. **¹H NMR (300 MHz, CDCl₃)** δ 2.91 (s, 12H), 4.52 (s, 2H), 5.27 (s, 1H), 5.82 (d, *J* = 3.1 Hz, 1H), 6.18 (d, *J* = 3.1 Hz, 1H), 6.68 (d, *J* = 8.8 Hz, 4H), 7.03 (d, *J* = 8.7 Hz, 4H). **¹³C NMR (100 MHz, CDCl₃)** δ 41.3, 49.7, 58.2, 108.8, 109.1, 113.2, 129.8, 131.0, 149.9, 153.6, 159.1.

Compound 297

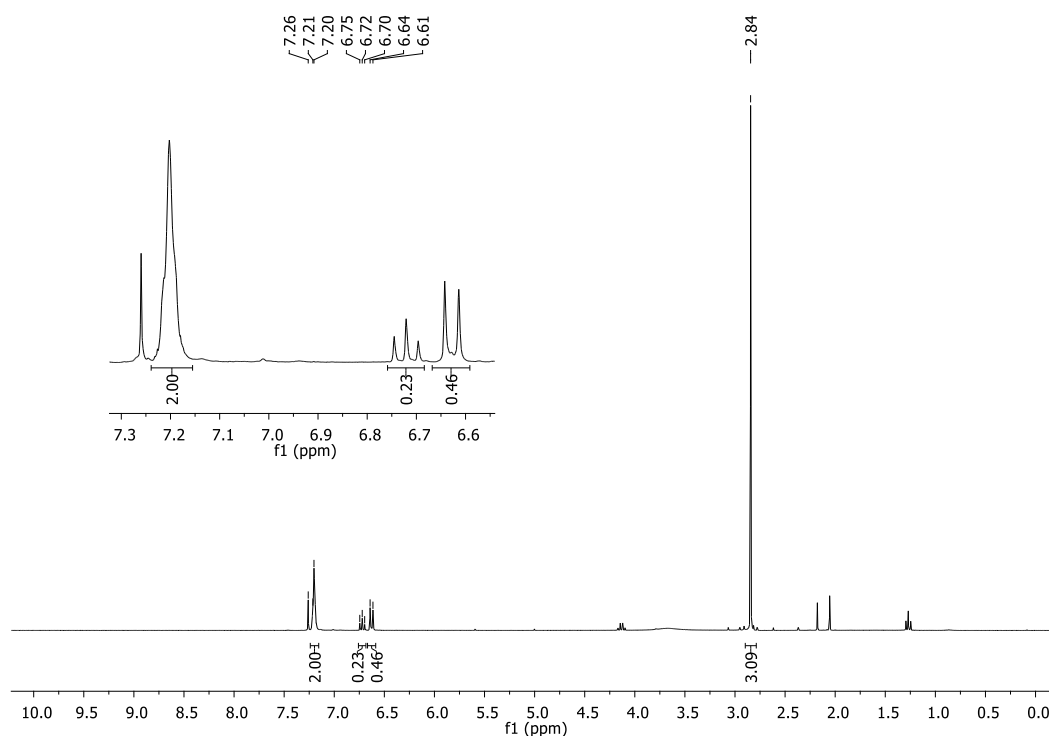
Isolated as a brown viscous liquid from the competitive experiment. **¹H NMR (300 MHz, CDCl₃)** δ 0.04 (s, 6H), 0.87 (s, 9H), 2.81 (s, 3H), 2.91 (s, 6H), 4.58 (s, 2H), 5.23 (s, 1H), 5.80 (d, *J* = 2.9 Hz, 1H), 6.12 (d, *J* = 3.0 Hz, 1H), 6.53 (d, *J* = 8.5 Hz, 2H), 6.66 (d, *J* = 8.7 Hz, 2H), 6.98 (d, *J* = 8.3 Hz, 2H), 7.03 (d, *J* = 8.5 Hz, 2H).

Compound 299 (Scheme III.47)

Following the general procedure, the product was isolated as an orange oil (63% yield). **¹H NMR (300 MHz, CDCl₃)** δ 0.11 (s, 6H), 0.93 (s, 9H), 4.77 (s, 2H), 6.42 (d, *J* = 3.4 Hz, 1H), 6.92 (d, *J* = 3.4 Hz, 1H), 7.22 (m, 3H), 7.37 (m, 2H), 7.22 (s, 1H). **¹³C NMR (100 MHz, CDCl₃)** δ -4.8, 18.9, 26.4, 59.3, 109.6, 117.9, 121.6, 126.6, 129.7, 148.5, 151.9, 152.2, 159.3.

Preparation of *N*-methylaniline-2,4,6- d_3 .

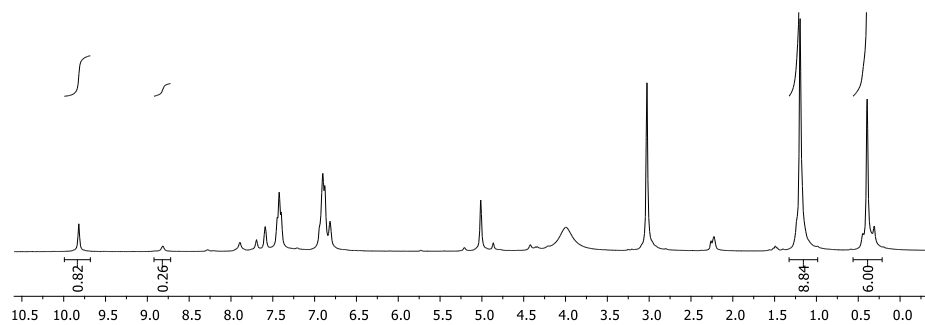
Acetyl chloride (1.5 mL) was slowly added to deuterium oxide (0.5 mL) with vigorous stirring at 0 °C. After 2 hours, *N*-methylaniline (0.2 mL) was slowly added and the reaction mixture was allowed to stir for 1 day at reflux. The reaction mixture was diluted and neutralized with NaHCO₃ sat. aq. solution and extracted with EtOAc. After careful solvent evaporation (40 °C, 150 mbar) the product was purified by column chromatography using hex/EtOAc to give the desired *N*-methylaniline with 80% D incorporation in *ortho* and *para* positions to the nitrogen (quantitative yield).



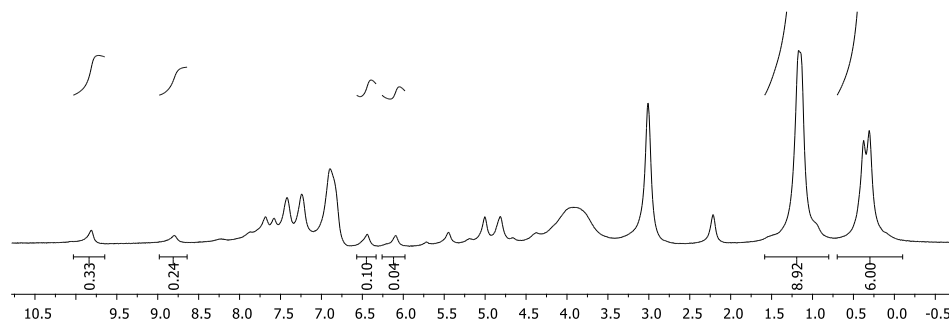
Intermolecular KIE experiment (Scheme III.53). To a 1:1 mixture of *N*-methylaniline and *N*-methylaniline-2,4,6- d_3 (6 equiv., ratio analyzed by ¹H NMR) and **148** (30 mg, 0.127 mmol, 1 equiv.) in anhydrous acetonitrile (1.3 mL, 0.1 M), Yb(OTf)₃ (10 mol%) was added. The reaction mixture was allowed to stir at 40 °C for 17 h under argon atmosphere. The solvent was evaporated and the crude reaction mixture was filtered through a pad of celite and analyzed by ¹H NMR.

Protocol for the reaction followed by ¹H NMR (Figure III.18). The general protocol was followed using anhydrous acetonitrile- d_3 (dried under molecular sieves for overnight). For the time described in the next spectra, the reaction mixture was transfer from the round bottom flask to the NMR tube, and then back again to the flask, under argon atmosphere.

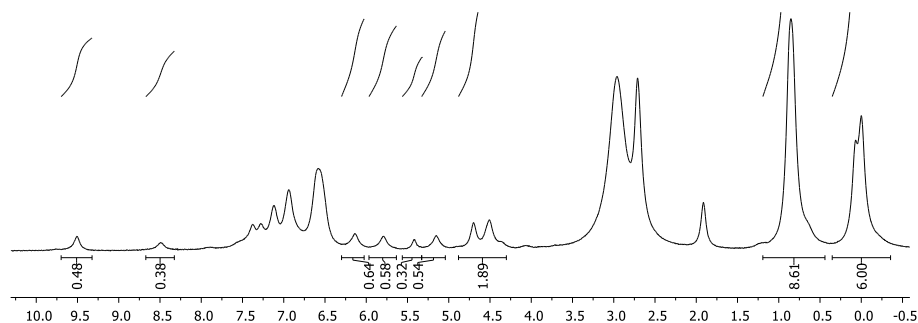
After 4 h:



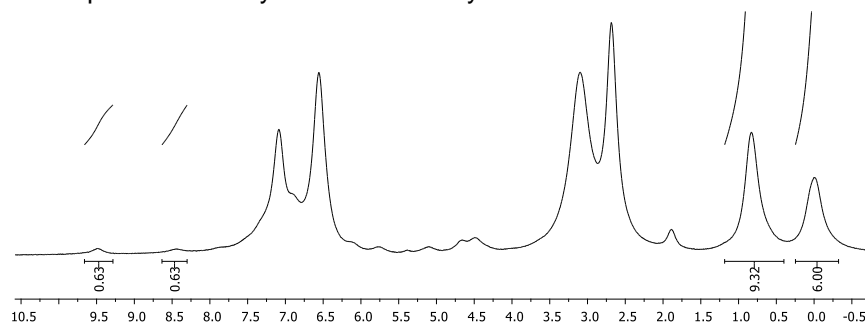
After 23 h:



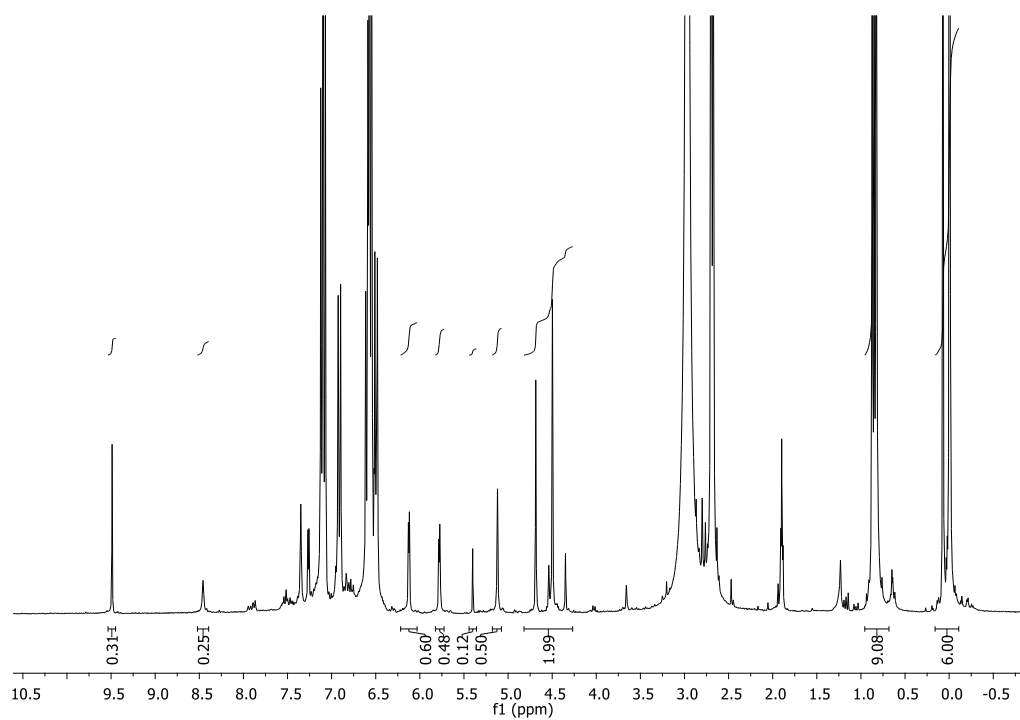
After 3 days:



After addition of 1 equiv. of *N*-methylaniline and 5 days:



After filtration through a pad o celite and 1 week in the freezer:



Chapter 4

Towards total synthesis of Modiolin, Fusanolide A and FR256523

In this chapter is described the work developed during my stay in the Max-Planck-Institut für Kohlenforschung (Germany) as a PhD exchange student from January 2013 to June 2013 under the supervision of Prof. Dr. Nuno Maulide. Herein is described the results towards the total synthesis of Modiolin and Fusanolide A and the synthesis of a building block for the total synthesis of FR256523.

IV. Towards total synthesis of Modiolin, Fusanolide A and FR256523	155
IV.1. Towards total synthesis of Modiolin and Fusanolide A	157
IV.1.1. Introduction	157
IV.1.2. Results	160
IV.2. Towards total synthesis of FR256523.....	171
IV.3. Conclusions and Perspectives.....	175
IV.4. Experimental	177
IV.4.1. General Remarks	177
IV.4.2. Towards total synthesis of Modiolin and Fusanolide A	177
IV.4.3. Towards total synthesis of FR256523.....	189

IV.1. Towards total synthesis of Modiolin and Fusanolide A

IV.1.1. Introduction

Conjugated dienoic carboxylates moieties are fundamental structural skeletons present in various natural products, such as those shown in **Figure IV.1**.

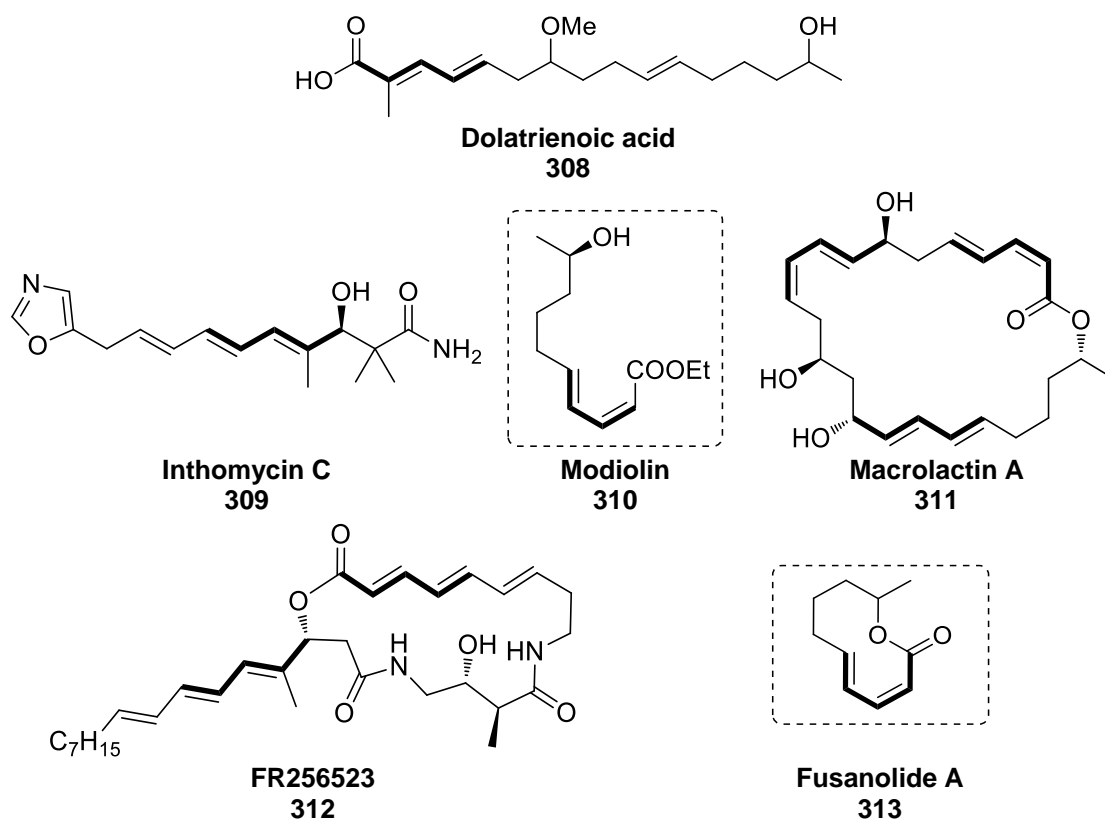
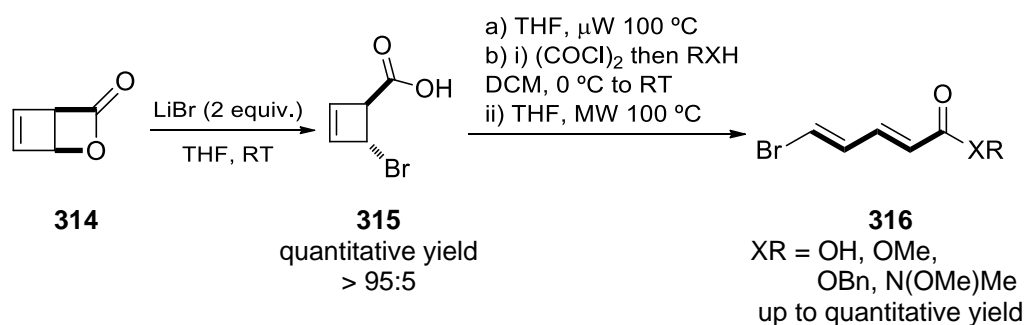


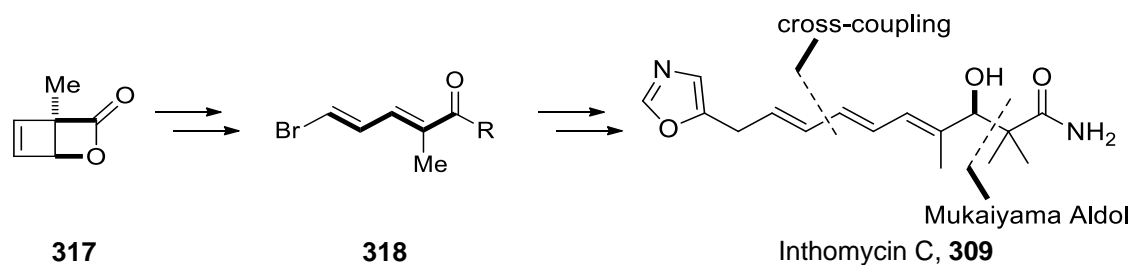
Figure IV.1. Selected examples of bioactive compounds bearing conjugated dienoic carboxylated moieties.

Very recently, Maulide *et al.* reported a direct synthetic route to functionalized and stereodefined diene carboxylate building blocks through the thermal 4 π -electrocyclic ring opening of readily available halocyclobutene precursors (**Scheme IV.1**).²⁶⁴⁻²⁶⁵



Scheme IV.1. Synthesis of halocyclobutenes and their ring-opening reactions

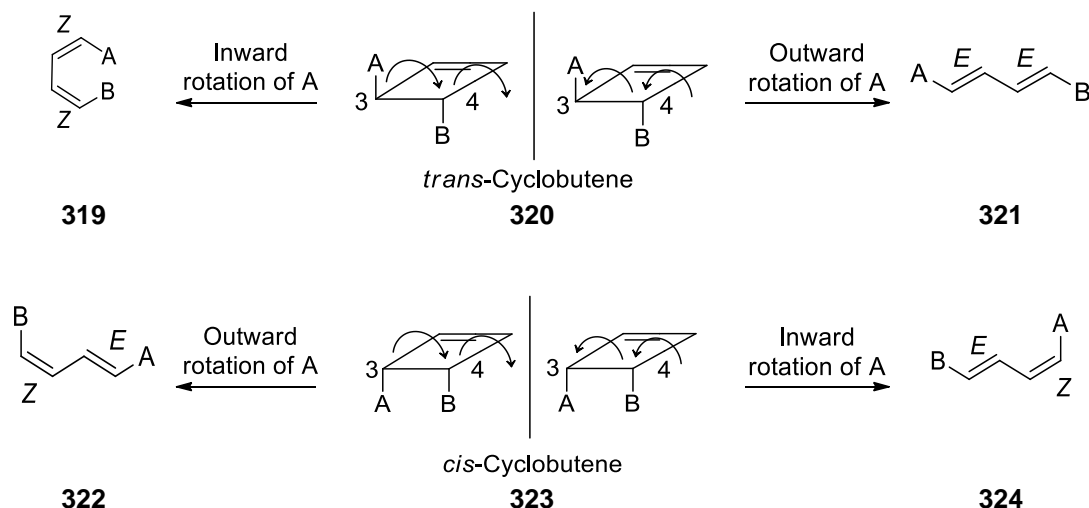
This methodology was successfully applied to the total synthesis of Inthomycin C **309**²⁶⁶ (Scheme IV.2).



Scheme IV.2. Total synthesis of Inthomycin C.

Extension of this approach to several other total syntheses of polyene natural products (e.g., concise synthesis of the southeastern fragment of Macrolactin A, **321**) was under exploration by Maulide group. Herein the results towards the total synthesis of Modiolin (**310**)²⁶⁷ and Fusanolide A (**313**) are discussed.

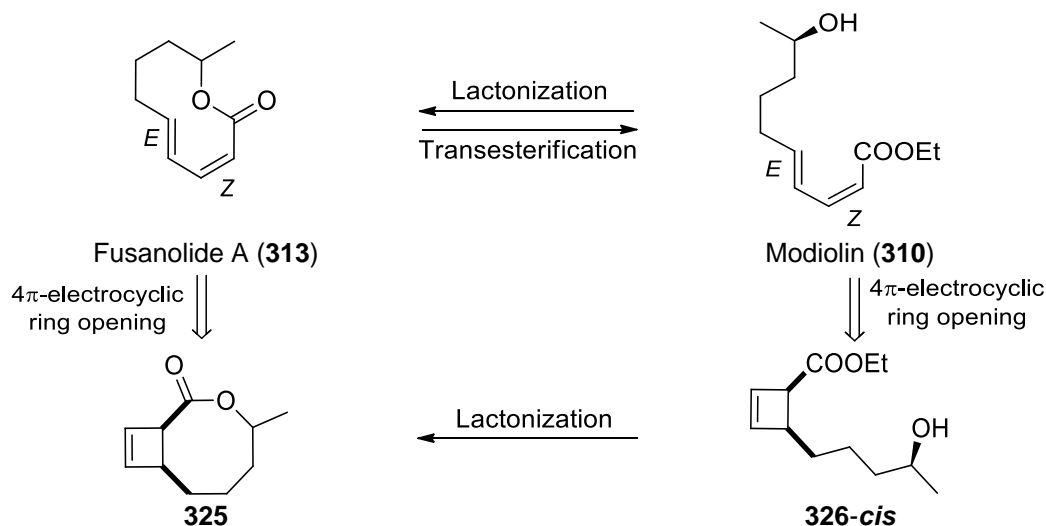
The above mentioned thermal 4π -electrocyclic ring opening of cyclobutenes is a well-established pericyclic reaction. This symmetry-allowed conrotatory transformation leads to either (*E,Z*)- or (*Z,E*)-diene products from a *cis*-3,4-disubstituted cyclobutene **323**, and (*E,E*)- or (*Z,Z*)-diene products from a *trans*-3,4-disubstituted cyclobutene **320** (Scheme IV.3).



Scheme IV.3. Conrotatory electrocyclic ring opening of substituted *cis* and *trans*-cyclobutenes.²⁶⁴

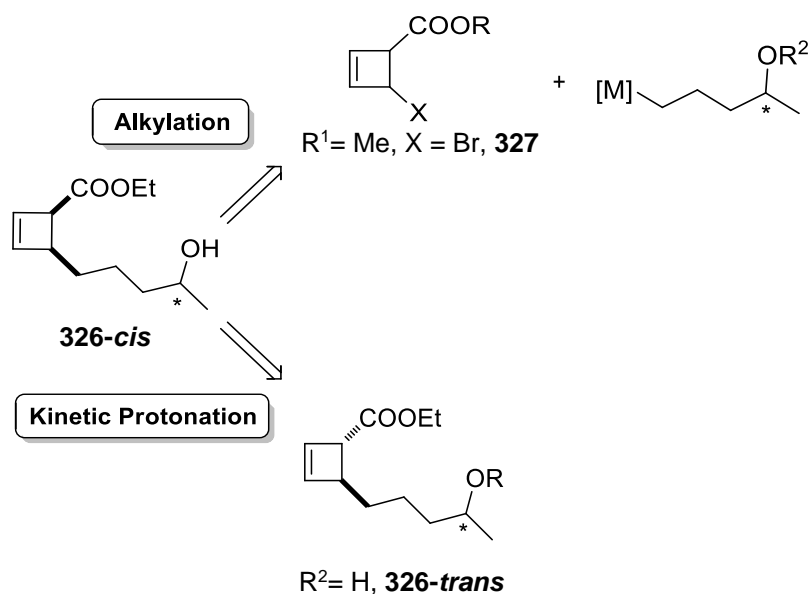
The inward or outward rotation of the substituents of the cyclobutene starting materials, crucial in determining the geometry of the diene products, can be predicted by a set of torquoselectivity rules deduced by Houk.²⁶⁸ Sterically demanding and electron-donating groups tend to rotate outward, whereas smaller and electron-withdrawing substituents (such as carboxylates) prefer inward rotation.

Both Modiolin (**310**) and Fusanolide A (**313**) natural products have a dienoic carboxylate structure which could be easily accessed from a ring-opening reaction of the corresponding *cis*-cyclobutenes. Therefore, a straightforward strategy for the synthesis of both natural products is proposed in **Scheme IV.4**. The ring-opening of a *cis*-cyclobutene bearing a carboxylate and the desired alkyl chain as substituents to generate the desired *Z,E*-diene is proposed for the last step of this retrosynthetic analysis. Moreover, the two natural products can be interconverted by macrolactonization or transesterification reactions.



Scheme IV.4. Retrosynthetic analysis for Fusanolide A and Modiolin.

The key step of this strategy is the construction of the required *cis*-cyclobutene **326-cis**. For that, two approaches were proposed: alkylation of a halocyclobutene (**327** was used as model substrate) or kinetic protonation of the **326-trans** isomer as depicted in **Scheme IV.5**.

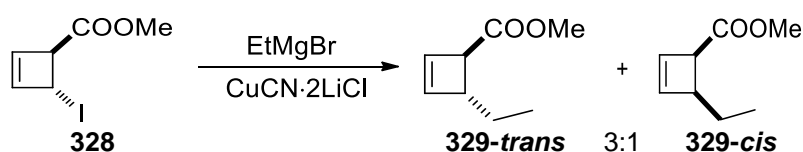


Scheme IV.5. Proposed strategies for the synthesis of the key cyclobutene **326-cis**.

IV.1.2. Results

Preliminary result

The reaction of organocopper reagent, prepared *in situ* by transmetallation of ethyl magnesium bromide and CuCN·2LiCl, with *trans*-methyl 4-iodocyclobut-2-ene carboxylate (**328**) resulted in the exclusive formation of both **329-cis** and **329-trans** as depicted in the **Scheme IV.6**. Despite the ratio favoring the undesired isomer *trans*, this result was promising because showed that only the desired alkylation was occurring.



Scheme IV.6. Alkylation of *trans* methyl 4-iodocyclobut-2-ene carboxylate (**328**) using monoorganocopper reagent (Experiment performed by Caroline Souris from Maulide group).

Alkylation strategy

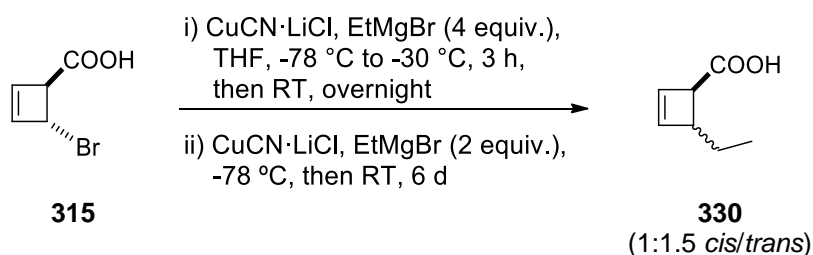
Gratifyingly, using the same conditions as before, the bromo derivative **327** offered a ratio of 3.7:1, favoring the desired product **329-cis** (**Table IV.1**, entry 1). However, the reaction was not completed, as starting material **328** was found in the crude reaction mixture by ^1H NMR analysis. Harsher conditions were tested to improve the starting material conversion, namely higher temperatures and longer times (**Table IV.1**, entries 2 and 3). Unfortunately, full conversion was never achieved even after overnight reaction at room temperature. Intriguingly, despite the good reproducibility of *cis/trans* ratio, starting material conversion was not in agreement with the harshness of the reaction conditions tested (**Table IV.1**, entry 2 vs. entry 3). Furthermore, no significant changes were observed from 1 to 6 h. Thus, degradation of the product and irreproducibility of the organocopper reagent preparation are hypothesis that could explain this unexpected result. Other types of organocopper alkylating agents reported in literature²⁶⁹⁻²⁷⁰ were also investigated yielding the undesired *trans* isomer as a major product (**Table IV.1**, entries 4-6).

Table IV.1. Alkylation of halocyclobutene **327**.

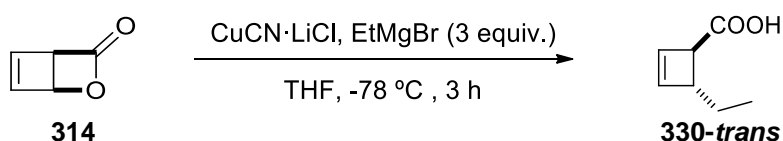
Entry	Solvent	Alkylating agent ^a	Temperature and time	cis/trans/327 ratio ^b
1	THF	CuCN·2LiCl + EtMgBr	-70 °C, 3 h	3.7 / 1.0 / 1.3
2	THF	CuCN·2LiCl + EtMgBr	-70 °C, 6 h, then RT overnight	3.8 / 1.0 / 1.9
3	THF	CuCN·2LiCl + EtMgBr	-70 °C to -30 °C in 3 h, -30 °C for 3 h and then RT overnight	3.6 / 1.0 / 4.0
4	Et ₂ O	Et ₂ Cu(CN)(MgBr) ₂	-70 °C to -30 °C in 2 h	1.0 / 2.4 / 0.1
5	THF	Et ₂ Cu(CN)(MgBr) ₂	-70 °C to -30 °C in 2 h	1.0 / 6.5 / 0.2
6	THF	EtCu(CN)(MgBr)	-70 °C to -30 °C in 2 h	1.0 / 1.5 / 1.2

^aAlkylating agent prepared in situ using described methods²⁶⁹⁻²⁷⁰ ^bRatio determined by ¹H NMR of crude reaction mixture after quenching with HCl and extraction with MTBE.

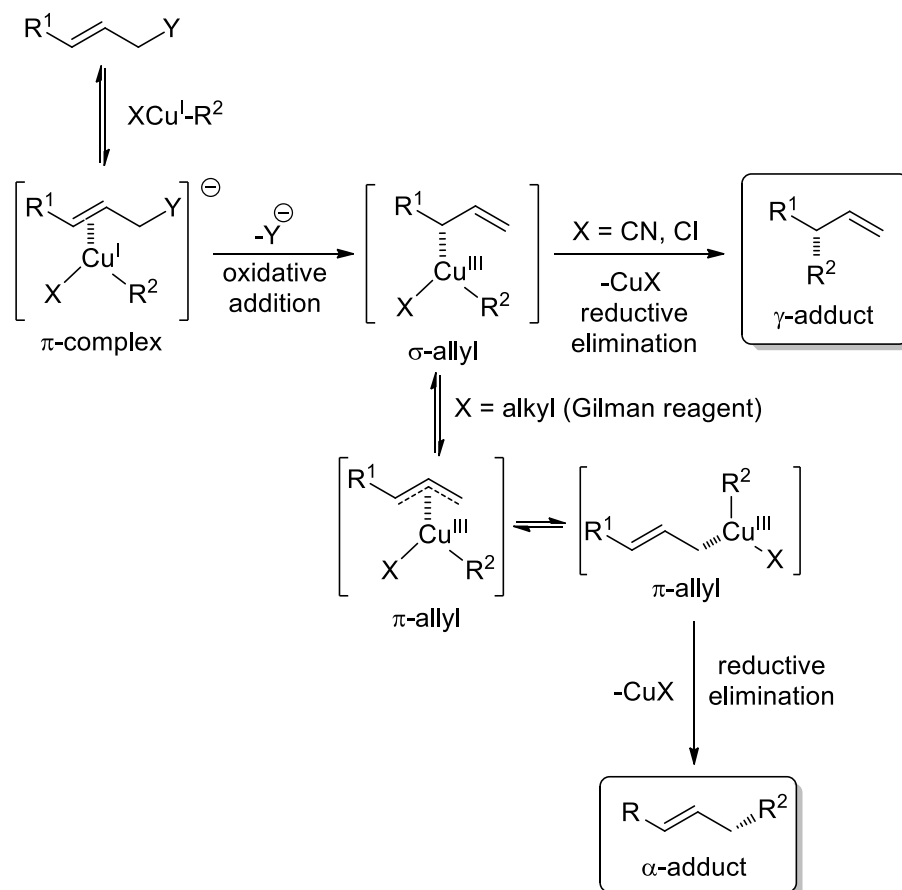
An interaction between the carboxylic acid moiety and the organocopper reagent was expected, to possibly result in the selective alkylation from the same side as the carboxylic moiety, favoring the formation of the *cis* isomer. However, the reaction of acid **315** afforded **330** in a *cis/trans* ratio of 1:1.5 (**Scheme IV.7**). Moreover, the reaction was again not complete even using a total of 6 equivalents of alkylating agent and 6 days reaction time at room temperature (a ratio **315/330** of 4:6 was observed by ¹H NMR of crude reaction mixture).

**Scheme IV.7.** Alkylation of carboxylic acid derivative **315** using organocopper reagent (ratio **315/330** in the end of the reaction was 4:6).

In addition, alkylation of lactone (1*S*,4*R*)-2-oxabicyclo[2.2.0]hex-5-en-3-one **314** offers exclusively the undesired *trans* product **330-trans** (**Scheme IV.8**).

**Scheme IV.8.** Alkylation of lactone **314**.

As mentioned above, these reactions gave only the two cited isomers as products and no other alkylation products. The reaction may proceed *via* an S_N2 displacement or *via* an oxidative addition followed by reductive elimination. For the second case, α - or γ -substitution can take place depending on the organocopper used. In contrast to monoalkylcopper species that offered the γ -adduct product, it is known that dialkylcopper species gives preferentially α -adduct products, which can be explained by the mechanism depicted in **Scheme IV.9**.²⁷¹⁻²⁷²

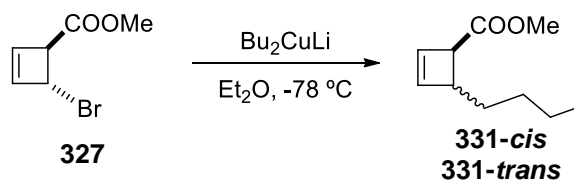


Scheme IV.9. General mechanism of organocopper(I)-mediated C-C bond formation.²⁷¹⁻²⁷²

Based on the assumption that this different reactivity could lead to a different *cis/trans* outcome, Gilman type reagents were investigated.²⁷¹⁻²⁷² Lithium dibutylcopper was prepared by reaction of *n*-butyl lithium and copper iodide, and reacted with **327**.²⁷³ Remarkably, selective formation of the desired **331-cis** isomer was obtained when 2 or 3 equivalents of alkylating agent were used (**Table IV.2**, entries 1 and 3). Furthermore, complete reactions were observed in very short reaction time. For commodity, the alkylating agent was changed from ethyl to butyl because *n*-butyl lithium is commercial available. Finally it is noteworthy to mention the formation of other cyclobutene-containing product for the reactions with selective formation of the *cis* isomer, which can explain the

lower isolated yields observed. This side-product was not isolated and the exact structure is unknown.

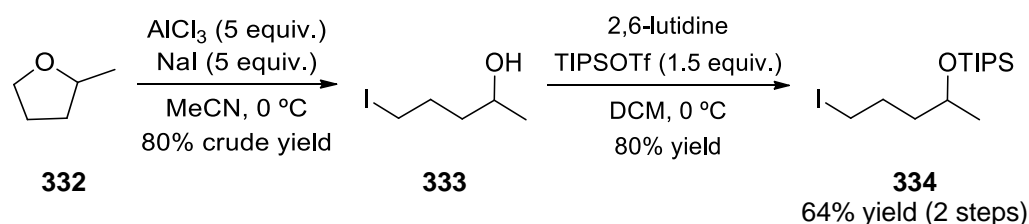
Table IV.2. Alkylation using dialkyl copper reagent.



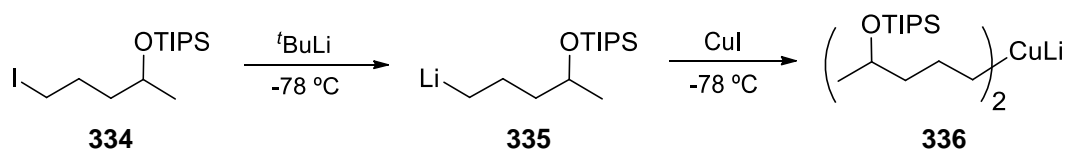
Entry	Bu_2CuLi (eq)	331- <i>cis</i> / <i>trans</i> /by-product ratio ^a	Isolated yield (%) of 331
1	2	7.6/1.0/0.7	43
2	1	1.8/1.0/NO	63
3	3	9.1/1.0/1.7	41
4	1 (addition for 2h)	0.9/1.0/NO	88

^aRatio determined by ^1H NMR of crude reaction mixture after quenching with HCl and extraction with MTBE. NO = not observed by ^1H NMR analysis

Encouraged by these results, we next aimed to improve the yield by reaction conditions optimization. Keeping in mind the structure of the desired natural product we decided to further continue the studies with the proper alkyl chain. Thus, Gilman reagent **336** (**Scheme IV.11**) would be necessary to yield the desired natural product precursor. Based on reported protocols, iodoalkyl **334**²⁷⁴ was obtained in 64% isolated yield (**Scheme IV.10**). Subsequently, lithium-iodide exchange followed by copper insertion was performed in order to synthesize the cited Gilman reagent **336** (**Scheme IV.11**).



Scheme IV.10. Synthesis of ((5-iodopentan-2-yl)oxy)triisopropylsilane (**334**).



Scheme IV.11. Proposed preparation of Gilman reagent **336**.

This reagent was then reacted *in situ* with **327** in the same conditions as performed before for Bu_2CuLi . Unfortunately, undesired *cis/trans* ratio was obtained for all the

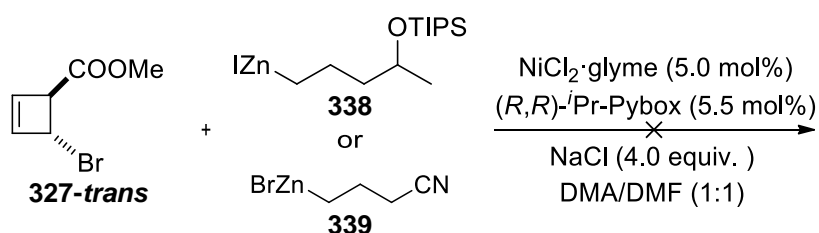
conditions tested together with low starting material conversion as summarized in **Table IV.3**. Since the outcome is similar to those obtained when monoalkylcopper reagents were used, it is reasonable to conclude that the dialkylcopper species **336** was not formed. An explanation for this could be the presence of OTIPS group that can interact with the copper center. To overcome this, titanium isopropoxide was added as additive to tentatively block the oxygen by coordination between the titanium and oxygen. However, selective formation of the *trans* isomer took place under this reaction conditions (**Table IV.3**, entry 3).

Table IV.3. Alkylation of **327** using dialkylcopper **336**.

Entry	336 (equiv.)	Additive	t / T	337-cis / 337-trans / 327 ratio	OTIPS
1	2		0.5 h / -78 °C	1/1.6/2.1	-
2	4	-	4 h / -78 °C 22 h / -78 °C to RT	-	Major product
3	2	Ti(O ⁱ Pr) ₄	2 h / -78 °C	0/1/1	traces

Taking into account these results it was decided to abandon this strategy, mainly because the reaction with desired alkyl chain **334** did not lead to a selective formation of the desired *cis*-cyclobutene product. Moreover, a very large amount of **334** would be necessary to perform the reaction under the actual reaction conditions. Thus, we next turned our attention toward the kinetic protonation strategy.

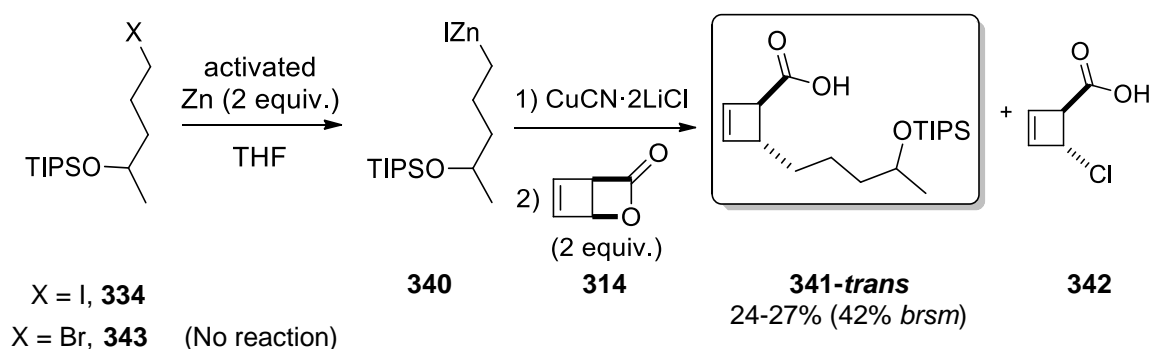
The reaction conditions reported by Fu *et al.* for the Nickel-catalyzed asymmetric Negishi cross-coupling of secondary allylic chlorides with alkylzincs were also investigated, but compound **327-trans** was not reactive under the conditions tested (**Scheme IV.12**).²⁷⁵



Scheme IV.12. Reaction of **327-trans** under the alkylation conditions reported by Fu *et al.*²⁷⁵

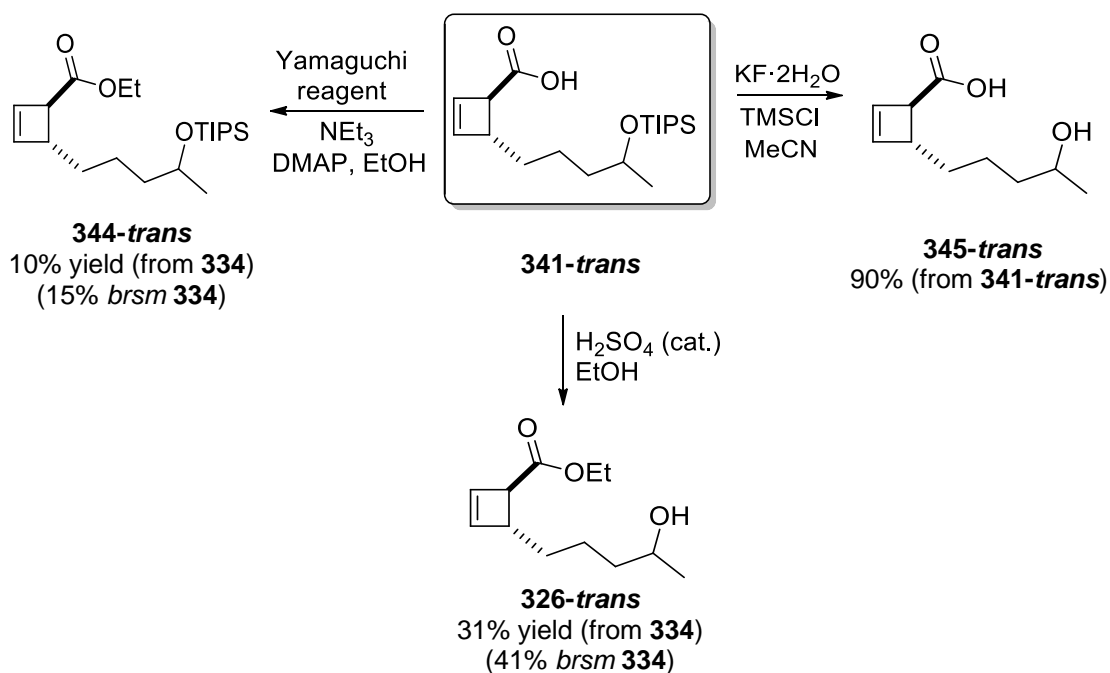
Kinetic Protonation strategy

Using reaction conditions optimized by Dr. Caroline Souris in Maulide lab for the same substrate, *trans* 4-(4-((triisopropylsilyl)oxy)pentyl) cyclobut-2-enecarboxylic acid (**341**) was prepared *via* organozinc chemistry as depicted in **Scheme IV.13**. Unfortunately, the yields obtained were around 30% (much lower compared to those reported by Dr. Caroline Souris). Several experimental conditions were investigated to improve the yield, such as solvent moisture, inert atmosphere and zinc and TMSCl sources. After a extensive study, it was concluded that zinc activation is the crucial step in this synthesis. The bromoalkyl derivative **343** was also tested but no zinc insertion occurred after overnight reaction at reflux temperature.



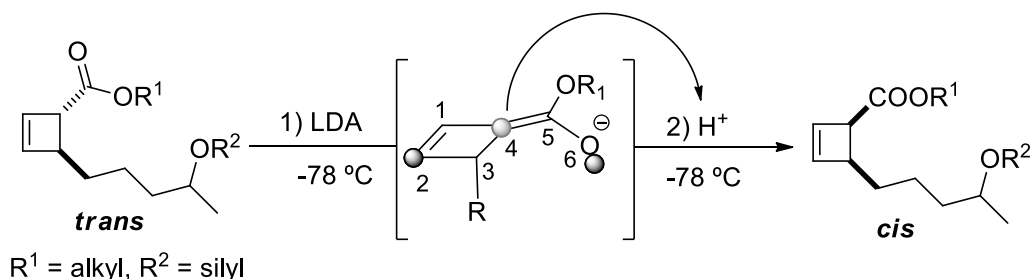
Scheme IV.13. Synthesis of **341-trans**. *brsm* = based on recovered starting material.

Several other derivatives were also prepared by employing benchmark methods as summarized in **Scheme IV.14**. Yamaguchi esterification condition offered the ethyl ester without deprotection of TIPS group (compound **344**)²⁷⁶ whereas the acid catalyzed esterification led to the formation of the unprotected alcohol **326**. Finally, TIPS deprotection promoted by KF/H₂O/TMSCl²⁷⁷ afforded the product **345**.



Scheme IV.14. Synthesis of cyclobutene derivatives **326-*trans***, **344-*trans*** and **345-*trans***.
brsm = based on recovered starting material.

The expected mode of action for the kinetic protonation to convert the *trans*-cyclobutene into the *cis* isomer is illustrated in **Scheme IV.15**. The most common proton sources described in the literature for kinetic protonation are 2,6-di-*tert*-butyl-4-methylphenol (BHT) and acetic acid.²⁷⁸⁻²⁹⁰ It is noteworthy to mention that the enolate obtained by reaction of the *trans* isomer with LDA contains three atoms (C2, C4 and O6, **Scheme IV.15**) that can react with the proton source. Gratifyingly, it was observed that only the desired carbon atom reacted with the proton source, allowing the quantitative isolation of the product (as a mixture of *cis*/*trans* isomers). Unfortunately, in this first attempt, a *cis*/*trans* ratio of 1:1.7 was obtained (**Table IV.4**, entry 1).



Scheme IV.15. Proposed mode of action for kinetic protonation.

Since it is not possible to directly analyze the *in situ* formation of the enolate, it was speculated that the reaction conditions were not effective enough to give full conversion of the starting material into the enolate. Thus, five equivalents of LDA prepared *in situ*, and

different reaction times were tested. However, this was not the case because the same ratio was observed for both 15 min and 2 h reaction time (**Table IV.4**, entries 2 and 3). Submitting substrate **344-trans** to the previous optimized reaction conditions led to a ratio of 1:1 (**Table IV.4**, entry 4).

During proton source screening, acetic acid was found to offer the better selectivity towards the *cis* isomer (**Table IV.4**, entry 5). Very surprisingly, quenching with HCl 1 M gave a *cis/trans* ratio of 1:2 which was not in agreement with the expected thermodynamic result of 0:1 (**Table IV.4**, entry 7). The more acidic phenol ethyl 2-hydroxybenzoate (ES) was also tested but only traces of product was observed and an unknown compound was obtained instead (**Table IV.4**, entry 6). Furthermore, the system HMPA/THF was used as solvent with no dramatic changes for the *cis/trans* ratio (**Table IV.4**, entry 8).

Table IV.4. Kinetic protonation experiments.^a

trans *cis/trans*

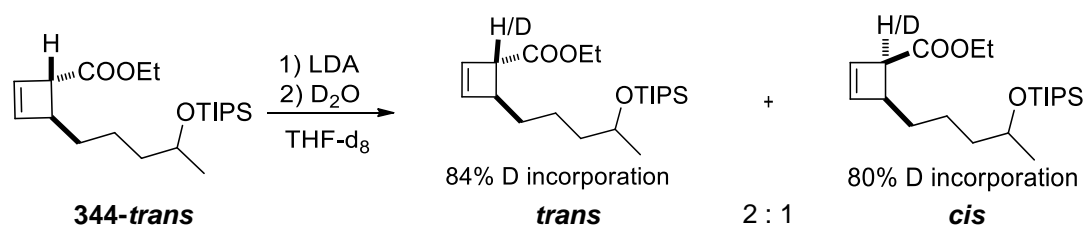
Entry	R ₁	R ₂	Compound	Proton source	<i>Cis/trans</i> ratio ^b
1 ^{c,d}	Et	H	326-trans	BHT	1:1.7
2 ^e	Et	H	326-trans	BHT	1:1.3
3 ^{c,e}	Et	H	326-trans	BHT	1:1.3
4	Et	TIPS	344-trans	BHT	1:1
5	Et	TIPS	344-trans	AcOH	1.2:1
6 ^f	Et	TIPS	344-trans	ES	traces
7	Et	TIPS	344-trans	HCl 1 M	1:2
8 ^{f,g}	Et	TIPS	344-trans	BHT	1:1.2
9	Et	TIPS	344-trans	D ₂ O	1:2
10 ^{f,h}	Et	TIPS	344-trans	D ₂ O	1:1.9
11	Et	TIPS	344-trans	TFA	1:1.6
12	Et	TIPS	344-trans	Pivalic acid	1:1.4
13 ^{i,j}	H	TIPS	345-trans	BHT	0:1
14 ^{i,k}	H	TIPS	345-trans	BHT	1:1.2

^aConditions for enolate formation: To a solution of *trans* compound in THF at -78 °C LDA (4 equiv., prepared *in situ*) was added. After 15 min the proton source was added at -78 °C and the reaction mixture was allowed to warm until room temperature.

^bDetermined by ¹H NMR of crude reaction mixture. ^c2 h for enolate formation.

^dCommercial LDA was used. ^e5 equiv. of LDA were used. ^f40 min at 0 °C for enolate formation. ^gHMPA (6 equiv.) was used as additive. ^hTHF-d₈ was used as solvent. ⁱ6 equiv. of LDA were used. ^j40 min at -78 °C for enolate formation. ^k3 h at 0 °C for enolate formation. BHT = 2,6-Di-*tert*-butyl-4-methylphenol. ES = Ethyl 2-hydroxybenzoate

To evaluate the deprotonation level, deuterated water was used as “proton source” to quench the reaction. As expected, the *cis/trans* ratio was similar to the one obtained using HCl 1 M. Surprisingly, incorporation of hydrogen in the *cis* product was observed (see result in **Scheme IV.16**), which is still not clear because the starting material was 100% *trans* and no proton sources were used. It was speculated that the protons could come from the aqueous work-up but reaction without workup and performed in dry THF- d_8 led to similar result (**Table IV.4**, entries 9 and 10).



Scheme IV.16. Kinetic deuteration experiment.

Since acetic acid offered the best *cis/trans* ratio, TFA and pivalic acid were also investigated to evaluate the steric and pKa effects. Unfortunately, the *trans* product was obtained as major product for both reactions (**Table IV.4**, entries 11 and 12). No other proton sources were tested because these are the most common ones.²⁷⁸⁻²⁹⁰ Moreover, according to the literature, no significant changes are observed when the proton source is changed, and so, no shift from *trans* to *cis* is expected for this substrate.

The fact that this molecule is not suitable for kinetic protonation is a reasonable explanation for the failure of this methodology. In fact, there is no significant steric difference between the two sides of the enolate plane for the selective proton source approach. In other words, the cyclobutene and the enolate are in the same plane and the substituent of the cyclobutene is a long aliphatic chain that not offer considerable steric effects (see **Figure IV.2**). It was speculated that the ethyl group from the carboxylate could interfere in the approach of the proton to the carbon center. However, using dienolate derivative in the kinetic protonation conditions led to a *cis/trans* ratio of 1:1.2 (**Table IV.4**, entry 13). As expected, the normal conditions were not harsh enough to form the dienolate. Therefore, harsher conditions were also tested, but no promising results favoring the *cis* isomer was observed (**Table IV.4**, entry 14).

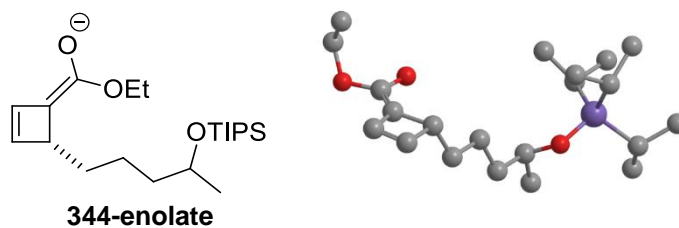


Figure IV.2. 3D structure of compound **344-enolate**.

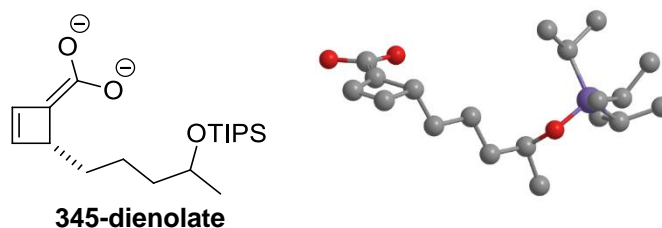


Figure IV.3. 3D structure of compound **345-dienolate**.

Looking for a more suitable derivative, it was expected that the corresponding lactone **346** would have significant different steric environment in the upper and bottom faces of the enolate (**Figure IV.4**) that could lead to an improved *cis/trans* ratio in kinetic protonation. Additionally, is also expected more stability for the *cis* isomer due to the constraint of the eight member ring. As a result, a simple thermodynamic protonation may take place to yield the *cis* isomer selectively.

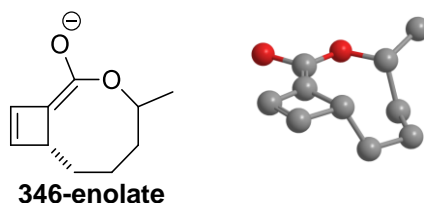
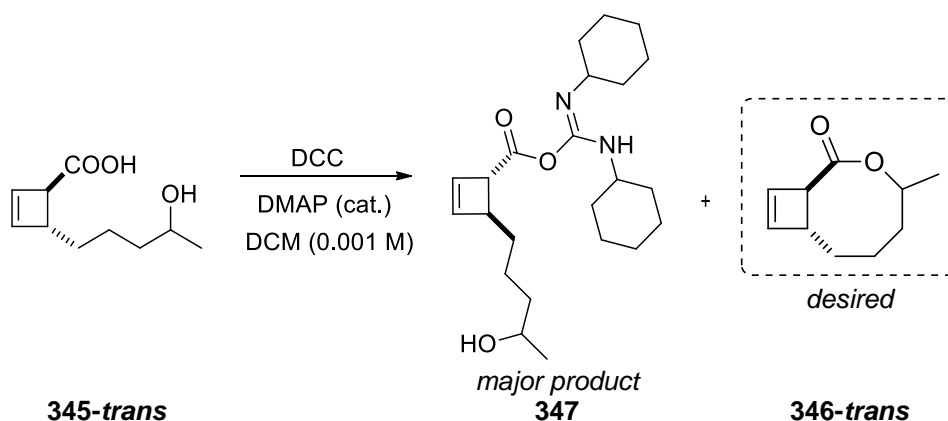


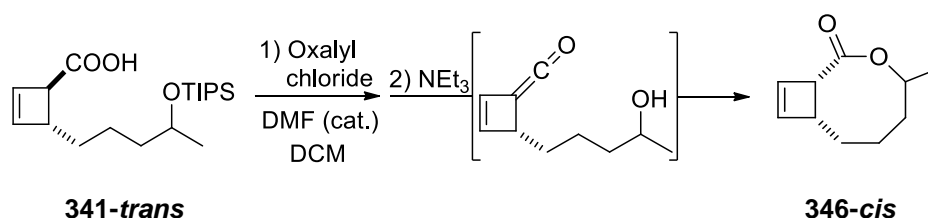
Figure IV.4. 3D structure of compound **346-enolate**.

Several known macrolactonization methods failed to yield the desired lactone (e.g., Yamaguchi esterification, Mitsunobu, $\text{Ac}_2\text{O}/\text{DMAP}$ and DCC/DMAP). DCC/DMAP coupling was found as the most promising method because gave the most selective reaction by NMR analysis. The known intermediate **347** of this reaction is suggested as the major product although the product was not fully characterized. The isolation of this type of intermediate suggests that the cyclization is not favorable for this ring size with a *trans*-cyclobutene (**Scheme IV.17**). Unfortunately, harsher conditions such as higher temperature cannot be used without avoiding the cyclobutene ring-opening process.



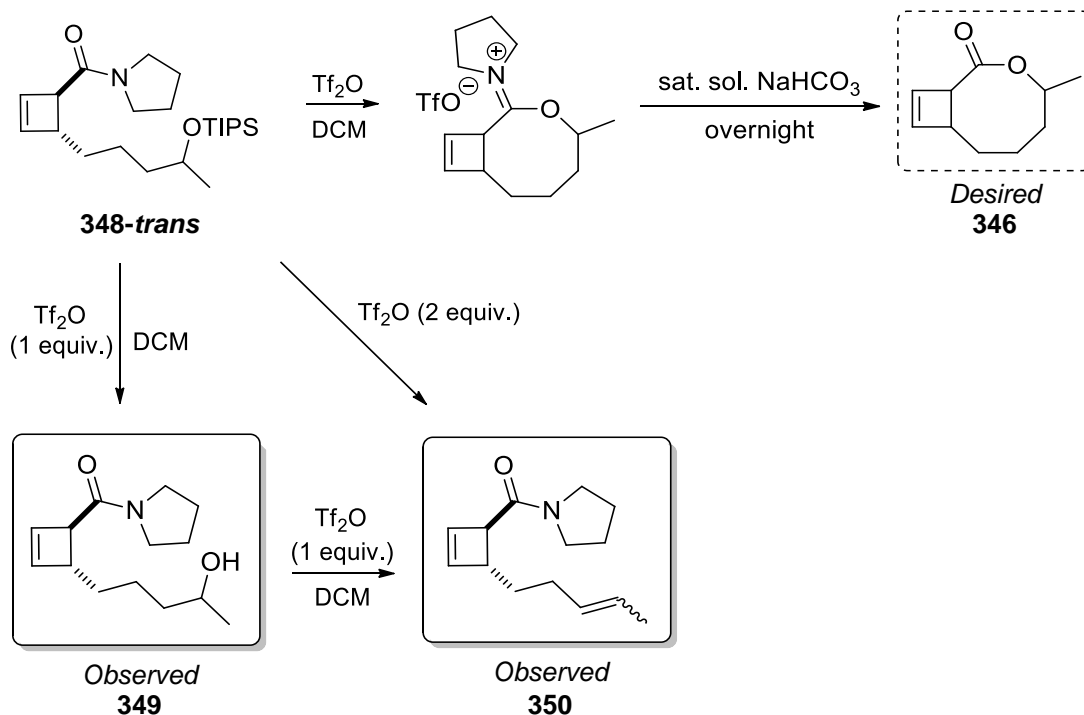
Scheme IV.17. Lactonization using DCC/DMAP.

Next, lactonization via ketene formation was also investigated. As illustrated in **Scheme IV.18**, the more stable **346-cis** isomer was expected as major product due to deprotonation of the α -proton of the carboxylic acid during ketene formation. Unfortunately, this approach was discarded after several attempts because an unselective reaction was taking place (complex ^1H NMR and more than 9 spots by TLC analysis). Additionally, the stepwise reaction was followed by *in situ* infra-red because distinct carbonyl groups are present during the reaction. However, due to the low concentration used (0.01 M), no signal was detectable.



Scheme IV.18. Proposed lactonization of **341-trans** via ketene intermediate.

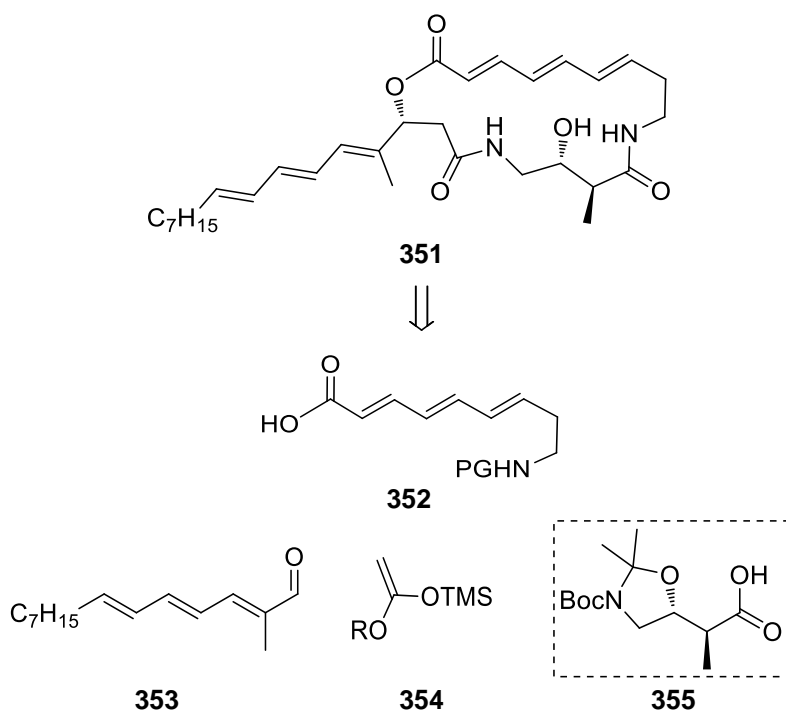
Finally, the esterification recently reported by Maulide *et al.*²⁹¹ was investigated for substrate **348-trans**. The reported methodology allows the lactonization of pyrrolidine amides and silyl protected alcohols via iminium ether intermediate as depicted in **Scheme IV.19**. After several attempts (quantity of triflic anhydride, temperature and concentration were screened) no cyclization was observed and alcohol elimination to yield the alkene **350** was taking place instead. Furthermore, reaction in the presence of water was also tested, giving the same outcome.



Scheme IV.19. Desired and observed products of the treatment of **348-*trans*** with triflic anhydride.

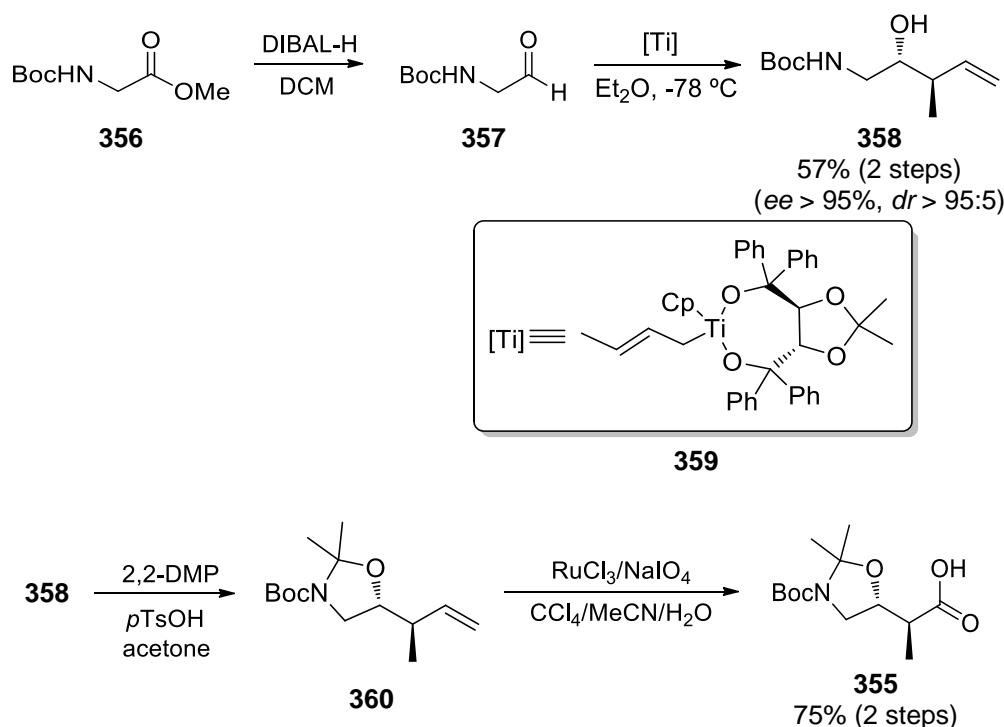
IV.2. Towards total synthesis of FR256523

Application of the above cited cyclobutene chemistry (**Section IV.1**) to the total synthesis of the recently isolated immunosuppressive agent FR256523 (**351**) was also currently under development in Maulide laboratory. The general synthons required for this total synthesis are depicted in **Scheme IV.20**. The exact retrosynthetic pathway was under development by Caroline Souris and Dr. Mohan Padmanaban from Maulide group. My goal in this collaboration was to prepare compound **355** using reported protocols.



Scheme IV.20. Retrosynthetic analysis for FR256523.

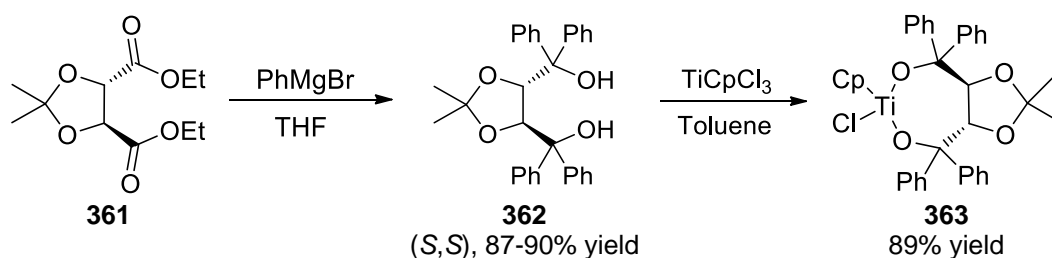
In the reported total synthesis of FR256523 (**351**) the authors prepared the (*S*)-2-[(*R*)-3-(Boc)-2,2-dimethyloxazolidin-5-yl]propanoic acid (**355**) according to **Scheme IV.21**.²⁹² Therein, *N*-Boc ethanolamine methyl ester (**356**) is reduced into the corresponded aldehyde **357** which undergoes diastereoselective crotyllation using the *in situ* prepared titanium complex **359** to afford the desired enantioenriched homoallylic alcohol **358**. Protection of both amine and alcohol and further oxidation of double bond into carboxylic acid gives the desired building block **355**.



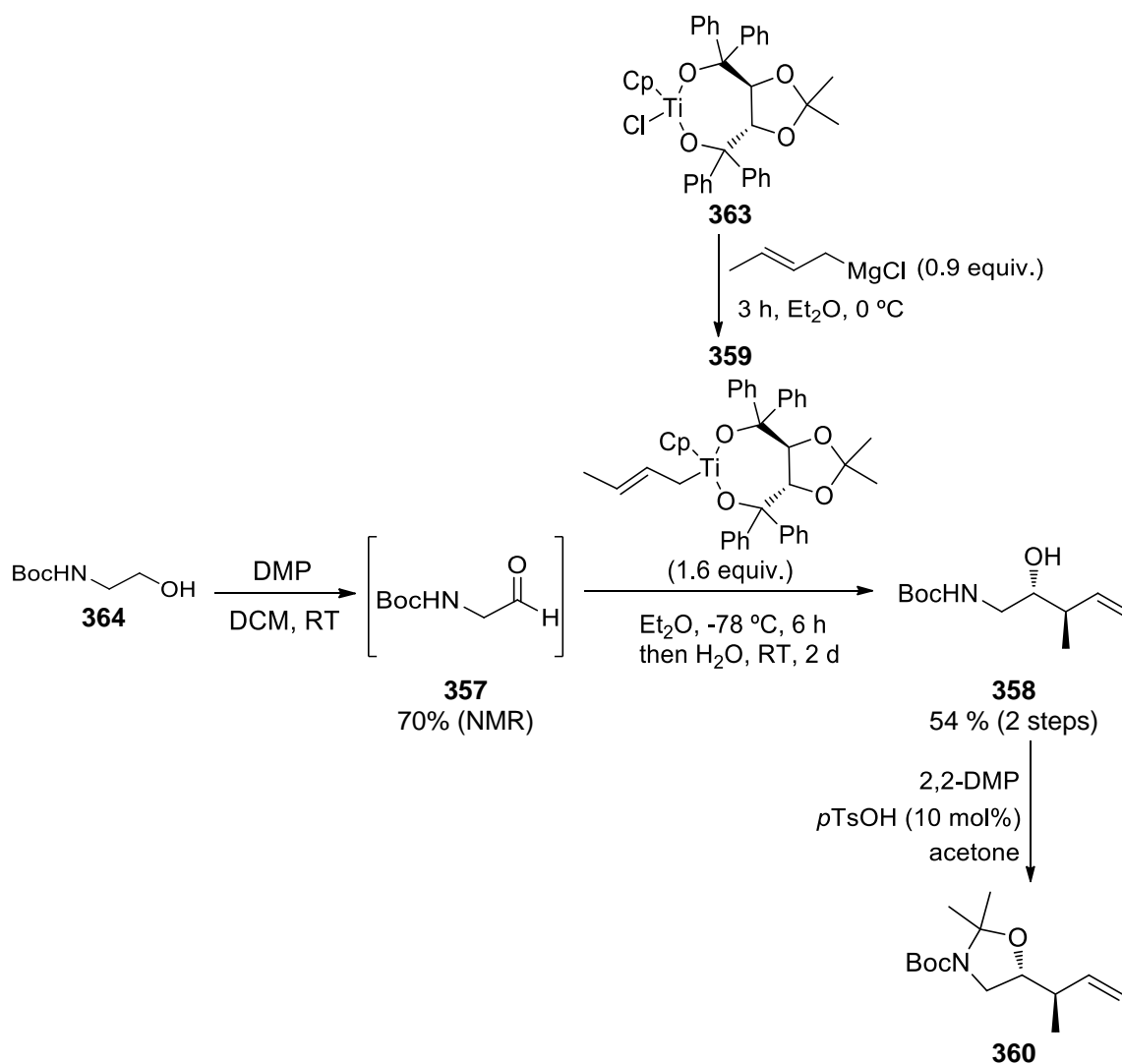
Scheme IV.21. Reported synthesis of desired building block **355**.²⁹²

Following the reported protocol for the reduction of ester **356** gave the desired aldehyde **357** in the range from 70 to 30%, performing a 1 or 25 mmol scale reaction respectively. Unsuccessful efforts were made to improve the yield such as using a new DIBAL-H commercial source, using a little excess of DIBAL-H (1.1 equiv.), longer reaction times and DIBAL-H addition time. The irreproducibility of this reaction led to the synthesis of the aldehyde *via* alcohol oxidation. After screening different oxidation methods such as TEMPO/BIAB and Dess-Martin periodinate, Dess-Martin oxidation was selected. This method was found to be reliable not only because of the reproducible good yields (70%, NMR yield) but also because no column chromatography purification is needed, which is important due to the instability of aldehyde **357**. With the desired aldehyde in hand, the next steps were performed as described in the literature.²⁹² The commercial source of aldehyde source was also tested but the obtained yield for the allylation is significantly lower, which can be due to purity issues.

The complete synthesis of the desired building block is summarized in **Scheme IV.23** and **Scheme IV.22**. This synthesis was performed in gram-scale (2 grams) and the desired compound stored as the protected homo allylic alcohol **360** because lower stability was expected for the acid **355**.



Scheme IV.22. Synthesis of titanium complex **363**.



Scheme IV.23. Synthesis of (*R*)-*tert*-butyl 5-((*R*)-but-3-en-2-yl)-2,2-dimethyloxazolidine-3-carboxylate (**360**).

Because the CH₂ protons from the 5-membered ring of compound **360** gave duplicated signals in ¹H NMR, it was initially thought that two diastereoisomers were present. However, the optical rotation was in good agreement with the literature, confirming the existence of only one diastereoisomer. Therefore, this behavior was believed to be due to the presence of two conformers of the 5-membered ring, although not so common to occur

at RT. This was confirmed by running a temperature series, showing that the 2 peaks merge into one once the exchange rate is fast enough so that NMR only detects the average (**Figure IV.5**).

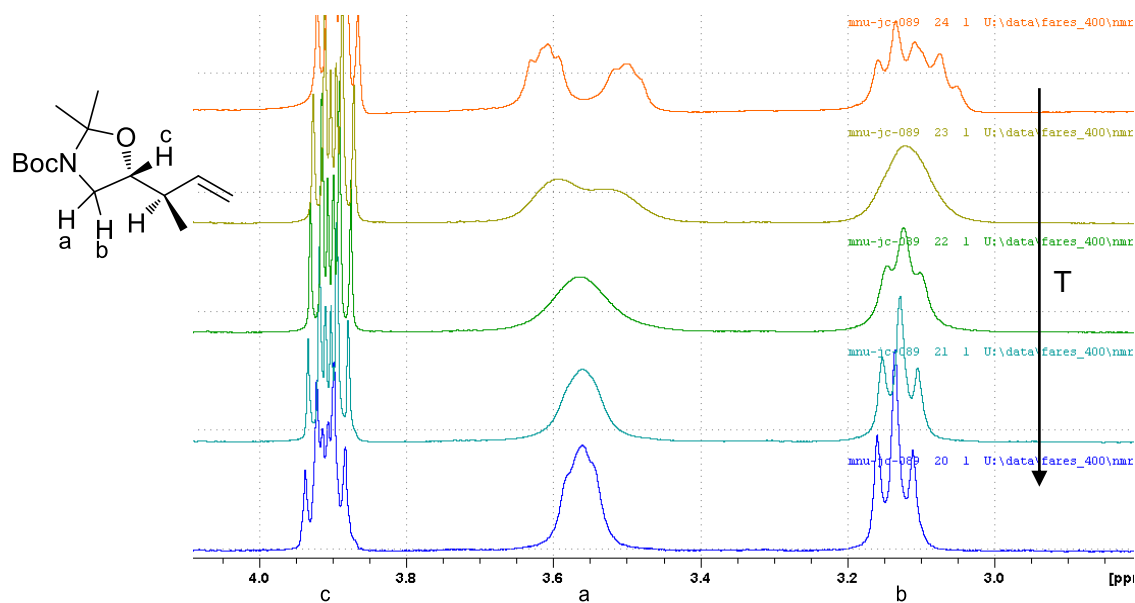
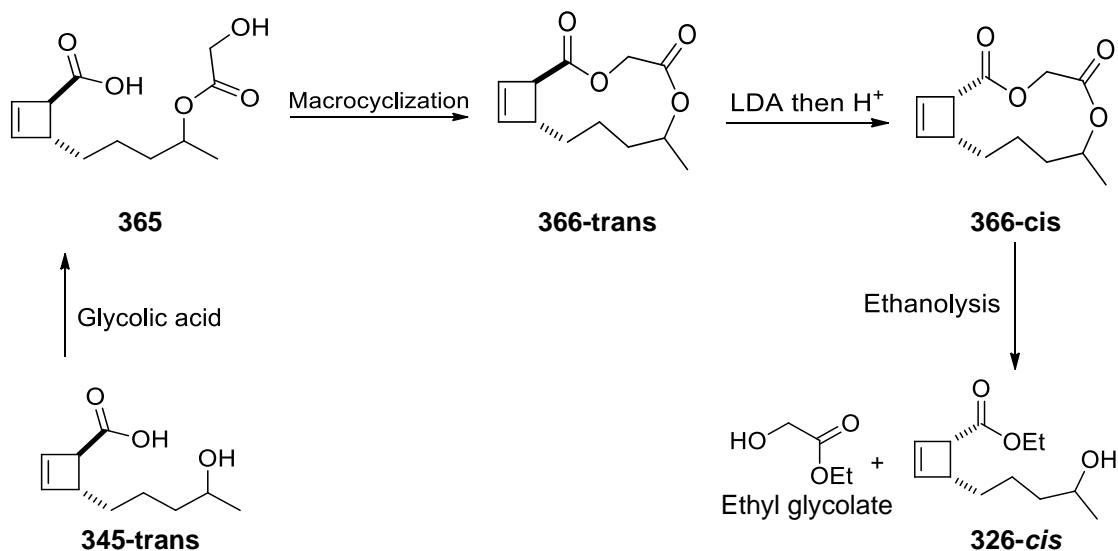


Figure IV.5. Temperature series experiment for compound **360**.

IV.3. Conclusions and Perspectives

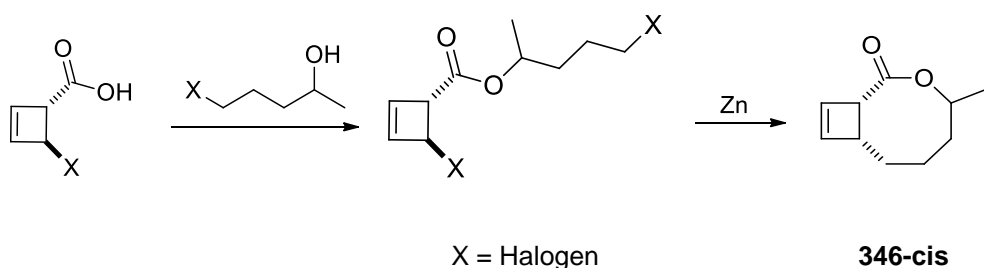
The main objective of this work was the total synthesis of two natural products, Modiolin and Fusanolide A, by taking advantage of the Maulide group expertise in the synthesis of functionalized and stereodefined diene carboxylates through the thermal 4π -electrocyclic ring-opening of cyclobutene precursors. For that, an 1,4-*cis*-substituted cyclobutene bearing a carboxylate and an alkyl chain was identified as the key intermediate. Two main strategies were proposed for its synthesis: one by direct alkylation of halocyclobutenes and the other by kinetic protonation of the easily synthesized *trans*-cyclobutene isomer. In the first case, promising results were obtained for a simple alkyl chain, but when the desired alkyl chain bearing a protected alcohol was used, undesired *cis/trans* ratio favoring the *trans* isomer was observed. In the second approach, the kinetic protonation, no promising results were observed for all the substrates tested.

Since the synthesis of the desired *cis*-cyclobutene was not accomplished, two different approaches are proposed. The first is related to the kinetic protonation approach, where an eleven member ring intermediate **366** is proposed for the synthesis of **326-*cis*** as shown in **Scheme IV.24**.



Scheme IV.24 Proposed macrocyclization approach for the synthesis of **326-trans**.

The second is related with the alkylation methodology. As shown in **Scheme IV.25**, an intramolecular alkylation is proposed for the synthesis of **346-cis**. This approach will only be possible if the alkyl zinc formation can take place at room temperature due to the cyclobutene instability.



Scheme IV.25. Proposed alkylation methodology to the synthesis of **346-cis**.

Finally, the synthesis of the building block (*R*)-*tert*-butyl 5-((*R*)-but-3-en-2-yl)-2,2-dimethyloxazolidine-3-carboxylate was successfully achieved following reported methods with some important modifications regarding the preparation of *tert*-butyl (2-oxoethyl)carbamate.

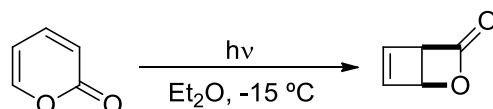
IV.4. Experimental

IV.4.1. General Remarks

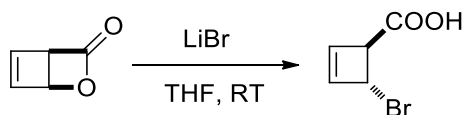
All glassware was oven dried at 100 °C before use and all reactions were performed under an atmosphere of argon unless otherwise stated. All solvents were distilled from appropriate drying agents prior to use. All reagents were used as received from commercial suppliers unless otherwise stated. Mass spectra were obtained using a Finnigan MAT 8200 or (70 eV) or an Agilent 5973 (70 eV) spectrometer, using electrospray ionization (ESI). All ^1H -NMR and ^{13}C -NMR experiments were recorded using Bruker AV-500 spectrometer at 300 K. Chemical shifts are quoted in ppm and coupling constants (J) are quoted in Hz. The 7.26 ppm resonance of residual CDCl_3 for proton spectra and 77 ppm resonance for carbon spectra were used as internal references. Reaction progress was monitored by thin layer chromatography (TLC) performed on aluminium plates coated with keiselgel F₂₅₄ with 0.2 mm thickness. Visualization was achieved by a combination of ultraviolet light (254 nm) and phosphomolybdic acid solution. Flash column chromatography was performed using silica gel 60 (230-400 mesh, Merck and co.). Microwave reactions were performed using a Discover SP CEM microwave.

IV.4.2. Towards total synthesis of Modiolin and Fusanolide A

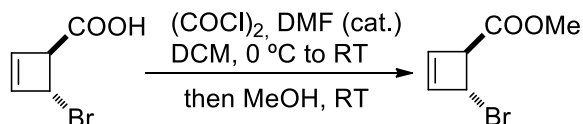
(1*S*,4*R*)-2-oxabicyclo[2.2.0]hex-5-en-3-one (**314**)



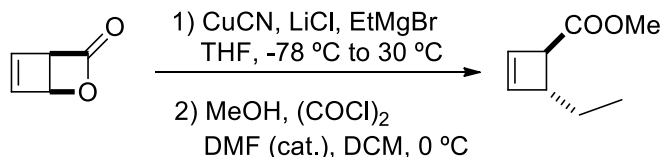
Prepared according to the literature.²⁹³ 2-Pyrone (500 mg, 5.2 mmol) was dissolved in degassed Et_2O (150 mL) and the resulting solution was irradiated at $-15\text{ }^\circ\text{C}$ using a water-cooled mercury arc lamp (Hanovia, 450 W) with a quartz filter. The reaction progress was followed by ^1H -NMR and usually 24 to 36 h was required to reach completion. After warming to room temperature, the solution was concentrated under vacuum in a cold bath to reach a volume of 5-10 mL and the concentration of the product was repeatedly assayed by ^1H NMR. Solutions of **314** were stored at $4\text{ }^\circ\text{C}$ and did not show any signs of decomposition after several weeks. The spectral data were in accordance with those reported in the literature.²⁹⁴ **^1H -NMR (500 MHz, CDCl_3)** δ 6.73 (app. t, $J = 3.5\text{ Hz}$, 1H), 6.54 (app. t, $J = 1.9\text{ Hz}$, 1H), 5.29 (dd, $J = 4.5, 1.9\text{ Hz}$, 1H), 4.39 (s, 1H).

(1*S*,4*R*)-4-bromocyclobut-2-enecarboxylic acid (315)

Prepared according to the literature.²⁶⁶ To a stirred solution of LiBr (1.0 mmol, 2.0 equiv.) in THF (25 mL) was added dropwise an ethereal solution of lactone (0.50 mmol) at RT. The resulting mixture was stirred for 1 h and water (15 mL) was added. The solution was acidified with 1 N HCl and extracted with EtOAc (3 x 15 mL). The combined organic layers were washed with brine, dried (Na₂SO₄) and solvents were removed under reduced pressure to afford the desired halocyclobutene. The spectral data were in accordance with those reported in the literature.²⁶⁶ **¹H-NMR (500 MHz, CDCl₃)** δ 6.36 (s, 1H), 6.27 (s, 1H), 5.09 (s, 1H), 3.91 (s, 1H).

(1*S*,4*R*)-methyl 4-bromocyclobut-2-enecarboxylate (327)

Prepared according to the literature.²⁶⁶ To a stirred solution of crude acid **315** (0.5 mmol) in DCM (0.1 M) was added DMF (0.1 mmol, 20 mol%) followed by (COCl)₂ (0.75 mmol, 1.5 equiv.) dropwise at 0 °C and the resulting mixture was stirred at 0 °C for 1 h. MeOH (1 mmol, 2.0 equiv.) was added at 0 °C and the reaction mixture was stirred for another 1 h at RT. Solvents were evaporated under reduced pressure and the residue was purified by column chromatography (pent/EtOAc) to give the desired ester. The spectral data were in accordance with those reported in the literature.²⁶⁶ **¹H-NMR (500 MHz, CDCl₃)** δ 6.33 (m, 1H), 6.25 (m, 1H), 5.07 (s, 1H), 3.88 (m, 1H), 3.73 (s, 3H).

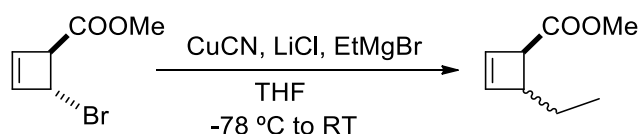
General alkylation method A:

In a flame dry flask, CuCN (1.6 mmol, 3.0 equiv.) and LiCl were charged. The flask was put under vacuum and backfilled with Argon three times. THF (5 mL) was added to the solids. The suspension was stirred for 20 min at RT until a greenish solution was obtained. On a side, in a flame dry flask, a solution of EtMgBr (3 M in Et₂O, 1.6 mmol, 3.0 equiv.) was added to THF (5 mL). The solution was cooled down at 0 °C. After 15 min, the CuCN·2LiCl THF solution was added dropwise to the Grignard. The solution becomes

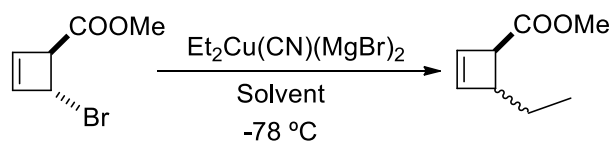
black at the end of the copper addition. The mixture was stirred for 30 min at 0 °C and then cooled down to -78 °C. After 15 min at -78 °C, an ethereal solution of lactone **314** (0.15-0.3 M, 0.52 mmol, 1.0 equiv.) was added dropwise to the solution. The mixture was stirred as described in **Table IV.1**, entries 1-3. The conversion was checked by TLC (pent/EtOAc 9.5/0.5). After full conversion, the solution was brought to RT, HCl 1 M was added. The reaction mixture was extracted with MTBE and the organic layer was washed with HCl and brine. The organic layer was dried over Na₂SO₄ and evaporated to afford the product.

The crude mixture of the acid was dissolved in DCM (0.05 M, 26 mL) and cooled down to 0 °C. After 15 min, (COCl)₂ (1.0 mmol, 2.0 equiv.) was added dropwise followed by the addition of one drop of DMF. The solution was stirred at 0 °C for 1 h. TLC was performed to check the conversion by quenching an aliquot of the reaction with MeOH. Dry MeOH (2 mL) was added to the mixture at 0 °C and the reaction mixture was stirred for another 1 h at RT. Solvents were evaporated and column chromatography purification (pent/EtOAc 9:1 to 7:3) afforded the desired product **329** as a mixture *cis/trans*.

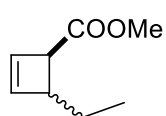
General alkylation method B:



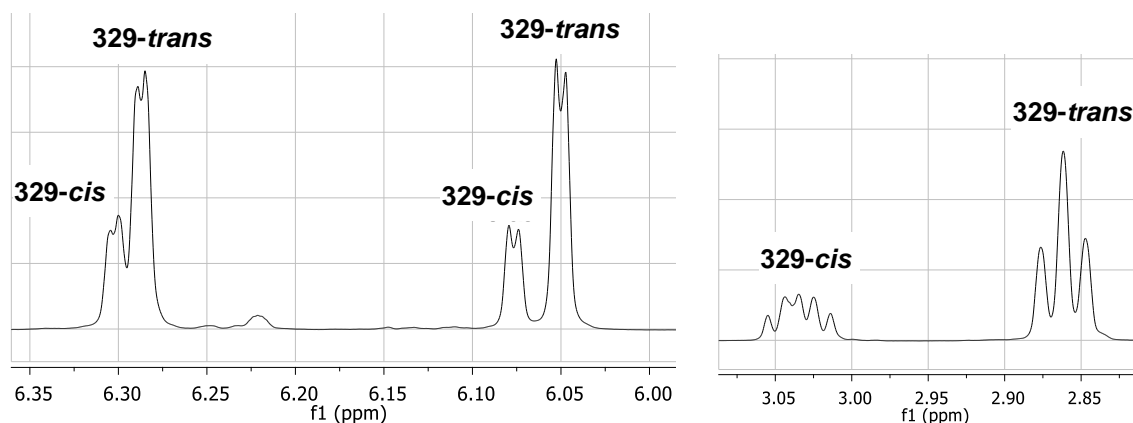
In a flame dry flask, CuCN (1.6 mmol, 3.0 equiv.) and LiCl were charged. The flask was put under vacuum and backfilled with Argon three times. THF (5 mL) was added to the solids. The suspension was stirred for 20 min at RT until a greenish solution was obtained. On a side, in a flame dry flask, a solution of EtMgBr (3 M in Et₂O, 1.6 mmol, 3.0 equiv.) was added to THF (5 mL). The solution was cooled down at 0 °C. After 15 min, the CuCN·2LiCl THF solution was added dropwise to the Grignard. The solution becomes black at the end of the copper addition. The mixture was stirred for 30 min at 0 °C and then cooled down to -78 °C. After 15 min at -78 °C, an ethereal solution of (1*S*,4*R*)-methyl 4-bromocyclobut-2-enecarboxylate (**327**) (0.15 M, 0.52 mmol, 1.0 equiv.) was added dropwise to the solution. The mixture was stirred as described in the report. The conversion was checked by TLC (pent/EtOAc 9.5:0.5). After full conversion, the solution was brought to RT, HCl 1 M was added. The reaction mixture was extracted with MTBE and the organic layer was washed with HCl and brine. The organic layer was dried over Na₂SO₄ and evaporated to afford the crude product that was analyzed by ¹H NMR.

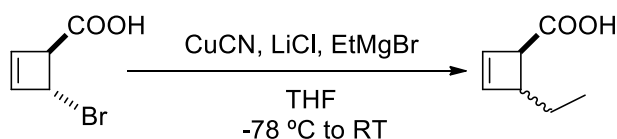
General alkylation method C (Table IV.1, entries 4-6):

The procedure is similar to those in the literature.²⁶⁹⁻²⁷⁰ In a flame dry flask, CuCN (0.8 mmol, 3.0 equiv.) was added. The flask was put under vacuum and backfilled with Argon three times. Solvent (5 mL) was added. The suspension was cooled down to -78 °C and EtMgBr (3 M in Et₂O, 1.6 mmol, 6.0 equiv.) was added dropwise. The mixture was stirred for 20 min at -60 °C. An ethereal solution of (1*S*,4*R*)-methyl 4-bromocyclobut-2-enecarboxylate (**327**) (0.15 M, 0.27 mmol, 1.0 equiv.) was added dropwise to the solution. The mixture was stirred for 1-2 h from -78 °C to -30 °C. The conversion was checked by TLC (pent/EtOAc 9.5:0.5). After full conversion, the solution was brought to RT, HCl 1 M was added. The reaction mixture was extracted with MTBE and the organic layer was washed with HCl and brine. The organic layer was dried over Na₂SO₄ and evaporated to afford the crude product that was analyzed by ¹H NMR.

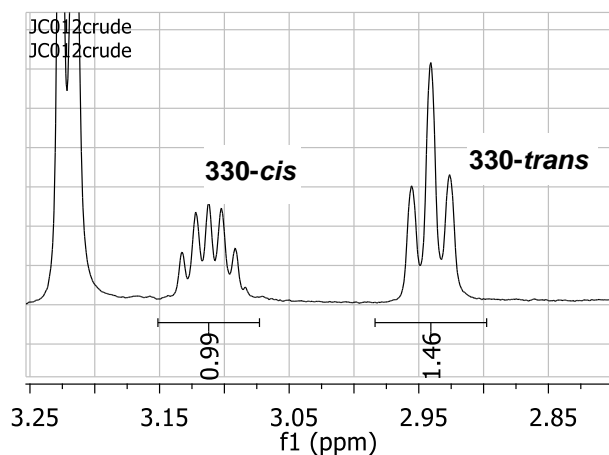
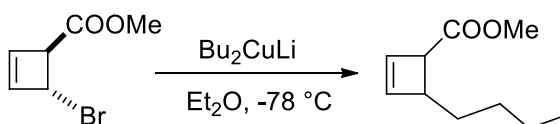
(1*R*)-methyl 4-ethylcyclobut-2-enecarboxylate (329)

329-*cis* ¹H-NMR (500 MHz, CDCl₃) δ 6.33 (d, 1H, *J* = 2.3 Hz), 6.09 (d, 1H, *J* = 2.7 Hz), 3.8 (m, 1H), 3.68 (s, 3H), 3.03 (q, 1H, *J* = 5.0 Hz), 1.67 (m, 2H), 0.88 (t, 3H, *J* = 7.4 Hz). **329-*trans* ¹H-NMR (500 MHz, CDCl₃)** δ 6.32 (d, 1H), 6.08 (d, 1H, *J* = 2.7 Hz), 3.68 (s, 3H), 3.17 (s, 1H), 2.88 (t, 1H, *J* = 7.3 Hz), 1.56 (m, 2H), 0.94 (t, 3H, *J* = 7.4 Hz).

Determination of *cis/trans* ratio:

(1*R*)-4-ethylcyclobut-2-enecarboxylic acid (330)

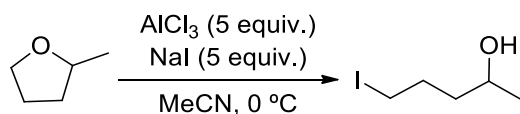
In a flame dry flask, CuCN (2.1 mmol, 4.0 equiv.) and LiCl (4.2 mmol, 8 equiv.) were charged. The flask was put under vacuum and backfilled with Argon three times. THF (6 mL) was added to the solids. The suspension was stirred for 1 h at RT until a greenish solution was obtained. On a side, in a flame dry flask, a solution of EtMgBr (3 M in Et₂O, 1.6 mmol, 3.0 equiv.) was added to THF (5 mL). The solution was cooled down at 0 °C. After 40 min, the CuCN·2LiCl THF solution was added dropwise to the Grignard. The solution becomes black at the end of the copper addition. The mixture was stirred for 40 min at 0 °C and then cooled down to -78 °C. After 15 min at -78 °C, an ethereal solution of (1*S*,4*R*)-4-bromocyclobut-2-enecarboxylic acid (**315**) (0.15 M, 0.52 mmol, 1.0 equiv.) was added dropwise to the solution. The mixture was stirred overnight from -78 °C to RT and then 2 more equivalents of alkylating agent were added as previously described. After 8 d HCl 1 M was added. The reaction mixture was extracted with MTBE and the organic layer was washed with HCl and brine. The organic layer was dried over Na₂SO₄ and evaporated to afford the crude product in trans/cis ratio 1.5:1, determined by ¹H NMR (see below).

**Methyl 4-butylcyclobut-2-enecarboxylate (331)**

Bu₂CuLi as prepared following reported procedure²⁷³: In a flame dry flask, CuI (0.52 mmol, 2.0 equiv.) was charged. The flask was put under vacuum and backfilled with Argon three times. Et₂O (4 mL) was added to the solid. The suspension was cooled down to -30

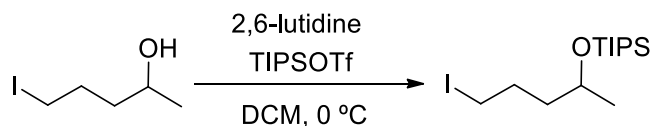
$^{\circ}\text{C}$ and *n*-BuLi (1.6 M, 1.4 mmol, 4.0 equiv.) was added dropwise. The mixture was stirred for 30 min at $-30\text{ }^{\circ}\text{C}$ and then cooled down to $-78\text{ }^{\circ}\text{C}$. A solution of (1*S*,4*R*)-methyl 4-bromocyclobut-2-enecarboxylate (**327**, 0.26 mmol, 1.0 equiv.) dissolved in Et₂O (4 mL) was added dropwise. The mixture was stirred for 30 min at $-78\text{ }^{\circ}\text{C}$, then HCl 1 M was added and the solution was brought to RT. The reaction mixture was extracted with MTBE and the organic layer was washed with HCl and brine. The organic layer was dried over Na₂SO₄ and evaporated to afford the crude product.

5-Iodopentan-2-ol (**333**)



Prepared according to the literature.²⁹⁵ 2-Methyltetrahydrofuran (2.8 mL, 27.8 mmol, 1 equiv.) was added to a solution of aluminum chloride (18 g, 135 mmol, 4.9 equiv.) and sodium iodide (20.3 g, 135 mmol) in acetonitrile (28 mL) at 0 °C. The mixture was stirred for 3 h at 0 °C, and a 1 M HCl aqueous solution was added until complete dissolution of salts. The aqueous layer was extracted with pentane, and the combined organic layers were dried over anhydrous Na₂SO₄ and then concentrated under reduced pressure. The iodoalcohol (4.94 g, 83% yield) was obtained as a yellow oil and used without further purification. The spectral data were in accordance with those reported in the literature.²⁹⁵ **¹H NMR (500 MHz, CDCl₃)** δ 3.90 (m, 1 H, *J* = 6 Hz), 3.45 (td, 2 H, *J* = 1.3, 5.5 Hz), 2.87 (s, 1 H), 2.03-1.89 (m, 2H), 1.64-1.56 (m, 2H), 1.24 (d, 3 H, *J* = 6.25 Hz).

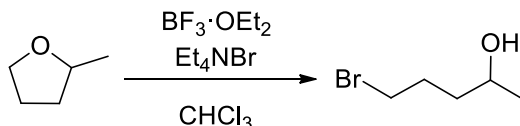
[(5-Iodopentan-2-yl)oxy]triisopropylsilane (**334**)



Prepared by a procedure similar to that in the literature.²⁹⁵ 2,6-Lutidine (16.8 mmol, 4 equiv.) and triisopropylsilyl triflate (6.31 mmol, 1.5 equiv.) were added successively to the crude mixture of 5-iodopentan-2-ol (**333**, 4.2 mmol, 1 equiv.) in dry DCM (10 mL) at 0 °C under nitrogen. After stirring for 2.5 h at RT, water (20 mL) was added, the layers separated and the aqueous layer extracted with DCM. The combined organic layers were dried over Na₂SO₄, evaporated under reduced pressure and the crude product was purified by column chromatography (pentane) to yield the pure product (65-75%) as a colorless oil. The spectral data were in accordance with those reported in the literature.²⁹⁵

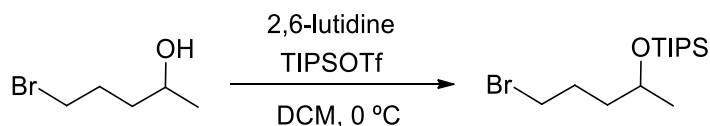
^1H NMR (500 MHz, CDCl_3) δ 3.99 (sext, 1H, J = 5.9 Hz), 3.01 (t, 2H, J = 7.0 Hz), 1.93-1.88 (m, 2H), 1.59-1.54 (m, 2H), 1.70 (d, 3H, J = 6.1 Hz), 1.06 (s, 21H).

5-bromopentan-2-ol

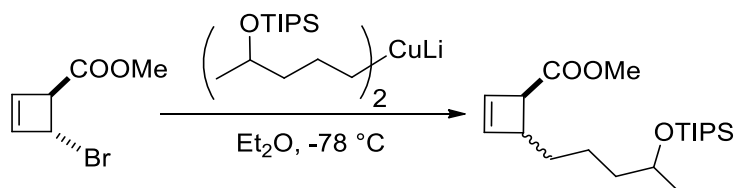


Prepared according to the literature.²⁹⁶ To a solution of tetraethylammonium bromide (4.3 g, 20.6 mmol, 1.1 equiv.) and 2-methyltetrahydrofuran (1.9 mL, 18.8 mmol, 1.0 equiv.) in anhydrous chloroform (25 mL) was added boron trifluoride etherate (2.6 mL, 20.5 mmol, 1.1 equiv.) and the reaction stirred at room temperature (18 °C) overnight (20 h). The reaction was quenched with saturated aqueous sodium bicarbonate, the aqueous layer was separated and extracted with DCM, the combined organic layers were washed with water (2 x 30 mL) and brine (30 mL), dried over Na_2SO_4 , filtered, and concentrated to give crude product (2.23 g, 71% yield). The spectral data were in accordance with those reported in the literature.²⁹⁶ **^1H NMR (500 MHz, CDCl_3)** δ 3.90 (m, 1 H, J = 6 Hz), 3.45 (td, 2 H, J = 1.3, 5.5 Hz), 2.87 (s, 1 H), 2.03-1.89 (m, 2H), 1.64-1.56 (m, 2H), 1.24 (d, 3 H, J = 6.25 Hz).

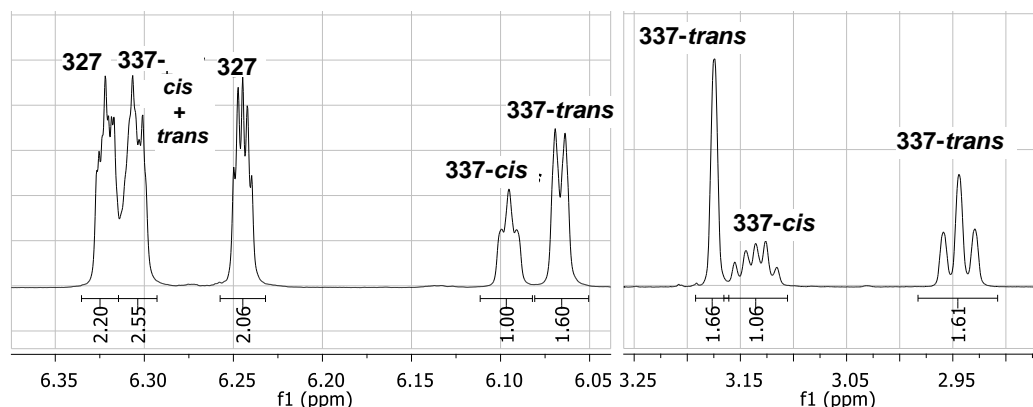
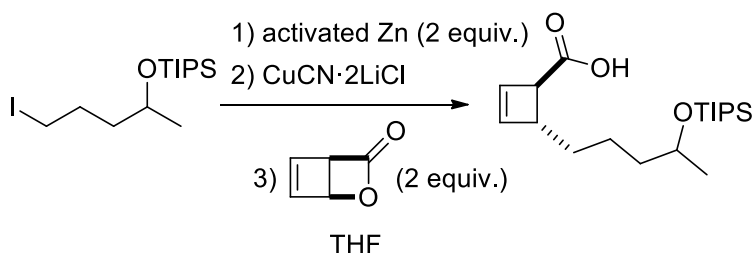
[(5-bromopentan-2-yl)oxy]triisopropylsilane (343)



Prepared by a procedure similar to that in the literature.²⁹⁵ 2,6-Lutidine (6.0 mL, 51.7 mmol, 3.9 equiv.) and triisopropylsilyl triflate (5.0 mL, 18.6 mmol, 1.4 equiv.) were added successively to the crude mixture of 5-bromopentan-2-ol (13.35 mmol, 1 equiv.) in dry DCM (34 mL) at 0 °C under nitrogen. After stirring for 4 h at RT, water was added, the layers separated and the aqueous layer extracted with DCM. The combined organic layers were dried over Na_2SO_4 , evaporated under reduced pressure and the crude product was purified by column chromatography (pent) to yield pure product (2.93 g, 68%) as a colorless oil. **^1H NMR (500 MHz, CDCl_3)** δ 4.00 (sext, 1H, J = 6.0 Hz), 3.42 (t, 2H, J = 6.8), 1.95-1.91 (m, 2H), 1.62-1.58 (m, 2H), 1.75 (d, 3H, J = 6.1 Hz), 1.06 (s, 21H).

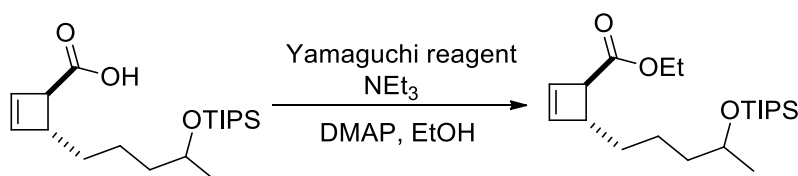
General alkylation method D (337):

In a flame dry flask [(5-iodopent-2-yl)oxy]triisopropylsilane (**334**, 0.552 mmol, 4.0 equiv.) and Et₂O (1 mL) were charged and cooled down to -78 °C. A solution of ^tBuLi (1.9 M in pentane) was added dropwise and the mixture allowed to stir for 10 min at -78 °C. In a separated flame dry flask, CuI (0.278 mmol, 2.0 equiv.) was charged. The flask was put under vacuum/backfilled with Argon three times. Et₂O (2 mL) was added to the solid. The suspension was cooled down to -40 °C and the solution of organolithium was added dropwise. The mixture was stirred for 30 min at -40 °C and then cooled down to -78 °C. A solution of (1*S*,4*R*)-methyl 4-bromocyclobut-2-enecarboxylate (**327**, 0.138 mmol, 1.0 equiv.) dissolved in Et₂O (2 mL) was added dropwise. The mixture was stirred for 30 min at -78 °C, then aqueous saturated solution of NH₄Cl (0.4 mL) and NH₃ (0.4 mL) were added and the solution was brought to RT. The reaction mixture was extracted with MTBE and the organic layer was washed with brine. The organic layers were dried over Na₂SO₄ and evaporated to afford the product as a mixture **337-trans**/**337-cis**/**327** summarized in **Table IV.3** as determined by ¹H NMR:

**(1*R*,4*R*)-4-(4-((triisopropylsilyl)oxy)pentyl)cyclobut-2-enecarboxylic acid (341-trans)**

Zinc powder was activated 12 h prior to the reaction. Metallic zinc powder was stirred with 1 N HCl for 5 min, filtered off and washed with *n*-pentane and then MTBE. The activated zinc powder was kept under vacuum for 12 h. In a flame dried flask, freshly activated zinc powder (438 mg, 6.7 mmol, 2.0 equiv.) was charged and the flask was evacuated and backfilled with Ar three times. THF (2.4 mL) was added followed by a catalytic amount of 1,2-dibromoethane (10 μ L). The mixture was heated with the heat gun for 1 min/cooled down for 1 min three times with high stirring. A catalytic amount of TMSCl (10 μ L) was added and the reaction mixture was stirred for 5 min at room temperature. (S)-((5-iodopentan-2-yl)oxy)triisopropylsilane (1.2 g, 3.24 mmol, 1.0 equiv.) was added dropwise and the suspension was stirred at 35 °C for 2-4 h (formation of the organozinc derivative was monitored by TLC analysis by quenching aliquots with HCl 1 M). In a separated flask, CuCN (291 mg, 3.25 mmol, 1.0 equiv.) and LiCl (275 mg, 6.50 mmol, 2.0 equiv.) were stirred in THF (6 mL) for 15-60 min until complete dissolution of the salts. The organozinc solution was diluted with THF (5 mL) and added dropwise to the solution of CuCN.2LiCl at -20 °C. The resulting mixture was stirred for 60 min at -20 °C, cooled down to -78 °C and an ethereal solution of (1*S*,4*R*)-2-oxabicyclo[2.2.0]hex-5-en-3-one (**314**, 0.1-0.3 M, 6.50 mmol, 2.0 equiv.) was added dropwise. The resulting mixture was warmed to -30 °C over 3 h and 1 N HCl was added (5 mL) dropwise. The solution was allowed to warm up to room temperature and diluted in EtOAc. The mixture was transferred in a separating funnel and the organic layer was washed with a saturated aqueous NH₄Cl solution. The aqueous layer was extracted with EtOAc. The combined organic layers were washed with brine, dried over Na₂SO₄, the solvent was removed under reduce pressure and the crude product was purified by column chromatography (pent/EtOAc from 1:0 to 7:3) to yield pure product. **¹H-NMR (500 MHz, CDCl₃)** δ 6.33 (d, *J* = 2.7 Hz, 1H), 6.08 (d, *J* = 2.7 Hz, 1H), 3.94-3.90 (m, 1H), 3.21 (s, 1H), 3.00 (t, *J* = 7.5 Hz, 1H), 1.61 - 1.60-151 (m, 3H), 1.46 - 1.39 (m, 3H), 1.15 (d, *J* = 6.0 Hz, 3H), 1.05 (s, 21H).

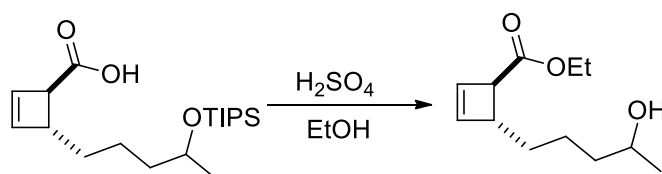
(1*R*,4*R*)-ethyl 4-(4-((triisopropylsilyl)oxy)pentyl)cyclobut-2-enecarboxylate (344-*trans*)



To the crude mixture of (1*R*,4*R*)-4-(4-((triisopropylsilyl)oxy)pentyl)cyclobut-2-enecarboxylic acid (**341-*trans***, 3.12 mmol, 1.0 equiv.) dissolved in THF (30 mL), triethylamine (6.45 mmol, 2.1 equiv.) and 2,4,6-trichlorobenzoyl chloride (3.24 mmol, 1.1 equiv.) were added at 0 °C and the mixture was allowed to stir. After 2.5 h degassed EtOH

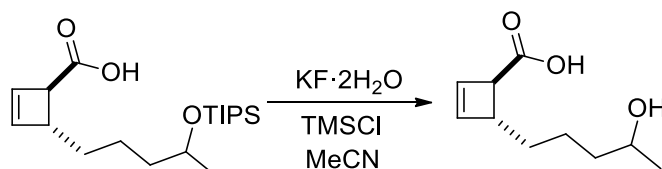
(17.1 mmol, 5.5 equiv.) and 4-dimethylaminopyridine (0.8 mmol, 0.25 equiv.) were added at 0 °C and the reaction mixture allowed to stir for 2.5 h from 0 °C to RT. The mixture was transferred in a separating funnel and the organic layer was washed with a saturated aqueous NH_4Cl solution. The aqueous layer was extracted with EtOAc. The combined organic layers were washed with brine, dried over Na_2SO_4 , the solvent was removed under reduce pressure and the crude product was purified by column chromatography (pent/EtOAc from 1:0 to 9:1) to yield pure product (10% yield, from ((5-iodopentan-2-yl)oxy)triisopropylsilane). **$^1\text{H-NMR}$ (500 MHz, CDCl_3)** δ 6.30 (d, $J = 2.7$ Hz, 1H), 6.08 (d, $J = 2.7$ Hz, 1H), 4.13 (q, 2H, $J = 7.12$ Hz), 3.95-3.89 (m, 1H), 3.16 (s, 1H), 2.94 (t, $J = 7.3$ Hz, 1H), 1.56-1.51 (m, 3H), 1.43 - 1.38 (m, 3H), 1.15 (d, $J = 6.1$ Hz, 3H), 1.05 (s, 21H).

(1*R*,4*R*)-ethyl 4-(4-hydroxypentyl)cyclobut-2-enecarboxylate (326-*trans*)



To the crude mixture of (1*R*,4*R*)-4-(4-((triisopropylsilyl)oxy)pentyl)cyclobut-2-enecarboxylic acid (1.6 mmol, 1.0 equiv.) dissolved in degassed EtOH (0.05 M), catalytic amount of H_2SO_4 conc. was added and the mixture was allowed to stir. The reaction was followed by TLC analysis and more H_2SO_4 conc. was added give full deprotection of TIPS. The mixture was transferred in a separating funnel, HCl 1 M was added, and the aqueous layer was extracted with EtOAc. The combined organic layers were washed with brine, dried over Na_2SO_4 , the solvent was removed under reduce pressure and the crude product was purified by column chromatography (pent/EtOAc from 1:0 to 7:1) to yield pure product (31% yield, 41% yield *brsm* ((5-iodopentan-2-yl)oxy)triisopropylsilane). **$^1\text{H-NMR}$ (500 MHz, CDCl_3)** δ 6.30 (d, $J = 2.8$ Hz, 1H), 6.08 (d, $J = 2.8$ Hz, 1H), 4.14 (q, 2H, $J = 7.12$ Hz), 3.82-3.78 (m, 1H), 3.17 (s, 1H), 2.95 (t, $J = 7.2$, 1H), 1.47-1.44 (m, 3H), 1.60 - 1.50 (m, 3H), 1.26 (t, $J = 7.1$, 3H), 1.19 (d, $J = 6.2$, 3H).

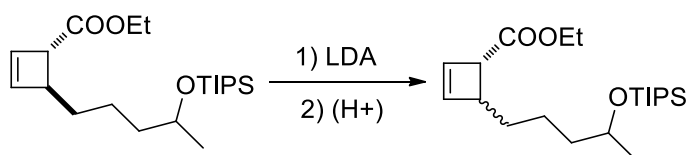
(1*R*,4*R*)-4-(4-hydroxypentyl)cyclobut-2-enecarboxylic acid (345-*trans*)



Following reported procedure²⁷⁷: To a stirred solution of TIPS ether **341-*trans*** (21.1 mg, 0.62 mmol) in MeCN (0.2 mL) was added powdered KF (4.7 mg, 0.81 mmol, 1.3 equiv.), followed by the addition of TMSCl (10 μL , 0.79 mmol, 1.3 equiv.) and H_2O (2 μL , 0.11

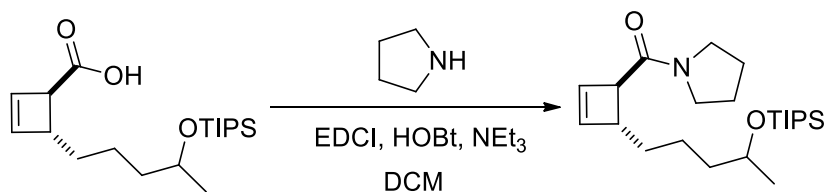
mmol, 1.8 equiv.) at RT. After vigorously stirring for 2 h, the reaction mixture was treated with aq. sat. sol. NaHCO_3 and extracted with CH_2Cl_2 . The combined extracts were washed with H_2O , brine, and dried over Na_2SO_4 . The solvent was evaporated in vacuum and the crude product was purified by filtration/column chromatography in a small pipette (pent/EtOAc from 7:3 to 4:6) to afford the desired product as a colorless oil (10 mg, 88%). **$^1\text{H-NMR}$ (500 MHz, CDCl_3)** δ 6.31 (d, $J = 2.8$ Hz, 1H), 6.07 (d, $J = 2.8$ Hz, 1H), 3.83-3.77 (m, 1H), 3.20 (s, 1H), 2.99 (t, $J = 7.4$ Hz, 1H), 1.56-1.55 (m, 2H), 1.51 - 1.37 (m, 4H), 1.18 (d, $J = 6.2$ Hz, 3H).

General procedure for kinetic protonation reaction (Table IV.4):



To lithium diisopropylamide (LDA, 15 μL , 0.104 mmol, 4.0 equiv.) in THF (0.2 mL) at -78°C , *n*-butyllithium solution (1.6 M, 71 μL , 0.113 mmol, 4.4 equiv.) was added and the mixture stirred for 10 min. A solution of starting material (10 mg, 0.026 mmol, 1.0 equiv.) was added dropwise and the mixture was allowed to stir for 15 min at this temperature. A cold (around -78°C) solution of proton source (0.239 mmol, 8.8 equiv.) dissolved in THF (0.1 mL) was added. The mixture was allowed to stir at -78°C for 5 min, then 15 min at 0°C and then brought to RT. The mixture was transferred in a separating funnel, HCl 1 M was added, and the aqueous layer was extracted with EtOAc. The combined organic layers were dried over Na_2SO_4 , the solvent was removed under reduce pressure and the crude product was analyzed by ^1H NMR.

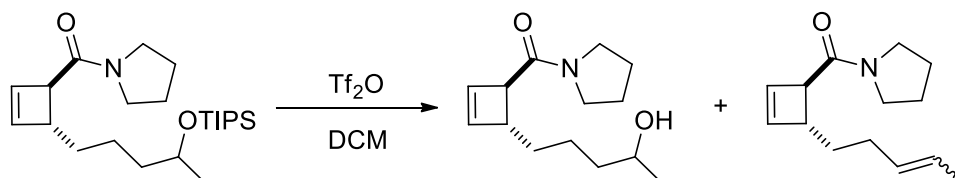
Pyrrolidin-1-yl((1R,4R)-4-(4-((triisopropylsilyl)oxy)pentyl)cyclobut-2-enyl)methanone (348-trans)



To a solution of (1R,4R)-4-(4-((triisopropylsilyl)oxy)pentyl)cyclobut-2-enecarboxylic acid (56.9 mg, 0.167 mmol, 1.0 equiv.) in DCM (1.7 mL), hydroxybenzotriazole (25 mg, 0.184 mmol, 1.1 equiv.), triethylamine (26 μL , 0.184 mmol, 1.1 equiv.), *N*-(3-dimethylaminopropyl)-*N'*-ethylcarbodiimide hydrochloride (35 mg, 0.184 mmol, 1.1 equiv.) and pyrrolidine (15 μL , 0.184 mmol, 1.1 equiv.) were added at 0°C . The resulting mixture was stirred overnight at RT. Evaporation of the solvent and purification by column chromatography (pent/EtOAc 7:3) afford the pure product (60 mg, 91%) as a colorless

liquid. **¹H NMR (500 MHz, CDCl₃)** δ 1.05 (s, 21H), 1.45 (d, 3H, *J* = 6.0 Hz), 1.33-1.52 (m, 6H), 1.85 (m, 2H, *J* = 6.8 Hz), 1.95 (m, 2H, *J* = 6.8 Hz), 3.05 (m, 1H), 3.26 (s, 1H), 3.41-3.48 (m, 4H), 3.92 (m, 1H, *J* = 5.3 Hz), 6.13 (d, 1H, *J* = 2.9 Hz), 6.35 (d, 1H, *J* = 2.9 Hz); **¹³C NMR (125 MHz, CDCl₃)** δ 12.5, 18.2, 23.4, 24.3, 26.2, 34.3, 40.0, 45.8, 46.5, 47.6, 51.9, 133.9, 142.5, 171.1.

General procedure for lactonization using triflic acid (349 and 350)

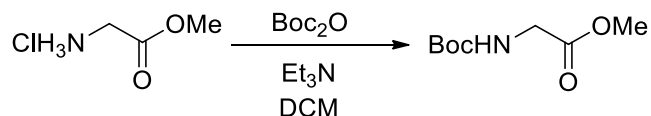


To a solution of pyrrolidin-1-yl((1*R*,4*R*)-4-((triisopropylsilyl)oxy)pentyl)cyclobut-2-en-1-yl)methanone in DCM, triflic anhydride was added and the reaction mixture allowed to stir. After completion of the reaction, an aqueous saturated solution of NaHCO₃ (same volume as DCM) was added and the reaction stirred vigorously overnight at room temperature. DCM extraction, dried over NaSO₄, filtration and solvent evaporation give the crude product mixture that was purified by column chromatography (pent/EtOAc from 7:3 to 4:6) to afford the different products. (1 equiv. of Tf₂O to yield **349** and 2 equiv. to yield **350** (as a *cis* and *trans* mixture (alkenes **a** and **b**), not separated, ratio 1:2)).

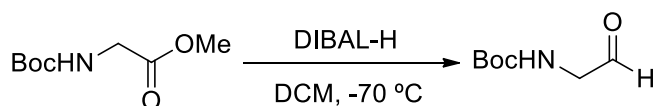
350: **¹H NMR (500 MHz, CDCl₃)** δ 1.53 (d, 3Ha, *J* = 6.6 Hz), 1.57 (d, 3Hb, *J* = 3.5 Hz), 1.60-1.68 (m, 2Ha + 2Hb), 1.75-1.81 (m, 4Ha + 4Hb, *J* = 6.8 Hz), 1.86-1.92 (m, 4Ha + 4Hb, *J* = 6.8 Hz), 1.92-2.18 (m, 2Ha + 2Hb), 3.00 (m, 1Ha + 1Hb), 3.20 (s, 1Hb), 3.22 (m, 1Ha), 3.33-3.43 (m, 4Ha + 4Hb), 5.29-5.43 (m, 2Ha + 2Hb), 6.06 (d, 1Hb, *J* = 2.7 Hz), 6.07 (d, 1Ha, *J* = 2.7 Hz), 6.28 (d, 1Hb, *J* = 2.7 Hz), 6.30 (d, 1Ha, *J* = 2.7 Hz). **¹³C NMR (125 MHz, CDCl₃)** δ 24.4, 26.2, 33.9, 45.8, 46.5, 47.3, 52.0, 124.2 (a) and 125.2 (b) 130.1 (a) and 130.8 (b), 134.0, 142.4, 171.1.

349: **¹H NMR (500 MHz, CDCl₃)** δ 1.11 (d, 3H, *J* = 5.8 Hz), 1.35-1.48 (m, 6H), 1.76-1.81 (m, 2H, *J* = 6.8 Hz), 1.86-1.92 (m, 2H, *J* = 6.8 Hz), 3.02 (t, 1H, *J* = 7.3 Hz), 3.20 (s, 1H), 3.37-3.41 (m, 4H), 3.73 (q, 1H, *J* = 5.9 Hz), 6.07 (d, 1H, *J* = 2.6 Hz), 6.28 (d, 1H, *J* = 2.6 Hz).

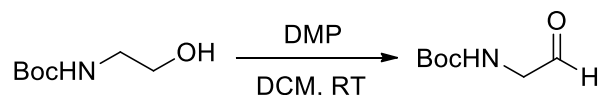
IV.4.3. Towards total synthesis of FR256523

***N*-Boc glycine methyl ester (356)**

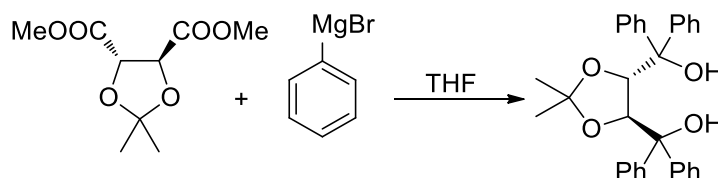
To a dry 250 mL round-bottom flask, glycine-O-methyl ester hydrochloride (5.1 g, 1 equiv., 39.8 mmol) and dry DCM (100 mL) were added and cooled down to 0 °C. Triethylamine (11.1 mL, 8.06 g, 2 equiv., 79.6 mmol) was added with stirring to the suspension. A solution of di-*tert*-butyl dicarbonate (8.69 g, 1 equiv., 39.8 mmol) in dry DCM (20 mL) was added dropwise to the suspension. The obtained solution was stirred overnight (17h) at room temperature. The solvent was removed and the obtained solid was dissolved in EtOAc (180 mL). The organic phase was washed with 0.9% w/w acetic solution in water (180 mL, pH=2-3), followed by a 5% w/w aqueous NaHCO₃ solution (180 mL, pH=8) and a saturated NaCl aqueous solution (100 mL). The organic phase was dried with anhydrous Na₂SO₄ and the solvent removed with a rotating evaporator and vacuum pump to obtain the product as colorless oil that became a white solid when stored at 20 °C (7.1 g, 94% yield). ¹H NMR (500 MHz, CDCl₃) δ 1.42 (m, 9H), 3.72 (s, 3H), 3.89 (s, 2H), 5.06 (s, 1H).

***tert*-Butyl (2-oxoethyl)carbamate (357), method A**

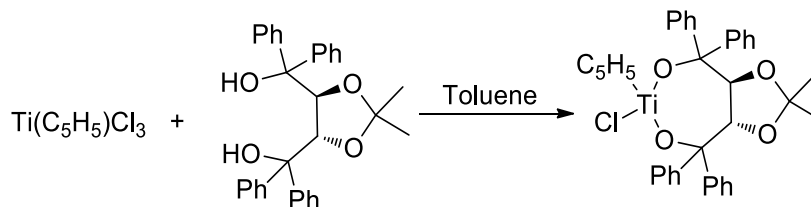
Prepared according to the literature.²⁹² DIBAL-H (1.0 M in toluene, 1.1 equiv) was added dropwise over 45 min *via* syringe pump to a solution of *N*-Boc glycine methyl ester (356, 1.0 equiv) in DCM (0.25 M) at -78 °C. After 1 h of stirring at -78 °C, the reaction mixture was hydrolyzed by adding a saturated aqueous solution of Rochelle's salt (same volume as DCM) and the mixture was allowed to warm to RT. The resulting gel was filtered over celite and the filtrate was concentrated under reduced pressure, to give the crude aldehyde as a colorless gel. This unstable compound was immediately used in the next step without purification. Yields vary from 30% (25 mmol scale) to 85% (1 mmol scale). The spectral data were in accordance with those reported in the literature.²⁹² ¹H NMR (500 MHz, CDCl₃) δ 1.46 (s, 9H), 4.08 (d, 2H, 4.6 Hz), 5.18 (s, 1H), 9.66 (s, 1H).

***tert*-Butyl (2-oxoethyl)carbamate (357), method B**

To a solution of *N*-Boc ethanolamine in commercial (not dried) DCM (0.1 M), Dess-Martin Periodinate was added as solid at RT. After 3 h stirring the reaction mixture was quenched by adding a solution 1:1 sat. aq. sol. NaHCO₃/ sat. aq. sol. Na₂S₂O₄ and stirred for 1 h. Extraction with DCM, dried over Na₂SO₄, filtered through celite and removal of solvent afforded the crude aldehyde (70% NMR yield using 1,3,5-metoxibenzene as internal standard).

((4S,5S)-2,2-dimethyl-1,3-dioxolane-4,5-diyl)bis(diphenylmethanol) (362)

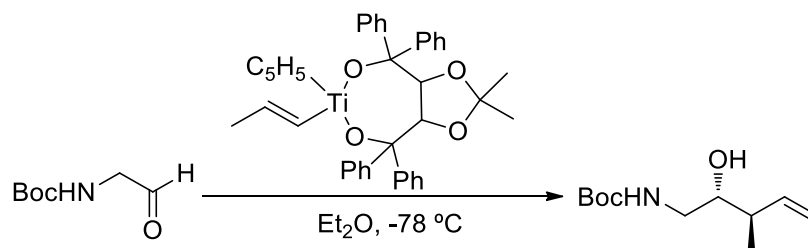
To a magnesium powder (4.37 g, 5 equiv.) in THF (12 mL), a solution of bromobenzene (19 mL, 5 equiv.) in THF (60 mL) was added. The reaction was stirred under controlled reflux until consumption of magnesium. Then THF (30 mL) was added to cool down the reaction. The commercial available (*S,S*)-ester was added slowly in THF (60 mL) at 0 °C. After 2h, the reaction mixture was hydrolyzed with sat. aq. NH₄Cl (200 mL) and extracted with MTBE (2 x 200 mL). The collected organic phases were dried over Na₂SO₄ and concentrated under vacuum. The product was recrystallized from MTBE/pentane and then washed with pentane to give a white solid (14.7 g, 87% yield). The spectral data were in accordance with those reported in the literature. ¹H NMR (500 MHz, CDCl₃) δ 0.96 (s, 6H), 3.85 (bs, 2H), 4.52 (s, 2H), 7.14-7.29 (m, 16H), 7.43-7.46 (m, 4H).

Cyclopentadienyl[(4S,trans)-2,2-dimethyl-α,α',α',α'-tetraphenyl-1,3-dioxolane-4,5-dimethanolato-O,O']titanium chloride (364)

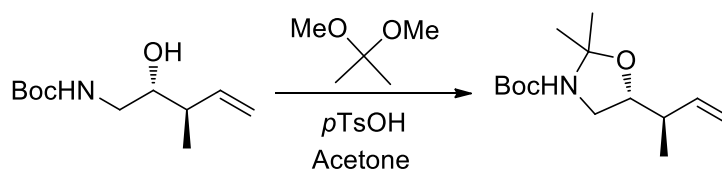
Prepared according to the literature.²⁹² To a solution of CpTiCl₃ in dry toluene (6.01 g, 27.4 mmol, 1.0 equiv.) at 110 °C, (*S,S*)-TADDOL (13.00 g, 27.9 mmol, 1.0 equiv.) was added as solid. The solution was stirred for 14h at reflux with argon bubbling in the solution. Then the solution was stirred for 12h at RT. without argon bubbling in the solution but still

under argon atmosphere. The solvent was removed until foam was obtained. For product recrystallization, Et₂O (69 mL) and *n*-pentane (206 mL) were added and the suspension stirred vigorously for 2-3 h. The solid obtained was filtered and washed with *n*-pentane (3 x 20 mL) to give a yellow solid (14.55 g, 89% yield). The spectral data were in accordance with those reported in the literature. ¹H NMR (500 MHz, CDCl₃) δ 0.96 (s, 6H), 3.85 (bs, 2H), 4.52 (s, 2H), 7.14-7.29 (m, 16H), 7.43-7.46 (m, 4H).

***tert*-Butyl ((2*R*,3*R*)-2-hydroxy-3-methylpent-4-en-1-yl)carbamate (358)**



Prepared according to the literature.²⁹² To a solution of cyclopentadienyl[(4*S*,*trans*)-2,2-dimethyl-α,α',α',α'-tetraphenyl-1,3-dioxolane-4,5-dimethanolato -O,O']titanium chloride (1.6 equiv.) in diethyl ether (0.08 M) at 0 °C, 2-butenylmagnesium chloride (0.5 M in THF, 1.3 equiv.) was added slowly and the mixture stirred for 3 h at 0 °C. The brown reaction mixture was cooled to -78 °C and a solution of *N*-Boc-2-aminoacetaldehyde (1 equiv.) in diethyl ether (0.31 M) was added dropwise. After 6 h at -78 °C, the reaction was quenched by addition of water (0.16 M). The reaction mixture was stirred for 48 h at r.t and then filtered over celite. The layers were separated and the aqueous phase was extracted with diethyl ether (3 x 100 mL). The combined organic extracts were washed with brine (150 mL), dried over Na₂SO₄ and concentrated in vacuum. The residue was diluted with *n*-pentane (60 mL) and filtered to remove ((4*S*,5*S*)-2,2-dimethyl-1,3-dioxolane-4,5-diyl)bis(diphenylmethanol). After removal of pentane under reduce pressure, purification of the residue by column chromatography provide the desired enantioenriched homoallylic alcohol as a colorless oil (yields: 50%-2.5 mmol scale, 72%-8.5 mmol scale and 80%-25 mmol scale). The physical and spectral data were in accordance with those reported in the literature.²⁹² ¹H NMR (500 MHz, CDCl₃) δ 1.05 (d, 3H, *J* = 6.85 Hz), 1.45 (s, 9H), 2.23 (sext, 1H, *J* = 7 Hz), 3.05-3.10 (m, 1H), 3.35-3.38 (ddd, 1H, *J* = 2.2, 6.2, 14.0 Hz), 3.47-3.49 (m, 1H), 4.92 (brs, 1H), 5.11-5.14 (m, 2H), 5.71-5.78 (m, 1H); [α]_D^{22°C} = -2.97 (*c* = 1.22, CHCl₃)

***tert*-Butyl (5*R*)-5-[(1*R*)-1-methylprop-2-en-1-yl]-2,2-dimethyloxazolidine-3-carboxylate (360)**

Prepared according to the literature.²⁹² To a solution of *tert*-Butyl ((2*R*,3*R*)-2-hydroxy-3-methylpent-4-en-1-yl)carbamate (1.0 equiv.) in acetone (0.1 M), 2,2-dimethoxypropane (18 equiv.) and *p*-toluenesulfonic acid monohydrate (0.1 equiv.) were successively added. After 10 min of stirring at RT, the reaction mixture was hydrolyzed by adding a saturated aqueous solution of NaHCO₃ (1/4 acetone volume). The layers were separated and the aqueous phase was extracted with DCM. The combined organic layers were washed with brine, dried over Na₂SO₄ and concentrated in vacuum. Purification of the residue by column chromatography (pent/EtOAc 19:1) furnished the desired compound as a colorless oil (yields from 56-70%). The physical and spectral data were in accordance with those reported in the literature.²⁹² **¹H NMR (500 MHz, CDCl₃)** δ 1.02 (d, 3H, *J* = 5.71 Hz), 1.45-1.57 (m, 15H), 2.37 (sext, 1H, *J* = 6.9 Hz), 3.08-3.18 (dt, 1H, *J* = 9.5, 31.1 Hz), 3.51-3.65 (dt, 1H, *J* = 8.2, 57 Hz), 3.89-3.94 (m, 1H), 5.06-5.11 (m, 2H), 5.80-5.86 (m, 1H); **¹³C NMR (125 MHz, CDCl₃)** δ 15.4, 24.2, 25.1, 26.0, 27.1, 28.5 (d), 40.4 (d), 48.7 (d), 77.0 (d), 79.4 and 80.0, 91.1 and 95.5, 115.1, 139.7, 152.0 and 152.4. [α]_D^{22°C} = -21,14 (*c* = 2.46, CHCl₃).

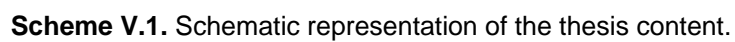
Conclusions

Two novel, integrated, simple and efficient methodologies for the preparation and isolation of HMF were developed, that overcome the major problem in big scale production of HMF that is the isolation and purification. The first one is the transformation of carbohydrates (mainly D-fructose) into HMF using TEAB as reaction medium and Amberlyst® 15 as catalyst. Remarkably, isolation of HMF was achieved in excellent yields and high purity without using other purification methods than simple cristalization of the reaction medium using renewable solvents (ethanol and EtOAc) followed by solvent evaporation. The second one is the integrated process for the production and isolation of HMF from D-glucose, by a combination of enzymatic D-glucose-D-fructose isomerization, selective D-fructose dehydration to HMF, and HMF isolation. Reutilization of the reaction medium and enzyme allowed the preparation of HMF in overall yields up to 87% and extremely high purity (>99 %). Cytotoxicity studies of the impact of HMF and derivatives in human skin fibroblast cells enabled the creation of potential guidelines for human exposure. It was observed that the di-aldehyde, di-hydroxymethyl, di-methyl derivatives are potentially more harmful than the di-carboxylic acid and HMF.

Valorization of HMF was investigated resulting in several methodologies for the creation of potential biologically active compounds. The selective ε -functionalization of HMF derivatives *via* trienamine intermediates was described for the first time. Several amines were successful applied producing a new highly functionalized skeleton. Specific patterns in 5-substituted furfural showed to be important to achieve good yields. Mechanistic studies suggested that formation of vinylogous iminium-ion is the rate limiting step, which is different from the known amine catalysis. DFT calculations were performed and corroborate the proposed mechanism. Preliminary biological assays results indicate that these new compounds exhibited promising antitumor activities when a cyclic secondary amine is present resulting. Furthermore, for piperazines, *N*-alkyl substituents offer better results then carboxyl groups. In other study, a mild and efficient synthesis of triarylmethanes bearing secondary anilines by Friedel-Crafts reaction of (hetero)aryl aldehydes and the corresponding secondary anilines catalyzed by ytterbium(III) triflate was reported. It was demonstrated that extreme high pressure (8970 bar) has a significant effect on the rate of the catalytic Friedel-Crafts alkylation. Several triarylmethanes were synthesized in 50-94% yield in 1 h at RT and 8970 bar. Several new triarylmethanes presented important antiproliferative activity against cancer cell lines, especially from colon origin (HT-29).

Finally, the total synthesis of two natural products, Modiolin and Fusanolide A, was explored by taking advantage of the Maulide group expertise in the synthesis of functionalized and stereodefined diene carboxylates through the thermal 4 π -electrocyclic ring-opening of cyclobutene precursors. The synthesis of the key 1,4-*cis*-substituted

cyclobutene bearing a carboxylate and an alkyl chain was tentatively synthesized by two different strategies: direct alkylation of halocyclobutenes and kinetic protonation of the easily synthesized *trans*-cyclobutene isomer. Unfortunately, a competitive methodology was not achieved.



References

1. Zhu, X.-F., *Nucleosides, Nucleotides Nucleic Acids*, **2000**, 19, 651.
2. Crimmins, M. T., *Tetrahedron*, **1998**, 54, 9229.
3. In *Name Reactions for Carbocyclic Ring Formations*; Li, J. J., Ed.; John Wiley & Sons, Inc., 2010.
4. Li, J. J. *Name Reactions: A Collection of Detailed Reaction Mechanisms*; Springer, 2003.
5. Liang, S.; Haunert, A.; Huber-Dirr, S.; Process for preparing cyclopentenone; US EP1422212; **2004**
6. Nazarov, I. N.; Zaretskaya, I. I., *Izv. Akad. Nauk. SSSR*, **1941**, Ser. Khim: 211.
7. Pauson, P. L.; Khand., I. U., *Ann. N.Y. Acad. Sci.*, **1977**, 295, 2.
8. Piancatelli, G.; Dauria, M.; Donofrio, F., *Synthesis*, **1994**, 867.
9. Fetizon, M.; Montaufier, M. T.; Rens, J., *J. Chem. Res. (S)*, **1982**, 9.
10. Nwaji, M. N.; Onyiriuk.Os, *Tetrahedron Lett.*, **1974**, 2255.
11. Kalaitzakis, D.; Triantafyllakis, M.; Alexopoulou, I.; Sofiadis, M.; Vassilikogiannakis, G., *Angew Chem Int Ed Engl*, **2014**.
12. Joule, J. A.; Mills, K. In *Heterocyclic Chemistry*; 5th ed.; Wiley-Blackwell, 2010.
13. Nanni, M.; Ta-machi, H.; Moriyama-shi, *Japanese Patent Disclosure Bulletin*, No. 57-62236, 15 April 1982.
14. Masayoshi, M.; Novel preparation of 4-hydroxy-2-cyclopentenone; Sumitomo chemical CO; JP57062236; **1983**
15. Curran, T. T.; Hay, D. A.; Koegel, C. P.; Evans, J. C., *Tetrahedron*, **1997**, 53, 1983.
16. Morgan, B. S.; Hoenner, D.; Evans, P.; Roberts, S. M., *Tetrahedron-Asymmetry*, **2004**, 15, 2807.
17. O'Byrne, A.; Murray, C.; Keegan, D.; Palacio, C.; Evans, P.; Morgan, B. S., *Org. Biomol. Chem.*, **2010**, 8, 539.
18. Beingessner, R. L.; Farand, J. A.; Barriault, L., *J. Org. Chem.*, **2010**, 75, 6337.
19. Basra, S. K.; Drew, M. G. B.; Mann, J.; Kane, P. D., *J. Chem. Soc., Perkin Trans. 1*, **2000**, 3592.
20. Becker, N.; Carreira, E. M., *Org. Lett.*, **2007**, 9, 3857.
21. Holland, H. L.; Brown, F. M.; Chenchiah, P. C.; Rao, J. A., *Can. J. Chem.*, **1990**, 68, 282.
22. Kruger, G.; Harde, C.; Bohlmann, F., *Tetrahedron Lett.*, **1985**, 26, 6027.
23. Watson, T. J. N.; Curran, T. T.; Hay, D. A.; Shah, R. S.; Wenstrup, D. L.; Webster, M. E., *Org. Process Res. Dev.*, **1998**, 2, 357.
24. Laumen, K.; Cyclopentene diols monoacetate derivatives; Novartis AG; WO2008/55874; **2008**
25. Ulbrich, K.; Kreitmeier, P.; Reiser, O., *Synlett*, **2010**, 2037.
26. Roche, S. P.; Aitken, D. J., *Eur. J. Org. Chem.*, **2010**, 5339.
27. Ghorpade, S. R.; Bastawade, K. B.; Gokhale, D. V.; Shinde, P. D.; Mahajan, V. A.; Kalkote, U. R.; Ravindranathan, T., *Tetrahedron-Asymmetry*, **1999**, 10, 4115.
28. Piancatelli, G.; Scettri, A.; Barbadoro, S., *Tetrahedron Lett.*, **1976**, 17, 3555.
29. Saito, K.; Yamachika, H.; US4371711; **1983**
30. Saito, K.; Yamachika, H.; US4356326; **1982**
31. Dohgane, I.; Yamachika, H.; Minai, M., *Tetrahedron*, **1978**, 34, 2775.
32. Islam, A. M.; Zemaity, M. T., *J. Am. Chem. Soc.*, **1957**, 79, 6023.
33. Eugster, O.; Eberhard, P., *Adv. Heterocycl. Chem.*, **1967**, 7, 377.
34. Faza, A. N.; Lopez, C. S.; Alvarez, R.; de Lera, I. R., *Chem. Eur. J.*, **2004**, 10, 4324.

REFERENCES

35. Shono, T.; Matsumura, Y.; Hamaguchi, H., *J. Chem. Soc. Chem. Commun.*, **1977**, 712.
36. Piancatelli, G.; Scettri, A., *Tetrahedron*, **1977**, 33, 69.
37. Csaky, A. G.; Mba, M.; Plumet, J., *Tetrahedron-Asymmetry*, **2004**, 15, 647.
38. Gurjar, M. K.; Wakharkar, R. D.; Singh, A. T.; Jaggi, M.; Borate, H. B.; Shinde, P. D.; Verma, R.; Rajendran, P.; Dutt, S.; Singh, G.; Sanna, V. K.; Singh, M. K.; Srivastava, S. K.; Mahajan, V. A.; Jadhav, V. H.; Dutta, K.; Krishnan, K.; Chaudhary, A.; Agarwal, S. K.; Mukherjee, R.; Burman, A. C., *J. Med. Chem.*, **2007**, 50, 1744.
39. D'Auria, M., *Heterocycles*, **2000**, 52, 185.
40. Paz Otero, M.; Santin, E. P.; Rodriguez-Barrios, F.; Vaz, B.; de Lera, A. R., *Bioorg. Med. Chem. Lett.*, **2009**, 19, 1883
41. Piancatelli, G.; Scettri, A., *Tetrahedron Lett.*, **1977**, 18, 1131.
42. Mico, A. D.; Piancatelli, G.; Cacurri, S.; Lappa, S., *Gazz. Chim. Ital.*, **1992**, 122, 415
43. DABUR RESEARCH FOUNDATION; US2003/229146; **2003**
44. D'auria, M.; Piancatelli, G.; Scettri, A., *Tetrahedron*, **1980**, 36, 3071.
45. Gilman, H.; Franz, R. A.; Hewlett, A. P.; Wright, G. F., *J. Am. Chem. Soc.*, **1950**, 72, 3.
46. D'Auria, M.; Piancatelli, G.; Scettri, A., *Tetrahedron*, **1980**, 36, 1877.
47. Piancatelli, G.; Catagnino, E., *Heterocycles*, **1985**, 23, 667.
48. Castagnino, E.; D'Auria, M.; De Mico, A.; D'Onofrio, F.; Piancatelli, G., *J. Chem. Soc. Chem. Commun.*, **1987**, 907.
49. Saito, K.; Takisawa, Y.; Yamachika, H., *Eur. Pat. 53842*, 1984; *Chem. Abstr.*, **1982**, 97, 162448g.
50. Collins, P. W.; Kramer, S. W.; Gullikson, G. W., *J. Med. Chem.*, **1987**, 30, 1952.
51. Rodriguez, A.; Nomen, M.; Spur, B. W.; Godfroid, J.-J., *Eur. J. Org. Chem.*, **1999**, 2655.
52. Henschke, J. P.; Liu, Y. L.; Huang, X. H.; Chen, Y. F.; Meng, D. C.; Xia, L. Z.; Wei, X. Q.; Xie, A. P.; Li, D. H.; Huang, Q.; Sun, T.; Wang, J.; Gu, X. B.; Huang, X. Y.; Wang, L. H.; Xiao, J.; Qiu, S. H., *Org. Process Res. Dev.*, **2012**, 16, 1905.
53. Fisher, D.; Palmer, L. I.; Cook, J. E.; Davis, J. E.; de Alaniz, J. R., *Tetrahedron*, **2014**, 70, 4105.
54. Yin, B. L.; Wu, Y. L.; Lai, J. Q., *Eur. J. Org. Chem.*, **2009**, 2695.
55. Veits, G. K.; Wenz, D. R.; deAlaniz, J. R., *Angew. Chem. Int. Ed.*, **2010**, 49, 9484
56. Palmer, L. I.; de Alaniz, J. R., *Angew. Chem. Int. Ed.*, **2011**, 50, 7167.
57. Liu, J. Q.; Shen, Q.; Yu, J. J.; Zhu, M. Y.; Han, J. W.; Wang, L. M., *Eur. J. Org. Chem.*, **2012**, 6933.
58. Huang, L.; Zhang, X. Y.; Li, J.; Ding, K.; Li, X. H.; Zheng, W. X.; Yin, B. L., *Eur. J. Org. Chem.*, **2014**, 338.
59. Yin, B. L.; Lai, J. Q.; Zhang, Z. R.; Jiang, H. F., *Adv. Synth. Catal.*, **2011**, 353, 1961.
60. Yin, B. L.; Huang, L.; Wang, X. J.; Liu, J. C.; Jiang, H. F., *Adv. Synth. Catal.*, **2013**, 355, 370.
61. Yin, B. A. L.; Huang, L.; Zhang, X. Y.; Ji, F. H.; Jiang, H. F., *J. Org. Chem.*, **2012**, 77, 6365.
62. Lewis, K. G.; Mulquiney, C. E., *Aust. J. Chem.*, **1979**, 32, 1079.
63. Lewis, K. G.; Mulquiney, C. E., *Chem. Ind.*, **1968**, 1249.
64. Lewis, K. G.; Mulquiney, C. E., *Aust. J. Chem.*, **1970**, 23, 2315.
65. Stenhouse, J., *Ann*, **1850**, 74, 278.

66. Stenhouse, J., *Ann*, **1870**, 156, 197.
67. Lewis, K. G.; Mulquiney, C. E., *Tetrahedron*, **1977**, 33, 463.
68. D'Arcy, B. R.; Lewis, K. G.; Mulquiney, C. E., *Aust. J. Chem.*, **1985**, 38, 953.
69. D'Arcy, B. R.; Lewis, K. G.; Mulquiney, C. E., *Aust. J. Chem.*, **1987**, 40, 509.
70. Wang, Q.-L.; Zhang, H.; Jiang, Y.-B., *Tetrahedron Lett.*, **2009**, 50, 29.
71. Schneider, G.; Schollmeyer, D.; Pindur, U., *Pharmazie*, **1998**, 53, 361
72. Li, S. W.; Batey, R. A., *Chem. Commun.*, **2007**, 3759.
73. Ramesh, D.; Reddy, T. S.; Narasimhulu, M.; Rajaram, S.; Suryakiran, N.; Mahesh, K. C.; Venkateswarlu, Y., *Chem. Lett.*, **2009**, 38, 586.
74. Procopio, A.; Costanzo, P.; Curini, M.; Nardi, M.; Oliverio, M.; Sindona, G., *ACS Sustainable Chem. Eng.*, **2013**, 1, 541.
75. Liu, J. Q.; Yu, J. J.; Zhu, M. Y.; Li, J.; Zheng, X. Z.; Wang, L. M., *Synthesis-Stuttgart*, **2013**, 45, 2165.
76. Helmy, S.; Leibfarth, F. A.; Oh, S.; Poelma, J. E.; Hawker, C. J.; de Alaniz, J. R., *J. Am. Chem. Soc.*, **2014**, 136, 8169.
77. Christensen, C. H.; Rass-Hansen, J.; Marsden, C. C.; Taarning, E.; Egeblad, K., *Chemsuschem*, **2008**, 1, 283.
78. Regalbuto, J. R., *Science*, **2009**, 325, 822.
79. Whitesides, G. M.; Crabtree, G. W., *Science*, **2007**, 315, 796.
80. Corma, A.; Iborra, S.; Velty, A., *Chem. Rev.*, **2007**, 107, 2411.
81. Gallezot, P., *Chem. Soc. Rev.*, **2012**, 41, 1538.
82. Roman-Leshkov, Y.; Barrett, C. J.; Liu, Z. Y.; Dumesic, J. A., *Nature*, **2007**, 447, 982.
83. Mascal, M.; Dutta, S., *Green Chem.*, **2011**, 13, 3101.
84. Mascal, M.; Dutta, S., *Green Chem.*, **2011**, 13, 40.
85. Stahlberg, T.; Fu, W. J.; Woodley, J. M.; Riisager, A., *Chemsuschem*, **2011**, 4, 451.
86. Climent, M. J.; Corma, A.; Iborra, S., *Green Chem.*, **2011**, 13, 520.
87. Rosatella, A. A.; Simeonov, S. P.; Frade, R. F. M.; Afonso, C. A. M., *Green Chem.*, **2011**, 13, 754.
88. Buntara, T.; Noel, S.; Phua, P. H.; Melian-Cabrera, I.; de Vries, J. G.; Heeres, H. J., *Angew. Chem. Int. Ed.*, **2011**, 50, 7083.
89. Nunes, J. P. M.; Veiros, L. F.; Vaz, P. D.; Afonso, C. A. M.; Caddick, S., *Tetrahedron*, **2011**, 67, 2779.
90. Nunes, J. P. M.; Afonso, C. A. M.; Caddick, S., *Rsc Advances*, **2013**, 3, 14975.
91. van Putten, R.-J.; van der Waal, J. C.; de Jong, E.; Rasrendra, C. B.; Heeres, H. J.; de Vries, J. G., *Chem. Rev.*, **2013**, 113, 1499.
92. Zhao, H. B.; Holladay, J. E.; Brown, H.; Zhang, Z. C., *Science*, **2007**, 316, 1597.
93. Li, C. Z.; Zhang, Z. H.; Zhao, Z. B. K., *Tetrahedron Lett.*, **2009**, 50, 5403.
94. Binder, J. B.; Raines, R. T., *J. Am. Chem. Soc.*, **2009**, 131, 1979.
95. Hu, S. Q.; Zhang, Z. F.; Song, J. L.; Zhou, Y. X.; Han, B. X., *Green Chem.*, **2009**, 11, 1746.
96. Rasrendra, C. B.; Soetedjo, J. N. M.; Makertihartha, I.; Adisasmito, S.; Heeres, H. J., *Top. Catal.*, **2012**, 55, 543.
97. Pagan-Torres, Y. J.; Wang, T. F.; Gallo, J. M. R.; Shanks, B. H.; Dumesic, J. A., *ACS Catal.*, **2012**, 2, 930.
98. Caes, B. R.; Palte, M. J.; Raines, R. T., *Chem. Sci.*, **2013**.
99. Gallo, J. M. R.; Alonso, D. M.; Mellmer, M. A.; Dumesic, J. A., *Green Chem.*, **2013**.
100. Jadhav, H.; Taarning, E.; Pedersen, C. M.; Bols, M., *Tetrahedron Lett.*, **2012**, 53, 983.

REFERENCES

101. Sigma-Aldrich; <http://www.sigmaaldrich.com>; 25/6/2014.
102. Shimizu, K.; Uozumi, R.; Satsuma, A., *Catal. Commun.*, **2009**, *10*, 1849.
103. Vigier, K. D. O.; Benguerba, A.; Barrault, J.; Jerome, F., *Green Chem.*, **2012**.
104. Wei, Z. J.; Liu, Y. X.; Thushara, D.; Ren, Q. L., *Green Chem.*, **2012**, *14*, 1220.
105. Bhosale, S. H.; Rao, M. B.; Deshpande, V. V., *Microbiol. Rev.*, **1996**, *60*, 280.
106. Vilonen, K. M.; Vuolanto, A.; Jokela, J.; Leisola, M. S. A.; Krause, A. O. I., *Biotechnol. Prog.*, **2004**, *20*, 1555.
107. Stahlberg, T.; Woodley, J. M.; Riisager, A., *Catal. Sci. Technol.*, **2012**, *2*, 291.
108. Visuri, K.; Klibanov, A. M., *Biotechnol. Bioeng.*, **1987**, *30*, 917.
109. Huang, R. L.; Qi, W.; Su, R. X.; He, Z. M., *Chem. Commun.*, **2010**, *46*, 1115.
110. Grande, P. M.; Bergs, C.; de Maria, P. D., *Chemsuschem*, **2012**, *5*, 1203.
111. Antal, M. J.; Mok, W. S. L.; Richards, G. N., *Carbohydr. Res.*, **1990**, *199*, 91.
112. Antal, M. J.; Leesomboon, T.; Mok, W. S.; Richards, G. N., *Carbohydr. Res.*, **1991**, *217*, 71.
113. Li, C. Z.; Zhao, Z. K.; Wang, A. Q.; Zheng, M. Y.; Zhang, T., *Carbohydr. Res.*, **2010**, *345*, 1846.
114. Amarasekara, A. S.; Williams, L. D.; Ebede, C. C., *Carbohydr. Res.*, **2008**, *343*, 3021.
115. Assary, R. S.; Redfern, P. C.; Greeley, J.; Curtiss, L. A., *J. Phys. Chem. B*, **2011**, *115*, 4341.
116. Horvat, J.; Klaić, B.; Metelko, B.; Sunjic, V., *Tetrahedron Lett.*, **1985**, *26*, 2111.
117. Zhang, J.; Weitz, E., *ACS Catal.*, **2012**, *2*, 1211.
118. Abraham, K.; Gürtler, R.; Berg, K.; Heinemeyer, G.; Lampen, A.; Appel, K. E., *Mol. Nutr. Food Res.*, **2011**.
119. Vinas, P.; Campillo, N.; Cordoba, M. H.; Candela, M., *Food Chem.*, **1992**, *44*, 67.
120. Archer, M. C.; Bruce, W. R.; Chan, C. C.; Corpet, D. E.; Medline, A.; Roncucci, L.; Stamp, D.; Zhang, X. M., *Environ. Health Perspect.*, **1992**, *98*, 195.
121. Zhang, X. M.; Chan, C. C.; Stamp, D.; Minkin, S.; Archer, M. C.; Bruce, W. R., *Carcinogenesis*, **1993**, *14*, 773.
122. Svendsen, C.; Husoy, T.; Glatt, H.; Paulsen, J. E.; Alexander, J., *Anticancer Res.*, **2009**, *29*, 1921.
123. Florian, S.; Bauer-Marinovic, M.; Taugner, F.; Dobbernack, G.; Monien, B. H.; Meinel, W.; Glatt, H., *Mol. Nutr. Food Res.*, **2012**, *56*, 593.
124. Godfrey, V. B.; Chen, L. J.; Griffin, R. J.; Lebetkin, E. H.; Burka, L. T., *J. Toxicol. Environ. Health A*, **1999**, *57*, 199.
125. Jellum, E.; Børresen, H. C.; Eldjarn, L., *Clin. Chim. Acta*, **1973**, *47*, 191.
126. Ronald, L.; Wu, X.; Gu, L., *J. Agric. Food Chem.*, **2006**, *54*, 3744.
127. Jobstl, D.; Husoy, T.; Alexander, J.; Bjellaas, T.; Leitner, E.; Murkovic, M., *Food Chem.*, **2010**, *123*, 814.
128. Lee, Y. C.; Shlyankevich, M.; Jeong, H. K.; Douglas, J. S.; Surh, Y. J., *Biochem. Biophys. Res. Commun.*, **1995**, *209*, 996.
129. Surh, Y. J.; Liem, A.; Miller, J. A.; Tannenbaum, S. R., *Carcinogenesis*, **1994**, *15*, 2375.
130. Bakhiya, N.; Monien, B.; Frank, H.; Seidel, A.; Glatt, H., *Biochem. Pharmacol.*, **2009**, *78*, 414.
131. Bluhm, K.; Heger, S.; Seiler, T. B.; Hallare, A. V.; Schaffer, A.; Hollert, H., *Energy Environ. Sci.*, **2012**, *5*, 7381.

132. Heger, S.; Bluhm, K.; Agler, M. T.; Maletz, S.; Schaffer, A.; Seiler, T. B.; Angenent, L. T.; Hollert, H., *Energy Environ. Sci.*, **2012**, 5, 9778.
133. States National Library of Medicine: ChemIDplus Advanced (<http://chem.sis.nlm.nih.gov/chemidplus>).
134. Musau, R. M.; Munavu, R. M., *Biomass*, **1987**, 13, 67.
135. Halliday, G. A.; Young, R. J.; Grushin, V. V., *Org. Lett.*, **2003**, 5, 2003.
136. Quotation from scienTEST, Germany.
137. Jadhav, H.; Taarning, E.; Pedersen, C. M.; Bols, M., *Tetrahedron Lett.*, **2012**, 53, 983.
138. Yuan, Z.; Xu, C. B.; Cheng, S. N.; Leitch, M., *Carbohydr. Res.*, **2011**, 346, 2019.
139. Cao, Q.; Guo, X. C.; Guan, J.; Mu, X. D.; Zhang, D. K., *Applied Catalysis a-General*, **2011**, 403, 98.
140. Svilen, P.; Coelho, J. A. S.; Afonso, C. A. M., *Chemsuschem*, **2012**, 5, 1388.
141. Monien, B. H.; Frank, H.; Seidel, A.; Glatt, H., *Chem. Res. Toxicol.*, **2009**, 22, 1123.
142. Sanda, K.; Rigal, L.; Gaset, A., *Carbohydr. Res.*, **1989**, 187, 15.
143. Cottier, L.; Descotes, G.; Eymard, L.; Rapp, K., *Synthesis*, **1995**, 303.
144. Cottier, L.; Descotes, G.; Soro, Y., *J. Carbohydr. Chem.*, **2005**, 24, 55.
145. Dai, H. L.; Shen, Q.; Zheng, J. B.; Li, J. Y.; Wen, R.; Li, J., *Lett. Org. Chem.*, **2011**, 8, 526.
146. Bognar, R.; Herczegh, P.; Zsely, M.; Batta, G., *Carbohydr. Res.*, **1987**, 164, 465.
147. CANON KABUSHIKI KAISHA; US2007/232815; **2007**
148. Antonio, J. P. M.; Frade, R. F. M.; Santos, F. M. F.; Coelho, J. A. S.; Afonso, C. A. M.; Gois, P. M. P.; Trindade, A. F., *Rsc Advances*, **2014**, 4, 29352.
149. Holzapfel, W. B.; Isaacs, N. S. *High-pressure techniques in chemistry and physics: A practical approach*; Oxford University Press, 1997.
150. Eldik, R. v.; Hubbard, C. D. *Chemistry under extreme or non-classical conditions*; John Wiley & Sons Inc, 1996.
151. Ballerini, E.; Minuti, L.; Piermatti, O., *J. Org. Chem.*, **2010**, 75, 4251.
152. Lyzwa, D.; Dudzinski, K.; Kwiatkowski, P., *Org. Lett.*, **2012**, 14, 1540.
153. Schettino, V.; Bini, R., *Chem. Soc. Rev.*, **2007**, 36, 869.
154. Bur, S. K.; Martin, S. F., *Tetrahedron*, **2001**, 57, 3221.
155. Casiraghi, G.; Battistini, L.; Curti, C.; Rassu, G.; Zanardi, F., *Chem. Rev.*, **2011**, 111, 3076.
156. Deiters, A.; Chen, K.; Eary, C. T.; Martin, S. F., *J. Am. Chem. Soc.*, **2003**, 125, 4541.
157. Ratjen, L.; Garcia-Garcia, P.; Lay, F.; Beck, M. E.; List, B., *Angew. Chem. Int. Ed.*, **2011**, 50, 754.
158. Zhou, Z.; Feng, X.; Yin, X.; Chen, Y. C., *Org. Lett.*, **2014**, 16, 2370.
159. Li, J.-L.; Yue, C.-Z.; Chen, P.-Q.; Xiao, Y.-C.; Chen, Y.-C., *Angewandte Chemie International Edition*, **2014**, 53, 5449.
160. Jia, Z. J.; Jiang, H.; Li, J. L.; Gschwend, B.; Li, Q. Z.; Yin, X.; Grouleff, J.; Chen, Y. C.; Jorgensen, K. A., *J. Am. Chem. Soc.*, **2011**, 133, 5053.
161. Mukherjee, S.; Yang, J. W.; Hoffmann, S.; List, B., *Chem. Rev.*, **2007**, 107, 5471.
162. Barbas, C. F., *Angew Chem Int Ed Engl*, **2008**, 47, 42.
163. Dondoni, A.; Massi, A., *Angew Chem Int Ed Engl*, **2008**, 47, 4638.
164. MacMillan, D. W. C., *Nature*, **2008**, 455, 304.
165. Melchiorre, P.; Marigo, M.; Carlone, A.; Bartoli, G., *Angew Chem Int Ed Engl*, **2008**, 47, 6138.
166. Ramachary, D. B.; Reddy, Y. V., *Eur. J. Org. Chem.*, **2012**, 865.

REFERENCES

167. Jensen, K. L.; Dickmeiss, G.; Jiang, H.; Albrecht, L.; Jorgensen, K. A., *Acc. Chem. Res.*, **2012**, *45*, 248.
168. Arceo, E.; Melchiorre, P., *Angew Chem Int Ed Engl*, **2012**, *51*, 5290.
169. Kumar, I.; Ramaraju, P.; Mir, N. A., *Org. Biomol. Chem.*, **2013**, *11*, 709.
170. Halskov, K. S.; Johansen, T. K.; Davis, R. L.; Steurer, M.; Jensen, F.; Jorgensen, K. A., *J. Am. Chem. Soc.*, **2012**, *134*, 12943.
171. Dell'Amico, L.; Albrecht, L.; Naicker, T.; Poulsen, P. H.; Jorgensen, K. A., *J. Am. Chem. Soc.*, **2013**, *135*, 8063.
172. Feng, X.; Zhou, Z.; Ma, C.; Yin, X.; Li, R.; Dong, L.; Chen, Y. C., *Angew Chem Int Ed Engl*, **2013**, *52*, 14173.
173. Reboredo, S.; Parra, A.; Alemán, J., *Asymmetric Organocatalysis*, **2013**, *1*.
174. Jiang, H.; Albrecht, L.; Jørgensen, K. A., *Chem. Sci.*, **2013**, *4*, 2287.
175. Dieckmann, A.; Breugst, M.; Houk, K. N., *J. Am. Chem. Soc.*, **2013**, *135*, 3237.
176. Lee, C. K.; Gong, J. S.; Lee, I. S. H., *J. Heterocycl. Chem.*, **1995**, *32*, 239.
177. Parr, R. G.; Yang, W. *Density Functional Theory of Atoms and Molecules*; Oxford University Press: New York, 1989.
178. Shchepinov, M. S.; Korshun, V. A., *Chem. Soc. Rev.*, **2003**, *32*, 170.
179. Nair, V.; Thomas, S.; Mathew, S. C.; Abhilash, K. G., *Tetrahedron*, **2006**, *62*, 6731.
180. Duxbury, D. F., *Chem. Rev.*, **1993**, *93*, 381.
181. Mason, C. D.; Nord, F. F., *J. Org. Chem.*, **1951**, *16*, 722.
182. Ghaisas, V. V.; Kane, B. J.; Nord, F. F., *J. Org. Chem.*, **1958**, *23*, 560.
183. Irie, M., *J. Am. Chem. Soc.*, **1983**, *105*, 2078.
184. Muthyala, R.; Katritzky, A. R.; Lan, X., *Dyes Pigm.*, **1994**, *25*, 303.
185. Urano, Y.; Kamiya, M.; Kanda, K.; Ueno, T.; Hirose, K.; Nagano, T., *J. Am. Chem. Soc.*, **2005**, *127*, 4888.
186. Abe, H.; Wang, J.; Furukawa, K.; Oki, K.; Uda, M.; Tsuneda, S.; Ito, Y., *Bioconjugate Chem.*, **2008**, *19*, 1219.
187. Kim, H. N.; Lee, M. H.; Kim, H. J.; Kim, J. S.; Yoon, J., *Chem. Soc. Rev.*, **2008**, *37*, 1465.
188. Beija, M.; Afonso, C. A. M.; Martinho, J. M. G., *Chem. Soc. Rev.*, **2009**, *38*, 2410.
189. Bhasikuttan, A. C.; Mohanty, J.; Nau, W. M.; Pal, H., *Angewandte Chemie International Edition*, **2007**, *46*, 4120.
190. Bindal, R. D.; Golab, J. T.; Katzenellenbogen, J. A., *J. Am. Chem. Soc.*, **1990**, *112*, 7861.
191. Bai, L.; Masukawa, N.; Yamaki, M.; Takagi, S., *Phytochemistry*, **1998**, *47*, 1637.
192. Jin, C.; Michetich, R. G.; Daneshtalab, M., *Phytochemistry*, **1999**, *50*, 505.
193. Wang, P.; Kozlowski, J.; Cushman, M., *J. Org. Chem.*, **1992**, *57*, 3861.
194. Al-Qawasmeh, R. A.; Lee, Y.; Cao, M.-Y.; Gu, X.; Vassilakos, A.; Wright, J. A.; Young, A., *Bioorg. Med. Chem. Lett.*, **2004**, *14*, 347.
195. Palchaudhuri, R.; Nesterenko, V.; Hergenrother, P. J., *J. Am. Chem. Soc.*, **2008**, *130*, 10274.
196. Gessner, T.; Mayer, U. In *Ullmann's Encyclopedia of Industrial Chemistry*; Wiley-VCH Verlag GmbH & Co. KGaA, 2000.
197. Benzaquen, L. R.; Brugnara, C.; Byers, H. R.; Gattoni-Celli, S.; Halperin, J. A., *Nat Med*, **1995**, *1*, 534.
198. Wulff, H.; Miller, M. J.; Hänsel, W.; Grissmer, S.; Cahalan, M. D.; Chandy, K. G., *P. N. A. S.*, **2000**, *97*, 8151.

199. Al-Qawasmeh, R. A.; Lee, Y.; Cao, M. Y.; Gu, X. P.; Vassilakos, A.; Wright, J. A.; Young, A., *Bioorg. Med. Chem. Lett.*, **2004**, 14, 347.
200. FINER JEFFREY T; CHABALA JOHN C; EVAN, L.; Triphenylmethane kinesin inhibitors; CYTOKINETICS INC; WO2002056880; **2002**
201. Dothager, R. S.; Putt, K. S.; Allen, B. J.; Leslie, B. J.; Nesterenko, V.; Hergenrother, P. J., *J. Am. Chem. Soc.*, **2005**, 127, 8686.
202. Oclarit, J. M.; Okada, H.; Ohta, S.; Kaminura, K.; Yamaoka, Y.; Iizuka, T.; Miyashiro, S.; Ikegami, S., *Microbios*, **1994**, 78, 7.
203. Shagufta; Srivastava, A. K.; Sharma, R.; Mishra, R.; Balapure, A. K.; Murthy, P. S. R.; Panda, G., *Bioorg. Med. Chem.*, **2006**, 14, 1497.
204. Klumpp, D. A.; Lau, S. F., *J. Org. Chem.*, **1999**, 64, 7309.
205. Klumpp, D. A.; Kindelin, P. J.; Li, A., *Tetrahedron Lett.*, **2005**, 46, 2931.
206. Saito, S.; Ohwada, T.; Shudo, K., *J. Am. Chem. Soc.*, **1995**, 117, 11081.
207. Esquivias, J.; Gómez Arrayás, R.; Carretero, J. C., *Angew. Chem. Int. Ed.*, **2006**, 45, 629.
208. Niwa, T.; Yorimitsu, H.; Oshima, K., *Org. Lett.*, **2007**, 9, 2373.
209. Lin, S.; Lu, X., *J. Org. Chem.*, **2007**, 72, 9757.
210. Yu, J. Y.; Kuwano, R., *Org. Lett.*, **2008**, 10, 973.
211. Katritzky, A. R.; Toader, D., *J. Org. Chem.*, **1997**, 62, 4137.
212. Makosza, M.; Surowiec, M.; Voskresensky, S., *Synthesis*, **2000**, 1237.
213. Podder, S.; Choudhury, J.; Roy, U. K.; Roy, S., *J. Org. Chem.*, **2007**, 72, 3100.
214. Nambo, M.; Crudden, C. M., *Angew. Chem. Int. Ed.*, **2014**, 53, 742.
215. Matthew, S. C.; Glasspoole, B. W.; Eisenberger, P.; Crudden, C. M., *J. Am. Chem. Soc.*, **2014**, 136, 5828.
216. Nair, V.; Abhilash, K. G.; Vidya, N., *Org. Lett.*, **2005**, 7, 5857.
217. Li, Z.; Duan, Z.; Kang, J.; Wang, H.; Yu, L.; Wu, Y., *Tetrahedron*, **2008**, 64, 1924.
218. Bardajee, G. R.; Jafarpour, F., *Cent. Eur. J. Chem.*, **2008**, 7, 138.
219. Jafarpour, F.; Bardajee, G. R.; Pirelahi, H.; Oroojpour, V.; Dehnamaki, H.; Rahmdel, S., *Chin. J. Chem.*, **2009**, 27, 1415.
220. Bardajee, G. R., *Beilstein J. Org. Chem.*, **2011**, 7, 135.
221. Guzman-Lucero, D.; Guzman, J.; Likhatchev, D.; Martinez-Palou, R., *Tetrahedron Lett.*, **2005**, 46, 1119.
222. Budin, G.; Chung, H. J.; Lee, H.; Weissleder, R., *Angew. Chem. Int. Ed.*, **2012**, 51, 7752.
223. Kaupp, G.; Schmeyers, J.; Boy, J., *J. prakt. Chem*, **2000**, 342, 269.
224. Murali, A.; Puppala, M.; Varghese, B.; Baskaran, S., *Eur. J. Org. Chem.*, **2011**, 5297.
225. Chiappe, C.; Piccioli, P.; Pieraccini, D., *Green Chem.*, **2006**, 8, 277.
226. Iranpoor, N.; Firouzabadi, H.; Nowrouzi, N.; Khalili, D., *Tetrahedron*, **2009**, 65, 3893.
227. Zhu, M. H.; Zhang, C.; Nwachukwu, J. C.; Srinivasan, S.; Cavett, V.; Zheng, Y. F.; Carlson, K. E.; Dong, C. N.; Katzenellenbogen, J. A.; Nettles, K. W.; Zhou, H. B., *Org. Biomol. Chem.*, **2012**, 10, 8692.
228. Atzrodt, J.; Derdau, V.; Fey, T.; Zimmermann, J., *Angew. Chem. Int. Ed.*, **2007**, 46, 7744.
229. Martins, A.; Lautens, M., *Org. Lett.*, **2008**, 10, 4351.
230. Simmons, E. M.; Hartwig, J. F., *Angew. Chem. Int. Ed.*, **2012**, 51, 3066.
231. Frisch, M. J.; Trucks, G. W.; Schlegel, H. B.; Scuseria, G. E.; Robb, M. A.; Cheeseman, J. R.; Scalmani, G.; Barone, V.; Mennucci, B.; Petersson, G. A.

REFERENCES

- Nakatsuji, H.; Caricato, M.; Li, X.; Hratchian, H. P.; Izmaylov, A. F.; Bloino, J.; Zheng, G.; Sonnenberg, J. L.; Hada, M.; Ehara, M.; Toyota, K.; Fukuda, R.; Hasegawa, J.; Ishida, M.; Nakajima, T.; Honda, Y.; Kitao, O.; Nakai, H.; Vreven, T.; Jr., J. A. M.; Peralta, J. E.; Ogliaro, F.; Bearpark, M.; Heyd, J. J.; Brothers, E.; Kudin, K. N.; Staroverov, V. N.; Kobayashi, R.; Normand, J.; Raghavachari, K.; Rendell, A.; Burant, J. C.; Iyengar, S. S.; Tomasi, J.; Cossi, M.; Rega, N.; Millam, J. M.; Klene, M.; Knox, J. E.; Cross, J. B.; Bakken, V.; Adamo, C.; Jaramillo, J.; Gomperts, R.; Stratmann, R. E.; Yazyev, O.; Austin, A. J.; Cammi, R.; Pomelli, C.; Ochterski, J. W.; Martin, R. L.; Morokuma, K.; Zakrzewski, V. G.; Voth, G. A.; Salvador, P.; Dannenberg, J. J.; Dapprich, S.; Daniels, A. D.; Ö. Farkas; Foresman, J. B.; Ortiz, J. V.; Cioslowski, J.; Fox, D. J.; GAUSSIAN 09 (Revision A.01), Gaussian, Inc.: Wallingford CT, 2009.
- 232.** Becke, A. D., *J. Chem. Phys.*, **1993**, 98, 5648.
- 233.** Ditchfie.R; Hehre, W. J.; Pople, J. A., *J. Chem. Phys.*, **1971**, 54, 724.
- 234.** Hehre, W. J.; Ditchfie.R; Pople, J. A., *J. Chem. Phys.*, **1972**, 56, 2257.
- 235.** Harihara.Pc; Pople, J. A., *Mol. Phys.*, **1974**, 27, 209.
- 236.** Gordon, M. S., *Chem. Phys. Lett.*, **1980**, 76, 163.
- 237.** Harihara.Pc; Pople, J. A., *Theor. Chim. Acta*, **1973**, 28, 213.
- 238.** Lee, C. T.; Yang, W. T.; Parr, R. G., *Physical Review B*, **1988**, 37, 785.
- 239.** Miehlich, B.; Savin, A.; Stoll, H.; Preuss, H., *Chem. Phys. Lett.*, **1989**, 157, 200.
- 240.** Peng, C. Y.; Ayala, P. Y.; Schlegel, H. B.; Frisch, M. J., *J. Comput. Chem.*, **1996**, 17, 49.
- 241.** Peng, C. Y.; Schlegel, H. B., *Isr. J. Chem.*, **1993**, 33, 449.
- 242.** Mclean, A. D.; Chandler, G. S., *J. Chem. Phys.*, **1980**, 72, 5639.
- 243.** Krishnan, R.; Binkley, J. S.; Seeger, R.; Pople, J. A., *J. Chem. Phys.*, **1980**, 72, 650.
- 244.** Wachters, A. J., *J. Chem. Phys.*, **1970**, 52, 1033.
- 245.** Raghavachari, K.; Trucks, G. W., *J. Chem. Phys.*, **1989**, 91, 1062.
- 246.** Hay, P. J., *J. Chem. Phys.*, **1977**, 66, 4377.
- 247.** Binning, R. C.; Curtiss, L. A., *J. Comput. Chem.*, **1990**, 11, 1206.
- 248.** McGrath, M. P.; Radom, L., *J. Chem. Phys.*, **1991**, 94, 511.
- 249.** Clark, T.; Chandrasekhar, J.; Spitznagel, G. W.; Schleyer, P. V., *J. Comput. Chem.*, **1983**, 4, 294.
- 250.** Frisch, M. J.; Pople, J. A.; Binkley, J. S., *J. Chem. Phys.*, **1984**, 80, 3265.
- 251.** Cancès, E.; Mennucci, B.; Tomasi, J., *J. Chem. Phys.*, **1997**, 107, 3032.
- 252.** Cossi, M.; Barone, V.; Mennucci, B.; Tomasi, J., *Chem. Phys. Lett.*, **1998**, 286, 253.
- 253.** Mennucci, B.; Tomasi, J., *J. Chem. Phys.*, **1997**, 106, 5151.
- 254.** Tomasi, J.; Mennucci, B.; Cammi, R., *Chem. Rev.*, **2005**, 105, 2999.
- 255.** Marenich, A. V.; Cramer, C. J.; Truhlar, D. G., *J. Phys. Chem. B*, **2009**, 113, 6378.
- 256.** Zhao, Y.; Truhlar, D. G., *Theor. Chem. Acc.*, **2008**, 120, 215.
- 257.** Zhao, Y.; Truhlar, D. G., *Acc. Chem. Res.*, **2008**, 41, 157.
- 258.** Zhao, Y.; Truhlar, D. G., *Chem. Phys. Lett.*, **2011**, 502, 1.
- 259.** Bruker Analytical Systems: Madison, WI, **2005**.
- 260.** Bruker Analytical Systems: Madison, WI, **2005**.
- 261.** Altomare, A.; Burla, M. C.; Camalli, M.; Cascarano, G. L.; Giacovazzo, C.; Guagliardi, A.; Moliterni, A. G. G.; Polidori, G.; Spagna, R., *J. Appl. Crystallogr.*, **1999**, 32, 115.
- 262.** Sheldrick, G. M., *Acta Crystallogr. Sect. A*, **2008**, 64, 112.
- 263.** Farrugia, L. J., *J. Appl. Cryst.*, **1999**, 32, 837.

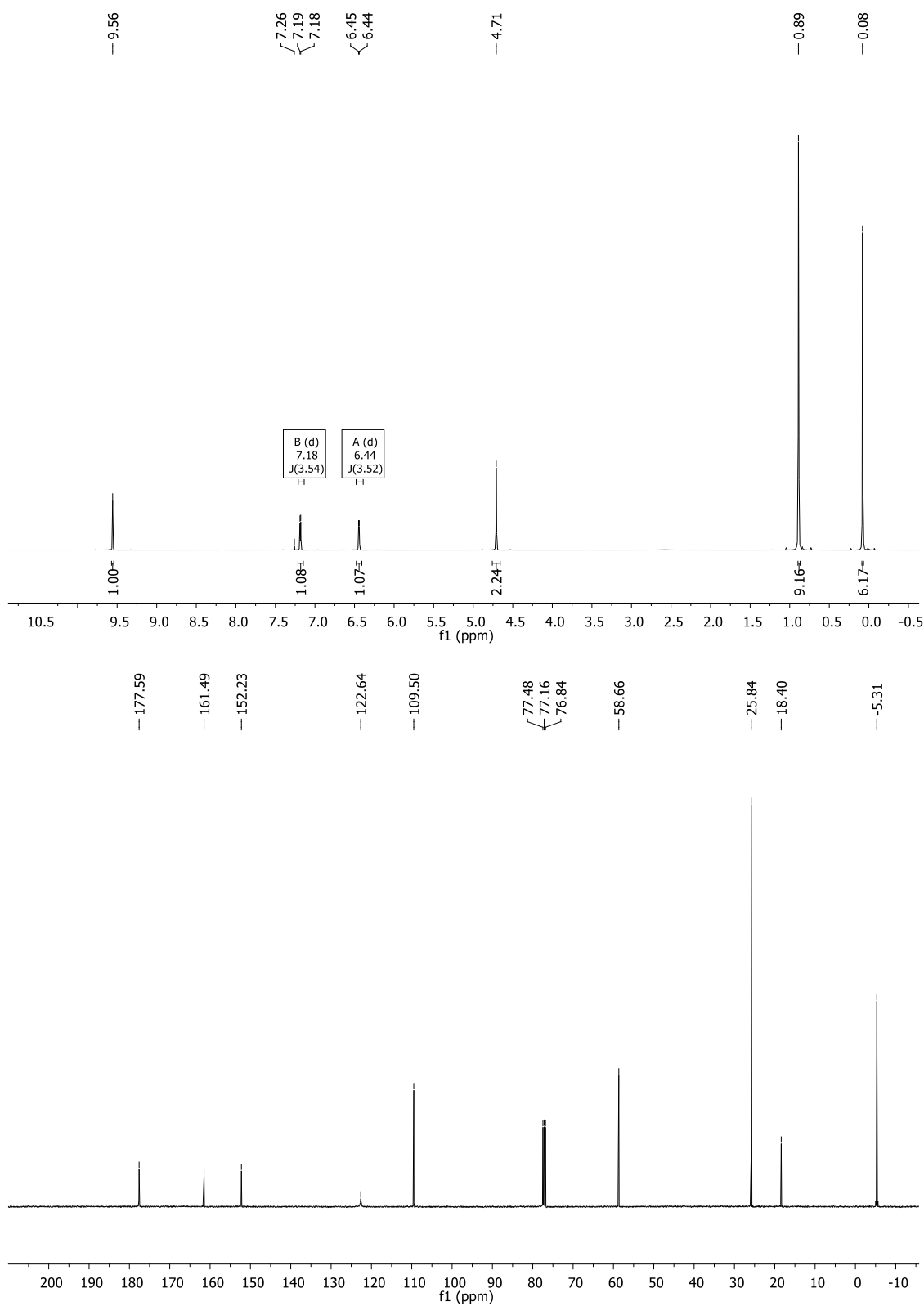
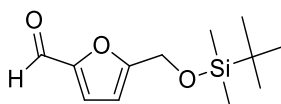
264. Souris, C.; Luparia, M.; Frebault, F.; Audisio, D.; Fares, C.; Goddard, R.; Maulide, N., *Chem. Eur. J.*, **2013**, *19*, 6566.
265. Souris, C.; Frebault, F.; Audisio, D.; Fares, C.; Maulide, N., *Synlett*, **2013**, *21*, 1286.
266. Souris, C.; Frébault, F.; Patel, A.; Audisio, D.; Houk, K. N.; Maulide, N., *Org. Lett.*, **2013**.
267. Tsuda, M.; Mugishima, T.; Komatsu, K.; Sone, T.; Tanaka, M.; Mikami, Y.; Kobayashi, J., *J. Nat. Prod.*, **2003**, *66*, 412.
268. Niwayama, S.; Kallel, E. A.; Spellmeyer, D. C.; Sheu, C. M.; Houk, K. N., *J. Org. Chem.*, **1996**, *61*, 2813.
269. Ito, M.; Matsuumi, M.; Murugesh, M. G.; Kobayashi, Y., *J. Org. Chem.*, **2001**, *66*, 5881.
270. Rieke, R. D.; Hanson, M. V., *Tetrahedron*, **1997**, *53*, 1925.
271. Yoshikai, N.; Nakamura, E., *Chem. Rev.*, **2012**, *112*, 2339.
272. Falciola, C. A.; Alexakis, A., *Eur. J. Org. Chem.*, **2008**, 3765.
273. Krishna, P. R.; Reddy, V. V. R.; Sharma, G. V. M., *Synthesis*, **2004**, 2107.
274. Node, M.; Kajimoto, T.; Nishide, K.; Fujita, E.; Fuji, K., *Tetrahedron Lett.*, **1984**, *25*, 219.
275. Son, S.; Fu, G. C., *J. Am. Chem. Soc.*, **2008**, *130*, 2756.
276. Dhimitruka, H.; SantaLucia, J., *Org. Lett.*, **2006**, *8*, 47.
277. Peng, Y.; Li, W. D. Z., *Synlett*, **2006**, 1165.
278. Morris, W. J.; Shair, M. D., *Tetrahedron Lett.*, **2010**, *51*, 4310.
279. Sperry, J.; Harris, E. B. J.; Brimble, M. A., *Org. Lett.*, **2010**, *12*, 420.
280. Casey, T. C.; Carlisle, J.; Tisselli, P.; Male, L.; Spencer, N.; Grainger, R. S., *J. Org. Chem.*, **2010**, *75*, 7461.
281. Engstrom, K.; Henry, R.; Hollis, L. S.; Kotecki, B.; Marsden, I.; Pu, Y. M.; Wagaw, S.; Wang, W. F., *J. Org. Chem.*, **2006**, *71*, 5369.
282. Zimmerman, H. E.; Wang, P. F., *J. Org. Chem.*, **2003**, *68*, 9226.
283. Eames, J.; Weerasooriya, N., *J. Chem. Res. (S)*, **2001**, 2.
284. Cohen, F.; Overman, L. E.; Sakata, S. K. L., *Org. Lett.*, **1999**, *1*, 2169.
285. Krause, N.; Ebert, S.; Haubrich, A., *Liebigs Ann-Recl*, **1997**, 2409.
286. Yasukata, T.; Koga, K., *Tetrahedron-Asymmetry*, **1993**, *4*, 35.
287. Awandi, D.; Henin, F.; Muzart, J.; Pete, J. P., *Tetrahedron-Asymmetry*, **1991**, *2*, 1101.
288. Compagnone, R. S.; Rapoport, H., *J. Org. Chem.*, **1986**, *51*, 1713.
289. Hirai, H.; Sawada, K.; Aratani, M.; Hashimoto, M., *Tetrahedron Lett.*, **1985**, *26*, 1739.
290. Takano, S.; Uchida, W.; Hatakeyama, S.; Ogasawara, K., *Chem. Lett.*, **1982**, 733.
291. Valerio, V.; Petkova, D.; Madelaine, C.; Maulide, N., *Chem. Eur. J.*, **2013**, *19*, 2606.
292. Amans, D.; Bellosta, V.; Cossy, J., *Chem. Eur. J.*, **2009**, *15*, 3457.
293. Frebault, F.; Oliveira, M. T.; Wostefeld, E.; Maulide, N., *J. Org. Chem.*, **2010**, *75*, 7962.
294. Corey, E. J.; Streith, J., *J. Am. Chem. Soc.*, **1964**, *86*, 950.
295. Lauzon, S.; Tremblay, F.; Gagnon, D.; Godbout, C.; Chabot, C.; Mercier-Shanks, C.; Perreault, S.; DeSeve, H.; Spino, C., *J. Org. Chem.*, **2008**, *73*, 6239.
296. Yadav, V. K.; Fallis, A. G., *J. Org. Chem.*, **1986**, *51*, 3372.

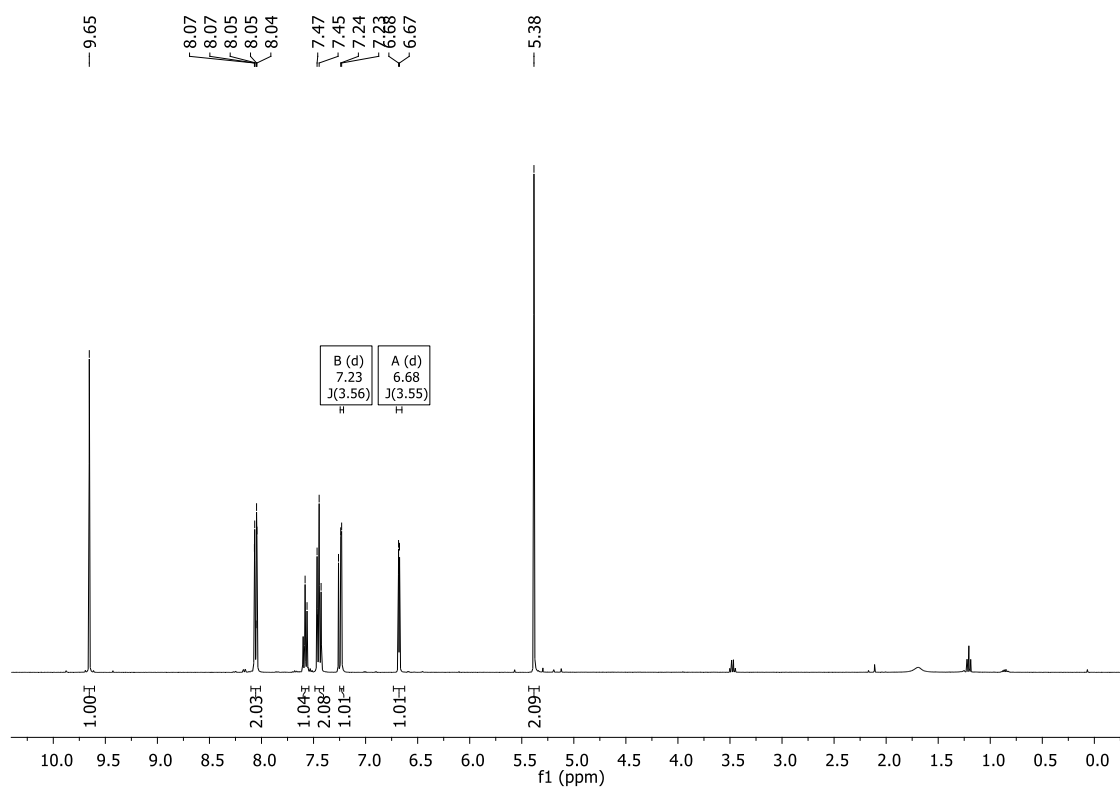
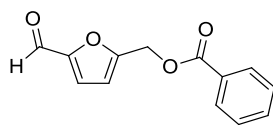
Supporting Information

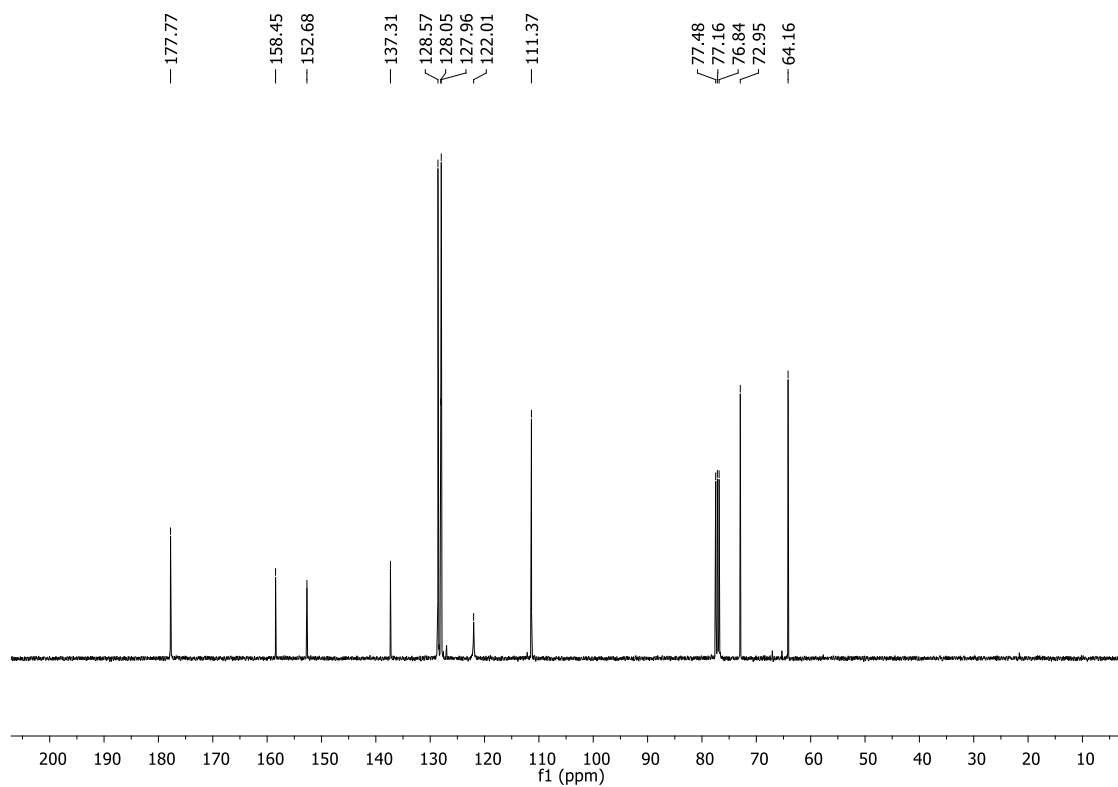
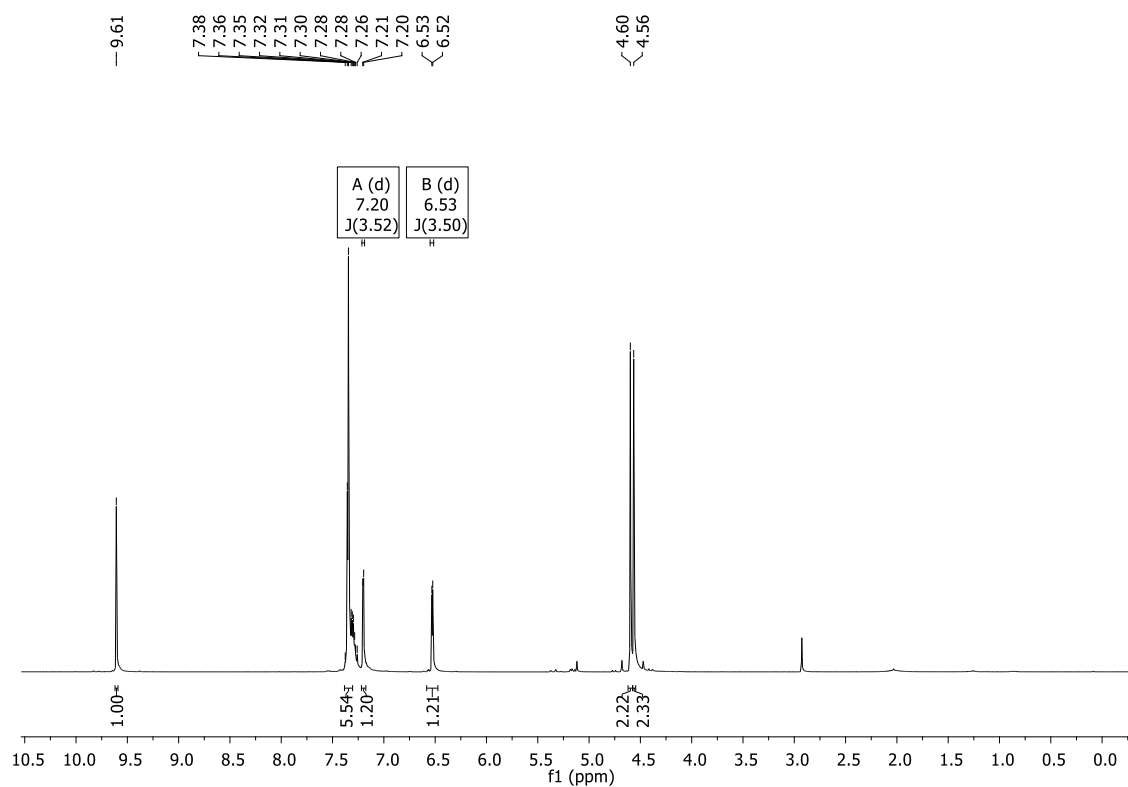
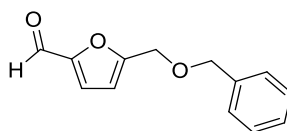
Supporting information for chapter III: Copies of NMR spectra and atomic coordinates for the optimized species

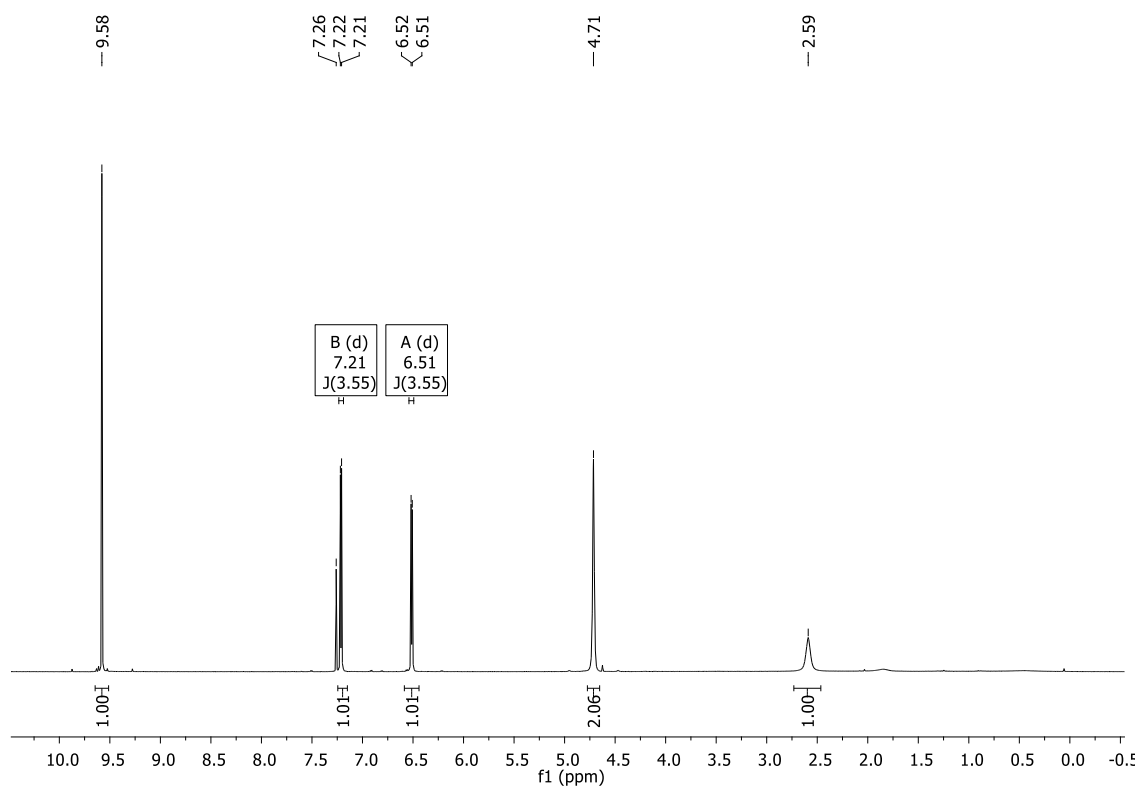
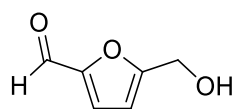
NMR Spectra of furfural derivatives	208
NMR Spectra of bisvinylogous Mannich addition products	215
NMR Spectra of Triarylmethanes	233
Atomic coordinates for all the optimized species	256

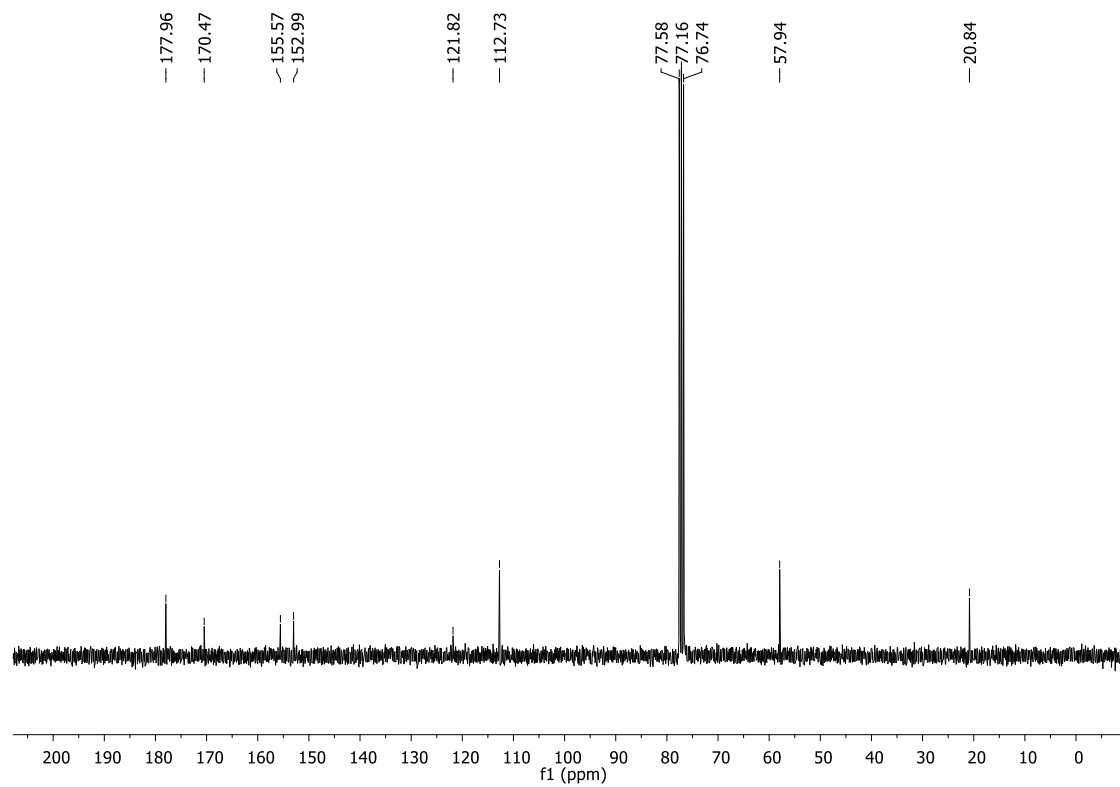
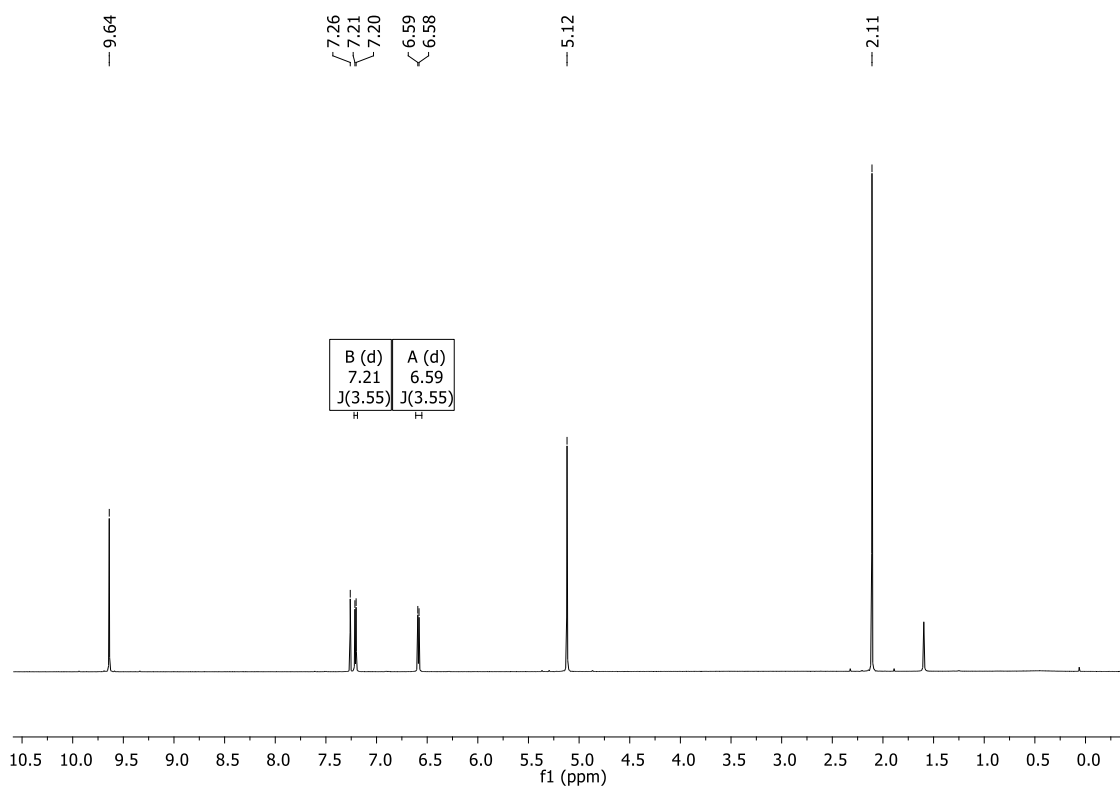
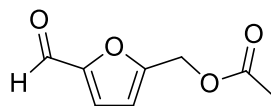
NMR Spectra of furfural derivatives

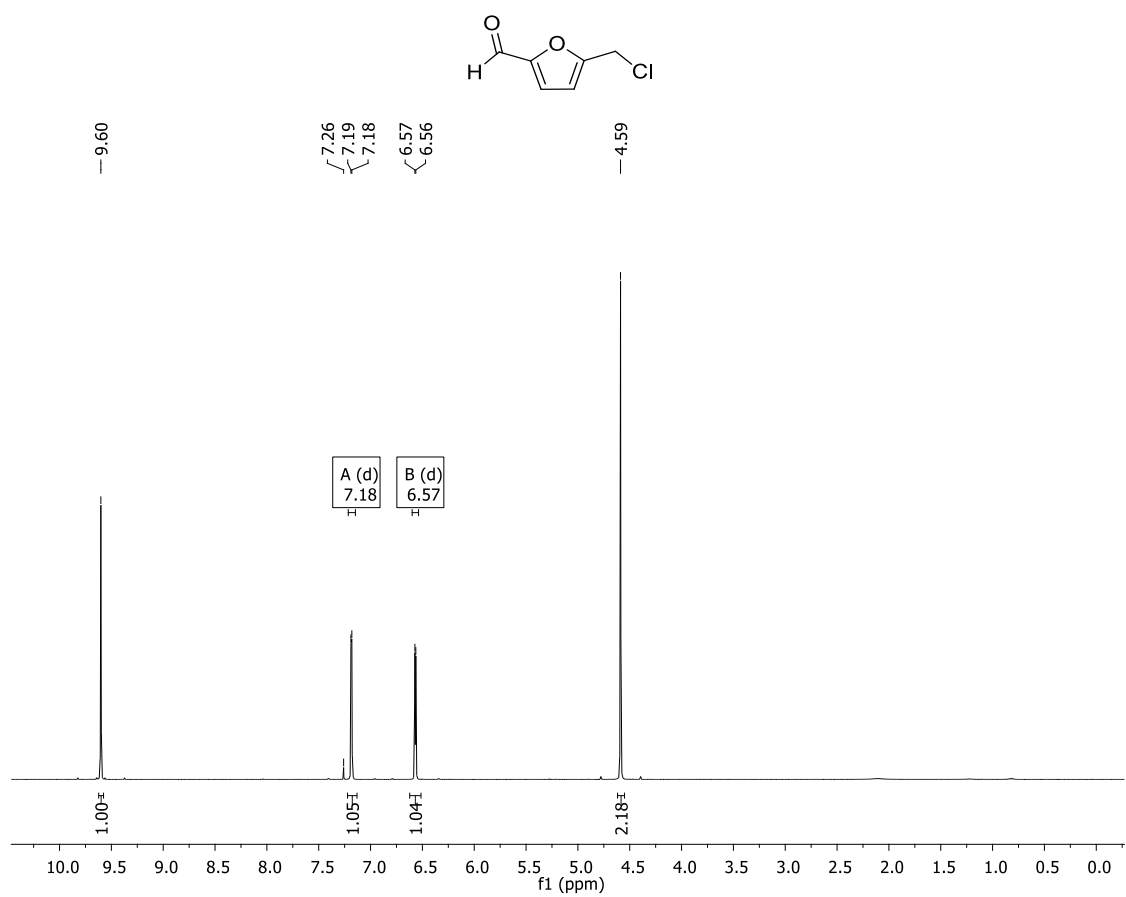




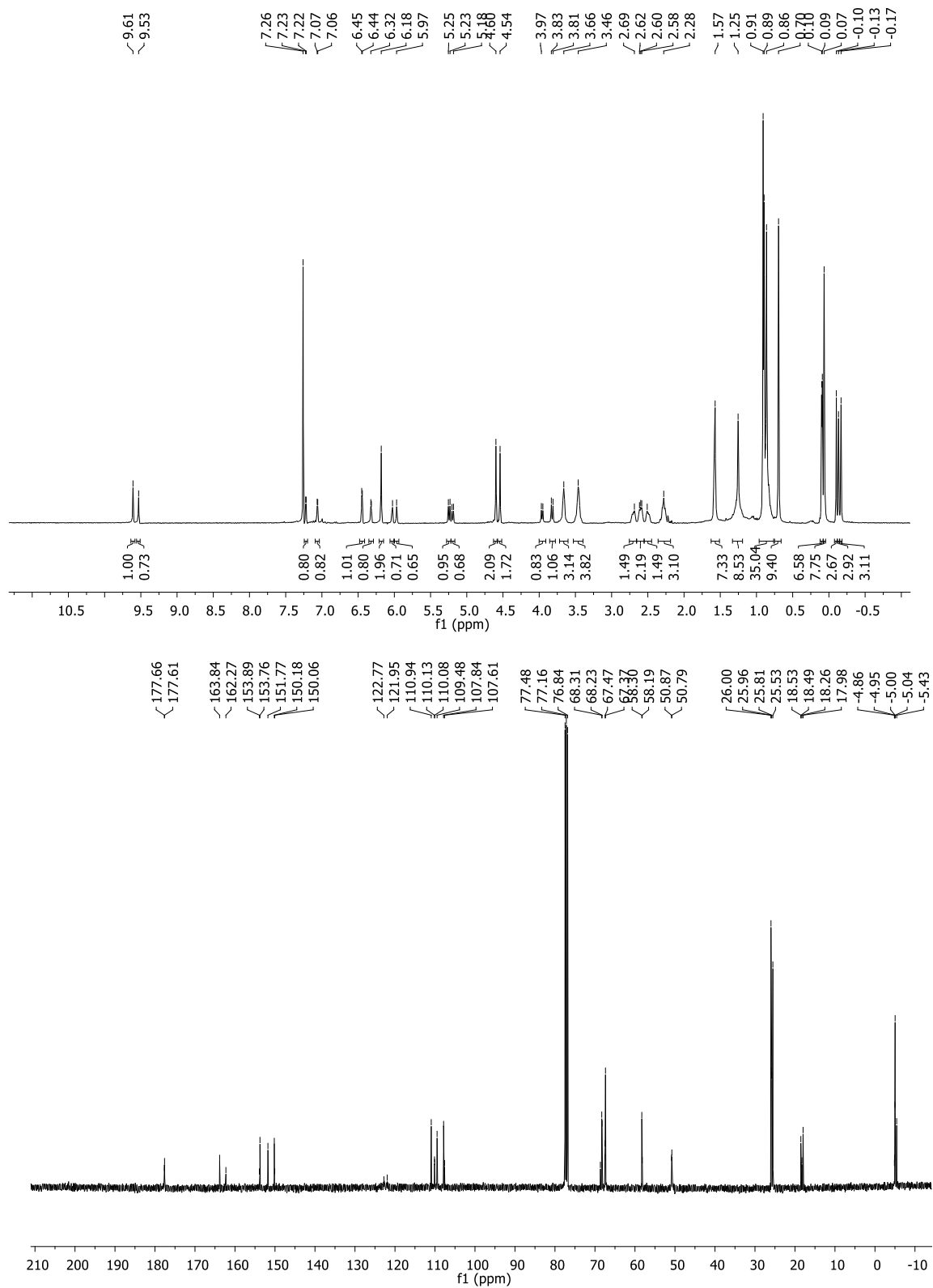
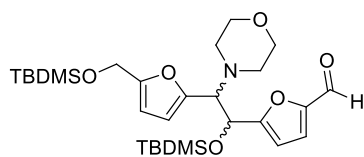


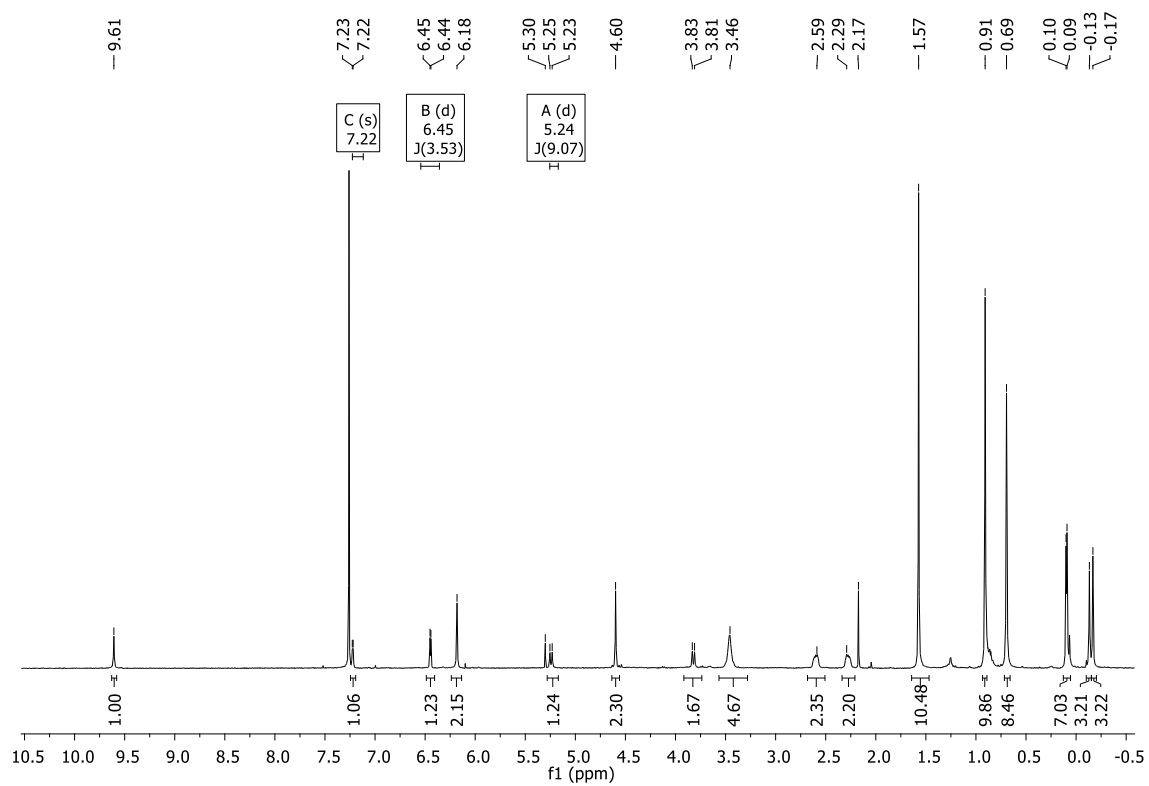


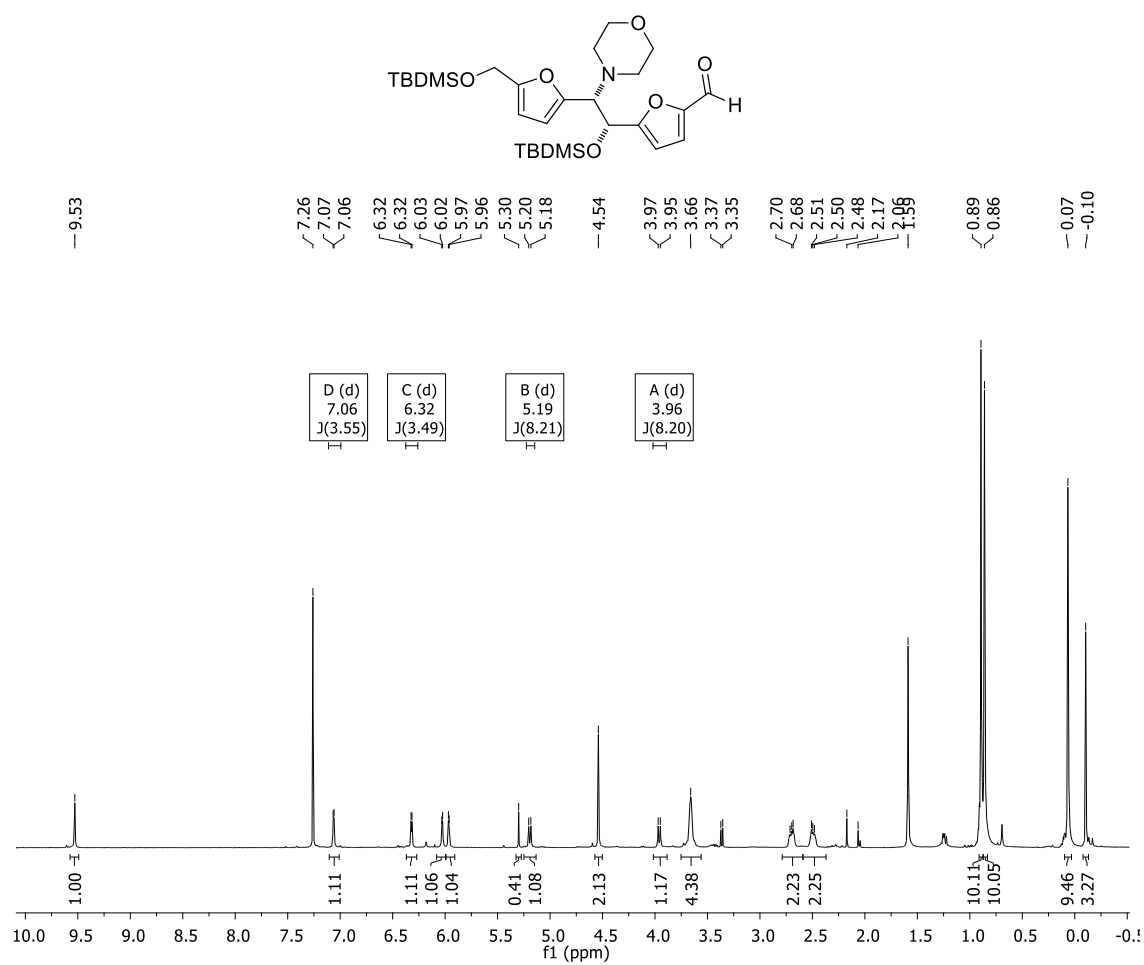


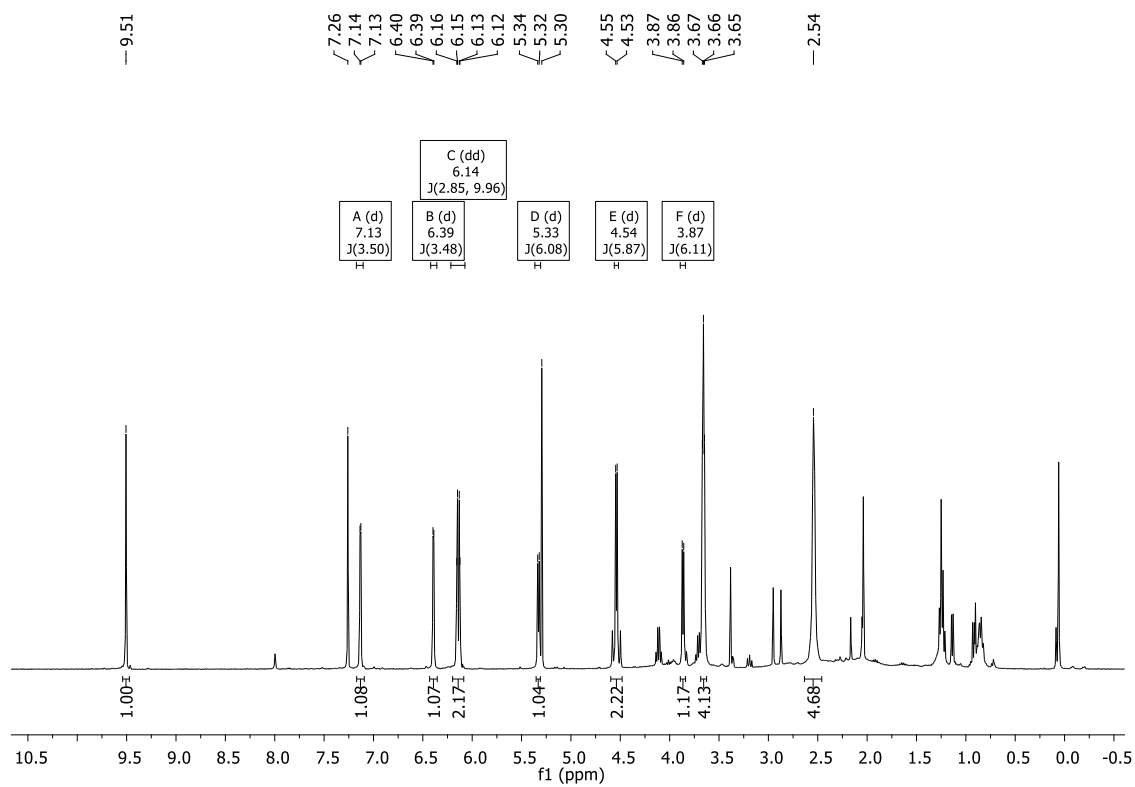
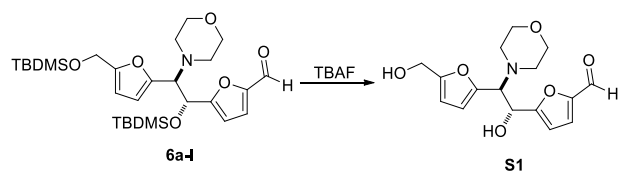


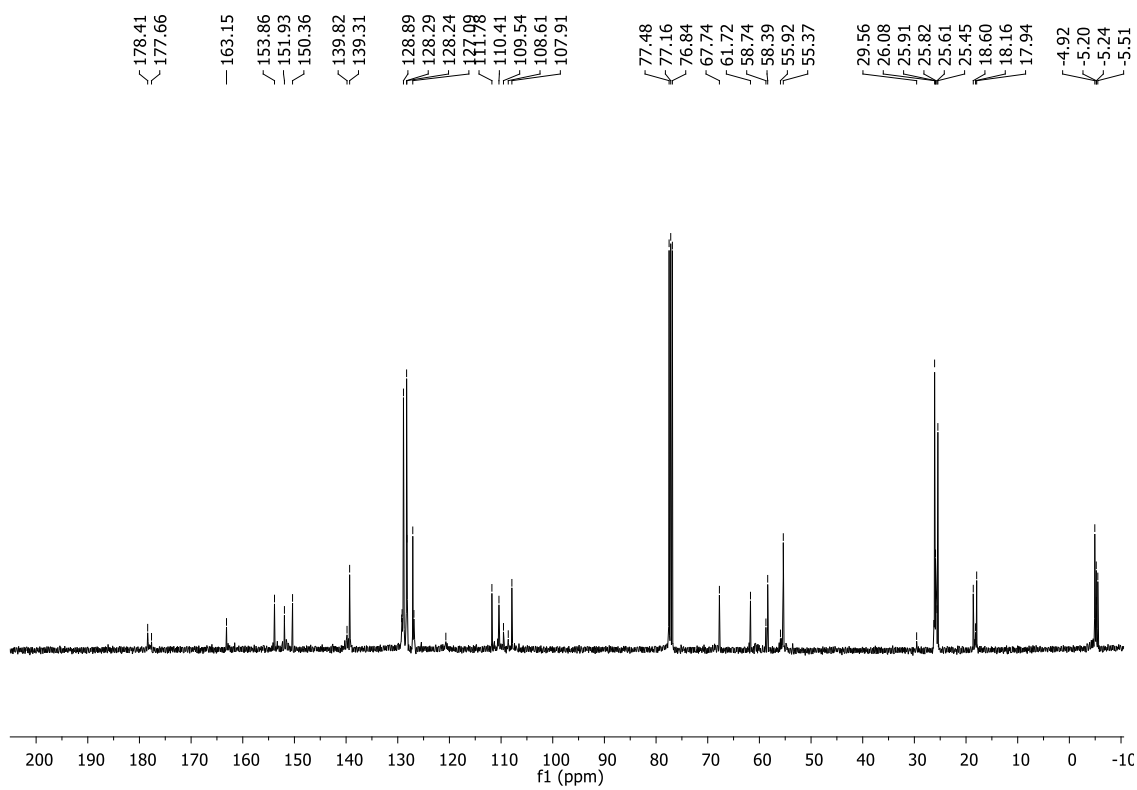
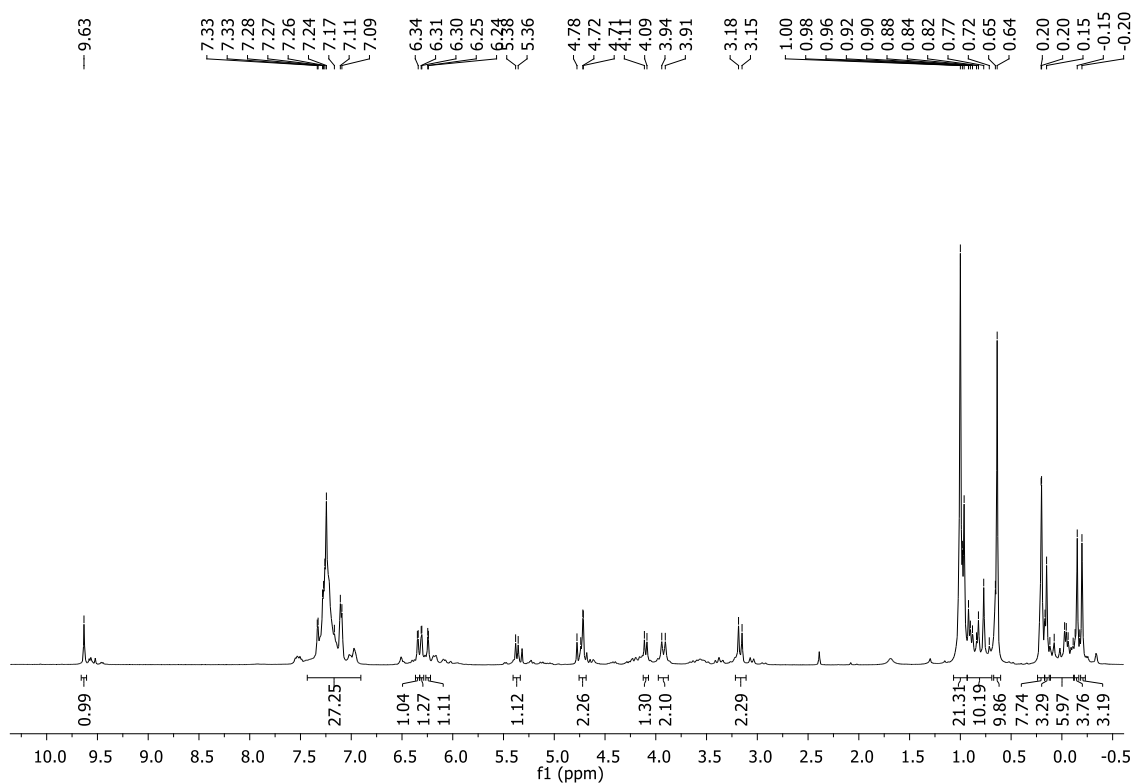
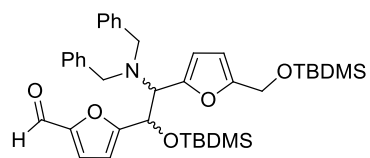
NMR Spectra of bisvinyllogous Mannich addition products

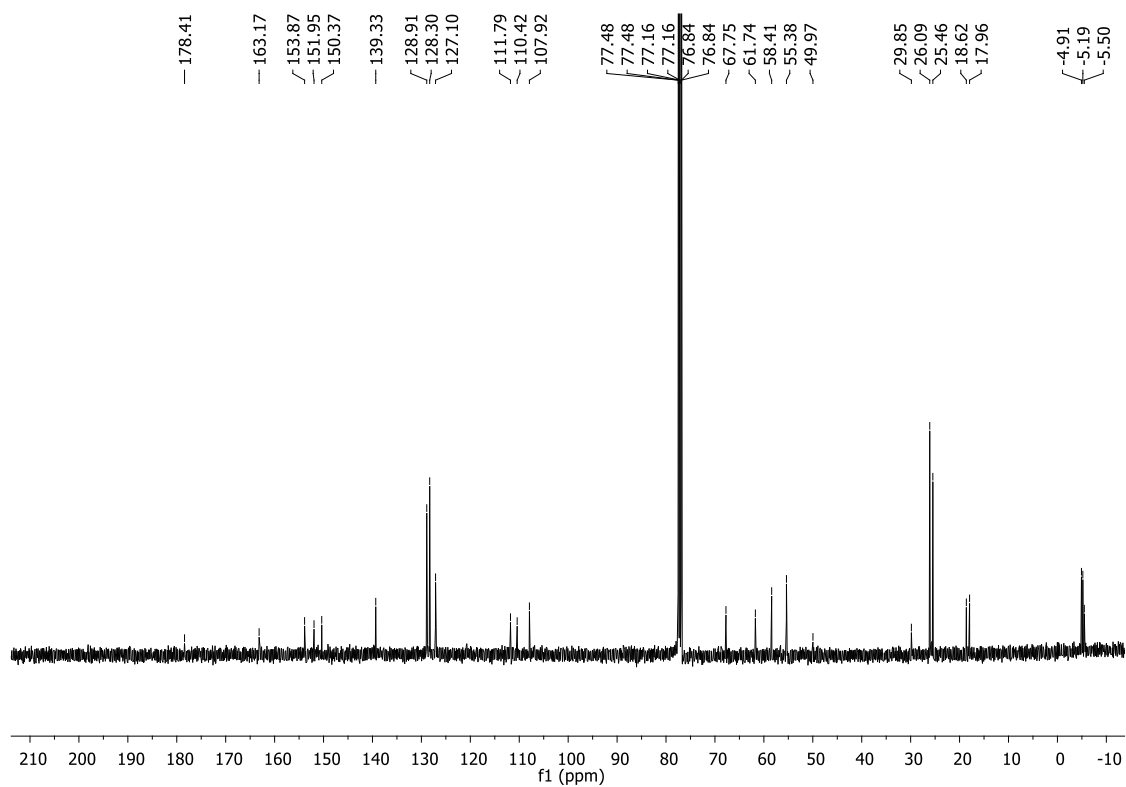
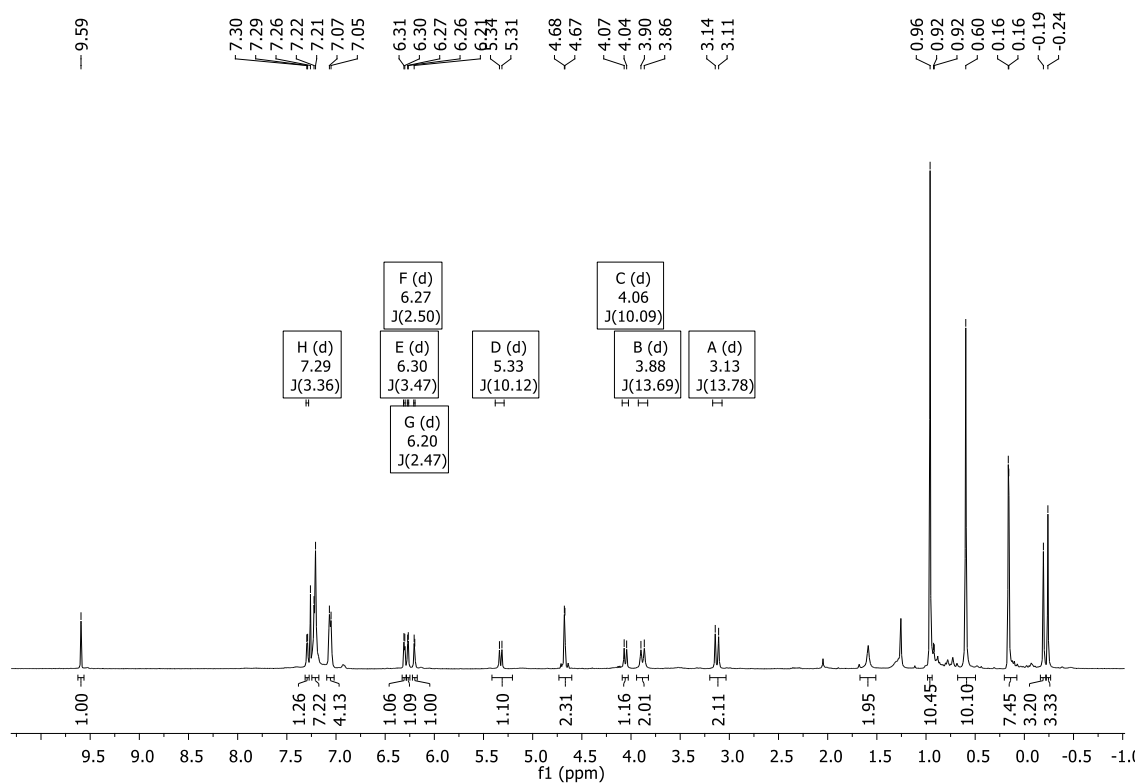
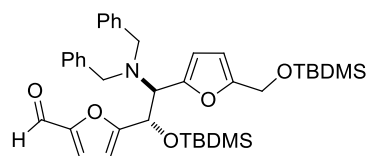


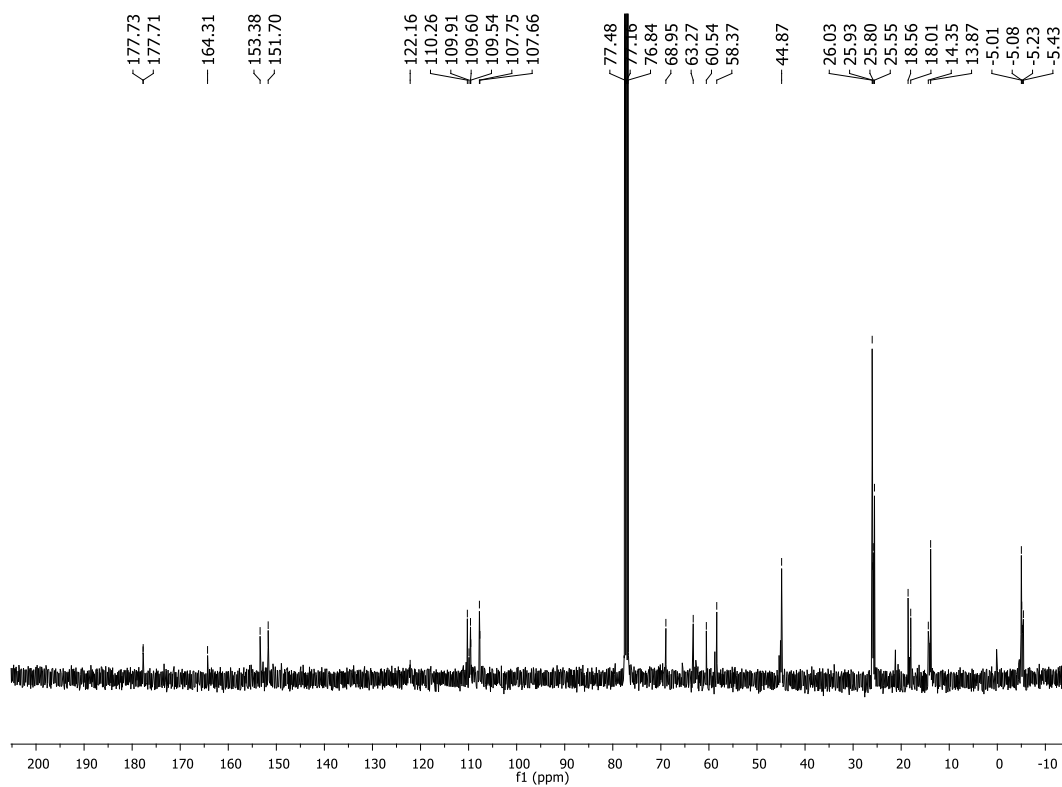
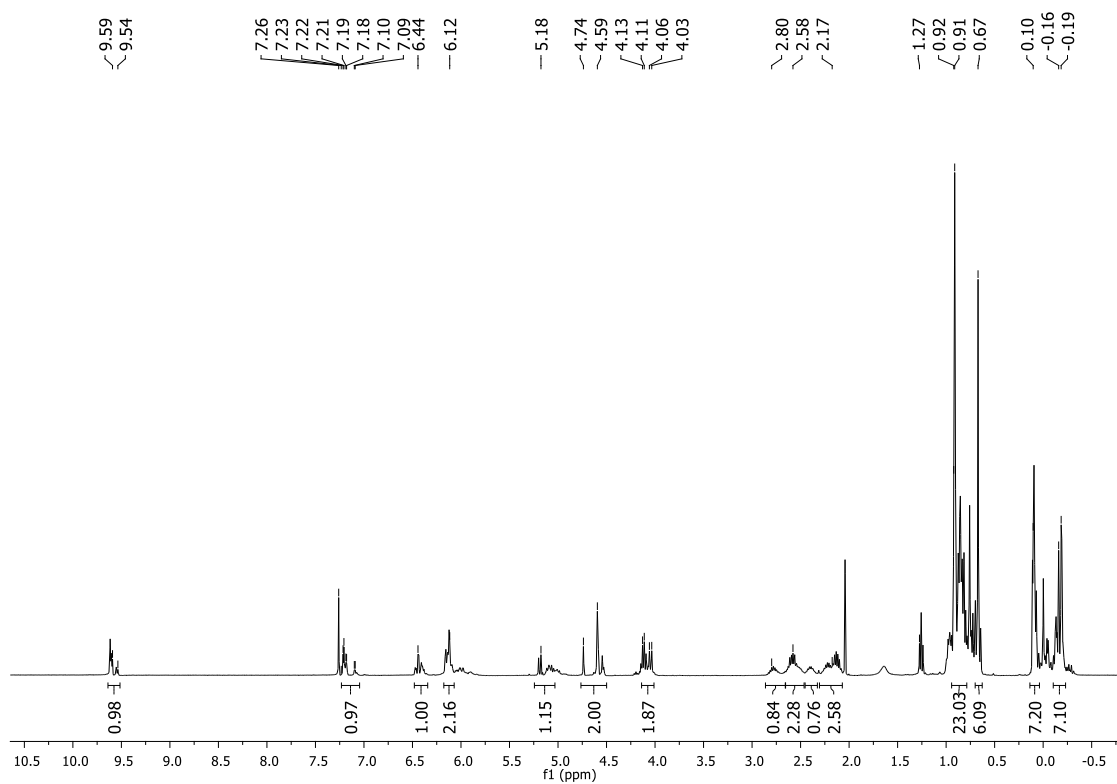
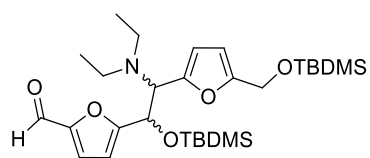


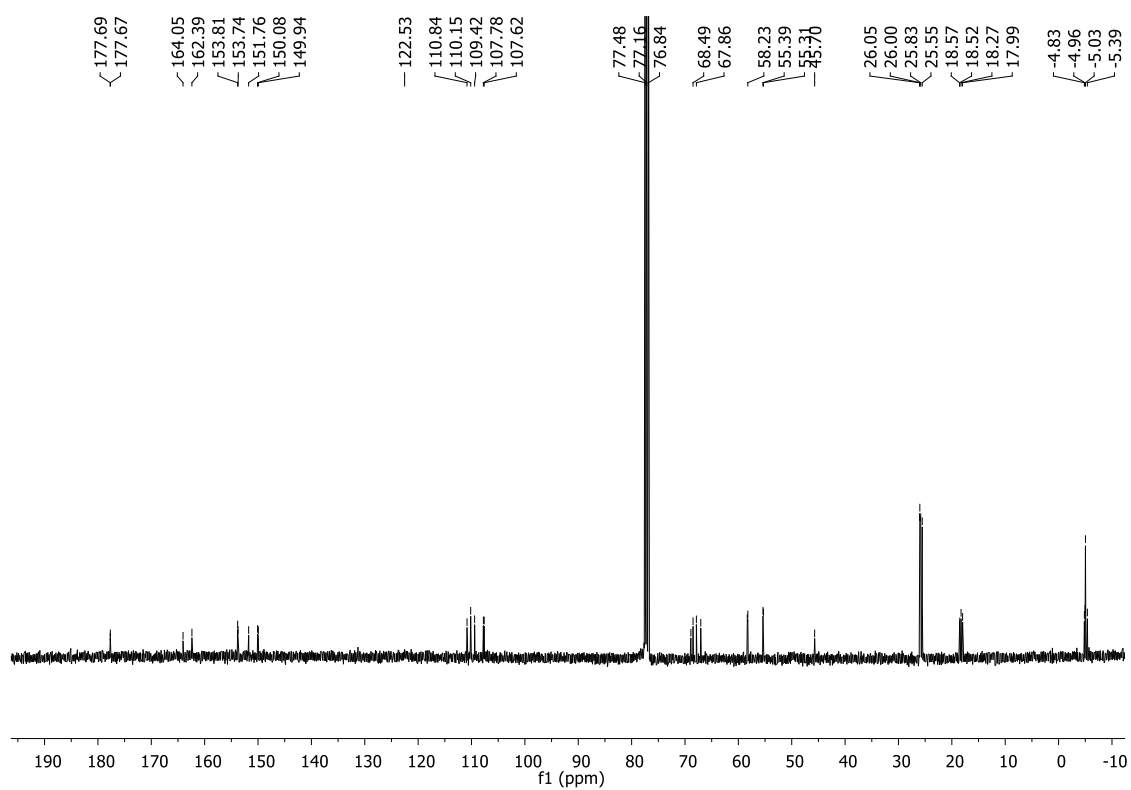
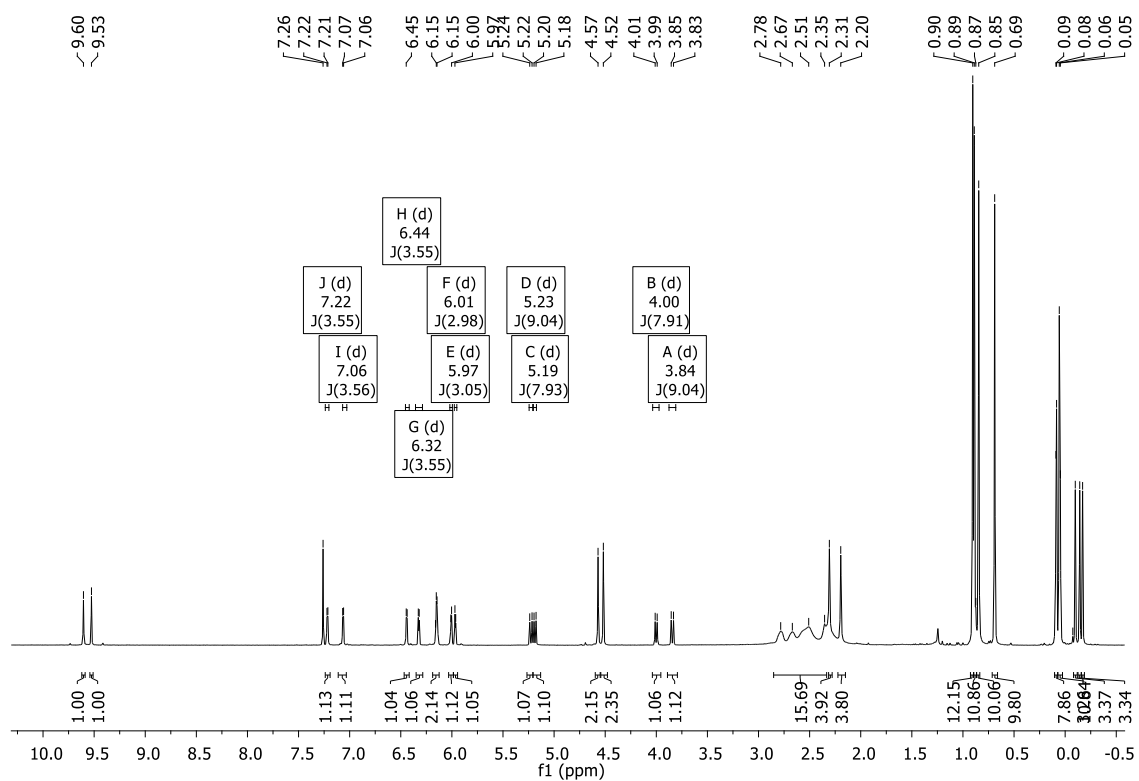
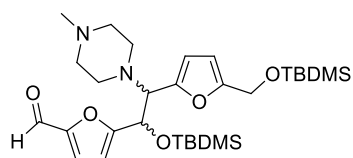


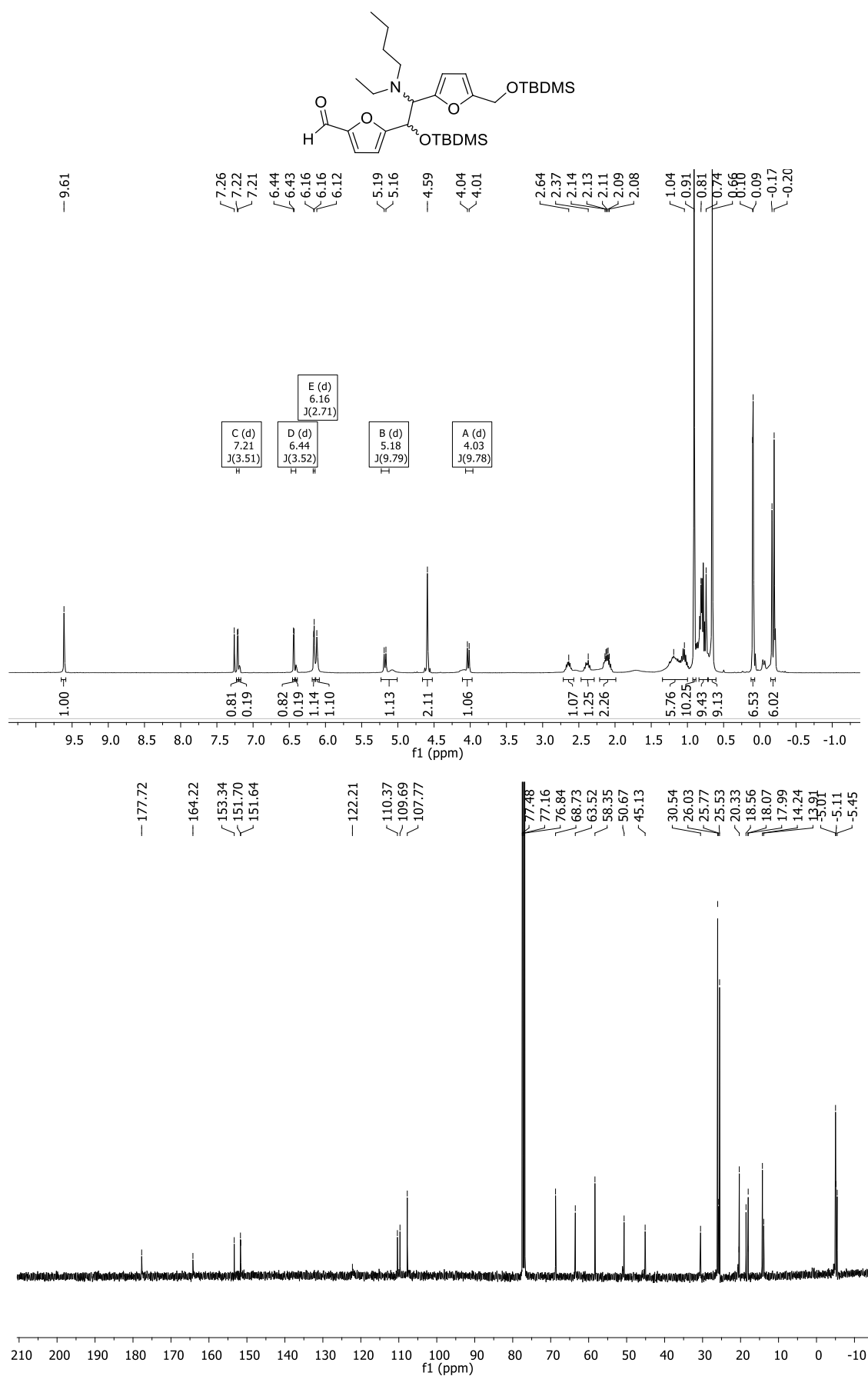


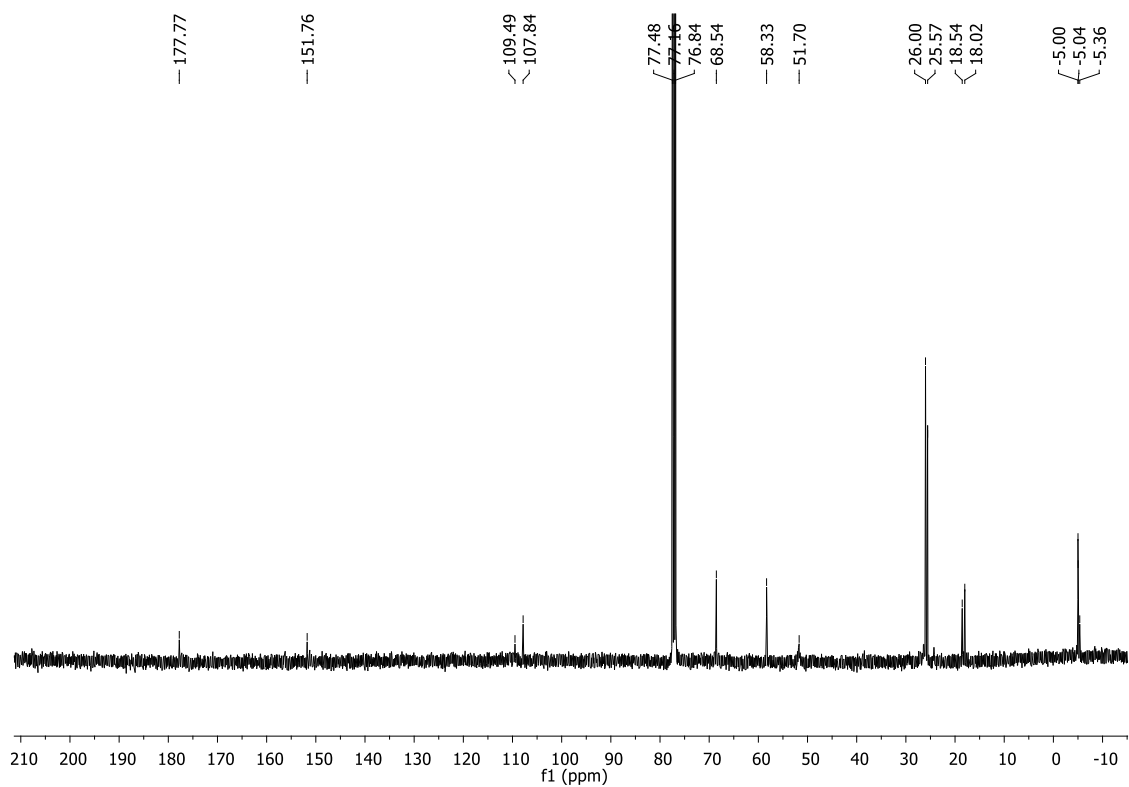
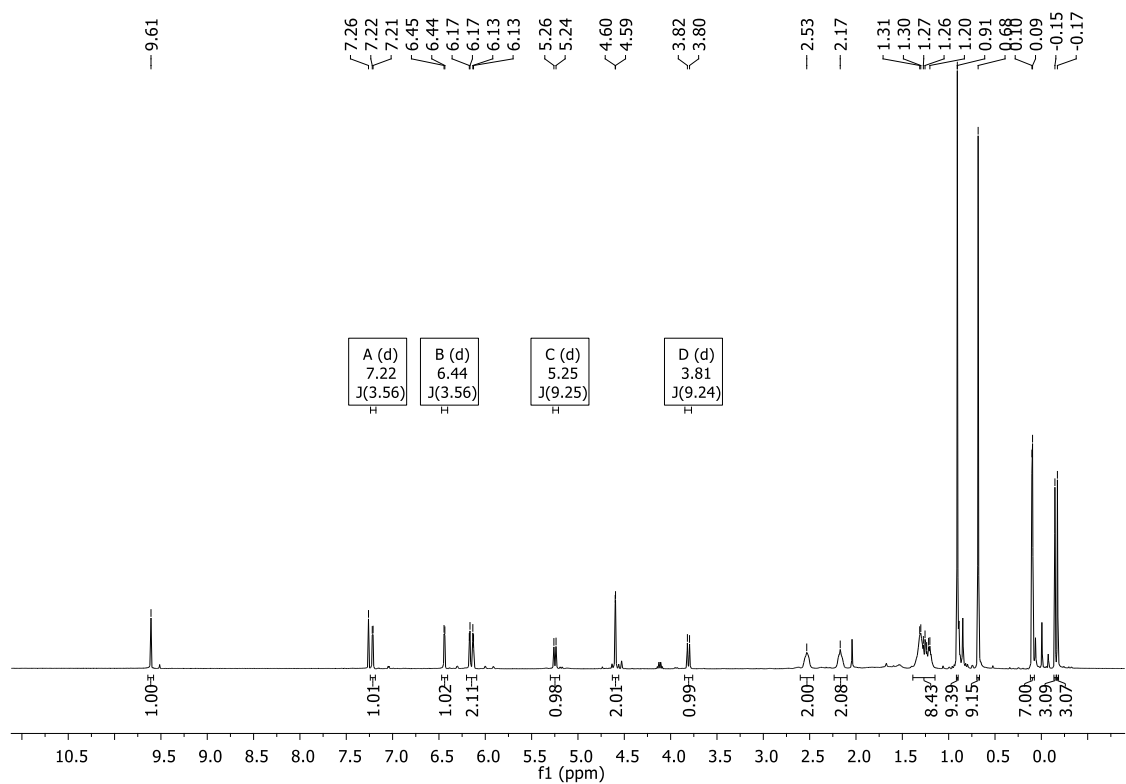
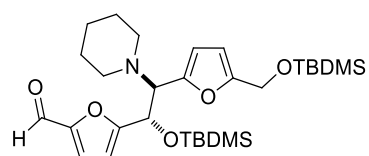


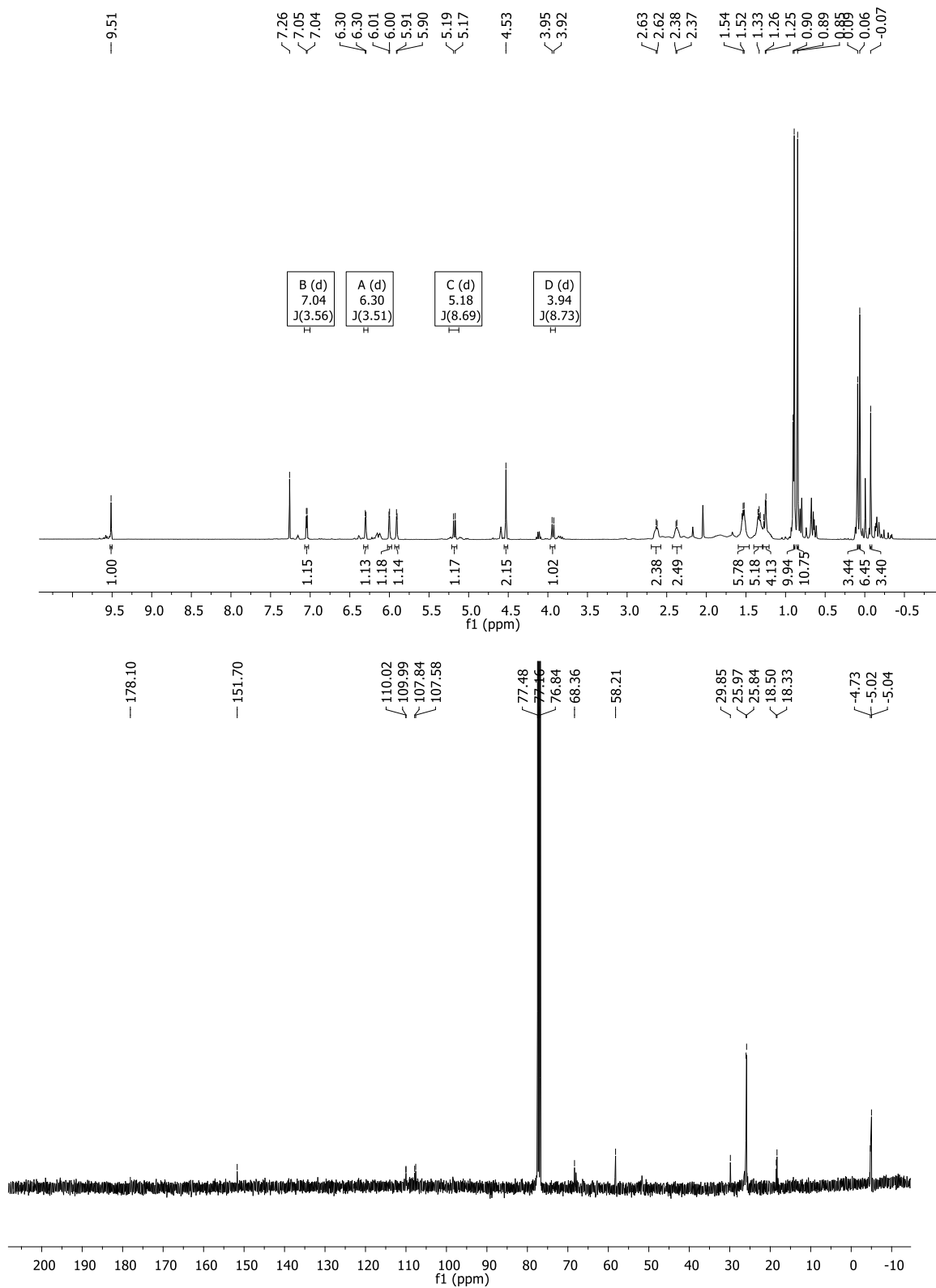
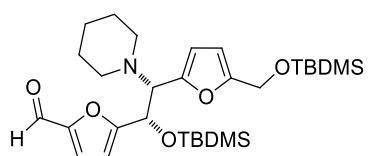


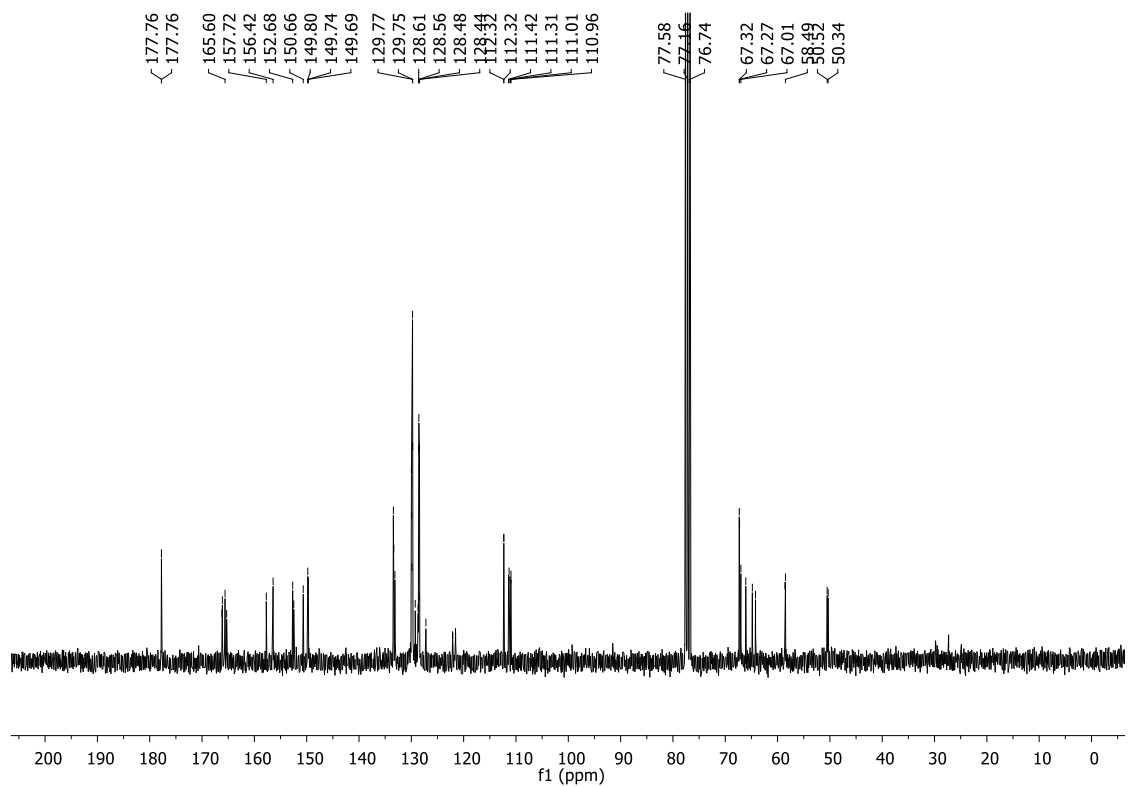
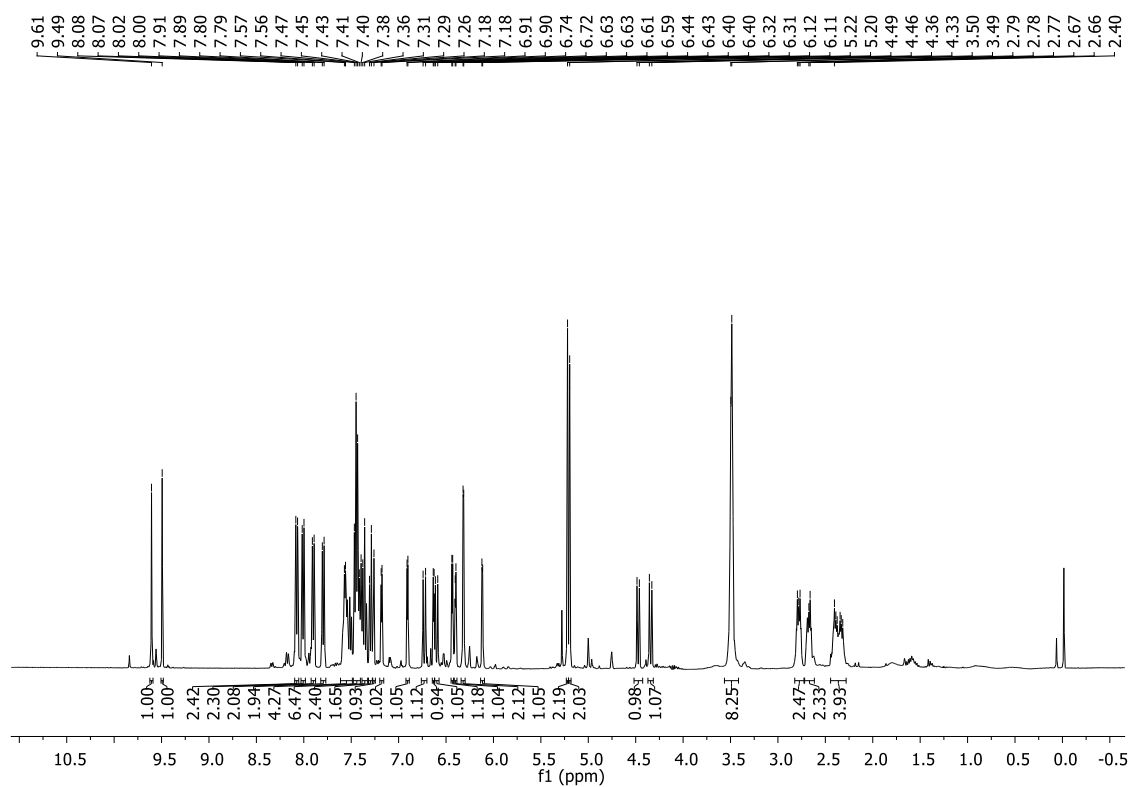
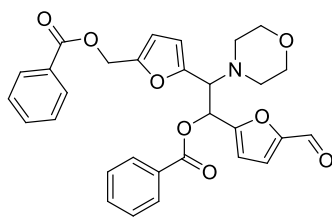


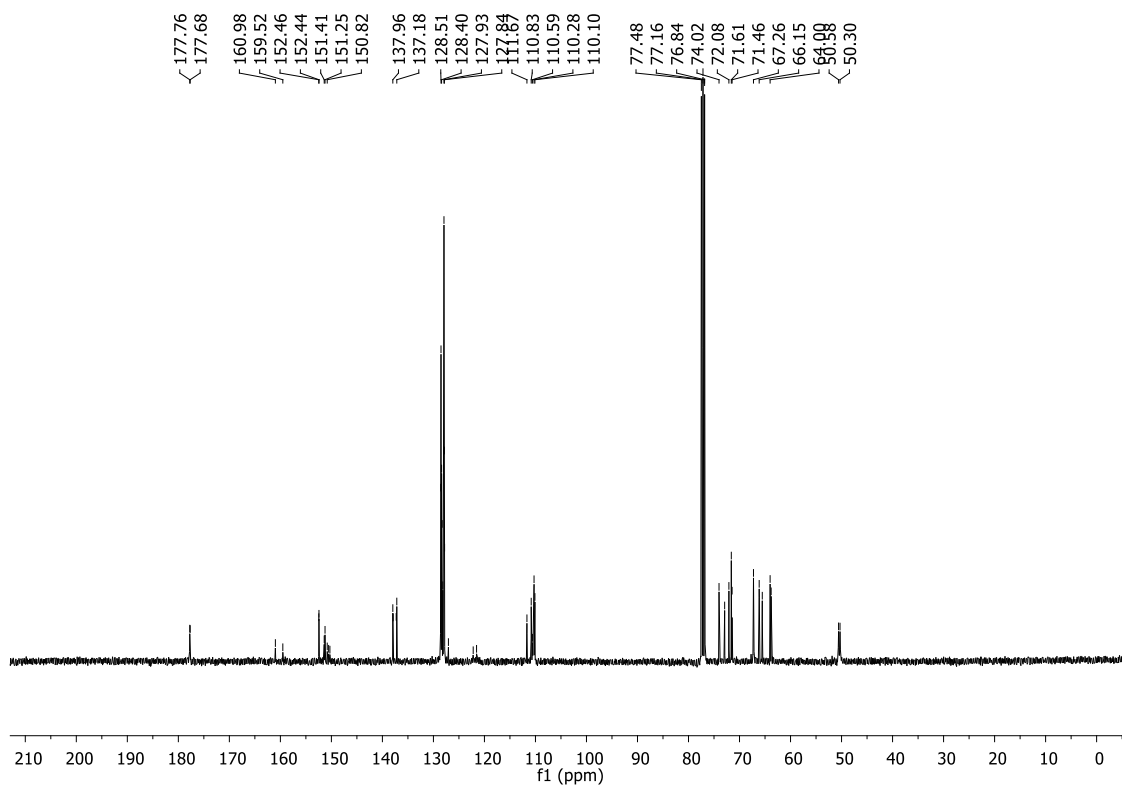
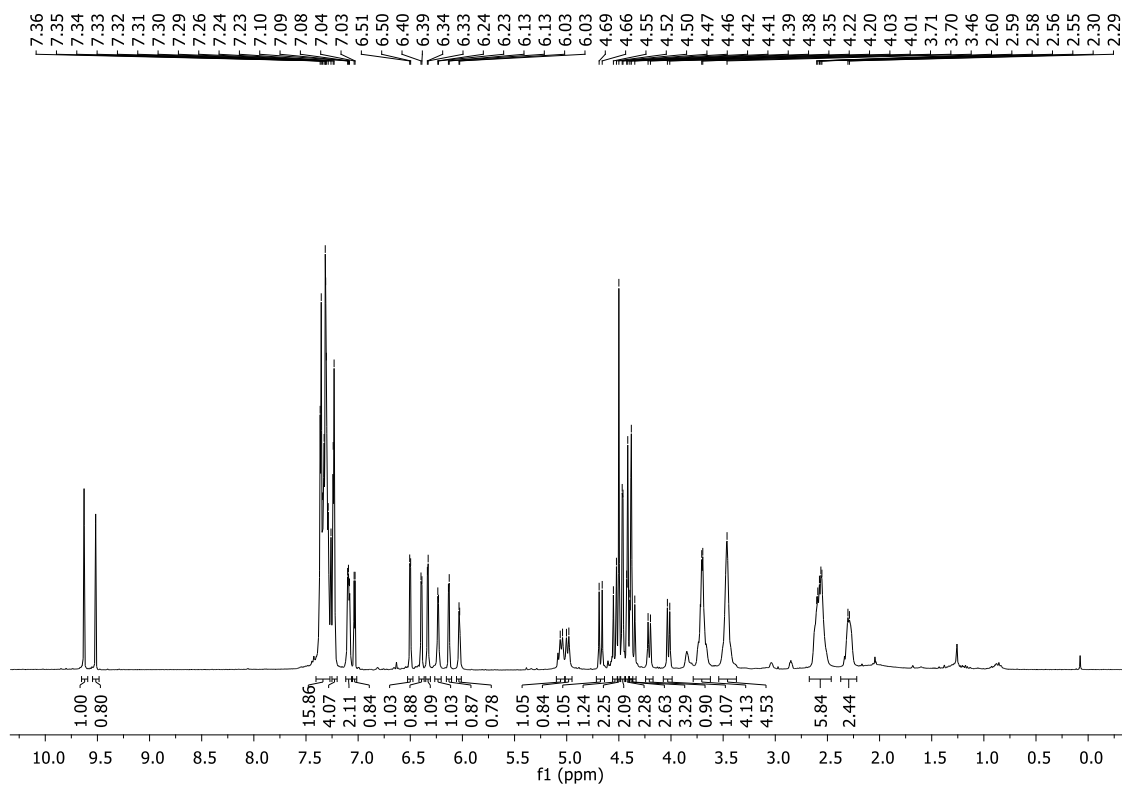
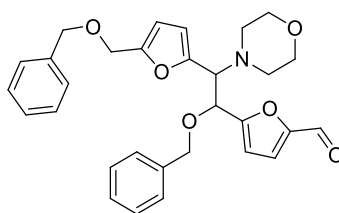


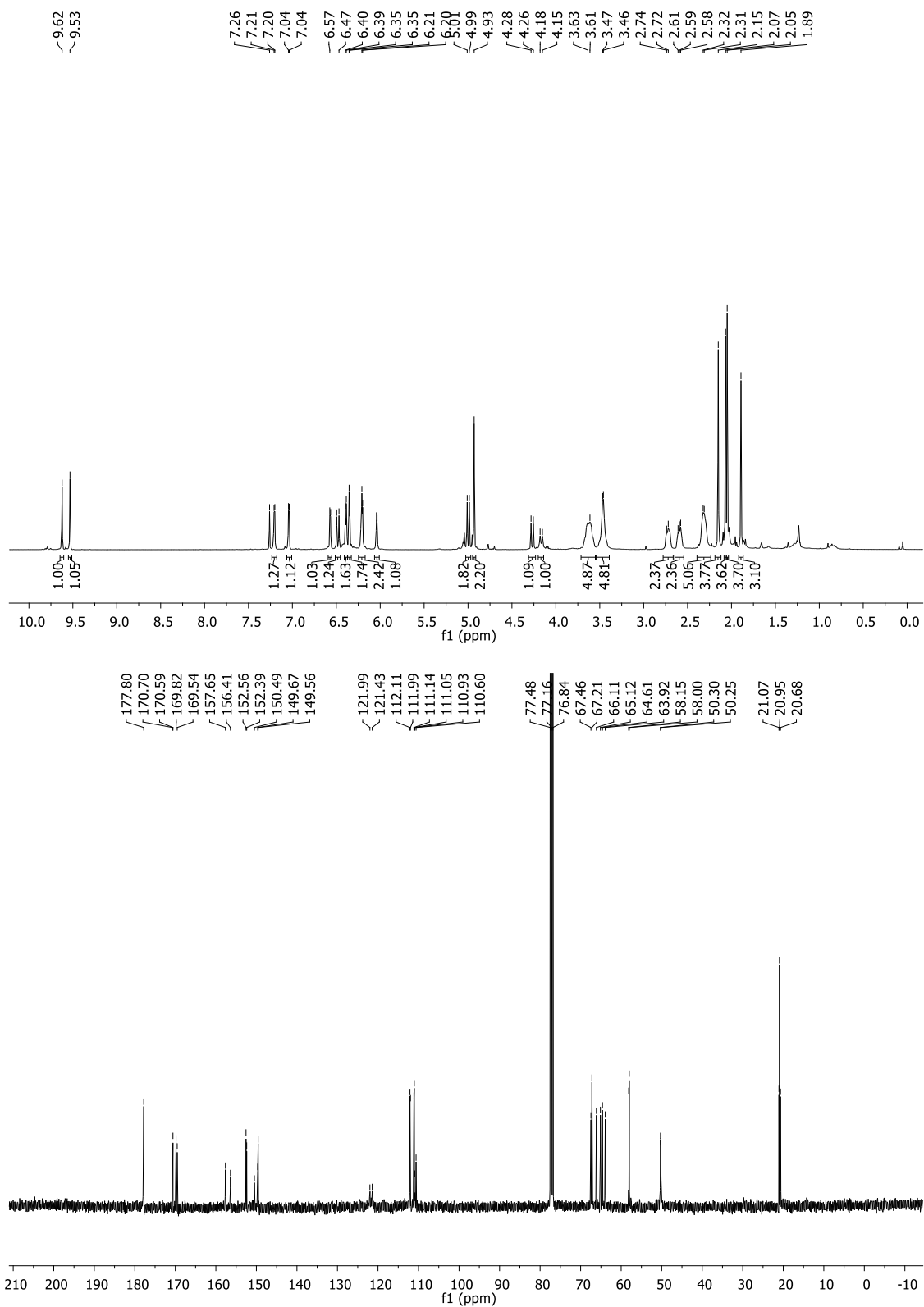
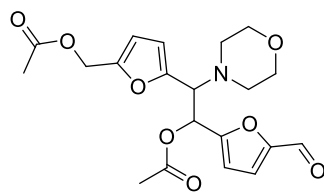


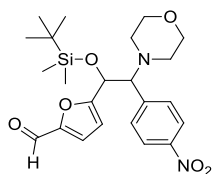




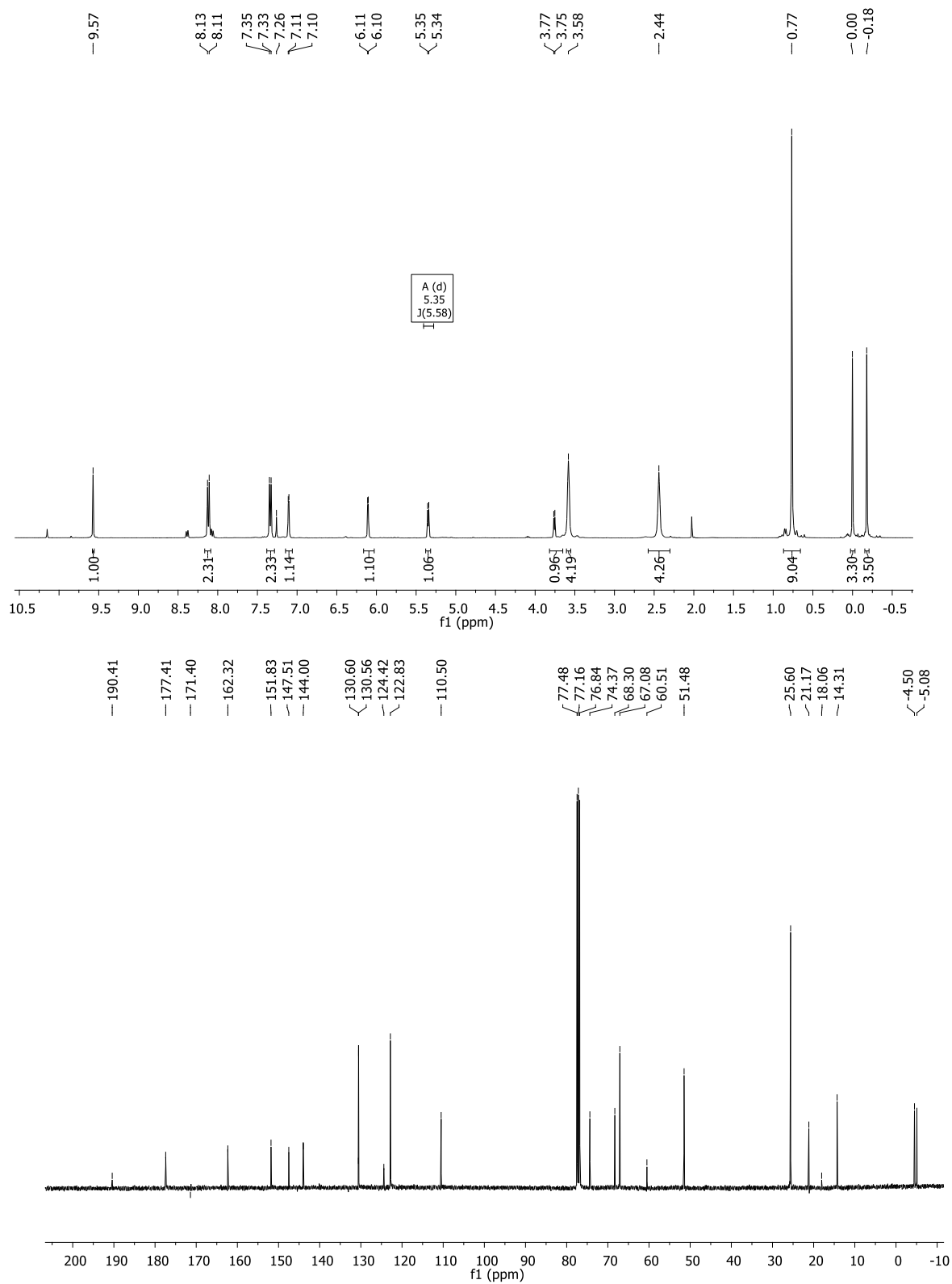




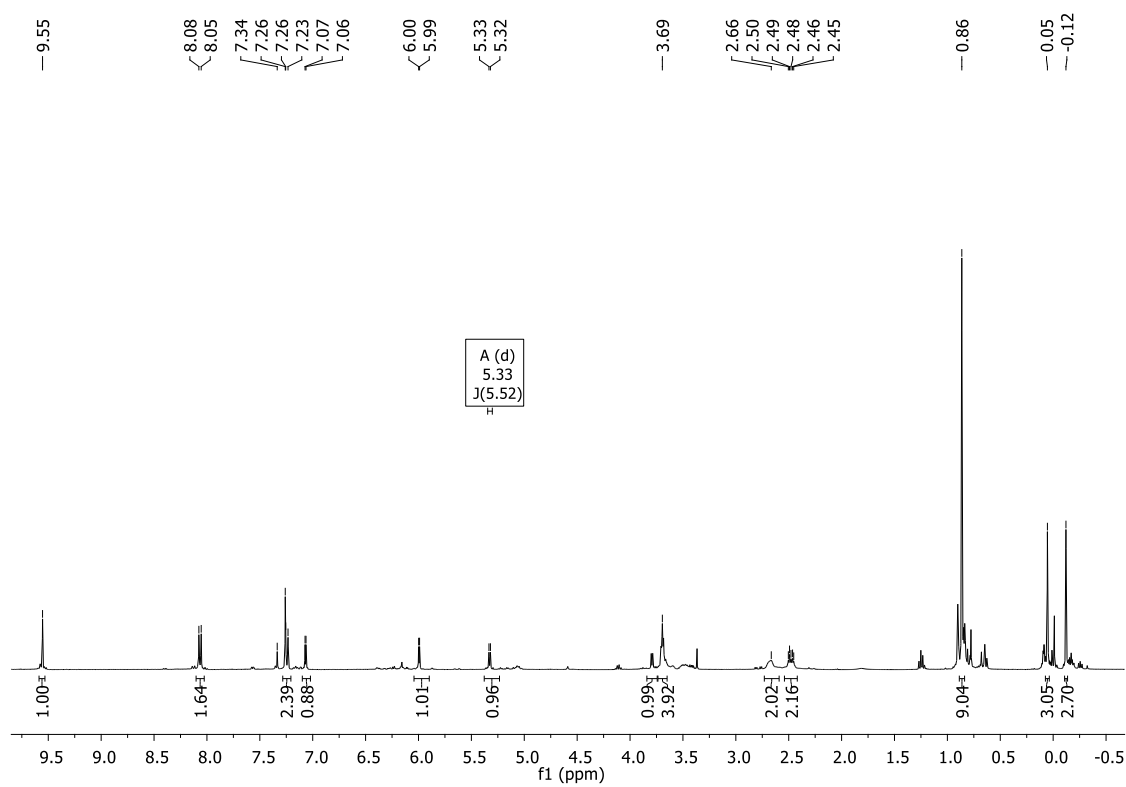


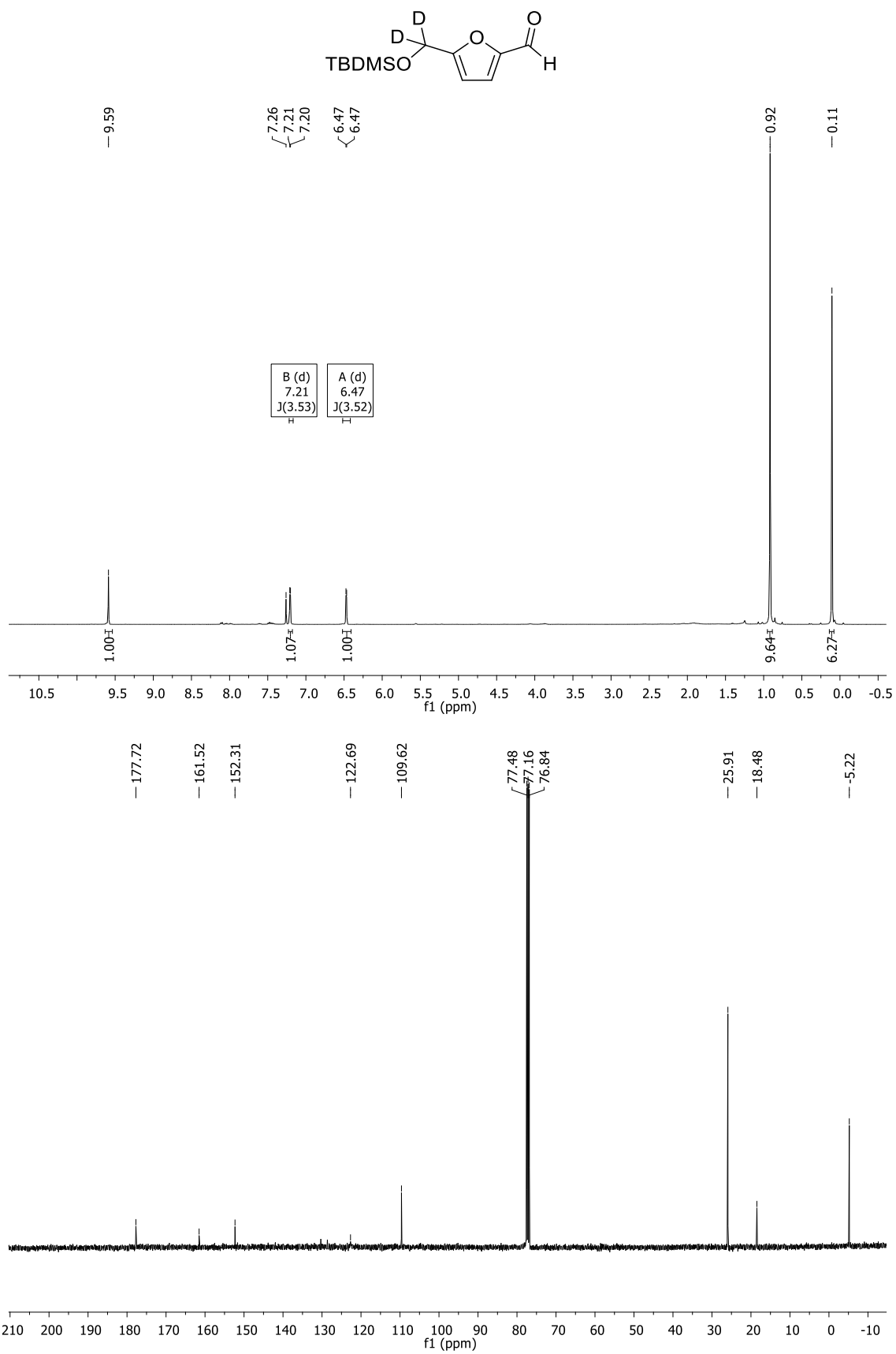


Isomer I

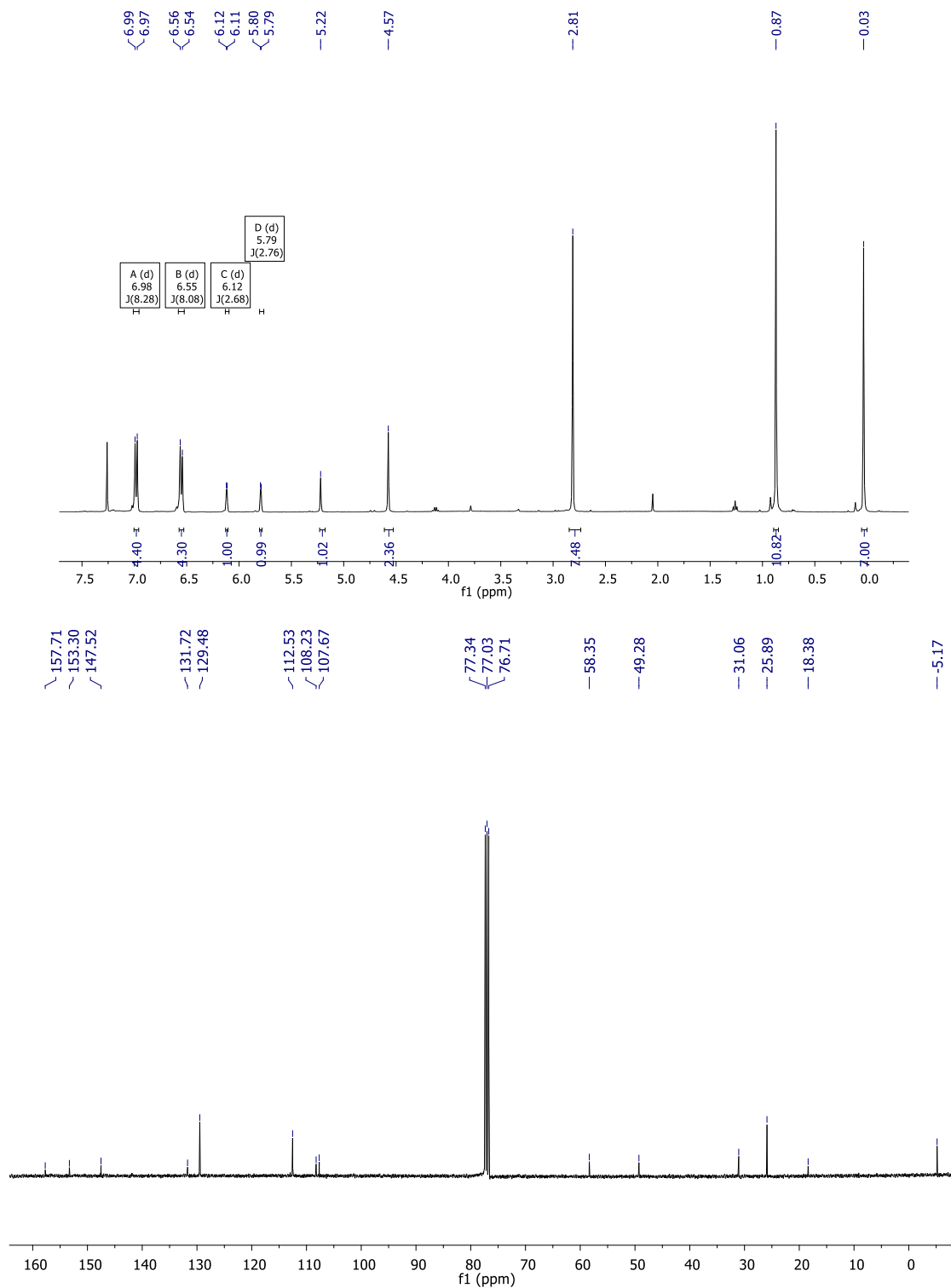
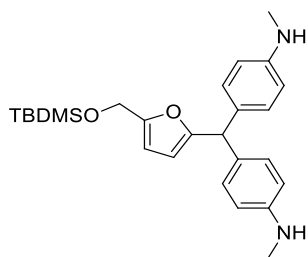


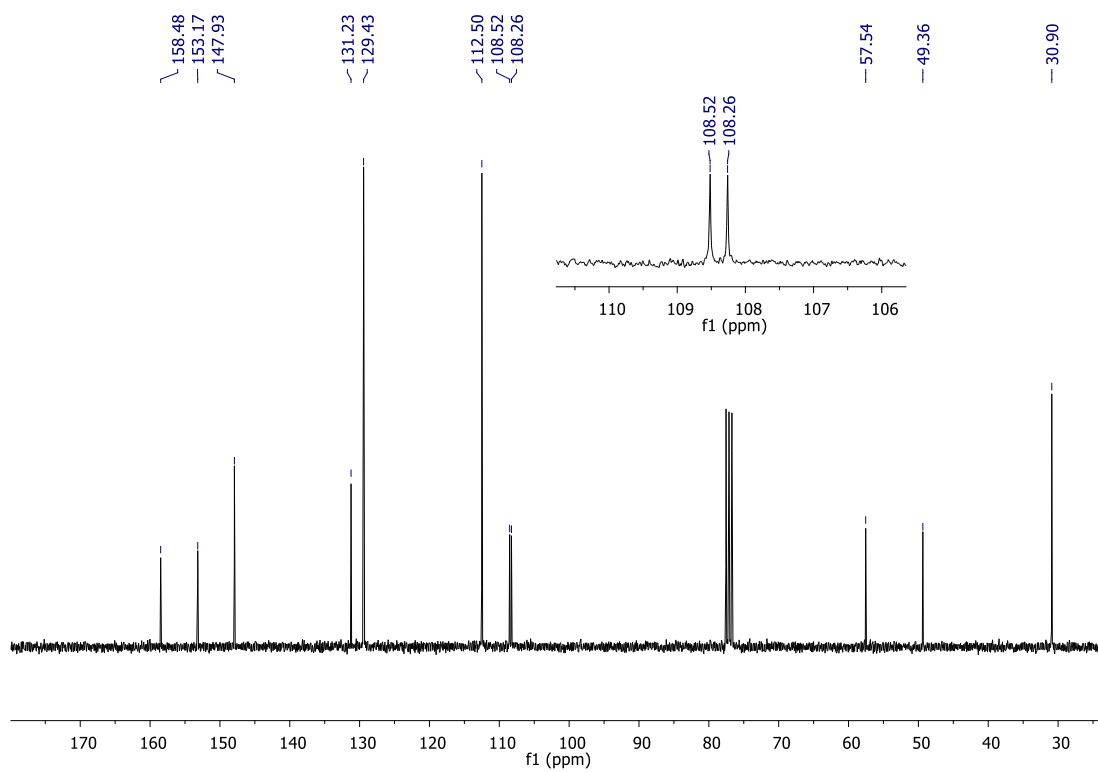
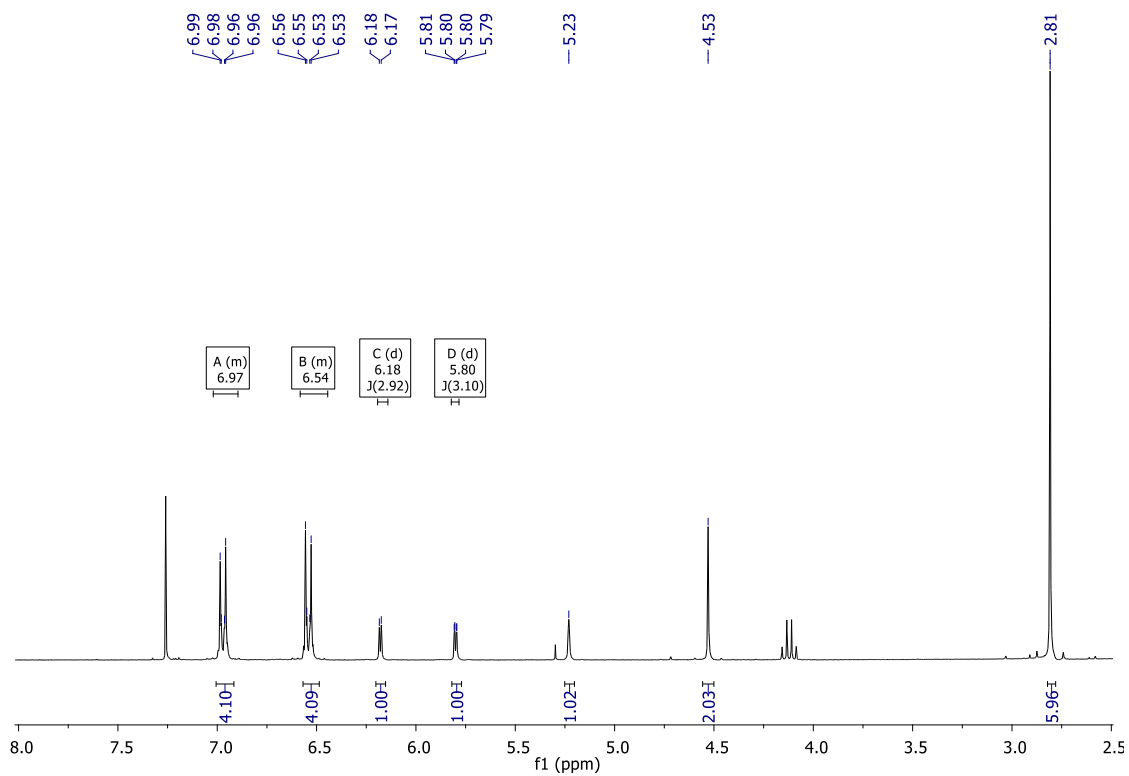
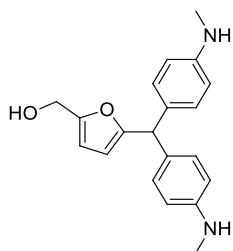
Isomer II

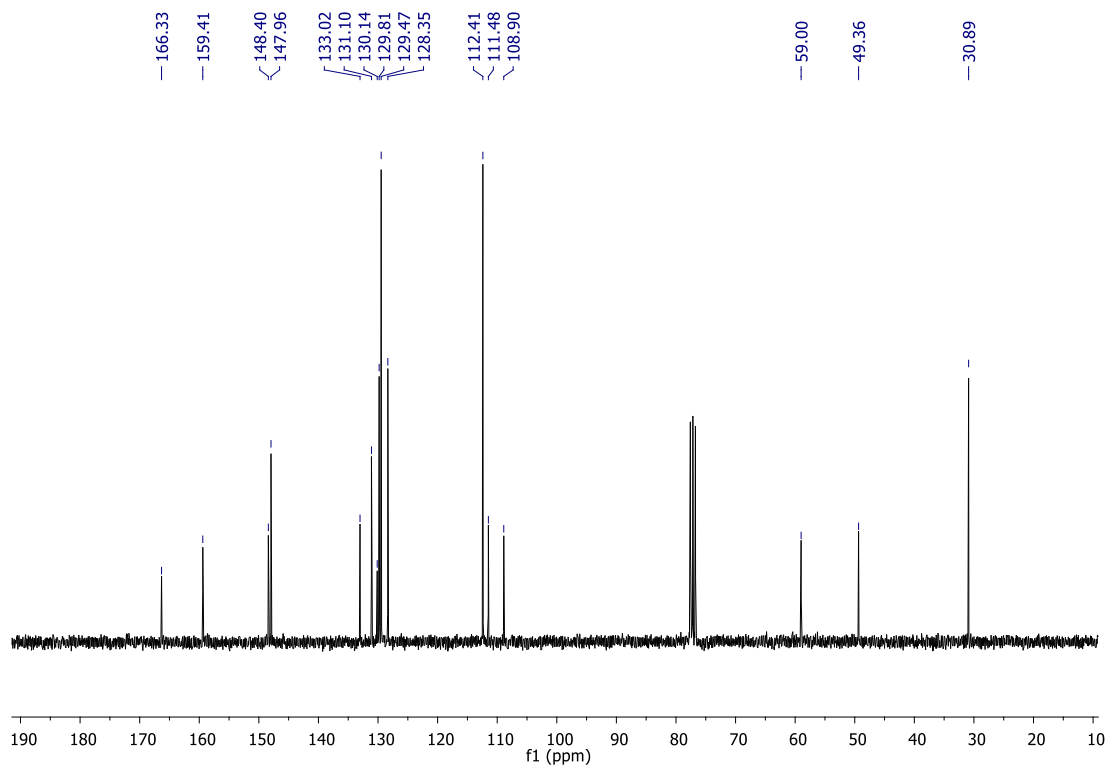
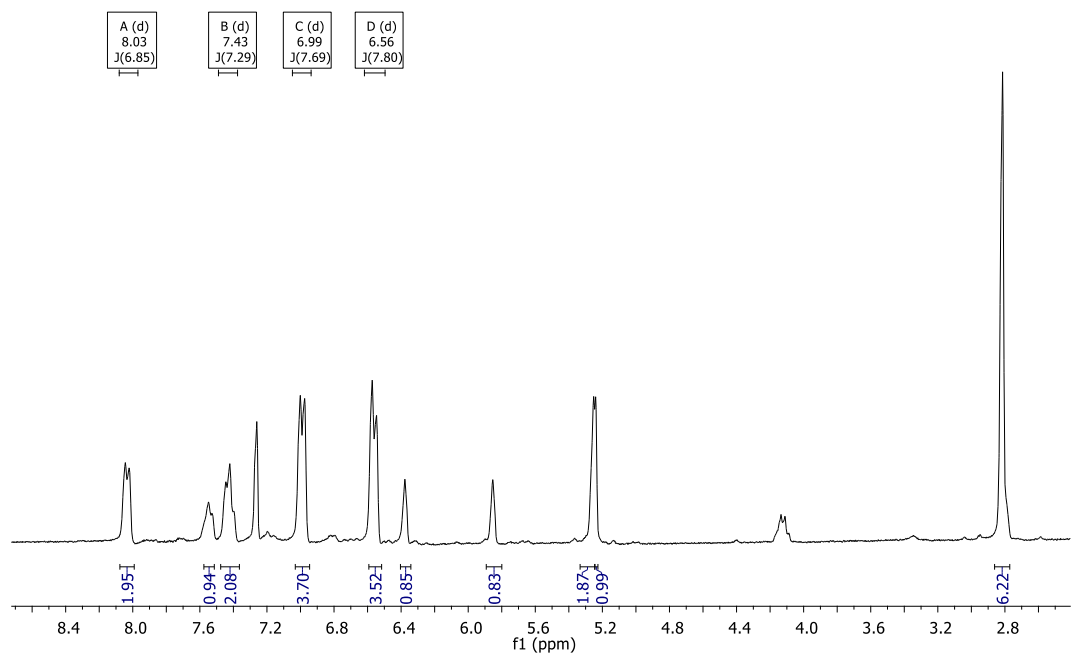
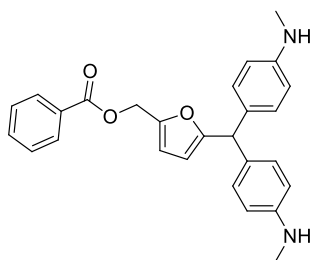


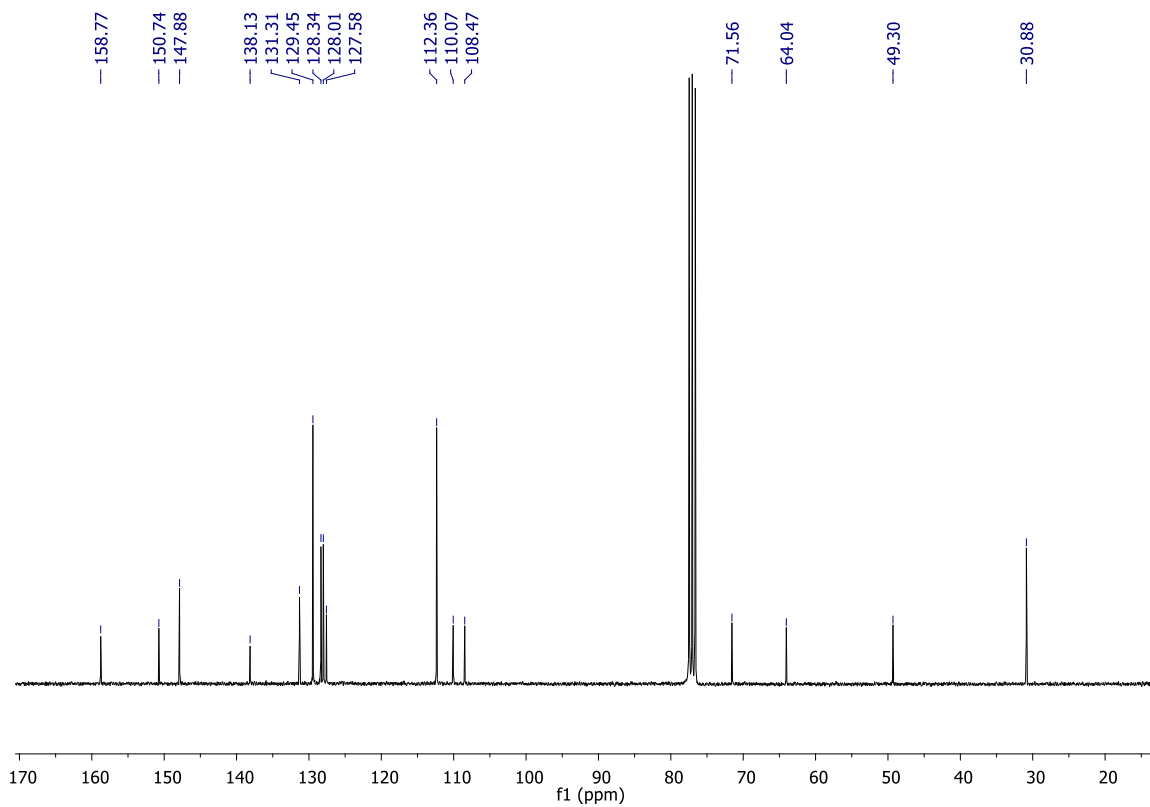
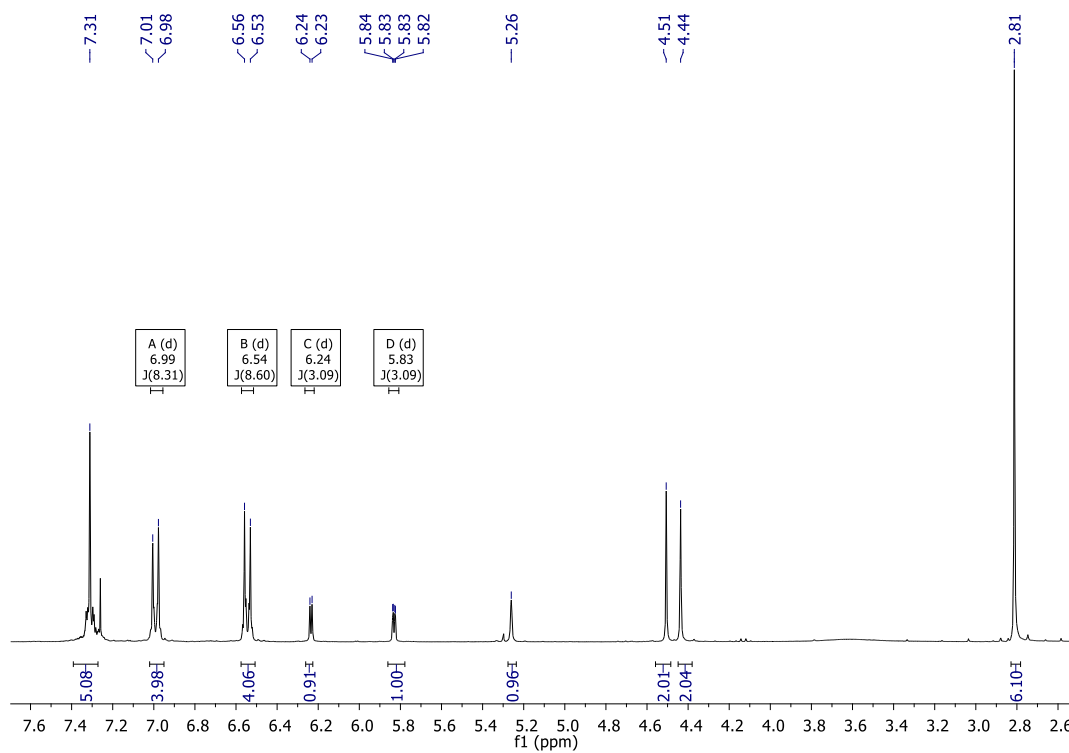
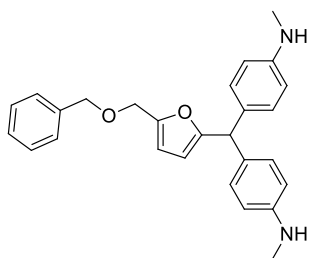


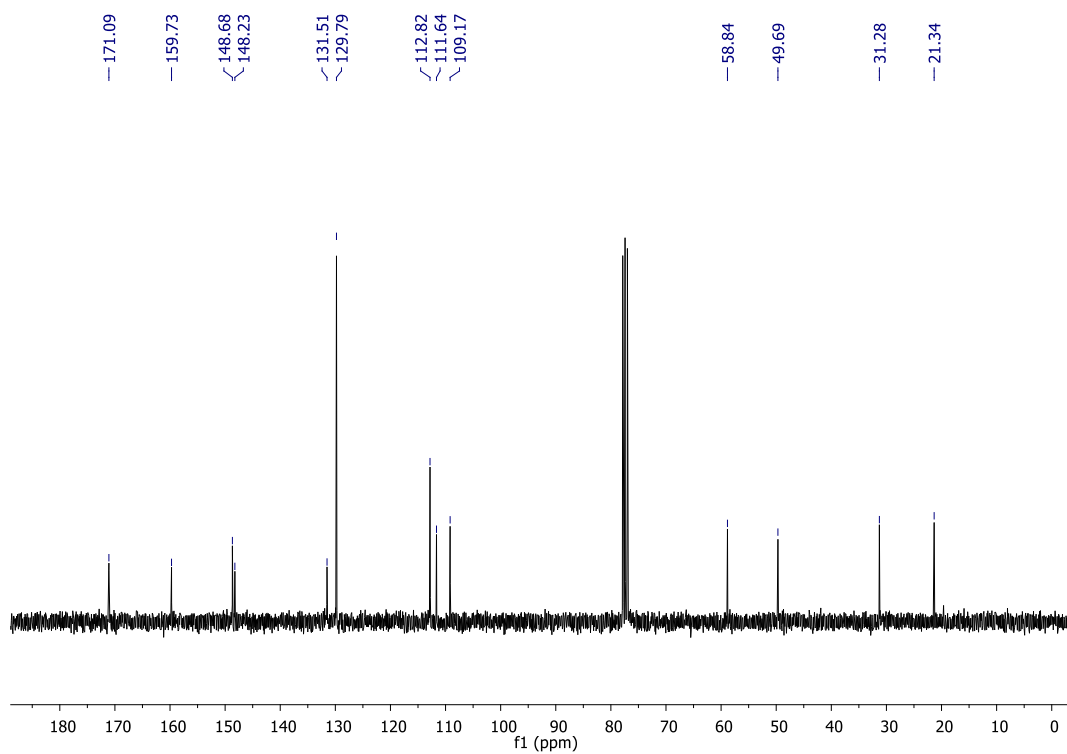
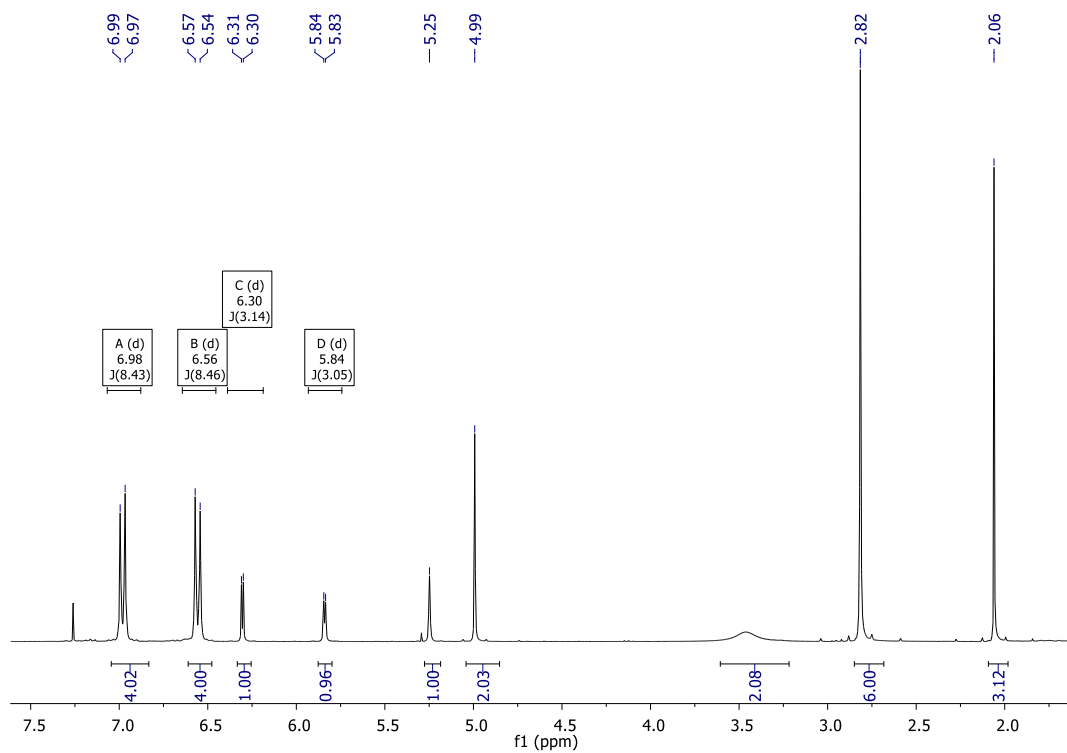
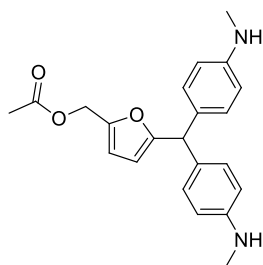
NMR Spectra of Triarylmethanes

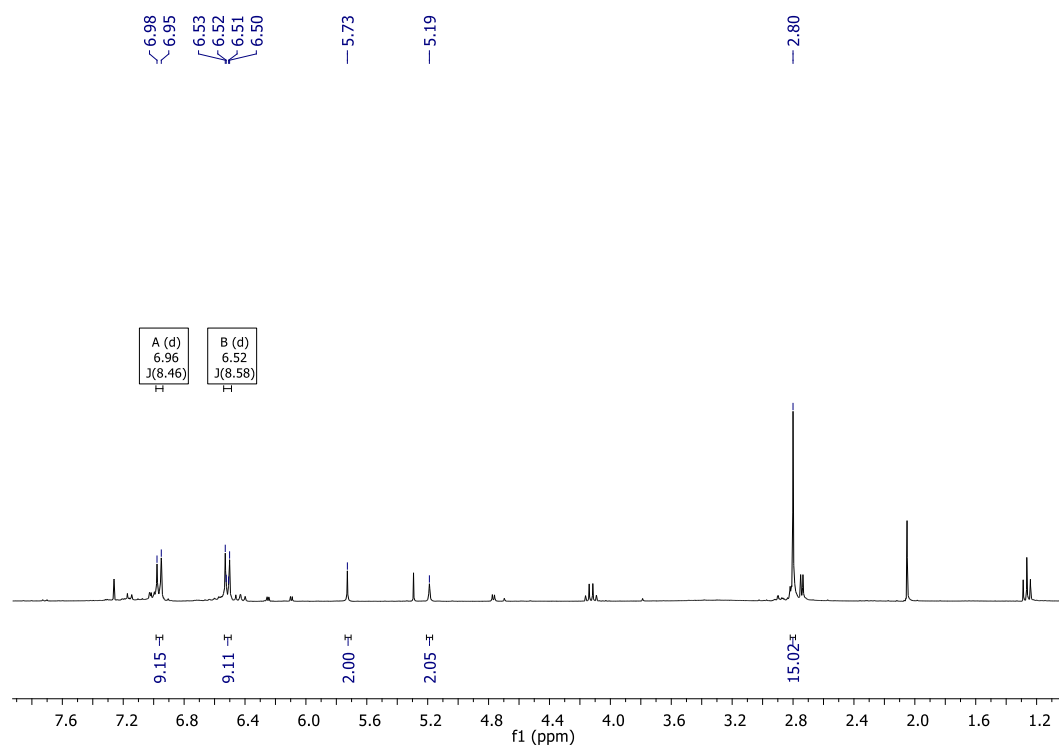
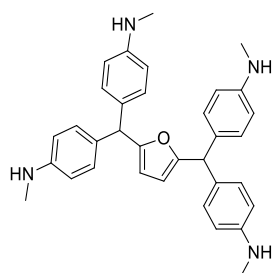


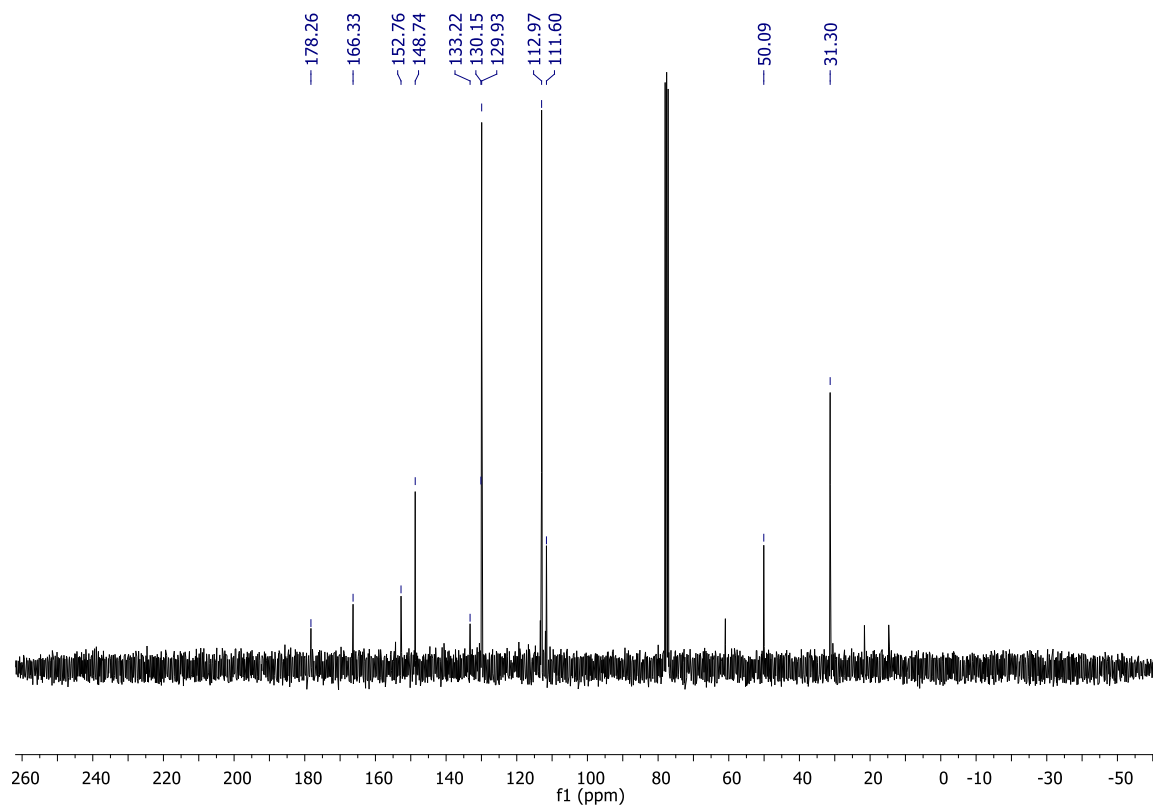
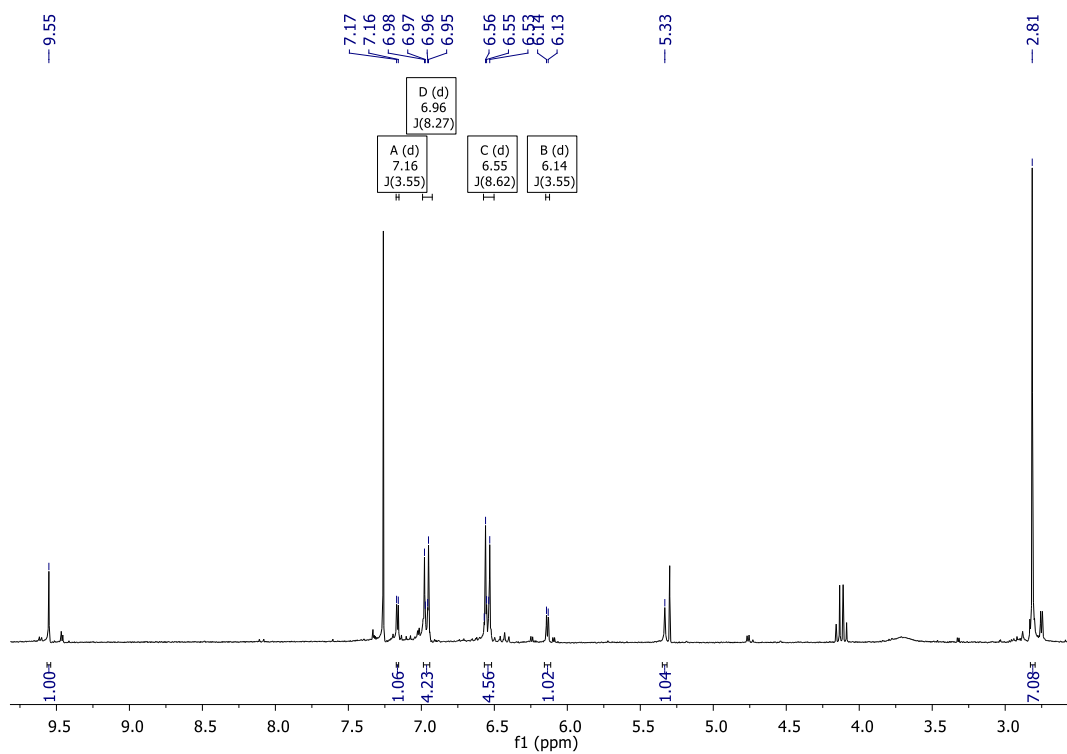
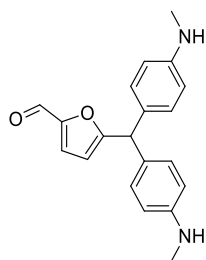


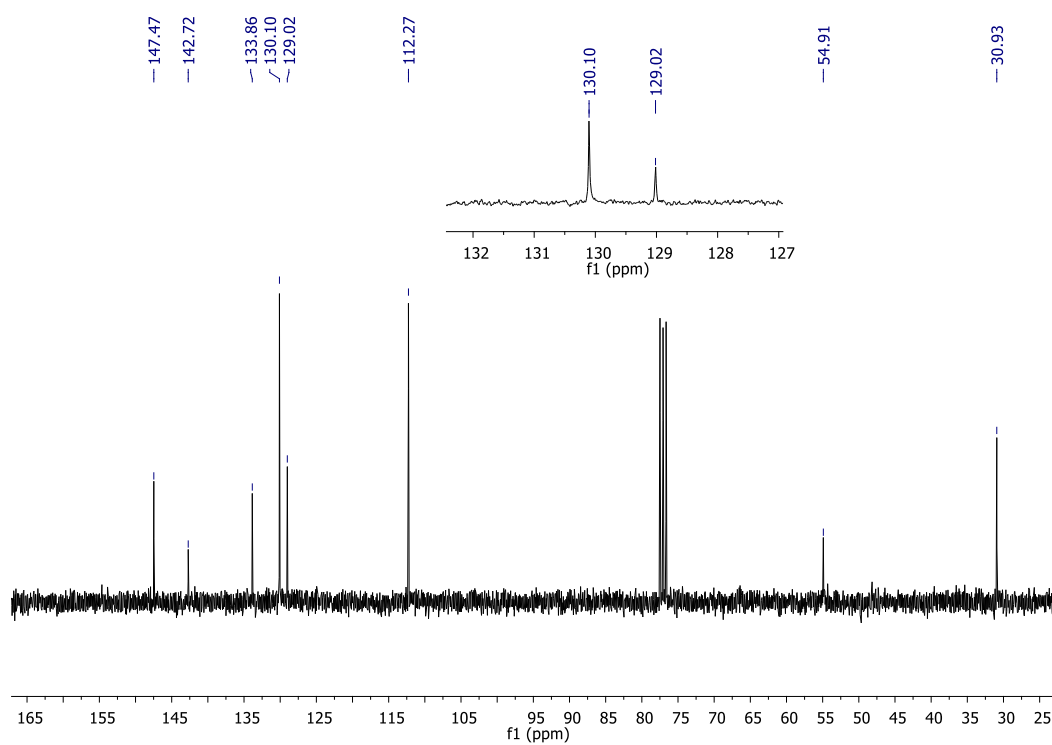
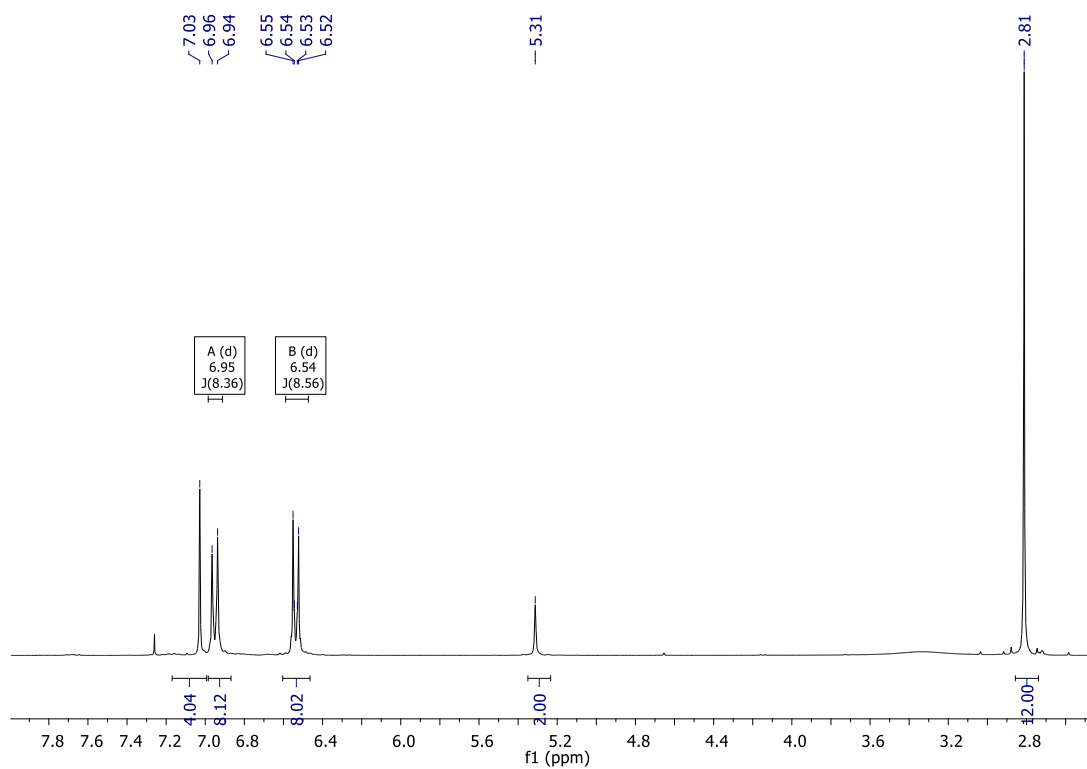
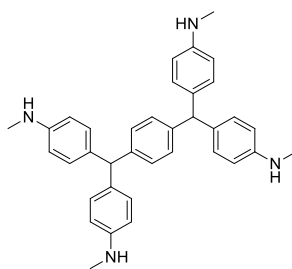


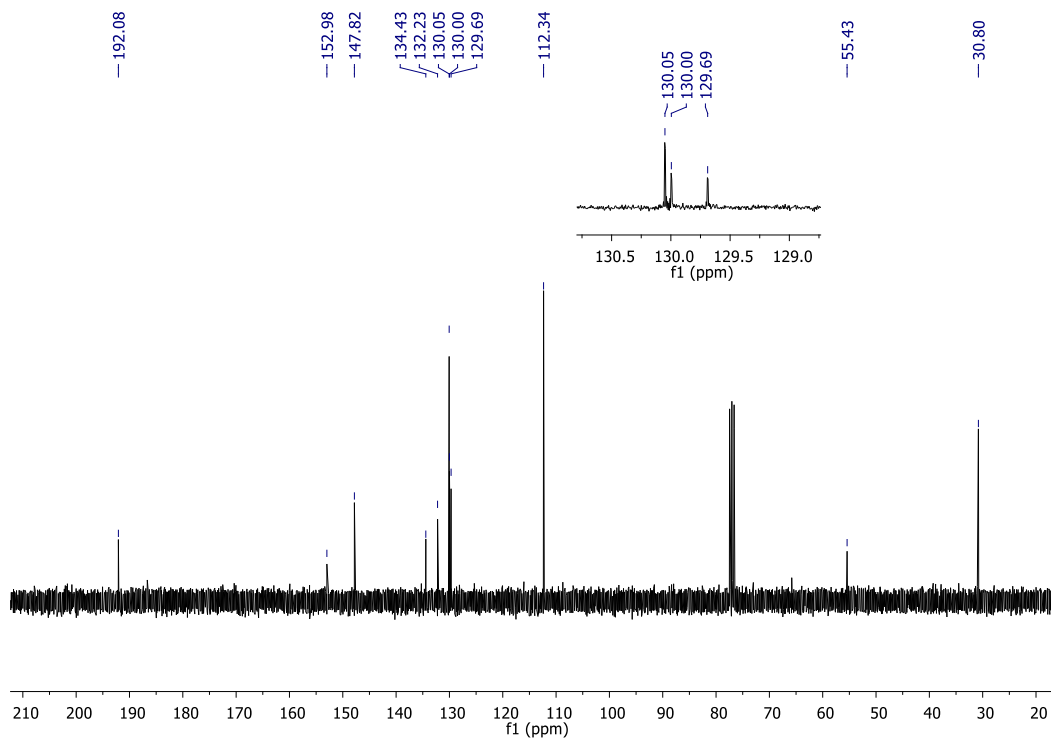
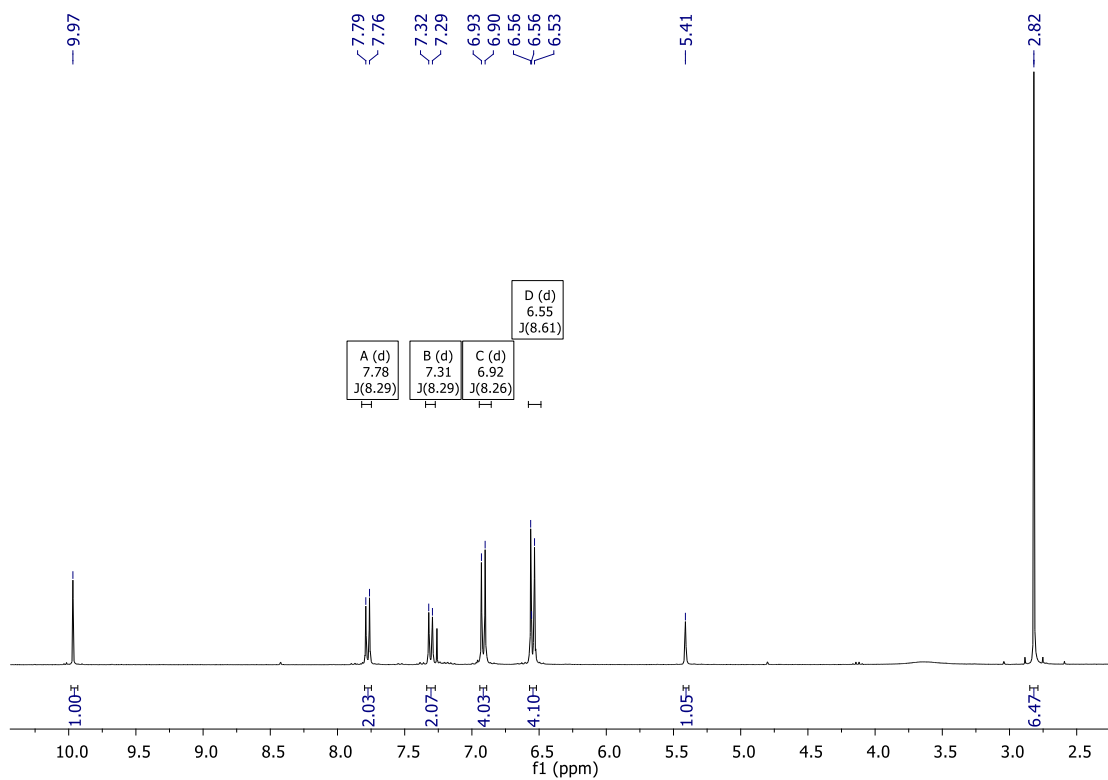
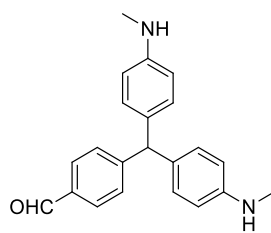


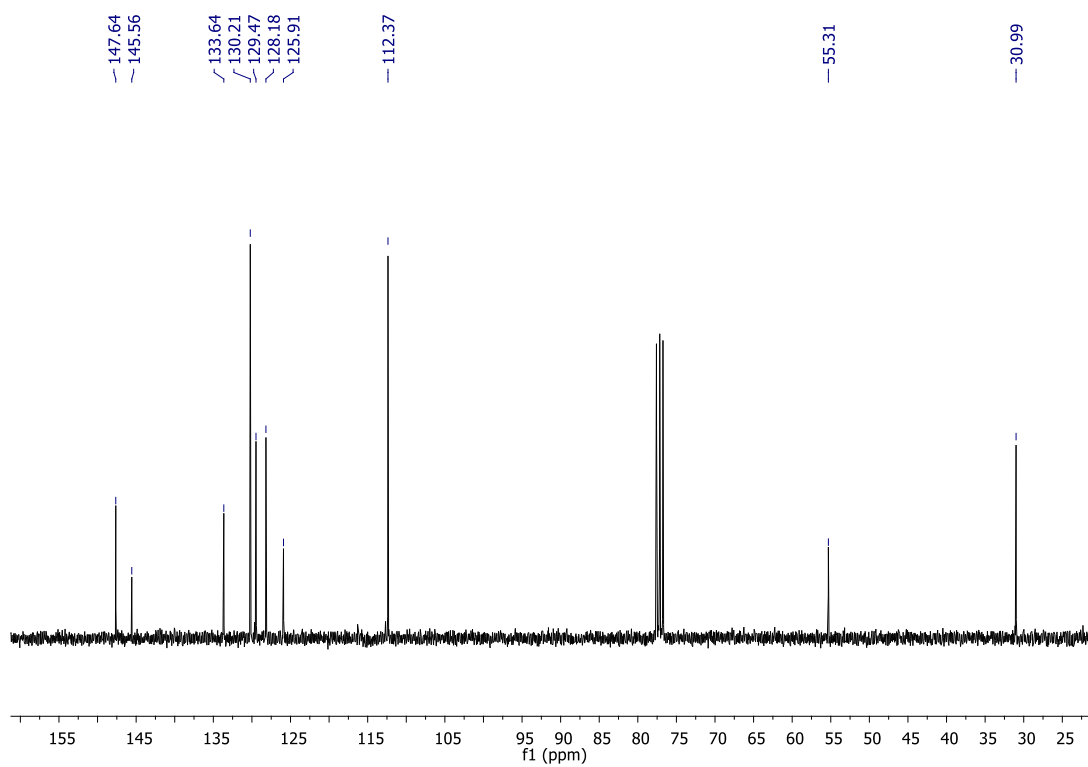
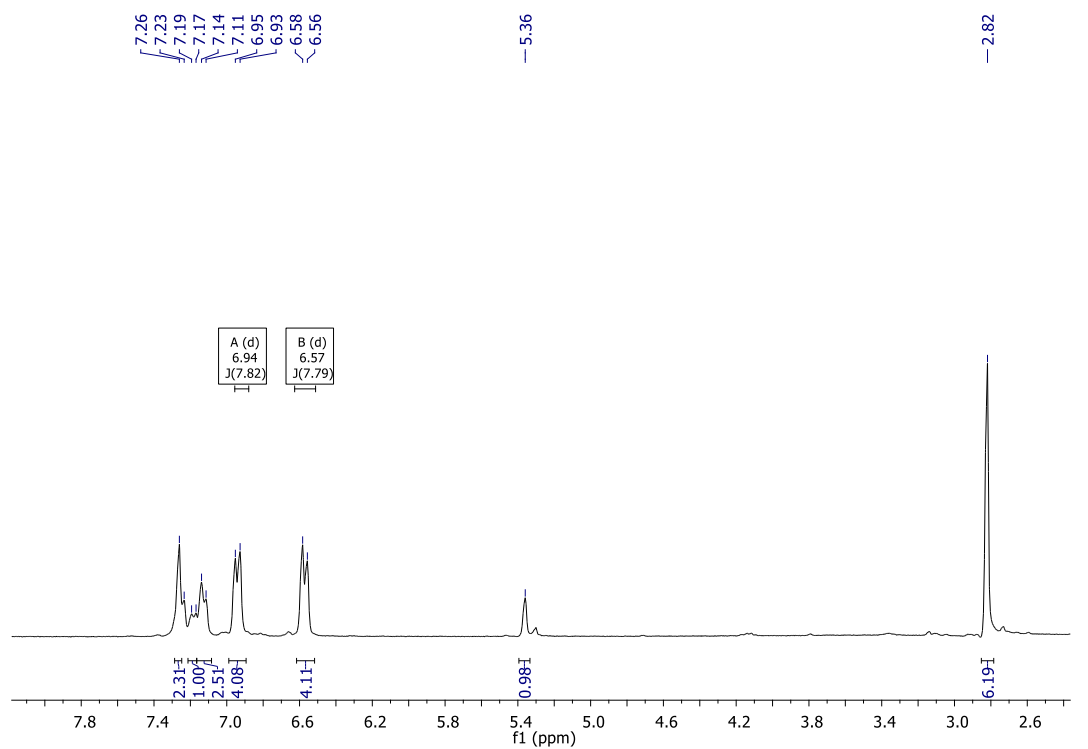
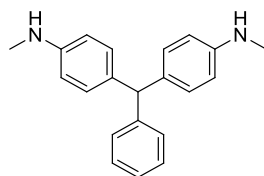


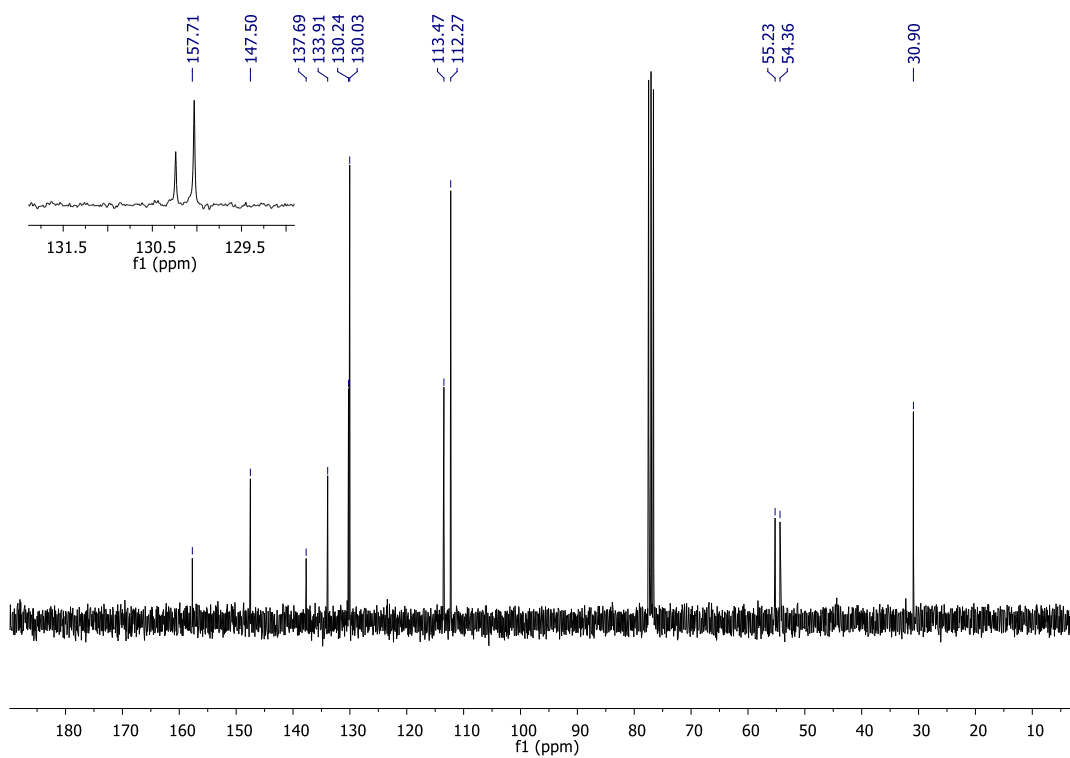
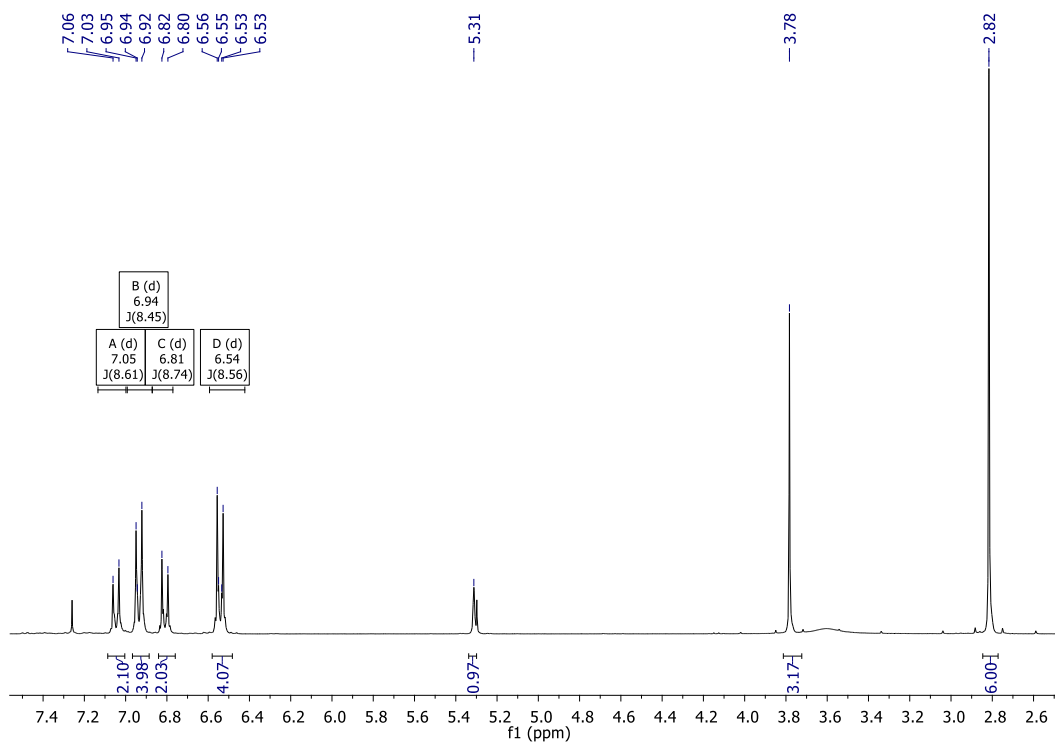
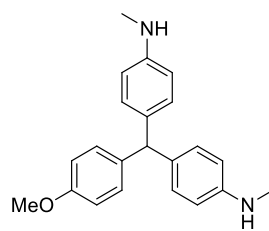


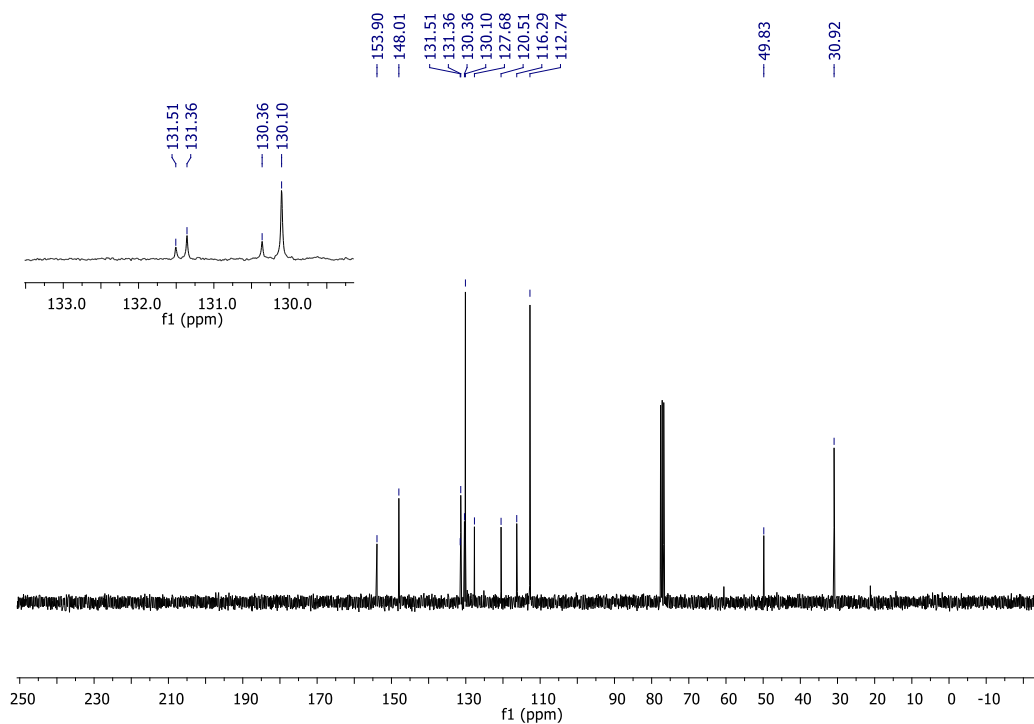
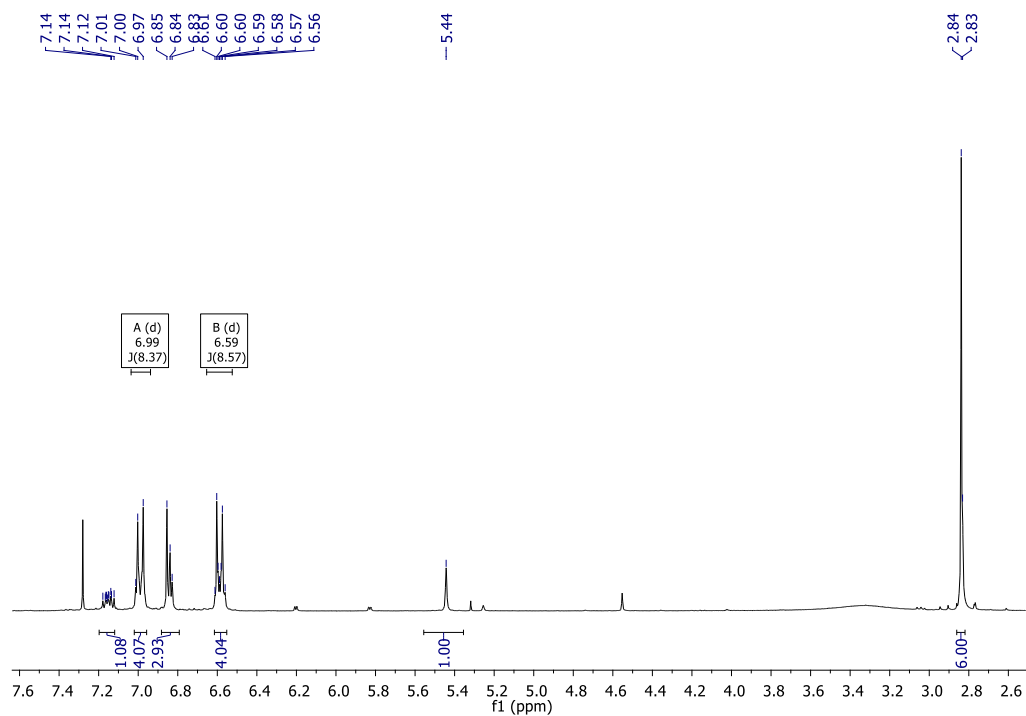
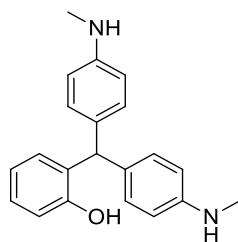


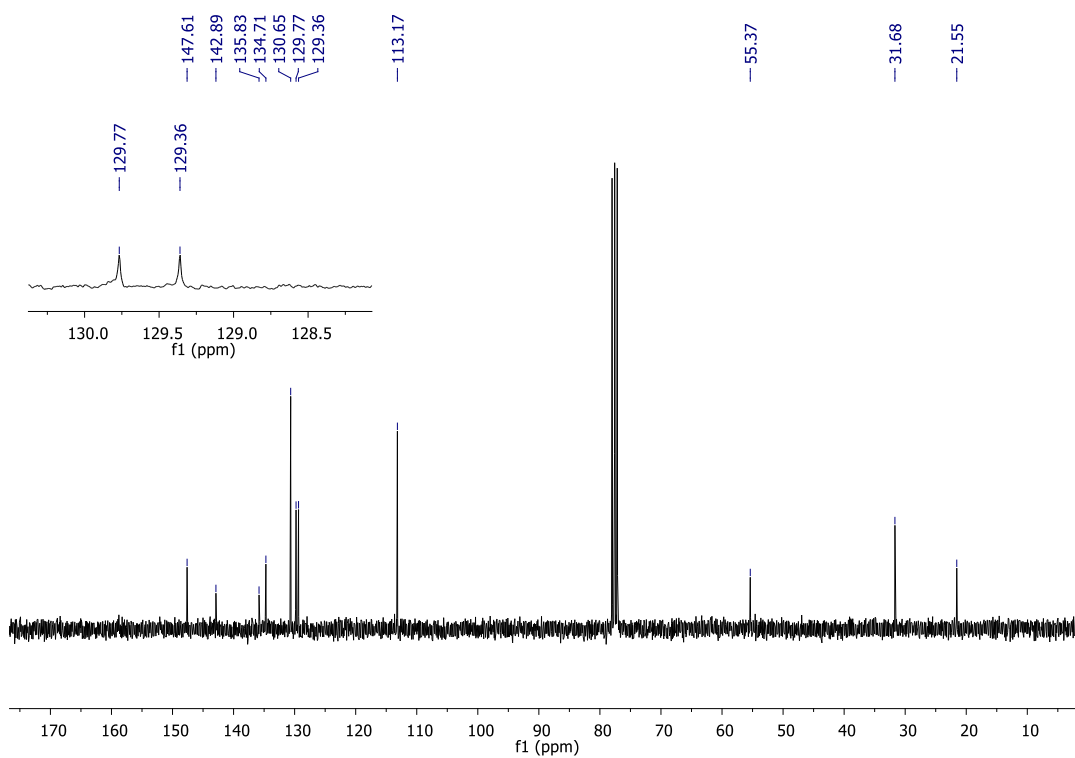
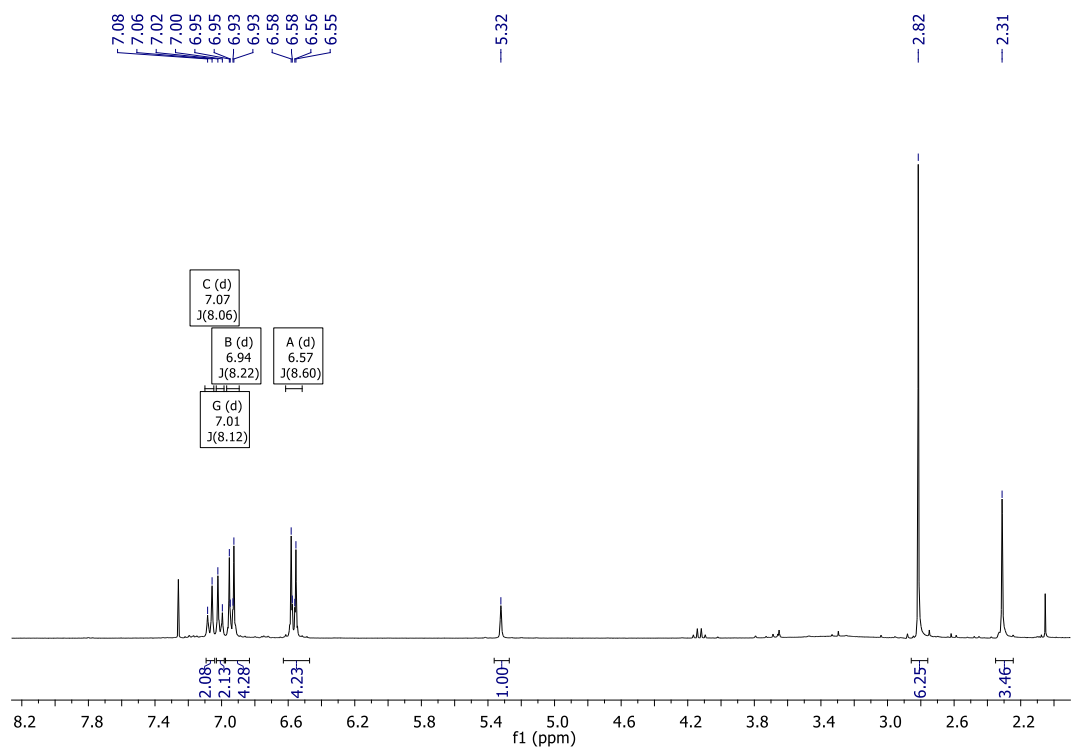
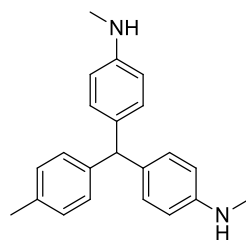


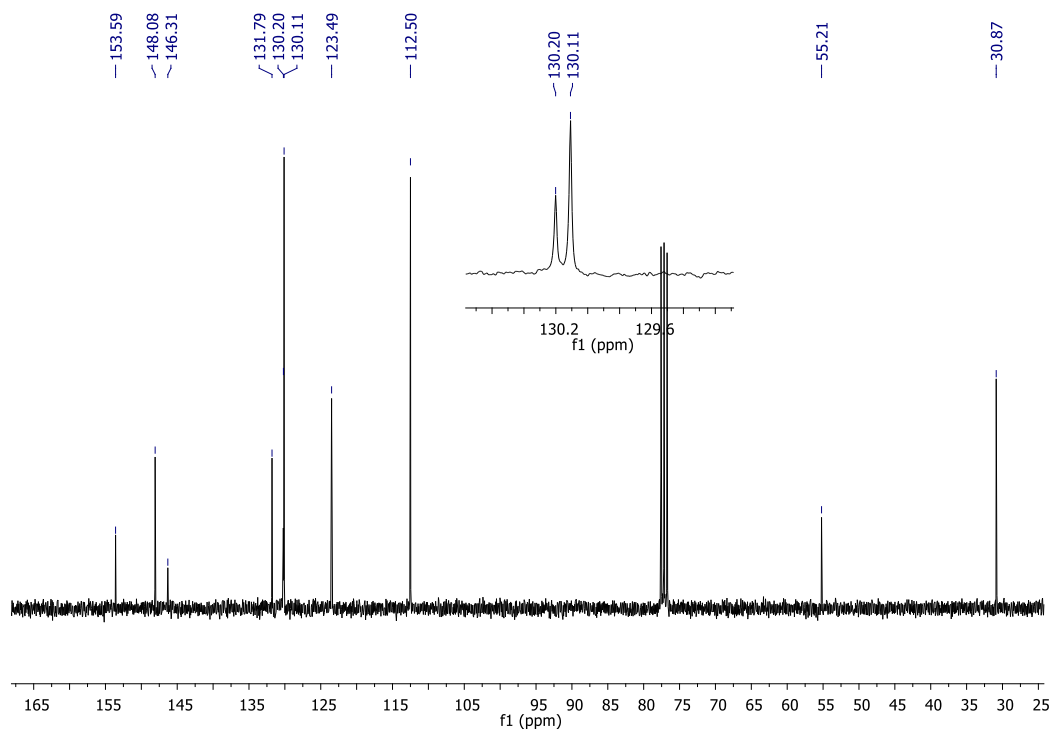
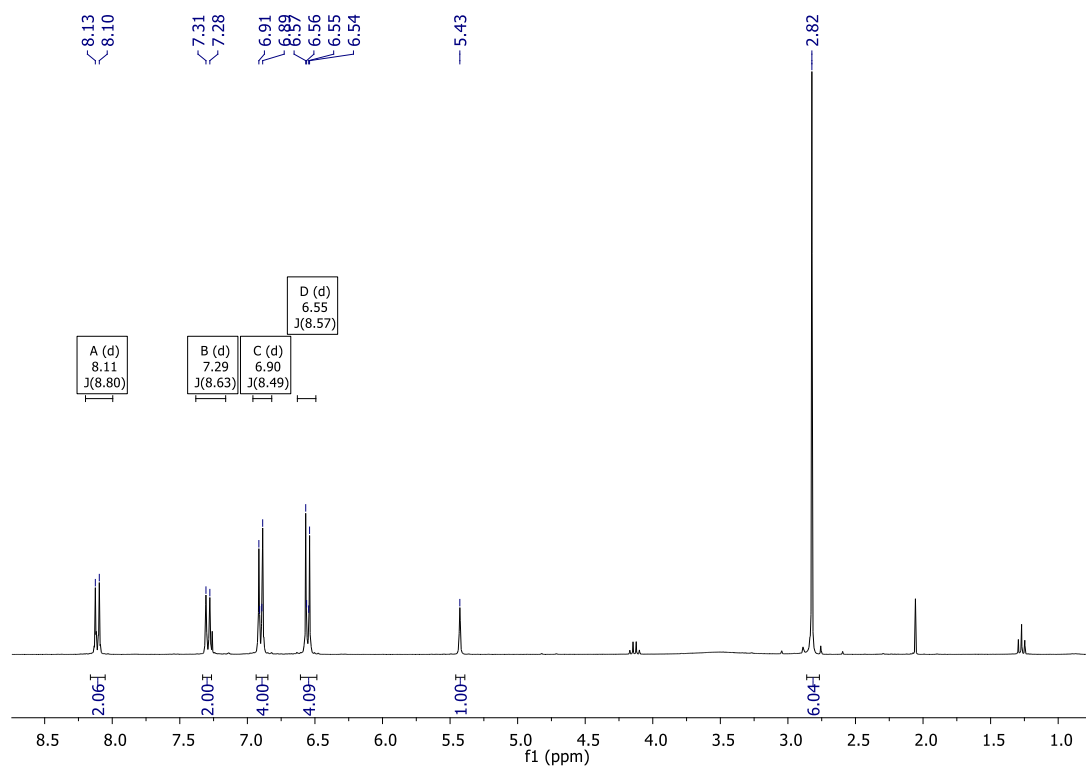
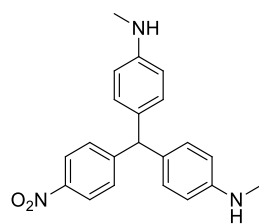


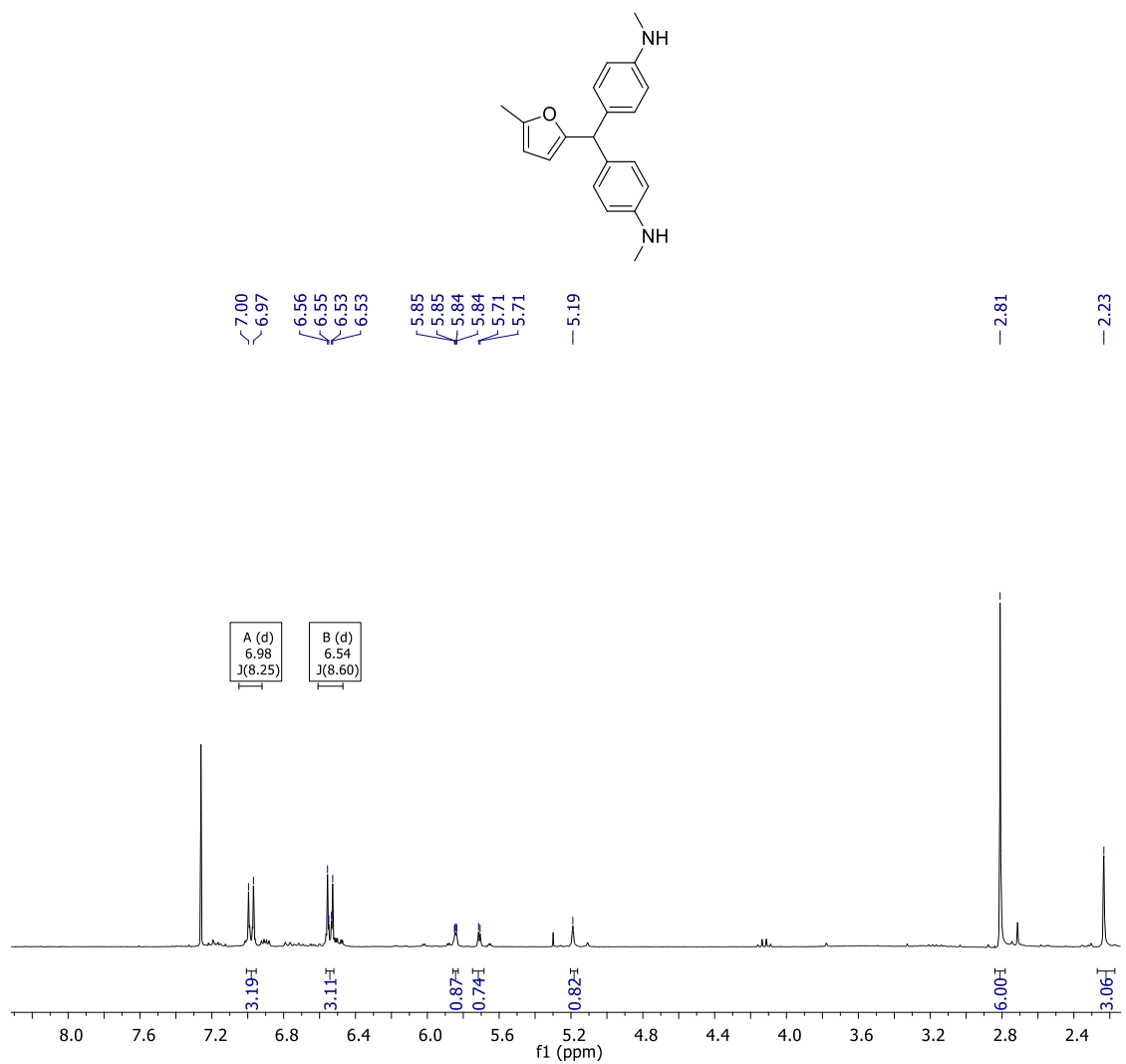


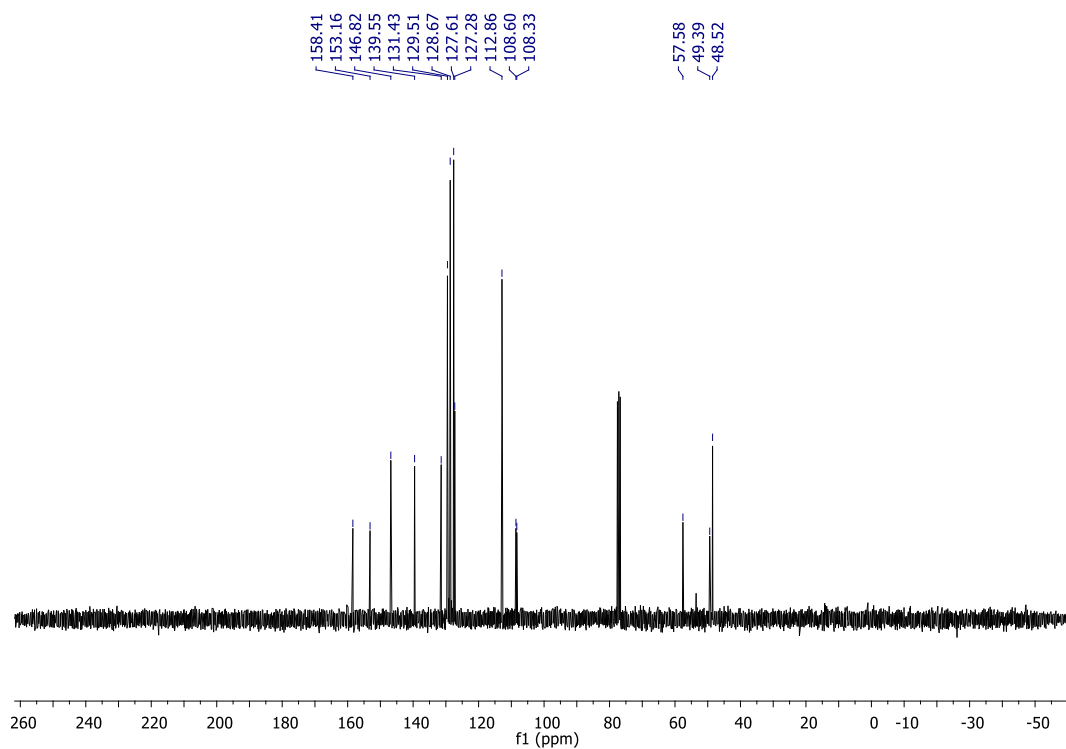
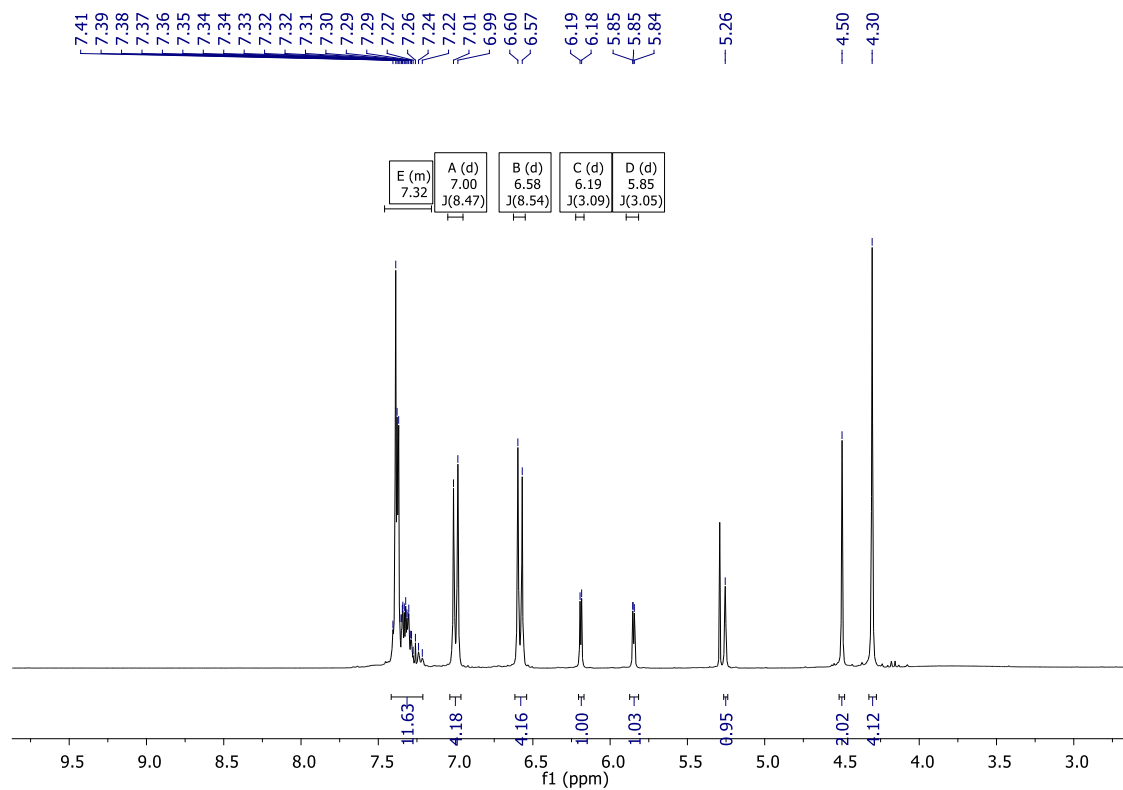
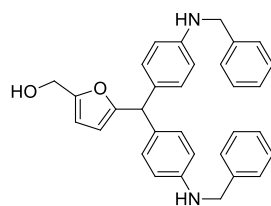


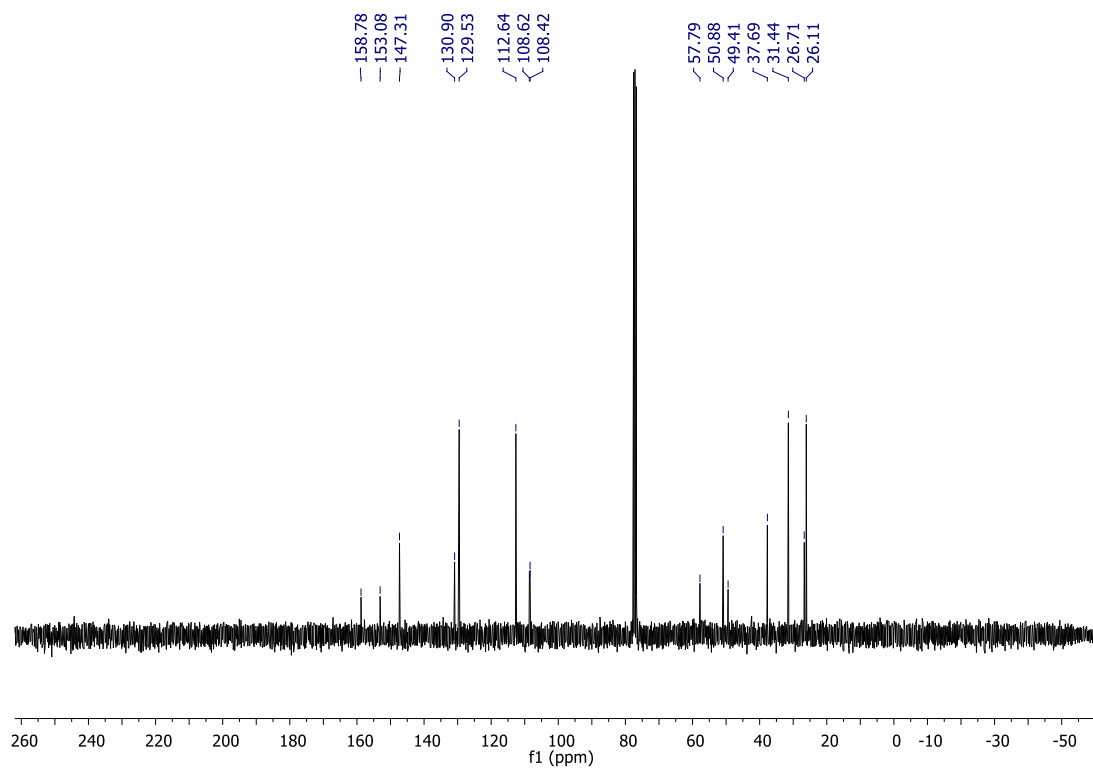
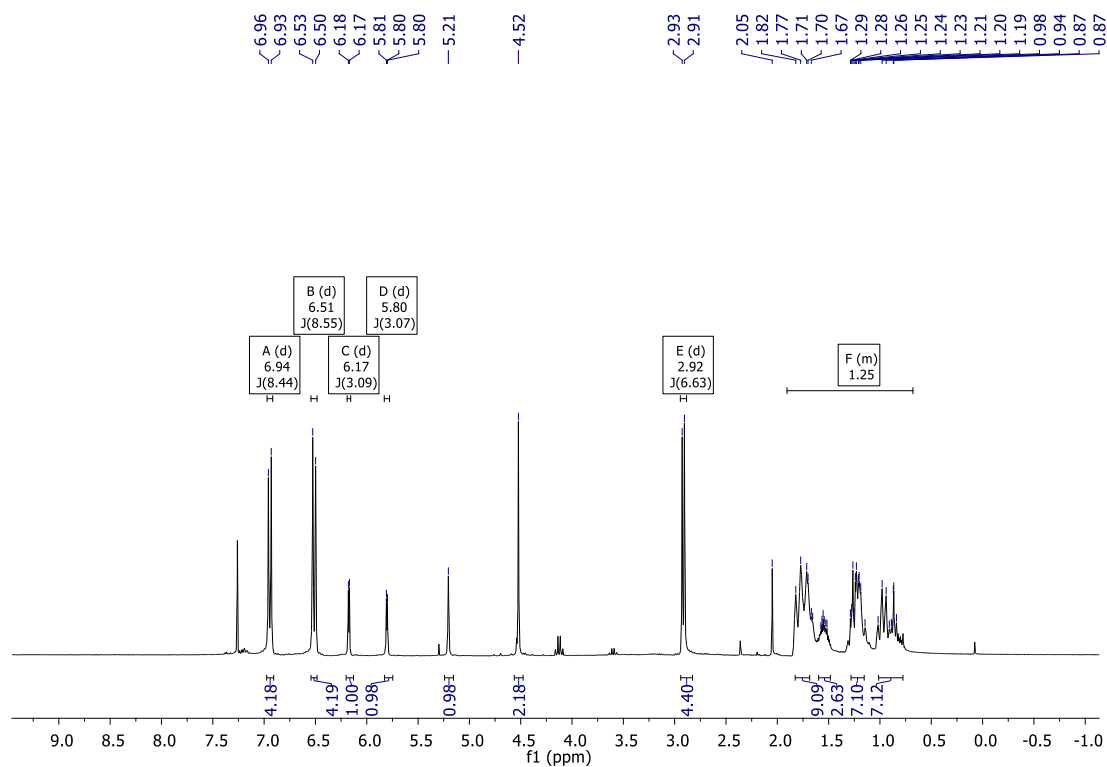
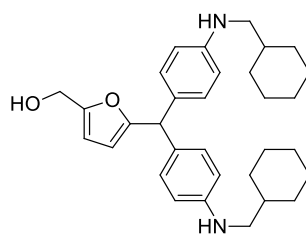


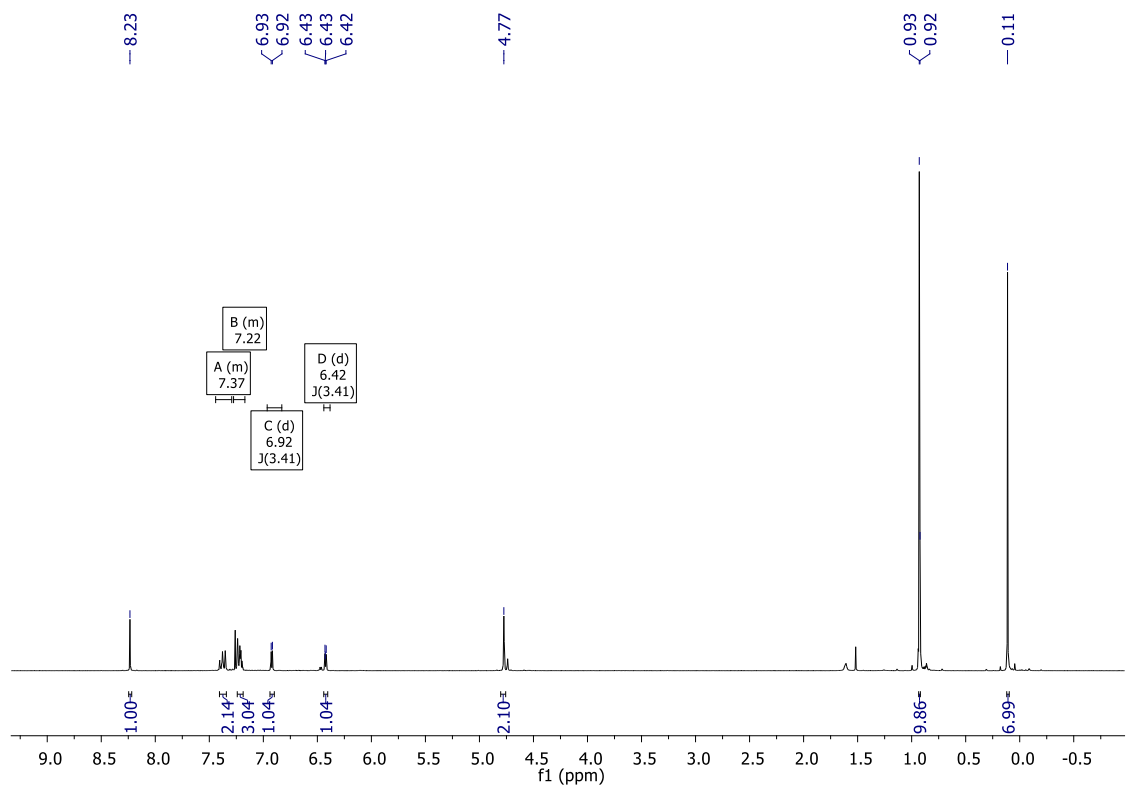


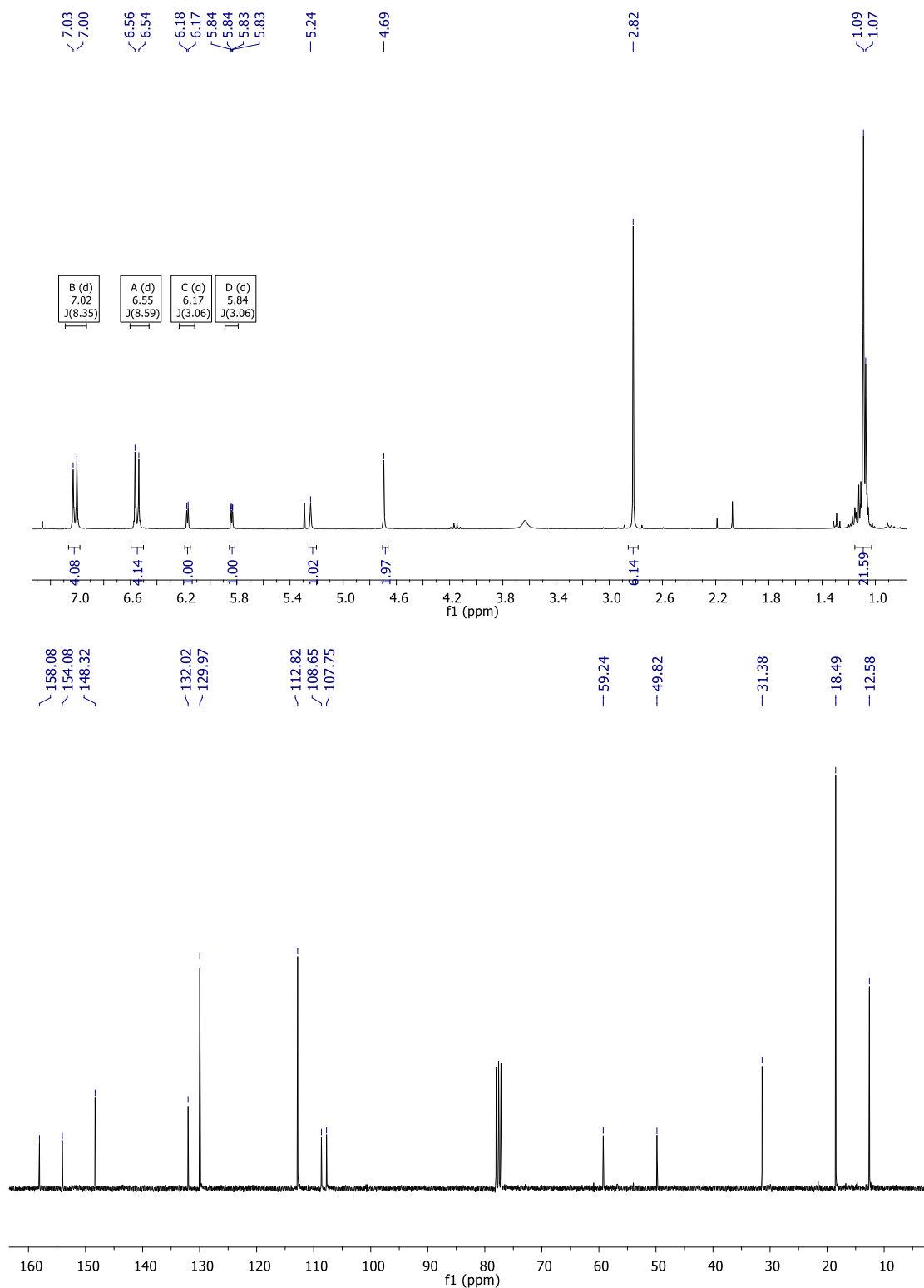
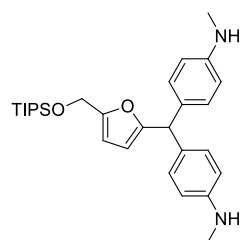


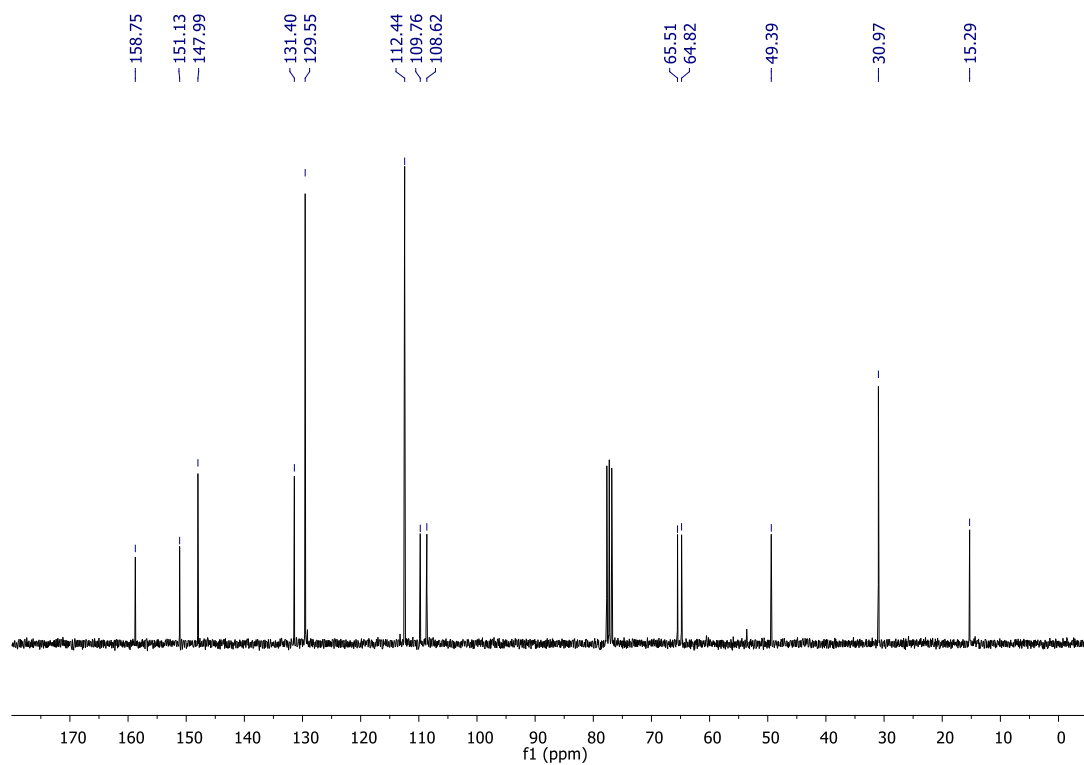
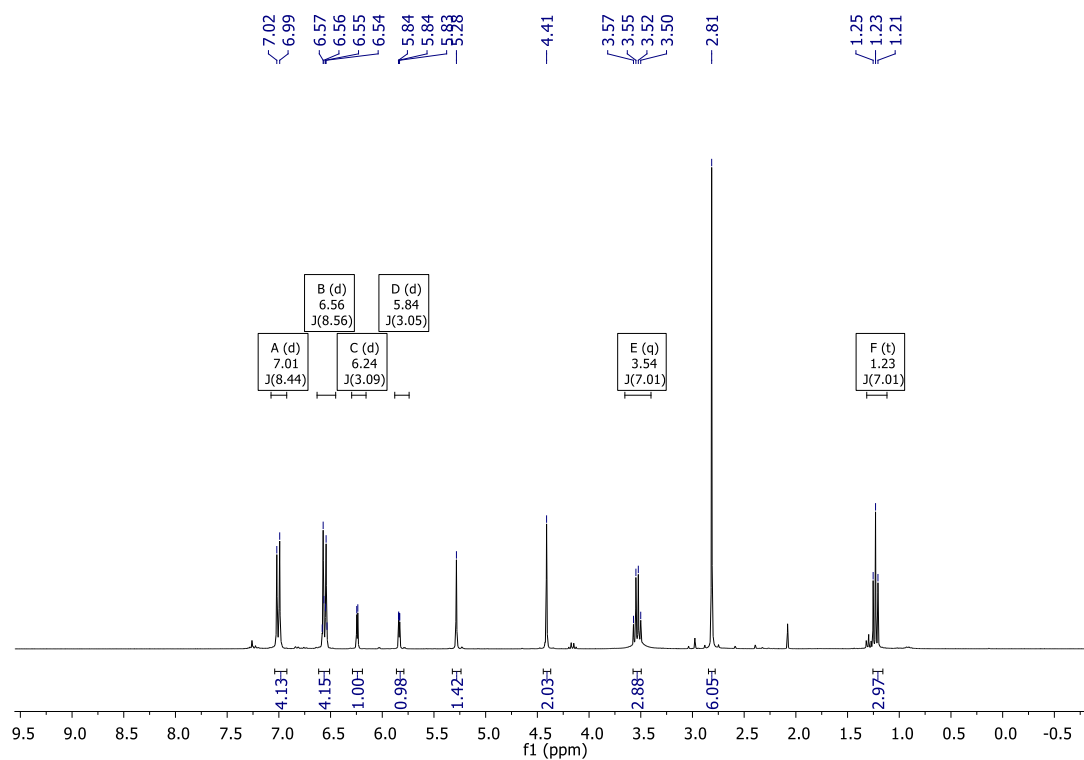
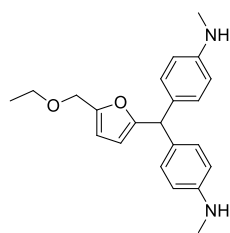


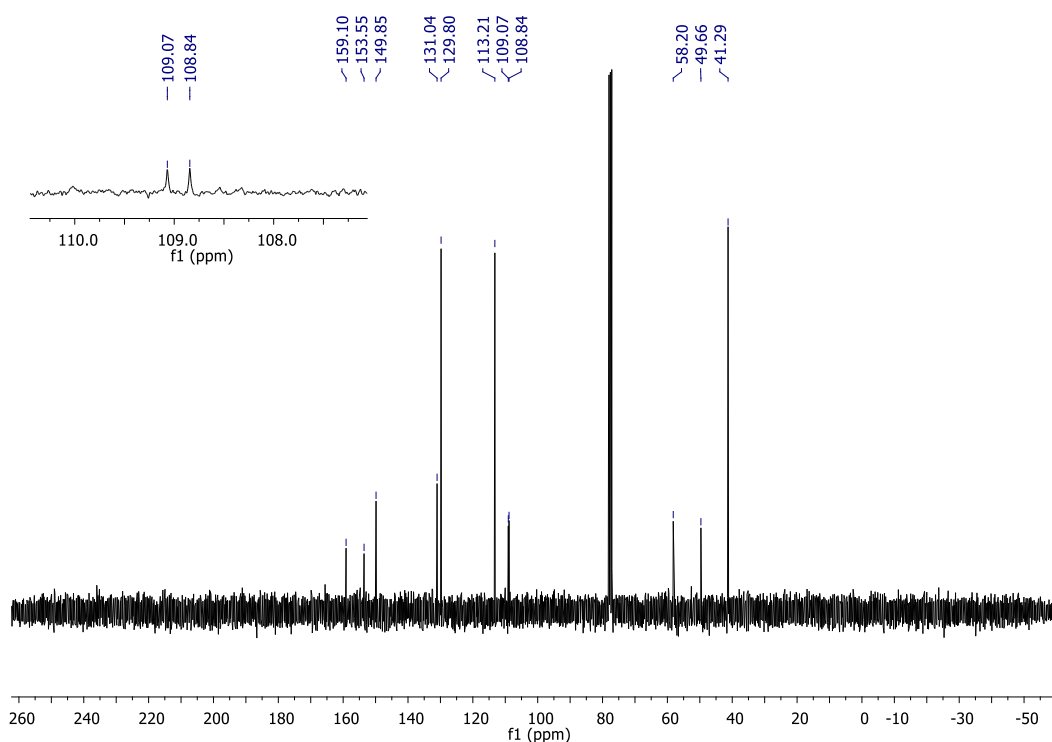
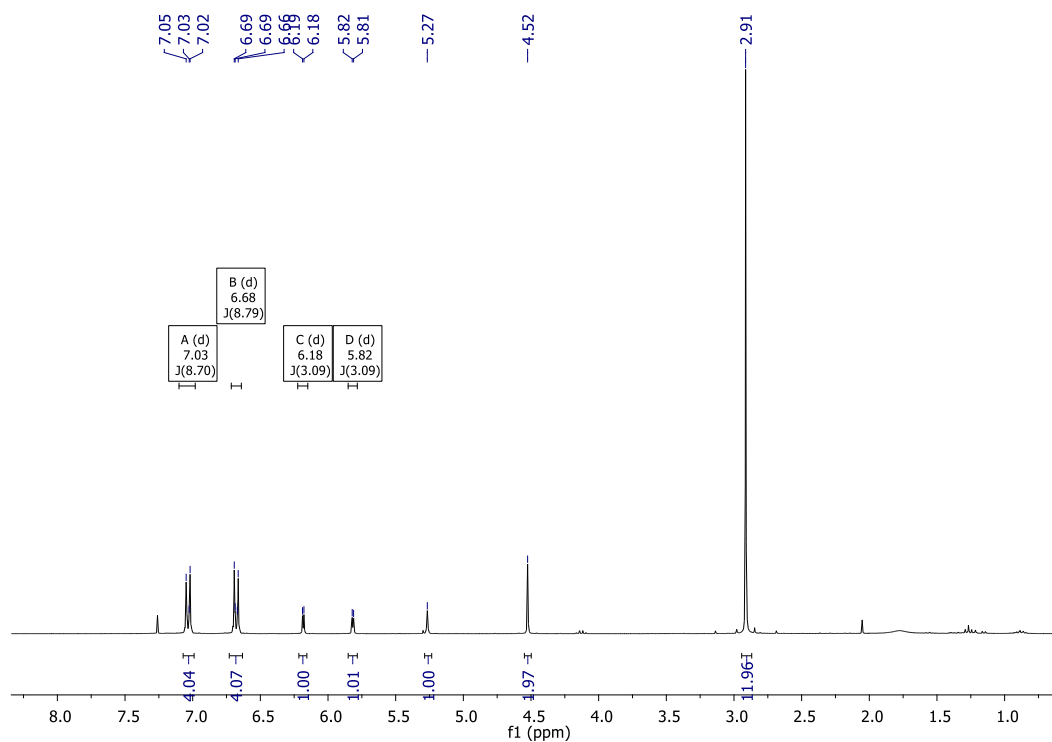
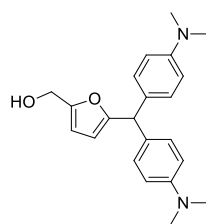


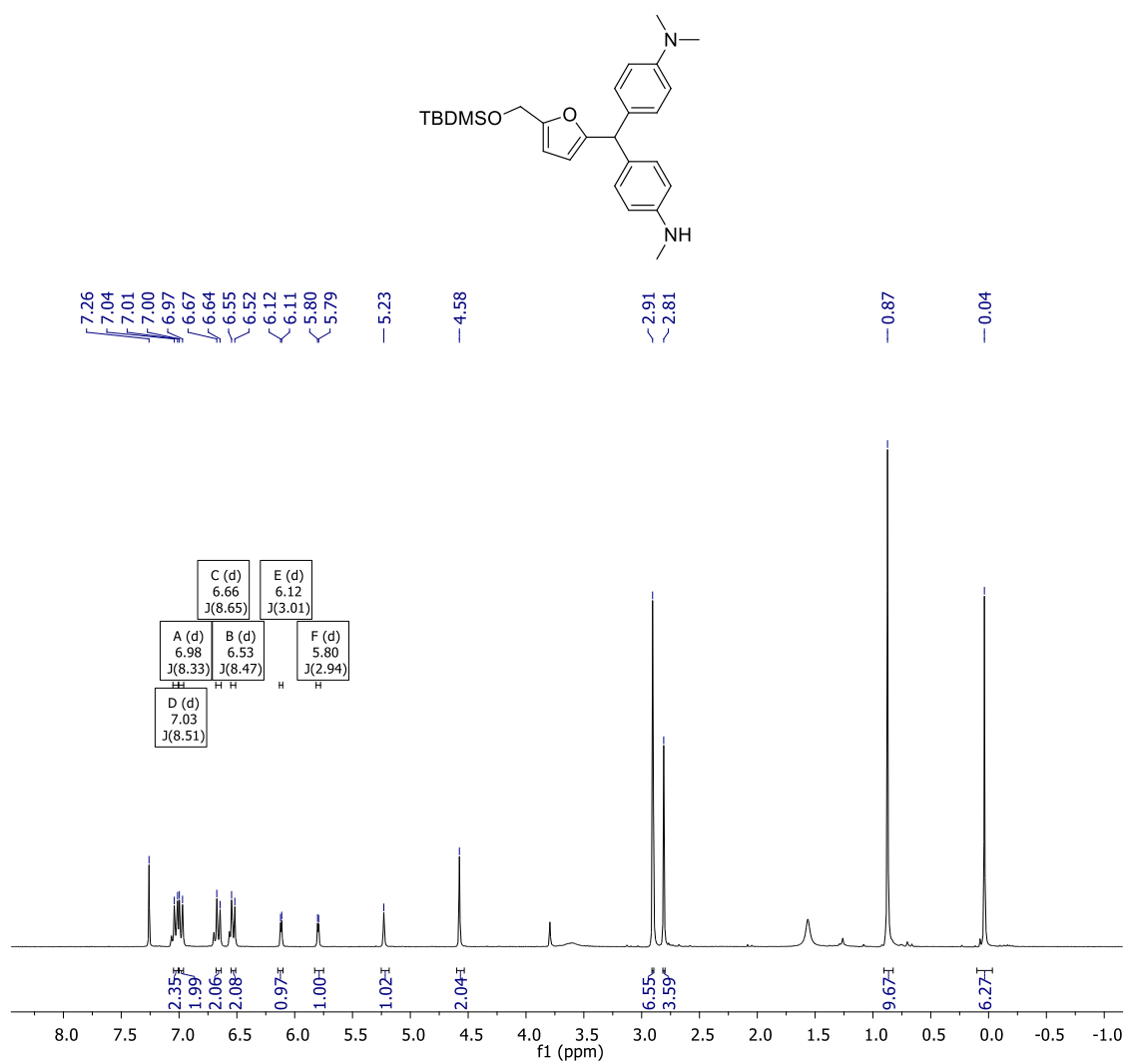












Atomic coordinates for all the optimized species

				8	0.000057000	-1.394054000	0.291929000
A				6	1.174829000	-0.755606000	-0.198403000
6	1.868295000	0.040588000	-0.006053000	6	1.205195000	0.718497000	0.199925000
6	1.986515000	1.405285000	0.008894000	1	-0.000040000	2.351997000	-0.087755000
6	3.382846000	1.673583000	0.014200000	1	-2.091079000	1.200227000	-0.229801000
6	4.022322000	0.456795000	0.002026000	1	-1.283322000	0.780981000	1.301533000
8	3.086687000	-0.549952000	-0.010452000	1	-1.220631000	-0.836479000	-1.296396000
6	0.688293000	-0.878712000	-0.016653000	1	-2.023432000	-1.295895000	0.231513000
6	5.433197000	0.117050000	0.001164000	1	2.023435000	-1.295620000	0.231659000
8	5.890121000	-1.012845000	-0.010471000	1	1.220991000	-0.836766000	-1.296422000
8	-0.491728000	-0.107297000	-0.011517000	1	1.283057000	0.780508000	1.301600000
14	-2.054877000	-0.750614000	0.009950000	1	2.091046000	1.200300000	-0.229639000
6	-3.189321000	0.784440000	-0.008627000				
6	-2.306102000	-1.839377000	-1.512674000				
6	-2.280889000	-1.791435000	1.569612000	B			
6	-4.669149000	0.342733000	0.010140000	6	-0.077992000	-2.315595000	-0.204253000
6	-2.923638000	1.615377000	-1.282643000	6	0.563378000	-3.032352000	-1.170940000
6	-2.907002000	1.662090000	1.230104000	6	1.957243000	-2.723894000	-1.056179000
1	1.169073000	2.108824000	0.015611000	6	2.068635000	-1.830792000	-0.032434000
1	3.865874000	2.640864000	0.025708000	8	0.836016000	-1.581165000	0.505486000
1	0.746356000	-1.525605000	-0.906401000	6	-1.505031000	-2.179105000	0.193492000
1	0.746032000	-1.542323000	0.860890000	6	3.239884000	-1.121596000	0.589854000
1	6.089370000	1.014822000	0.012797000	7	3.451715000	0.224395000	0.047775000
1	-2.136620000	-1.283182000	-2.440053000	8	-1.988955000	-0.885059000	-0.148615000
1	-3.324522000	-2.241811000	-1.545483000	14	-3.470346000	-0.231800000	0.311740000
1	-1.623247000	-2.696257000	-1.509741000	6	-3.351527000	1.590432000	-0.249020000
1	-2.094245000	-1.206926000	2.475928000	6	-4.876654000	-1.152583000	-0.552940000
1	-3.298878000	-2.191201000	1.632552000	6	-3.699008000	-0.386834000	2.182440000
1	-1.598851000	-2.648938000	1.581453000	6	-4.671675000	2.331842000	0.052246000
1	-5.327711000	1.221493000	0.000614000	6	-3.068584000	1.648995000	-1.765855000
1	-4.916201000	-0.235946000	0.907615000	6	-2.195128000	2.283874000	0.503087000
1	-4.929772000	-0.265390000	-0.863609000	6	4.387186000	0.995270000	0.880371000
1	-1.880492000	1.941654000	-1.340476000	6	4.753227000	2.293854000	0.169409000
1	-3.149383000	1.051745000	-2.194778000	8	3.596488000	3.067261000	-0.119224000
1	-3.556507000	2.513101000	-1.289863000	6	2.682882000	2.326930000	-0.918591000
1	-3.543548000	2.557198000	1.214762000	6	2.256309000	1.026955000	-0.239203000
1	-1.864789000	1.995220000	1.260108000	8	4.432104000	-1.866180000	0.400834000
1	-3.116505000	1.131488000	2.165643000	1	0.097500000	-3.704021000	-1.877922000
Morpholine				1	2.769501000	-3.125385000	-1.643456000
7	0.000022000	1.364253000	-0.325703000	1	-2.076335000	-2.962959000	-0.322285000
6	-1.205274000	0.718372000	0.199902000	1	-1.603514000	-2.350099000	1.275334000
6	-1.174857000	-0.755696000	-0.198392000	1	3.078041000	-1.097057000	1.681453000
				1	-4.904669000	-2.205490000	-0.250140000
				1	-4.768124000	-1.125132000	-1.641659000

1	-5.850782000	-0.718730000	-0.301500000				
1	-4.624766000	0.103497000	2.503714000	B'			
1	-3.767670000	-1.435103000	2.494002000	6	-5.535266000	-2.778504000	-1.179590000
1	-2.871311000	0.070027000	2.734209000	6	-3.532831000	-1.461831000	0.258996000
1	-5.521591000	1.893960000	-0.483582000	6	-4.278807000	-2.540457000	-1.753445000
1	-4.598567000	3.382401000	-0.259942000	6	-5.763605000	-2.343499000	0.134226000
1	-4.912476000	2.329475000	1.121704000	6	-3.274290000	-1.885534000	-1.044214000
1	-2.970308000	2.692544000	-2.095298000	6	-4.771258000	-1.690775000	0.860395000
1	-2.140924000	1.127287000	-2.020397000	6	-6.609180000	-3.514457000	-1.943392000
1	-3.878007000	1.199095000	-2.352052000	16	-2.264324000	-0.608370000	1.178253000
1	-2.367649000	2.308014000	1.584824000	8	-0.949037000	-0.939707000	0.596738000
1	-1.241104000	1.776520000	0.327644000	8	-2.500818000	-0.821631000	2.602052000
1	-2.090419000	3.324486000	0.166764000	8	-2.576441000	0.927296000	0.800447000
1	3.942531000	1.235374000	1.864135000	6	2.876569000	0.814999000	-2.096335000
1	5.282277000	0.391331000	1.052262000	6	3.297901000	2.012748000	-2.591698000
1	5.393271000	2.913205000	0.804474000	6	2.306827000	2.984859000	-2.232252000
1	5.298361000	2.061487000	-0.760352000	6	1.353382000	2.313704000	-1.528406000
1	1.815410000	2.973123000	-1.079870000	8	1.678159000	0.986382000	-1.450826000
1	3.136412000	2.093862000	-1.895955000	6	3.428285000	-0.569824000	-2.123577000
1	1.688553000	1.267165000	0.677012000	6	0.029692000	2.692727000	-0.923948000
1	1.593160000	0.473586000	-0.908268000	8	-0.199039000	1.858208000	0.265752000
1	4.731929000	-1.629282000	-0.490395000	7	-0.045307000	4.080971000	-0.641838000
				6	-1.373350000	4.704764000	-0.595045000
				6	-1.956473000	4.762470000	0.821401000
				8	-1.044888000	5.399780000	1.708317000
pTSA				6	0.192192000	4.692611000	1.766416000
6	2.670598000	0.007596000	0.027725000	6	0.852853000	4.633222000	0.385411000
6	-0.120429000	-0.007865000	-0.075580000	8	3.698826000	-1.025887000	-0.810383000
6	1.959651000	-1.201160000	0.032181000	14	3.365780000	-2.560243000	-0.189269000
6	1.948875000	1.208609000	-0.032089000	6	3.506769000	-2.329512000	1.700321000
6	0.568485000	-1.220243000	-0.023088000	6	1.644156000	-3.125346000	-0.719561000
6	0.557471000	1.211787000	-0.084576000	6	4.642766000	-3.787580000	-0.853448000
6	4.179429000	0.015491000	0.052273000	6	2.510469000	-1.244291000	2.164029000
16	-1.901469000	-0.017587000	-0.131491000	6	4.939067000	-1.884840000	2.068064000
8	-2.280145000	-0.076404000	1.473152000	6	3.185991000	-3.657260000	2.420247000
8	-2.344094000	-1.271457000	-0.724532000	1	-4.082494000	-2.875768000	-2.768161000
8	-2.384399000	1.277707000	-0.614801000	1	-6.730611000	-2.522618000	0.596445000
1	2.503019000	-2.140957000	0.075348000	1	-2.298456000	-1.715487000	-1.485185000
1	2.483810000	2.154267000	-0.041281000	1	-4.943473000	-1.368797000	1.881311000
1	0.021314000	-2.156214000	-0.034537000	1	-6.440991000	-3.462553000	-3.022431000
1	0.001144000	2.140538000	-0.145112000	1	-7.601520000	-3.104806000	-1.732335000
1	4.576144000	-0.866846000	0.561962000	1	-6.630492000	-4.575093000	-1.664555000
1	4.567139000	0.905230000	0.556313000	1	-1.689113000	1.377515000	0.603312000
1	4.585725000	0.014776000	-0.966628000	1	4.212329000	2.185315000	-3.141086000
1	-2.830173000	0.706541000	1.646152000	1	2.301513000	4.040239000	-2.458620000

1	2.716064000	-1.232941000	-2.636971000	8	-1.328986000	1.226894000	1.355716000
1	4.348844000	-0.553969000	-2.722178000	6	-3.484459000	0.526502000	2.232715000
1	-0.777169000	2.460887000	-1.633975000	6	0.800707000	2.053490000	0.655575000
1	0.211318000	0.981452000	0.142377000	8	0.169729000	1.495641000	-0.937657000
1	-2.048963000	4.168454000	-1.269869000	7	1.659302000	3.071206000	0.453228000
1	-1.274965000	5.733038000	-0.968194000	6	3.081461000	2.802060000	0.166240000
1	-2.200692000	3.751324000	1.183044000	6	3.441032000	3.184314000	-1.271702000
1	-2.872740000	5.361403000	0.833063000	8	3.062382000	4.530120000	-1.546508000
1	0.826815000	5.241266000	2.469413000	6	1.661411000	4.696846000	-1.401030000
1	0.032775000	3.675214000	2.150291000	6	1.218656000	4.413365000	0.039023000
1	1.126583000	5.652558000	0.081821000	8	-3.953701000	0.177066000	0.949545000
1	1.767043000	4.036451000	0.423443000	14	-4.134147000	-1.395757000	0.341792000
1	1.431398000	-4.117884000	-0.306507000	6	-4.258002000	-1.146336000	-1.546664000
1	1.564138000	-3.214471000	-1.809230000	6	-2.665913000	-2.467975000	0.839423000
1	0.859078000	-2.445716000	-0.375024000	6	-5.715249000	-2.138256000	1.066935000
1	5.664713000	-3.471953000	-0.621483000	6	-2.979461000	-0.451379000	-2.064706000
1	4.496332000	-4.788426000	-0.432064000	6	-5.481012000	-0.266070000	-1.883044000
1	4.566057000	-3.880863000	-1.942978000	6	-4.408039000	-2.515535000	-2.245338000
1	2.589422000	-1.097112000	3.249983000	1	3.411076000	-2.947058000	2.957441000
1	1.471297000	-1.510678000	1.944947000	1	5.960637000	-3.438343000	-0.463459000
1	2.717791000	-0.283423000	1.682180000	1	1.669119000	-1.919881000	1.501944000
1	5.018013000	-1.717660000	3.151119000	1	4.219010000	-2.419381000	-1.907609000
1	5.686865000	-2.640377000	1.800838000	1	5.732608000	-3.655583000	3.274444000
1	5.211084000	-0.950469000	1.566648000	1	6.870056000	-3.637678000	1.916545000
1	2.164244000	-3.997430000	2.218172000	1	5.795109000	-5.015211000	2.150339000
1	3.873019000	-4.461400000	2.131040000	1	1.024422000	0.995517000	-1.312984000
1	3.275099000	-3.530569000	3.507618000	1	-2.888300000	3.302519000	3.347463000
TS ₁				1	-0.460123000	4.188277000	2.461751000
				1	-3.098012000	-0.348584000	2.776969000
				1	-4.295579000	0.951937000	2.838876000
				1	1.295499000	1.115938000	0.899260000
				1	-0.388790000	0.711745000	-0.740011000
				1	3.286410000	1.742988000	0.332365000
				1	3.681076000	3.400122000	0.863628000
				1	2.963645000	2.489876000	-1.976300000
				1	4.524023000	3.127233000	-1.409883000
				1	1.435294000	5.734950000	-1.661409000
6	4.813675000	-3.260955000	1.353744000	1	1.116630000	4.031526000	-2.088108000
6	2.855916000	-2.085326000	-0.276284000	1	1.671152000	5.152291000	0.712021000
6	3.598298000	-2.823157000	1.893648000	1	0.133610000	4.479552000	0.119410000
6	5.025568000	-3.099845000	-0.024077000	1	-2.808461000	-3.486733000	0.461087000
6	2.619568000	-2.238941000	1.088530000	1	-2.573787000	-2.550644000	1.928909000
6	4.056958000	-2.522237000	-0.839943000	1	-1.715566000	-2.096960000	0.443351000
6	5.858132000	-3.922282000	2.221213000	1	-6.589213000	-1.514401000	0.855580000
16	1.624859000	-1.309069000	-1.330347000	1	-5.910204000	-3.138462000	0.664417000
8	0.365872000	-1.238898000	-0.522466000				
8	1.572485000	-2.079508000	-2.577833000				
8	2.152654000	0.121178000	-1.532060000				
6	-2.400147000	1.551217000	2.135195000				
6	-2.207797000	2.785346000	2.686954000				
6	-0.942705000	3.254919000	2.213102000				
6	-0.453572000	2.275762000	1.393264000				

1	-5.636388000	-2.238252000	2.155774000	6	2.264987000	-3.679652000	1.869652000
1	-3.044150000	-0.300671000	-3.150904000	1	-5.450698000	-2.822044000	-2.465089000
1	-2.078699000	-1.043193000	-1.870569000	1	-5.838868000	-2.518144000	1.801120000
1	-2.848064000	0.533244000	-1.602869000	1	-3.340748000	-1.511050000	-2.361382000
1	-5.538257000	-0.094475000	-2.966707000	1	-3.727699000	-1.208418000	1.894958000
1	-6.423497000	-0.735957000	-1.578880000	1	-7.589938000	-3.447790000	-1.339243000
1	-5.420118000	0.711829000	-1.394358000	1	-7.738948000	-3.340037000	0.422333000
1	-3.545926000	-3.166029000	-2.062218000	1	-6.840545000	-4.669419000	-0.310897000
1	-5.309869000	-3.048572000	-1.921585000	1	-0.479137000	1.224601000	1.645511000
1	-4.484809000	-2.379328000	-3.332377000	1	4.944388000	2.901478000	-1.124131000
B''				1	2.720169000	4.368935000	-0.644967000
6	-5.790083000	-2.778552000	-0.337409000	1	3.771335000	-0.508488000	-2.503959000
6	-3.401931000	-1.306949000	-0.224860000	1	5.267337000	0.244980000	-1.924610000
6	-5.072171000	-2.482026000	-1.504068000	1	-0.271539000	1.637400000	-1.321741000
6	-5.289615000	-2.311830000	0.885627000	1	0.852430000	1.135658000	2.410204000
6	-3.885252000	-1.753297000	-1.455273000	1	-2.212433000	2.467010000	-1.116401000
6	-4.103692000	-1.582346000	0.948995000	1	-2.190087000	4.241631000	-1.401445000
6	-7.058144000	-3.597138000	-0.394681000	1	-2.556070000	2.820978000	1.286175000
16	-1.835155000	-0.426890000	-0.147076000	1	-3.760911000	3.805726000	0.417569000
8	-1.743865000	0.328438000	-1.442721000	1	-0.590664000	5.707142000	2.080163000
8	-0.766339000	-1.440317000	0.025397000	1	-0.686777000	3.922978000	2.224145000
8	-1.970480000	0.498181000	1.032842000	1	-0.059584000	5.523902000	-0.313019000
6	3.503046000	1.265973000	-1.371651000	1	1.023114000	4.437833000	0.612085000
6	3.922024000	2.553359000	-1.120788000	1	1.784848000	-3.667739000	-1.383288000
6	2.760245000	3.311192000	-0.855174000	1	2.343940000	-2.407622000	-2.471372000
6	1.685332000	2.442684000	-0.956398000	1	1.221636000	-2.013526000	-1.146689000
8	2.159811000	1.196107000	-1.293955000	1	5.816961000	-3.448370000	-0.109021000
6	4.237977000	-0.011192000	-1.642553000	1	4.563722000	-4.654081000	-0.439842000
6	0.264573000	2.505452000	-0.918388000	1	5.152854000	-3.615701000	-1.739294000
8	0.325920000	1.743666000	1.877120000	1	1.927680000	-1.185340000	2.966821000
7	-0.486641000	3.478016000	-0.477486000	1	1.273858000	-1.157453000	1.319356000
6	-1.955839000	3.439935000	-0.690819000	1	2.741943000	-0.235600000	1.705434000
6	-2.694806000	3.683871000	0.624739000	1	4.063498000	-2.365347000	3.516206000
8	-2.247358000	4.890938000	1.236881000	1	4.972878000	-3.255796000	2.290923000
6	-0.875719000	4.783380000	1.568579000	1	4.951911000	-1.485045000	2.263541000
6	-0.005275000	4.623905000	0.310596000	1	1.322470000	-3.699911000	1.313300000
8	4.246558000	-0.820732000	-0.491534000	1	2.826309000	-4.591277000	1.630305000
14	3.559373000	-2.361924000	-0.275738000	1	2.014246000	-3.727167000	2.938069000
6	3.074801000	-2.398244000	1.571630000	[pTSA-OH]⁻			
6	2.092124000	-2.616196000	-1.424819000	6	2.878534000	0.176821000	-0.002904000
6	4.898379000	-3.636939000	-0.673364000	6	0.107774000	-0.323623000	0.001127000
6	2.201001000	-1.167774000	1.900959000	6	2.385423000	-1.131275000	-0.008203000
6	4.341520000	-2.374959000	2.453117000				

6	1.952988000	1.233338000	0.002868000	1	-2.033597000	2.843206000	0.147698000
6	1.010204000	-1.383485000	-0.005788000	1	4.181529000	1.789433000	-0.678495000
6	0.581771000	0.994729000	0.005011000	1	-3.775542000	1.019360000	2.532300000
6	4.364764000	0.454739000	0.003553000	1	-2.966147000	-0.546572000	2.690978000
16	-1.681775000	-0.637187000	0.002026000	1	-4.668584000	-0.463617000	2.227892000
8	-1.816157000	-2.113383000	0.011197000	1	-5.459645000	0.728623000	-0.622239000
8	-2.168715000	0.025738000	-1.247455000	1	-4.526900000	2.166682000	-0.239162000
8	-2.169219000	0.040585000	1.243547000	1	-4.185783000	1.264777000	-1.723026000
1	3.085455000	-1.965354000	-0.014549000	1	-4.772531000	-2.513277000	0.513256000
1	2.316602000	2.259877000	0.005085000	1	-4.268664000	-3.380458000	-0.938008000
1	0.617803000	-2.394952000	-0.009790000	1	-5.131876000	-1.849816000	-1.089811000
1	-0.131054000	1.816531000	0.007956000	1	-1.862985000	-3.463905000	-0.140730000
1	4.943812000	-0.470090000	-0.084372000	1	-1.014387000	-1.984443000	0.338700000
1	4.679778000	0.954290000	0.928870000	1	-2.322464000	-2.626100000	1.344204000
1	4.657476000	1.110668000	-0.825686000	1	-3.223035000	-0.968995000	-2.590069000
8	-2.364096000	2.641604000	-0.006774000	1	-1.552590000	-0.991553000	-2.008140000
1	-2.404604000	1.997396000	0.724343000	1	-2.379792000	-2.507413000	-2.405874000
1	-2.400134000	2.002809000	-0.742380000	1	4.753664000	-1.258120000	-1.640016000
C				1	5.533297000	0.113407000	-0.810282000
				1	6.083969000	-2.143571000	0.238526000
				1	5.276620000	-1.040340000	1.381786000
				1	2.179708000	-2.859247000	1.034010000
6	0.032588000	2.434266000	0.186482000	1	2.931572000	-1.471483000	1.860416000
6	0.654436000	3.650053000	-0.037608000	1	2.312333000	-1.702775000	-1.141338000
6	2.002279000	3.364765000	-0.305616000	1	1.469938000	-0.643321000	0.013182000
6	2.139729000	1.980384000	-0.240712000	C'			
8	0.919024000	1.426649000	0.069298000				
6	-1.369496000	2.073922000	0.570600000				
6	3.289522000	1.205242000	-0.467077000				
7	3.459840000	-0.097470000	-0.474482000	6	-0.313601000	0.478533000	2.193083000
8	-1.671699000	0.782783000	0.128785000	6	0.035689000	0.299383000	3.519567000
14	-3.228474000	0.080261000	0.271270000	6	1.314818000	-0.282906000	3.524864000
6	-3.015989000	-1.647470000	-0.503977000	6	1.688570000	-0.440646000	2.193348000
6	-3.692884000	0.016933000	2.097246000	8	0.677103000	0.030663000	1.390112000
6	-4.454172000	1.160496000	-0.667203000	6	-1.488168000	1.109050000	1.509463000
6	-4.376646000	-2.380285000	-0.499742000	6	2.904427000	-0.925734000	1.677335000
6	-1.995802000	-2.472063000	0.310382000	7	3.307986000	-1.078772000	0.437171000
6	-2.513757000	-1.514015000	-1.958093000	8	-1.916355000	0.338758000	0.409396000
6	4.797785000	-0.687155000	-0.706808000	14	-3.267191000	-0.705749000	0.420935000
6	5.147973000	-1.624902000	0.457486000	6	-3.314145000	-1.415967000	-1.347369000
8	4.147807000	-2.611924000	0.616331000	6	-2.994292000	-2.040065000	1.729326000
6	2.889523000	-2.037565000	0.917139000	6	-4.804491000	0.295587000	0.849327000
6	2.418353000	-1.119808000	-0.220201000	6	-4.457350000	-2.451017000	-1.453679000
1	0.180528000	4.620309000	-0.015507000	6	-1.973835000	-2.108433000	-1.676892000
1	2.789039000	4.070813000	-0.534564000	6	-3.559668000	-0.283107000	-2.367866000
1	-1.449640000	2.160161000	1.668815000	6	4.700071000	-1.495755000	0.147297000

6	4.704629000	-2.645211000	-0.865582000	1	-0.119279000	4.027567000	-2.553946000
8	4.007993000	-2.267664000	-2.035850000	1	-1.439626000	3.019534000	-1.912528000
6	2.648479000	-1.994149000	-1.752285000				
6	2.495789000	-0.819176000	-0.776877000				
1	-0.568185000	0.562810000	4.375324000	TS₂			
1	1.905194000	-0.562556000	4.386975000	6	-0.199035000	1.140956000	1.748319000
1	-2.269597000	1.273202000	2.263707000	6	0.319465000	1.947549000	2.798461000
1	-1.168456000	2.096695000	1.134459000	6	1.689612000	1.949551000	2.668321000
1	3.632748000	-1.191701000	2.439382000	6	2.024979000	1.161423000	1.544697000
1	-2.860105000	-1.604603000	2.726130000	8	0.835258000	0.679562000	0.991371000
1	-2.115373000	-2.655768000	1.512505000	6	-1.526226000	0.896523000	1.344278000
1	-3.859604000	-2.708534000	1.789927000	6	3.278509000	0.864651000	1.051556000
1	-5.699784000	-0.334473000	0.813257000	7	3.673271000	0.114971000	0.015781000
1	-4.753882000	0.715064000	1.860290000	8	-1.770246000	-0.118756000	0.408872000
1	-4.953290000	1.125482000	0.152085000	14	-2.221714000	-1.703429000	0.880573000
1	-4.313957000	-3.298146000	-0.773909000	6	-2.311095000	-2.685059000	-0.753912000
1	-4.505520000	-2.857329000	-2.471966000	6	-0.922407000	-2.388341000	2.064134000
1	-5.435997000	-2.008382000	-1.237902000	6	-3.887609000	-1.613826000	1.760424000
1	-1.999936000	-2.519759000	-2.694334000	6	-2.709988000	-4.146579000	-0.445241000
1	-1.136178000	-1.404108000	-1.623745000	6	-0.936095000	-2.674997000	-1.456368000
1	-1.763318000	-2.941113000	-0.995949000	6	-3.363403000	-2.065714000	-1.698596000
1	-4.524097000	0.211252000	-2.209557000	6	5.099466000	-0.002872000	-0.329059000
1	-2.778005000	0.482688000	-2.320665000	6	5.476187000	-1.479201000	-0.485836000
1	-3.567429000	-0.687459000	-3.388392000	8	4.634951000	-2.109885000	-1.437125000
1	5.218723000	-0.631349000	-0.281076000	6	3.276554000	-2.064847000	-1.034568000
1	5.190273000	-1.781029000	1.080783000	6	2.786125000	-0.618894000	-0.901088000
1	5.733780000	-2.869421000	-1.154976000	1	-0.270536000	2.429674000	3.564331000
1	4.261024000	-3.546909000	-0.415112000	1	2.405413000	2.443679000	3.311951000
1	2.167721000	-1.733416000	-2.697481000	1	-2.257848000	0.987184000	2.153670000
1	2.152231000	-2.887167000	-1.341692000	1	-1.905330000	2.103898000	0.514245000
1	2.845990000	0.117033000	-1.226860000	1	4.090474000	1.325722000	1.606562000
1	1.454048000	-0.693830000	-0.494995000	1	-0.818422000	-1.753409000	2.950498000
7	-0.248720000	3.894772000	-0.414192000	1	0.062724000	-2.469359000	1.594952000
6	1.146123000	4.301596000	-0.206517000	1	-1.207937000	-3.385507000	2.415689000
6	2.027382000	3.060598000	-0.313668000	1	-4.215081000	-2.612481000	2.068506000
8	1.866299000	2.397137000	-1.567136000	1	-3.831844000	-1.006098000	2.670353000
6	0.497376000	2.085838000	-1.850153000	1	-4.670731000	-1.191803000	1.122859000
6	-0.397655000	3.317151000	-1.756874000	1	-1.983478000	-4.644808000	0.206031000
1	-0.861994000	4.699530000	-0.314584000	1	-2.763557000	-4.727831000	-1.374507000
1	1.485369000	5.044092000	-0.948984000	1	-3.692621000	-4.214058000	0.034033000
1	1.255942000	4.744393000	0.789261000	1	-0.984334000	-3.239375000	-2.396596000
1	3.085377000	3.329360000	-0.244411000	1	-0.612661000	-1.656182000	-1.697429000
1	1.779301000	2.373889000	0.511676000	1	-0.160193000	-3.140770000	-0.838068000
1	0.485639000	1.675013000	-2.863536000	1	-4.364742000	-2.063117000	-1.254702000
1	0.124869000	1.323351000	-1.150387000	1	-3.110635000	-1.033937000	-1.967095000

1	-3.423924000	-2.641146000	-2.631319000	8	4.599127000	-1.475369000	-2.240952000
1	5.276227000	0.519994000	-1.277547000	6	3.331590000	-1.794335000	-1.691556000
1	5.701181000	0.472716000	0.449253000	6	2.766437000	-0.622165000	-0.885708000
1	6.500148000	-1.566476000	-0.856996000	1	0.080966000	0.995708000	4.484467000
1	5.409486000	-1.987207000	0.489214000	1	2.713092000	1.089847000	4.037210000
1	2.698984000	-2.581458000	-1.804961000	1	-2.108262000	0.258259000	2.828223000
1	3.139168000	-2.593027000	-0.077541000	1	-1.231834000	2.479933000	0.809187000
1	2.827702000	-0.129537000	-1.882913000	1	4.247010000	0.552276000	1.971170000
1	1.763020000	-0.587191000	-0.533531000	1	-1.093671000	-2.938165000	2.354803000
7	-2.371186000	2.971536000	-0.240053000	1	-0.257373000	-3.044015000	0.802937000
6	-1.394407000	4.090492000	-0.417093000	1	-1.608243000	-4.131106000	1.160301000
6	-0.219932000	3.603775000	-1.265780000	1	-4.557085000	-2.900076000	1.404464000
8	-0.668979000	3.093384000	-2.508868000	1	-3.936260000	-1.739079000	2.571764000
6	-1.524673000	1.972109000	-2.325263000	1	-4.800188000	-1.170717000	1.135459000
6	-2.777806000	2.365767000	-1.548725000	1	-2.728743000	-4.234545000	-1.259805000
1	-3.200776000	3.316854000	0.245398000	1	-3.453049000	-3.522951000	-2.701847000
1	-1.898177000	4.924009000	-0.917187000	1	-4.326809000	-3.476024000	-1.169918000
1	-1.062379000	4.414762000	0.572983000	1	-1.418716000	-2.065325000	-3.109301000
1	0.445557000	4.442581000	-1.483002000	1	-0.772927000	-1.026771000	-1.829730000
1	0.350861000	2.838248000	-0.717712000	1	-0.637745000	-2.785687000	-1.699268000
1	-1.803846000	1.618396000	-3.320078000	1	-4.559267000	-0.896749000	-1.403887000
1	-1.003110000	1.162784000	-1.794316000	1	-3.125348000	0.085202000	-1.741949000
1	-3.357796000	3.103903000	-2.112592000	1	-3.726677000	-1.044434000	-2.953849000
1	-3.398781000	1.493585000	-1.336513000	1	5.104288000	0.912482000	-1.018002000
D'				1	5.771895000	0.171614000	0.452966000
				1	6.491515000	-0.978301000	-1.705631000
				1	5.667098000	-2.067743000	-0.558901000
				1	2.671871000	-2.026365000	-2.532131000
				1	3.404724000	-2.682936000	-1.044598000
				1	2.568989000	0.218493000	-1.571904000
				1	1.831125000	-0.906820000	-0.405373000
				7	-1.454134000	2.197313000	-0.152827000
				6	-2.643653000	2.973600000	-0.649721000
				6	-2.245542000	4.435512000	-0.842054000
				8	-1.131706000	4.543283000	-1.711120000
				6	0.014486000	3.895387000	-1.185340000
				6	-0.237016000	2.399344000	-1.017607000
				1	-1.670961000	1.167420000	-0.042605000
				1	-2.940609000	2.524589000	-1.599942000
				1	-3.453090000	2.853944000	0.074132000
				1	-3.069804000	4.983368000	-1.303426000
				1	-2.027505000	4.903004000	0.132703000
				1	0.828674000	4.055480000	-1.895234000
				1	0.307774000	4.343958000	-0.221547000
6	5.539306000	-1.191783000	-1.213848000	1	-0.455208000	1.932998000	-1.981205000

1 0.591829000 1.876598000 -0.536714000

D

6 2.148128000 -0.267342000 -0.198641000

6 1.659992000 1.033010000 0.207805000

6 0.304695000 1.017946000 0.161252000

6 -0.110191000 -0.289686000 -0.283107000

8 1.027185000 -1.052114000 -0.502016000

6 3.358492000 -0.865213000 -0.335467000

6 -1.335418000 -0.812231000 -0.494643000

7 4.643214000 -0.331152000 -0.249943000

8 -2.461155000 -0.043136000 -0.345169000

14 -3.954339000 -0.609042000 0.222182000

6 -5.145317000 0.846465000 -0.104638000

6 -4.440456000 -2.162420000 -0.736308000

6 -3.804063000 -1.025883000 2.055788000

6 -6.554031000 0.502818000 0.426229000

6 -4.627818000 2.113021000 0.610949000

6 -5.224569000 1.124792000 -1.621099000

6 5.636438000 -1.180761000 0.414879000

6 7.044170000 -0.693312000 0.087424000

8 7.204603000 0.675455000 0.436888000

6 6.281568000 1.481434000 -0.281430000

6 4.834188000 1.087914000 0.015782000

1 2.277425000 1.859960000 0.523475000

1 -0.375057000 1.817981000 0.416030000

1 3.341734000 -1.918091000 -0.603848000

1 -1.456822000 -1.833878000 -0.843679000

1 -5.447566000 -2.492624000 -0.458524000

1 -3.759294000 -2.993479000 -0.523104000

1 -4.430552000 -1.992567000 -1.817390000

1 -4.735926000 -1.443888000 2.452108000

1 -3.014899000 -1.769487000 2.211682000

1 -3.548079000 -0.144980000 2.652635000

1 -7.244137000 1.337067000 0.241385000

1 -6.976821000 -0.380418000 -0.066426000

1 -6.553910000 0.316278000 1.506209000

1 -5.300922000 2.959978000 0.420092000

1 -3.630372000 2.393376000 0.258488000

1 -4.575224000 1.978369000 1.697247000

1 -5.884880000 1.980488000 -1.817805000

1 -4.240321000 1.359939000 -2.038414000

1 -5.628592000 0.269341000 -2.174078000

1 5.507475000 -2.211146000 0.065964000

1 5.493337000 -1.176263000 1.509283000

1 7.244763000 -0.836476000 -0.986862000

1 7.786751000 -1.254358000 0.661708000

1 6.462605000 2.515737000 0.024621000

1 6.467306000 1.396193000 -1.364396000

1 4.592890000 1.343604000 1.063400000

1 4.167406000 1.659052000 -0.637032000

[Morpholine-H]⁺

7 0.002343000 1.381110000 0.224422000

6 1.264451000 0.659536000 -0.230330000

6 1.173054000 -0.801380000 0.207305000

8 -0.002882000 -1.402578000 -0.300732000

6 -1.175838000 -0.796531000 0.208447000

6 -1.261923000 0.663562000 -0.231405000

1 0.002095000 1.441746000 1.249539000

1 0.004306000 2.346140000 -0.121236000

1 2.121359000 1.179267000 0.203903000

1 1.291525000 0.743543000 -1.318550000

1 1.213435000 -0.877659000 1.306347000

1 2.024312000 -1.350579000 -0.200444000

1 -2.029787000 -1.343028000 -0.197267000

1 -1.214851000 -0.870692000 1.307699000

1 -1.286710000 0.745686000 -1.319800000

1 -2.117493000 1.187312000 0.200615000

DC-II

6 -0.519046000 1.750778000 -1.529988000

6 -0.115263000 1.558678000 -2.846320000

6 1.291435000 1.495776000 -2.836576000

6 1.687025000 1.656910000 -1.524494000

8 0.608649000 1.796704000 -0.728389000

6 -1.736305000 1.836304000 -0.813944000

7 -2.921987000 2.224969000 -1.273364000

6 3.043248000 1.888809000 -0.928330000

8 3.147361000 1.392514000 0.381019000

6 -4.978911000 3.387226000 -0.568654000

6 -4.116684000 2.135330000 -0.413063000

6 -3.198927000 2.604456000 -2.665904000

6 -4.140035000 3.817112000 -2.699731000

8 -5.307026000 3.593916000 -1.933377000

14 3.963990000 2.243714000 1.615596000

6 3.214049000 3.969546000 1.765942000

6	1.139773000	-1.758368000	-0.909058000	1	-2.736511000	-0.940823000	-1.254399000
6	1.168375000	-1.741953000	0.521733000	1	6.352775000	2.901134000	1.931907000
6	-0.083064000	-1.442678000	0.974568000	1	5.921315000	2.952712000	0.225549000
6	-0.929705000	-1.275203000	-0.171651000	1	6.246502000	1.399870000	1.004252000
8	-0.172095000	-1.461352000	-1.305612000	1	4.214692000	1.286114000	5.299172000
6	2.026363000	-1.975447000	-1.931506000	1	3.962675000	2.880088000	4.586247000
7	3.312022000	-2.428500000	-1.903697000	1	5.450056000	1.979898000	4.247888000
6	-2.254161000	-0.966601000	-0.280805000	1	4.102349000	-0.823473000	3.890845000
8	-3.039591000	-0.802621000	0.827170000	1	3.839917000	-0.727445000	2.141211000
6	3.681618000	1.199532000	3.185125000	1	5.367456000	-0.176375000	2.843524000
6	5.786444000	2.381983000	1.151323000	1	1.710483000	2.050182000	3.666172000
6	4.368262000	1.881539000	4.390003000	1	1.997606000	0.450070000	4.352774000
6	4.283570000	-0.209952000	2.998472000	1	1.635786000	0.621585000	2.623740000
6	2.168259000	1.075084000	3.465989000	1	-2.086614000	-3.666916000	1.613277000
14	-3.970945000	-2.031638000	1.596720000	1	-3.633812000	-4.476772000	1.873785000
6	-3.134220000	-3.691105000	1.297636000	1	-3.153764000	-3.987806000	0.244517000
6	-5.755958000	-2.002291000	0.903044000	1	-4.221093000	-0.519016000	3.572891000
6	-3.924930000	-1.560707000	3.415697000	1	-2.918008000	-1.687465000	3.826443000
6	-6.484617000	-0.714631000	1.342553000	1	-4.601555000	-2.189754000	4.003788000
6	-6.525928000	-3.223423000	1.457268000	1	-7.499065000	-0.686647000	0.924292000
6	-5.741044000	-2.078162000	-0.638713000	1	-5.965886000	0.188245000	0.999930000
6	5.193062000	-3.649789000	-0.895288000	1	-6.579756000	-0.648909000	2.431264000
6	4.006134000	-2.714159000	-0.649139000	1	-7.565427000	-3.206576000	1.105218000
6	4.181740000	-2.089556000	-3.038393000	1	-6.087843000	-4.171130000	1.127719000
6	5.332583000	-3.085792000	-3.148761000	1	-6.558449000	-3.230330000	2.552761000
8	6.041137000	-3.163389000	-1.921836000	1	-5.233936000	-2.977730000	-1.005127000
1	-0.754625000	1.426215000	-3.705845000	1	-6.766144000	-2.102505000	-1.030609000
1	1.943900000	1.356697000	-3.686112000	1	-5.245205000	-1.208539000	-1.086412000
1	-1.666273000	1.705919000	0.260222000	1	5.798235000	-3.724965000	0.011503000
1	3.783197000	1.423872000	-1.595207000	1	4.821773000	-4.654103000	-1.152988000
1	3.227957000	2.975511000	-0.970672000	1	3.307020000	-3.208242000	0.029689000
1	-5.918909000	3.257087000	-0.027588000	1	4.347346000	-1.778895000	-0.178217000
1	-4.455347000	4.264977000	-0.158803000	1	3.582701000	-2.098211000	-3.954511000
1	-3.797243000	1.984395000	0.619501000	1	4.595433000	-1.076993000	-2.907704000
1	-4.692226000	1.254952000	-0.720787000	1	6.043633000	-2.755651000	-3.910093000
1	-2.261700000	2.859375000	-3.159679000	1	4.946086000	-4.077205000	-3.432783000
1	-3.659415000	1.754065000	-3.185067000				
1	-4.458189000	3.999235000	-3.728966000				
1	-3.602656000	4.707107000	-2.336402000	TS_{3-II}			
1	3.687159000	4.520660000	2.585876000	6	0.709759000	-1.583713000	-1.323090000
1	3.362504000	4.567692000	0.860141000	6	0.693696000	-1.332800000	-2.678810000
1	2.139269000	3.929437000	1.968125000	6	-0.665026000	-1.384617000	-3.087341000
1	2.041163000	-1.899912000	1.134961000	6	-1.403740000	-1.668436000	-1.966429000
1	-0.400076000	-1.326729000	2.000183000	8	-0.584545000	-1.776714000	-0.889956000
1	1.631535000	-1.813973000	-2.930398000	6	1.673086000	-1.617237000	-0.252086000

7	2.882564000	-2.190758000	-0.289925000	1	2.915369000	-2.529357000	-2.358522000
6	-2.844472000	-2.039113000	-1.786151000	1	4.352183000	-1.703501000	-1.707375000
8	-3.378741000	-1.553719000	-0.575387000	1	4.988981000	-3.999283000	-2.246927000
6	4.324067000	-3.756783000	0.936963000	1	3.574283000	-4.657978000	-1.387283000
6	3.661868000	-2.378781000	0.948506000	1	-3.488033000	-4.647587000	1.739966000
6	3.614890000	-2.496233000	-1.523256000	1	-2.856995000	-4.662992000	0.099383000
6	4.323791000	-3.850898000	-1.392906000	1	-2.064776000	-3.675887000	1.333992000
8	5.122971000	-3.909095000	-0.226125000	1	-1.616013000	2.333220000	1.927936000
14	-4.169918000	-2.567241000	0.542285000	1	0.894927000	1.568813000	2.395176000
6	-3.037090000	-4.017257000	0.965936000	1	-2.022990000	1.707049000	-2.084416000
6	-1.133694000	1.899757000	-0.207010000	1	2.502636000	0.720132000	-1.198943000
6	-0.893083000	2.022596000	1.188713000	1	-6.289915000	-3.887334000	0.449695000
6	0.397005000	1.624656000	1.438951000	1	-5.554112000	-3.787634000	-1.146837000
6	0.979306000	1.267725000	0.187732000	1	-6.446251000	-2.405418000	-0.502725000
8	0.046090000	1.427919000	-0.795715000	1	-5.458292000	-1.611799000	4.006673000
6	-2.184742000	2.080499000	-1.077427000	1	-4.699254000	-3.116226000	3.483780000
7	-3.373640000	2.688995000	-0.884190000	1	-6.237340000	-2.602722000	2.771979000
6	2.225281000	0.767239000	-0.149582000	1	-5.526516000	0.429156000	2.484268000
8	3.232506000	0.733460000	0.777495000	1	-4.848777000	0.348183000	0.845784000
6	-4.500703000	-1.450010000	2.052248000	1	-6.332138000	-0.530561000	1.242369000
6	-5.761004000	-3.215788000	-0.235153000	1	-2.545637000	-1.782190000	3.004468000
6	-5.266021000	-2.246923000	3.132213000	1	-3.346429000	-0.287518000	3.493955000
6	-5.350097000	-0.233942000	1.626267000	1	-2.575164000	-0.400135000	1.899428000
6	-3.162450000	-0.953396000	2.639651000	1	2.614704000	3.712092000	1.504217000
14	4.373054000	1.990579000	1.081206000	1	4.174087000	4.466309000	1.166119000
6	3.506192000	3.649929000	0.872617000	1	3.194954000	3.833871000	-0.160464000
6	5.864775000	1.831821000	-0.110249000	1	5.232333000	0.680421000	3.032873000
6	4.864042000	1.698222000	2.871469000	1	4.007599000	1.852732000	3.535835000
6	6.670965000	0.547602000	0.178926000	1	5.652830000	2.388867000	3.187050000
6	6.788630000	3.054952000	0.100836000	1	7.529704000	0.476485000	-0.501005000
6	5.398070000	1.810767000	-1.582116000	1	6.072206000	-0.359255000	0.034523000
6	-4.710593000	4.507936000	0.090309000	1	7.065524000	0.528307000	1.200104000
6	-3.741130000	3.353443000	0.368053000	1	7.671959000	2.975297000	-0.545478000
6	-4.485854000	2.402029000	-1.804089000	1	6.289804000	3.997423000	-0.147390000
6	-5.387469000	3.625120000	-1.955200000	1	7.151932000	3.127701000	1.132068000
8	-5.818530000	4.084937000	-0.684053000	1	4.814567000	2.699179000	-1.847797000
1	1.541292000	-1.090097000	-3.302674000	1	6.264272000	1.779638000	-2.255535000
1	-1.048629000	-1.241298000	-4.087241000	1	4.786588000	0.927915000	-1.804185000
1	1.236224000	-1.554215000	0.738501000	1	-5.105741000	4.890706000	1.034401000
1	-3.401923000	-1.641218000	-2.645150000	1	-4.174998000	5.322676000	-0.422023000
1	-2.919044000	-3.136469000	-1.851802000	1	-2.834752000	3.753345000	0.827905000
1	4.989183000	-3.855275000	1.798218000	1	-4.199698000	2.632303000	1.058795000
1	3.561116000	-4.549387000	0.988048000	1	-4.071463000	2.107859000	-2.772825000
1	2.992551000	-2.267306000	1.804375000	1	-5.071564000	1.559838000	-1.410892000
1	4.427643000	-1.601571000	1.008737000	1	-6.283407000	3.360791000	-2.522085000

1	-4.853539000	4.424991000	-2.492168000	8	-5.145649000	4.876241000	-0.733475000
				1	1.271066000	-0.902142000	-3.038984000
				1	-1.178449000	-1.938878000	-3.659632000
E-II				1	1.452197000	-1.504431000	0.954881000
6	0.774744000	-1.618812000	-1.027714000	1	-3.001984000	-3.383434000	-2.129704000
6	0.585714000	-1.393324000	-2.363188000	1	-2.294384000	-4.027407000	-0.636307000
6	-0.701695000	-1.927747000	-2.689798000	1	5.250972000	-3.984451000	1.676019000
6	-1.217058000	-2.436835000	-1.534069000	1	3.953846000	-4.678536000	0.665606000
8	-0.323457000	-2.253007000	-0.513642000	1	3.047135000	-2.736570000	1.868444000
6	1.875274000	-1.336229000	-0.040624000	1	4.403894000	-1.722632000	1.341605000
7	2.983712000	-2.258457000	-0.168590000	1	3.164097000	-2.110101000	-2.248523000
6	-2.503874000	-3.103046000	-1.192631000	1	4.467591000	-1.287599000	-1.356997000
8	-3.328031000	-2.226867000	-0.426553000	1	5.389773000	-3.318583000	-2.312971000
6	4.602556000	-3.801062000	0.815095000	1	4.044169000	-4.301565000	-1.675015000
6	3.750750000	-2.554684000	1.047820000	1	-4.876145000	-4.291402000	2.454323000
6	3.811218000	-2.173342000	-1.368327000	1	-3.705889000	-4.927370000	1.307823000
6	4.683681000	-3.425048000	-1.485099000	1	-3.238868000	-3.621623000	2.402049000
8	5.454079000	-3.623711000	-0.310049000	1	-1.440753000	2.218255000	2.086067000
14	-4.636701000	-2.743098000	0.510804000	1	0.949904000	1.053552000	2.495285000
6	-4.057106000	-4.006180000	1.785311000	1	-1.727530000	1.998717000	-2.001027000
6	-0.930184000	1.962905000	-0.061070000	1	2.526697000	0.482302000	-1.113382000
6	-0.745499000	1.898951000	1.324531000	1	-6.833349000	-3.820431000	-0.014958000
6	0.488529000	1.282904000	1.546970000	1	-5.573130000	-4.418038000	-1.088873000
6	1.020859000	0.987371000	0.296056000	1	-6.291260000	-2.830194000	-1.377189000
8	0.182312000	1.395714000	-0.667766000	1	-6.830811000	-0.502031000	2.712116000
6	-1.924448000	2.322884000	-0.982264000	1	-6.231878000	-2.130229000	3.034683000
7	-3.055818000	2.974330000	-0.802610000	1	-7.313516000	-1.838020000	1.664772000
6	2.249275000	0.220834000	-0.083353000	1	-6.007554000	0.824459000	0.705852000
8	3.282458000	0.466453000	0.832631000	1	-4.818068000	0.114944000	-0.417363000
6	-5.254055000	-1.128108000	1.334301000	1	-6.482235000	-0.483935000	-0.377663000
6	-5.954649000	-3.517633000	-0.594616000	1	-3.829943000	-1.178636000	3.011931000
6	-6.473869000	-1.423729000	2.233232000	1	-4.463797000	0.426644000	2.649098000
6	-5.661442000	-0.113022000	0.245170000	1	-3.232939000	-0.309602000	1.592768000
6	-4.126658000	-0.515898000	2.192179000	1	2.467456000	3.573671000	1.175512000
14	4.284845000	1.849011000	0.993680000	1	3.950789000	4.270408000	0.528548000
6	3.303150000	3.388172000	0.493578000	1	2.902677000	3.326081000	-0.524104000
6	5.869422000	1.699855000	-0.069900000	1	5.161349000	0.950960000	3.152443000
6	4.673292000	1.876441000	2.832075000	1	3.758215000	1.990063000	3.422644000
6	6.671840000	0.433800000	0.302338000	1	5.336494000	2.708485000	3.088978000
6	6.756355000	2.939093000	0.204476000	1	7.593047000	0.384809000	-0.292418000
6	5.526900000	1.670019000	-1.575845000	1	6.116902000	-0.490394000	0.115246000
6	-4.124961000	4.935030000	0.242029000	1	6.970201000	0.435278000	1.356371000
6	-3.493003000	3.555049000	0.479855000	1	7.675107000	2.876645000	-0.392293000
6	-4.053324000	3.059987000	-1.894714000	1	6.261429000	3.877977000	-0.066903000
6	-4.621985000	4.476601000	-1.987761000	1	7.060895000	3.008460000	1.254273000

1	4.993244000	2.572054000	-1.895892000	6	2.509871000	3.672555000	-0.083065000
1	6.446223000	1.610482000	-2.172428000	6	1.398166000	2.870877000	2.763812000
1	4.915713000	0.801548000	-1.846359000	6	3.557023000	2.557186000	0.119476000
1	-4.581983000	5.284522000	1.170501000	6	3.122496000	5.028160000	0.337324000
1	-3.343750000	5.651540000	-0.055614000	6	2.115055000	3.735339000	-1.574544000
1	-2.629406000	3.658532000	1.135451000	7	-6.645699000	0.316942000	-0.421788000
1	-4.217202000	2.871769000	0.937740000	6	-9.085619000	0.062478000	-0.481800000
1	-3.577459000	2.757061000	-2.830107000	6	-7.843550000	0.109812000	0.409291000
1	-4.858092000	2.354078000	-1.661367000	6	-6.859693000	0.709425000	-1.806562000
1	-5.446398000	4.492417000	-2.703957000	6	-7.884676000	-0.228500000	-2.490774000
1	-3.845789000	5.178861000	-2.328787000	8	-8.839213000	-0.778851000	-1.591705000
DC-I				1	0.040289000	-1.586106000	3.435016000
6	0.594175000	-1.713893000	1.293299000	1	2.706893000	-1.464977000	3.812467000
6	0.796507000	-1.633049000	2.666102000	1	-0.179333000	-1.632703000	-0.666511000
6	2.189724000	-1.550980000	2.868045000	1	4.825087000	-1.298327000	2.013716000
6	2.775689000	-1.597999000	1.620025000	1	4.461751000	-2.741859000	1.064987000
8	1.827288000	-1.682286000	0.667683000	1	-4.184828000	-3.596840000	-1.329285000
6	-0.473870000	-1.798651000	0.365105000	1	-2.731904000	-4.431662000	-0.722934000
7	-1.724800000	-2.178975000	0.546026000	1	-2.097509000	-2.150021000	-1.521017000
6	4.208299000	-1.675895000	1.186178000	1	-3.377193000	-1.435647000	-0.506551000
8	4.420410000	-0.948204000	0.008912000	1	-1.545845000	-2.610913000	2.594447000
6	-3.418628000	-3.588474000	-0.550711000	1	-2.967570000	-1.642896000	2.129360000
6	-2.661557000	-2.259440000	-0.592198000	1	-3.719030000	-3.920014000	2.679415000
6	-2.330837000	-2.489642000	1.850400000	1	-2.473224000	-4.642484000	1.632665000
6	-3.151682000	-3.783897000	1.755668000	1	5.288754000	-0.551648000	-3.654235000
8	-4.084259000	-3.731680000	0.693652000	1	3.669729000	-0.706899000	-2.960758000
14	5.386147000	-1.419155000	-1.314511000	1	4.694295000	0.659882000	-2.509635000
6	4.700292000	-0.408924000	-2.741972000	1	-4.411100000	2.124109000	-2.083621000
6	-4.251570000	0.925643000	-0.197194000	1	-1.824174000	2.612665000	-1.720228000
6	-3.792997000	1.743066000	-1.284243000	1	-5.438692000	-0.071529000	1.199367000
6	-2.468744000	2.005382000	-1.102266000	1	-0.766418000	0.869234000	1.735948000
6	-2.056122000	1.364639000	0.115061000	1	5.610648000	-3.554647000	-2.568537000
8	-3.149278000	0.698369000	0.649193000	1	4.053221000	-3.487503000	-1.743924000
6	-5.440753000	0.382054000	0.211023000	1	5.521362000	-3.911683000	-0.848252000
6	-0.859348000	1.337692000	0.759684000	1	9.140341000	-1.190168000	-1.979830000
8	0.234614000	1.961698000	0.243358000	1	7.791987000	-0.909067000	-3.082002000
6	7.222043000	-1.017498000	-0.953704000	1	8.033228000	-2.509626000	-2.362189000
6	5.119877000	-3.263126000	-1.633658000	1	8.774477000	-1.574604000	0.475605000
6	8.086096000	-1.432985000	-2.165764000	1	7.170731000	-1.482208000	1.199521000
6	7.711892000	-1.782536000	0.294926000	1	7.611188000	-2.867958000	0.183348000
6	7.383033000	0.498656000	-0.709113000	1	7.108039000	1.087001000	-1.591074000
14	0.971202000	3.325938000	0.982827000	1	8.427799000	0.738728000	-0.471955000
6	-0.270110000	4.742196000	0.964266000	1	6.766509000	0.843884000	0.128007000
				1	-1.215160000	4.439072000	1.427233000
				1	0.109114000	5.602575000	1.525709000

1	-0.491610000	5.080605000	-0.052761000	6	-5.635720000	0.318735000	0.275729000
1	1.990266000	1.951987000	2.818093000	6	-1.025124000	1.078269000	0.806644000
1	0.495376000	2.729273000	3.367884000	8	0.067160000	1.703999000	0.280050000
1	1.979188000	3.668737000	3.238921000	6	7.401064000	-1.045472000	-0.821689000
1	4.434248000	2.744347000	-0.514326000	6	5.069737000	-2.937577000	-1.767853000
1	3.169599000	1.567407000	-0.141014000	6	8.255668000	-1.464188000	-2.039610000
1	3.914075000	2.515765000	1.154578000	6	7.744645000	-1.969496000	0.367119000
1	4.024809000	5.232801000	-0.253173000	6	7.743885000	0.411010000	-0.439563000
1	2.432006000	5.862394000	0.173137000	14	0.690161000	3.189000000	0.894956000
1	3.420079000	5.040345000	1.392352000	6	-0.684661000	4.476616000	0.803982000
1	1.379551000	4.523571000	-1.772255000	6	2.161661000	3.605773000	-0.236652000
1	2.997366000	3.955710000	-2.189670000	6	1.187524000	2.919669000	2.692433000
1	1.694999000	2.786131000	-1.921445000	6	3.330011000	2.632118000	0.025234000
1	-9.923443000	-0.367728000	0.071497000	6	2.628263000	5.049560000	0.061413000
1	-9.382420000	1.073400000	-0.801217000	6	1.738081000	3.505710000	-1.718194000
1	-7.947148000	0.910390000	1.155659000	7	-6.831545000	0.224900000	-0.331503000
1	-7.737739000	-0.842891000	0.942787000	6	-9.263955000	-0.128523000	-0.378670000
1	-5.912054000	0.628464000	-2.341550000	6	-8.025175000	-0.016492000	0.508680000
1	-7.181250000	1.759495000	-1.873287000	6	-7.060352000	0.495556000	-1.748565000
1	-7.370762000	-1.083725000	-2.939511000	6	-8.041241000	-0.533070000	-2.361209000
1	-8.387385000	0.327250000	-3.296519000	8	-9.000538000	-1.028690000	-1.436466000
TS_{3-I}				1	0.158898000	-1.008171000	3.476089000
6	0.676214000	-1.175652000	1.343079000	1	2.851356000	-1.124517000	3.815223000
6	0.902374000	-1.114855000	2.699287000	1	-0.202628000	-0.903265000	-0.575625000
6	2.312729000	-1.154465000	2.879283000	1	4.934642000	-1.247098000	2.011188000
6	2.865861000	-1.244569000	1.628520000	1	4.387125000	-2.549936000	0.952878000
8	1.884596000	-1.241433000	0.688724000	1	-3.549837000	-3.811187000	-1.456339000
6	-0.464063000	-1.159308000	0.446048000	1	-1.890462000	-4.236946000	-0.964259000
7	-1.532996000	-1.971242000	0.565954000	1	-1.985192000	-1.801314000	-1.473722000
6	4.270628000	-1.475426000	1.166176000	1	-3.381966000	-1.621384000	-0.384682000
8	4.581328000	-0.690441000	0.040926000	1	-1.165027000	-2.544218000	2.548253000
6	-2.789016000	-3.665006000	-0.685355000	1	-2.828842000	-2.009299000	2.213318000
6	-2.452525000	-2.176578000	-0.560112000	1	-2.855520000	-4.445760000	2.481136000
6	-1.977018000	-2.581607000	1.822871000	1	-1.489633000	-4.638643000	1.353833000
6	-2.385224000	-4.040181000	1.582053000	1	5.655257000	-0.148282000	-3.547837000
8	-3.332374000	-4.148788000	0.532422000	1	4.010451000	-0.096632000	-2.899818000
14	5.544537000	-1.175459000	-1.273368000	1	5.217640000	1.061792000	-2.333230000
6	5.067305000	0.022827000	-2.640160000	1	-4.492591000	1.744732000	-2.204418000
6	-4.420791000	0.777284000	-0.192600000	1	-1.885002000	2.164849000	-1.820486000
6	-3.914538000	1.438363000	-1.345244000	1	-5.632813000	-0.012765000	1.311329000
6	-2.573705000	1.667126000	-1.154727000	1	-1.047965000	0.897047000	1.878641000
6	-2.237065000	1.162579000	0.131579000	1	5.566029000	-3.210926000	-2.705435000
8	-3.355769000	0.629325000	0.707502000	1	3.989911000	-3.012275000	-1.936744000
				1	5.347136000	-3.694098000	-1.026923000
				1	9.323434000	-1.377506000	-1.799800000

1	8.069293000	-0.829493000	-2.913054000	6	-1.859652000	-2.214668000	1.927282000
1	8.074219000	-2.503860000	-2.334170000	6	-2.318417000	-3.671594000	1.996985000
1	8.817987000	-1.916010000	0.591700000	8	-3.169224000	-3.991989000	0.901782000
1	7.213928000	-1.679843000	1.281059000	14	5.820757000	-1.069939000	-1.293326000
1	7.511830000	-3.019811000	0.158770000	6	5.331166000	0.245266000	-2.547815000
1	7.575623000	1.103163000	-1.271692000	6	-4.520247000	0.639135000	-0.344775000
1	8.802302000	0.492782000	-0.158885000	6	-3.979432000	1.234287000	-1.490316000
1	7.148509000	0.760753000	0.410869000	6	-2.602694000	1.351458000	-1.285665000
1	-1.581010000	4.142385000	1.337251000	6	-2.341023000	0.830480000	-0.023315000
1	-0.360999000	5.413266000	1.270024000	8	-3.481763000	0.423869000	0.553350000
1	-0.974350000	4.703091000	-0.226886000	6	-5.764054000	0.238749000	0.166309000
1	1.884582000	2.083600000	2.799312000	6	-1.057003000	0.654475000	0.719175000
1	0.317507000	2.719489000	3.327489000	8	-0.137761000	1.599078000	0.241797000
1	1.674551000	3.815419000	3.093122000	6	7.655714000	-0.900545000	-0.767501000
1	4.171364000	2.870104000	-0.638916000	6	5.457598000	-2.788670000	-1.993385000
1	3.058003000	1.588352000	-0.155883000	6	8.575255000	-1.166833000	-1.979540000
1	3.702789000	2.708069000	1.052423000	6	7.989340000	-1.914262000	0.348075000
1	3.493753000	5.299576000	-0.565261000	6	7.910854000	0.527378000	-0.239286000
1	1.849596000	5.790283000	-0.150487000	14	0.244658000	3.136636000	0.886196000
1	2.940458000	5.177898000	1.104427000	6	-1.249687000	4.274133000	0.662456000
1	0.918188000	4.192090000	-1.960589000	6	1.745504000	3.691898000	-0.144992000
1	2.581498000	3.768521000	-2.369735000	6	0.617437000	2.984639000	2.726423000
1	1.421235000	2.491044000	-1.979642000	6	2.953083000	2.771514000	0.140156000
1	-10.093078000	-0.541889000	0.199544000	6	2.111959000	5.145823000	0.231124000
1	-9.577759000	0.858307000	-0.751546000	6	1.406177000	3.627948000	-1.650306000
1	-8.146254000	0.796200000	1.236218000	7	-6.951362000	0.183161000	-0.400048000
1	-7.881267000	-0.955399000	1.054846000	6	-9.305401000	-0.561146000	-0.468063000
1	-6.110729000	0.418692000	-2.278185000	6	-8.138089000	-0.152377000	0.437149000
1	-7.428554000	1.521761000	-1.878635000	6	-7.233484000	0.443521000	-1.817699000
1	-7.490748000	-1.407057000	-2.721243000	6	-8.019335000	-0.745127000	-2.430717000
1	-8.538924000	-0.065017000	-3.223014000	8	-8.819236000	-1.424618000	-1.475814000
				1	0.506813000	-0.318962000	3.397207000
				1	3.169237000	-0.872689000	3.644789000
				1	-0.072842000	-0.754735000	-0.566987000
				1	5.032035000	-1.790313000	1.830958000
				1	4.263148000	-2.712665000	0.530477000
				1	-3.158718000	-4.129016000	-1.122818000
				1	-1.588402000	-4.485035000	-0.354041000
				1	-1.435423000	-2.283393000	-1.420758000
				1	-2.948735000	-1.765041000	-0.644322000
				1	-1.128440000	-2.031349000	2.720008000
				1	-2.731902000	-1.560979000	2.107844000
				1	-2.896475000	-3.849069000	2.907975000
				1	-1.439614000	-4.334094000	1.999912000
				1	5.976214000	0.229145000	-3.432571000
E-I							
6	0.858853000	-0.860224000	1.300948000				
6	1.173824000	-0.651374000	2.614643000				
6	2.571156000	-0.935880000	2.747218000				
6	3.013931000	-1.298744000	1.509474000				
8	1.974184000	-1.257789000	0.620051000				
6	-0.395641000	-0.782079000	0.478634000				
7	-1.230258000	-1.959973000	0.633962000				
6	4.344558000	-1.711864000	0.978480000				
8	4.813469000	-0.768604000	0.031147000				
6	-2.472156000	-3.829579000	-0.325669000				
6	-2.036359000	-2.374897000	-0.509015000				

1	4.301270000	0.081901000	-2.882094000
1	5.382238000	1.247745000	-2.112374000
1	-4.518066000	1.570526000	-2.363637000
1	-1.864914000	1.771950000	-1.951096000
1	-5.736302000	-0.075944000	1.207419000
1	-1.268018000	0.758457000	1.793346000
1	5.996076000	-2.931748000	-2.936510000
1	4.389299000	-2.902055000	-2.208510000
1	5.754041000	-3.604242000	-1.326052000
1	9.628769000	-1.058212000	-1.689240000
1	8.392978000	-0.461797000	-2.798370000
1	8.453052000	-2.180761000	-2.376782000
1	9.046504000	-1.834477000	0.634402000
1	7.397042000	-1.734984000	1.252399000
1	7.818597000	-2.949523000	0.031813000
1	7.738496000	1.284997000	-1.011434000
1	8.952133000	0.633069000	0.093576000
1	7.264727000	0.765208000	0.612599000
1	-2.131140000	3.891838000	1.190401000
1	-1.038323000	5.266381000	1.075587000
1	-1.520078000	4.406713000	-0.389833000
1	1.432193000	2.281889000	2.918181000
1	-0.257028000	2.654464000	3.298730000
1	0.908990000	3.960248000	3.130804000
1	3.811755000	3.081718000	-0.469417000
1	2.744515000	1.723920000	-0.096479000
1	3.268114000	2.821674000	1.187793000